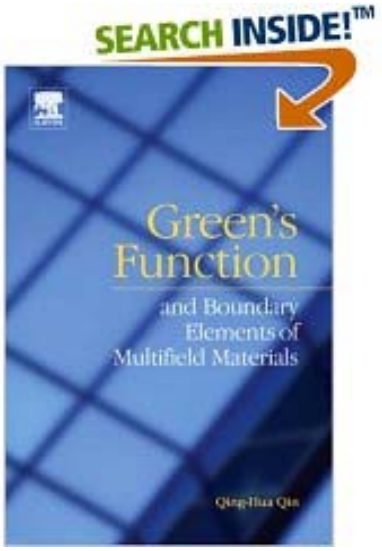
SEARCH INSIDE!™
Green's Function
and Boundary Elements of Multifield Materials
Qing-Hua Qin

Preface

Green's functions play an important role in the solution of numerous problems in the mechanics and physics of solids. It is the heart of many analytical and numerical techniques such as singular-integral-equation methods, boundary-element methods, eigenstrain approaches, and dislocation methods. In general, the term "Green's function" refers to a function, associated with a given boundary value problem, which appears as an integrand for an integral representation of the solution to the problem. In 1828, an English miller from Nottingham published a mathematical essay on Green's function. Although the essay generated little response at that time, Green's function, however, had since found wide applications in areas ranging from classical electrostatics to modern multi-field theory. Research to date on Green's function and the corresponding boundary element formulation of multi-field materials has resulted in the publication of a great deal of new information and has led to improvements in design and fabrication practices. Articles have been published in a wide range of journals attracting the attention of both researchers and practitioners with backgrounds in the mechanics of solids, applied physics, applied mathematics, mechanical engineering and materials science. However, no extensive, detailed treatment of this subject has been available up to the present. It now appears timely to collect significant information and to present a unified treatment of these useful but scattered results. These results should be made available to professional engineers, research scientists, workers and students in applied mechanics and material engineering, e.g. physicists, metallurgists and materials scientists. The objective of this book is to fill this gap, so that readers can obtain a sound knowledge of Green's function and its boundary element implementation of multi-field materials and structures. This volume details the development of each of the techniques and ideas, beginning with a description of the basic concept of Green's function from a mathematical point of view. From there we progress to the derivation and construction of Green's function for multifield problems including piezoelectric, thermopiezoelectric, and magnetoelectroelastic problems and show how they arise naturally in the response of multi-field solid to external loads.

Green's function and boundary elements of multifield materials is written for researchers, postgraduate students and professional engineers in the areas of solid mechanics, Physical science and engineering, applied mathematics, mechanical engineering, and materials science. Little mathematical knowledge beyond the usual calculus is required, although convenience matrix presentation is used throughout the book.

This book consists of six chapters and three appendices. The first chapter gives a brief description of Green's function and linear theory of multi-field material in order to establish notation and to provide a common source for reference in later chapters. It describes in detail the method of deriving Green's function and boundary value equations of multi-field problems. Chapter 2 deals with Green's function of piezoelectric materials, beginning with a discussion of Green's function by Radon transforms and ending with a brief description of dynamic Green's function in three-dimensional piezoelectric solids. Chapter 3 presents Green's functions in theropiezoelectric problems. Green's functions of infinite thermopiezoelectric solids with a half-plane boundary, a bimaterial interface, an elliptic, an arbitrarily shaped hole, and elliptic inclusion are presented. Chapter 4 is concerned with applications of Green's function to magnetoelectroelastic problem. Chapter 5 describes the development of boundary element formulation using the reciprocity theorem and the Green's function described in the previous chapters. The final chapter talks about an alternative boundary element formulation which is

suitable for modelling multi-field problem with discontinuity and demonstrate the power and versatility of the discontinuity boundary element formulation in treating fracture problems of multi-field materials.

I am indebted to a number of individuals in academic circles and organizations who have contributed in different, but important, ways to the preparation of this book. In particular, I wish to extend my appreciation to X.Q. Feng, E. Pan, and S.W. Yu. Special thanks go to Jonathan Agbenyega and other staff members of Elsevier for their commitment to excellence in all aspects of the publication of this book. Finally, I wish to acknowledge the individuals and organizations cited in the book for permission to use their material. Thanks are particularly to Elsevier, John Wiley & Sons, and Birkhäuser Verlag at Basel of Switzerland for their permission to use the invaluable materials published by them.

Acknowledgements

Pages 26–27:
Dunn ML, Electroelastic Green's functions for transversely isotropic media and their application to the solution of inclusion and inhomogeneity problems, Int J Eng Sci, 32, 119–131, 1994

Pages 29–31:
Dunn ML and Wienecke HA, Green's functions for transversely isotropic piezoelectric solids, Int J Solids Struct, 33, 4571–4581, 1996

Section 2.8:
Lu P and Williams FW, Green's function of piezoelectric materials, with an elliptic hole or inclusion, Int J Solids Struct, 35, 651–664, 1998

Section 2.10:
Chen BJ, Xiao ZM and Liew KM, A line dislocation interacting with a semi-infinite crack in piezoelectric solid, Int J Eng Sci, 42, 1–11, 2004

Section 2.11:
Chen BJ, Liew KM and Xiao ZM, Green's function for anti-plane problems in piezoelectric media with a finite crack, Int J Solids Struct, 41, 5285–5300, 2004

Section 2.12:
Wang X and Zhong Z, Two-dimensional time-harmonic dynamic Green's functions in transversely isotropic piezoelectric solids, Mech Res Commun, 30, 589–593, 2003

Section 3.7:
Qin QH, Thermoelectroelastic solution on elliptic inclusions and its application to crack-inclusion problems, Appl Math Modelling 25, 1–23, 2000

Section 4.2:
Pan E, Three dimensional Green's functions in anisotropic magnetoelectroelastic bimaterials, Z Angew Math Phys, 53, 815–838, 2002

Section 4.3:
Hou PF, Ding HJ and Chen JY, Green's function for transversely isotropic magnetoelectroelastic media, Int J Eng Sci, 43, 826–858, 2005

Section 4.4:
Li JY, Magnetoelectric Green's functions and their application to the inclusion and inhomogeneity problems, Int J Solids Struct, 39, 4201–4213, 2002

Section 4.7:
Liu J, Liu X, Zhao Y. Green's functions for anisotropic magnetoelectroelastic solids with an elliptical cavity or a crack. Int J Eng Sci, 39, 1405–1418, 2001

Section 5.4:
Kogl M and Gaul L, A boundary element method for transient piezoelectric analysis, Eng Analysis Boun Elements, 24, 591–598, 2000

Section 5.5:
Davi G and Milazzo A, Multidomain boundary integral formulation for piezoelectric materials fracture mechanics, Int J Solids Srtuc, 38, 7065–7078, 2001

Notations

$\mathbf{a}$	matrix defined in Eq (1.118)
$\mathbf{A}$	matrix defined in Eq (1.130)
$\mathbf{b}$	matrix defined in Eq (1.122) or line dislocation in Eq (2.61)
$\mathbf{B}$	matrix defined in Eq (1.130)
b_i	body force per unit volume
b_e	electric charge density
b_m	body electric current
B_i	magnetic induction
C_{ijkl} (or c_{ij})	elastic stiffness constant
C_v	specific heat per unit mass
D_i	electric displacement
E	Young's modulus
e_{mij}	piezoelectric constant
$\tilde{e}_{lij}$	piezomagnetic constants
E_i	electric field
E_{iJMl}	generalied material constant defined in Eq (1.115)
F	Lekhnitskii stress function in Eq (1.148)
f_{ij}	elastic compliance
g	Gibbs energy function
G	shear modulus
g_{ij}	inverse piezoelectric constants
h_i	heat flow
$\overline{h}_n$	prescribed surface heat flow
h^*	line heat source
$\mathbf{h}(z)$	function defined in Eq (2.99)
H_i	magnetic field
k	$=(k_{11}k_{22}-k_{12}^2)^{1/2}$ defined after Eq (3.2)
k_{ij}	constant of heat conduction
$K_{MN}(\mathbf{n})$	$=E_{iMNj}n_in_j$ defined in Eq (2.306)
$\mathbf{M}^{(j)}$	$=-i\mathbf{B}^{(j)}\mathbf{A}^{(j)-1}$ defined after Eq (2.85)
n_i	unit vector outward normal to boundary Γ
p_i	eigenvalue of the material equation determined from Eq (1.118)
q_0	$=\hat{T}/4\pi i+h^*/4\pi k$ defined in Eq (3.6)
$\overline{q}_s$	prescribed surface charge
$\mathbf{q}_0$	generalized line force
$\mathbf{q}^*$	$=\mathbf{A}^T\mathbf{q}_0+\mathbf{B}^T\mathbf{b}$ defined in Eq (2.70)
s	entropy density
S, H, L	matrices defined in Eq (1.142)
T	small temperature change
$\overline{t}_i$	prescribed surface traction
T^a	absolute temperature
T_0	reference temperature
$\hat{T}$	line temperature discontinuity
U	internal energy density
u_i	mechanical displacement
U_i	displacement and electric potential defined in Eq (1.114)
V	induction function in Eq (1.148)

ν_i	pyromagnetic constants or material eigenvalues in Section 2.3
z_α^*	$= z_\alpha / p_\alpha$
α_{ij}	electromagnetic constants
β_{ij}	dielectric impermeability
Γ	boundary of solution domain Ω
δ	variational symbol or Dirac delta function
δ_{ij}	Kronecker delta
ε_{ij} (or ε_p)	strain
κ_{ij}	dielectric constant
λ	Lamé constant
λ_{ij}	thermal-stress coefficient
μ_{ij}	magnetic permeabilities
Π_{ij}	stress and electric displacement defined in Eq (1.114)
ρ	mass density
σ_{ij} (or σ_p)	stress
υ	Poisson's ratio
ϕ	electric potential
$\boldsymbol{\varphi}$	Generalized stress function defined in Eq (1.121)
χ_i	pyroelectric coefficient
ψ	magnetic potential
∇_2	$= \dfrac{\partial^2}{\partial x^2} + \dfrac{\partial^2}{\partial y^2}$, two-dimensional Laplacian operator

Chapter 1 Introduction

1.1 Foundation of Green's function

Green's function is a basic solution to a linear differential equation, a building block that can be used to construct many useful solutions. In heat conduction, we know that the Green's function represents the temperature at a field point due to a unit heat source applied at the source point. In elastostatics, the Green's function stands for the displacement in the solid due to the application of a unit point force. In general, the exact form of Green's function depends on the differential equation, the body shape, and the types of boundary condition present. Green's functions are named in honor of British mathematician and physicist George Green (1793-1841), who pioneered the concept in the 1830s. To show how Green's function arises, and to initiate further study of the method, a typical one-dimensional boundary value problem is first considered and solved by fairly elementary methods.

Consider a taut string of length l whose transverse displacement, $u(x)$, is governed by the following differential equation (see Chapter 1 in [1])

$$u''(x) + \lambda^2 u(x) = -f(x); \qquad 0 \le x \le l \tag{1.1}$$

and by the boundary conditions

$$u(0) = u(l) = 0 \tag{1.2}$$

where the prime $'$ stands for differentiation, λ is a known constant, and $f(x)$ is a known function of x. To solve the boundary value problem (1.1) and (1.2) we employ the method of variation of parameters. To this end, we start by considering the characteristic equation of the associated homogeneous equation to Eq (1.1): $r^2 + \lambda^2 = 0$, which factors $(r + i\lambda)(r - i\lambda)$ having the roots $r_1 = -i\lambda$ and $r_2 = i\lambda$, where $i = \sqrt{-1}$. The general solution of the associated homogeneous equation is then given by

$$u(x) = c_1 e^{i\lambda x} + c_2 e^{-i\lambda x} \tag{1.3}$$

Noting that $e^{i\lambda x} = \cos\lambda x + i\sin\lambda x$, Eq (1.3) can be rearranged in the form

$$u(x) = A\cos\lambda x + B\sin\lambda x \tag{1.4}$$

where $A = c_1 + c_2$ and $B = i(c_1 - c_2)$. By the method of variation of parameters, we assume that A and B are unknown functions of x such that

$$u(x) = A(x)\cos\lambda x + B(x)\sin\lambda x \tag{1.5}$$

Now we have two unknown functions here and so two equations are required to determine the two unknowns. The first equation can be obtained by plugging the proposed solution (1.5) into Eq (1.1). The second equation can come from a variety of places. We are going to obtain our second equation simply by making an assumption that will make our work easier. This can be done by setting[1]

$$A'(x)\cos\lambda x + B'(x)\sin\lambda x = 0 \tag{1.6}$$

Using Eq (1.6) we can then find that Eq (1.5) constitutes a solution provided that

$$-\lambda A'(x)\sin\lambda x + \lambda B'(x)\cos\lambda x = -f(x) \tag{1.7}$$

Solving Eqs (1.6) and (1.7), we obtain

$$A'(x)=\frac{f(x)\sin\lambda x}{\lambda};\qquad B'(x)=\frac{-f(x)\cos\lambda x}{\lambda} \tag{1.8}$$

Thus, the functions A and B can be written in the form

$$A(x)=\frac{1}{\lambda}\int f(x)\sin\lambda x dx+c;\qquad B(x)=-\frac{1}{\lambda}\int f(x)\cos\lambda x dx+d \tag{1.9}$$

where c and d are two constants to be determined by the boundary conditions (1.2). Substituting Eq (1.9) into (1.5) we have

$$u(x)=\frac{\cos\lambda x}{\lambda}\int_c^x f(y)\sin\lambda y dy-\frac{\sin\lambda x}{\lambda}\int_d^x f(y)\cos\lambda y dy \tag{1.10}$$

After some mathematical manipulation we arrive at

$$\begin{aligned}u(x)&=\int_0^x\frac{f(y)\sin\lambda y\sin\lambda(l-x)}{\lambda\sin\lambda l}dy+\int_x^l\frac{f(y)\sin\lambda x\sin\lambda(l-y)}{\lambda\sin\lambda l}dy\\&=\int_0^x f(y)G(x,y)dy\end{aligned} \tag{1.11}$$

in which the function $G(x,y)$ is a two-point function of (x,y), known as the Green's function for the boundary value problem (1.1) and (1.2). It is defined as[1]

$$G(x,y)=\begin{cases}\dfrac{\sin\lambda y\sin\lambda(l-x)}{\lambda\sin\lambda l};& 0\le y\le x,\\[2ex]\dfrac{\sin\lambda x\sin\lambda(l-y)}{\lambda\sin\lambda l};& x\le y\le l\end{cases} \tag{1.12}$$

where x is usually known as field point(or observation point) and y the source point. It can be seen from Eqs (1.11) and (1.12) that the two-point Green's function, $G(x,y)$, is independent of the force term $f(x)$, and depends only upon the differential equation considered and the boundary conditions which are imposed. Consequently, the solution to all such problems as that examined above but having different forcing terms is known in the form of Eq (1.11) once the kernel $G(x,y)$ has been determined.

The Green's function $G(x,y)$ associated with the above boundary value problem can also be defined by the following auxiliary boundary value problem:

$$G''+\lambda^2 G=-\delta(x-y);\qquad x\ne y \tag{1.13}$$

$$G(0,y)=G(l,y)=0 \tag{1.14}$$

where y is fixed and $0<y<l$. $\delta(x-y)$ is a two point symbolic function known as the Dirac delta function, which is discussed in the next section. Although the problem (1.13) and (1.14) is quite similar to the boundary value problem (1.1) and (1.2), the forcing function in Eq (1.13) is a Dirac delta function rather than an arbitrary function $f(x)$. This means that solving the problem for G will be somewhat simpler than solving the corresponding problem for u, and once G has been found for a particular differential operator, say L, and set of boundary conditions, the function G may be used for solving (1.1) and (1.2) for any number of times where only the function $f(x)$ changes from time to time. It is this feature of Green's function, coupled with its

physical interpretation, that makes it most useful in engineering applications.

The discussion above is for a simple and quite special operator only. To prepare the way for further study of such functions and their use in solving boundary value problems, let us consider a more general boundary value problem:

$$Lu(x) = -f(x), \tag{1.15}$$

$$u(a) = \alpha, \quad u(b) = \beta \tag{1.16}$$

where we introduce as a separate quantity for our consideration the differential operator L [in Eq (1.1), $L = d^2/dx^2 + \lambda^2$], a and b are the boundary points of the solution domain, and α and β are two prescribed constants. Since this is a linear problem the solution to Eqs (1.15) and (1.16) can be assumed to consist of a particular part u_p and a homogeneous part u_h as $u = u_h + u_p$, where u_p satisfies the boundary value problem

$$Lu_p(x) = -f(x); \; u_p(a) = u_p(b) = 0 \tag{1.17}$$

and u_h is the solution of

$$Lu_h(x) = 0; \; u_h(a) = \alpha; \; u_h(b) = \beta \tag{1.18}$$

For a second-order linear ordinary differential operator, the general solution for u_h is of the form

$$u_h = c_1 u_1(x) + c_2 u_2(x) \tag{1.19}$$

where u_1 and u_2 are linearly independent solutions of the homogeneous differential equation $(1.18)_1$, and the constants c_1 and c_2 are determined by imposing the non-homogeneous boundary conditions $(1.18)_{2,3}$. To determine the particular solution u_p, Eq $(1.17)_1$ is rewritten as

$$u_p(x) = -L^{-1}(x) f(x) \tag{1.20}$$

where L^{-1} is the inverse of the differential operator L. Since L is a differential operator, it is reasonable to expect its inverse to be an integral operator. We expect the usual properties of inverse to hold:

$$LL^{-1} = L^{-1}L = I \tag{1.21}$$

where I is the identity operator. On the other hand, if we consider the problem as an example of heat conduction, $f(x)$ would be the distribution function of heat source density. We first consider the heat source concentrated at a point y, and $G(x, y)$ is a function of the temperature representing a unit of heat source at the point y and satisfying the boundary conditions. Because of the continuity of $f(x)$, all other solutions are simply superpositions of this function. Therefore, the particular solution should be

$$u_p(x) = \int_a^b G(x, y) f(y) dy \tag{1.22}$$

The consistency of Eqs (1.20) and (1.22) yields

$$-L^{-1}f(x)=\int_a^b G(x,y)f(y)dy \tag{1.23}$$

If we formally apply the differential operator L to both sides of (1.23), and assume commutativity of L with integration, we find that

$$f(x)=-\int_a^b L[G(x,y)]f(y)dy \tag{1.24}$$

This will lead to

$$L[G(x,y)]=-\boldsymbol{\delta}(x-y) \tag{1.25}$$

Besides, the boundary conditions $(1.17)_{2,3}$ require that

$$u_p(a)=\int_a^b G(a,y)f(y)dy=0;\qquad u_p(b)=\int_a^b G(b,y)f(y)dy=0 \tag{1.26}$$

Since $f(y)$ can represent any functions of y, the relations (1.26) are possible only if

$$G(a,y)=G(b,y)=0 \tag{1.27}$$

Therefore the Green's function we are seeking is a solution of the boundary value problem

$$\begin{cases} L[G(x,y)]=-\boldsymbol{\delta}(x-y) \\ G(a,y)=G(b,y)=0 \end{cases} \tag{1.28}$$

As an illustration, consider the two-dimensional Laplace's operator

$$L=\nabla_2=\frac{\partial^2}{\partial x_1^2}+\frac{\partial^2}{\partial x_2^2} \tag{1.29}$$

The Green's function for this particular differential operator is known to be

$$G(\mathbf{x},\mathbf{y})=-\frac{1}{2\pi}\ln r \tag{1.30}$$

where $\mathbf{x}=(x_1,x_2)$ and $\mathbf{y}=(y_1,y_2)$ are two position vectors in two-dimensional space and

$$r=\left[(x_1-y_1)^2+(x_2-y_2)^2\right]^{1/2} \tag{1.31}$$

It can be seen that the Green's function here represents the potential at the observation point **x** due to a point charge at the source point **y**. It is also found that the Green's function depends on the distance between the source and observation point only.

From the discussion above it is as yet unclear how the Green's functions for a given differential operator can be derived. In the rest of this section we follow the results given in [2] to show the procedure for deriving Green's functions using Fourier transform. To this end, consider the Helmholtz equation in three dimensions:

$$Lu=\left[\frac{\partial^2}{dx_1^2}+\frac{\partial^2}{dx_2^2}+\frac{\partial^2}{dx_3^2}+\lambda^2\right]u=(\nabla_3+\lambda^2)u=0 \tag{1.32}$$

where ∇_3 is the three-dimensional Laplace's operator. From the discussion above the related free-space (no boundary conditions are specified) Green's function can be obtained by considering

$$L(\mathbf{x})G(\mathbf{x},\mathbf{y}) = -\delta(\mathbf{x}-\mathbf{y}) \tag{1.33}$$

where $\mathbf{x} = (x_1, x_2, x_3)$ and $\mathbf{y} = (y_1, y_2, y_3)$ are two position vectors in three-dimensional space, and

$$\delta(\mathbf{x}-\mathbf{y}) = \delta(x_1 - y_1)\delta(x_2 - y_2)\delta(x_3 - y_3) \tag{1.34}$$

is the three-dimensional Dirac delta function. The differential equation (1.33) can be solved using a variety of methods. Here we use the Fourier transform method given in [2] to solve this problem. Since we are calculating only the free-space component of the Green's function, we can use a single variable **r**=**x**-**y**, as the free-space Green's function will depend only on the relative distance between points **x** and **y** and not on their absolute positions. We begin by defining a Fourier transform pair [2]

$$\hat{u}(\boldsymbol{\xi}) = \frac{1}{(2\pi)^3}\int_{-\infty}^{\infty} u(\mathbf{r})e^{-i\boldsymbol{\xi}\cdot\mathbf{r}}d\mathbf{r}, \quad u(\mathbf{r}) = \int_{-\infty}^{\infty}\hat{u}(\boldsymbol{\xi})e^{i\boldsymbol{\xi}\cdot\mathbf{r}}d\boldsymbol{\xi} \tag{1.35}$$

where $\boldsymbol{\xi} = (\xi_1, \xi_2, \xi_3)$ represents the coordinates in the frequency domain. Applying the forward transformation $(1.35)_1$ to Eq (1.33) for the Green's function we obtain

$$\hat{G}(\boldsymbol{\xi}) = \frac{1}{(2\pi)^3(\xi^2 - \lambda^2)} \tag{1.36}$$

where $\xi^2 = \boldsymbol{\xi}\cdot\boldsymbol{\xi}$. The Green's function in physical space is then given through the inverse integral

$$\begin{aligned} G(\mathbf{r}) &= \frac{1}{(2\pi)^3}\int_{-\infty}^{\infty}\frac{e^{i\boldsymbol{\xi}\cdot\mathbf{r}}}{(\xi^2-\lambda^2)}d\boldsymbol{\xi} \\ &= \frac{\pi}{ir(2\pi)^3}\left\{\int_{-\infty}^{\infty}\frac{\xi e^{ir\xi}}{(\xi^2-\lambda^2)}d\xi - \int_{-\infty}^{\infty}\frac{\xi e^{-ir\xi}}{(\xi^2-\lambda^2)}d\xi\right\} \\ &= \frac{\pi}{ir(2\pi)^3}\{R_1 - R_2\} \end{aligned} \tag{1.37}$$

where $r = \sqrt{\mathbf{r}\cdot\mathbf{r}} = [(x_1-y_1)^2 + (x_2-y_2)^2 + (x_3-y_3)^2]^{1/2}$ and the integrals R_1 and R_2 can be evaluated by considering a contour in the complex ξ space [2]:

$$R_1 = \lim_{\varepsilon\to 0}\int_{-\infty}^{\infty}\frac{\xi e^{ir\xi}d\xi}{(\xi-(\lambda+i\varepsilon))(\xi+(\lambda+i\varepsilon))} = i\pi e^{i\lambda r} \tag{1.38}$$

$$R_2 = \lim_{\varepsilon\to 0}\int_{-\infty}^{\infty}\frac{\xi e^{-ir\xi}d\xi}{(\xi-(\lambda+i\varepsilon))(\xi+(\lambda+i\varepsilon))} = -i\pi e^{i\lambda r} \tag{1.39}$$

The Green's function is then given by

$$G(\mathbf{r}) = \frac{\pi}{ir(2\pi)^3}\{i\pi e^{i\lambda r} + i\pi e^{i\lambda r}\} = \frac{1}{4\pi r}e^{ir\lambda} \tag{1.40}$$

1.2 Dirac delta function

Having already used the concept of the Dirac delta function in Section 1.1 above, we

now introduce it in a way which demonstrates how this concept fits into the familiar realm of functions and integrals, and we provide some physical interpretations. The Dirac delta function is important in the study of phenomena of a point action or an impulsive force, such as an action which is highly localized in space and/or time, including the point force in solid mechanics; the impulsive force in rigid body dynamics; the point mass in gravitational field theory; and the point heat source in the theory of heat conduction. The point action or the impulse is usually described by the Dirac delta function $\delta(x)$ [2,3]. The function $\delta(x)$ is defined to be zero when $x \neq 0$, and infinite at $x = 0$ in such a way that the area under the function is unity. With this in mind, a concise definition of $\delta(x)$ can be given in the form

$$\delta(x) = 0 \text{ if } x \neq 0; \ \int_{-a}^{b} \delta(x)dx = 1 \tag{1.40}$$

for any $a > 0$ and $b > 0$. This is a weak definition of $\delta(x)$, since the limits of integration are never precisely zero. The definition (1.40) is, however, sufficient for work with Green's functions [2]. Alternatively, $\delta(x)$ can also be mathematically defined as

$$\delta(x) = \begin{cases} 0 & (x \neq 0) \\ \infty & (x = 0) \end{cases} \tag{1.41}$$

As mentioned in [2,3], the Dirac delta function has several special properties which are useful for deriving Green's functions. They are:

(i) Physical dimension of $\delta(x)$
Since the definition of the Dirac delta function requires that the product $\delta(x)dx$ is dimensionless, the dimension of $\delta(x)$ is the inverse of its argument x.

(ii) Sifting property. If function $f(x)$ is continuous at $x = y$, we have

$$\int_a^b \delta(x-y)f(y)dy = \begin{cases} f(x) & \text{if } a < x < b \\ 0 & \text{if } x \notin [a,b] \end{cases} \tag{1.42}$$

(iii) Unit impulse property. With a any real constant, we have

$$\delta(ax) = \frac{1}{|a|}\delta(x) \tag{1.43}$$

(iv) Derivative property

$$\int_{-a}^{b} f(x)\delta'(x)dx = -f'(0) \tag{1.44}$$

(v) Integral property.

$$\int_{-\infty}^{x} \delta(y)dy = H(x); \ \frac{dH(x-y)}{dx} = \delta(x-y) \tag{1.45}$$

where $H(x)$ is the Heaviside unit step function defined as

$$H(x) = \begin{cases} 0 & \text{if } x < 0 \\ 1 & \text{if } x > 0 \end{cases} \tag{1.46}$$

(vi) If $f(x)$ has real roots x_n (i.e. $f(x_n)=0$), then

$$\delta(f(x))=\sum_n \frac{\delta(x-x_n)}{|f'(x_n)|} \tag{1.47}$$

The sum applies to all real roots. The proof of these properties can be found in [2,4,5].

1.3 Basic equations of piezoelectricity

In this section, we recall briefly the three-dimensional formulation of linear piezoelectricity that appeared in [6-9]. Here, a three-dimensional Cartesian coordinate system is adopted where the position vector is denoted by **x** (or x_i). In this book, both conventional indicial notation x_i and traditional Cartesian notation (x, y, z) are utilized. In the case of indicial notation we invoke the summation convention over repeated indices. Moreover, vectors, tensors and their matrix representations are denoted by bold-face letters. The three-dimensional constitutive equations for linear piezoelectricity can be derived by considering the full Gibbs energy function per unit volume g [9]

$$g=U-E_m D_m-T^a s \tag{1.48}$$

where U, s, D_m and E_m are the internal energy density, entropy density, electric displacement and electric field, respectively, $T^a=T_0+T$ is the absolute temperature, where T_0 is the reference temperature, and T a small temperature change: $|T|<<T_0$. The electric field E_i is defined by

$$E_i=-\phi_{,i}, \tag{1.49}$$

in which ϕ is electric potential, a comma followed by arguments denotes partial differentiation with respect to the arguments. From the exact differential

$$dg=\sigma_{ij}d\varepsilon_{ij}-D_m dE_m-sdT \tag{1.50}$$

where σ_{ij} and ε_{ij} are respectively stress and strain, while ε_{ij} is defined by

$$\varepsilon_{ij}=\frac{1}{2}(u_{i,j}+u_{j,i}), \tag{1.51}$$

in which u_i is elastic displacement, we obtain

$$s=-\left[\frac{\partial g}{\partial T}\right]_{\varepsilon,E},\quad \sigma_{ij}=\left[\frac{\partial g}{\partial \varepsilon_{ij}}\right]_{T,E},\quad D_m=-\left[\frac{\partial g}{\partial E_m}\right]_{\varepsilon,T} \tag{1.52}$$

When the function g is expanded with respect to T, ε_{ij} and E_m within the scope of linear interactions, we have

$$g=\frac{1}{2}\left(T\frac{\partial}{\partial T}+\varepsilon_{ij}\frac{\partial}{\partial \varepsilon_{ij}}+E_m\frac{\partial}{\partial E_m}\right)\left(T\frac{\partial}{\partial T}+\varepsilon_{kl}\frac{\partial}{\partial \varepsilon_{kl}}+E_n\frac{\partial}{\partial E_n}\right)g \tag{1.53}$$

The following constants can then be defined for developing a linear constitutive relation corresponding to the functional g:

$$c_{ijkl}^{(T,E)}=\left[\frac{\partial^2 g}{\partial\varepsilon_{ij}\partial\varepsilon_{kl}}\right]_{T,E},\quad \kappa_{nm}^{(\varepsilon,T)}=-\left[\frac{\partial^2 g}{\partial E_n\partial E_m}\right]_{\varepsilon,T},\quad \frac{\rho C_v^{(\varepsilon,E)}}{T_0}=-\left[\frac{\partial^2 g}{\partial T^2}\right]_{\varepsilon,E},$$

$$e_{mij}^{(T)} = -\left[\frac{\partial^2 g}{\partial \varepsilon_{ij}\partial E_m}\right]_T, \quad \lambda_{ij}^{(E)} = -\left[\frac{\partial^2 g}{\partial \varepsilon_{ij}\partial T}\right]_E, \quad \chi_m^{(\varepsilon)} = -\left[\frac{\partial^2 g}{\partial T \partial E_m}\right]_\varepsilon \tag{1.54}$$

where $c_{ijkl}^{(T,E)}$ are the elastic moduli measured at a constant electric field and temperature, $\kappa_{nm}^{(\varepsilon,T)}$ the dielectric constants measured at a constant strain and temperature, ρ mass density, $C_v^{(\varepsilon,E)}$ specific heat per unit mass, $e_{mij}^{(T)}$ the piezoelectric coefficients measured at a constant temperature, $\lambda_{ij}^{(E)}$ the thermal-stress coefficients measured at a constant electric field, and $\chi_m^{(\varepsilon)}$ the pyroelectric coefficients measured at a constant strain.

When the function g is differentiated according to Eq (1.50), and the above constants are used, we find

$$\begin{aligned} s &= \frac{\rho C_v}{T_0} T + \lambda_{ij}\varepsilon_{ij} + \chi_m E_m, \\ \sigma_{ij} &= -\lambda_{ij} T + c_{ijkl}\varepsilon_{kl} - e_{mij} E_m, \\ D_n &= \chi_n T + e_{nij}\varepsilon_{ij} + \kappa_{mn} E_m \end{aligned} \tag{1.55}$$

A set of these three equations is the constitutive relation in the coupled system. It should be noted that the superscripts "ε", "T" and "E" appearing in Eq (1.54) have been dropped here. To simplify subsequent writing, we omit them in the remaining part of this book. Using the notation defined above, the Gibbs function per unit volume can now be expressed as [9]:

$$g = \frac{1}{2} c_{ijkl}\varepsilon_{ij}\varepsilon_{kl} - \frac{1}{2}\kappa_{ij} E_i E_j - \frac{\rho C_v}{2T_0} T^2 - e_{ijk} E_i \varepsilon_{jk} - \chi_m T E_m - \lambda_{ij} T \varepsilon_{ij} \tag{1.56}$$

Having defined the material constants, the related divergence equations and boundary conditions can be derived by considering the modified Biot's variational principle [9,10]

$$\delta \int_\Omega (B + 2F) d\Omega - \int_\Omega (b_i \delta u_i + b_e \delta\phi)\, d\Omega - \int_\Gamma \left(\bar{t}_i \delta u_i - \bar{q}_s \delta\phi - \bar{h}_n \frac{\delta T}{T_0} \right) d\Gamma = 0 \tag{1.57}$$

where δ is the variational symbol, Ω and Γ are the domain and boundary of the material, b_i and b_e are the body force per unit volume and electric charge density, $\bar{t}_i$, $\bar{q}_s$ and $\bar{h}_n$ are the applied surface traction, applied surface charge, and prescribed surface heat flow, respectively, B and F are Biot's generalized free energy density and the dissipation function, which are respectively defined by [10,11] as

$$B = U - T_0 s = g + E_i D_i + Ts, \quad F = \frac{1}{2T_0} k_{ij} T_{,i} T_{,j} \tag{1.58}$$

in which k_{ij} is the heat conduction coefficient.

The variational principle (1.57) provides the following results:

$$\sigma_{ij,j} + b_i = 0, \quad D_{i,i} + b_e = 0, \quad h_{i,i} = -T_0 \Delta s, \tag{1.59}$$

$$\sigma_{ij} n_j = \bar{t}_i, \quad D_i n_i = -\bar{q}_s, \quad h_i n_i = \bar{h}_n \tag{1.60}$$

and the constitutive equations (1.55), where n_i is the outer unit normal vector to Γ, and h_i is heat flow. Eqs (1.59) are the elastic equilibrium equations, Gauss' law of electrostatics, and the heat conduction equation, respectively; Eqs (1.60) are boundary conditions and Eq (1.55) the constitutive equations.

In this discussion we have shown how a thermal system, as a third system, affects to a greater or lesser degree the elastic, dielectric, and piezoelectric constants. It is therefore necessary to specify the thermal condition, i.e. whether it is isothermal or adiabatic. Since most electromechanical measurements are made under an alternating field or stress, the observed constants are adiabatic. On the other hand, discussion of phase transformation in solid-state physics requires knowledge of isothermal constants. In fact, the distinction between isothermal and adiabatic constants is rarely mentioned because electrical-to-thermal and mechanical-to-thermal couplings are rather weak, except in a few special cases. Therefore, it is worthwhile to pay attention to an electromechanically coupled system.

At a constant temperature, Eqs (1.55) are reduced to

$$\sigma_{ij} = c_{ijkl}\varepsilon_{kl} - e_{mij}E_m, \qquad D_n = e_{nij}\varepsilon_{ij} + \kappa_{mn}E_m \tag{1.61}$$

In addition to the constitutive relation (1.61) above, three other forms of constitutive representation are commonly used in the stationary theory of linear piezoelectricity to describe the coupled interaction between elastic and electric variables. Each type has its own different set of independent variables and corresponds to a different thermodynamic function, as listed in Table 1.1. Although all equations are actually tonsorial, the indices have been omitted for brevity. It should be pointed out that an alternative derivation of formulae is merely a transformation from one type of relation to another. Some relationships between various constants occurring in the four types are as follows:

$$\begin{aligned}
&\beta_{np}\kappa_{pm} = \delta_{nm}, \ \beta^{\varepsilon}_{\mathrm{nm}} - \beta^{\sigma}_{\mathrm{nm}} = g_{nkl}h_{nkl}, \ \kappa^{\sigma}_{nm} - \kappa^{\varepsilon}_{nm} = d_{nkl}e_{mkl}, \\
&c^{D}_{ijkl} - c^{E}_{ijkl} = e_{mij}h_{mkl}, \ f^{E}_{ijkl} - f^{D}_{ijkl} = d_{mij}g_{mkl}, \ d_{nij} = \kappa^{\sigma}_{nm}g_{mij} = e_{nkl}f^{E}_{klij}, \\
&e_{nij} = \kappa^{\varepsilon}_{nm}h_{mij} = d_{nkl}c^{E}_{klij}, \ g_{nij} = \beta^{\sigma}_{nm}d_{mij} = h_{nkl}f^{D}_{klij}, \ h_{nij} = \beta^{\varepsilon}_{nm}e_{mij} = g_{nkl}c^{D}_{klij}
\end{aligned} \tag{1.62}$$

Table 1.1 Four types of fundamental electroelastic relations

Independent variables	Constitutive relations	Thermodynamic functional
ε, **E**	$\begin{cases}\boldsymbol{\sigma} = \mathbf{c}^{E}\boldsymbol{\varepsilon} - \mathbf{e}^{T}\mathbf{E} \\ \mathbf{D} = \mathbf{e}\boldsymbol{\varepsilon} + \boldsymbol{\kappa}^{\varepsilon}\mathbf{E}\end{cases}$	Electric Gibbs energy $g_0 = \frac{1}{2}\mathbf{c}^{E}\boldsymbol{\varepsilon}^2 - \frac{1}{2}\boldsymbol{\kappa}^{\varepsilon}\mathbf{E}^2 - \mathbf{e}\boldsymbol{\varepsilon}\mathbf{E}$
ε, **D**	$\begin{cases}\boldsymbol{\sigma} = \mathbf{c}^{D}\boldsymbol{\varepsilon} - \mathbf{h}^{T}\mathbf{D} \\ \mathbf{E} = -\mathbf{h}\boldsymbol{\varepsilon} + \boldsymbol{\beta}^{\varepsilon}\mathbf{D}\end{cases}$	Helmholtz free energy $g_1 = g_0 + \mathbf{E}\mathbf{D}$
σ,**E**	$\begin{cases}\boldsymbol{\varepsilon} = \mathbf{f}^{E}\boldsymbol{\sigma} + \mathbf{d}^{T}\mathbf{E} \\ \mathbf{D} = \mathbf{d}\boldsymbol{\sigma} + \boldsymbol{\kappa}^{\sigma}\mathbf{E}\end{cases}$	Gibbs free energy $g_2 = g_0 - \boldsymbol{\sigma}\boldsymbol{\varepsilon}$
σ, **D**	$\begin{cases}\boldsymbol{\varepsilon} = \mathbf{f}^{D}\boldsymbol{\sigma} + \mathbf{g}^{T}\mathbf{D} \\ \mathbf{E} = -\mathbf{g}\boldsymbol{\sigma} + \boldsymbol{\beta}^{\sigma}\mathbf{D}\end{cases}$	Elastic Gibbs energy $g_3 = g_0 + \mathbf{E}\mathbf{D} - \boldsymbol{\sigma}\boldsymbol{\varepsilon}$

The material constants can be reduced by the following consideration. According to definition (1.51) we may write $\varepsilon_{ij}=\varepsilon_{ji}$. It follows that

$$c_{ijkm} = c_{ijmk} \tag{1.63}$$

Further, from $\sigma_{ij} = \sigma_{ji}$ we have

$$c_{ijkm} = c_{jikm},\ e_{kij} = e_{kji} \tag{1.64}$$

In view of these properties, it is useful to introduce the so-called two-index notation or compressed matrix notation [12]. Two-index notation involves replacing *ij* or *km* by *p* or *q*, i.e. $c_{ijkm}=c_{pq}$, $e_{ikm}=e_{iq}$, $\sigma_{ij}=\sigma_p$, where *i*, *j*, *k*, *m* take the values 1-3, and *p*, *q* assume the values 1-6 according to the replacements $11\to 1$, $22\to 2$, $33\to 3$, 23 or $32\to 4$, 13 or $31\to 5$, 12 or $21\to 6$. With the two-index system, the constitutive relations (1.61) then become

$$\sigma_p = c_{pq}\varepsilon_q - \varepsilon_{kp}E_k,\quad D_i = e_{iq}\varepsilon_q + \kappa_{ik}E_k, \tag{1.65}$$

in which

$$\varepsilon_p = \begin{cases} \varepsilon_{ij}, & \text{when } i = j, \\ 2\varepsilon_{ij}, & \text{when } i \neq j \end{cases} \tag{1.66}$$

In addition, the elastic, piezoelectric and dielectric constants can now be written in matrix form since they all are described by two indices. The arrays for an arbitrarily anisotropic material are

$$\mathbf{c} = \begin{bmatrix} c_{11} & c_{12} & c_{13} & c_{14} & c_{15} & c_{16} \\ c_{12} & c_{22} & c_{23} & c_{24} & c_{25} & c_{26} \\ c_{13} & c_{23} & c_{33} & c_{34} & c_{35} & c_{36} \\ c_{14} & c_{24} & c_{34} & c_{44} & c_{45} & c_{46} \\ c_{15} & c_{25} & c_{35} & c_{45} & c_{55} & c_{56} \\ c_{16} & c_{26} & c_{36} & c_{46} & c_{56} & c_{66} \end{bmatrix}, \tag{1.67}$$

$$\mathbf{e} = \begin{bmatrix} e_{11} & e_{12} & e_{13} & e_{14} & e_{15} & e_{16} \\ e_{21} & e_{22} & e_{23} & e_{24} & e_{25} & e_{26} \\ e_{31} & e_{32} & e_{33} & e_{34} & e_{35} & e_{36} \end{bmatrix}, \tag{1.68}$$

$$\boldsymbol{\kappa} = \begin{bmatrix} \kappa_{11} & \kappa_{12} & \kappa_{13} \\ \kappa_{12} & \kappa_{22} & \kappa_{23} \\ \kappa_{13} & \kappa_{23} & \kappa_{33} \end{bmatrix} \tag{1.69}$$

It can be seen that there are 21+18+6=45 independent constants for this material type. The matrices for a material with monoclinic symmetry, with x_1 the diagonal axis (Class 2), are

$$\mathbf{c}=\begin{bmatrix} c_{11} & c_{12} & c_{13} & c_{14} & 0 & 0 \\ c_{12} & c_{22} & c_{23} & c_{24} & 0 & 0 \\ c_{13} & c_{23} & c_{33} & c_{34} & 0 & 0 \\ c_{14} & c_{24} & c_{34} & c_{44} & 0 & 0 \\ 0 & 0 & 0 & 0 & c_{55} & c_{56} \\ 0 & 0 & 0 & 0 & c_{56} & c_{66} \end{bmatrix}, \tag{1.70}$$

$$\mathbf{e}=\begin{bmatrix} e_{11} & e_{12} & e_{13} & e_{14} & 0 & 0 \\ 0 & 0 & 0 & 0 & e_{25} & e_{26} \\ 0 & 0 & 0 & 0 & e_{35} & e_{36} \end{bmatrix}, \tag{1.71}$$

$$\boldsymbol{\kappa}=\begin{bmatrix} \kappa_{11} & 0 & 0 \\ 0 & \kappa_{22} & \kappa_{23} \\ 0 & \kappa_{23} & \kappa_{33} \end{bmatrix} \tag{1.72}$$

This type of material symmetry reduces the number of independent constants to 25. For a transversely isotropic material with x_3 in the poling direction (Class C_{6v}=6 mm), the related material matrices are

$$\mathbf{c}=\begin{bmatrix} c_{11} & c_{12} & c_{13} & 0 & 0 & 0 \\ c_{12} & c_{22} & c_{23} & 0 & 0 & 0 \\ c_{13} & c_{23} & c_{33} & 0 & 0 & 0 \\ 0 & 0 & 0 & c_{44} & 0 & 0 \\ 0 & 0 & 0 & 0 & c_{44} & 0 \\ 0 & 0 & 0 & 0 & 0 & \frac{1}{2}(c_{11}-c_{12}) \end{bmatrix}, \tag{1.73}$$

$$\mathbf{e}=\begin{bmatrix} 0 & 0 & 0 & 0 & e_{15} & 0 \\ 0 & 0 & 0 & e_{15} & 0 & 0 \\ e_{31} & e_{31} & e_{33} & 0 & 0 & 0 \end{bmatrix}, \tag{1.74}$$

$$\boldsymbol{\kappa}=\begin{bmatrix} \kappa_{11} & 0 & 0 \\ 0 & \kappa_{11} & 0 \\ 0 & 0 & \kappa_{33} \end{bmatrix} \tag{1.75}$$

Thus it is clear that a material with this type of symmetry is described by ten independent material constants. This category of material is important because the corresponding polarized ceramics have high piezoelectric coupling. Finally, an isotropic dielectric material has arrays which are similar to the arrays for transversely isotropic materials, except that there are some additional relations among the material constants. They are

$$e_{ip}=0 \quad \text{for all values of } i \text{ and } p, \tag{1.76}$$

$$c_{12}=c_{13}=\lambda, \quad c_{11}=c_{33}=\lambda+2G, \quad c_{44}=c_{66}=G, \quad \kappa_{11}=\kappa_{33} \tag{1.77}$$

where $G=E/2(1+\upsilon)$ is the shear modulus of elasticity, $\lambda=2G\upsilon/(1-2\upsilon)$ is the Lamé constant and E, υ are Young's modulus and Poisson's ratio, respectively. In the MKS system the material constants and the variables mentioned above are measured in the following units: $[c_{ij}]=\mathrm{Nm}^{-2}$, $[e_{ij}]=\mathrm{N(Vm)}^{-1}=\mathrm{Cm}^{-2}$, $[\kappa_{ij}]=\mathrm{C}^2\mathrm{N}^{-1}\mathrm{m}^{-2}=\mathrm{NV}^{-2}$, $[\sigma_{ij}]=\mathrm{Nm}^{-2}$, $[\varepsilon_{ij}]=\mathrm{mm}^{-1}$, $[D_i]=\mathrm{Cm}^{-2}=\mathrm{N(Vm)}^{-1}$, $[E_i]=\mathrm{NC}^{-1}=\mathrm{Vm}^{-1}$, $[\phi]=\mathrm{V}$. For poled barium-titanate ($BaTiO_3$) and lead-zirconate-titanate, these physical constants are of the orders: $c_{ij}\sim 10^{11}\,\mathrm{Nm}^{-2}$, $e_{ij}\sim 10\,\mathrm{Nm}^{-2}$, $\kappa_{ij}\sim 10^{-8}\,\mathrm{NV}^{-2}$.

Substitution of Eqs (1.49) and (1.51) into Eq (1.65), and later into Eq (1.59), results in

$$c_{11}u_{1,11}+\frac{1}{2}(c_{11}+c_{12})u_{2,12}+(c_{13}+c_{44})u_{3,13}+\frac{1}{2}(c_{11}-c_{12})u_{1,22} + c_{44}u_{1,33}+(e_{31}+e_{15})\phi_{,13}+b_1=0, \tag{1.78}$$

$$c_{11}u_{2,22}+\frac{1}{2}(c_{11}+c_{12})u_{1,12}+(c_{13}+c_{44})u_{3,23}+\frac{1}{2}(c_{11}-c_{12})u_{2,11} + c_{44}u_{2,33}+(e_{31}+e_{15})\phi_{,23}+b_2=0, \tag{1.79}$$

$$c_{44}u_{3,11}+(c_{44}+c_{13})(u_{1,31}+u_{2,32})+c_{44}u_{3,22}+c_{33}u_{3,33} + e_{15}(\phi_{,11}+\phi_{,22})+e_{33}\phi_{,33}+b_3=0, \tag{1.80}$$

$$e_{15}(u_{3,11}+u_{3,22})+(e_{15}+e_{31})(u_{1,31}+u_{2,32}) + e_{33}u_{3,33}-\kappa_{11}(\phi_{,11}+\phi_{,22})-\kappa_{33}\phi_{,33}+b_e=0, \tag{1.81}$$

for transversely isotropic materials (Class C_{6v}=6 mm) with x_3 as the poling direction and the x_1-x_2 plane as the isotropic plane. This type of material is adopted in the most of following chapters.

1.4 Linear theory of magnetoelectroelastic materials

1.4.1 Basic equations of general anisotropy

In the previous section, the linear theory of piezoelectricity was presented. Extension of the theory to include magnetic effect is described in this section. For a linear magnetoelectroelastic solid, the governing equations of the mechanical and electric fields are in the same form as those of Eqs (1.49), (1.51), and $(1.59)_{1,2}$. The magnetic field is governed by the following equations

$$B_{i,i}+b_m=0\,;\quad H_i=-\psi_{,i} \tag{1.82}$$

where b_m is the body electric current; $B_i, H_i,$ and ψ are the magnetic induction, magnetic field, and magnetic potential, respectively. Eqs (1.49), (1.51), and $(1.59)_{1,2}$ are coupled to Eq (1.82) through following constitutive relations [13]

$$\left.\begin{aligned}\sigma_{ij}&=c_{ijkl}\varepsilon_{kl}-e_{lij}E_l-\tilde{e}_{lij}H_l\\ D_i&=e_{ikl}\varepsilon_{kl}+\kappa_{il}E_l+\alpha_{il}H_l\\ B_i&=\tilde{e}_{ikl}\varepsilon_{kl}+\alpha_{il}E_l+\mu_{il}H_l\end{aligned}\right\} \tag{1.83}$$

where $\tilde{e}_{lij}, \alpha_{ij},$ and μ_{ij} are respectively piezomagnetic constants, electromagnetic constants, and magnetic permeabilities. Let Γ be the boundary of the solution domain Ω of the magnetoelectroelastic solid considered, then the boundary conditions

can be given in the form [13]

$$u_i = \overline{u}_i \qquad (\text{on } \Gamma_u) \tag{1.84}$$

$$t_i = \sigma_{ij} n_j = \overline{t}_i \qquad (\text{on } \Gamma_t) \tag{1.85}$$

$$\phi = \overline{\phi} \qquad (\text{on } \Gamma_\phi) \tag{1.86}$$

$$D_n = D_i n_i = -\overline{q}_s \quad (\text{on } \Gamma_D) \tag{1.87}$$

$$\psi = \overline{\psi} \qquad (\text{on } \Gamma_\psi) \tag{1.88}$$

$$B_n = B_i n_i = \overline{m} \quad (\text{on } \Gamma_B) \tag{1.89}$$

Where a bar over a variable indicates that the variable is prescribed, and $\Gamma = \Gamma_u \cup \Gamma_t = \Gamma_\phi \cup \Gamma_D = \Gamma_\psi \cup \Gamma_B$. Obviously, the first four equations (1.84)-(1.87) are the electric and mechanical boundary conditions which are the same as those presented in Section 1.3, and the remaining two are for magnetic field. Eqs (1.49), (1.51), and $(1.59)_{1,2}$, (1.82)-(1.89) constitute the complete set of equations of a linear magnetoelectroelastic solid. This set of equations is coupled among magnetic, electric, and mechanical fields.

It should be mentioned that there are eight equivalent constitutive representations commonly used in the stationary theory of linear magnetoelectroelastic solid to describe the coupled interaction among elastic, electric, and magnetic variables [14]. Table 1.2 lists the eight forms of constitutive relations, and the corresponding independent variables and generalized Gibbs energy functionals. In Table 1.2, $\mathbf{c}$ and $\mathbf{s}$ are elastic stiffness and compliance tensors, $\boldsymbol{\kappa}$ and $\boldsymbol{\beta}$ are permittivity and impermittivity tensors, $\boldsymbol{\mu}$ and $\boldsymbol{\nu}$ are permeability and reluctivity tensors, $\boldsymbol{\alpha}$, $\boldsymbol{\lambda}$, $\boldsymbol{\eta}$, and $\boldsymbol{\zeta}$ are magnetoelectric constants, $\mathbf{e}$, $\mathbf{h}$, $\mathbf{d}$, and $\mathbf{g}$ are piezoelectric constants, and $\tilde{\mathbf{e}}$, $\tilde{\mathbf{h}}$, $\tilde{\mathbf{d}}$ and $\tilde{\mathbf{g}}$ are piezomagnetic constants.

1.4.2 Transversely isotropic simplification

If the magnetoelectroelastic solid considered is transversely isotropic, the equations described in Section 1.4.1 can be further simplified [15]. In a fixed rectangular coordinate system (x,y,z), the constitutive equations of a transversely isotropic magnetoelectroelastic solid with the isotropic plane perpendicular to z axis can be expressed in the following form

$$\begin{aligned}
\sigma_{xx} &= c_{11}u_{1,x} + c_{12}u_{2,y} + c_{13}u_{3,z} + e_{31}\phi_{,z} - \tilde{e}_{31}\psi_{,z} \\
\sigma_{yy} &= c_{12}u_{1,x} + c_{11}u_{2,y} + c_{13}u_{3,z} + e_{31}\phi_{,z} - \tilde{e}_{31}\psi_{,z} \\
\sigma_{zz} &= c_{13}u_{1,x} + c_{13}u_{2,y} + c_{33}u_{3,z} + e_{33}\phi_{,z} - \tilde{e}_{33}\psi_{,z} \\
\sigma_{yz} &= c_{44}(u_{2,z} + u_{3,y}) + e_{15}\phi_{,y} - \tilde{e}_{15}\psi_{,y} \\
\sigma_{xz} &= c_{44}(u_{1,z} + u_{3,x}) + e_{15}\phi_{,x} - \tilde{e}_{15}\psi_{,x} \\
\sigma_{xy} &= c_{66}(u_{1,y} + u_{2,x})
\end{aligned} \tag{1.90}$$

$$\begin{aligned}
D_x &= e_{15}(u_{1,z} + u_{3,x}) - \kappa_{11}\phi_{,x} - \alpha_{11}\psi_{,x} \\
D_y &= e_{15}(u_{2,z} + u_{3,y}) - \kappa_{11}\phi_{,y} - \alpha_{11}\psi_{,y} \\
D_z &= e_{31}(u_{1,x} + u_{2,y}) - e_{33}u_{3,z} - \kappa_{33}\phi_{,z} - \alpha_{33}\psi_{,z}
\end{aligned} \tag{1.91}$$

Table 1.2 Eight types of constitutive models[14]

Independent variables	Constitutive relations	Thermodynamic functional
ε, E,H	$\begin{cases}\boldsymbol{\sigma}=\mathbf{c}\boldsymbol{\varepsilon}-\mathbf{e}^T\mathbf{E}-\tilde{\mathbf{e}}^T\mathbf{H}\\ \mathbf{D}=\mathbf{e}\boldsymbol{\varepsilon}+\boldsymbol{\kappa}\mathbf{E}+\boldsymbol{\alpha}\mathbf{H}\\ \mathbf{B}=\tilde{\mathbf{e}}\boldsymbol{\varepsilon}+\boldsymbol{\alpha}\mathbf{E}+\boldsymbol{\mu}\mathbf{H}\end{cases}$	$\Pi_1=\frac{1}{2}(\mathbf{c}\boldsymbol{\varepsilon}^2-\boldsymbol{\kappa}\mathbf{E}^2-\boldsymbol{\mu}\mathbf{H}^2)$ $-\mathbf{e}\boldsymbol{\varepsilon}\mathbf{E}-\tilde{\mathbf{e}}\boldsymbol{\varepsilon}\mathbf{H}-\boldsymbol{\alpha}\mathbf{E}\mathbf{H}$
ε, D,H	$\begin{cases}\boldsymbol{\sigma}=\mathbf{c}\boldsymbol{\varepsilon}-\mathbf{h}^T\mathbf{D}-\tilde{\mathbf{e}}^T\mathbf{H}\\ \mathbf{E}=-\mathbf{h}\boldsymbol{\varepsilon}+\boldsymbol{\beta}\mathbf{D}-\boldsymbol{\zeta}\mathbf{H}\\ \mathbf{B}=\tilde{\mathbf{e}}\boldsymbol{\varepsilon}+\boldsymbol{\zeta}\mathbf{D}+\boldsymbol{\mu}\mathbf{H}\end{cases}$	$\Pi_2=\Pi_1+\mathbf{D}\mathbf{E}$
ε, E,B	$\begin{cases}\boldsymbol{\sigma}=\mathbf{c}\boldsymbol{\varepsilon}-\mathbf{e}^T\mathbf{E}-\tilde{\mathbf{h}}^T\mathbf{B}\\ \mathbf{D}=\mathbf{e}\boldsymbol{\varepsilon}+\boldsymbol{\kappa}\mathbf{E}+\boldsymbol{\eta}\mathbf{B}\\ \mathbf{H}=-\tilde{\mathbf{h}}\boldsymbol{\varepsilon}-\boldsymbol{\eta}\mathbf{E}+\boldsymbol{\nu}\mathbf{B}\end{cases}$	$\Pi_3=\Pi_1+\mathbf{B}\mathbf{H}$
ε, D,B	$\begin{cases}\boldsymbol{\sigma}=\mathbf{c}\boldsymbol{\varepsilon}-\mathbf{h}^T\mathbf{D}-\tilde{\mathbf{h}}^T\mathbf{B}\\ \mathbf{E}=-\mathbf{h}\boldsymbol{\varepsilon}+\boldsymbol{\beta}\mathbf{D}-\boldsymbol{\lambda}\mathbf{B}\\ \mathbf{H}=\tilde{\mathbf{h}}\boldsymbol{\varepsilon}-\boldsymbol{\lambda}\mathbf{D}+\boldsymbol{\nu}\mathbf{B}\end{cases}$	$\Pi_4=\Pi_1+\mathbf{D}\mathbf{E}+\mathbf{B}\mathbf{H}$
σ, D,B	$\begin{cases}\boldsymbol{\varepsilon}=\mathbf{s}\boldsymbol{\sigma}+\mathbf{g}^T\mathbf{D}+\tilde{\mathbf{g}}^T\mathbf{B}\\ \mathbf{E}=-\mathbf{g}\boldsymbol{\sigma}+\boldsymbol{\beta}\mathbf{D}-\boldsymbol{\lambda}\mathbf{B}\\ \mathbf{H}=\tilde{\mathbf{g}}\boldsymbol{\sigma}-\boldsymbol{\lambda}\mathbf{D}+\boldsymbol{\nu}\mathbf{B}\end{cases}$	$\Pi_5=\Pi_1+\mathbf{D}\mathbf{E}+\mathbf{B}\mathbf{H}-\boldsymbol{\sigma}\boldsymbol{\varepsilon}$
σ, E,B	$\begin{cases}\boldsymbol{\varepsilon}=\mathbf{s}\boldsymbol{\sigma}+\mathbf{d}^T\mathbf{E}+\tilde{\mathbf{g}}^T\mathbf{B}\\ \mathbf{D}=\mathbf{d}\boldsymbol{\sigma}+\boldsymbol{\kappa}\mathbf{E}+\boldsymbol{\eta}\mathbf{B}\\ \mathbf{H}=-\tilde{\mathbf{g}}\boldsymbol{\sigma}-\boldsymbol{\eta}\mathbf{E}+\boldsymbol{\nu}\mathbf{B}\end{cases}$	$\Pi_6=\Pi_1+\mathbf{B}\mathbf{H}-\boldsymbol{\sigma}\boldsymbol{\varepsilon}$
σ, D,H	$\begin{cases}\boldsymbol{\varepsilon}=\mathbf{s}\boldsymbol{\sigma}+\mathbf{g}^T\mathbf{D}+\tilde{\mathbf{d}}^T\mathbf{H}\\ \mathbf{E}=-\mathbf{g}\boldsymbol{\sigma}+\boldsymbol{\beta}\mathbf{D}-\boldsymbol{\zeta}\mathbf{H}\\ \mathbf{B}=\tilde{\mathbf{d}}\boldsymbol{\sigma}+\boldsymbol{\zeta}\mathbf{D}+\boldsymbol{\mu}\mathbf{H}\end{cases}$	$\Pi_7=\Pi_1+\mathbf{D}\mathbf{E}-\boldsymbol{\sigma}\boldsymbol{\varepsilon}$
σ, E,H	$\begin{cases}\boldsymbol{\varepsilon}=\mathbf{s}\boldsymbol{\sigma}+\mathbf{d}^T\mathbf{E}+\tilde{\mathbf{d}}^T\mathbf{H}\\ \mathbf{D}=\mathbf{d}\boldsymbol{\sigma}+\boldsymbol{\kappa}\mathbf{E}+\boldsymbol{\alpha}\mathbf{H}\\ \mathbf{B}=\tilde{\mathbf{d}}\boldsymbol{\sigma}+\boldsymbol{\alpha}\mathbf{E}+\boldsymbol{\mu}\mathbf{H}\end{cases}$	$\Pi_8=\Pi_1-\boldsymbol{\sigma}\boldsymbol{\varepsilon}$

$$\begin{aligned}B_x&=\tilde{e}_{15}(u_{1,z}+u_{3,x})+\alpha_{11}\phi_{,x}-\mu_{11}\psi_{,x}\\ B_y&=\tilde{e}_{15}(u_{2,z}+u_{3,y})+\alpha_{11}\phi_{,y}-\mu_{11}\psi_{,y}\\ B_z&=\tilde{e}_{31}(u_{1,x}+u_{2,y})+\tilde{e}_{33}u_{3,z}+\alpha_{33}\phi_{,z}-\mu_{33}\psi_{,z}\end{aligned}\tag{1.92}$$

The governing equations $(1.59)_{1,2}$ and $(1.82)_1$ are now replaced by

$$\begin{aligned}&c_{11}u_{1,xx}+\frac{1}{2}(c_{11}-c_{12})u_{1,yy}+\frac{1}{2}(c_{11}+c_{12})u_{2,xy}+(c_{13}+c_{44})u_{3,xz}\\ &+c_{44}u_{1,zz}+(e_{31}+e_{15})\phi_{,xz}-(\tilde{e}_{15}+\tilde{e}_{31})\psi_{,xz}+b_1=0,\end{aligned}\tag{1.93}$$

$$c_{11}u_{2,yy}+\frac{1}{2}(c_{11}-c_{12})u_{2,xx}+\frac{1}{2}(c_{11}+c_{12})u_{1,xy}+(c_{13}+c_{44})u_{3,yz} \\ +c_{44}u_{2,zz}+(e_{31}+e_{15})\phi_{,yz}-(\tilde{e}_{15}+\tilde{e}_{31})\psi_{,yz}+b_2=0, \tag{1.94}$$

$$c_{44}(u_{3,xx}+u_{3,yy})+(c_{44}+c_{13})(u_{1,xz}+u_{2,yz})+c_{33}u_{3,33} \\ +e_{15}(\phi_{,xx}+\phi_{,yy})+e_{33}\phi_{,zz}-\tilde{e}_{33}\psi_{,zz}-\tilde{e}_{15}(\psi_{,xx}+\psi_{,yy})+b_3=0, \tag{1.95}$$

$$e_{15}(u_{3,xx}+u_{3,yy})+(e_{15}+e_{31})(u_{1,xz}+u_{2,yz})+e_{33}u_{3,zz} \\ -\kappa_{11}(\phi_{,xx}+\phi_{,yy})-\kappa_{33}\phi_{,zz}-\alpha_{11}(\psi_{,xx}+\psi_{,yy})-\alpha_{33}\psi_{,zz}+b_e=0, \tag{1.96}$$

$$\tilde{e}_{15}(u_{3,xx}+u_{3,yy})+(\tilde{e}_{15}+\tilde{e}_{31})(u_{1,xz}+u_{2,yz})+\tilde{e}_{33}u_{3,zz} \\ +\alpha_{11}(\phi_{,xx}+\phi_{,yy})+\alpha_{33}\phi_{,zz}-\mu_{11}(\psi_{,xx}+\psi_{,yy})-\mu_{33}\psi_{,zz}+b_m=0, \tag{1.97}$$

Equations (1.90)-(1.97) are used in later chapters.

1.4.3 Extension to include thermal effect

The equations presented in Section 1.4.1 can be extended to include thermal effects if the temperature field does not fully couple with the magnetoelectroelastic field, that is, if the magnetoelectroelastic field can be affected by the temperature field through constitutive relations but the temperature field is not affected by the magnetoelectroelastic field. Under such assumptions the governing equations of thermomagnetoelectroelastic problem can be expressed as [16]

$$\sigma_{ij,j}+b_i=0\,,\quad D_{i,i}+b_e=0,\quad B_{i,i}+b_m=0 \tag{1.98}$$

$$\left.\begin{aligned}\sigma_{ij}&=c_{ijkl}\varepsilon_{kl}-e_{lij}E_l-\tilde{e}_{lij}H_l-\lambda_{ij}T\\ D_i&=e_{ikl}\varepsilon_{kl}+\kappa_{il}E_l+\alpha_{il}H_l+\chi_iT\\ B_i&=\tilde{e}_{ikl}\varepsilon_{kl}+\alpha_{il}E_l+\mu_{il}H_l-\nu_iT\end{aligned}\right\} \tag{1.99}$$

$$\varepsilon_{ij}=\frac{1}{2}(u_{i,j}+u_{j,i})\,,\qquad E_i=-\phi_{,i},\quad H_i=-\psi_{,i} \tag{1.100}$$

$$h_{i,i}=0,\qquad h_i=-k_{ij}T_{,j} \tag{1.101}$$

where ν_i are pyromagnetic coefficients. The boundary conditions of the thermomagnetoelectroelastic problem are still defined by Eqs (1.84)-(1.89) together with the boundary conditions for the thermal field.

1.4.4 Variational formulation

Taking $\Pi_1(\boldsymbol{\varepsilon},\mathbf{E},\mathbf{H})$ (see Table 1.2) as an example, we now present a variational principle for a magnetoelectroelastic solid in the domain Ω bounded by Γ. First the explicit expression of $\Pi_1(\boldsymbol{\varepsilon},\mathbf{E},\mathbf{H})$ in terms of ε_{ij}, E_i and H_i is presented:

$$\Pi_1=\frac{1}{2}c_{ijkl}\varepsilon_{ij}\varepsilon_{kl}-\frac{1}{2}\kappa_{ij}E_iE_j-\frac{1}{2}\mu_{ij}H_iH_j-e_{ijk}E_i\varepsilon_{jk}-\tilde{e}_{ijk}H_i\varepsilon_{jk}-\alpha_{ij}E_iH_j \tag{1.102}$$

which results in the following constitutive relations

$$\sigma_{ij}=\frac{\partial \Pi_1}{\partial \varepsilon_{ij}},\quad D_i=-\frac{\partial \Pi_1}{\partial E_i},\quad B_i=-\frac{\partial \Pi_1}{\partial H_i} \tag{1.103}$$

Then, based on the variational functional $\Pi_1(\boldsymbol{\varepsilon},\mathbf{E},\mathbf{H})$ and the basic equations (1.49), (1.51), and $(1.59)_{1,2}$, (1.82)-(1.89), a variational principle can be constructed in the form

$$\delta\left[\int_\Omega(\Pi_1-b_iu_i-b_e\phi-b_m\psi)d\Omega-\int_{\Gamma_t}\bar{t}_iu_id\Gamma-\int_{\Gamma_D}\bar{D}_n\phi d\Gamma-\int_{\Gamma_B}\bar{m}\psi d\Gamma\right]=0 \tag{1.104}$$

in which Eqs (1.83), (1.84), (1.86), and (1.88) are assumed to be satisfied, *a priori*.

We now proceed to show that Eqs $(1.59)_{1,2}$, $(1.82)_1$, (1.85), (1.87), and (1.89) can be derived from Eq (1.104) for the independent variables δu_i, $\delta\phi$, and $\delta\psi$. Noting the variation of Π_1 expressed by

$$\begin{aligned}\delta\Pi_1=&c_{ijkl}\varepsilon_{kl}\delta\varepsilon_{ij}-e_{ijk}(E_k\delta\varepsilon_{ij}+\varepsilon_{jk}\delta E_i)-\kappa_{ij}E_j\delta E_i-\mu_{ij}H_j\delta H_i\\&-\tilde{e}_{ijk}(H_k\delta\varepsilon_{ij}+\varepsilon_{jk}\delta H_i)-\alpha_{ij}(E_j\delta H_i+H_j\delta E_i)\\=&\sigma_{ij}\delta\varepsilon_{ij}-D_i\delta E_i-B_i\delta H_i,\end{aligned} \tag{1.105}$$

Eq (1.104) can be further written as

$$\begin{aligned}&\int_\Omega(\sigma_{ij}\delta\varepsilon_{ij}-D_i\delta E_i-B_i\delta H_i-b_i\delta u_i-b_e\delta\phi-b_m\delta\psi)d\Omega\\&-\int_{\Gamma_t}\bar{t}_i\delta u_id\Gamma-\int_{\Gamma_D}\bar{D}_n\delta\phi d\Gamma-\int_{\Gamma_B}\bar{m}\delta\psi d\Gamma=0\end{aligned} \tag{1.106}$$

Making use of Eqs (1.49), (1.51), and $(1.82)_2$, the variables can be expressed as

$$\delta\varepsilon_{ij}=\frac{1}{2}(\delta u_{j,i}+\delta u_{i,j}),\quad \delta E_i=-\delta\phi_{,i},\quad \delta H_i=-\delta\psi_{,i} \tag{1.107}$$

By substituting Eq (1.107) into Eq (1.106) and employing the chain rule of differentiation, integration by parts, the divergence theorem, and the boundary conditions (1.84), (1.86), (1.88), the first three terms of Eq (1.106), with the substitution of Eq (1.103), become

$$\begin{aligned}\int_\Omega\sigma_{ij}\delta\varepsilon_{ij}d\Omega&=\int_{\Gamma_t}\sigma_{ij}n_j\delta u_id\Gamma-\int_\Omega\sigma_{ij,j}\delta u_jd\Gamma\\&=\int_{\Gamma_t}t_i\delta u_id\Gamma-\int_\Omega\sigma_{ij,j}\delta u_jd\Gamma\end{aligned} \tag{1.108}$$

$$\begin{aligned}-\int_\Omega D_i\delta E_id\Omega&=\int_{\Gamma_D}D_in_i\delta\phi d\Gamma-\int_\Omega D_{i,i}\delta\phi d\Gamma\\&=\int_{\Gamma_D}D_n\delta\phi d\Gamma-\int_\Omega D_{i,i}\delta\phi d\Gamma\end{aligned} \tag{1.109}$$

$$\begin{aligned}-\int_\Omega B_i\delta H_id\Omega&=\int_{\Gamma_D}B_in_i\delta\psi d\Gamma-\int_\Omega B_{i,i}\delta\psi d\Gamma\\&=\int_{\Gamma_D}B_n\delta\psi d\Gamma-\int_\Omega B_{i,i}\delta\psi d\Gamma\end{aligned} \tag{1.110}$$

Then, with substitution of Eqs (1.108)-(1.110) into Eq (1.106), we have

$$\begin{aligned}&\int_{\Omega}[(\sigma_{ij,j}+b_i)\delta u_i+(D_{i,i}+b_e)\delta\phi+(B_{i,i}+b_m)\delta\psi]d\Omega\\&-\int_{\Gamma_t}(t_i-\bar{t})_i\delta u_i d\Gamma-\int_{\Gamma_D}(D_n-\bar{D}_n)\delta\phi d\Gamma-\int_{\Gamma_B}(B_n-\bar{m})\delta\psi d\Gamma=0\end{aligned}\tag{1.111}$$

The above equation must be satisfied for independent variables $\delta u_i, \delta\phi,$ and $\delta\psi$. Hence, the volume integrals lead to Eqs $(1.59)_{1,2}$ and $(1.82)_1$, and the surface integrals yield boundary conditions (1.85), (1.87), and (1.89). Similarly, we can present variational principles for the other seven thermodynamic functionals ($\Pi_2 \sim \Pi_8$) in a straightforward way.

1.5 Two solution procedures in anisotropic multifield materials

For two-dimensional deformations in a general anisotropic multifield material, in which all fields depend on x_1 and x_2 (or x_3) only, there are two powerful solution procedures in the literature. One is Lekhnitskii's approach [17], which starts with equilibrated stress functions, followed by compatibility equations. This approach is discussed in Section 1.5.2. Another is Stroh's formalism [18], which starts with the displacements, electric potential, and magnetic potential, followed by equilibrium equations. The equivalence of these two formalisms has been discussed by Suo [19]. The details of Stroh's formulation are given in the following section.

1.5.1 Solution with Stroh formalism

To treat a multifield variable system (elastic, electric, and magnetic fields in piezoelectric/piezomagnetic materials) on an equal footing and reduce the amount of writing, the shorthand notation given by Barnett and Lothe [20] is employed here. With this shorthand notation, the governing equation $(1.59)_{1,2}$, $(1.82)_1$ and the constitutive relationship (1.83) can be rewritten as

$$\Pi_{iJ,i}+b_J=0,\tag{1.112}$$

$$\Pi_{iJ}=E_{iJKm}U_{K,m},\tag{1.113}$$

where $b_4=b_e$ and $b_5=b_m$, and

$$\Pi_{iJ}=\begin{cases}\sigma_{ij}, & J\le 3,\\ D_i, & J=4,\\ B_i, & J=5,\end{cases}\qquad U_M=\begin{cases}u_m, & M\le 3,\\ \phi, & M=4,\\ \psi, & M=5,\end{cases}\tag{1.114}$$

$$E_{iJMn}=\begin{cases}c_{ijmn}, & J,M\le 3,\\ e_{nij}, & J\le 3, M=4,\\ \tilde{e}_{nij}, & J\le 3, M=5,\\ e_{imn}, & J=4, M\le 3,\\ -\kappa_{in}, & J=4, M=4,\\ -\alpha_{in}, & J=4, M=5,\\ \tilde{e}_{imn}, & J=5, M\le 3,\\ -\alpha_{in}, & J=5, M=4,\\ -\mu_{in} & J=5, M=5,\end{cases}\tag{1.115}$$

Denoting $\mathbf{U} = \{u_1\ u_2\ u_3\ \phi\ \psi\}^T$, where the superscript T stands for the transpose, a

general solution can be obtained by considering an arbitrary function of the form [20]

$$\mathbf{U} = \mathbf{a}f(z), \tag{1.116}$$

$$z = x_1 + px_2 \tag{1.117}$$

where p and $\mathbf{a}$ are determined by inserting Eq (1.116) into Eq (1.113), and later into Eq (1.112), $f(z)$ is an arbitrary function of z. In the absence of any body force, body electric current, and free charge distribution, that is, b_J=0 (J=1-5), we have

$$[\mathbf{Q} + p(\mathbf{R} + \mathbf{R}^T) + p^2\mathbf{T}]\mathbf{a} = 0 \tag{1.118}$$

where $\mathbf{Q}$, $\mathbf{R}$ and $\mathbf{T}$ are 5×5 real matrices whose components are

$$Q_{IK} = E_{1IK1}, \quad R_{IK} = E_{1IK2}, \quad T_{IK} = E_{2IK2} \tag{1.119}$$

The stress, magnetic induction, and electric displacement (SMED) obtained by substituting Eq (1.116) into Eq (1.113) can be written in terms of a SMED function $\boldsymbol{\varphi}$ as

$$\boldsymbol{\Pi}_{1J} = -\boldsymbol{\varphi}_{J,2}, \ \boldsymbol{\Pi}_{2J} = \boldsymbol{\varphi}_{J,1}, \tag{1.120}$$

where

$$\boldsymbol{\varphi} = \mathbf{b}f(z), \tag{1.121}$$

$$\mathbf{b} = (\mathbf{R}^T + p\mathbf{T})\mathbf{a} = -p^{-1}(\mathbf{Q} + p\mathbf{R})\mathbf{a} \tag{1.122}$$

The second equality in Eq (1.122) follows from Eq (1.118). It suffices therefore to consider only the SMED function $\boldsymbol{\varphi}$ because the stresses σ_{ij}, magnetic induction B_i and the electric displacement D_i can be obtained by differentiation of $\boldsymbol{\varphi}$.

There are ten eigenvalues p from Eq (1.118) which consist of five pairs of complex conjugates [20]. If $p_J, \mathbf{a}_J (J = 1, 2, \cdots, 10)$ are the eigenvalues and the associated eigenvectors, let

$$\operatorname{Im} p_J > 0, \ p_{J+5} = \overline{p}_J, \ \mathbf{a}_{J+5} = \overline{\mathbf{a}}_J, \ \mathbf{b}_{J+5} = \overline{\mathbf{b}}_J, \qquad (J\text{=1-5}) \tag{1.123}$$

where "Im" stands for the imaginary part of a complex number and the overbar denotes a complex conjugate. Assuming that p_J are distinct, the general solutions for $\mathbf{U}$ and $\boldsymbol{\varphi}$ obtained by superposing ten solutions of the form of Eqs (1.116) and (1.121) are

$$\mathbf{U} = \sum_{J=1}^{5} \{\mathbf{a}_J f_J(z_J) + \overline{\mathbf{a}}_J f_{J+5}(\overline{z}_J)\}, \tag{1.124}$$

$$\boldsymbol{\varphi} = \sum_{J=1}^{5} \{\mathbf{b}_J f_J(z_J) + \overline{\mathbf{b}}_J f_{J+5}(\overline{z}_J)\} \tag{1.125}$$

In Eqs (1.124) and (1.125), $f_J (J = 1, 2, \cdots, 10)$ are arbitrary functions of their argument and

$$z_J = x_1 + p_J x_2 \tag{1.126}$$

In most applications f_J assume the same functional form, so that we may write

$$f_J(z_J) = q_J f(z_J), \quad f_{J+5}(\overline{z}_J) = \overline{q}_J f(\overline{z}_J), \qquad (J=1\text{-}5) \qquad (1.127)$$

where q_J are complex constants to be determined. The second equation of Eq (1.127) is used for obtaining real solutions for **U** and $\boldsymbol{\varphi}$. Expressions (1.124) and (1.125) can then be written in a compact form:

$$\mathbf{U} = 2\,\mathrm{Re}\{\mathbf{A}\mathbf{f}(z)\} = 2\,\mathrm{Re}\{\mathbf{A}\langle f(z_\alpha)\rangle\mathbf{q}\}, \qquad (1.128)$$

$$\boldsymbol{\varphi} = 2\,\mathrm{Re}\{\mathbf{B}\mathbf{f}(z)\} = 2\,\mathrm{Re}\{\mathbf{B}\langle f(z_\alpha)\rangle\mathbf{q}\}, \qquad (1.129)$$

in which "Re" stands for the real part of a complex number, $\mathbf{f}(z)=\{f_1(z_1)\ f_2(z_2)\ f_3(z_3)\ f_4(z_4)\ f_5(z_5)\}^T$, **A**, **B** are 5×5 complex matrices defined by

$$\mathbf{A} = [\mathbf{a}_1\ \mathbf{a}_2\ \mathbf{a}_3\ \mathbf{a}_4\ \mathbf{a}_5], \quad \mathbf{B} = [\mathbf{b}_1\ \mathbf{b}_2\ \mathbf{b}_3\ \mathbf{b}_4\ \mathbf{b}_5] \qquad (1.130)$$

and $\langle f(z_\alpha)\rangle$ is a diagonal matrix

$$\langle f(z_\alpha)\rangle = \mathrm{diag}\,[f(z_1)f(z_2)f(z_3)f(z_4)f(z_5)] \qquad (1.131)$$

For a given problem, it is clear that all that is required is to determine the unknown function $f(z_J)$ and the complex constant vector **q**.

In the following, we present some identities concerning matrices **A** and **B** which will be used in later chapters. For this purpose, Eq (1.122) is rewritten as

$$\begin{bmatrix} -\mathbf{R}^T & \mathbf{I} \\ -\mathbf{Q} & \mathbf{0} \end{bmatrix} \begin{Bmatrix} \mathbf{a} \\ \mathbf{b} \end{Bmatrix} = p \begin{bmatrix} \mathbf{T} & \mathbf{0} \\ \mathbf{R} & \mathbf{I} \end{bmatrix} \begin{Bmatrix} \mathbf{a} \\ \mathbf{b} \end{Bmatrix} \qquad (1.132)$$

where **I** is the identity matrix. Since $\mathbf{T}^{-1}$ exists, we can reduce Eq (1.132) to

$$\mathbf{N}\boldsymbol{\xi} = p\boldsymbol{\xi} \qquad (1.133)$$

where

$$\mathbf{N} = \begin{bmatrix} \mathbf{N}_1 & \mathbf{N}_2 \\ \mathbf{N}_3 & \mathbf{N}_1^T \end{bmatrix}, \quad \boldsymbol{\xi} = \begin{Bmatrix} \mathbf{a} \\ \mathbf{b} \end{Bmatrix} \qquad (1.134)$$

$$\mathbf{N}_1 = -\mathbf{T}^{-1}\mathbf{R}^T, \ \ \mathbf{N}_2 = \mathbf{T}^{-1} = \mathbf{N}_2^T, \ \ \mathbf{N}_3 = \mathbf{R}\mathbf{T}^{-1}\mathbf{R}^T - \mathbf{Q} = \mathbf{N}_3^T \qquad (1.135)$$

The 10×10 matrix **N** is the generalization of the 6×6 matrix **N** for anisotropic elastic materials.

Eq (1.133) is a standard eigenrelation in the ten-dimensional space. The vector $\boldsymbol{\xi}$ in Eq (1.133) is a right eigenvector. The left eigenvector $\boldsymbol{\eta}$ is defined by

$$\boldsymbol{\eta}^T\mathbf{N} = p\boldsymbol{\eta}^T, \quad \mathbf{N}^T\boldsymbol{\eta} = p\boldsymbol{\eta}, \qquad (1.136)$$

and can be shown to be [20]

$$\boldsymbol{\eta} = \begin{Bmatrix} \mathbf{b} \\ \mathbf{a} \end{Bmatrix} \qquad (1.137)$$

Normalization of $\boldsymbol{\xi}_I$ and $\boldsymbol{\eta}_J$ (which are orthogonal to each other) gives

$$\boldsymbol{\eta}_J^T \boldsymbol{\xi}_K = \delta_{JK} \tag{1.138}$$

where δ_{JK} is the Kronecker delta. Making use of Eqs (1.123), (1.128), (1.129), $(1.134)_2$ and (1.137), Eq (1.138) can be written as

$$\begin{bmatrix} \mathbf{B}^T & \mathbf{A}^T \\ \overline{\mathbf{B}}^T & \overline{\mathbf{A}}^T \end{bmatrix} \begin{bmatrix} \mathbf{A} & \overline{\mathbf{A}} \\ \mathbf{B} & \overline{\mathbf{B}} \end{bmatrix} = \begin{bmatrix} \mathbf{I} & 0 \\ 0 & \mathbf{I} \end{bmatrix} \tag{1.139}$$

This is the orthogonal relation. The two 10×10 matrices on the left-hand side of Eq (1.139) are the inverse of each other. Their product commutes so that

$$\begin{bmatrix} \mathbf{A} & \overline{\mathbf{A}} \\ \mathbf{B} & \overline{\mathbf{B}} \end{bmatrix} \begin{bmatrix} \mathbf{B}^T & \mathbf{A}^T \\ \overline{\mathbf{B}}^T & \overline{\mathbf{A}}^T \end{bmatrix} = \begin{bmatrix} \mathbf{I} & 0 \\ 0 & \mathbf{I} \end{bmatrix} \tag{1.140}$$

This is the closure relation and is equivalent to

$$\mathbf{A}\mathbf{B}^T + \overline{\mathbf{A}}\overline{\mathbf{B}}^T = \mathbf{B}\mathbf{A}^T + \overline{\mathbf{B}}\overline{\mathbf{A}}^T = \mathbf{I}, \quad \mathbf{A}\mathbf{A}^T + \overline{\mathbf{A}}\overline{\mathbf{A}}^T = \mathbf{B}\mathbf{B}^T + \overline{\mathbf{B}}\overline{\mathbf{B}}^T = 0 \tag{1.141}$$

Equations $(1.141)_{1,2}$ tell us that the real part of $\mathbf{A}\mathbf{B}^T$ is $\mathbf{I}/2$ while Eq $(1.141)_{3,4}$ imply that $\mathbf{A}\mathbf{A}^T$ and $\mathbf{B}\mathbf{B}^T$ are purely imaginary. Hence, the three Barnett-Lothe tensors **S**, **H**, **L**, defined by

$$\mathbf{S} = i(2\mathbf{A}\mathbf{B}^T - \mathbf{I}), \quad \mathbf{H} = 2i\mathbf{A}\mathbf{A}^T, \quad \mathbf{L} = -2i\mathbf{B}\mathbf{B}^T, \tag{1.142}$$

are real. It is clear that **H** and **L** are symmetric.

1.5.2 Solution with Lekhnitskii formalism

The mathematical method known as Lekhnitskii formalism was originally developed to solve two-dimensional problems in anisotropic elastic materials [17]. The evolution of the method and a number of extensions to electroelastic problems were described in [22-25]. In this section the Lekhnitskii formalism used in linear piezoelectricity is briefly summarized. For a complete derivation and discussion, the reader is referred to [9, 17, 22-25].

Consider a two-dimensional piezoelectric plate, where the material is transversely isotropic and coupling between in-plane stresses and in-plane electric fields takes place. For a Cartesian coordinate system *Oxyz*, choose the *z*-axis as the poling direction, and denote the coordinates *x* and *z* by x_1 and x_2 in order to generate a compacted notation. If a plain strain problem is considered, it requires that

$$\varepsilon_{33} = \varepsilon_{23} = \varepsilon_{13} = E_3 = 0 \tag{1.143}$$

By substitution of Eq (1.143) into Eq (1.61), we have

$$\begin{Bmatrix} \sigma_{11} \\ \sigma_{22} \\ \sigma_{12} \\ D_1 \\ D_2 \end{Bmatrix} = \begin{bmatrix} c_{11} & c_{12} & 0 & 0 & e_{21} \\ c_{12} & c_{22} & 0 & 0 & e_{22} \\ 0 & 0 & c_{33} & e_{13} & 0 \\ 0 & 0 & e_{13} & -\kappa_{11} & 0 \\ e_{21} & e_{22} & 0 & 0 & -\kappa_{22} \end{bmatrix} \begin{Bmatrix} \varepsilon_{11} \\ \varepsilon_{22} \\ 2\varepsilon_{12} \\ -E_1 \\ -E_2 \end{Bmatrix}, \tag{1.144}$$

or inversely

$$\begin{Bmatrix} \varepsilon_{11} \\ \varepsilon_{22} \\ 2\varepsilon_{12} \\ -E_1 \\ -E_2 \end{Bmatrix} = \begin{bmatrix} f_{11} & f_{12} & 0 & 0 & g_{21} \\ f_{12} & f_{22} & 0 & 0 & g_{22} \\ 0 & 0 & f_{33} & g_{13} & 0 \\ 0 & 0 & g_{13} & -\beta_{11} & 0 \\ g_{31} & g_{33} & 0 & 0 & -\beta_{22} \end{bmatrix} \begin{Bmatrix} \sigma_{11} \\ \sigma_{22} \\ \sigma_{12} \\ D_1 \\ D_2 \end{Bmatrix} \tag{1.145}$$

in which f_{ij} is the elastic compliance tensor of the material, g_{ij} is the piezoelectric tensor and β_{ij} is the dielectric impermeability tensor. In the constitutive equations (1.144) and (1.145), $-E_i$ is used instead of E_i because it allows the construction of a symmetric generalized linear response matrix which will prove to be advantageous.

From the constitutive equations (1.145), we observe that D_2 produces normal strains ε_{11} and ε_{22}, while the stress component σ_{12} induces an electric field E_1, and σ_{11} and σ_{22} produce E_2. Equation (1.144) constitutes a system of five equations in ten unknowns. Additional equations are provided by elastic equilibrium and Gauss' law

$$\sigma_{11,1} + \sigma_{12,2} = 0, \quad \sigma_{12,1} + \sigma_{22,2} = 0, \quad D_{1,1} + D_{2,2} = 0, \tag{1.146}$$

in which the absence of body forces and free electric volume charge has been assumed, and by one elastic and one electric compatibility condition

$$\varepsilon_{11,22} + \varepsilon_{22,11} - 2\varepsilon_{12,12} = 0, \quad E_{1,2} - E_{2,1} = 0 \tag{1.147}$$

Having formulated the electroelastic problem, we seek a solution to Eqs (1.145)-(1.147) subjected to a given loading and boundary condition. To this end, the well-known Lekhnitskii stress function F and induction function V satisfying the foregoing equilibrium equations are introduced as follows [9,22]:

$$\sigma_{11} = F_{,22}, \ \ \sigma_{22} = F_{,11}, \ \ \sigma_{12} = -F_{,12}, \ \ D_1 = V_{,2}, \ \ D_2 = -V_{,1} \tag{1.148}$$

Inserting Eq (1.148) into Eq (1.145), and later into Eq (1.147) leads to

$$L_4 F - L_3 V = 0, \qquad L_3 F + L_2 V = 0 \tag{1.149}$$

where

$$\begin{aligned} L_4 &= f_{22}\frac{\partial^4}{\partial x_1^4} + f_{11}\frac{\partial^4}{\partial x_2^4} + (2f_{12} + f_{33})\frac{\partial^4}{\partial x_1^2 \partial x_2^2}, \\ L_3 &= g_{22}\frac{\partial^3}{\partial x_1^3} + (g_{21} + g_{13})\frac{\partial^3}{\partial x_1 \partial x_2^2}, \qquad L_2 = \beta_{22}\frac{\partial^2}{\partial x_1^2} + \beta_{11}\frac{\partial^2}{\partial x_2^2} \end{aligned} \tag{1.150}$$

Note that if the problem was purely mechanical, L_4 would be the only nonzero operator and its form would coincide with the plane anisotropic case discussed, among others, by Lekhnitskii [17]. In order to solve Eq (1.149) we reduce the system to a single partial differential equation of order six in either F or V. Choosing F, we obtain

$$(L_4L_2 + L_3L_3)F = 0 \tag{1.151}$$

As discussed in [17] within the framework of anisotropic elasticity, Eq (1.151) can be solved by assuming a solution of $F(z)$ such that

$$F(z) = F(x_1 + px_2), \qquad p = \alpha + i\beta \tag{1.152}$$

where α and β are real numbers. By introducing Eq (1.152) into Eq (1.151), and using the chain rule of differentiation, an expression of the form $\{\cdot\}F^{(6)} = 0$ is obtained. A nontrivial solution follows by setting the characteristic equation (i.e., L_4L_2+L_3L_3) equal to zero, namely

$$\begin{aligned} &f_{11}\beta_{11}p^6 + (f_{11}\beta_{22} + f_{33}\beta_{11} + 2f_{12}\beta_{11} + g_{21}^2 + g_{13}^2 + 2g_{21}g_{13})p^4 \\ &\quad + (f_{22}\beta_{11} + 2f_{12}\beta_{22} + f_{33}\beta_{22} + 2g_{21}g_{22} + 2g_{13}g_{22})p^2 + f_{22}\beta_{22} + g_{22}^2 = 0 \end{aligned} \tag{1.153}$$

Owing to the particular material symmetry of the piezoelectric solid under investigation, the polynomial is expressed in terms of even powers of p. This allows us to solve Eq (1.153) analytically, rendering

$$p_1 = i\beta_1, \;\; p_2 = \alpha_2 + i\beta_2, \;\; p_3 = -\alpha_2 + i\beta_2, \;\; p_4 = \overline{p}_1, \;\; p_5 = \overline{p}_2, \;\; p_6 = \overline{p}_3 \tag{1.154}$$

where β_1, α_2 and β_2 depend on the material constants. Once the roots p_j, j=1, 2, 3 are known, the solution for stress function F is written as

$$F(x_1, x_2) = 2\,\mathrm{Re}\sum_{j=1}^{3} F_j(z_j) \tag{1.155}$$

The next step is to find the function V using one of Eqs (1.149). If we consider L_3F=-L_2V, assuming solutions of the form $F(z_k)$ and $V(z_k)$, we have

$$V_k''(z_k) = \varpi_k(p_k)F_k'''(z_k) \tag{1.156}$$

where primes indicate differentiation with respect to the related argument, and

$$\varpi_k(p_k) = -\frac{(g_{21} + g_{13})p_k^2 + g_{22}}{\beta_{11}p_k^2 + \beta_{22}} \tag{1.157}$$

Integration of Eq (1.156) leads to

$$V_k(z_k) = \varpi_k(p_k)F_k'(z_k) \tag{1.158}$$

It should be noted here that the arbitrary constants of integration could be set equal to zero [22]. Thus, the solution for the induction function can be expressed as follows:

$$V(x_1, x_2) = 2\,\mathrm{Re}\sum_{j=1}^{3} V_j(z_j) = 2\,\mathrm{Re}\sum_{j=1}^{3} \varpi_j F_j'(z_j) \tag{1.159}$$

With the aid of Eqs (1.155) and (1.159) we can obtain expressions for the stress and electric displacement components. Using Eqs (1.148), (1.155) and (1.159), we obtain

$$\begin{Bmatrix} \sigma_{11} \\ \sigma_{22} \\ \sigma_{12} \end{Bmatrix} = 2\,\mathrm{Re}\sum_{k=1}^{3} \begin{Bmatrix} p_k^2 \\ 1 \\ -p_k \end{Bmatrix} \Phi_k'(z_k), \qquad \begin{Bmatrix} D_1 \\ D_2 \end{Bmatrix} = 2\,\mathrm{Re}\sum_{k=1}^{3} \begin{Bmatrix} \varpi_k p_k \\ -\varpi_k \end{Bmatrix} \Phi_k'(z_k) \tag{1.160}$$

where $\Phi_k(z_k) = F_k'(z_k)$.

Finally, using the constitutive equations in conjunction with Eq (1.160) allows us to find expressions for the strain and electric field. They are

$$\begin{Bmatrix} \varepsilon_{11} \\ \varepsilon_{22} \\ 2\varepsilon_{12} \end{Bmatrix} = 2\,\mathrm{Re}\sum_{k=1}^{3} \begin{bmatrix} p_k^* \\ q_k^* \\ r_k^* \end{bmatrix} \Phi_k'(z_k), \quad \begin{Bmatrix} E_1 \\ E_2 \end{Bmatrix} = -\sum_{k=1}^{3} \begin{bmatrix} t_k^* \\ v_k^* \end{bmatrix} \Phi_k'(z_k) \tag{1.161}$$

where

$$\begin{aligned} &p_k^* = f_{11}p_k^2 + f_{12} - g_{21}\varpi_k,\ q_k^* = (f_{12}p_k^2 + f_{22} - g_{22}\varpi_k)/p_k, \\ &r_k^* = (g_{13}\varpi_k - f_{33})p_k,\ \ t_k^* = -(g_{13} + \beta_{11}\varpi_k)p_k,\ v_k^* = g_{21}p_k^2 + g_{22} + \beta_{22}\varpi_k \end{aligned} \tag{1.162}$$

Substitution of Eqs (1.56) and (1.58) into Eq (1.161), and then integration of the normal strains and the electric field E = -grad ϕ produces

$$\begin{Bmatrix} u_1 \\ u_2 \\ \phi \end{Bmatrix} = 2\,\mathrm{Re}\sum_{k=1}^{3} \begin{Bmatrix} p_k^* \\ q_k^* \\ t_k^* \end{Bmatrix} \Phi_k(z_k) + \begin{Bmatrix} \omega_0 x_2 + u_0 \\ -\omega_0 x_1 + v_0 \\ \phi_0 \end{Bmatrix} \tag{1.163}$$

where the constants ω_0, u_0, v_0 represent rigid body displacements, and ϕ_0 is a reference potential.

Recapitulating, based on the procedure above, the plane strain piezoelectric problem is reduced to one of finding three complex potentials, Φ_1, Φ_2 and Φ_3, in some region Ω of the material. Each potential is a function of a different generalized complex variable $z_k = x_1 + p_k x_2$.

References

[1] Roach GF, Green's functions: Introductory theory with applications, London:Van Nostrand Reinhold, 1970

[2] Barton G, Elements of Green's functions and propagation: potentials, diffusion, and waves, Oxford: Clarendon Press, 1989

[3] Greenberg MD, Application of Green's functions in science and engineering, Englewood Cliffs: Prentice-Hall, 1971

[4] Lighthill MJ, Introduction to Fourier analysis and generalized functions, Cambridge: Cambridge University Press, 1958

[5] Schwartz L, Mathematics for the physical sciences, Paris: Hermann, 1966

[6] Cady WG, Piezoelectricity, vols. 1 & 2, New York: Dover Publishers, 1964

[7] Tiersten HF, Linear piezoelectric plate vibrations, New York: Plenum Press, 1964
[8] Parton VZ and Kudryavtsev BA, Electromagnetoelasticity, piezoelectrics and electrically conductive solids, New York: Gordon and Breach Science Publishers, 1988
[9] Qin QH, Fracture mechanics of piezoelectric materials, Southampton: WIT Press, 2001
[10] Biot MA, Thermoelasticity and irreversible thermodynamics, J Appl Phys, 27, 240-253, 1956
[11] Mindlin RD, Equations of high frequency vibrations of thermopiezo-electric crystal plates, Int J Solids Struct, 10, 625-637, 1974
[12] Nye JF, Physical properties of crystals: their representation by tensors and matrices, Oxford: Clarendon Press, 1972
[13] Lee PCY, A variational principle for the equations of piezoelectromagnetism in elastic dielectric crystals, J Appl Phys, 6, 7470-7473, 1991
[14] Soh AK and Liu JX, On the constitutive equations of magnetoelectroelastic solids, J Intelligent Mat Sys Struc, 16, 597-602, 2005
[15] Hou PF, Ding HJ and Chen JY, Green's function for transversely isotropic magnetoelectroelastic media, Int J Eng Sci, 43, 826-858, 2005
[16] Gao CF and Noda N, Thermal-induced interfacial cracking of magnetoelectroelastic materials, Int J Eng Sci, 42, 1347-1360, 2004
[17] Lekhnitskii SG, Theory of elasticity of an anisotropic elastic body, San Francisco: Holden-Day, Inc., 1963
[18] Stroh AN, Dislocations and cracks in anisotropic elasticity, Phil Mag, 3, 625-646, 1958
[19] Suo Z, Singularities, interfaces and cracks in dissimilar anisotropic media. Proc R Soc Lond, A427, 331-358, 1990
[20] Barnett DM and Lothe J, Dislocations and line charges in anisotropic piezoelectric insulators, Phys Stat Sol(b), 67, 105-111, 1975
[21] Chung MY and Ting TCT, The Green function for a piezoelectric piezomagnetic magnetoelectric anisotropic elastic medium with an elliptic hole or rigid inclusion, Phil Mag Letters, 72, 405-410, 1995
[22] Sosa H, Plane problems in piezoelectric media with defects, Int J Solids Struct, 28, 491-505, 1991
[23] Qin QH, A new solution for thermopiezoelectric solid with an insulated elliptic hole, Acta Mechanica Sinica, 14, 157-170, 1998
[24] Qin QH and Mai YW, A new thermoelectroelastic solution for piezoelectric materials with various openings, Acta Mechanica, 138, 97-111, 1999
[25] Wang SS and Choi I, The interface crack between dissimilar anisotropic composite materials, J Appl Mech, 50, 169-178, 1983

Chapter 2 Green's function of electroelastic problem

2.1 Introduction

Green's function plays an important role in the solution of numerous problems in the mechanics and physics of solids. It is at the heart of many analytical and numerical methods such as singular integral equation methods, boundary element methods, eigenstrain approaches, and dislocation methods [1-3]. Extensive studies have been carried out on static Green's functions in anisotropic piezoelectric solids. Benveniste [4] studied three-dimensional (3D) solutions in piezoelectric solids using the Fourier transform. Chen [5] and Chen and Lin [6] expressed the infinite body Green's functions and their derivatives as the contour integrals over the unit circle using 3D Fourier transforms. Dunn [7] obtained explicit Green's functions for transversely isotropic piezoelectric solids using the Radon transform, coordinator transformation, and evaluation of residues in sequence. However, the expressions of this solution are very complicated, so that it is difficult to verify and inconvenient to use. Lee and Jiang [8] obtained a two-dimensional (2D) fundamental solution for an infinite plane by using double Fourier transform. Sosa and Castro [9] obtained the solutions to the problem of concentrated loads acting at the boundary of a 2D half-plane by means of a state-space method in conjunction with the Fourier transform. Using the potential function approach, Dunn and Wienecke [10] and Ding et al [11,12] presented closed form solutions of transversely isotropic piezoelectric materials where displacements and electric potential are derivable from two potential functions. Pan [13] gave expressions for 2D piezoelectric Green's functions and their boundary integral equations for dealing with fracture problems. Gao and Fan [14] obtained the Green's functions of a piezoelectric plane containing an elliptic hole. Norris [15] discussed the derivation of dynamic Green's functions for problems dealing with 2D dynamic piezoelectricity. Khutoryansky and Sosa [16] further examined the dynamic Green's function of piezoelectric materials and gave a general representation formula of the governing equations of transient piezoelectricity through a generalization of the reciprocal theorem and the plane wave transform method. Qin [17] presented Green's functions for 2D piezoelectric materials with holes of various shapes and applied them to establish boundary singular integral equations. Qin and Mai [18] also derived explicit Green's functions for an interface crack subject to an edge dislocation in various piezoelectric bimaterial combinations. Pan and Yuan [19] gave 3D Green's functions for anisotropic piezoelectric bimaterials. They showed that the 3D bimaterial Green's function can be expressed in terms of a full-space part or the Kelvin-type solution and a complementary part or the Mindlin-type part. Studies in [6,20] suggested a numerical algorithm to compute the derivatives of the piezoelectric Green's function. Green's functions for piezoelectric materials can also be found in [21,22] for half-plane; [23,24] for semi-infinite crack; [25] for two-phase piezoelectric composites; [26] for anti-plane arc-crack; [27,28] for an impermeable elliptic hole or crack; [14,29] for a permeable elliptic hole; [30] for the case of collinear permeable cracks; and [31,32] for straight permeable interface cracks between two dissimilar piezoelectric media.

In this chapter, we begin with an introduction to free space Green's function of piezoelectricity with some typical approaches including the Radon transform method, the potential function approach, and the Fourier transform scheme. This is followed by discussion about extension of the results to problems with half-plane, bimaterials, interface crack, elliptic hole and inclusion, arbitrarily shaped hole, semi-infinite crack, and anti-plane problems. Finally, applications of the Green's function approach to

dynamic problems are described.

2.2 Green's function by Radon transforms

Applications of the Radon transform to deriving Green's function of electroelastic problems have been studied by Dunn [7] and Pan and Tonon [20] for transversely isotropic piezoelectricity, Hill and Farris [33] for three-dimensional piezoelectricity where the resulting solution is represented by a line integral that is evaluated numerically using standard Gaussian quadrature, Denda et al [34] for time-harmonic problems of 2D piezoelectricity, and Ma and Wang [35] and Wang and Zhang [36] for 3D dynamic problems. In this section we follow the results given in [7].

Consider a 3D electroelastic problem of a piezoelectric solid, where the field quantities depend on the coordinates x_1 and x_2 only. Using the shorthand notation described in Section 1.5, the governing equations $(1.59)_{1,2}$ and constitutive relation (1.65) can be written as

$$E_{iJMn}U_{J,in} + b_M = 0, \quad \Pi_{iJ} = E_{iJMn}U_{M,n} \tag{2.1}$$

where the generalized displacement U_J, stress Π_{iJ}, stiffness constant E_{iJMn} are different from those in Eqs (1.114) and (1.115) which were initially for magnetoelectroelastic problems. These constants are now defined by

$$\Pi_{iJ} = \begin{cases} \sigma_{ij}, & J \le 3, \\ D_i & J = 4, \end{cases} \qquad U_J = \begin{cases} u_J,, & J \le 3, \\ \phi & J = 4, \end{cases} \tag{2.2}$$

$$E_{iJMn} = \begin{cases} c_{ijmn}, & J, M \le 3, \\ e_{nij}, & J \le 3, M = 4, \\ e_{imn}, & J = 4, M \le 3, \\ -\kappa_{in}, & J = 4, M = 4 \end{cases} \tag{2.3}$$

By comparing Eq (1.33), the Green's function corresponding to Eq (2.1) is defined by the following differential equation

$$E_{iJMn}G_{MR,in}(\mathbf{x}-\hat{\mathbf{x}}) + \delta_{JR}\delta(\mathbf{x}-\hat{\mathbf{x}}) = 0 \tag{2.4}$$

where the components $G_{IJ}(\mathbf{x}-\hat{\mathbf{x}})$ represent the elastic displacement at $\mathbf{x}$ in the x_I-direction (for I=1,2,3) or the electric potential (for I=4) due to a unit point force at $\hat{\mathbf{x}}$ in the x_J-direction (for J=1,2,3), or a unit point charge at $\hat{\mathbf{x}}$ (for J=4), and δ_{JR} is the generalized Kronecker delta. The boundary conditions on $G_{IJ}(\mathbf{x}-\hat{\mathbf{x}})$ are that they and their first spatial partial derivative must vanish as $|\mathbf{x}-\hat{\mathbf{x}}| \to \infty$.

The Green's function $G_{IJ}(\mathbf{x}-\hat{\mathbf{x}})$ can be obtained by applying the Radon transform (see Appendix A for details) to Eq (2.4)[7]:

$$K_{JM}(\mathbf{n})\frac{\partial^2}{\partial\omega^2}\hat{G}_{MR}(\mathbf{n},\omega-\mathbf{n}\cdot\hat{\mathbf{x}}) + \delta_{JR}\delta(\omega-\mathbf{n}\cdot\hat{\mathbf{x}}) = 0 \tag{2.5}$$

where $K_{JM}(\mathbf{n}) = E_{iJMl}n_i n_l$, $\mathbf{n}$ and ω are variables in the transformed space, and $\hat{G}$ is the Radon transform of G defined in Appendix A.

$$\hat{G}_{MR}(\mathbf{n},\omega-\mathbf{n}\cdot\hat{\mathbf{x}}) = \iint\limits_{\mathbf{n}\cdot\mathbf{x}=\omega} G_{MR}(\mathbf{x}-\hat{\mathbf{x}})dS(\mathbf{x}) \tag{2.6}$$

Here the integration is to be performed over the infinite plane $\mathbf{n}\cdot\mathbf{x}=\omega$. The inverse transform of Eq (2.6) yields

$$G_{MR}(\mathbf{x}-\hat{\mathbf{x}}) = \frac{1}{8\pi^2}\iint\limits_{S^2}\left[\frac{\partial^2\hat{G}_{MR}(\mathbf{n},\omega-\mathbf{n}\cdot\hat{\mathbf{x}})}{\partial\omega^2}\right]_{\mathbf{n}\cdot\mathbf{x}=\omega} dS(\mathbf{n}) \tag{2.7}$$

where S^2 represents the surface of the unit sphere $|\mathbf{n}|=1$. Making use of Eq (2.7), the inversion of Eq (2.5) followed by some manipulation yields

$$G_{MR}(\mathbf{x}-\hat{\mathbf{x}}) = \frac{1}{8\pi^2|\mathbf{x}-\hat{\mathbf{x}}|}\iint\limits_{S^2} K^{-1}_{MR}(\mathbf{n})\delta(\mathbf{n}\cdot\mathbf{t})dS(\mathbf{n}) \tag{2.8}$$

where $K_{JM}(\mathbf{n})K^{-1}_{MR}(\mathbf{n}) = \delta_{JR}$ and **t** is defined as a unit vector in the direction of $\mathbf{x}-\hat{\mathbf{x}}$ (see Fig. 2.1). The integral expression (2.8) for the extended Green's displacement components is similar to the expressions obtained by Chen [5] and Deeg [37].

The surface integral in Eq (2.8) can be converted to a contour integral by considering the coordinate system defined by the three mutually orthogonal vectors **t**-**m**-**d** (see Fig. 2.1) and utilizing the well-known properties of the Dirac delta function to yield [7]:

$$G_{MR}(\mathbf{x}-\hat{\mathbf{x}}) = \frac{1}{8\pi^2|\mathbf{x}-\hat{\mathbf{x}}|}\int\limits_{S^1} K^{-1}_{MR}(\mathbf{n})dS \tag{2.9}$$

where S^1 is the contour $|\mathbf{n}|=1$ which lies in the **m**-**d** plane normal to $\mathbf{x}-\hat{\mathbf{x}}$. Equation (2.9) is analogous to the contour integral obtained by Synge [38] for the Green's function for anisotropic elasticity. As mentioned in [7], the contour integral in Eq (2.9) can be evaluated numerically for arbitrary anisotropy and explicitly for the case of transversely isotropic material symmetry. Such explicit expression can be found in [7,20].

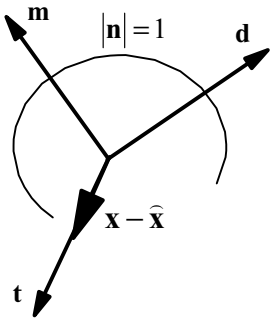

Fig. 2.1 Definition for the mutually orthogonal unit vectors **m**, **d** and **t**

2.3 Green's function by the potential function approach

The Green's function described in Section 2.2 for a transversely isotropic

piezoelectricity can also be solved by the potential function approach, which is based on expressing the four unknowns u, v, w, ϕ in terms of two potential functions $g(x, y, z)$ and $\varpi(x, y, z)$, in such a way that [10]

$$u = \left[(c_{13}e_{15} - c_{44}e_{31}) \frac{\partial^2}{\partial x \partial z} \nabla_2 + [(c_{44} + c_{13})e_{33} - c_{33}(e_{15} + e_{31})] \frac{\partial^4}{\partial x \partial z^3} \right] g - \frac{\partial \varpi}{\partial y} \quad (2.10)$$

$$v = \left[(c_{13}e_{15} - c_{44}e_{31}) \frac{\partial^2}{\partial y \partial z} \nabla_2 + [(c_{44} + c_{13})e_{33} - c_{33}(e_{15} + e_{31})] \frac{\partial^4}{\partial y \partial z^3} \right] g + \frac{\partial \varpi}{\partial x} \quad (2.11)$$

$$w = \left[-c_{11}e_{15}\nabla_2\nabla_2 - c_{44}e_{33} \frac{\partial^4}{\partial z^4} + [c_{13}(e_{15} + e_{31}) + c_{44}e_{31} - c_{11}e_{33}] \frac{\partial^2}{\partial z^2} \nabla_2 \right] g \quad (2.12)$$

$$\phi = \left[c_{11}c_{44}\nabla_2\nabla_2 + c_{44}c_{33} \frac{\partial^4}{\partial z^4} + (c_{11}c_{33} - 2c_{44}c_{13} - c_{13}^2) \frac{\partial^2}{\partial z^2} \nabla_2 \right] g \quad (2.13)$$

where ∇_2 is the 2D Laplace's operator defined in Eq (1.29). Substituting Eqs (2.10)-(2.13) into Eqs (1.78)-(1.81) and after some manipulation, we have

$$\left(\nabla_2 + \frac{\partial^2}{v_0^2 \partial z^2} \right) \varpi = 0, \quad \left(\nabla_2 + \frac{\partial^2}{v_1^2 \partial z^2} \right) \left(\nabla_2 + \frac{\partial^2}{v_2^2 \partial z^2} \right) \left(\nabla_2 + \frac{\partial^2}{v_3^2 \partial z^2} \right) g = 0 \quad (2.14)$$

in which all force terms b_i are assumed to be zero for simplicity, and $v_0 = (c_{66}/c_{44})^{1/2}$, v_i^2 are the three roots of the characteristic equation:

$$av^6 + bv^4 + cv^2 + d = 0 \quad (2.15)$$

with

$$a = c_{11}(\kappa_{11}c_{44} + e_{15}^2)$$

$$b = c_{11}(\kappa_{11}c_{33} + 2e_{15}e_{33}) - \kappa_{11}c_{13}(c_{13} + 2c_{44}) + c_{44}(\kappa_{33}c_{11} + e_{31}^2) - 2e_{15}c_{13}(e_{31} + e_{15})$$

$$c = c_{33}[\kappa_{11}c_{44} + \kappa_{33}c_{11} + e_{31}(e_{31} + e_{15})] - c_{13}\kappa_{33}(c_{13} + 2c_{44}) + (e_{31} + e_{15})(c_{33}e_{15} - 2c_{13}e_{33}) + e_{33}(c_{11}e_{33} - 2c_{44}e_{31})$$

$$d = c_{44}(\kappa_{33}c_{33} + e_{33}^2)$$

The three roots v_i^2 are easily obtained using the well-known solution for a cubic equation. Either all three roots are real or one is real and the other two are complex conjugates.

Based on the general solution (2.10)-(2.13), Dunn and Wienecke [10] presented a complete set of Green's functions by considering following two problems: (i) a point charge and a point force directed along the z-axis, both acting at the origin; and (ii) a point force at the origin directed along the x-axis. In the following we present some results given in [10] in order to provide a brief introduction to the potential function approach of Green's function. The reader may refer to [10-12] for more detail.

(i) Green's function for a point charge and point force in the z-direction

In this case the problem is axially symmetric about the *z*-axis and the potential functions *g* and ϖ can be assumed in the form [10]:

$$\begin{aligned} &\varpi = 0 \\ &g = \sum_{i=1}^{3} A_i f(\mathbf{x}_i) = \sum_{i=1}^{3} A_i [Q_1(\mathbf{x}_i) z_i \ln R_i^* + Q_2(\mathbf{x}_i) R_i + Q_3(\mathbf{x}_i) z_i] \end{aligned} \tag{2.16}$$

where A_i are unknown constants, $\mathbf{x}_i = (x, y, z_i)$, and

$$R_i = \sqrt{x^2 + y^2 + z_i^2}, \quad R_i^* = R_i + z_i, \quad z_i = v_i z \tag{2.17}$$

$$\begin{aligned} Q_j(\mathbf{x}_i) = {} & q_{j0} + q_{j1} x + q_{j2} y + q_{j3} z_i + q_{j4} xy + q_{j5} x z_i + q_{j6} y z_i \\ & + q_{j7} x^2 + q_{j8} y^2 + q_{j9} z_i^2 \qquad (j = 1, 2, 3) \end{aligned} \tag{2.18}$$

The linear relation between the functions *g* and *f* in Eq (2.16) requires that *f* also satisfy the *z*-weighted harmonic:

$$\left(\nabla^2 + \frac{\partial^2}{\partial z_i^2} \right) f = 0 \tag{2.19}$$

To find the explicit form of *f* the thirty q_{ij} are determined using Eq (2.19). After substantial computation, Dunn and Wienecke [10] found that *f* can be expressed in the form

$$f(\mathbf{x}_i) = 3(3R_i^2 - 5z_i^2) z_i \ln R_i^* - (4R_i^2 - 15z_i^2) R_i - 6z_i^3 \tag{2.20}$$

Substituting Eq (2.20) into (2.16), and later into Eqs (2.10)-(2.13), yields

$$\begin{aligned} &u = \sum_{i=1}^{3} A_i \lambda_i^{uv} \frac{x}{R_i R_i^*}, \quad v = \sum_{i=1}^{3} A_i \lambda_i^{uv} \frac{y}{R_i R_i^*}, \\ &w = \sum_{i=1}^{3} A_i \lambda_i^{w} \frac{1}{R_i}, \qquad \phi = \sum_{i=1}^{3} A_i \lambda_i^{\phi} \frac{1}{R_i} \end{aligned} \tag{2.21}$$

where

$$\begin{aligned} \lambda_i^{uv} &= [(c_{13} + c_{44}) e_{33} - c_{33}(e_{31} + e_{15})] v_i^3 + (c_{44} e_{31} - c_{13} e_{15}) v_i \\ \lambda_i^{w} &= -c_{44} e_{33} v_i^4 - [e_{31}(c_{13} + c_{44}) - e_{33} c_{11} + e_{15} c_{13}] v_i^2 - e_{15} c_{11} \\ \lambda_i^{\phi} &= c_{44} c_{33} v_i^4 + [c_{13}(c_{13} + 2c_{44}) - c_{11} c_{33}] v_i^2 + c_{11} c_{44} \end{aligned} \tag{2.22}$$

There are three unknowns A_i in Eq (2.21). We then need to find three conditions to determine the three unknowns. The fact that displacements *u* and *v* are bounded on the *z*-axis leads to

$$\sum_{i=1}^{3} A_i \lambda_i^{uv} = 0 \tag{2.23}$$

The remaining two equations can be established by considering the requirements of the force and charge balance. These requirements are enforced by integrating the traction and normal component of the electric displacement over the surface of a small spherical cavity centered at the origin, and requiring these to balance the point

force P_z and the point charge Q. These conditions lead to

$$\sum_{i=1}^{3} A_i \frac{n_i^a}{v_i^2 - 1} = \frac{P_z}{2\pi}, \quad \sum_{i=1}^{3} A_i \frac{n_i^e}{v_i^2 - 1} = \frac{Q}{2\pi} \tag{2.24}$$

where

$$\begin{aligned} n_i^a &= 2[\lambda_i^{uv}(c_{13} + c_{44}v_i^2) + v_i\lambda_i^w(c_{44} - c_{33}) + v_i\lambda_i^\phi(e_{15} - e_{33})] \\ n_i^e &= 2[-\lambda_i^{uv}(e_{15}v_i^2 + e_{31}) + v_i\lambda_i^w(e_{33} - e_{15}) + v_i\lambda_i^\phi(\kappa_{11} - \kappa_{33})] \end{aligned} \tag{2.25}$$

The Green's functions can then be obtained by setting P_z and Q to be unity and solving Eqs (2.23) and (2.24) for A_i.

(ii) Green's function for a point force P_x in the x-direction
As with the treatment for the point force in z-direction, the potential functions g and ϖ are assumed in the form:

$$\begin{aligned} g &= \sum_{i=1}^{3} D_i \left[Q_4(\mathbf{x}_i) x \ln R_i^* + Q_5(\mathbf{x}_i) \frac{xz_i}{R_i^*} + Q_6(\mathbf{x}_i) x \right] \\ \varpi &= \frac{-D_0 y}{R_0^*} \end{aligned} \tag{2.26}$$

where Q_j (j=4-6) are quadratic polynomials defined by Eq (2.18). With a treatment similar to that in (i) above, we can express the function g in the form [10]

$$g = \sum_{i=1}^{3} D_i \left[3(R_i^2 - 5z_i^2) x \ln R_i^* + (13R_i^2 - 15z_i^2) \frac{xz_i}{R_i^*} + 4xz_i^2 \right] \tag{2.27}$$

Substitution of Eqs $(2.26)_2$ and (2.27) into Eqs (2.10)-(2.13) leads to

$$\begin{aligned} u &= D_0 \left[\frac{1}{R_0^*} - \frac{y^2}{R_0 R_0^{*2}} \right] - \sum_{i=1}^{3} D_i \lambda_i^{uv} \left[\frac{1}{R_i^*} - \frac{x^2}{R_i R_i^{*2}} \right], \quad w = \sum_{i=1}^{3} D_i \lambda_i^w \frac{x}{R_i R_i^*}, \\ v &= D_0 \frac{xy}{R_0 R_0^{*2}} + \sum_{i=1}^{3} D_i \lambda_i^{uv} \frac{xy}{R_i R_i^{*2}}, \qquad \phi = \sum_{i=1}^{3} D_i \lambda_i^\phi \frac{x}{R_i R_i^*} \end{aligned} \tag{2.28}$$

There are four unknowns D_i (i=0-3) in Eq (2.28), which can be determined by enforcing both the requirement that the solution be bounded on the z-axis and the force balance condition. The fact that the displacements u and v are bounded on the z-axis leads to

$$D_0 v_0 + \sum_{i=1}^{3} D_i v_i \lambda_i^{uv} = 0 \tag{2.29}$$

Requiring that w and ϕ be bounded on the z-axis leads to the following two equations:

$$\sum_{i=1}^{3} D_i \lambda_i^w = 0, \quad \sum_{i=1}^{3} D_i \lambda_i^\phi = 0 \tag{2.30}$$

The single remaining equation can be obtained by considering the force balance in the x-direction:

$$D_0 v_0 c_{44} + \sum_{i=1}^{3} D_i \frac{n_i^t}{v_i^2 - 1} = \frac{P_x}{2\pi} \tag{2.31}$$

where

$$n_i^t = v_i \lambda_i^{uv}(c_{44} - c_{11}) + \lambda_i^w (c_{13} v_i^2 + c_{44}) + \lambda_i^\phi (e_{31} v_i^2 + e_{15}) \tag{2.32}$$

The unknowns D_i can thus be determined from Eqs (2.30)-(2.32). Having determined all the unknowns A_i and D_i, the fundamental solutions (2.10)-(2.13) can be explicitly expressed in terms of material constants and generalized coordinates in the form [22]

$$\begin{Bmatrix} u \\ v \\ w \\ \phi \end{Bmatrix} = \begin{bmatrix} G_{11} & G_{12} & G_{13} & G_{14} \\ G_{21} & G_{22} & G_{23} & G_{24} \\ G_{31} & G_{32} & G_{33} & G_{34} \\ G_{41} & G_{42} & G_{43} & G_{44} \end{bmatrix} \begin{Bmatrix} P_x \\ P_y \\ P_z \\ -Q \end{Bmatrix} \tag{2.33}$$

where G_{ij}, defined in Eq (2.4), are given by

$$G_{11} = \frac{x^2 D_0}{R_0 R_0^{*2}} - \sum_{i=1}^{3} D_i \lambda_i^{uv} \frac{y^2 + z_i^2 + z_i R_i}{R_i R_i^{*2}}, \quad G_{12} = G_{21} = \frac{xyD_0}{R_0 R_0^{*2}} + \sum_{i=1}^{3} D_i \lambda_i^{uv} \frac{xy}{R_i R_i^{*2}},$$

$$G_{13} = G_{31} = \sum_{i=1}^{3} B_i \lambda_i^{uv} \frac{x}{R_i R_i^*} = \sum_{i=1}^{3} D_i \lambda_i^{w} \frac{x}{R_i R_i^*},$$

$$G_{14} = G_{41} = -\sum_{i=1}^{3} A_i \lambda_i^{uv} \frac{x}{R_i R_i^*} = \sum_{i=1}^{3} D_i \lambda_i^{\phi} \frac{x}{R_i R_i^*}, \quad G_{22} = \frac{y^2 D_0}{R_0 R_0^{*2}} - \sum_{i=1}^{3} D_i \lambda_i^{uv} \frac{x^2 + z_i^2 + z_i R_i}{R_i R_i^{*2}},$$

$$G_{23} = G_{32} = \sum_{i=1}^{3} B_i \lambda_i^{uv} \frac{y}{R_i R_i^*} = \sum_{i=1}^{3} D_i \lambda_i^{w} \frac{y}{R_i R_i^*},$$

$$G_{24} = G_{42} = -\sum_{i=1}^{3} A_i \lambda_i^{uv} \frac{y}{R_i R_i^*} = \sum_{i=1}^{3} D_i \lambda_i^{\phi} \frac{y}{R_i R_i^*},$$

$$G_{33} = \sum_{i=1}^{3} B_i \lambda_i^{w} \frac{1}{R_i}, \quad G_{34} = G_{43} = -\sum_{i=1}^{3} A_i \lambda_i^{w} \frac{1}{R_i} = \sum_{i=1}^{3} B_i \lambda_i^{\phi} \frac{1}{R_i},$$

$$G_{44} = -\sum_{i=1}^{3} A_i \lambda_i^{\phi} \frac{1}{R_i} \tag{2.34}$$

with

$$A_1 = \frac{1}{4\pi\gamma_e} \frac{(v_1^2 - 1)(v_2^2 - 1)(v_3^2 - 1)}{v_1 (v_1^2 - v_2^2)(v_1^2 - v_3^2)}$$

$$B_1 = \frac{1}{4\pi\gamma_a} (v_1^2 - 1)[n_2^e \lambda_3^{uv} (v_3^2 - 1) - n_3^e \lambda_2^{uv} (v_2^2 - 1)] \tag{2.35}$$

$$D_0 = \frac{1}{4\pi c_{44} v_0}, \qquad D_1 = \frac{1}{4\pi\gamma_t} \frac{\lambda_2^\phi \lambda_3^w - \lambda_3^\phi \lambda_2^w}{c_{44}}.$$

The constants A_2, B_2, D_2, A_3, B_3, and D_3 are obtained from A_1, B_1, and D_1 by cyclically

permuting the indices 1, 2, and 3. The constants γ_a, γ_e, and γ_t appearing in Eq (2.35) are

$$\gamma_a = (v_1^2 - 1)\lambda_1^{uv}(n_2^a n_3^e - n_3^a n_2^e) + (v_2^2 - 1)\lambda_2^{uv}(n_3^a n_1^e - n_1^a n_3^e) + (v_3^2 - 1)\lambda_3^{uv}(n_1^a n_2^e - n_2^a n_1^e) \quad (2.36)$$

$$\begin{aligned}\gamma_e = {} & (\kappa_{11} - \kappa_{33})[c_{11}(c_{44} - c_{33}) + c_{44}(c_{33} + 2c_{13}) + c_{13}^2] + c_{11}(e_{33} - e_{15}^2)^2 \\ & + c_{33}(e_{31} + e_{15})^2 - c_{44}(e_{33} + e_{31})^2 + 2c_{13}[e_{15}(e_{15} + e_{31} - e_{33}) - e_{33}e_{31}]\end{aligned} \quad (2.37)$$

$$\gamma_t = v_1\lambda_1^{uv}(\lambda_3^{\phi}\lambda_2^{w} - \lambda_2^{\phi}\lambda_3^{w}) + v_2\lambda_2^{uv}(\lambda_1^{\phi}\lambda_3^{w} - \lambda_3^{\phi}\lambda_1^{w}) + v_3\lambda_3^{uv}(\lambda_2^{\phi}\lambda_1^{w} - \lambda_1^{\phi}\lambda_2^{w}) \quad (2.38)$$

2.4 Green's function by Fourier transforms

In this section, we briefly examine the application of Fourier transform techniques to the fundamental solution of piezoelectric materials. Lee and Jiang [8] used Fourier transform techniques to derive Green's functions of 2D piezoelectric material. They began with considering a plain strain problem of a transversely isotropic piezoelectric solid with the symmetry of a hexagonal class. The solid is subjected to a point force F_i and a point electric charge Ψ at the source point ξ. Note that F_i and Ψ are unity, but are used here as a bookkeeping device [8]. If the $x_2 - x_3$ plane is the isotropic plane, one can employ either the $x_1 - x_2$ or $x_1 - x_3$ plane for the study of plane electromechanical phenomena. Choosing the former, the plain strain problem is defined by Eqs (1.144) and (1.145). Recently, Li and Wang [39] extended Lee and Jiang's formulation to the case of three-dimensional problem. The discussion below focus on the results presented in [8] and [39].

Making use of Eqs (1.49), (1.(51), (1.144), and noting that w=0 or constant in the case of plane strain, Eq $(1.59)_{1,2}$ can be written in the form

$$\begin{bmatrix} c_{11}\dfrac{\partial^2}{\partial x_1^2} + c_{33}\dfrac{\partial^2}{\partial x_2^2} & (c_{12} + c_{33})\dfrac{\partial^2}{\partial x_1 \partial x_2} & (e_{21} + e_{13})\dfrac{\partial^2}{\partial x_1 \partial x_2} \\ (c_{12} + c_{33})\dfrac{\partial^2}{\partial x_1 \partial x_2} & c_{33}\dfrac{\partial^2}{\partial x_1^2} + c_{22}\dfrac{\partial^2}{\partial x_2^2} & e_{13}\dfrac{\partial^2}{\partial x_1^2} + e_{22}\dfrac{\partial^2}{\partial x_2^2} \\ -(e_{21} + e_{13})\dfrac{\partial^2}{\partial x_1 \partial x_2} & -e_{13}\dfrac{\partial^2}{\partial x_1^2} - e_{22}\dfrac{\partial^2}{\partial x_2^2} & \kappa_{11}\dfrac{\partial^2}{\partial x_1^2} + \kappa_{22}\dfrac{\partial^2}{\partial x_2^2} \end{bmatrix} \begin{Bmatrix} u \\ v \\ \phi \end{Bmatrix} + \begin{Bmatrix} F_1\delta(\xi, \mathbf{x}) \\ F_2\delta(\xi, \mathbf{x}) \\ \Psi\delta(\xi, \mathbf{x}) \end{Bmatrix} = 0 \quad (2.39)$$

After applying the double Fourier transform which is defined by:

$$\hat{f}(\lambda_1, \lambda_2) = \frac{1}{2\pi}\int_{-\infty}^{\infty}\int_{-\infty}^{\infty} f(x_1, x_2)e^{-i(\lambda_1 x_1 + \lambda_2 x_2)}dx_1 dx_2 \quad (2.40)$$

Eq (2.39) may be further written as [8]

$$\begin{Bmatrix} \hat{u} \\ \hat{v} \\ \hat{\phi} \end{Bmatrix} = \frac{1}{2\pi}\begin{bmatrix} A_{11} & A_{12} & -A_{13} \\ A_{12} & A_{22} & -A_{23} \\ A_{13} & A_{23} & -A_{33} \end{bmatrix} \begin{Bmatrix} \hat{F}_1 \\ \hat{F}_2 \\ \hat{\Psi} \end{Bmatrix} \quad (2.41)$$

where

$$A_{11}=(\alpha_{11}\lambda_1^4+\beta_{11}\lambda_1^2\lambda_2^2+\gamma_{11}\lambda_2^4)N^{-1},\quad A_{12}=(\alpha_{12}\lambda_1^3\lambda_2+\beta_{12}\lambda_1\lambda_2^3)N^{-1},$$
$$A_{13}=(\alpha_{13}\lambda_1^3\lambda_2+\beta_{13}\lambda_1\lambda_2^3)N^{-1},\qquad A_{22}=(\alpha_{22}\lambda_1^4+\beta_{22}\lambda_1^2\lambda_2^2+\gamma_{22}\lambda_2^4)N^{-1},\qquad (2.42)$$
$$A_{23}=(\alpha_{23}\lambda_1^4+\beta_{23}\lambda_1^2\lambda_2^2+\gamma_{23}\lambda_2^4)N^{-1},\quad A_{33}=(\alpha_{33}\lambda_1^4+\beta_{33}\lambda_1^2\lambda_2^2+\gamma_{33}\lambda_2^4)N^{-1},$$

$$N(\lambda_1,\lambda_2)=\lambda^6+\kappa_1\lambda_1^4\lambda_2^2+\kappa_2\lambda_1^2\lambda_2^4+\kappa_3\lambda_2^6 \qquad (2.43)$$

In Eq (2.42), constants α_{ij}, β_{ij}, γ_{ij}, and κ_i are given by

$$\alpha_{11}=(e_{13}^2+c_{33}\kappa_{11})P,\quad \beta_{11}=(2e_{13}e_{22}+c_{22}\kappa_{11}+c_{33}\kappa_{22})P,\quad \gamma_{11}=(e_{22}^2+c_{22}\kappa_{22})P,$$

$$\alpha_{12}=-(c_{12}\kappa_{11}+c_{33}\kappa_{11}+e_{13}^2+e_{13}e_{21})P,\quad \beta_{12}=-(c_{12}\kappa_{22}+c_{33}\kappa_{22}+e_{13}e_{22}+e_{22}e_{21})P,$$

$$\alpha_{13}=(c_{12}e_{13}-c_{33}e_{21})P,\quad \beta_{13}=(c_{12}e_{22}+c_{33}e_{22}-e_{13}c_{22}-e_{21}c_{22})P,$$

$$\alpha_{22}=c_{11}\kappa_{11}P,\quad \beta_{22}=(2e_{13}e_{21}+c_{11}\kappa_{22}+e_{13}^2+e_{21}^2+c_{33}\kappa_{11})P,\quad \gamma_{22}=c_{33}\kappa_{22}P,$$

$$\alpha_{23}=-c_{11}e_{13}P,\quad \beta_{23}=(c_{12}e_{13}-c_{11}e_{22}+e_{21}c_{12}+e_{21}c_{33})P,\quad \gamma_{23}=-c_{33}e_{22}P,$$

$$\alpha_{33}=-c_{11}c_{33}P,\quad \beta_{33}=(c_{12}^2-c_{11}c_{22}+2c_{33}c_{12})P,\quad \gamma_{33}=-c_{33}c_{22}P,$$

$$\kappa_1=(c_{11}c_{22}\kappa_{11}+2c_{11}e_{13}e_{22}-2c_{12}e_{13}^2+c_{11}c_{33}\kappa_{22}-2c_{12}c_{33}\kappa_{11}$$
$$-2c_{12}e_{21}e_{13}+e_{21}^2c_{33}-c_{12}^2\kappa_{11})P,$$

$$\kappa_2=(2e_{13}e_{21}c_{22}-2c_{33}e_{21}e_{22}-2c_{12}e_{22}e_{13}-c_{12}^2\kappa_{22}-2c_{12}c_{33}\kappa_{22}$$
$$+c_{22}c_{33}\kappa_{11}-2c_{12}e_{22}e_{21}+e_{13}^2c_{22}+c_{11}c_{22}\kappa_{22}+e_{22}^2c_{11}+e_{21}^2c_{22})P,$$

$$\kappa_3=(c_{33}e_{22}^2+c_{33}c_{22}\kappa_{22})P, \qquad (2.44)$$

where

$$P=(c_{11}e_{13}^2+c_{11}c_{33}\kappa_{11})^{-1} \qquad (2.45)$$

Applying the Fourier inversion defined by

$$f(x_1,x_2)=\frac{1}{2\pi}\int_{-\infty}^{\infty}\int_{-\infty}^{\infty}\hat{f}(\lambda_1,\lambda_2)e^{i(\lambda_1x_1+\lambda_2x_2)}d\lambda_1d\lambda_2 \qquad (2.46)$$

to Eq (2.41), followed by some manipulation, yields the Green's function in the original space:

$$G_{11}(\boldsymbol{\xi},\mathbf{x})=\frac{1}{2\pi}(\alpha_{11}I_4+\beta_{11}I_2+\gamma_{11}I_0),\quad G_{12}(\boldsymbol{\xi},\mathbf{x})=G_{21}(\boldsymbol{\xi},\mathbf{x})=\frac{1}{2\pi}(\alpha_{12}I_3+\beta_{12}I_1),$$

$$G_{22}(\boldsymbol{\xi},\mathbf{x})=\frac{1}{2\pi}(\alpha_{22}I_4+\beta_{22}I_2+\gamma_{22}I_0),\quad G_{31}(\boldsymbol{\xi},\mathbf{x})=-G_{13}(\boldsymbol{\xi},\mathbf{x})=\frac{1}{2\pi}(\alpha_{13}I_3+\beta_{13}I_1), \qquad (2.47)$$

$$G_{33}(\boldsymbol{\xi},\mathbf{x})=-\frac{1}{2\pi}(\alpha_{33}I_4+\beta_{33}I_2+\gamma_{33}I_0),\ G_{32}(\boldsymbol{\xi},\mathbf{x})=-G_{23}(\boldsymbol{\xi},\mathbf{x})=\frac{1}{2\pi}(\alpha_{23}I_4+\beta_{23}I_2+\gamma_{23}I_0)$$

where

$$I_m = \frac{1}{2\pi}\int_{-\infty}^{\infty}\int_{-\infty}^{\infty}\frac{\lambda_1^m\lambda_2^{4-m}}{N(\lambda_1,\lambda_2)}e^{i(\lambda_1 x_1+\lambda_2 x_2)}d\lambda_1 d\lambda_2 \tag{2.48}$$

and the components $G_{ij}(\mathbf{x},\boldsymbol{\xi})$ represent the elastic displacement at **x** in the x_i-direction (for i=1,2), or the electric potential (for i=3) due to a unit point force at $\boldsymbol{\xi}$ in the x_j-direction (for j=1,2), or a unit point charge at $\boldsymbol{\xi}$ (for j=3).

It is now clear that all that is required is to evaluate the integral (2.48). In what follows we describe Lee and Jiang's approach presented in [8] for calculating the integral I_m. They indicated that the explicit expression of I_m depends on the roots of the equation $N(\lambda_1,\lambda_2)=0$. In general there are two independent sets of roots:

$$\begin{aligned} &1)\quad \lambda_1 = \pm ip_0\lambda_2, \quad \lambda_1 = \pm(p_1 \pm iq_1)\lambda_2; \\ &2)\quad \lambda_1 = \pm ip_0\lambda_2, \quad \lambda_1 = \pm(p_1 \pm q_1)\lambda_2 \end{aligned} \tag{2.49}$$

where p_0, p_1 and q_1 are real positive numbers. Taking the first set of roots as an example, $N(\lambda_1,\lambda_2)$ can be factored into the following form:

$$N(\lambda_1,\lambda_2) = \left(\lambda_1^2+(p_0\lambda_2)^2\right)\left((\lambda_1-p_1\lambda_2)^2+(q_1\lambda_2)^2\right)\left((\lambda_1+p_1\lambda_2)^2+(q_1\lambda_2)^2\right) \tag{2.50}$$

The integral (2.48) can then be evaluated using the residue theorem for the variable λ_1 and by considering the so-called Hadamard's finite part [40]. As a result, I_m may be written in the form

$$I_m = \sum_{i=1}^{6} R_{mi}L_i, \quad (m=0,1,2,3,4) \tag{2.51}$$

in which

$$R_{01}=Q,\ \ R_{02}=0,\ \ R_{03}=R_{05}=-\frac{Q}{2},\ \ R_{04}=-R_{06}=\frac{1}{4p_1}(p_0^2-q_1^2+3p_1^2)Q,$$

$$R_{11}=0,\ \ R_{12}=R_{21}=-p_0^2Q,\ \ R_{13}=-R_{15}=\frac{1}{4p_1}(p_0^2-q_1^2-p_1^2)Q,$$

$$R_{14}=R_{16}=\frac{1}{2}(q_1^2+p_1^2)Q,\ \ R_{22}=0,\ \ R_{23}=R_{25}=\frac{1}{2}p_0^2Q,$$

$$R_{24}=-R_{26}=-\frac{1}{4p_1}(p_0^2q_1^2+p_0^2p_1^2-p_1^4-2p_1^2q_1^2-q_1^4)Q,\ \ R_{31}=0,$$

$$R_{32}=p_0^4Q,\ \ R_{33}=-R_{35}=\frac{1}{4p_1}(3p_0^2p_1^2-p_0^2q_1^2+p_1^4+2p_1^2q_1^2+q_1^4)Q,$$

$$R_{34}=R_{36}=-\frac{1}{2}(q_1^2+p_1^2)p_0^2Q,\ \ R_{41}=p_0^4Q, R_{42}=0,$$

$$R_{43}=R_{45}=\frac{1}{2}(2p_0^2p_1^2-2p_0^2q_1^2+p_1^4+2p_1^2q_1^2+q_1^4)Q,$$

$$R_{44}=-R_{46}=-\frac{1}{4p_1}(2p_0^2p_1^2q_1^2-p_0^2q_1^4+3q_1^2p_1^4+3p_1^2q_1^4+q_1^6+p_1^6)Q,$$

$$L_1 = -\frac{1}{p_0}\ln\sqrt{p_0^2\overline{x}_1^2 + \overline{x}_2^2}, \quad L_2 = -\frac{1}{p_0^2}\tan^{-1}\left(\frac{p_0\overline{x}_1}{\overline{x}_2}\right),$$

$$L_3 = -\frac{1}{q_1}\ln\sqrt{(p_1\overline{x}_1 + \overline{x}_2)^2 + (q_1\overline{x}_1)^2},$$

$$L_4 = \frac{p_1}{q_1\eta}\left[-\ln\sqrt{\left(\overline{x}_1 + \frac{p_1}{\eta}\overline{x}_2\right)^2 + \left(\frac{q_1}{\eta}\overline{x}_2\right)^2} + \tan^{-1}\left(\frac{\eta\overline{x}_1 + p_1\overline{x}_2}{q_1\overline{x}_2}\right)\right],$$

$$L_5 = -\frac{1}{q_1}\ln\sqrt{(\overline{x}_2 - p_1\overline{x}_1)^2 + (q_1\overline{x}_1)^2},$$

$$L_6 = \frac{p_1}{q_1\eta}\left[\ln\sqrt{\left(\overline{x}_1 - \frac{p_1}{\eta}\overline{x}_2\right)^2 + \left(\frac{q_1}{\eta}\overline{x}_2\right)^2} - \tan^{-1}\left(\frac{\eta\overline{x}_1 - p_1\overline{x}_2}{q_1\overline{x}_2}\right)\right] \tag{2.52}$$

with

$$\overline{x}_1 = \xi_1 - x_1, \ \ \overline{x}_2 = \xi_2 - x_2, \ \eta = p_1^2 + q_1^2$$

$$Q = \frac{1}{2\pi}(q_1^4 - 2p_0^2q_1^2 + 2p_1^2q_1^2 + p_0^4 + 2p_0^1p_1^2 + p_1^4)^{-1} \tag{2.53}$$

The Green's function obtained above is suitable for two-dimensional piezoelectric material only. Extension of the formulation to three-dimensional material is straightforward [39]. To this end, taking the Fourier transform in the x_1-, x_2- and x_3- directions for $G_{MR}(\mathbf{x})$ in Eq (2.4), we have [39]

$$\hat{G}_{MR}(\boldsymbol{\xi}) = \int_{-\infty}^{\infty} G_{MR}(\mathbf{x})e^{i\mathbf{x}\cdot\boldsymbol{\xi}}d\mathbf{x} \tag{2.54}$$

where $\boldsymbol{\xi} = \{\xi_1, \ \xi_2, \ \xi_3\}$, and the inverse of the Fourier transform (2.54) gives

$$G_{MR}(\mathbf{x}) = \frac{1}{8\pi^3}\int_{-\infty}^{\infty}\hat{G}_{MR}(\boldsymbol{\xi})e^{-i\mathbf{x}\cdot\boldsymbol{\xi}}d\boldsymbol{\xi} \tag{2.55}$$

Then Eq (2.4) turns into a set of algebraic equations

$$E_{iJMl}\hat{G}_{MR}(\boldsymbol{\xi})\xi_i\xi_l = \delta_{JR} \tag{2.56}$$

Solving Eq (2.56) provides

$$\hat{G}_{MR}(\boldsymbol{\xi}) = K_{JM}^{-1}(\boldsymbol{\xi})\delta_{JR} = K_{RM}^{-1}(\boldsymbol{\xi}) \tag{2.57}$$

Taking the Fourier inverse transform (2.57), we obtain

$$G_{MR}(\mathbf{x}) = \frac{1}{8\pi^3}\int_{-\infty}^{\infty}K_{MR}^{-1}(\boldsymbol{\xi})e^{-i\mathbf{x}\cdot\boldsymbol{\xi}}d\boldsymbol{\xi} = \frac{1}{8\pi^3}\int_{-\infty}^{\infty}\frac{A_{MR}(\boldsymbol{\xi})}{D(\boldsymbol{\xi})}e^{-i\mathbf{x}\cdot\boldsymbol{\xi}}d\boldsymbol{\xi} \tag{2.58}$$

Replacing $\boldsymbol{\xi}$ in Eq (2.58) with -$\boldsymbol{\xi}$, we have[39]

$$G_{MR}(\mathbf{x}) = \frac{1}{8\pi^3}\int_{-\infty}^{\infty}\frac{A_{MR}(\boldsymbol{\xi})}{D(\boldsymbol{\xi})}e^{i\mathbf{x}\cdot\boldsymbol{\xi}}d\boldsymbol{\xi} \tag{2.59}$$

where D($\boldsymbol{\xi}$) and $A_{MR}(\boldsymbol{\xi})$ are the determinant and adjoint of matrix $K_{MR}(\boldsymbol{\xi})$, respectively. Li and Wang [39] provided further expressions of $G_{MR}(\mathbf{x})$ by defining the volume element d$\boldsymbol{\xi}$ as $d\boldsymbol{\xi}=\xi^2 d\xi dS$, where $|\boldsymbol{\xi}|=(\xi_i\xi_i)^{1/2}$ and S is the surface element on the unit sphere S^2 in the $\boldsymbol{\xi}$-space, centred at the origin of the coordinates ξ_i (see Fig. 2.2).

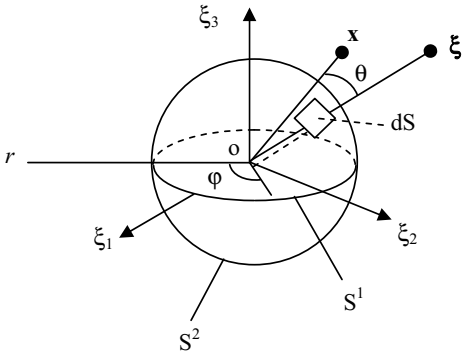

Fig. 2.2 The unit sphere S^2 in the $\boldsymbol{\xi}$-space; S^1 is the unit circle on S^2 intersected by the plane perpendicular to $\mathbf{x}$; r is a local polar coordinate [39]

By adding Eqs (2.58) and (2.59), we obtain under the sphere coordinate system

$$G_{MR}(\mathbf{x})=\frac{1}{16\pi^3}\int_{-\infty}^{\infty} d|\boldsymbol{\xi}|\int_{S^2}\frac{A_{MR}(\boldsymbol{\xi}^0)}{D(\boldsymbol{\xi}^0)}e^{i|\mathbf{x}||\boldsymbol{\xi}|\mathbf{x}^0\cdot\boldsymbol{\xi}^0}dS(\boldsymbol{\xi}^0) \tag{2.60}$$

where

$$\boldsymbol{\xi}^0=\frac{\boldsymbol{\xi}}{|\boldsymbol{\xi}|},\qquad \mathbf{x}^0=\frac{\mathbf{x}}{|\mathbf{x}|},\qquad |\mathbf{x}|=(x_i x_i)^{1/2} \tag{2.61}$$

Integrating Eq (2.60) with respect to $\boldsymbol{\xi}$ leads to

$$G_{MR}(\mathbf{x})=\frac{1}{8\pi^2}\int_{S^2}\delta(|\mathbf{x}|\mathbf{x}^0\cdot\boldsymbol{\xi}^0)\frac{A_{MR}(\boldsymbol{\xi}^0)}{D(\boldsymbol{\xi}^0)}dS(\boldsymbol{\xi}^0) \tag{2.62}$$

Denoting the angle between $\boldsymbol{\xi}$ and $\mathbf{x}$ by θ, we have

$$\boldsymbol{\xi}^0\cdot\mathbf{x}^0=\cos\theta,\quad d(\boldsymbol{\xi}^0\cdot\mathbf{x}^0)=-\sin\theta d\theta,\quad dS(\boldsymbol{\xi}^0)=\sin\theta d\theta d\varphi \tag{2.63}$$

where φ is defined on the plane perpendicular to $\mathbf{x}$. Substituting Eq (2.63) into Eq (2.62), we obtain

$$G_{MR}(\mathbf{x})=\frac{1}{8\pi^2}\int_{-1}^{1} d(\mathbf{x}^0\cdot\boldsymbol{\xi}^0)\delta(|\mathbf{x}|\mathbf{x}^0\cdot\boldsymbol{\xi}^0)\int_0^{2\pi}\frac{A_{MR}(\boldsymbol{\xi}^0)}{D(\boldsymbol{\xi}^0)}d\varphi=\frac{1}{8\pi^2|\mathbf{x}|}\oint_{S^1}\frac{A_{MR}(\boldsymbol{\xi}^0)}{D(\boldsymbol{\xi}^0)}d\varphi \tag{2.64}$$

Thus $G_{MR}(\mathbf{x})$ can be expressed by a line integral along S^1 which lies on the plane perpendicular to $\mathbf{x}$. Eq (2.64) can be further simplified by considering $\boldsymbol{\xi}^0=e^{i\varphi}$ as

$$G_{MR}(\mathbf{x})=\frac{1}{4\pi^2|\mathbf{x}|}\int_{-\pi/2}^{\pi/2}\frac{A_{MR}(e^{i\varphi})}{D(e^{i\varphi})}d\varphi \tag{2.65}$$

Defining $\varphi = \arctan\zeta$ and $R = \sqrt{1+\zeta^2}$ (see Fig. 2.3), and substituting them into Eq (2.65), we have

$$G_{MR}(\mathbf{x}) = \frac{1}{4\pi^2|\mathbf{x}|}\int_{-\infty}^{\infty}\frac{A_{MR}(Re^{i\arctan\zeta})}{D(Re^{i\arctan\zeta})}d\zeta = \frac{1}{4\pi^2|\mathbf{x}|}\int_{-\infty}^{\infty}\frac{A_{MR}(\mathbf{p}+\zeta\mathbf{q})}{D(\mathbf{p}+\zeta\mathbf{q})}d\zeta \qquad (2.66)$$

where **p** and **q** are two unit vectors and $\mathbf{p}\perp\mathbf{q}$ (see Fig. 2.3).

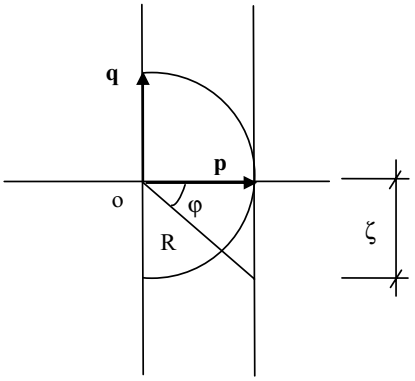

Fig. 2.3 The unit vector **p** and **q** on the plane where the unit circle S^1 is located

Considering that Eq (2.4) are elliptic and the coefficients in $D(\xi)$ are all real, $D(\xi)$ has no real root and all imaginary roots occur in complex conjugate pairs. Therefore the eight-order polynomial equation of ζ

$$D(\mathbf{p}+\zeta\mathbf{q}) = 0 \qquad (2.67)$$

has eight roots, four of them being the conjugate of the remainder. With these roots, $D(\mathbf{p}+\zeta\mathbf{q})$ can be expressed as

$$D(\mathbf{p}+\zeta\mathbf{q}) = \sum_{k=0}^{8} a_{k+1}\zeta^k = a_9\prod_{m=1}^{4}(\zeta-\zeta_m)(\zeta-\overline{\zeta}_m) \qquad (2.68)$$

where $\mathrm{Im}(\zeta_m) > 0$ (m=1,2,3,4) and $\overline{\zeta}_m$ is the complex conjugate of ζ_m.

According to the residual theory of complex integrals, Eq (2.66) can be further written as

$$G_{MR}(\mathbf{x}) = -\frac{1}{2\pi|\mathbf{x}|}\mathrm{Im}\sum_{m=1}^{4}\frac{A_{MR}(\mathbf{p}+\zeta\mathbf{q})}{a_9(\zeta_m-\overline{\zeta}_m)\prod_{k=1,k\neq m}^{4}(\zeta_m-\zeta_k)(\zeta_m-\overline{\zeta}_k)} \qquad (2.69)$$

in which the roots of $D(\mathbf{p}+\zeta\mathbf{q})$ are assumed to be distinct from each other.

2.5 Half-plane problem

In the previous sections, we derived Green's function in free space using the Radon transform, the potential function approach, and the Fourier transform. Green's functions for piezoelectric solids with defects such as a half-plane boundary, bimaterial interface, and an elliptic hole boundary are discussed in the remaining sections of this chapter. In this section, Green's functions in a half-plane piezoelectric solid subjected to a line force-charge $\mathbf{q}_0$ and a generalized line dislocation **b** are presented through use of Stroh's formalism. The boundary condition on the infinite straight boundary of the half-plane is free of surface traction-charge. Owing to the linear property of the problem, the principle of superposition is used and this problem can be divided into two problems (see Fig. 2.4): (i) An infinite piezoelectric plate is subjected to the line force-charge $\mathbf{q}_0$ and the line dislocation **b** both located at $z_0(x_{10}, x_{20})$ in an infinite domain; and (ii) the infinite straight boundary of the half-plane is subjected to loadings making the surface traction-charge free.

We start by considering an infinite domain subjected to a line force-charge $\mathbf{q}_0$ and a line dislocation **b**, both located at $z_0(x_{10}, x_{20})$. The general solution (1.128) and (1.129) is in this case in the form [2,41,42]

$$\mathbf{U} = 2\,\mathrm{Re}\{\mathbf{A}\langle \ln(z_\alpha - z_{\alpha 0})\rangle \mathbf{q}_f\}, \qquad \boldsymbol{\varphi} = 2\,\mathrm{Re}\{\mathbf{B}\langle \ln(z_\alpha - z_{\alpha 0})\rangle \mathbf{q}_f\} \tag{2.70}$$

where $\mathbf{q}_f$ is a complex vector to be determined, **A** and **B** are now 4×4 matrices (5×5 matrix in Section 1.5) expressed by

$$\mathbf{A} = [\mathbf{a}_1\ \mathbf{a}_2\ \mathbf{a}_3\ \mathbf{a}_4], \quad \mathbf{B} = [\mathbf{b}_1\ \mathbf{b}_2\ \mathbf{b}_3\ \mathbf{b}_4] \tag{2.71}$$

and

$$\mathbf{U} = \{u_1\ u_2\ u_3\ \phi\}^T, \quad \boldsymbol{\varphi} = \{\varphi_1\ \varphi_2\ \varphi_3\ \varphi_4\}^T,$$

$$z_\alpha = x_1 + p_\alpha x_2, \qquad z_{\alpha 0} = x_{10} + p_\alpha x_{20}, \quad (\alpha = 1-4) \tag{2.72}$$

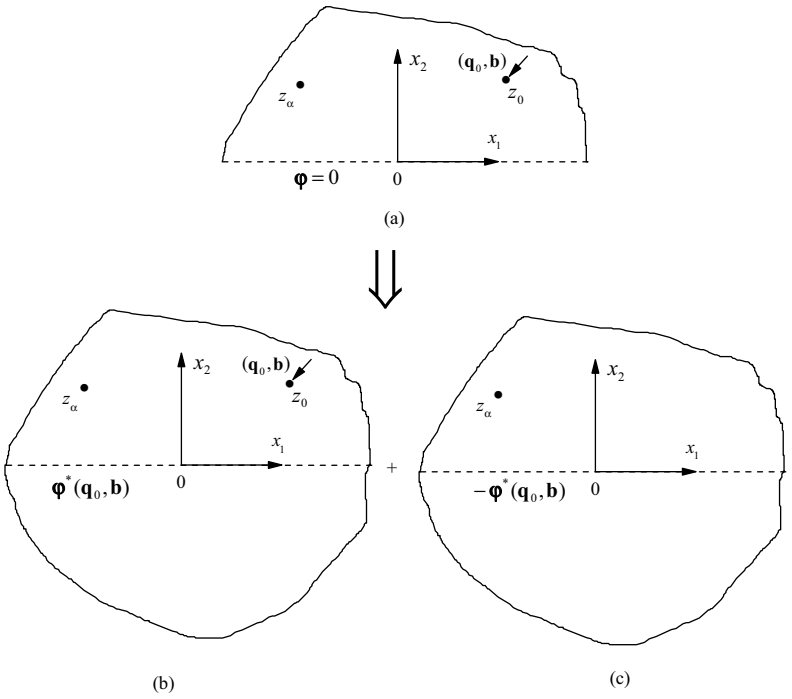

Fig. 2.4 (a) Half-plane subjected to $\mathbf{q}_0$ and $\mathbf{b}$; (b) problem (i), $\boldsymbol{\varphi}^*$ is induced by $\mathbf{q}_0$ and $\mathbf{b}$ at x_2=0; (c) problem (ii)

Since $\ln(z_\alpha - z_{\alpha 0})$ is a multi-valued function we introduce a cut along the line defined by $x_2=x_{20}$ and $x_1 \le x_{10}$. Using the polar coordinate system (r,θ) with its origin at $z_0(x_{10}, x_{20})$ and θ=0 being parallel to the x_1-axis, the solution (2.70) applies to

$$-\pi < \theta < \pi, \qquad r>0 \tag{2.73}$$

Therefore

$$\ln(z_\alpha - z_{\alpha 0}) = \ln r \pm i\pi, \qquad \text{at } \theta = \pm\pi \text{ for } \alpha = 1\text{-}4 \tag{2.74}$$

Due to this relation, Eq (2.70) must satisfy the conditions

$$\mathbf{U}(\pi) - \mathbf{U}(-\pi) = \mathbf{b}, \quad \boldsymbol{\varphi}(\pi) - \boldsymbol{\varphi}(-\pi) = \mathbf{q}_0 \tag{2.75}$$

which lead to

$$4\pi \,\mathrm{Re}(i\mathbf{A}\mathbf{q}_f) = \mathbf{b}, \qquad 4\pi \,\mathrm{Re}(i\mathbf{B}\mathbf{q}_f) = \mathbf{q}_0 \tag{2.76}$$

It is easy to prove that Eq (2.76) satisfy following equilibrium conditions of the force and single-valued conditions of the generalized displacement **U**:

$$\int_C d\boldsymbol{\varphi} = \mathbf{q}_0, \quad \int_C d\mathbf{U} = \mathbf{b} \tag{2.77}$$

where C represents an arbitrary closed curve enclosing the point z_0.

Eq (2.76) can be written as

$$\begin{bmatrix} \mathbf{A} & \overline{\mathbf{A}} \\ \mathbf{B} & \overline{\mathbf{B}} \end{bmatrix} \begin{Bmatrix} i\mathbf{q}_f \\ -i\overline{\mathbf{q}}_f \end{Bmatrix} = \frac{1}{2\pi} \begin{Bmatrix} \mathbf{b} \\ \mathbf{q}_0 \end{Bmatrix} \tag{2.78}$$

It follows from Eq (1.139) that

$$\begin{Bmatrix} i\mathbf{q}_f \\ -i\overline{\mathbf{q}}_f \end{Bmatrix} = \frac{1}{2\pi} \begin{bmatrix} \mathbf{B}^T & \mathbf{A}^T \\ \overline{\mathbf{B}}^T & \overline{\mathbf{A}}^T \end{bmatrix} \begin{Bmatrix} \mathbf{b} \\ \mathbf{q}_0 \end{Bmatrix} \tag{2.79}$$

Hence

$$\mathbf{q}_f = \frac{1}{2\pi i}\left(\mathbf{A}^T\mathbf{q}_0 + \mathbf{B}^T\mathbf{b}\right) \tag{2.80}$$

The traction-charge on the half-plane boundary induced by the applied $\mathbf{q}_0$ and $\mathbf{b}$ is then given as

$$\mathbf{\Pi}_{2J}^I(x_1) = \left\{\sigma_{12}^I \ \sigma_{22}^I \ \sigma_{32}^I \ D_2^I\right\}^T = \boldsymbol{\varphi}_{J,1}^I = \frac{1}{\pi}\mathrm{Im}\left\{\mathbf{B}\left\langle\frac{1}{x_1 - z_{\alpha 0}}\right\rangle(\mathbf{A}^T\mathbf{q}_0 + \mathbf{B}^T\mathbf{b})\right\} \tag{2.81}$$

Therefore the second problem is the half-plane solid subjected to loading of $\mathbf{\Pi}_{2J}^{II}(x_1) = -\mathbf{\Pi}_{2J}^{I}(x_1)$ at the infinite straight boundary of the half-plane, which is equivalent to the condition that

$$\boldsymbol{\varphi} = \boldsymbol{\varphi}^I + \boldsymbol{\varphi}^{II} = 0 \qquad \text{at } x_2 = 0 \tag{2.82}$$

where the following relations have been used [2]:

$$\mathbf{\Pi}_n = \boldsymbol{\varphi}_{,s} \tag{2.83}$$

where n is the normal direction of the boundary, s is the arc length measured along the half-plane boundary, $\mathbf{\Pi}_n$ represents the surface traction-charge vector. Integrating Eq (2.83) and ignoring the induced integral constant, which represents rigid body motion, results in Eq (2.82).

Therefore, to satisfy the boundary condition on the infinite straight boundary (2.82), the solution can be assumed in the form [2,43]

$$\mathbf{U} = \mathbf{U}^I + \mathbf{U}^{II} = \frac{1}{\pi}\mathrm{Im}\{\mathbf{A}\left\langle\ln(z_\alpha - z_{\alpha 0})\right\rangle\mathbf{q}^*\} + \sum_{\beta=1}^{4}\frac{1}{\pi}\mathrm{Im}\{\mathbf{A}\left\langle\ln(z_\alpha - \overline{z}_{\beta 0})\right\rangle\mathbf{q}_\beta\}, \tag{2.84}$$

$$\boldsymbol{\varphi} = \boldsymbol{\varphi}^I + \boldsymbol{\varphi}^{II} = \frac{1}{\pi}\mathrm{Im}\{\mathbf{B}\left\langle\ln(z_\alpha - z_{\alpha 0})\right\rangle\mathbf{q}^*\} + \sum_{\beta=1}^{4}\frac{1}{\pi}\mathrm{Im}\{\mathbf{B}\left\langle\ln(z_\alpha - \overline{z}_{\beta 0})\right\rangle\mathbf{q}_\beta\} \tag{2.85}$$

where $\mathbf{q}_\beta$ are unknown constants to be determined and

$$\mathbf{q}^* = \mathbf{A}^T\mathbf{q}_0 + \mathbf{B}^T\mathbf{b} \tag{2.86}$$

Substituting Eq (2.85) into Eq (2.82) yields

$$\boldsymbol{\varphi} = \frac{1}{\pi}\mathrm{Im}\{\mathbf{B}\left\langle\ln(x_1 - z_{\alpha 0})\right\rangle\mathbf{q}^*\} + \sum_{\beta=1}^{4}\frac{1}{\pi}\mathrm{Im}\{\ln(z_\alpha - \overline{z}_{\beta 0})\mathbf{B}\mathbf{q}_\beta\} = 0 \tag{2.87}$$

Noting that $\mathrm{Im}(f) = -\mathrm{Im}(\bar{f})$, we have

$$\mathrm{Im}\{\mathbf{B}\langle \ln(x_1 - z_{\alpha 0})\rangle \mathbf{q}^*\} = -\mathrm{Im}\{\bar{\mathbf{B}}\langle \ln(x_1 - \bar{z}_{\alpha 0})\rangle \bar{\mathbf{q}}^*\}, \tag{2.88}$$

and

$$\langle \ln(x_1 - \bar{z}_{\alpha 0})\rangle = \sum_{\beta=1}^{4} \ln(x_1 - \bar{z}_{\beta 0})\mathbf{I}_\beta, \tag{2.89}$$

where

$$\mathbf{I}_i = \langle \delta_{i\alpha} \rangle = \mathrm{diag}[\delta_{i1}, \delta_{i2}, \delta_{i3}, \delta_{i4}] \tag{2.90}$$

Equation (2.87) now yields

$$\mathbf{q}_\beta = \mathbf{B}^{-1}\bar{\mathbf{B}}\mathbf{I}_\beta \bar{\mathbf{q}}^* = \mathbf{B}^{-1}\bar{\mathbf{B}}\mathbf{I}_\beta(\bar{\mathbf{A}}^T\mathbf{q}_0 + \bar{\mathbf{B}}^T\mathbf{b}) \tag{2.91}$$

If the boundary $x_2 = 0$ is a rigid surface, then

$$\mathbf{U} = 0, \quad \text{at } x_2 = 0 \tag{2.92}$$

The same procedure shows that the solution is given by Eqs (2.84) and (2.85) with

$$\mathbf{q}_\beta = \mathbf{A}^{-1}\bar{\mathbf{A}}\mathbf{I}_\beta(\bar{\mathbf{A}}^T\mathbf{q}_0 + \bar{\mathbf{B}}^T\mathbf{b}) \tag{2.93}$$

2.6 Solution of bimaterial problems

We now consider a bimaterial piezoelectric plate subjected to a line force-charge $\mathbf{q}_0$ and a line dislocation **b**, both located in the upper half-plane at $z_0(x_{10}, x_{20})$, for which the upper half-plane $(x_2 > 0)$ is occupied by material 1, and the lower half-plane $(x_2 < 0)$ is occupied by material 2 (see Fig. 2.5). They are rigidly bonded together so that

$$\mathbf{U}^{(1)} = \mathbf{U}^{(2)}, \quad \boldsymbol{\varphi}^{(1)} = \boldsymbol{\varphi}^{(2)}, \quad \text{at } x_2 = 0 \tag{2.94}$$

where the superscripts (1) and (2) label the quantities relating to materials 1 and 2. The equality of traction-charge continuity comes from the relation $\partial\boldsymbol{\varphi}/\partial s = \boldsymbol{\Pi}_n$, where $\boldsymbol{\Pi}_n$ is the surface traction-charge vector on a curve boundary (the interface in the bimaterial problem). When points along the interface are considered, integration of $\boldsymbol{\Pi}_n^{(1)} = \boldsymbol{\Pi}_n^{(2)}$ provides $\boldsymbol{\varphi}^{(1)} = \boldsymbol{\varphi}^{(2)}$, since the integration constants which correspond to rigid body motion can be neglected.

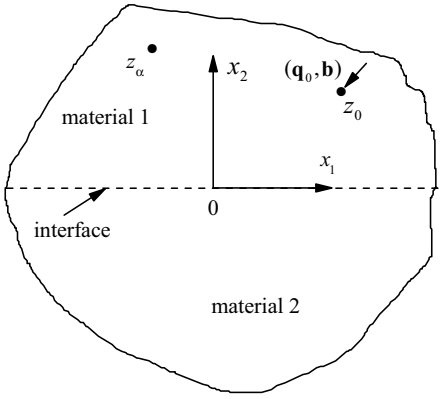

Fig. 2.5 Bimaterial plate subjected to $\mathbf{q}_0$ and $\mathbf{b}$

To satisfy the continuity condition (2.94) on the interface of the bimaterial plate, the Green's function solution may be assumed, in a similar way as treated in the half-plane problem, in the form [2,43]

$$\mathbf{U}^{(1)} = \frac{1}{\pi}\mathrm{Im}\{\mathbf{A}^{(1)}\left\langle \ln(z_\alpha^{(1)} - z_{\alpha 0}^{(1)})\right\rangle \mathbf{q}^{(1)*}\} + \sum_{\beta=1}^{4}\frac{1}{\pi}\mathrm{Im}\{\mathbf{A}^{(1)}\left\langle \ln(z_\alpha^{(1)} - \bar{z}_{\beta 0}^{(1)})\right\rangle \mathbf{q}_\beta^{(1)}\}, \tag{2.95}$$

$$\boldsymbol{\varphi}^{(1)} = \frac{1}{\pi}\mathrm{Im}\{\mathbf{B}^{(1)}\left\langle \ln(z_\alpha^{(1)} - z_{\alpha 0}^{(1)})\right\rangle \mathbf{q}^{(1)*}\} + \sum_{\beta=1}^{4}\frac{1}{\pi}\mathrm{Im}\{\mathbf{B}^{(1)}\left\langle \ln(z_\alpha^{(1)} - \bar{z}_{\beta 0}^{(1)})\right\rangle \mathbf{q}_\beta^{(1)}\} \tag{2.96}$$

for material 1 in $x_2>0$ and

$$\mathbf{U}^{(2)} = \sum_{\beta=1}^{4}\frac{1}{\pi}\mathrm{Im}\{\mathbf{A}^{(2)}\left\langle \ln(z_\alpha^{(2)} - z_{\beta 0}^{(1)})\right\rangle \mathbf{q}_\beta^{(2)}\}, \tag{2.97}$$

$$\varphi^{(2)} = \sum_{\beta=1}^{4}\frac{1}{\pi}\mathrm{Im}\{\mathbf{B}^{(2)}\left\langle \ln(z_\alpha^{(2)} - z_{\beta 0}^{(1)})\right\rangle \mathbf{q}_\beta^{(2)}\} \tag{2.98}$$

for material 2 in $x_2<0$, where $\mathbf{q}^{(1)*} = \mathbf{A}^{(1)T}\mathbf{q}_0 + \mathbf{B}^{(1)T}\mathbf{b}$, and $\mathbf{q}_\beta^{(1)}$, $\mathbf{q}_\beta^{(2)}$ are unknown constant vectors which are determined by substituting (2.95)-(2.98) into (2.94). Following the derivation in Section 2.5, we obtain

$$\mathbf{A}^{(1)}\mathbf{q}_\beta^{(1)} + \bar{\mathbf{A}}^{(2)}\bar{\mathbf{q}}_\beta^{(2)} = \bar{\mathbf{A}}^{(1)}\mathbf{I}_\beta\bar{\mathbf{q}}^{(1)*}, \qquad \mathbf{B}^{(1)}\mathbf{q}_\beta^{(1)} + \bar{\mathbf{B}}^{(2)}\bar{\mathbf{q}}_\beta^{(2)} = \bar{\mathbf{B}}^{(1)}\mathbf{I}_\beta\bar{\mathbf{q}}^{(1)*}. \tag{2.99}$$

Solving Eq (2.99) yields

$$\mathbf{q}_\beta^{(1)} = \mathbf{B}^{(1)-1}[\mathbf{I} - 2(\mathbf{M}^{(1)-1} + \bar{\mathbf{M}}^{(2)-1})^{-1}\mathbf{L}^{(1)-1}]\bar{\mathbf{B}}^{(1)}\mathbf{I}_\beta\bar{\mathbf{q}}^{(1)*}, \tag{2.100}$$

$$\mathbf{q}_\beta^{(2)} = 2\mathbf{B}^{(2)-1}(\bar{\mathbf{M}}^{(1)-1} + \mathbf{M}^{(2)-1})^{-1}\mathbf{L}^{(1)-1}\mathbf{B}^{(1)}\mathbf{I}_\beta\mathbf{q}^{(1)*}, \tag{2.101}$$

where $\mathbf{M}^{(j)} = -i\mathbf{B}^{(j)}\mathbf{A}^{(j)-1}$ is the surface impedance matrix.

2.7 Bimaterial solid with an interface crack

In the previous section we presented the Green's function for a bimaterial solid without cracks. This section discusses the Green's function for a bimaterial system with an interface crack subjected to a line force-charge $\mathbf{q}_0$ and a generalized line

dislocation **b**. Material combinations of the bimaterial system here may be piezoelectric-piezoelectric (PP), piezoelectric-anisotropic conductor (PAC), piezoelectric-isotropic dielectric (PID), or piezoelectric-isotropic conductor (PIC). The focus is on the fundamental solution of a bimaterial solid with an interface crack subjected to loadings $\mathbf{q}_0$ and **b** [2].

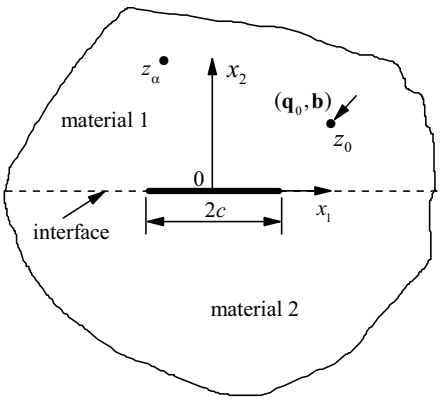

Fig. 2.6 Geometry of the interface crack system

The geometrical configuration analysed is depicted in Fig. 2.6. A crack of length $2c$ is shown lying along the interface between two dissimilar materials, subjected to loadings $\mathbf{q}_0$ and **b** at z_0 in material 1. In the following, Green's functions satisfying the traction-charge free conditions on the faces of the interface crack are derived by way of the Stroh formalism and the solution for bimaterials due to loadings $\mathbf{q}_0$ and **b**. It is clear from Eq (1.128) that the Green's function of **U** for the cracked medium subject to a line force-charge $\mathbf{q}_0$ and a generalized line dislocation **b** can be determined if the solution of **f**(z) in Eq (1.128) is known. Therefore our focus here is to determine the function **f**(z).

(a) *Green's function in a cracked homogeneous material (HM)*
Consider the problem of a two-dimensional infinite piezoelectric medium (see Fig. 2.6, in which material 1 is the same as material 2 in this case). If the generalized loadings $\mathbf{q}_0$ and **b** are located at $z_0(x_{10}, x_{20})$, the electroelastic solution **f**(z) in Eq (1.128) is [2]

$$\mathbf{f}_0(\mathbf{z}) = \langle f_0(z_\alpha) \rangle = \frac{\mathbf{q}^*}{2\pi i} \langle \ln(z_\alpha - z_{\alpha 0}) \rangle \tag{2.102}$$

where $\mathbf{q}^*$ is defined in Eq (2.86). The expression for $\mathbf{f}_0(z)$ is obtained by imposing $\mathbf{q}_0$ net traction-charge in a circuit around the source point z_0, and by demanding that the jumps in **U** be given by $\mathbf{b} = \{\Delta u_1 \ \Delta u_2 \ \Delta u_3 \ \Delta\varphi\}^T$, where Δu is the jump for the quantity u across the dislocation line, and the generalized line force $\mathbf{q}_0 = \{q_{01} \ q_{02} \ q_{03} \ q_{04}\}^T$, in which q_{0i} $(i \le 3)$ represents components of a line

-distributed force vector and q_{04} stands for a line electric charge. In the presence of an interface crack, however, the solution for a line force-charge $\mathbf{q}_0$ and a generalized line dislocation **b** is no longer given by $\mathbf{f}_0(z)$ alone. In addition to the conditions imposed at z_0, the boundary conditions for the interface crack must be satisfied. This can be accomplished by evaluating the traction-charge on the crack faces due to the generalized loadings and introducing an appropriate function $\mathbf{f}_I(z)$ to cancel the traction-charge on the crack faces. Substituting for $\mathbf{f}_0(z)$ from Eq (2.102) into Eq (1.129), and then into Eq (1.120), the traction-charge on the crack surface induced by $\mathbf{q}_0$ and **b** alone at z_0 is of the form

$$\mathbf{t}(x)=\mathbf{B}\mathbf{f}_0'(x)+\overline{\mathbf{B}}\overline{\mathbf{f}_0'(x)}=\frac{1}{2\pi i}\mathbf{B}\left\langle\frac{1}{x-z_{0\alpha}}\right\rangle\mathbf{q}^*-\frac{1}{2\pi i}\overline{\mathbf{B}}\left\langle\frac{1}{x-\overline{z}_{0\alpha}}\right\rangle\overline{\mathbf{q}}^* \tag{2.103}$$

The prescribed traction-charge, -$\mathbf{t}(x_1)$ acting on the crack faces, leads to the following Hilbert problem [44]:

$$\mathbf{B}\mathbf{f}_I'(z)=-\frac{\chi(z)}{2\pi i}\int_{-c}^{c}\frac{\mathbf{t}(x)dx}{\chi^+(x)(x-z)}+\mathbf{c}\chi(z) \tag{2.104}$$

where $\chi(z)$ is the basic Plemelj function defined as

$$\chi(z)=(z^2-c^2)^{-1/2} \tag{2.105}$$

Using contour integration one is finally led to

$$\mathbf{f}_I'(z)=-\frac{1}{2\pi i}\mathbf{F}_*(z,z_0)\mathbf{q}^*+\frac{1}{2\pi i}\mathbf{B}^{-1}\overline{\mathbf{B}}\mathbf{F}_*(z,\overline{z}_0)\overline{\mathbf{q}}^*,\quad \mathbf{c}=\frac{\mathbf{B}\mathbf{q}^*}{2\pi i} \tag{2.106}$$

where

$$\mathbf{F}_*(z,z_0)=\frac{1}{2}\left\langle\frac{1}{z_\alpha-z_{0\alpha}}\left[1-\frac{\chi(z_\alpha)}{\chi(z_{0\alpha})}\right]\right\rangle \tag{2.107}$$

The functions defined in Eqs (2.102) and (2.106) together provide a Green's function for the crack problem:

$$\mathbf{f}'(z)=\mathbf{f}_0'(z)+\mathbf{f}_I'(z)=\frac{1}{2\pi i}\left\{\left[\left\langle\frac{1}{z_\alpha-z_{0\alpha}}\right\rangle-\mathbf{F}_*(z,z_0)\right]\mathbf{q}^*+\mathbf{B}^{-1}\overline{\mathbf{B}}\mathbf{F}_*(z,\overline{z}_0)\overline{\mathbf{q}}^*\right\} \tag{2.108}$$

It is obvious that the singularity is contained in $\mathbf{f}_0(z)$ and the crack interactions are accounted for by $\mathbf{f}_I(z)$. The integration of Eq (2.108) with respect to z provides $\mathbf{f}(z)$, and then substituting the result of $\mathbf{f}(z)$ into Eqs (1.128) and (1.129), neglecting the integration constants which correspond to rigid body motion, yields the Green's functions for **U** and $\boldsymbol{\varphi}$.

(b) *Green's function in a PP bimaterial*

The solutions due to loadings $\mathbf{q}_0$ and **b** for this bimaterial group (in this case, materials 1 and 2 are both piezoelectric, but the material constants are different) were provided in the previous section (Section 2.6). Using those solutions, the functions

$\mathbf{f}_0(z^{(i)})$ are given by

$$\mathbf{f}_0^{(1)}(z^{(1)}) = \frac{1}{2\pi i}\left\{\left\langle \ln(z_*^{(1)} - z_{0*}^{(1)})\right\rangle \mathbf{q}^{(1)*} + \sum_{k=1}^{4}\left\langle \ln(z_*^{(1)} - \overline{z}_{0k}^{(1)})\right\rangle \mathbf{B}_k^* \overline{\mathbf{q}}^{(1)*}\right\}, \tag{2.109}$$

for material 1 (x_2>0), and

$$\mathbf{f}_0^{(2)}(z^{(2)}) = \frac{1}{2\pi i}\sum_{k=1}^{4}\left\langle \ln(z_\alpha^{(2)} - z_{0k}^{(1)})\right\rangle \mathbf{B}_k^{**} \mathbf{q}^{(1)*}, \tag{2.110}$$

for material 2 (x_2<0), where $\mathbf{q}^{(1)*}$ is the same as in Eq (2.95) and

$$\mathbf{B}_k^* = \mathbf{B}^{(1)-1}[\mathbf{I} - 2(\mathbf{M}^{(1)-1} + \overline{\mathbf{M}}^{(2)-1})^{-1}\mathbf{L}^{(1)-1}]\overline{\mathbf{B}}^{(1)}\mathbf{I}_k, \tag{2.111}$$

$$\mathbf{B}_k^{**} = \mathbf{B}^{(2)-1}(\overline{\mathbf{M}}^{(1)-1} + \mathbf{M}^{(2)-1})^{-1}\mathbf{L}^{(1)-1}\mathbf{B}^{(1)}\mathbf{I}_k. \tag{2.112}$$

The interface traction-charge induced by the generalized loading $\mathbf{q}^{(1)*}$ is then of the form

$$\mathbf{t}(x) = \mathbf{B}^{(2)}\mathbf{f}_0'^{(2)}(x) + \overline{\mathbf{B}}^{(2)}\overline{\mathbf{f}}_0'^{(2)}(x) = \mathbf{F}_{**}(x)\mathbf{q}^{(1)*} + \overline{\mathbf{F}}_{**}(x)\overline{\mathbf{q}}^{(1)*} \tag{2.113}$$

where

$$\mathbf{F}_{**}(x) = \frac{1}{2\pi i}\sum_{k=1}^{4}\frac{\mathbf{B}^{(2)}\mathbf{B}_k^{**}}{x - z_{0k}^{(1)}} \tag{2.114}$$

This traction-charge vector, $\mathbf{t}(x)$, can be removed by superposing a solution with the traction-charge, $-\mathbf{t}(x)$, induced by the potential $\mathbf{f}_I(z)$. The solution for $\mathbf{f}_I(z)$ can be obtained by setting

$$\mathbf{h}(z) = \begin{cases} \mathbf{B}^{(1)}\mathbf{f}_I'^{(1)}(z), & \text{in material 1,} \\ \mathbf{H}^{-1}\overline{\mathbf{H}}\mathbf{B}^{(2)}\mathbf{f}_I'^{(2)}(z), & \text{in material 2,} \end{cases} \tag{2.115}$$

where $\mathbf{H} = -\mathbf{M}^{(1)} - \overline{\mathbf{M}}^{(2)}$.

The function $\mathbf{h}(z)$ defined above, together with prescribed traction-charge, $-\mathbf{t}(x)$, on the crack faces, yields the following non-homogeneous Hilbert problem:

$$\mathbf{h}^+(x) + \overline{\mathbf{H}}^{-1}\mathbf{H}\mathbf{h}^-(x) = -\mathbf{t}(x) \tag{2.116}$$

Writing the quantities $\mathbf{h}(x)$ and $\mathbf{t}(x)$ in their components in the sense of the eigenvectors $\mathbf{w}$, $\mathbf{w}_3$ and $\mathbf{w}_4$ as [45]:

$$\begin{aligned} \mathbf{h}(x) &= h_1(x)\mathbf{w} + h_2(x)\overline{\mathbf{w}} + h_3(x)\mathbf{w}_3 + h_4(x)\mathbf{w}_4, \\ \mathbf{t}(x) &= t(x)\mathbf{w} + \overline{t}(x)\overline{\mathbf{w}} + t_3(x)\mathbf{w}_3 + t_4(x)\mathbf{w}_4, \end{aligned} \tag{2.117}$$

we obtain

$$
\begin{aligned}
h_1(z) &= -\frac{\chi(z)}{2\pi i}\int_{-c}^{c}\frac{t(x)dx}{\chi^+(x)(x-z)} + c_1\chi(z),\\
h_2(z) &= -\frac{\overline{\chi}(z)}{2\pi i}\int_{-c}^{c}\frac{\overline{t}(x)dx}{\overline{\chi}^+(x)(x-z)} + c_2\chi(z),\\
h_3(z) &= -\frac{\chi_3(z)}{2\pi i}\int_{-c}^{c}\frac{t_3(x)dx}{\chi_3^+(x)(x-z)} + c_3\chi(z),\\
h_4(z) &= -\frac{\chi_4(z)}{2\pi i}\int_{-c}^{c}\frac{t_4(x)dx}{\chi_4^+(x)(x-z)} + c_4\chi(z)
\end{aligned}
\tag{2.118}
$$

where $\mathbf{w}$, $\mathbf{w}_3$ and $\mathbf{w}_4$ are eigenvectors and have been defined in [2], and

$$
\begin{aligned}
\chi(z) &= (z+c)^{-1/2-i\varepsilon}(z-c)^{-1/2+i\varepsilon},\\
\chi_3(z) &= (z+c)^{-1/2-\kappa}(z-c)^{-1/2+\kappa},\\
\chi_4(z) &= (z+c)^{-1/2+\kappa}(z-c)^{-1/2-\kappa}
\end{aligned}
\tag{2.119}
$$

The functions h_i and t_i are evaluated by taking inner products with $\mathbf{w}$, $\mathbf{w}_3$ and $\mathbf{w}_4$, respectively, i.e.

$$
\begin{aligned}
&h_1(x) = \frac{\overline{\mathbf{w}}^T\mathbf{H}\mathbf{h}(x)}{\overline{\mathbf{w}}^T\mathbf{H}\mathbf{w}},\ h_2(x) = \frac{\mathbf{w}^T\mathbf{H}\mathbf{h}(x)}{\mathbf{w}^T\mathbf{H}\overline{\mathbf{w}}},\ h_3(x) = \frac{\mathbf{w}_4^T\mathbf{H}\mathbf{h}(x)}{\mathbf{w}_4^T\mathbf{H}\mathbf{w}_3},\\
&h_4(x) = \frac{\mathbf{w}_3^T\mathbf{H}\mathbf{h}(x)}{\mathbf{w}_3^T\mathbf{H}\mathbf{w}_4},\quad t = \frac{\overline{\mathbf{w}}^T\mathbf{H}\mathbf{t}(x)}{\overline{\mathbf{w}}^T\mathbf{H}\mathbf{w}},\quad t_3 = \frac{\mathbf{w}_4^T\mathbf{H}\mathbf{t}(x)}{\mathbf{w}_4^T\mathbf{H}\mathbf{w}_3},\ t_4 = \frac{\mathbf{w}_3^T\mathbf{H}\mathbf{t}(x)}{\mathbf{w}_3^T\mathbf{H}\mathbf{w}_4}
\end{aligned}
\tag{2.120}
$$

The contour integration of Eq (2.118) provides

$$
h_1(z) = \frac{\overline{\mathbf{w}}^T\mathbf{H}}{\overline{\mathbf{w}}^T\mathbf{H}\mathbf{w}}\sum_{k=1}^{4}[\mathbf{F}(\varepsilon,\chi,z,z_{0k}^{(1)},\mathbf{B}^{(2)},\mathbf{B}_k^{**}\mathbf{q}^{(1)*}) + \mathbf{F}(\varepsilon,\chi,z,\overline{z}_{0k}^{(1)},\overline{\mathbf{B}}^{(2)},\overline{\mathbf{B}}_k^{**}\overline{\mathbf{q}}^{(1)*})], \tag{2.121}
$$

$$
h_2(z) = \frac{\mathbf{w}^T\mathbf{H}}{\mathbf{w}^T\mathbf{H}\overline{\mathbf{w}}}\sum_{k=1}^{4}[\mathbf{F}(-\varepsilon,\overline{\chi},z,z_{0k}^{(1)},\mathbf{B}^{(2)},\mathbf{B}_k^{**}\mathbf{q}^{(1)*}) + \mathbf{F}(-\varepsilon,\overline{\chi},z,\overline{z}_{0k}^{(1)},\overline{\mathbf{B}}^{(2)},\overline{\mathbf{B}}_k^{**}\overline{\mathbf{q}}^{(1)*})], \tag{2.122}
$$

$$
h_3(z) = \frac{\mathbf{w}_4^T\mathbf{H}}{\mathbf{w}_4^T\mathbf{H}\mathbf{w}_3}\sum_{k=1}^{4}[\mathbf{F}(-i\kappa,\chi_3,z,z_{0k}^{(1)},\mathbf{B}^{(2)},\mathbf{B}_k^{**}\mathbf{q}^{(1)*}) + \mathbf{F}(-i\kappa,\chi_3,z,\overline{z}_{0k}^{(1)},\overline{\mathbf{B}}^{(2)},\overline{\mathbf{B}}_k^{**}\overline{\mathbf{q}}^{(1)*})], \tag{2.123}
$$

$$
h_4(z) = \frac{\mathbf{w}_3^T\mathbf{H}}{\mathbf{w}_3^T\mathbf{H}\mathbf{w}_4}\sum_{k=1}^{4}[\mathbf{F}(i\kappa,\chi_4,z,z_{0k}^{(1)},\mathbf{B}^{(2)},\mathbf{B}_k^{**}\mathbf{q}^{(1)*}) + \mathbf{F}(i\kappa,\chi_4,z,\overline{z}_{0k}^{(1)},\overline{\mathbf{B}}^{(2)},\overline{\mathbf{B}}_k^{**}\overline{\mathbf{q}}^{(1)*})], \tag{2.124}
$$

$$
\begin{aligned}
c_1 &= -\frac{\overline{\mathbf{w}}^T\mathbf{H}}{\overline{\mathbf{w}}^T\mathbf{H}\mathbf{w}}\frac{\mathbf{X}_*}{1+e^{-2\pi\varepsilon}},\quad c_2 = -\frac{\mathbf{w}^T\mathbf{H}}{\mathbf{w}^T\mathbf{H}\overline{\mathbf{w}}}\frac{\mathbf{X}_*}{1+e^{2\pi\varepsilon}},\\
c_3 &= -\frac{\mathbf{w}_4^T\mathbf{H}}{\mathbf{w}_4^T\mathbf{H}\mathbf{w}_3}\frac{\mathbf{X}_*}{1+e^{2i\pi\kappa}},\quad c_4 = -\frac{\mathbf{w}_3^T\mathbf{H}}{\mathbf{w}_3^T\mathbf{H}\mathbf{w}_4}\frac{\mathbf{X}_*}{1+e^{-2i\pi\kappa}}
\end{aligned}
\tag{2.125}
$$

where

$$\mathbf{F}(r,\chi,z,z_{0k},\mathbf{X},\mathbf{Y}) = -\frac{\mathbf{XY}}{(1+e^{-2\pi r})}\left[1-\frac{\chi(z)}{\chi(z_{0k})}\right]\frac{1}{z-z_{0k}},$$
$$\mathbf{X}_* = \sum_{k=1}^{4}(\mathbf{B}^{(2)}\mathbf{B}_k^{**}\mathbf{q}^{(1)*} + \overline{\mathbf{B}}^{(2)}\overline{\mathbf{B}}_k^{**}\overline{\mathbf{q}}^{(1)*}). \tag{2.126}$$

Once $h_i(z)$ has been obtained, the functions $\mathbf{f}_I'^{(j)}(z)$ can be evaluated through use of Eqs (2.115) and (2.117).

(c) *Green's function in a PAC bimaterial*

In (b) the solutions for a PP bimaterial due to loadings $\mathbf{q}_0$ and $\mathbf{b}$ were presented. Here we extend these solutions to the case of a PAC bimaterial. When one of the two materials, say material 2, is an anisotropic conductor, the interface condition (2.94) should be changed to

$$\begin{Bmatrix} u_1 \\ u_2 \\ u_3 \\ \phi \end{Bmatrix}^{(1)} = \begin{Bmatrix} u_1 \\ u_2 \\ u_3 \\ 0 \end{Bmatrix}^{(2)}, \quad \begin{Bmatrix} \varphi_1 \\ \varphi_2 \\ \varphi_3 \\ \varphi_4 \end{Bmatrix}^{(1)} = \begin{Bmatrix} \varphi_1 \\ \varphi_2 \\ \varphi_3 \\ 0 \end{Bmatrix}^{(2)}. \tag{2.127}$$

Further inside the conductor, we have

$$D_i^{(2)} = E_i^{(2)} = 0. \tag{2.128}$$

The formulations presented in (b) are still available if the following modifications are made:

$$\mathbf{A}^{(2)} = \begin{bmatrix} \mathbf{A}_{(3\times3)} & 0 \\ 0 & 1 \end{bmatrix}, \quad \mathbf{B}^{(2)} = \begin{bmatrix} \mathbf{B}_{(3\times3)} & 0 \\ 0 & 1 \end{bmatrix}, \tag{2.129}$$

$$p_4^{(2)} = i, \quad \mathbf{q}_\beta^{(2)} = \{q_{\beta1}^{(2)} \; q_{\beta2}^{(2)} \; q_{\beta3}^{(2)} \; 0\}, \qquad (\beta=1,2,3,4) \tag{2.130}$$

where $\mathbf{A}_{(3\times3)}$ and $\mathbf{B}_{(3\times3)}$ are well-defined material matrices for anisotropic elastic materials (see [43], for example).

(d) *Green's function in a PID bimaterial*

In this subsection we consider a PID bimaterial for which the upper half-plane (x_2>0) is occupied by a piezoelectric material (material 1), and the lower half-plane (x_2<0) is occupied by an isotropic dielectric material (material 2). For simplicity a plane strain deformation only is considered here. Thus the related interface condition is reduced to

$$\begin{Bmatrix} u_1 \\ u_2 \\ \phi \end{Bmatrix}^{(1)} = \begin{Bmatrix} u_1 \\ u_2 \\ \phi \end{Bmatrix}^{(2)}, \quad \begin{Bmatrix} \varphi_1 \\ \varphi_2 \\ \varphi_3 \end{Bmatrix}^{(1)} = \begin{Bmatrix} \varphi_1 \\ \varphi_2 \\ \varphi_3 \end{Bmatrix}^{(2)}, \qquad \text{at } x_2=0 \tag{2.131}$$

(d1) *General solutions for isotropic dielectric material*

The general solutions for an isotropic dielectric material can be assumed in the form

$$u_i = 2\,\mathrm{Re}[v_i f(z)], \quad \varphi_i = 2\,\mathrm{Re}[h_i f(z)], \quad z = x_1 + p x_2 \tag{2.132}$$

where $\mathbf{v}(=\{v_i\})$ and $\mathbf{h}(=\{h_i\})$ are determined by

$$\begin{aligned} &[\mathbf{Q} + p(\mathbf{R} + \mathbf{R}^T) + p^2\mathbf{T}]\mathbf{v} = 0, \\ &\mathbf{h} = (\mathbf{R}^T + p\mathbf{T})\mathbf{v} \end{aligned} \tag{2.133}$$

For an isotropic dielectric material, the 3×3 matrices **Q**, **R** and **T** are in the form

$$\mathbf{Q} = \begin{bmatrix} \lambda + 2G & 0 & 0 \\ 0 & G & 0 \\ 0 & 0 & -\varepsilon_0 \end{bmatrix}, \quad \mathbf{R} = \begin{bmatrix} 0 & \lambda & 0 \\ G & 0 & 0 \\ 0 & 0 & 0 \end{bmatrix}, \quad \mathbf{T} = \begin{bmatrix} G & 0 & 0 \\ 0 & \lambda + 2G & 0 \\ 0 & 0 & -\varepsilon_0 \end{bmatrix} \tag{2.134}$$

where ε_0 is the dielectric constant of the isotropic dielectric material, and λ and G are the Lamé constants [46] defined by

$$\lambda = \frac{E\mu}{(1+\mu)(1-2\mu)}, \quad G = \frac{E}{2(1+\mu)} \tag{2.135}$$

Since $p=i$ is a double root, a second independent solution can be written as

$$u_i = 2\,\mathrm{Re}\left\{\frac{\partial}{\partial p}[v_i f(z)]\right\}, \quad \varphi_i = 2\,\mathrm{Re}\left\{\frac{\partial}{\partial p}[h_i f(z)]\right\}, \tag{2.136}$$

where

$$\mathbf{v} = \mathbf{v}_p = \frac{1}{2G}\{1\ i\ 0\}, \quad \mathbf{h} = \mathbf{h}_p = \{i\ 1\ 0\} \tag{2.137}$$

for plane elastic deformation, and

$$\mathbf{v} = \mathbf{v}_e = \frac{-1}{\varepsilon_0}\{0\ 0\ 1\}, \quad \mathbf{h} = \mathbf{h}_e = \{0\ 0\ i\} \tag{2.138}$$

for electric field. Following the method of Ting and Chou [46], the complete general solutions can be expressed as

$$\mathbf{U} = \mathbf{A}\mathbf{q} f(z) + \frac{z-\bar{z}}{2i}\mathbf{v}_p q_2 f'(z), \quad \boldsymbol{\varphi} = \mathbf{B}\mathbf{q} f(z) + \frac{z-\bar{z}}{2i}\mathbf{h}_p q_2 f'(z), \tag{2.139}$$

$$\mathbf{A} = \frac{1}{2G}\begin{bmatrix} 1 & (1-2k)i & 0 \\ i & -2k & 0 \\ 0 & 0 & -2G\varepsilon_0^{-1} \end{bmatrix}, \quad \mathbf{B} = \begin{bmatrix} i & 0 & 0 \\ -1 & -i & 0 \\ 0 & 0 & i \end{bmatrix} \tag{2.140}$$

where $\mathbf{q}=\{q_1\ q_2\ q_3\}^T$ are constants to be determined, and

$$k = \frac{\lambda + 2G}{\lambda + G} \tag{2.141}$$

(d2) *Green's function for homogeneous isotropic materials*
For simplicity and conciseness of the following discussion, we consider here a line dislocation **b**, rather than a generalized loading $\mathbf{q}^*$, applied to an infinite plate at the point $z_0(=x_{10}+ix_{20})$. The function $f(z)$ in Eq (2.139), in this case, can be assumed as

$$f(z)=\ln(z-z_0) \tag{2.142}$$

The condition

$$\int_C d\mathbf{U}=\mathbf{b}, \qquad \text{for any closed curve } C \text{ enclosing the point } z_0 \tag{2.143}$$

yields

$$\mathbf{q}=\mathbf{q}_0=\{q_{10}\ q_{20}\ q_{30}\}^T=\frac{1}{2\pi i}\mathbf{A}^*\mathbf{b}, \tag{2.144}$$

where

$$\mathbf{A}^*=\frac{1}{1-4k}\begin{bmatrix}-4kG & -(2-4k)iG & 0\\ -2iG & 2G & 0\\ 0 & 0 & -\varepsilon_0(1-4k)\end{bmatrix} \tag{2.145}$$

(d3) *Green's function for PID bimaterials*
(d3.1) z_0 *located in isotropic dielectric material (material 2).* Consider a PID bimaterial for which a line dislocation **b** is applied at $z_0(=x_{10}+ix_{20}, \quad x_{20}<0)$. The interface condition (2.94) suggests that the solution can be assumed in the form:

$$\mathbf{U}^{(1)}=\frac{1}{\pi}\mathrm{Im}[\mathbf{A}^{(1)}\langle\ln(z_\alpha-z_0)\rangle\mathbf{q}_1], \qquad \boldsymbol{\varphi}^{(1)}=\frac{1}{\pi}\mathrm{Im}[\mathbf{B}^{(1)}\langle\ln(z_\alpha-z_0)\rangle\mathbf{q}_1] \tag{2.146}$$

for material 1 in $x_2>0$ and

$$\begin{aligned}\mathbf{U}^{(2)}&=\frac{1}{\pi}\mathrm{Im}\left[\mathbf{A}^{(2)}\mathbf{A}^*\mathbf{b}\ln(z-z_0)+\frac{\pi(z-\bar{z})\mathbf{v}_p q_{20}}{(z-z_0)}+\mathbf{A}^{(2)}\mathbf{q}_2\ln(z-\bar{z}_0)\right],\\ \boldsymbol{\varphi}^{(2)}&=\frac{1}{\pi}\mathrm{Im}\left[\mathbf{B}_2\mathbf{A}^*\mathbf{b}\ln(z-z_0)+\frac{\pi(z-\bar{z})\mathbf{h}_p q_{20}}{(z-z_0)}+\mathbf{B}^{(2)}\mathbf{q}_2\ln(z-\bar{z}_0)\right]\end{aligned} \tag{2.147}$$

for material 2 in $x_2<0$, where $\mathbf{q}_1$ and $\mathbf{q}_2$ are unknowns to be determined. The substitution of Eqs (2.146) and (2.147) into Eq (2.94), yields

$$\bar{\mathbf{A}}^{(1)}\bar{\mathbf{q}}_1+\mathbf{A}^{(2)}\mathbf{q}_2=\bar{\mathbf{A}}^{(2)}\bar{\mathbf{A}}^*\mathbf{b}, \quad \bar{\mathbf{B}}^{(1)}\bar{\mathbf{q}}_1+\mathbf{B}^{(2)}\mathbf{q}_2=\bar{\mathbf{B}}^{(2)}\bar{\mathbf{A}}^*\mathbf{b} \tag{2.148}$$

Solving Eq (2.148), we have

$$\mathbf{q}_1=\mathbf{B}^a\mathbf{b}, \quad \mathbf{q}_2=\mathbf{B}^b\mathbf{b}, \tag{2.149}$$

where

$$\begin{aligned}\mathbf{B}^a &= (\overline{\mathbf{B}}^{(2)-1}\mathbf{B}^{(1)} - \overline{\mathbf{A}}^{(2)-1}\mathbf{A}^{(1)})^{-1}(\overline{\mathbf{B}}^{(2)-1}\mathbf{B}^{(2)} - \overline{\mathbf{A}}^{(2)-1}\mathbf{A}^{(2)})\mathbf{A}^*,\\ \mathbf{B}^b &= (\overline{\mathbf{B}}^{(1)-1}\mathbf{B}^{(2)} - \overline{\mathbf{A}}^{(1)-1}\mathbf{A}^{(2)})^{-1}(\overline{\mathbf{B}}^{(1)-1}\overline{\mathbf{B}}^{(2)} - \overline{\mathbf{A}}^{(1)-1}\overline{\mathbf{A}}^{(2)})\overline{\mathbf{A}}^*\end{aligned} \tag{2.150}$$

(d3.2) z_0 *located in piezoelectric material* (*material 1*). When the single dislocation **b** is applied at z_0 with $x_{20} > 0$, the electroelastic solution can be assumed in the form

$$\mathbf{U}^{(1)} = \frac{1}{\pi}\mathrm{Im}[\mathbf{A}^{(1)}\langle \ln(z_\alpha - z_{0\alpha}\rangle \mathbf{B}^{(1)T}\mathbf{b}] + \frac{1}{\pi}\mathrm{Im}\sum_{\beta=1}^{3}[\mathbf{A}^{(1)}\langle \ln(z_\alpha - \overline{z}_{0\beta}\rangle \mathbf{q}_\beta^{(1)}], \tag{2.151}$$

$$\boldsymbol{\varphi}^{(1)} = \frac{1}{\pi}\mathrm{Im}[\mathbf{B}^{(1)}\langle \ln(z_\alpha - z_{0\alpha}\rangle \mathbf{B}^{(1)T}\mathbf{b}] + \frac{1}{\pi}\mathrm{Im}\sum_{\beta=1}^{3}[\mathbf{B}^{(1)}\langle \ln(z_\alpha - \overline{z}_{0\beta}\rangle \mathbf{q}_\beta^{(1)}] \tag{2.152}$$

for material 1 in x_2>0 and

$$\mathbf{U}^{(2)} = \frac{1}{\pi}\mathrm{Im}\sum_{\beta=1}^{3}[\mathbf{A}^{(2)}\langle \ln(z - z_{0\beta}\rangle \mathbf{q}_\beta^{(2)}] \tag{2.153}$$

$$\boldsymbol{\varphi}^{(2)} = \frac{1}{\pi}\mathrm{Im}\sum_{\beta=1}^{3}[\mathbf{B}^{(2)}\langle \ln(z - z_{0\beta}\rangle \mathbf{q}_\beta^{(2)}] \tag{2.154}$$

for material 2 in x_2<0. Substituting Eqs (2.151)-(2.154) into Eq (2.94), we find the solution has the same form as that given in (b) except that all matrices here are 3×3 matrices.

The interface traction-charge vector induced by the dislocation **b** is, then, of the form

$$\mathbf{t}(x) = \boldsymbol{\varphi}_{,1}^{(1)} = 2\,\mathrm{Re}[\mathbf{B}^{(1)}\mathbf{f}_0'^{(1)}] = \frac{1}{\pi}\mathrm{Im}\left[\frac{1}{x - z_0}\mathbf{B}^{(1)}\mathbf{B}^a\mathbf{b}\right] \tag{2.155}$$

for z_0 in material 2 and

$$\mathbf{t}(x) = \boldsymbol{\varphi}_{,1}^{(2)} = 2\,\mathrm{Re}[\mathbf{B}^{(2)}\mathbf{f}_0'^{(2)}] = \frac{1}{\pi}\mathrm{Im}\left[\sum_{\beta=1}^{3}\mathbf{B}^{(2)}\left\langle\frac{1}{x - z_{0\beta}}\right\rangle\mathbf{q}_\beta^{(2)}\right] = [\mathbf{F}_{**}(x) + \overline{\mathbf{F}}_{**}(x)]\mathbf{b} \tag{2.156}$$

for z_0 in material 1.

Similar to the treatment in (b), the traction-charge $\mathbf{t}(x)$ given in Eq (2.155) [or Eq (2.156)] can be removed by superposing a solution with the traction-charge, $-\mathbf{t}(x)$, induced by the potential $\mathbf{f}_I(z)$. The solution for $\mathbf{f}_I(z)$ can also be obtained by setting

$$\mathbf{h}(z) = \begin{cases}\mathbf{B}^{(1)}\mathbf{f}_I'^{(1)}(z), & \text{in material 1,}\\ \mathbf{H}^{-1}\overline{\mathbf{H}}\mathbf{B}^{(2)}\mathbf{f}_I'^{(2)}(z), & \text{in material 2}\end{cases} \tag{2.157}$$

The subsequent derivation is the same as that in (b) except that

$$\chi(z) = (z+c)^{-1/2-i\varepsilon}(z-c)^{-1/2+i\varepsilon},$$
$$\chi_3(z) = (z+c)^{-1/2}(z-c)^{-1/2} \tag{2.158}$$

where ε is determined in a similar manner to that of Suo et al [45].

(e) *Green's function in a PIC bimaterial*
As treated in (c), the solutions for a PIC bimaterial due to a single dislocation can be obtained based on the results given in (d). When one of the two materials, say material 2, is an isotropic conductor, the interface condition (2.94) should be changed to

$$\begin{Bmatrix} u_1 \\ u_2 \\ \varphi \end{Bmatrix}^{(1)} = \begin{Bmatrix} u_1 \\ u_2 \\ 0 \end{Bmatrix}^{(2)}, \quad \begin{Bmatrix} \phi_1 \\ \phi_2 \\ \phi_3 \end{Bmatrix}^{(1)} = \begin{Bmatrix} \phi_1 \\ \phi_2 \\ 0 \end{Bmatrix}^{(2)}, \qquad \text{at } x_2=0. \tag{2.159}$$

The formulations presented in subsection (d) are still available if the following modification is made:

$$\mathbf{q}_2 = \{q_{21}\ q_{22}\ 0\} \tag{2.160}$$

2.8 Elliptic hole and inclusion
The problem of determining Green's functions in a piezoelectric plate with an elliptic hole has been studied by Gao and Fan [14] and Lu et al [29] for a permeable elliptic hole, Liu et al [27] and Lu and Williams [28] for an impermeable elliptic hole or a crack, and Cheung and Ting [47] for an inclusion or elliptic hole in an infinite piezoelectric plate. More recently, Zhou et al [48] presented Green's function for elliptic hole and small crack problems. Here we follow the results given in [28,48].

2.8.1 Mapping of an ellipse to a unit circle
When the boundary of a linear piezoelectric plate has the shape of an ellipse, it is convenient to transform the ellipse to a unit circle before solving the problem. Let us consider an infinite two-dimensional piezoelectric material containing an elliptic hole, where the material is transversely isotropic and coupling between in-plane stress and in-plane electric fields takes place. The geometric equation of an ellipse Γ (see Fig. 2.7) can be expressed as

$$x_1 = a\cos\theta, \quad x_2 = b\sin\theta, \quad \rho(\theta) = (a^2\cos^2\theta + b^2\sin^2\theta)^{1/2},$$
$$\mathbf{n} = \left\{\frac{dx_1}{ds}, \frac{dx_2}{ds}, 0\right\}^T, \quad \mathbf{m} = \left\{-\frac{dx_2}{ds}, \frac{dx_1}{ds}, 0\right\}^T, \quad ds = \rho(\theta)d\theta \tag{2.161}$$

where θ is a real parameter and a, b are the half-length of the major and minor axes respectively of the ellipse (see Fig. 2.7), **m** and **n** are the unit vectors tangential and normal to the elliptic boundary respectively, and s is the infinitesimal arc length of the ellipse. To transform the ellipse to a unit circle, consider the mapping [49]

$$z_k = c_k\zeta_k + d_k\zeta_k^{-1} \tag{2.162}$$

where c_k and d_k are constants to be chosen such that the ellipse is mapped into a unit circle. Thus, when x_1 and x_2 are given by Eq (2.161), $\zeta_k = e^{i\theta}$. Hence

$$\begin{aligned} z_k = x_1 + p_k x_2 &= a\cos\theta + p_k b\sin\theta = c_k e^{i\theta} + d_k e^{-i\theta} \\ &= c_k(\cos\theta + i\sin\theta) + d_k(\cos\theta - i\sin\theta) \end{aligned} \tag{2.163}$$

from which we obtain

$$c_k = \frac{1}{2}(a - ip_k b), \quad d_k = \frac{1}{2}(a + ip_k b) \tag{2.164}$$

One of the two solutions for ζ in Eq (2.162) is

$$\zeta_{k1} = \frac{z_k + (z_k^2 - 4c_k d_k)^{1/2}}{2c_k} \tag{2.165}$$

This solution has the property that $|\zeta_{k1}| \to \infty$ as $|z_k| \to \infty$. The other solution is given by

$$\zeta_{k2} = \frac{z_k - (z_k^2 - 4c_k d_k)^{1/2}}{2c_k} \tag{2.166}$$

This solution has the property that $|\zeta_{k2}| \to 0$ as $|z_k| \to \infty$ [49].

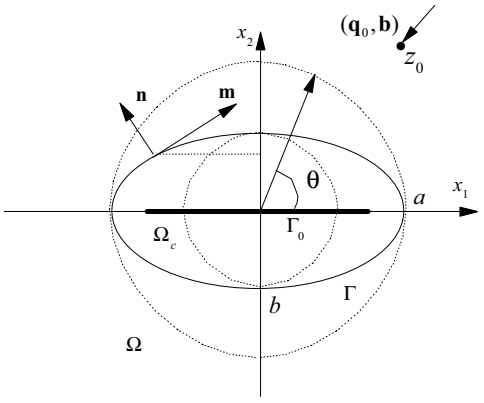

Fig. 2.7 Geometry of the elliptic hole problem

The mapping (2.162) is one-to-one mapping for points outside the ellipse in the (x_1,x_2)-plane to points outside the circle in the ζ_k-plane if the roots of

$$dz_k / d\zeta_k = c_k - d_k \zeta_k^{-2} = 0 \tag{2.167}$$

are located inside the unit circle, i.e. $|\zeta_k| < 1$. Let the roots be $\pm\breve{\zeta}_k$, where

$$\breve{\zeta}_k = \sqrt{\frac{d_k}{c_k}} \tag{2.168}$$

The inequality $\left|\breve{\zeta}_k\right| = \left|(d_k / c_k)^{1/2}\right| < 1$ can be proved by considering $p_k = \alpha + i\beta$, where α and β are real. It is evident that

$$\zeta_k \overline{\zeta}_k = \frac{d_k \overline{d}_k}{c_k \overline{c}_k} = \frac{(a - b\beta)^2 + (b\alpha)^2}{(a + b\beta)^2 + (b\alpha)^2} < 1 \tag{2.169}$$

Therefore $\pm\breve{\zeta}_k$ are inside the unit circle, which ensures that the mapping is one-to-one mapping. However, the mapping in not conformal [49]. The angle between any two line elements in the (x_1,x_2)-plane is in general different from the angle between the corresponding elements in the ζ_k-plane.

2.8.2 Green's functions for a piezoelectric plate with an elliptic hole

Consider an infinite piezoelectric plate with an elliptic hole subjected to a generalized line dislocation **b** and a generalized line force $\mathbf{q}_0$ at a point $z_0(x_{10},x_{20})$ outside the ellipse (see Fig. 2.7). The hole is assumed to be filled with a homogeneous gas of dielectric constant κ_0, and is free of mechanical traction. On the hole boundary the normal component of electric displacement and the electric potential are continuous. We therefore have boundary conditions on the contour Γ:

$$\sigma_{nn} = \sigma_{nm} = \sigma_{n3} = 0, \quad D_n = -\kappa_0 \frac{\partial \phi^c}{\partial m} = D_n^c, \quad \phi = \phi^c \tag{2.170}$$

where n and m respectively represent the normal and tangent to the hole boundary (Fig. 2.7). σ_{nn} and σ_{nm} are the normal and shear stresses along the hole boundary, D_n is the normal component of electric displacement vector, superscript c indicates the quantity associated with the hole medium.

Similar to the treatment in Section 2.5 for half-plane problems, this problem can also be divided into two subproblems [48]: (i) a homogeneous infinite piezoelectric medium is subjected to the generalized line dislocation **b** and the traction-charge $\mathbf{q}_0$ both at the point $z_0(x_{10},x_{20})$; and (ii) the boundary of the elliptic hole is subjected to loadings which make the hole boundary traction free and normal electric displacement and electric potential to be continuous across rim of the hole.

For the case in which the generalized line dislocation **b** and the traction-charge $\mathbf{q}_0$ are applied at a point $z_0(x_{10},x_{20})$ in a homogeneous infinite piezoelectric medium, the equilibrium conditions of the force and the single-valued conditions of the generalized displacement are still defined by Eq (2.77). In order to satisfy the jump conditions defined by Eq (2.77), the arbitrary function in Eqs (1.128) and (1.129) is chosen to be

$$f(z_\alpha) = \ln(\zeta_\alpha - \zeta_{\alpha 0}) \tag{2.171}$$

where ζ_α and z_α are related by Eq (2.162) and

$$\zeta_{\alpha 0} = \frac{z_{\alpha 0} + (z_{\alpha 0}^2 - 4c_k d_k)^{1/2}}{2c_k}, \quad z_{\alpha 0} = x_{10} + p_\alpha x_{20} \tag{2.172}$$

Substituting Eq (2.171) into Eqs (1.128) and (1.129), and later into Eq (2.77), we obtain the first basic solution [47]

$$\mathbf{U}^I = 2\,\mathrm{Re}\{\mathbf{A}\langle \ln(z_\alpha - z_{\alpha 0})\rangle \mathbf{q}_f\}, \qquad \boldsymbol{\varphi}^I = 2\,\mathrm{Re}\{\mathbf{B}\langle \ln(z_\alpha - z_{\alpha 0})\rangle \mathbf{q}_f\} \tag{2.173}$$

where $\mathbf{q}_f$ is given in Eq (2.80).

The Green's function can be easily obtained if the surface traction and the normal component of the electric displacement vanish on the hole boundary. This means that $\boldsymbol{\varphi} = 0$ on the hole boundary. The general Green's function solution in this case can be assumed in the form [50]

$$\mathbf{U} = \mathbf{U}^I + \mathbf{U}^{II} = \frac{1}{\pi}\mathrm{Im}\{\mathbf{A}\langle \ln(\zeta_\alpha - \zeta_{\alpha 0})\rangle \mathbf{q}^*\} + \sum_{\beta=1}^{4}\frac{1}{\pi}\mathrm{Im}\{\mathbf{A}\langle \ln(\zeta_\alpha^{-1} - \overline{\zeta}_{\beta 0})\rangle \mathbf{q}_\beta\}, \quad (2.174)$$

$$\boldsymbol{\varphi} = \boldsymbol{\varphi}^I + \boldsymbol{\varphi}^{II} = \frac{1}{\pi}\mathrm{Im}\{\mathbf{B}\langle \ln(\zeta_\alpha - \zeta_{\alpha 0})\rangle \mathbf{q}^*\} + \sum_{\beta=1}^{4}\frac{1}{\pi}\mathrm{Im}\{\mathbf{B}\langle \ln(\zeta_\alpha^{-1} - \overline{\zeta}_{\beta 0})\rangle \mathbf{q}_\beta\} \quad (2.175)$$

in which $\mathbf{q}^*$ is given in Eq (2.86). Making use of the condition $\boldsymbol{\varphi} = 0$ and the expression $\zeta_\alpha = e^{i\theta}$ on the hole boundary, we have

$$\mathrm{Im}\{\mathbf{B}\langle \ln(e^{i\theta} - \zeta_{\alpha 0})\mathbf{q}^*\rangle\} + \mathrm{Im}\left\{\sum_{\beta=1}^{4}\ln(e^{-i\theta} - \overline{\zeta}_{\beta 0})\mathbf{B}\mathbf{q}_\beta\right\} = 0 \quad (2.176)$$

The first term can be replaced by the negative of its complex conjugate, that is

$$\begin{aligned}\mathrm{Im}\{\mathbf{B}\langle \ln(e^{i\theta} - \zeta_{\alpha 0})\mathbf{q}^*\rangle\} &= -\mathrm{Im}\{\overline{\mathbf{B}}\langle \ln(e^{-i\theta} - \overline{\zeta}_{\alpha 0})\overline{\mathbf{q}}^*\rangle\} \\ &= -\mathrm{Im}\left\{\sum_{\beta=1}^{4}\ln(e^{-i\theta} - \overline{\zeta}_{\beta 0})\overline{\mathbf{B}}\mathbf{I}_\beta\overline{\mathbf{q}}^*\right\}\end{aligned} \quad (2.177)$$

Substituting Eq (2.177) into (2.176) yields

$$\mathbf{q}_\beta = \mathbf{B}^{-1}\overline{\mathbf{B}}\mathbf{I}_\beta\overline{\mathbf{q}}^* \quad (2.178)$$

If the ellipse is a rigid inclusion with vanishing elastic displacement and electric potential, we have **U**=0. A similar derivation gives [50]

$$\mathbf{q}_\beta = \mathbf{A}^{-1}\overline{\mathbf{A}}\mathbf{I}_\beta\overline{\mathbf{q}}^* \quad (2.179)$$

If the hole is assumed to be filled with a homogeneous gas of dielectric constant κ_0, the boundary condition on the hole boundary is defined by Eq (2.170). In this case, the induced electric potential ϕ^c inside the hole should be considered and can be expressed as [48]:

$$\phi^c(z) = 2\,\mathrm{Re}[f^c(z)], \quad E_i^c = -\phi^c_{,i}, \quad z = x_1 + ix_2 \quad (2.180)$$

The electric potential ϕ^c in the hole can be solved from the differential equation

$$\phi^c_{,ii} = 0 \quad (2.181)$$

To solve the problem above, consider the single-valued mapping function

$$z = c_0\zeta_0 + d_0\zeta_0^{-1}, \quad c_0 = \frac{a+b}{2}, \quad d_0 = \frac{a-b}{2} \quad (2.182)$$

The roots of $dz/d\zeta_0 = 0$ are $\zeta_{01,2} = \pm\sqrt{\dfrac{1-e}{1+e}}$, where $e=b/a$. Thus, mapping of the

region of the hole, denoted by Ω_c, can be achieved by excluding a straight line Γ_0 along x_1 and of length $2a\sqrt{1-e^2}$ from the ellipse (Fig. 2.7). In this case, the mapping function (2.182) will transform Γ and Γ_0 (Fig. 2.7) into the ring of outer and inner circles with radii $r_{out}=1$ and $r_{in}=\sqrt{\dfrac{1-e}{1+e}}$, respectively.

Considering the differential equation (2.181) and the mapping function (2.182), $f^c(z)$ in Eq (2.180), defined in the annular ring mentioned above, can be expressed by Laurent's expansion as [48]

$$f^c(\zeta_0)=\sum_{k=-\infty}^{\infty} a_{0k}\zeta_0^k \tag{2.183}$$

where a_{0k} is a complex constant to be determined. To ensure the function f^c is single-valued inside the hole and along the straight line Γ_0, the following condition must be satisfied [2]

$$f^c(r_{in}e^{i\theta})=f^c(r_{in}e^{-i\theta}) \tag{2.184}$$

from which the relations between a_{0k} and a_{-0k} in Eq (2.183) can be determined as $a_{-0k}=r_{in}^{2k}a_{0k}$. Therefore $f^c(z)$ can be further written as

$$f^c(\zeta_0)=\sum_{k=1}^{\infty} a_{0k}(\zeta_0^k+r_{in}^{2k}\zeta_0^{-k}) \tag{2.185}$$

Substituting (2.185) into Eq $(2.170)_2$ and noting that $\zeta_0=e^{i\theta}$ on the hole boundary, we have

$$D_n^c\big|_{\Gamma}=-\frac{2\kappa_0}{r_{in}}\sum_{k=1}^{\infty}\left\{[-k\left(1+r_{in}^{2k}\right)\operatorname{Im}a_{0k}]\sin(n\theta)+[k\left(1-r_{in}^{2k}\right)\operatorname{Re}a_{0k}]\cos(n\theta)\right\} \tag{2.186}$$

In order to provide analytical solutions outside the ellipse,

$$\begin{aligned}
\mathbf{f}^{II}(\mathbf{z})&=\sum_{k=1}^{\infty}\left\langle\zeta_\alpha^{-k}\right\rangle(\mathbf{A}^T\mathbf{g}_k+\mathbf{B}^T\mathbf{h}_k),\\
\mathbf{U}^{II}&=2\sum_{k=1}^{\infty}\operatorname{Re}\left[\mathbf{A}\left\langle\zeta_\alpha^{-k}\right\rangle(\mathbf{A}^T\mathbf{g}_k+\mathbf{B}^T\mathbf{h}_k)\right],\\
\boldsymbol{\varphi}^{II}&=2\sum_{k=1}^{\infty}\operatorname{Re}\left[\mathbf{B}\left\langle\zeta_\alpha^{-k}\right\rangle(\mathbf{A}^T\mathbf{g}_k+\mathbf{B}^T\mathbf{h}_k)\right]
\end{aligned} \tag{2.187}$$

are assumed for problem (ii) defined in the second paragraph after Eq (2.170), where $\mathbf{g}_k$ and $\mathbf{h}_k$ are real constants to be determined. Noting that $\zeta_\alpha=e^{i\theta}$ on the hole boundary, Eq (2.187) can be further written as

$$\begin{aligned}
\mathbf{U}^{II}\big|_{\Gamma}&=\sum_{k=1}^{\infty}[\cos(k\theta)\mathbf{h}_k-\sin(k\theta)\hat{\mathbf{h}}_k],\\
\boldsymbol{\varphi}^{II}\big|_{\Gamma}&=\sum_{k=1}^{\infty}[\cos(k\theta)\mathbf{g}_k-\sin(k\theta)\hat{\mathbf{g}}_k],\\
\boldsymbol{\Pi}_n^{II}\big|_{\Gamma}&=-\frac{1}{\rho(\theta)}\sum_{k=1}^{\infty}\{k[\sin(k\theta)\mathbf{g}_k+\cos(k\theta)\hat{\mathbf{g}}_k]\}
\end{aligned} \tag{2.188}$$

where

$$\hat{\mathbf{h}}_k = \mathbf{S}\mathbf{h}_k + \mathbf{H}\mathbf{g}_k, \quad \hat{\mathbf{g}}_k = \mathbf{S}^T\mathbf{g}_k - \mathbf{L}\mathbf{h}_k \tag{2.189}$$

where **S**, **H**, and **L** are defined in Eq (1.142).

In addition, in order to obtain $\mathbf{g}_k$ and $\mathbf{h}_k$ from the boundary condition (2.170), the solution $\mathbf{U}^I$ and $\boldsymbol{\varphi}^I$ should also be expressed in terms of $\sin(k\theta)$ and $\cos(k\theta)$. In doing so, Eq $(2.173)_2$ is rewritten as

$$\boldsymbol{\varphi}^I = \frac{1}{\pi}\mathrm{Im}\left\{\mathbf{B}\left\langle \ln(\zeta_\alpha - \zeta_{\alpha 0}) + \ln\left[c_\alpha\left(1 - \frac{d_\alpha / c_\alpha}{\zeta_\alpha \zeta_{\alpha 0}}\right)\right]\right\rangle \mathbf{q}^*\right\} \tag{2.190}$$

in which the relation

$$\ln(z_\alpha - z_{\alpha 0}) = \ln(\zeta_\alpha - \zeta_{\alpha 0}) + \ln\left[c_\alpha\left(1 - \frac{d_\alpha / c_\alpha}{\zeta_\alpha \zeta_{\alpha 0}}\right)\right] \tag{2.191}$$

has been used. Along the unit circle boundary, it follows that

$$\boldsymbol{\varphi}^I\big|_\Gamma = \frac{1}{\pi}\mathrm{Im}\left\{\mathbf{B}\left\langle \ln(e^{i\theta} - \zeta_{\alpha 0}) + \ln\left[c_\alpha\left(1 - \frac{d_\alpha / c_\alpha}{\zeta_{\alpha 0}} e^{-i\theta}\right)\right]\right\rangle \mathbf{q}^*\right\} \tag{2.192}$$

Making use of the series representation

$$\ln(1 - x) = -\sum_{k=1}^{\infty} \frac{1}{k} x^k, \tag{2.193}$$

Eq (2.192) can be further written as

$$\boldsymbol{\varphi}^I\big|_\Gamma = \frac{1}{\pi}\mathrm{Im}\left\{\mathbf{B}\left\langle \ln(-c_\alpha \zeta_{\alpha 0}) - \frac{1}{k}\sum_{k=1}^{\infty}\left[\left(\frac{e^{i\theta}}{\zeta_{\alpha 0}}\right)^k + \left(\frac{d_\alpha e^{-i\theta}}{c_\alpha \zeta_{\alpha 0}}\right)^k\right]\right\rangle \mathbf{q}^*\right\} \tag{2.194}$$

where $e^{ik\theta} = \cos(k\theta) + i\sin(k\theta)$. Therefore the traction-charge vector $\boldsymbol{\Pi}_n$ on the elliptic boundary Γ can obtained as

$$\boldsymbol{\Pi}_n^I\big|_\Gamma = (\boldsymbol{\varphi}_{,s}^I)\big|_\Gamma = \frac{1}{\pi\rho(\theta)}\mathrm{Im}\left\{i\mathbf{B}\left\langle \sum_{k=1}^{\infty}\left[\left(\frac{d_\alpha e^{-i\theta}}{c_\alpha \zeta_{\alpha 0}}\right)^k - \left(\frac{e^{i\theta}}{\zeta_{\alpha 0}}\right)^k\right]\right\rangle \mathbf{q}^*\right\} \tag{2.195}$$

To ensure that the Green's functions satisfy the traction-free and electric displacement conditions as well as electric potential continuous condition on the interface of the elliptic hole and its outer infinite piezoelectric solid of the original problem, a generalized surface traction $\mathbf{t}_n$ must be applied to the elliptic boundary in problem (ii), where

$$\mathbf{t}_n = -\boldsymbol{\Pi}_n^I\big|_\Gamma - \boldsymbol{\Pi}_n^{II}\big|_\Gamma + D_n^c\big|_\Gamma \mathbf{i}_4, \quad \mathbf{i}_4 = \{0,0,0,1\}^T \tag{2.196}$$

The substitution of Eqs (2.186), $(2.188)_3$, and (2.195) into Eq (2.196) provides [48]

$$\mathbf{g}_k = \mathbf{g}_k^{(1)} + \mathbf{g}_k^{(2)}, \quad \hat{\mathbf{g}}_k = \hat{\mathbf{g}}_k^{(1)} + \hat{\mathbf{g}}_k^{(2)},$$

$$\mathbf{g}_k^{(1)} = \frac{1}{k\pi}\mathrm{Im}\left[\mathbf{B}\left\langle\left(\frac{d_\alpha}{c_\alpha\zeta_{\alpha 0}}\right)^k + \left(\frac{1}{\zeta_{\alpha 0}}\right)^k\right\rangle\mathbf{q}^*\right],$$

$$\hat{\mathbf{g}}_k^{(1)} = \frac{1}{k\pi}\mathrm{Re}\left[\mathbf{B}\left\langle\left(\frac{d_\alpha}{c_\alpha\zeta_{\alpha 0}}\right)^k - \left(\frac{1}{\zeta_{\alpha 0}}\right)^k\right\rangle\mathbf{q}^*\right],$$

$$\mathbf{g}_k^{(2)} = -2\kappa_0(1+(d_0/c_0)^k\,\mathrm{Im}[a_{0k}]\mathbf{i}_4,$$

$$\hat{\mathbf{g}}_k^{(2)} = 2\kappa_0(1-(d_0/c_0)^k\,\mathrm{Re}[a_{0k}]\mathbf{i}_4, \tag{2.197}$$

in which a_{0k} in $(2.197)_{4,5}$ is still unknown, which can be determined by imposing the condition of electric potential continuity across the elliptic hole boundary. It should be mentioned that $\mathbf{g}_k$ and $\hat{\mathbf{g}}_k$ are divided into two parts: the first part is associated with the traction-free condition, and the second with the conditions of electric potential and electric displacement continuity across the elliptic hole boundary.

Making use of Eqs $(2.187)_3$, (2.190), and combining them with Eqs (2.191) and (2.197), we can finally obtain the generalized stress function outside the ellipse as

$$\begin{aligned}\boldsymbol{\varphi} = \frac{1}{\pi}\mathrm{Im}\{\mathbf{B}\langle\ln(\zeta_\alpha-\zeta_{\alpha 0})\rangle\mathbf{q}^*\} + \sum_{\beta=1}^{4}\frac{1}{\pi}\mathrm{Im}\{\mathbf{B}\langle\ln(\zeta_\alpha^{-1}-\overline{\zeta}_{\beta 0})\rangle\mathbf{B}^{-1}\overline{\mathbf{B}}\mathbf{I}_\beta\overline{\mathbf{q}}^*\} \\ + 2\kappa_0\sum_{k=1}^{\infty}\mathrm{Im}[\mathbf{B}\langle\zeta_\alpha^{-k}\rangle\mathbf{B}^{-1}\{\overline{a}_{0k}-(d_0/c_0)^k a_{0k}\}\mathbf{i}_4]\end{aligned} \tag{2.198}$$

in which following relations have been used:

$$\begin{aligned}&\sum_{k=1}^{\infty}\zeta_\alpha^{-k}\overline{\zeta}_{\beta 0}^{-k}/k = -\ln(1-\zeta_\alpha^{-1}\overline{\zeta}_{\beta 0}^{-1}), \quad \text{if } \left|\zeta_\alpha^{-1}\overline{\zeta}_{\beta 0}^{-1}\right|<1, \\ &2(\mathbf{A}^T+\mathbf{B}^T\mathbf{L}^{-1}\mathbf{S}^T) = \mathbf{B}^{-1}, \quad 2\mathbf{B}^T\mathbf{L}^{-1} = i\mathbf{B}\end{aligned} \tag{2.199}$$

The constants a_{0k} in Eq (2.198) can be determined in the following way. In order to use the condition of electric potential continuity $\phi = \phi^c$ across the elliptic hole boundary, ϕ^c in Eq (2.180) is rewritten in terms of θ as

$$\phi^c\big|_\Gamma = 2\,\mathrm{Re}[f^c(e^{i\theta})] = 2\,\mathrm{Re}\sum_{k=1}^{\infty}a_{0k}\left[\left\{1+\left(\frac{d_0}{c_0}\right)^k\right\}\cos(k\theta)+i\left\{1-\left(\frac{d_0}{c_0}\right)^k\right\}\sin(k\theta)\right] \tag{2.200}$$

Comparing Eqs $(2.173)_1$ and $(2.188)_1$ with Eq (2.200) and using the single-valued condition yields

$$(\mathbf{h}_k)_4 = 2(1+(d_0/c_0)^k)\,\mathrm{Re}[a_{0k}], \quad (\hat{\mathbf{h}}_k)_4 = 2(1-(d_0/c_0)^k)\,\mathrm{Im}[a_{0k}], \tag{2.201}$$

for $k \geq 1$.

Substituting Eqs (2.197) and (2.201) into Eq (2.189), we have

$$\begin{aligned} &2[(1+(d_0/c_0)^k)+\kappa_0(1-(d_0/c_0)^k)L_{44}^{-1}]\mathrm{Re}[a_{0k}] \\ &\qquad +2\kappa_0(1+(d_0/c_0)^k)L_{4i}^{-1}S_{i4}^T]\mathrm{Im}[a_{0k}]=C_{1k} \\ &2[(1-(d_0/c_0)^k)+\kappa_0(1+(d_0/c_0)^k)L_{44}^{-1}]\mathrm{Im}[a_{0k}] \\ &\qquad -2\kappa_0(1-(d_0/c_0)^k)L_{4i}^{-1}S_{i4}^T]\mathrm{Re}[a_{0k}]=C_{2k} \end{aligned} \tag{2.202}$$

in which C_{1k} and C_{2k} are real constants given by

$$C_{1k}=\frac{L_{4j}^{-1}}{k\pi}\left\{S_{ji}^T\,\mathrm{Im}\left[\mathbf{B}\left\langle\frac{1+(d_\alpha/c_\alpha)^k}{\zeta_{\alpha 0}^k}\right\rangle\mathbf{q}^*\right]+\mathrm{Re}\left[\mathbf{B}\left\langle\frac{1-(d_\alpha/c_\alpha)^k}{\zeta_{\alpha 0}^k}\right\rangle\mathbf{q}^*\right]\right\},$$

$$C_{2k}=\frac{L_{4j}^{-1}}{k\pi}\left\{\mathrm{Im}\left[\mathbf{B}\left\langle\frac{1+(d_\alpha/c_\alpha)^k}{\zeta_{\alpha 0}^k}\right\rangle\mathbf{q}^*\right]-S_{ji}^T\,\mathrm{Re}\left[\mathbf{B}\left\langle\frac{1-(d_\alpha/c_\alpha)^k}{\zeta_{\alpha 0}^k}\right\rangle\mathbf{q}^*\right]\right\} \tag{2.203}$$

Solving Eq (2.202) for a_{0k}, we have

$$a_{0k}=\alpha_k/\beta_k,\qquad C_k=C_{1k}+iC_{2k}$$

$$\alpha_k=\frac{1}{2}[\bar{C}_k(d_0/c_0)^k(1-\kappa_0L_{44}^{-1}+i\kappa_0L_{4j}^{-1}S_{j4}^T)-C_k(1+\kappa_0L_{44}^{-1}+i\kappa_0L_{4j}^{-1}S_{j4}^T)],$$

$$\beta_k=\{(1-(d_0/c_0)^{2k}[1-(\kappa_0L_{44}^{-1})^2-(\kappa_0L_{4j}^{-1}S_{j4}^T)^2]-2\kappa_0(1+(d_0/c_0)^{2k})L_{44}^{-1}\}, \tag{2.204}$$

where L_{ij} are components of matrix **L** defined in Eq (1.142).

2.8.3 Green's function of piezoelectric matrix with an inclusion

In Section 2.8.2, Green's function for a piezoelectric solid with an elliptic hole was presented. We now extend the results to the case of a piezoelectric solid with a piezoelectric inclusion. The discussion follows the results presented in [28].

When the hole considered in Section 2.8.2 becomes an inclusion, the condition (2.170) is replaced by

$$\mathbf{U}^M=\mathbf{U}^I,\quad \boldsymbol{\varphi}^M=\boldsymbol{\varphi}^I,\quad \text{on }\Gamma \tag{2.205}$$

provided that the matrix and the elliptic inclusion are bonded perfectly along the bonded interface, where the superscripts *M* and *I* label the quantities relating to the matrix and inclusion, respectively.

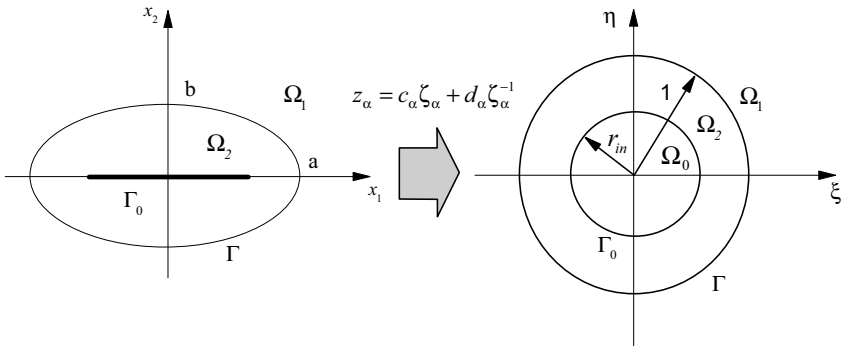

(a) z_α – plane (b) ζ–plane

Fig. 2.8 Geometry of elliptic inclusion problem

Let a generalized line dislocation **b** and a line force-charge $\mathbf{q}_0$ be applied at a point $z_0(x_{10},x_{20})$ in the region of matrix (in Ω_1), as shown in Fig. 2.8. The Green's functions for such a problem may be expressed in the following form [28]

$$\begin{aligned}\mathbf{U}^M &= 2\,\mathrm{Re}[\mathbf{A}^M\{\mathbf{f}_0(\boldsymbol{\zeta}^M)+\mathbf{f}_1(\boldsymbol{\zeta}^M)\}],\\ \boldsymbol{\varphi}^M &= 2\,\mathrm{Re}[\mathbf{B}^M\{\mathbf{f}_0(\boldsymbol{\zeta}^M)+\mathbf{f}_1(\boldsymbol{\zeta}^M)\}]\end{aligned} \tag{2.206}$$

for the matrix material, and

$$\begin{aligned}\mathbf{U}^I &= 2\,\mathrm{Re}[\mathbf{A}^I\mathbf{f}_2(\boldsymbol{\zeta}^I)],\\ \boldsymbol{\varphi}^I &= 2\,\mathrm{Re}[\mathbf{B}^I\mathbf{f}_2(\boldsymbol{\zeta}^I)]\end{aligned} \tag{2.207}$$

for the inclusion, where $\boldsymbol{\zeta}^x=\{\zeta_1^x,\zeta_2^x,\zeta_3^x,\zeta_4^x\}^T$, ($x$=*M,I*), and the relation between ζ_α^x and z_α^x ($z_\alpha^x = x_1 + p_\alpha^x x_2$) are defined by Eq (2.162). $\mathbf{f}_0$ represents the singular solution for homogeneous media for the generalized line dislocation **b** and a line force-charge $\mathbf{q}_0$, which was obtained in Section 2.5, and can be written as

$$\mathbf{f}_0(\boldsymbol{\zeta}^M) = \left\langle f_0(\zeta_\alpha^M)\right\rangle \mathbf{q}_f = \frac{1}{2\pi i}\left\langle \ln(\zeta_\alpha^M - \zeta_{\alpha 0}^M)\right\rangle \mathbf{q}^{M*} \tag{2.208}$$

where $\mathbf{q}^{M*} = (\mathbf{A}^M)^T\mathbf{q}_0 + (\mathbf{B}^M)^T\mathbf{b}$. $\mathbf{f}_1$ and $\mathbf{f}_2$ are the functions corresponding to the perturbed field, due to the existence of the inclusion, of matrix and inclusion, respectively. They are holomorphic in the regions Ω_1 and Ω_2, respectively (see Fig. 2.8). In the $\boldsymbol{\zeta}$-plane, Ω_1 is the region outside the unit circle while Ω_2 is the region of the annular ring between the unit circle and the circle of radius $r_{in} = \left|\sqrt{\dfrac{a+ibp_\alpha^I}{a-ibp_\alpha^I}}\right|$.

Noting that $\mathbf{f}_2$ is holomorphic in the annular ring Ω_2 mentioned above, it can be represented by Laurent's series as

$$\mathbf{f}_2(\boldsymbol{\zeta}^I) = \sum_{j=-\infty}^{\infty}\left\langle \left(\zeta_\alpha^I\right)^j\right\rangle \mathbf{c}_j \tag{2.209}$$

whose coefficients $\mathbf{c}_j$ can be related by means of the condition (2.184) in the following

manner:

$$\mathbf{c}_{-j}=\mathbf{\Gamma}_j^*\mathbf{c}_j,\quad \mathbf{\Gamma}_j^*=\left\langle\Gamma_{j\alpha}^*\right\rangle=\left\langle\left(\frac{a+ibp_\alpha^I}{a-ibp_\alpha^I}\right)^j\right\rangle. \tag{2.210}$$

Therefore, Eq (2.209) can be further written as

$$\mathbf{f}_2(\zeta^I)=\sum_{j=1}^{\infty}\left\langle\left(\zeta_\alpha^I\right)^j+\Gamma_{j\alpha}^*\left(\zeta_\alpha^I\right)^{-j}\right\rangle\mathbf{c}_j \tag{2.211}$$

in which the constant $\mathbf{c}_0$, which represents the rigid body motion, is neglected. Substituting Eq (2.211) into Eq $(2.207)_2$ and using the continuouity condition $(2.205)_2$ and $\zeta_\alpha^M\big|_\Gamma=\zeta_\alpha^I\big|_\Gamma=e^{i\theta}=\sigma$ along the interface, yields

$$\begin{aligned}&\mathbf{B}^M\mathbf{f}_1(\sigma)+\overline{\mathbf{B}}^M\overline{\mathbf{f}_0(\sigma)}-\sum_{k=1}^{\infty}\{\overline{\mathbf{B}}^I\overline{\mathbf{c}}_k+\mathbf{B}^I\mathbf{\Gamma}_k^*\mathbf{c}_k\}\sigma^{-k}\\&\qquad=-\overline{\mathbf{B}}^M\overline{\mathbf{f}_1(\sigma)}-\mathbf{B}^M\mathbf{f}_0(\sigma)+\sum_{k=1}^{\infty}\{\mathbf{B}^I\mathbf{c}_k+\overline{\mathbf{B}}^I\overline{\mathbf{\Gamma}}_k^*\overline{\mathbf{c}}_k\}\sigma^k\end{aligned} \tag{2.212}$$

One of the important properties of holomorphic functions used in the method of analytic continuation is that if the function $f(\zeta)$ is holomorphic in Ω_1, the region outside the ellipse, (or $\Omega_0+\Omega_2$), then $\overline{f(1/\overline{\zeta})}$ is holomorphic in $\Omega_0+\Omega_2$ (or Ω_1), Ω_0 denoting the region inside the circle of radius r_{in}. According to this property, we may introduce a function which is holomorphic in the entire domain including the interface boundary, i.e. [28]

$$\omega(\zeta)=\begin{cases}\mathbf{B}^M\mathbf{f}_1(\zeta)+\overline{\mathbf{B}}^M\overline{\mathbf{f}_0(1/\overline{\zeta})}-\sum_{j=1}^{\infty}[\overline{\mathbf{B}}^I\overline{\mathbf{c}}_j+\mathbf{B}^I\mathbf{\Gamma}_j^*\mathbf{c}_j]\zeta^{-j}, & \zeta\in\Omega_1,\\ -\overline{\mathbf{B}}^M\overline{\mathbf{f}_1(1/\overline{\zeta})}-\mathbf{B}^M\mathbf{f}_0(\zeta)+\sum_{j=1}^{\infty}[\mathbf{B}^I\mathbf{c}_j+\overline{\mathbf{B}}^I\overline{\mathbf{\Gamma}}_j^*\overline{\mathbf{c}}_j]\zeta^j, & \zeta\in\Omega_0+\Omega_2,\end{cases} \tag{2.213}$$

where the function $\omega(\boldsymbol{\zeta})$ is holomorphic and single valued in the whole plane. By Liouville's theorem, we have $\omega(\boldsymbol{\zeta})$=constant. However, constant function $\mathbf{f}$ corresponds to rigid body motion, which may be neglected. Thus, by letting $\omega(\boldsymbol{\zeta})$=0, we have

$$\begin{aligned}&\sum_{j=1}^{\infty}[\overline{\mathbf{B}}^I\overline{\mathbf{c}}_j+\mathbf{B}^I\mathbf{\Gamma}_j^*\mathbf{c}_j]\zeta^{-j}=\mathbf{B}^M\mathbf{f}_1(\zeta)+\overline{\mathbf{B}}^M\overline{\mathbf{f}_0(1/\overline{\zeta})}, && \zeta\in\Omega_1,\\&\sum_{j=1}^{\infty}[\mathbf{B}^I\mathbf{c}_j+\overline{\mathbf{B}}^I\overline{\mathbf{\Gamma}}_j^*\overline{\mathbf{c}}_j]\zeta^j=\overline{\mathbf{B}}^M\overline{\mathbf{f}_1(1/\overline{\zeta})}+\mathbf{B}^M\mathbf{f}_0(\zeta), && \zeta\in\Omega_0+\Omega_2\end{aligned} \tag{2.214}$$

Similarly, the continuity condition $(2.205)_1$ gives

$$\begin{aligned}&\sum_{j=1}^{\infty}[\overline{\mathbf{A}}^I\overline{\mathbf{c}}_j+\mathbf{A}^I\mathbf{\Gamma}_j^*\mathbf{c}_j]\zeta^{-j}=\mathbf{A}^M\mathbf{f}_1(\zeta)+\overline{\mathbf{A}}^M\overline{\mathbf{f}_0(1/\overline{\zeta})}, && \zeta\in\Omega_1,\\&\sum_{j=1}^{\infty}[\mathbf{A}^I\mathbf{c}_j+\overline{\mathbf{A}}^I\overline{\mathbf{\Gamma}}_j^*\overline{\mathbf{c}}_j]\zeta^j=\overline{\mathbf{A}}^M\overline{\mathbf{f}_1(1/\overline{\zeta})}+\mathbf{A}^M\mathbf{f}_0(\zeta), && \zeta\in\Omega_0+\Omega_2\end{aligned} \tag{2.215}$$

The equations $(2.214)_2$ and $(2.215)_2$ provide

$$\mathbf{f}_0(\zeta)=\sum_{k=1}^{\infty} i(\mathbf{A}^M)^T\{(\bar{\mathbf{M}}^M+\mathbf{M}^I)\mathbf{A}^I\mathbf{c}_k+(\bar{\mathbf{M}}^M-\bar{\mathbf{M}}^I)\bar{\mathbf{A}}^I\bar{\boldsymbol{\Gamma}}_k^*\bar{\mathbf{c}}_k\}\zeta^k \tag{2.216}$$

where

$$\mathbf{M}^x=-i\mathbf{B}^x(\mathbf{A}^x)^{-1}, \qquad (x=I,M) \tag{2.217}$$

With the use of series representation

$$f_0(x)=\sum_{k=1}^{\infty} e_k x^k, \quad e_k=\frac{f_0^{(k)}(0)}{k!}, \tag{2.218}$$

of $\mathbf{f}_0$ from Eq (2.208), and comparing the coefficient $\mathbf{c}_k$ of the corresponding terms in Eq (2.216), we have

$$\mathbf{c}_k=(\mathbf{G}_0-\bar{\mathbf{G}}_k\bar{\mathbf{G}}_0^{-1}\mathbf{G}_k)^{-1}(\mathbf{t}_k-\bar{\mathbf{G}}_k\bar{\mathbf{G}}_0^{-1}\bar{\mathbf{t}}_k), \quad k=1,2,\cdots,\infty, \tag{2.219}$$

where

$$\begin{aligned}&\mathbf{G}_0=(\bar{\mathbf{M}}^M+\mathbf{M}^I)\mathbf{A}^I, \quad \mathbf{G}_k=(\mathbf{M}^M-\mathbf{M}^I)\mathbf{A}^I\boldsymbol{\Gamma}_k^*,\\ &\mathbf{t}_k=\frac{1}{2\pi}(\mathbf{A}^M)^{-T}\left\langle\frac{1}{k}\left(\frac{1}{\zeta_\alpha}\right)^k\right\rangle\mathbf{q}^{M*}\end{aligned} \tag{2.220}$$

With the solution obtained for $\mathbf{c}_k$, $\mathbf{f}_1$ can be obtained from Eqs $(2.214)_1$ and $(2.215)_1$. The functions $\mathbf{f}_0$, $\mathbf{f}_1$ and $\mathbf{f}_2$ can then be further written as

$$\begin{aligned}&\mathbf{f}_0(\zeta^M)=\frac{1}{2\pi i}\left\langle\ln(\zeta_\alpha^M-\zeta_{\alpha 0}^M\right\rangle\mathbf{q}^{M*},\\ &\mathbf{f}_1(\zeta^M)=\sum_{k=1}^{\infty}(\mathbf{B}^M)^{-1}\left\langle(\zeta_\alpha^M)^{-k}\right\rangle(\bar{\mathbf{B}}^I\bar{\mathbf{c}}_k+\mathbf{B}^I\boldsymbol{\Gamma}_k^*\mathbf{c}_k)-(\mathbf{B}^M)^{-1}\bar{\mathbf{B}}^M\bar{\mathbf{f}}_0(1/\zeta^M),\\ &\mathbf{f}_2(\zeta^I)=\sum_{k=1}^{\infty}\{\left\langle(\zeta_\alpha^I)^k\right\rangle+\left\langle(\zeta_\alpha^I)^{-k}\right\rangle\boldsymbol{\Gamma}_k^*\}\mathbf{c}_k\end{aligned} \tag{2.221}$$

The Green's functions $\mathbf{U}^x$ and $\boldsymbol{\varphi}^x$ $(x=I,M)$ can thus be obtained by substituting the results (2.221) into Eqs (2.206) and (2.207).

2.9 Arbitrarily shaped hole

In this section, we present Green's functions for holes of various shapes embedded in an infinite plane piezoelectric plate subjected to a line force-charge $\mathbf{q}_0$ and generalized line dislocations $\mathbf{b}$ (Fig. 2.9). The Green's functions satisfying traction free and exact electric boundary conditions along the hole boundary are derived using Lekhnitskii's formalism and the technique of one-to-one mapping. A detailed discussion of the critical points for the mapping function of a piezoelectric plate with polygonal holes is also presented. Study shows that the transformation function (2.223) below is nonsingle-valued. A simple approach is presented to treat such a situation. This section details the development given in [17].

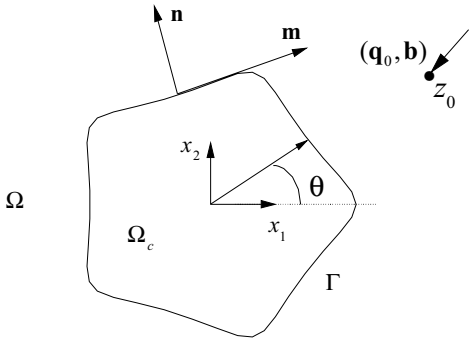

Fig. 2.9 Geometry of a particular hole (a=1, e=1, m=4, γ=0.1)

2.9.1 One-to-one mapping

Consider an infinite two-dimensional piezoelectric material containing a hole of various contours, where the material is transversely isotropic and coupling between in-plane stress and in-plane electric fields takes place. The constitutive relation used here is defined by Eq (1.144). The contour of the hole considered, say Γ (see Fig. 2.9), in this section is represented by

$$x_1 = a(\cos\theta + \gamma e_{m1}\cos m\theta), \quad x_2 = ae(\sin\theta - \gamma e_{m1}\sin m\theta) \tag{2.222}$$

where θ is a real parameter (see Fig. 2.9), $e_{ij} = 1$ if $i \neq j$; $e_{ij} = 0$ if $i = j$, $0<e\leq 1$, m is an integer and the same value exists for subscripts and for the argument of functions. By appropriate selection of the parameters e, m and γ, we can obtain various special kinds of hole, such as ellipse (m=1), circle (m=e=1), triangle (m=2), square (m=3) and pentagon (m=4). Since complex mapping is a fundamental tool used to find the solution of hole problems, the transformation [2]

$$z_k = a(a_{1k}\zeta_k + a_{2k}\zeta_k^{-1} + e_{m1}a_{3k}\zeta_k^{m} + e_{m1}a_{4k}\zeta_k^{-m}), \tag{2.223}$$

in which

$$\begin{aligned} a_{1k} &= (1 - ip_k e)/2, \qquad a_{2k} = (1 + ip_k e)/2, \\ a_{3k} &= \gamma(1 + ip_k e)/2, \quad a_{4k} = \gamma(1 - ip_k e)/2 \end{aligned} \tag{2.224}$$

is used to map the contour of the hole onto a unit circle in the ζ-plane. For a particular value of z_k, there exist 2m roots for ζ_k in Eq (2.223). Numerical study of Eq (2.223) shows that half of the roots are located outside the unit circle and the remaining roots are inside it. Thus the transformation (2.223) will be single-valued for m=1 (ellipse) since only one root locates outside the unit circle. For m>1, however, the transformation (2.223) is multi-valued as there are m roots located outside the unit circle. The question is, which root should be chosen. To determine this, some numerical investigation has been performed and typical results are listed in Tables 2.1-2.3 for a=e=1 and γ=0.1. In these tables, p_k= $-0.2291853 + 1.003833i$, which is one of the eigenvalues of material $BaTiO_3$ used in [2], $|\zeta|^2 = \zeta\overline{\zeta}$, and ζ_{ki} is the ith

root of ζ_k for Eq (2.223). It is found from the tables that the magnitudes among the m-roots are obviously different from each other. Numerical study in [2] showed that the root, say ζ_k^*, whose magnitude has the minimum value among the m-roots, can provide acceptable results. So we choose ζ_k^* as the solution for Eq (2.223) in our analysis. Hence, the entire z_k-plane is now mapped onto part of the ζ_k-plane with a one-to-one transformation. Moreover, it is interesting to see from Tables 2.1-2.3 that the real and imaginary parts of ζ_k^* always retain the same symbol as those of z_k, i.e., sign[Im(z_k)]= sign[Im(ζ_k^*)] and sign[Re(z_k)]= sign[Re(ζ_k^*)], where sign(x) is defined by

$$\text{Sign}(x)=\begin{cases}1 & \text{if } x>0\\ 0 & \text{if } x=0\\ -1 & \text{if } x<0\end{cases} \tag{2.225}$$

which means that ζ_k^* and z_k are always situated in the same quadrant of a rectangular coordinate system.

Next, to find a single-valued mapping of the region Ω_c (see Fig. 2.9), occupied by vacuum(or air), let

$$z = a(a_{1c}\zeta + a_{2c}\zeta^{-1} + e_{m1}a_{3c}\zeta^{m} + e_{m1}a_{4c}\zeta^{-m}) \tag{2.226}$$

where $z = x_1 + ix_2$, and

$$\begin{aligned} a_{1c} &= (1+e)/2, \quad a_{2c} = (1-e)/2,\\ a_{3c} &= \gamma(1-e)/2, \quad a_{4c} = \gamma(1+e)/2 \end{aligned} \tag{2.227}$$

Table 2.1: The properties of solution ξ_{kj} (j=1-m) for m=2

z_k	5+5p_k	-5+5p_k	-5-5p_k	5-5p_k
ξ_{k1}	7.51-91.75i	16.35-92.73i	16.30-82.84i	5.156-81.59i
$\lvert\xi_{k1}\rvert$	92.06	94.16	84.43	81.74
ξ_{k2}	3.97+4.52i	-4.885+5.4757i	-4.85-4.41i	6.294-5.65i
$\lvert\xi_{k2}\rvert$	6.016	7.338	6.555	8.458

Table 2.2: The properties of solution ξ_{kj} (j=1-m) for m=3

z_k	5+5p_k	-5+5p_k	-5-5p_k	5-5p_k
ξ_{k1}	6.02-8.63i	8.96-8.07i	9.39-5.05i	-8.96+8.07i
$\lvert\xi_{k1}\rvert$	10.52	12.06	10.66	12.06
ξ_{k2}	-9.39+5.05i	-7.73+0.784i	-6.02+8.63i	7.73-0.784i
$\lvert\xi_{k2}\rvert$	10.66	7.770	10.52	7.770
ξ_{k3}	3.38+3.60i	-1.221+7.274i	-3.38-3.60i	1.221-7.274i
$\lvert\xi_{k3}\rvert$	4.938	7.376	4.938	7.376

Table 2.3: The properties of solution ξ_{kj} (j=1-m) for m=4

z_k	5+5p_k	-5+5p_k	-5-5p_k	5-5p_k
ξ_{k1}	-4.69-3.22i	4.58-2.98i	5.23-1.53i	-5.31-1.88i
$\lvert\xi_{k1}\rvert$	5.689	5.464	5.449	5.633
ξ_{k2}	-2.02+4.43i	1.94+4.68i	-4.43-0.16i	4.78+0.30i
$\lvert\xi_{k2}\rvert$	4.869	5.066	4.433	4.789
ξ_{k3}	3.71-3.61i	-3.52-4.15i	0.436+5.58i	-0.94+5.75i
$\lvert\xi_{k3}\rvert$	5.177	5.442	5.597	5.826
ξ_{k4}	3.01+2.41i	-3.49+2.45i	-1.255-3.90i	1.46-4.15i
$\lvert\xi_{k4}\rvert$	3.856	4.264	4.097	4.399

The roots of $dz/d\zeta = 0$ represent the critical points for transformation (2.226) and can be obtained by solving

$$a_{1c} - a_{2c}\zeta^{-2} + me_{m1}a_{3c}\zeta^{m-1} - me_{m1}a_{4c}\zeta^{-m-1} = 0 \tag{2.228}$$

The analytical solution of Eq.(2.228) is, in general, not easy to find for m>1. For simplicity, we consider following two cases only:

(i) m=1(ellipse). Solving Eq.(2.228), we have

$$\zeta_{1,2} = \pm\sqrt{\frac{1-e}{1+e}} \tag{2.229}$$

Thus, the mapping of the region Ω_c can be performed by excluding a straight line Γ_0 along x_1 and of length $2a\sqrt{1-e^2}$ from the ellipse. In this case the function

$$z = a(a_{1c}\zeta + a_{2c}\zeta^{-1}) \tag{2.230}$$

will transform Γ and Γ_0 (see Fig. 2.8) into the ring of outer and inner circles with radii $r_{out} = 1$ and $r_{in} = \sqrt{\frac{1-e}{1+e}}$, respectively.

(ii) m>1 and e=1. In this case the mapping function (2.226) becomes

$$z = a(a_{1c}\zeta + a_{4c}\zeta^{-m}) \tag{2.231}$$

The roots of equation (2.228) can then be easily found as

$$\zeta_0 = \sqrt[m+1]{m\gamma} \tag{2.232}$$

In practice, γ is a small number. If we assume $m\gamma$<1, the function (2.231) will transform the lines Γ and Γ_0 (a straight line along x_1-axis and of length $a(m\gamma)^{\frac{1}{m+1}}(1+m^{-1})$) into an annular circle with inner and outer radii $r_{in} = \sqrt[m+1]{m\gamma}$ and r_{out}=1, respectively.

2.9.2 Green's function for electroelastic field

Consider an infinite piezoelectric plate containing a hole subjected to a line force-charge $\mathbf{q}_0$ and a generalized line dislocation $\mathbf{b}$, both located at $z_0(x_{10},x_{20})$. The hole surface is assumed to be free of traction, but the normal component of electric

displacement and the electric potential are continuous along the hole boundary. We therefore have the following boundary conditions:

along the hole boundary:

$$\sigma_{nn} = 0, \quad \sigma_{nm} = 0, \quad D_n = -\varepsilon_0 \frac{\partial \varphi^c}{\partial n}, \quad \varphi = \varphi^c \tag{2.233}$$

at infinity:

$$\sigma_{ij} \to 0, \quad D_i \to 0 \tag{2.234}$$

where n and m, respectively, stand for the normal and tangent to the hole boundary (Fig. 2.9). σ_{nn} and σ_{nm} are the normal and shear stresses along the boundary, ε_0 is the dielectric constant of vacuum, superscript c indicates the quantity associated with the hole medium.

It can be shown that the electroelastic boundary conditions (2.233) can be expressed in terms of complex potentials in the form [2]:

$$\begin{aligned} &2\,\mathrm{Re}\sum_{k=1}^{3}\Phi_k = 0, \quad 2\,\mathrm{Re}\sum_{k=1}^{3}\{p_k\Phi_k\} = 0, \\ &2\,\mathrm{Re}\sum_{k=1}^{3}\{\varpi_k\Phi_k\} = -\kappa_0\int_0^s \frac{\partial \varphi^c}{\partial n}ds, \quad 2\,\mathrm{Re}\sum_{k=1}^{3}\{t_k^*\Phi_k\} = \varphi^c, \end{aligned} \tag{2.235}$$

where s is arc length of Γ, and ϖ_k and t_k^* are defined by Eqs (1.157) and (1.162). Noting that [10]

$$\frac{\partial \varphi^c(x_1 + ix_2)}{\partial n} = -i\frac{\partial \varphi^c(x_1 + ix_2)}{\partial m} \tag{2.236}$$

Eq $(2.235)_3$ can be further simplified as

$$2\,\mathrm{Re}\sum_{k=1}^{3}\{\varpi_k\Phi_k\} = 2\,\mathrm{Re}\{i\kappa_0 F(z)\} \tag{2.237}$$

where

$$\varphi^c(z) = F(z) + \overline{F(z)} \tag{2.238}$$

Conditions (2.234) and (2.235) suggest that the complex potentials Φ_k be chosen as

$$\Phi_k(z_k) = g_k \ln(\zeta_k - \zeta_{k0}) + \Phi_{k0}(\zeta_k) \tag{2.239}$$

where

$$\Phi_{k0}(\zeta_k) = a_{k0} + \sum_{i=1}^{\infty} a_{ki}\zeta_k^{-i} \qquad \text{in } \Omega \tag{2.240}$$

while the function $F(\zeta)$ may be assumed as

$$F(\zeta) = b_0 + \sum_{k=1}^{\infty} b_k \zeta^{-k} \tag{2.241}$$

for the case of a crack, and

$$F(\zeta) = \sum_{k=-\infty}^{\infty} b_k \zeta^k \tag{2.242}$$

for the other holes in which the coefficients have the following relation [11]:

$$b_{-k} = r_{in}^{2k} b_k \tag{2.243}$$

Here g_k are complex constants which can be determined from following conditions:

$$\int_C \mathbf{A}^* d\boldsymbol{\Phi} = \mathbf{b} \quad \text{and} \quad \int_C \mathbf{B}^* d\boldsymbol{\Phi} = \mathbf{q}_0 \quad \text{for any closed curve C enclosing the point } \boldsymbol{\zeta}_0 \tag{2.244}$$

where

$$\boldsymbol{\zeta}_0 = \{\zeta_{10}\ \zeta_{20}\ \zeta_{30}\}^T, \quad \boldsymbol{\Phi} = \{\Phi_1\ \Phi_2\ \Phi_3\}^T \tag{2.245}$$

$$\mathbf{A}^* = \begin{bmatrix} p_1^* & p_2^* & p_3^* \\ q_1^* & q_2^* & q_3^* \\ t_1^* & t_2^* & t_3^* \end{bmatrix}, \qquad \mathbf{B}^* = \begin{bmatrix} -p_1 & -p_2 & -p_3 \\ 1 & 1 & 1 \\ -\varpi_1 & -\varpi_2 & -\varpi_3 \end{bmatrix} \tag{2.246}$$

Substituting Eq. (2.239) into Eq. (2.244), leads to

$$\mathbf{g} = \{g_1\ g_2\ g_3\}^3 = \frac{1}{2\pi i}(\bar{\mathbf{A}}^{*-1}\mathbf{A}^* - \bar{\mathbf{B}}^{*-1}\mathbf{B}^*)^{-1}(\bar{\mathbf{A}}^{*-1}\mathbf{b} - \bar{\mathbf{B}}^{*-1}\mathbf{q}_0) \tag{2.247}$$

Using the solution (2.247) and expression (2.239), the boundary conditions (2.235) can be further written as

$$\sum_{k=1}^{3}[\Phi_{k0}(\sigma) + \overline{\Phi_{k0}(\sigma)} + \sum_{m=1}^{\infty}(g_k e_{km}\sigma^m + \bar{g}_k \bar{e}_{km}\sigma^{-m})] = 0 \tag{2.248}$$

$$\sum_{k=1}^{3}[p_k\Phi_{k0}(\sigma) + \bar{p}_k\overline{\Phi_{k0}(\sigma)} + \sum_{m=1}^{\infty}(p_k g_k e_{km}\sigma^m + \bar{p}_k\bar{g}_k\bar{e}_{km}\sigma^{-m})] = 0 \tag{2.249}$$

$$\sum_{k=1}^{3}[\varpi_k\Phi_{k0}(\sigma) + \bar{\varpi}_k\overline{\Phi_{k0}(\sigma)} + \sum_{m=1}^{\infty}(\varpi_k g_k e_{km}\sigma^m + \bar{\varpi}_k\bar{g}_k\bar{e}_{km}\sigma^{-m})] = i\kappa_0[F(\sigma) - \overline{F(\sigma)}] \tag{2.250}$$

$$\sum_{k=1}^{3}[t_k^*\Phi_{k0}(\sigma) + \bar{t}_k^*\overline{\Phi_{k0}(\sigma)} + \sum_{m=1}^{\infty}(t_k^* g_k e_{km}\sigma^m + \bar{t}_k^*\bar{g}_k\bar{e}_{km}\sigma^{-m})] = F(\sigma) + \overline{F(\sigma)} \tag{2.251}$$

where $\sigma = e^{i\theta}$ denotes the point located on the unit circle.

During the derivation of Eqs. (2.248)-(2.251), the series representation for function $\ln(\zeta_k - \zeta_{k0})$ has been employed. In fact, for a function $f(x)$, the series representation may be written in the form:

$$f(x) = \sum_{k=1}^{\infty} e_k x^k, \quad e_k = \frac{f^{(k)}(0)}{k!} = \frac{1}{2\pi i}\int_C \frac{f(x)}{x^{k+1}}dx \tag{2.252}$$

Thus, the function $\ln(\zeta_k - \zeta_{k0})$ can be expressed as

$$\ln(\zeta_k - \zeta_{k0}) = \sum_{m=1}^{\infty} e_{km}\zeta^m, \qquad e_{km} = -\frac{\zeta_{k0}^{-m}}{m} \tag{2.253}$$

The substitution of Eqs. (2.240)~(2.242) into Eqs. (2.248)~(2.251), yields

$$\sum_{k=1}^{3}(a_{ki} + \bar{g}_k\bar{e}_{ki}) = 0, \quad \sum_{k=1}^{3}(p_k a_{ki} + \bar{p}_k\bar{g}_k\bar{e}_{ki}) = 0, \quad \sum_{k=1}^{3}(\chi_{ki}a_{ki} + \bar{t}_{ki}\bar{a}_{ki}) = l_i \tag{2.254}$$

where

$$t_{ki} = \varpi_k + i\kappa_0 t_k^*, \quad \chi_{ki} = 0, \quad l_i = \sum_{k=1}^{3} (\varpi_k - i\kappa_0 t_k^*) g_k e_{ki} \tag{2.255}$$

$$b_i = \sum_{k=1}^{3} (t_k^* g_k e_{ki} - \overline{t}_k^* \overline{a}_{ki}) \tag{2.256}$$

for cracks, and

$$\begin{aligned} &\overline{t}_{ki} = \overline{\varpi}_k - \frac{i\kappa_0}{1-r_{in}^{4i}}(1+r_{in}^{4i})\overline{t}_k^*, \quad \chi_{ki} = \frac{2i\kappa_0 r_{in}^{2i} t_k^*}{1-r_{in}^{4i}}, \\ &l_i = \sum_{k=1}^{3} \{\varpi_k g_k e_{ki} + \frac{i\kappa_0}{1-r_{in}^{4i}}[2r_{in}^{2i}\overline{t}_k^* \overline{g}_k \overline{e}_{ki} - (1+r_{in}^{4i}) t_k^* g_k e_{ki}]\}, \end{aligned} \tag{2.257}$$

$$b_i = \frac{1}{1-r_{in}^{4i}} \sum_{k=1}^{3} [t_k^* g_k e_{ki} - \overline{t}_k^* \overline{a}_{ki} - r_{in}^{2i}(\overline{t}_k^* \overline{g}_k \overline{e}_{ki} - t_k^* a_{ki})] \tag{2.258}$$

for the other holes. Solving Eqs. (2.254), one obtains

$$\mathbf{a}_i = \mathbf{E}_i \mathbf{g} + \mathbf{F}_i \overline{\mathbf{g}} \tag{2.259}$$

where

$$\mathbf{a}_i = \{a_{1i}\ a_{2i}\ a_{3i}\}^T \tag{2.260}$$

$$\mathbf{E}_i = (\mathbf{P}_i - \mathbf{Q}_i \overline{\mathbf{P}}_i^{-1} \overline{\mathbf{Q}}_i)^{-1} (\mathbf{E}_i^* - \mathbf{Q}_i \overline{\mathbf{P}}_i^{-1} \overline{\mathbf{F}}_i^*) \tag{2.261}$$

$$\mathbf{F}_i = (\mathbf{P}_i - \mathbf{Q}_i \overline{\mathbf{P}}_i^{-1} \overline{\mathbf{Q}}_i)^{-1} (\mathbf{F}_i^* - \mathbf{Q}_i \overline{\mathbf{P}}_i^{-1} \overline{\mathbf{E}}_i^*) \tag{2.262}$$

$$\mathbf{P}_i = \begin{bmatrix} 1 & 1 & 1 \\ p_1 & p_2 & p_3 \\ \chi_{1i} & \chi_{2i} & \chi_{3i} \end{bmatrix}, \quad \mathbf{Q}_i = \begin{bmatrix} 0 & 0 & 0 \\ 0 & 0 & 0 \\ \overline{t}_{1i} & \overline{t}_{2i} & \overline{t}_{3i} \end{bmatrix} \tag{2.263}$$

$$\mathbf{E}_i^* = \begin{bmatrix} 0 & 0 & 0 \\ 0 & 0 & 0 \\ b_{1i}^* & b_{2i}^* & b_{3i}^* \end{bmatrix}, \quad \mathbf{F}_i^* = \begin{bmatrix} -\overline{e}_{1i} & -\overline{e}_{2i} & -\overline{e}_{3i} \\ -\overline{e}_{1i}\overline{p}_1 & -\overline{e}_{2i}\overline{p}_2 & -\overline{e}_{3i}\overline{p}_3 \\ b_{1i}^{**} & b_{2i}^{**} & b_{3i}^{**} \end{bmatrix} \tag{2.264}$$

in which

$$b_{ki}^* = (\varpi_k - i\kappa_0 t_k^*) e_{ki}, \quad b_{ki}^{**} = 0 \tag{2.265}$$

for cracks, and

$$b_{ki}^* = [\varpi_k - \frac{i\kappa_0(1+r_{in}^{4i})}{1-r_{in}^{4i}} t_k^*] e_{ki}, \quad b_{ki}^{**} = \frac{2i\kappa_0 r_{in}^{2i}}{1-r_{in}^{4i}} \overline{t}_k^* \overline{e}_{ki} \tag{2.266}$$

for other holes. Using the expression (2.259), the potential solution, $\mathbf{\Phi}$, can further be written as

$$\mathbf{\Phi} = \left\langle \ln(\zeta_\alpha - \zeta_{\alpha 0}) \right\rangle \mathbf{g} + \sum_{i=1}^{\infty} \left\langle \zeta_\alpha^{-i} \right\rangle (\mathbf{E}_i \mathbf{g} + \mathbf{F}_i \overline{\mathbf{g}}) \tag{2.267}$$

where $\left\langle f_\alpha \right\rangle = \mathrm{diag}[f_1 f_2 f_3]$ represents a diagonal matrix. Therefore, the Green's function of **U** can be written as

$$\mathbf{U} = \{u_1, u_2, \phi\}^T = 2\,\mathrm{Re}[\mathbf{A}^*\{\langle \ln(\zeta_\alpha - \zeta_{\alpha 0})\rangle \mathbf{g} + \sum_{i=1}^{\infty} \langle \zeta_\alpha^{-i} \rangle (\mathbf{E}_i \mathbf{g} + \mathbf{F}_i \bar{\mathbf{g}})\}] \tag{2.268}$$

2.10 Semi-infinite cracks

Consider an infinite piezoelectric solid with a semi-infinite crack L_c along the negative direction of the x_1-axis, as shown in Fig. 2.10. The infinite piezoelectric solid is loaded by a line force-charge $\mathbf{q}_0$ and a generalized line dislocation **b**, both located at $z_0(x_{10},x_{20})$[51]. The crack faces are assumed to be free of mechanical forces and external electric charge. Therefore, along the crack faces, we have

$$\boldsymbol{\varphi}\big|_{L_c} = 0 \tag{2.269}$$

We introduce the mapping function [51]

$$z_\alpha = \zeta_\alpha^2 \tag{2.270}$$

which maps the crack faces $\theta = \pm\pi$ in the z-plane into the imaginary axis in the ζ-plane (see Fig. 2.10). Based on the mapping function (2.270), the corresponding Green's function of **U** and $\boldsymbol{\varphi}$ may be assumed in the following form [2,50]

$$\mathbf{U} = \frac{1}{\pi}\mathrm{Im}\{\mathbf{A}\langle \ln(\zeta_\alpha - \zeta_{\alpha 0})\rangle \mathbf{q}^*\} + \sum_{\beta=1}^{4} \frac{1}{\pi}\mathrm{Im}\{\mathbf{A}\langle \ln(-\zeta_\alpha - \overline{\zeta}_{\beta 0})\rangle \mathbf{q}_\beta\}, \tag{2.271}$$

$$\boldsymbol{\varphi} = \frac{1}{\pi}\mathrm{Im}\{\mathbf{B}\langle \ln(\zeta_\alpha - \zeta_{\alpha 0})\rangle \mathbf{q}^*\} + \sum_{\beta=1}^{4} \frac{1}{\pi}\mathrm{Im}\{\mathbf{B}\langle \ln(-\zeta_\alpha - \overline{\zeta}_{\beta 0})\rangle \mathbf{q}_\beta\} \tag{2.272}$$

where $\mathbf{q}^*$ is defined by Eq (2.86).

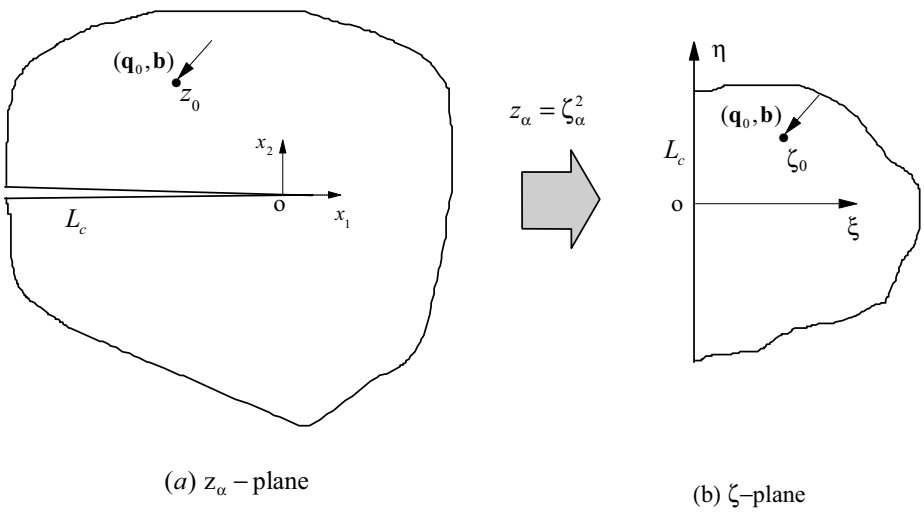

(*a*) z_α – plane (b) ζ–plane

Fig. 2.10 Geometry of the semi-infinite crack system

The substitution of Eq (2.272) into Eq (2.269) leads to

$$\mathrm{Im}\{\mathbf{B}\left\langle \ln(\zeta_c-\zeta_{\alpha 0})\right\rangle \mathbf{q}^*\}+\sum_{\beta=1}^{4}\mathrm{Im}\{\ln(-\zeta_c-\overline{\zeta}_{\beta 0})\mathbf{B}\mathbf{q}_\beta\}=0 \tag{2.273}$$

where ζ_c is the value of ζ_α along the imaginary axis [51]. Noting that $\overline{\zeta}_c=-\zeta_c$ holds along the imaginary axis, the first term in Eq (2.273) can be replaced by the negative of its complex conjugate:

$$\begin{aligned}\mathrm{Im}\{\mathbf{B}\left\langle \ln(\zeta_c-\zeta_{\alpha 0})\mathbf{q}^*\right\rangle\} &= -\mathrm{Im}\{\overline{\mathbf{B}}\left\langle \ln(-\zeta_c-\overline{\zeta}_{\alpha 0})\overline{\mathbf{q}}^*\right\rangle\}\\ &= -\mathrm{Im}\left\{\sum_{\beta=1}^{4}\ln(-\zeta_c-\overline{\zeta}_{\beta 0})\overline{\mathbf{B}}\mathbf{I}_\beta\overline{\mathbf{q}}^*\right\}\end{aligned} \tag{2.274}$$

Equation (2.273) then yields

$$\mathbf{q}_\beta=\mathbf{B}^{-1}\overline{\mathbf{B}}\mathbf{I}_\beta\overline{\mathbf{q}}^* \tag{2.275}$$

which is in the same form as that in Eq (2.178). Therefore the Green's function can be written in terms of z_α as

$$\mathbf{U}=\frac{1}{\pi}\mathrm{Im}\{\mathbf{A}\left\langle \ln(\sqrt{z_\alpha}-\sqrt{z_{\alpha 0}})\right\rangle \mathbf{q}^*\}+\sum_{\beta=1}^{4}\frac{1}{\pi}\mathrm{Im}\{\mathbf{A}\left\langle \ln(-\sqrt{z_\alpha}-\sqrt{\overline{z}_{\alpha 0}})\right\rangle \mathbf{B}^{-1}\overline{\mathbf{B}}\mathbf{I}_\beta\overline{\mathbf{q}}^*\}, \tag{2.276}$$

$$\boldsymbol{\varphi}=\frac{1}{\pi}\mathrm{Im}\{\mathbf{B}\left\langle \ln(\sqrt{z_\alpha}-\sqrt{z_{\alpha 0}})\right\rangle \mathbf{q}^*\}+\sum_{\beta=1}^{4}\frac{1}{\pi}\mathrm{Im}\{\mathbf{B}\left\langle \ln(-\sqrt{z_\alpha}-\sqrt{\overline{z}_{\alpha 0}})\right\rangle \mathbf{B}^{-1}\overline{\mathbf{B}}\mathbf{I}_\beta\overline{\mathbf{q}}^*\} \tag{2.277}$$

2.11 Anti-plane problems in a cracked solid

In this section, Green's function for anti-plane problems in an piezoelectric solid with a crack is presented based on the complex variable method and the perturbation technique. The discussion is based on the results given in [52].

2.11.1 Basic equations of anti-plane problem

In the case of anti-plane shear deformation involving only out-of-plane displacement u_z and in-plane electric fields, whose variables are independent of the longitudinal coordinate z,

$$u_x=u_y=0,\quad u_z=u_z(x,y),\quad \phi=\phi(x,y) \tag{2.278}$$

The differential governing equations $(1.59)_{1,2}$ are thus reduced to

$$c_{44}\nabla_2 u_z+e_{15}\nabla_2\phi=0,\qquad e_{15}\nabla_2 u_z-\kappa_{11}\nabla_2\phi=0 \qquad \text{in } \Omega \tag{2.279}$$

with the constitutive equations

$$\begin{Bmatrix}\sigma_{xz}\\ \sigma_{yz}\\ D_x\\ D_y\end{Bmatrix}=\begin{bmatrix}c_{44} & 0 & -e_{15} & 0\\ 0 & c_{44} & 0 & -e_{15}\\ e_{15} & 0 & \kappa_{11} & 0\\ 0 & e_{15} & 0 & \kappa_{11}\end{bmatrix}\begin{Bmatrix}\gamma_{xz}\\ \gamma_{yz}\\ E_x\\ E_y\end{Bmatrix} \tag{2.280}$$

or

$$\begin{Bmatrix} \gamma_{xz} \\ \gamma_{yz} \\ E_x \\ E_y \end{Bmatrix} = \begin{bmatrix} f_{44} & 0 & g_{15} & 0 \\ 0 & f_{44} & 0 & g_{15} \\ -g_{15} & 0 & \beta_{11} & 0 \\ 0 & -g_{15} & 0 & \beta_{11} \end{bmatrix} \begin{Bmatrix} \sigma_{xz} \\ \sigma_{yz} \\ D_x \\ D_y \end{Bmatrix} \tag{2.281}$$

where ∇_2 is the 2D Laplace's operator defined by Eq (1.29), γ_{xz}, γ_{yz} and E_x, E_y are, respectively, shear strains and electric fields given by

$$\gamma_{xz} = \frac{\partial u_z}{\partial x}, \quad \gamma_{yz} = \frac{\partial u_z}{\partial y}, \quad E_x = -\frac{\partial \phi}{\partial x}, \quad E_y = -\frac{\partial \phi}{\partial y} \tag{2.282}$$

The constants f_{44}, g_{15} and β_{11} are defined by the relations:

$$f_{44} = \frac{\kappa_{11}}{\Delta}, \quad g_{15} = \frac{e_{15}}{\Delta}, \quad \beta_{11} = \frac{c_{44}}{\Delta}, \quad \Delta = c_{44}\kappa_{11} + e_{15}^2 \tag{2.283}$$

It is obvious from Eq (2.279) that it requires

$$c_{44}\kappa_{11} + e_{15}^2 \neq 0 \tag{2.284}$$

to have a non-trivial solution for the out-of-plane displacement and in-plane electric fields. With the relation (2.284), Eq (2.279) results in

$$\nabla_2 u_z = 0, \qquad \nabla_2 \phi = 0 \tag{2.285}$$

If we let the harmonic functions u_z and ϕ be the imaginary parts of some complex potentials of the variable $z=x_1+ix_2$:

$$u_z = \mathrm{Im}[u(z)], \quad \phi = \mathrm{Im}[\psi(z)], \tag{2.286}$$

then the generalized strain and stress fields can be expressed as

$$\begin{aligned} &\gamma_{23} + i\gamma_{13} = W(z), \quad E_2 + iE_1 = -\Phi(z), \\ &\tau_{23} + i\tau_{13} = c_{44}W(z) + e_{15}\Phi(z), \quad D_2 + iD_1 = e_{15}W(z) - \kappa_{11}\Phi(z) \end{aligned} \tag{2.287}$$

where $W(z) = u'(z)$, $\Phi(z) = \phi'(z)$, and the prime denotes the derivative with respect to the argument z.

The mechanical boundary conditions on the crack faces are

$$\tau_{23}(x)^+ = \tau_{23}(x)^- = 0, \quad |x| < a, \tag{2.288}$$

$$u_z(x)^- = u_z(x)^-, |x| \geq a \tag{2.289}$$

where the superscripts '+' and '-' refer, respectively, to the upper and lower crack faces. The electric boundary conditions over the crack surface are given by [52]

$$\begin{aligned} &E_2(x)^+ = E_2(x)^- = C_r E_0(x), \quad |x| < a, \\ &\phi(x)^+ = \phi(x)^-, \qquad\qquad\quad |x| \geq a, \end{aligned} \tag{2.290}$$

where $E_0(x)$ is the boundary value of $E_y(z)$ on the crack faces due to external

loading without the disturbance of the crack. C_r is referred to as the electric crack condition parameter [52].

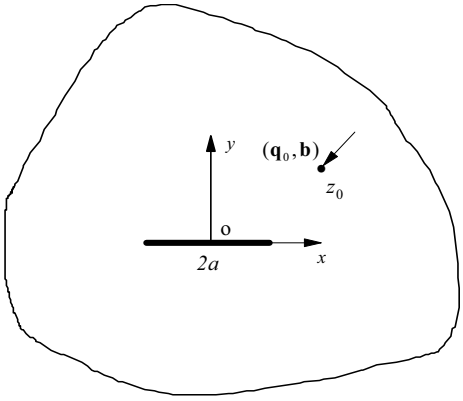

Fig. 2.11 Anti-plane solid with a finite crack

2.11.2 Green's function of the anti-plane problem

To obtain the Green's function of the anti-plane problem described above, assume that a screw dislocation b_z, a line force f, a line charge q, and an electric potential jump b_ϕ are located at a point $z_0(x_0,y_0)$ in an infinite piezoelectric plate (see Fig. 2.11). Using the concept of perturbation technique, the complex potential W and Φ can be assumed in the form [52]

$$W(z) = W_0(z) + W_1(z), \quad \Phi(z) = \Phi_0(z) + \Phi_1(z), \tag{2.291}$$

where $W_1(z)$ and $\Phi_1(z)$ are two analytical functions corresponding to the perturbed field due to the existence of the crack. $W_0(z)$ and $\Phi_0(z)$ are associated with the unperturbed fields without the crack, and can be written as

$$W_0(z) = \frac{(A_1 + iA_2)}{z - z_0}, \quad \Phi_0(z) = \frac{(B_1 + iB_2)}{z - z_0}, \tag{2.292}$$

where A_1, A_2, B_1, and B_2 are constants which can be determined from the following conditions:

$$\int_C \tau_{3j} n_j ds = -f, \quad \int_C D_j n_j ds = q, \tag{2.293}$$

$$\int_C \frac{\partial u_z}{\partial s} ds = b_z, \quad \int_C \frac{\partial \phi}{\partial s} ds = b_\phi \tag{2.294}$$

Substituting Eq (2.286) into Eqs (2.293) and (2.294) yields

$$A_1 = \frac{b_z}{2\pi}, \ A_2 = \frac{e_{15}q - \kappa_{11}f}{2\pi(c_{44}\kappa_{11} + e_{15}^2)}, \ B_1 = \frac{b_\phi}{2\pi}, \ B_2 = -\frac{c_{44}q + e_{15}f}{2\pi(c_{44}\kappa_{11} + e_{15}^2)}, \tag{2.295}$$

Making use of Eq $(2.287)_3$, the condition (2.288) yields

$$c_{44}[W(x)^+ + \overline{W}(x)^-] + e_{15}[\Phi(x)^+ + \overline{\Phi}(x)^-] = 0, \quad |x| < a \tag{2.296}$$

and

$$c_{44}[W(x)^- + \overline{W}(x)^+] + e_{15}[\Phi(x)^- + \overline{\Phi}(x)^+] = 0, \quad |x| < a \tag{2.297}$$

The subtraction and addition of Eqs (2.296) and (2.297), respectively, provides

$$\begin{aligned} &c_{44}\{[W(x) - \overline{W}(x)]^+ - [W(x) - \overline{W}(x)]^-\} \\ &\quad + e_{15}\{[\Phi(x) - \overline{\Phi}(x)]^+ - [\Phi(x) - \overline{\Phi}(x)]^-\} = 0, \quad |x| < a \end{aligned} \tag{2.298}$$

and

$$\begin{aligned} &c_{44}\{[W(x) + \overline{W}(x)]^+ + [W(x) + \overline{W}(x)]^-\} \\ &\quad + e_{15}\{[\Phi(x) + \overline{\Phi}(x)]^+ + [\Phi(x) + \overline{\Phi}(x)]^-\} = 0, \quad |x| < a \end{aligned} \tag{2.299}$$

Substituting Eq (2.291) into Eqs (2.298) and (2.299), we have

$$\begin{aligned} &c_{44}\{[W_1(x) - \overline{W}_1(x)]^+ - [W_1(x) - \overline{W}_1(x)]^-\} \\ &\quad + e_{15}\{[\Phi_1(x) - \overline{\Phi}_1(x)]^+ - [\Phi_1(x) - \overline{\Phi}_1(x)]^-\} = 0, \quad |x| < a \end{aligned} \tag{2.300}$$

$$\begin{aligned} &c_{44}\{[W_1(x) + \overline{W}_1(x)]^+ + [W_1(x) + \overline{W}_1(x)]^-\} \\ &\quad + e_{15}\{[\Phi_1(x) + \overline{\Phi}_1(x)]^+ + [\Phi_1(x) + \overline{\Phi}_1(x)]^-\} = -2F_0(x), \quad |x| < a \end{aligned} \tag{2.301}$$

where

$$F_0(x) = c_{44}\left(\frac{A_1 + iA_2}{x - z_0} + \frac{A_1 - iA_2}{x - \overline{z}_0}\right) + e_{15}\left(\frac{B_1 + iB_2}{x - z_0} + \frac{B_1 - iB_2}{x - \overline{z}_0}\right) \tag{2.302}$$

The solution for Eqs (2.300) and (2.301) can be written as [44]

$$c_{44}W_1(z) + e_{15}\Phi_1(z) = -c_{44}F_w(z) - e_{15}F_\phi(z), \tag{2.303}$$

in which

$$\begin{aligned} F_w(z) = &\frac{A_1 + iA_2}{2(z - z_0)} + \frac{A_1 - iA_2}{2(z - \overline{z}_0)} - \frac{A_1 + iA_2}{2\sqrt{z^2 - a^2}}\left(\frac{\sqrt{z_0^2 - a^2}}{z - z_0} + 1\right) \\ &- \frac{A_1 - iA_2}{2\sqrt{z^2 - a^2}}\left(\frac{\sqrt{\overline{z}_0^2 - a^2}}{z - \overline{z}_0} + 1\right), \end{aligned} \tag{2.304}$$

$$\begin{aligned} F_\phi(z) = &\frac{B_1 + iB_2}{2(z - z_0)} + \frac{B_1 - iB_2}{2(z - \overline{z}_0)} - \frac{B_1 + iB_2}{2\sqrt{z^2 - a^2}}\left(\frac{\sqrt{z_0^2 - a^2}}{z - z_0} + 1\right) \\ &- \frac{B_1 - iB_2}{2\sqrt{z^2 - a^2}}\left(\frac{\sqrt{\overline{z}_0^2 - a^2}}{z - \overline{z}_0} + 1\right) \end{aligned} \tag{2.305}$$

In a similar way, the condition (2.290) provides

$$\Phi_1(z) = (C_r - 1)F_\phi(z) \tag{2.306}$$

Substituting Eq (2.306) into Eq (2.303), we have

$$W_1(z) = -F_w(z) - \frac{C_r e_{15}}{c_{44}} F_\phi(z) \tag{2.307}$$

Chen et al [52] indicated that the solutions (2.306) and (2.307) correctly recover both the impermeable and permeable crack solutions as limiting cases. The impermeable crack solution is obtained by letting C_r=0, while the permeable crack solution is achieved by setting C_r=1. The Green's function of u_z and ϕ are obtained by integrating Eqs (2.306) and (2.307) with respect to z, i.e.

$$u_z(z) = \mathrm{Im}[(A_1 + iA_2)\ln(z - z_0) - \int\{F_w(z) + \frac{C_r e_{15}}{c_{44}} F_\phi(z)\}dz] \tag{2.308}$$

$$\phi(z) = \mathrm{Im}[(B_1 + iB_2)\ln(z - z_0) + (C_r - 1)\int F_\phi(z)dz] \tag{2.309}$$

in which the integral constants representing rigid body motion have been ignored.

2.12 Dynamic Green's function

2.12.1 Dynamic anti-plane problem [53]

Green's function of the dynamic anti-plane problem for a piezoelectric plate subjected to a time harmonic line force $fe^{i\omega t}$ and a line charge $qe^{i\omega t}$ at the origin of the plate, with ω being the circular frequency, is presented in this section. Since the anti-plane problem contains only the out-of-plane displacement u_z and electric potential ϕ, which are functions of the plane coordinates x_1 and x_2, the governing differential equations can be written as

$$\begin{aligned} &c_{44}\nabla_2 u_z + e_{15}\nabla_2\phi + \rho\omega^2 u_z = -f\delta(x_1)\delta(x_2), \\ &e_{15}\nabla_2 u_z - \kappa_{11}\nabla_2\phi = q\delta(x_1)\delta(x_2) \end{aligned} \tag{2.310}$$

where ρ is the mass density of the piezoelectric plate. When $c_{44}\kappa_{11} + e_{15}^2 \neq 0$, Eq (2.310) may be further written as

$$\begin{aligned} &\nabla_2 u_z + \frac{\rho\omega^2\kappa_{11}}{c_{44}\kappa_{11} + e_{15}^2} u_z = \frac{e_{15}q - \kappa_{11}f}{c_{44}\kappa_{11} + e_{15}^2}\delta(x_1)\delta(x_2), \\ &\nabla_2\phi + \frac{\rho\omega^2 e_{15}}{c_{44}\kappa_{11} + e_{15}^2} u_z = \frac{-e_{15}f - c_{44}q}{c_{44}\kappa_{11} + e_{15}^2}\delta(x_1)\delta(x_2) \end{aligned} \tag{2.311}$$

Making use of the new function [53]

$$\mu = \phi - \frac{e_{15}}{\kappa_{11}} u_z \tag{2.312}$$

Eq (2.311) can be converted to the following equivalent system:

$$\begin{aligned} &\nabla_2 u_z + k^2 u_z = \frac{e_{15}q - \kappa_{11}f}{c_{44}\kappa_{11} + e_{15}^2}\delta(x_1)\delta(x_2), \\ &\nabla_2\mu = \frac{q}{\kappa_{11}}\delta(x_1)\delta(x_2) \end{aligned} \tag{2.313}$$

where k is the wave number given by

$$k = \omega\sqrt{\frac{\rho\kappa_{11}}{c_{44}\kappa_{11} + e_{15}^2}} \tag{2.314}$$

It is evident from Eq (2.313) that the original problem is equivalent to the determination of the Green's functions for the 2D Helmholtz equation as well as for the 2D Laplace equation, which are well-known in the literature [53] as

$$u_z = -i\frac{e_{15}q - \kappa_{11}f}{4(c_{44}\kappa_{11} + e_{15}^2)}H_0^{(1)}(kr), \quad \mu = -\frac{q}{2\pi\kappa_{11}}\ln r, \tag{2.315}$$

where $H_0^{(1)}$ is the zeroth order Hankel function of the first kind. From Eq (2.312) one obtains the explicit expression of ϕ as

$$\phi = -\frac{q}{2\pi\kappa_{11}}\ln r - i\frac{e_{15}(e_{15}q - \kappa_{11}f)}{4\kappa_{11}(c_{44}\kappa_{11} + e_{15}^2)}H_0^{(1)}(kr) \tag{2.316}$$

2.12.2 3D Dynamic Green's function

In this section, the Radon transform is used to derive 3D dynamic Green's functions. The discussion follows the results presented in [54].

Consider a homogeneous piezoelectric solid whose motion in the Euclidean space is described in terms of the independent variables $\mathbf{x} = \{x_i\}$ and t. The piezoelectric solid is subjected to an impulsive mechanical point force and an impulsive electric point charge at the origin $\mathbf{x}$=0. The Green's function of this problem is governed by the following differential equations:

$$E_{iJKl}G_{KM,il}(\mathbf{x},t) - \rho\delta_{JK}^{*}\ddot{G}_{KM}(\mathbf{x},t) = -\delta_{JM}\delta(\mathbf{x})\delta(t), \tag{2.317}$$

and the initial conditions

$$G_{KM}(\mathbf{x},t) = 0, \qquad \text{for } t < 0, \tag{2.318}$$

where the dots over a variable denote temporal derivatives, G_{KM} denotes Green's function of displacement in the x_k-direction (K=1,2,3) or electric potential (K=4) at the field point $\mathbf{x}$ due to an impulsive point force in the x_M-direction (M=1,2,3) or an impulsive electric charge (M=4) at the source point $\mathbf{x}$=0, and δ_{JK}^{*} is the generalized Kronecker delta defined by

$$\delta_{JK}^{*} = \begin{cases} \delta_{JK}, & J,K = 1,2,3, \\ 0, & \text{otherwise} \end{cases} \tag{2.319}$$

The Green's function $G_{IJ}(\mathbf{x},t)$ can be obtained by applying the Radon transform defined by (2.6) to Eqs (2.317) and (2.318) [7]

$$K_{JK}(\mathbf{n})\frac{\partial^2\hat{G}_{KM}(\omega,t)}{\partial\omega^2} - \rho\delta_{JK}^{*}\frac{\partial^2\hat{G}_{KM}(\omega,t)}{\partial t^2} = -\delta_{JM}\delta(\omega)\delta(t), \tag{2.320}$$

$$\hat{G}_{KM}(\omega,t) = 0, \qquad \text{for } t < 0, \tag{2.321}$$

where ω is the parameter of the radon transform which is defined by $\omega = \mathbf{n}\cdot\mathbf{x}$ with $\mathbf{n}$ being a unit vector, and $K_{IJ}(\mathbf{n})$ is the generalized Christoffel tensor used in Eq (2.5)

and is rewritten here for convenience

$$K_{JK}(\mathbf{n}) = E_{iJKl} n_i n_l \tag{2.322}$$

We consider, as the first step, the Green's function due to a mechanical point load. Eq (2.320) can be, in this case, rewritten as

$$K_{jk}\frac{\partial^2 \hat{G}_{km}(\omega,t)}{\partial \omega^2} + K_{j4}\frac{\partial^2 \hat{G}_{4m}(\omega,t)}{\partial \omega^2} - \rho\delta_{jk}\frac{\partial^2 \hat{G}_{km}(\omega,t)}{\partial t^2} = -\delta_{jm}\delta(\omega)\delta(t), \tag{2.323}$$

$$K_{4k}\frac{\partial^2 \hat{G}_{km}(\omega,t)}{\partial \omega^2} + K_{44}\frac{\partial^2 \hat{G}_{4m}(\omega,t)}{\partial \omega^2} = 0 \tag{2.324}$$

Solving Eq (2.324) for $\hat{G}_{4m,\omega\omega}$, and then substituting it back to Eq (2.323), we have

$$L_{jk}\frac{\partial^2 \hat{G}_{km}(\omega,t)}{\partial \omega^2} - \rho\delta_{jk}\frac{\partial^2 \hat{G}_{km}(\omega,t)}{\partial t^2} = -\delta_{jm}\delta(\omega)\delta(t), \tag{2.325}$$

where $L_{jk} = K_{jk} - K_{j4}K_{4k}/K_{44}$. It is obvious that the solution of Eq (2.325) depends on the eigenvalues of the matrix L_{jk}. The eigenvalues, denoted by λ_q, are the roots of the characteristic equation [54]

$$\det(L_{jk} - \lambda\delta_{jk}) = 0 \tag{2.326}$$

If λ_q are all distinct, L_{jk} can be expressed in terms of λ_q as

$$L_{jk} = \sum_{q=1}^{3} \lambda_q P_{jk}^q, \tag{2.327}$$

where P_{jk}^q are the projection operators of the matrix L_{jk} with the following properties [55]

$$P_{ji}^p P_{ik}^q = \delta_{pq} P_{jk}^q, \quad \sum_{q=1}^{3} P_{ji}^q = \delta_{ji} \tag{2.328}$$

They are given by [54]

$$P_{jk}^q = \frac{A_{jk}^q}{A_{ii}^q}, \quad A_{jk}^q = \mathrm{adj}(L_{jk} - \lambda_q\delta_{jk}) \tag{2.329}$$

where 'adj' represents the adjoint matrix of a square matrix. If λ_q is not a simple root, the projectors can be determined indirectly by using Eq (2.328). For example, when $\lambda_1 \neq \lambda_2 = \lambda_3$, P_{jk}^1 is given by Eq (2.329), while $P_{jk}^2 = 1 - P_{jk}^1$.

By multiplying both sides of Eq (2.325) by P_{ij}^q and using the properties of the projection operators (2.327) and (2.328), we have

$$\left(\lambda_q\frac{\partial^2}{\partial \omega^2} - \rho\frac{\partial^2}{\partial t^2}\right) P_{ij}^q \hat{G}_{jm}(\omega,t) = -P_{im}^q \delta(\omega)\delta(t), \tag{2.330}$$

It should be mentioned that in Eq (2.330) and in the sequel the summation convention does not apply to the suffix q whenever λ_q appears. For each fixed q, i and m, Eq (2.330) represents a one-dimensional wave equation which, together with Eq (2.321),

can be solved by using the well-known d'Alembert solution. The result is

$$P_{ij}^{q}\hat{G}_{jm}(\omega,t)=-\frac{H(t)P_{im}^{q}}{2\rho c_q}[H(\omega+c_q t)-H(\omega-c_q t)] \tag{2.331}$$

where $H(t)$ is defined in Eq (1.46) and $c_q=\sqrt{\lambda_q/\rho}$. Using Eq (2.328), we obtain [54]

$$\hat{G}_{jm}(\omega,t)=H(t)\sum_{q=1}^{Q}\frac{P_{im}^{q}}{2\rho c_q}[H(\omega+c_q t)-H(\omega-c_q t)] \tag{2.332}$$

where Q is the number of distinct roots of Eq (2.326). Making use of Eq (A7) in Appendix A, the inversion of Eq (2.332) followed by some manipulation yields

$$G_{im}(\mathbf{x},t)=-\frac{H(t)}{16\pi^2}\int_{|\mathbf{n}|=1}\sum_{q=1}^{Q}\frac{P_{im}^{q}}{\lambda_q}[\dot{\delta}(c_q t+\mathbf{n}\cdot\mathbf{x})+\dot{\delta}(c_q t-\mathbf{n}\cdot\mathbf{x})]d\mathbf{n} \tag{2.333}$$

Since the two δ-function terms in the integration above yield the same contribution to G_{im}, Eq (2.243) can be further written as

$$G_{im}(\mathbf{x},t)=-\frac{H(t)}{8\pi^2}\int_{|\mathbf{n}|=1}\sum_{q=1}^{Q}\frac{P_{im}^{q}}{\lambda_q}\dot{\delta}(c_q t+\mathbf{n}\cdot\mathbf{x})d\mathbf{n} \tag{2.334}$$

Substituting Eq (2.332) into Eq (2.334), we have

$$\hat{G}_{4m}(\omega,t)=-H(t)\sum_{q=1}^{Q}\frac{K_{4k}P_{km}^{q}}{2\rho c_q K_{44}}[H(\omega+c_q t)-H(\omega-c_q t)] \tag{2.335}$$

Applying the inverse Radon transform to Eq (2.335) we obtain

$$G_{4m}(\mathbf{x},t)=\frac{H(t)}{8\pi^2}\int_{|\mathbf{n}|=1}\sum_{q=1}^{Q}\frac{K_{4i}P_{im}^{q}}{K_{44}\lambda_q}\dot{\delta}(c_q t+\mathbf{n}\cdot\mathbf{x})d\mathbf{n} \tag{2.336}$$

Eq (2.334) and (2.336) represent the Green's functions due to a mechanical point force. Following essentially the same procedure above, the corresponding Green's functions due to an electric point charge can be obtained. The results are

$$G_{m4}(\mathbf{x},t)=\frac{H(t)}{8\pi^2}\int_{|\mathbf{n}|=1}\sum_{q=1}^{Q}\frac{K_{k4}P_{mk}^{q}}{K_{44}\lambda_q}\dot{\delta}(c_q t+\mathbf{n}\cdot\mathbf{x})d\mathbf{n}, \tag{2.337}$$

$$G_{44}(\mathbf{x},t)=-\frac{H(t)}{8\pi^2}\int_{|\mathbf{n}|=1}\sum_{q=1}^{Q}\frac{K_{4i}P_{im}^{q}K_{m4}}{K_{44}^{2}\lambda_q}\dot{\delta}(c_q t+\mathbf{n}\cdot\mathbf{x})d\mathbf{n}-\frac{\delta(t)}{4\pi R\sqrt{\Lambda}}, \tag{2.338}$$

where

$$\Lambda=\det[\kappa_{ij}],\quad R=\sqrt{\kappa_{ij}^{-1}x_i x_j}, \tag{2.339}$$

with κ_{ij}^{-1} being the inverse components of the dielectric permittivity tensor κ_{ij}. Eqs (2.334), (2.336)-(2.338) can be rewritten in a unified form as

$$G_{IJ}(\mathbf{x},t)=-\frac{H(t)}{8\pi^2}\int_{|\mathbf{n}|=1}\sum_{q=1}^{Q}\frac{\bar{P}_{IJ}^{q}}{\lambda_q}\dot{\delta}(c_q t+\mathbf{n}\cdot\mathbf{x})d\mathbf{n}-\frac{\delta_{4I}\delta_{4J}\delta(t)}{4\pi R\sqrt{\Lambda}} \tag{2.340}$$

where

$$\bar{P}_{IJ}^{q}=\begin{cases} P_{ij}^{q} & I,J=1,2,3, \\ -\dfrac{K_{k4}P_{ik}^{q}}{K_{44}} & I=1,2,3,\quad J=4, \\ \dfrac{K_{4k}P_{kl}^{q}K_{l4}}{K_{44}^{2}} & I=J=4. \end{cases} \tag{2.341}$$

2.13 Green's functions for an infinite medium with a crack

In this section, Green's functions for an infinite medium containing a conducting crack or an impermeable crack are presented based on extended Lekhnitskii's formalism and distributed dislocation modelling. The discussion fellows the results presented in [56].

2.13.1 Green' function for line force/charge

Consider a concentrated line force/charge $\mathbf{P}(P_1, P_2, P_3)$, i.e., horizontal force P_1, vertical force P_2, and electric charge P_3, applied at $\mathbf{z}^0(x_0, y_0)$. The complete Green's functions of an infinite medium were given in Stroh formalism in Section 2.5. With extended Lekhnitskii's formalism, the corresponding expressions of Green's functions can be obtained by substituting the following potentials [56]

$$\Phi_k(z_k)=\frac{1}{2\pi i}\ln(z_k-z_k^0)s_{ki}^{*}P_i \tag{2.342}$$

into Eqs (1.160) and (1.163), where $\Phi_k(z_k)$ is defined in Eq (1.160), and

$$\begin{aligned}
&[s_{ij}^{*}]=[g_{ij}^{*}]^{-1} \\
&g_{1j}^{*}=p_j+\bar{p}_i f_{ij}^{*},\quad g_{2j}^{*}=1+f_{2j}^{*},\quad g_{3j}^{*}=\varpi_j+\bar{\varpi}_i f_{ij}^{*} \\
&f_{1j}^{*}=[q_j^{*}(\bar{p}_2^{*}\bar{t}_3^{*}-\bar{p}_3^{*}\bar{t}_2^{*})-p_j^{*}(\bar{q}_2^{*}\bar{t}_3^{*}-\bar{q}_3^{*}\bar{t}_2^{*})-t_j^{*}(\bar{p}_2^{*}\bar{q}_3^{*}-\bar{p}_3^{*}\bar{q}_2^{*})]/\Delta_1^{*} \\
&f_{2j}^{*}=[p_j^{*}(\bar{q}_1^{*}\bar{t}_3^{*}-\bar{q}_3^{*}\bar{t}_1^{*})-q_j^{*}(\bar{p}_1^{*}\bar{t}_3^{*}-\bar{p}_3^{*}\bar{t}_1^{*})-t_j^{*}(\bar{p}_3^{*}\bar{q}_1^{*}-\bar{p}_1^{*}\bar{q}_3^{*})]/\Delta_1^{*} \\
&f_{3j}^{*}=[q_j^{*}(\bar{p}_1^{*}\bar{t}_2^{*}-\bar{p}_2^{*}\bar{t}_1^{*})-p_j^{*}(\bar{q}_1^{*}\bar{t}_2^{*}-\bar{q}_2^{*}\bar{t}_1^{*})-t_j^{*}(\bar{p}_1^{*}\bar{q}_2^{*}-\bar{p}_2^{*}\bar{q}_1^{*})]/\Delta_1^{*} \\
&\Delta_1^{*}=\bar{p}_1^{*}(\bar{q}_2^{*}\bar{t}_3^{*}-\bar{q}_3^{*}\bar{t}_2^{*})-p_2^{*}(\bar{q}_1^{*}\bar{t}_3^{*}-\bar{q}_3^{*}\bar{t}_1^{*})+p_3^{*}(\bar{q}_1^{*}\bar{t}_2^{*}-\bar{q}_2^{*}\bar{t}_1^{*})
\end{aligned} \tag{2.343}$$

where overbar denotes the complex conjugate of a complex-valued quantity, p_i, ϖ_i, p_i^{*}, q_i^{*}, and t_i^{*} are defined in Eqs (1.154), (1.157) and (1.162).

2.13.2 Green's function for a solid with a crack [56]

In this subsection, Green's functions for an infinite medium containing either an impermeable crack or a conducting crack are presented based on extended Lekhnitskii's formalism. Since this is a linear problem it can be decomposed into two

simple subproblems as shown in Fig. 2.12 (b) and (c). The solution to the subproblem (b)

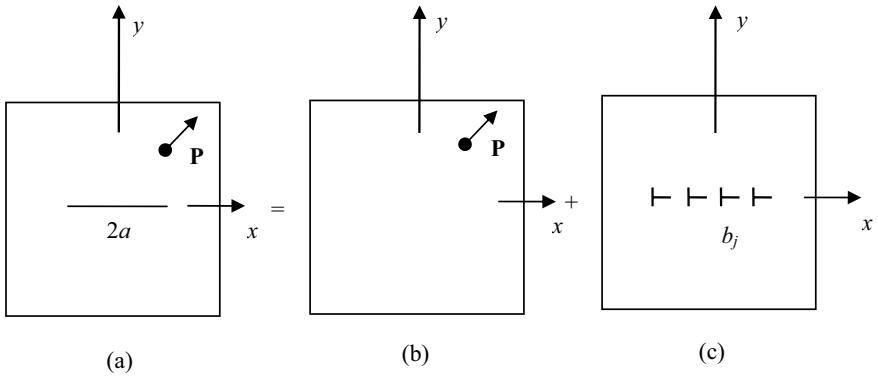

Fig. 2.12 Decomposition used to derive Green's function with a crack[56]

was given by Eq (2.342). For the subproblem in Fig. 2.12(c), a continuous generalized dislocation field with densities **b** is utilized to model the crack. The resultant electroelastic fields on the crack faces due to the line force/charge and distributed dislocation field should satisfy the corresponding boundary conditions. Let us consider first the case of an impermeable crack. The boundary conditions on the crack faces in this case are

$$\sigma_{yy} = 0, \quad \sigma_{xy} = 0, \quad D_y = 0, \quad (-a \le x \le a) \tag{2.344}$$

The solution for problem (c) satisfying the boundary condition of Eq (2.344) is obtained based on the solution (2.70) for a single generalized edge dislocation. The dislocation field **b** is then obtained by enforcing the boundary conditions of Eq (2.344). The final results for the potential functions $\Phi_k(z_k)$ corresponding to the subproblem in Fig 2.12(c) are obtained as

$$\Phi_k(z_k) = \frac{s_{ki}}{2\pi i} \mathrm{Im} \sum_{j=1}^{3} \left[v_{ji} \ln \frac{\sqrt{(z_j^0)^2 - a^2}\sqrt{z_j^2 - a^2} + z_j^0 z_j - a^2}{z_j - z_j^0} s_{jn}^* P_n \right] \tag{2.345}$$

where s_{ij} and v_{ij} are given by [56]

$$
\begin{aligned}
&[s_{ij}]=[g_{ij}]^{-1}\\
&g_{1j}=\overline{p}_j^*+\overline{p}_i^* f_{ij}\,,\quad g_{2j}=q_j^*+\overline{q}_i^* f_{ij}\,,\quad g_{3j}=t_j^*+\overline{t}_i^* f_{ij}\\
&f_{1j}=[\overline{p}_3\varpi_2-\overline{p}_2\varpi_3+p_j\overline{\varpi}_3-p_j\overline{\varpi}_2-\varpi_j\overline{p}_3+\varpi_j\overline{p}_2)]/\Delta_1\\
&f_{2j}=[p_1\overline{\varpi}_3-p_3\overline{\varpi}_1-p_j\overline{\varpi}_3+p_j\overline{\varpi}_1-\varpi_j\overline{p}_1+\varpi_j\overline{p}_3)]/\Delta_1\\
&f_{3j}^*=[\overline{p}_2\overline{\varpi}_1-\overline{p}_1\overline{\varpi}_2-p_j\overline{\varpi}_1+p_j\overline{\varpi}_2-\varpi_j\overline{p}_2+\varpi_j\overline{p}_1)]/\Delta_1\\
&\Delta_1=\overline{p}_1(\overline{\varpi}_2-\overline{\varpi}_3)+\overline{p}_2(\overline{\varpi}_3-\overline{\varpi}_1)+\overline{p}_3(\overline{\varpi}_1-\overline{\varpi}_2)
\end{aligned}
\tag{2.346}
$$

$$
v_{ij}=u_{j1}-p_i u_{j2}-\varpi_i u_{j3} \tag{2.347}
$$

with

$$
[u_{ij}]=[r_{ij}]^{-1} \tag{2.348}
$$

and

$$
\{r_{1j},r_{2j},r_{3j}\}^T=\mathrm{Im}\sum_{n=1}^{3}\{1,-p_n,-\varpi_n\}^T s_{nj} \tag{2.249}
$$

Superposition of Eqs (2.342) and (2.345) yields the complex potential functions corresponding to Green's functions for an impermeable crack.

Similar, for an infinite medium containing a conducting crack whose boundary conditions are defined by

$$
\sigma_{yy}=0,\quad \sigma_{xy}=0,\quad E_x=0,\quad (-a\le x\le a)\,, \tag{2.350}
$$

the potential functions $\Phi_k(z_k)$ corresponding to the subproblem in Fig 2.12(c) can be obtained as [56]

$$
\Phi_k(z_k)=\frac{\hat{s}_{ki}}{2\pi i}\,\mathrm{Im}\sum_{j=1}^{3}\left[\hat{v}_{ji}\ln\frac{\sqrt{(z_j^0)^2-a^2}\sqrt{z_j^2-a^2}+z_j^0 z_j-a^2}{z_j-z_j^0}s_{jn}^* P_n\right] \tag{2.351}
$$

where coefficients are given by

$$
\begin{aligned}
&[\hat{s}_{ij}]=[\hat{g}_{ij}]^{-1}\\
&\hat{g}_{1j}=\overline{p}_j^*+\overline{p}_i^*\hat{f}_{ij}\,,\quad \hat{g}_{2j}=q_j^*+\overline{q}_i^*\hat{f}_{ij}\,,\quad \hat{g}_{3j}=\varpi_j+\overline{\varpi}_i\hat{f}_{ij}\\
&\hat{f}_{1j}=[\overline{p}_3\overline{t}_2^*-\overline{p}_2\overline{t}_3^*+p_j\overline{t}_3^*-p_j\overline{t}_2^*-t_j^*\overline{p}_3+t_j^*\overline{p}_2)]/\hat{\Delta}_1\\
&f_{2j}=[\overline{p}_1\overline{t}_3^*-\overline{p}_3\overline{t}_1^*-p_j\overline{t}_3^*+p_j\overline{t}_1^*-t_j^*\overline{p}_1+t_j^*\overline{p}_3)]/\hat{\Delta}_1\\
&f_{3j}^*=[\overline{p}_2\overline{t}_1^*-\overline{p}_1\overline{t}_2^*-p_j\overline{t}_1^*+p_j\overline{t}_2^*-t_j^*\overline{p}_2+t_j^*\overline{p}_1)]/\hat{\Delta}_1\\
&\hat{\Delta}_1=\overline{p}_1(\overline{t}_2^*-\overline{t}_3^*)+\overline{p}_2(\overline{t}_3^*-\overline{t}_1^*)+\overline{p}_3(\overline{t}_1^*-\overline{t}_2^*)
\end{aligned}
\tag{2.352}
$$

$$\hat{v}_{ij} = \hat{u}_{j1} - p_i \hat{u}_{j2} - t_i^* \hat{u}_{j3} \tag{2.353}$$

with

$$[\hat{u}_{ij}] = [\hat{r}_{ij}]^{-1} \tag{2.354}$$

and

$$\{\hat{r}_{1j}, \hat{r}_{2j}, \hat{r}_{3j}\}^T = \mathrm{Im} \sum_{n=1}^{3} \{1, -p_n, -t_n^*\}^T \hat{s}_{nj} \tag{2.355}$$

Superposition of Eqs (2.342) and (2.351) yields the complex potential functions corresponding to the Green's functions for a conducting crack.

2.14 Approximate expressions of Green's function

In this section we present a review of the approximate expressions of Green's function developed in [57]. In that paper, the authors concentrated on developing approximate Green's functions for two-dimensional transversely isotropic materials subjected to line force/charge. The constitutive relation and differential equations are, in this case, governed by Eqs (1.144) and (1.146). The corresponding Green's function for the two-dimensional electroelastic problem are obtained by solving Eq (2.39). For the convenience of the following derivation, Eq (2.39) is rewritten as

$$\mathbf{L}(\nabla_{\mathbf{x}})\mathbf{G}(\boldsymbol{\xi} - \mathbf{x}) = \delta(\boldsymbol{\xi} - \mathbf{x})\mathbf{I}_3 \tag{2.356}$$

where $\mathbf{I}_3$ is the 3×3 unit matrix, and

$$\mathbf{L}(\nabla_{\mathbf{x}}) = -\begin{bmatrix} c_{11}\dfrac{\partial^2}{\partial x_1^2} + c_{33}\dfrac{\partial^2}{\partial x_2^2} & (c_{12}+c_{33})\dfrac{\partial^2}{\partial x_1 \partial x_2} & (e_{21}+e_{13})\dfrac{\partial^2}{\partial x_1 \partial x_2} \\ (c_{12}+c_{33})\dfrac{\partial^2}{\partial x_1 \partial x_2} & c_{33}\dfrac{\partial^2}{\partial x_1^2} + c_{22}\dfrac{\partial^2}{\partial x_2^2} & e_{13}\dfrac{\partial^2}{\partial x_1^2} + e_{22}\dfrac{\partial^2}{\partial x_2^2} \\ -(e_{21}+e_{13})\dfrac{\partial^2}{\partial x_1 \partial x_2} & -e_{13}\dfrac{\partial^2}{\partial x_1^2} - e_{22}\dfrac{\partial^2}{\partial x_2^2} & \kappa_{11}\dfrac{\partial^2}{\partial x_1^2} + \kappa_{22}\dfrac{\partial^2}{\partial x_2^2} \end{bmatrix} \tag{2.357}$$

In [57], the authors indicated that Eq (2.356) can be solved by the plane wave decomposition approach [16]. That is, **G** is represented over the unit circle $|\mathbf{n}| = 1$ in terms of its transformed function **g** as follows

$$\mathbf{G}(\boldsymbol{\xi} - \mathbf{x}) = \int_{|\mathbf{n}|=1} \mathbf{g}(\mathbf{n}, \omega) d\beta = \int_0^{2\pi} \mathbf{g}(\mathbf{n}, \omega) d\beta \tag{2.358}$$

where $\omega = (\boldsymbol{\xi} - \mathbf{x}) \cdot \mathbf{n}$ in which $\xi_1 - x_1 = |\boldsymbol{\xi} - \mathbf{x}| \cos\theta$, $\xi_2 - x_2 = |\boldsymbol{\xi} - \mathbf{x}| \sin\theta$, $\mathbf{n}=(n_1,n_2)$ $=(\cos\beta, \sin\beta)$. Substituting Eq (2.358) into Eq (2.356) and using the chain rule leads to

$$\mathbf{L}(\nabla_{\mathbf{x}}) \int_0^{2\pi} \mathbf{g}(\mathbf{n}, \omega) d\beta = \int_0^{2\pi} \mathbf{L}(\mathbf{n}) \frac{\partial^2}{\partial \omega^2} \mathbf{g}(\mathbf{n}, \omega) d\beta = \delta(\boldsymbol{\xi} - \mathbf{x})\mathbf{I}_3 \tag{2.359}$$

where

$$\mathbf{L}(\mathbf{n}) = -\begin{bmatrix} A_{11} & A_{12} & A_{13} \\ A_{12} & A_{22} & A_{23} \\ A_{13} & A_{23} & A_{33} \end{bmatrix} \tag{2.360}$$

with

$$\begin{aligned} &A_{11} = c_{11}n_1^2 + c_{33}n_2^2, \quad A_{12} = (c_{12} + c_{33})n_1 n_2, \quad A_{13} = (e_{21} + e_{13})n_1 n_2, \\ &A_{22} = c_{33}n_1^2 + c_{22}n_2^2, \quad A_{23} = e_{13}n_1^2 + e_{22}n_2^2, \qquad A_{33} = \kappa_{11}n_1^2 + \kappa_{22}n_2^2 \end{aligned} \tag{2.361}$$

For obtaining explicit expression of the function $\mathbf{g}(\mathbf{n},\omega)$ in Eq (2.359), consider the function

$$f(\boldsymbol{\xi} - \mathbf{x}) = a\int_0^{2\pi} \ln\left|(\boldsymbol{\xi} - \mathbf{x})\cdot\mathbf{n}\right| d\beta \tag{2.362}$$

Since

$$\ln\left|(\boldsymbol{\xi} - \mathbf{x})\cdot\mathbf{n}\right| = \ln\left[\left|\boldsymbol{\xi} - \mathbf{x}\right|\left|\frac{\boldsymbol{\xi} - \mathbf{x}}{|\boldsymbol{\xi} - \mathbf{x}|}\cdot\mathbf{n}\right|\right] = \ln\left|\boldsymbol{\xi} - \mathbf{x}\right| + \ln\left|\cos(\beta - \theta)\right|, \tag{2.363}$$

it follows that

$$f(\boldsymbol{\xi} - \mathbf{x}) = 2\pi\ln\left|(\boldsymbol{\xi} - \mathbf{x})\right| + a\int_0^{2\pi} \ln\left|\cos(\beta - \theta)\right| d\beta \tag{2.364}$$

where the second term is a constant. Using the identity [57]

$$\delta(\boldsymbol{\xi} - \mathbf{x}) = \frac{1}{2\pi}\nabla_2 \ln\left|(\boldsymbol{\xi} - \mathbf{x})\right| \tag{2.365}$$

where

$$\nabla_2 = \frac{\partial^2}{\partial x_1^2} + \frac{\partial^2}{\partial x_2^2}, \tag{2.366}$$

and then by applying ∇_2 to Eq (2.362) and taking $a = 1/4\pi^2$, we have

$$\delta(\boldsymbol{\xi} - \mathbf{x}) = \nabla_2 f(\boldsymbol{\xi} - \mathbf{x}) = \frac{1}{4\pi^2}\int_0^{2\pi} \frac{\partial^2}{\partial\omega^2}\ln\left|\omega\right| d\beta \tag{2.367}$$

By comparing Eq (2.367) with Eq $(2.359)_2$, we obtain

$$\mathbf{L}(\mathbf{n})\mathbf{g}(\mathbf{n},\omega) = \frac{1}{4\pi^2}\ln\left|\omega\right|\mathbf{I}_3 \tag{2.368}$$

Consequently

$$\mathbf{g}(\mathbf{n},\omega) = \frac{1}{4\pi^2}\mathbf{L}^{-1}(\mathbf{n})\ln\left|\omega\right| \tag{2.369}$$

To simplify the calculation of $\mathbf{g}(\mathbf{n},\omega)$ in Eq (2.369) and avoid making use of numerical integration in Eq (2.358), express the coefficients L_{ij}^{-1} as a Fourier series in terms of the parameter β such that [57]

$$L_{ij}^{-1}(\beta)=\frac{a_{ij}^{(0)}}{2}+\sum_{k=1}^{\infty}[a_{ij}^{(k)}\cos(2k\beta)+b_{ij}^{(k)}\sin(2k\beta)] \tag{2.370}$$

where

$$a_{ij}^{(k)}=\frac{1}{\pi}\int_0^{2\pi}L_{ij}^{-1}(\beta)\cos(2k\beta)d\beta \qquad (k=1,2,3,\ldots) \tag{2.371}$$

$$b_{ij}^{(k)}=\frac{1}{\pi}\int_0^{2\pi}L_{ij}^{-1}(\beta)\sin(2k\beta)d\beta \qquad (k=1,2,3,\ldots) \tag{2.372}$$

It should be mentioned that the periodicity property of $L_{ij}(\beta)=L_{ij}(\beta+\pi)$ has been used in Eq (2.370).

Substituting Eq (2.370) into Eq (2.369) and subsequently into Eq (2.358) and integrating yields

$$G_{ij}(\boldsymbol{\xi}-\mathbf{x})=\frac{1}{4\pi}\left\{a_{ij}^{(0)}\ln|\boldsymbol{\xi}-\mathbf{x}|+\sum_{k=1}^{\infty}\frac{(-1)^{k+1}}{k}[a_{ij}^{(k)}\cos(2k\beta)+b_{ij}^{(k)}\sin(2k\beta)]\right\}+\text{const.} \tag{2.373}$$

where the constant term is associated with rigid displacement or a reference potential and can be omitted in engineering analysis.

As indicated by Khutoryansky et al [57], the approximate Green's function has the following features:

(a) The coefficients $a_{ij}^{(k)}$ and $b_{ij}^{(k)}$ need to be calculated only once for each integral independently of the value $\boldsymbol{\xi}$-$\mathbf{x}$.

(b) $L_{ij}^{-1}(\beta)$ is a rational function of cos2β and sin2β with the denominator being a cubic polynomial of cos2β. Using the roots of this polynomial one can calculate exactly all the coefficients $a_{ij}^{(k)}$ and $b_{ij}^{(k)}$.

(c) For most piezoelectric materials these coefficients decrease very rapidly as $k\to\infty$. Therefore, instead of Eq (2.373) we can use the following approximate Green's functions

$$G_{ij}(\boldsymbol{\xi}-\mathbf{x})\approx\frac{1}{4\pi}\left\{a_{ij}^{(0)}\ln|\boldsymbol{\xi}-\mathbf{x}|+\sum_{k=1}^{m}\frac{(-1)^{k+1}}{k}[a_{ij}^{(k)}\cos(2k\beta)+b_{ij}^{(k)}\sin(2k\beta)]\right\} \tag{2.374}$$

where *m* should be chosen to satisfy the required accuracy.

2.15 Green's functions for time-dependent thermo-piezoelectricity

Applications of Radon transform technique to deriving Green's functions of time-dependent thermo-piezoelectricity are discussed in this section. The presentation here is from the development in [58].

For a thermo-piezoelectric solid under quasi-static conditions, its differential equations governing mechanical and electric behaviour were defined in Eq (1.59) and constitutive equations were given in Eq (1.55). In terms of entropy balance, the heat conduction equation $(1.59)_3$ is rewritten as

$$h_{i,i}+T_0\dot{s}+b_t=0 \tag{2.375}$$

in order to include the effect of heat source density b_t, where $T=T^a-T_0<<T_0$ is assumed.

The Fourier law for heat conduction of anisotropic solid is

$$h_i = k_{ij}\Phi_j \tag{2.376}$$

where $\Phi_j = -T_{,j}$ is the temperature gradient.

2.15.1 Green's functions

Consider a solid which is subjected to a point force F_i, a point electric charge F_e, and a point heat source F_t at the source point $\hat{\mathbf{x}}$. Note that F_i, F_e, and F_t are unity, but are used here as a bookkeeping device [58]. Making use of Eqs (1.49), (1,51), (1.55), and (2.376), Eqs $(1.55)_{1,2}$ and (2.375) can be written in the form [58]

$$\left(c_{ijkl} + \frac{T_0\lambda_{ij}\lambda_{kl}}{\rho c_v}\right)u_{k,lj} + \left(e_{ijl} - \frac{T_0\lambda_{ij}\chi_l}{\rho c_v}\right)\phi_{,lj} - \frac{T_0\lambda_{ij}}{\rho c_v}s_{,j} + F_i\delta(\mathbf{x}-\hat{\mathbf{x}})H(t) = 0 \tag{2.377}$$

$$\left(e_{lij} - \frac{T_0\lambda_{ij}\chi_l}{\rho c_v}\right)u_{i,jl} - \left(\kappa_{ik} - \frac{T_0\chi_i\chi_k}{\rho c_v}\right)\phi_{,ik} + \frac{T_0\chi_i}{\rho c_v}s_{,i} + F_e\delta(\mathbf{x}-\hat{\mathbf{x}})H(t) = 0 \tag{2.378}$$

$$k_{ij}T_{,ij} - T_0\dot{s} + F_t\delta(\mathbf{x}-\hat{\mathbf{x}})\delta(t) = 0 \tag{2.379}$$

where $H(t)$ is the Heaviside step function.

Applying the Radon transform to both sides of Eqs (2.377) and (2.378) leads to

$$\left(c_{ijkl} + \frac{T_0\lambda_{ij}\lambda_{kl}}{\rho c_v}\right)n_j n_l \hat{u}_k'' + \left(e_{ijl} - \frac{T_0\lambda_{ij}\chi_l}{\rho c_v}\right)n_j n_l \hat{\phi}'' - \frac{T_0\lambda_{ij}}{\rho c_v}n_j\hat{s}' + F_i\delta(\omega)H(t) = 0 \tag{2.380}$$

$$\left(e_{lij} - \frac{T_0\lambda_{ij}\chi_l}{\rho c_v}\right)n_l n_j \hat{u}_i'' - \left(\kappa_{ik} - \frac{T_0\chi_i\chi_k}{\rho c_v}\right)n_i n_k \hat{\phi}'' + \frac{T_0\chi_i}{\rho c_v}n_i\hat{s}' + F_e\delta(\omega)H(t) = 0 \tag{2.381}$$

where $\omega = \mathbf{n}\cdot\mathbf{x}$, ω and $\mathbf{n}$ are defined in Eq (A1) and Fig. 2.1.

Solving the above two equations simultaneously for $\hat{u}_k''$ and $\hat{\phi}''$ in terms of $\hat{s}'$ yields

$$\hat{u}_k'' = -c_k\hat{s}' - h_{ki}F_i\delta(\omega)H(t) - d_kF_e\delta(\omega)H(t) \tag{2.382}$$

$$\hat{\phi}'' = -e\hat{s}' - r_iF_i\delta(\omega)H(t) - qF_e\delta(\omega)H(t) \tag{2.383}$$

where

$$[h_{ik}] = [b_{ik}]^{-1} \tag{2.384}$$

$$b_{ik} = \left(c_{ijkl} + \frac{T_0\lambda_{ij}\lambda_{kl}}{\rho c_v}\right)n_j n_l + \frac{1}{a}\left[e_{ijl}e_{mnk} - \left(\frac{T_0}{\rho c_v}\right)^2\lambda_{ij}\lambda_{kn}\chi_l\chi_m\right]n_j n_n n_m n_l \tag{2.385}$$

$$a = \left(\kappa_{ik} - \frac{T_0\chi_i\chi_k}{\rho c_v}\right)n_i n_k \tag{2.386}$$

$$c_k = \left(-\frac{1}{a}e_{ijl}\chi_m n_j n_l n_m + \frac{T_0}{a\rho c_v}\lambda_{ij}\chi_l\chi_m n_j n_l n_m - \frac{T_0}{\rho c_v}\lambda_{ij}n_j\right)h_{ki} \tag{2.387}$$

$$d_i = -\frac{1}{a}\left(e_{kml} - \frac{T_0\lambda_{kl}\chi_m}{\rho c_v}\right)n_m n_l h_{ki} \tag{2.388}$$

$$e = \frac{c_k}{a}\left(e_{ilk} + \frac{T_0}{\rho c_v}\lambda_{kl}\chi_i\right)n_i n_l + \frac{T_0}{a\rho c_v}\chi_i n_i \tag{2.389}$$

$$r_i = \frac{1}{a}\left(e_{mlk} + \frac{T_0\lambda_{kl}\chi_m}{\rho c_v}\right)n_m n_l h_{ki} \tag{2.390}$$

$$q = \frac{1}{a}\left[1 + \left(e_{ilk} + \frac{T_0}{\rho c_v}\lambda_{kl}\chi_i\right)n_i n_l d_k\right] \tag{2.391}$$

Applying the Radon transform to Eq $(1.55)_1$ and taking the derivative with respect to ω twice, we have

$$\hat{T}'' = \frac{T_0\left(\hat{s}'' - \lambda_{ij}n_j u_i''' + n_i\chi_i\hat{\phi}'''\right)}{\rho c_v} \tag{2.392}$$

Making use of Eqs (2.382) and (2.383), the relation between $\hat{T}''$ and $\hat{s}''$ can be obtained as

$$\hat{T}'' = g\hat{s}'' + (v_i F_i + wF_e)\delta'(\omega)H(t) \tag{2.393}$$

where

$$g = \frac{T_0}{\rho c_v}(1 + \lambda_{ij}c_i n_j - \chi_i n_i e) \tag{2.394}$$

$$v_i = \frac{T_0}{\rho c_v}(\lambda_{km}h_{ki}n_m - \chi_j n_j r_i) \tag{2.395}$$

$$w = \frac{T_0}{\rho c_v}(\lambda_{km}d_k n_m - \chi_j n_j q) \tag{2.396}$$

Applying the Radon transform to Eq (2.379) leads to

$$k_{ij}n_i n_j\hat{T}'' - T_0\dot{\hat{s}} + F_t\delta(\omega)\delta(t) = 0 \tag{2.397}$$

To eliminate $\hat{T}''$ from Eq (2.397), substituting Eq (2.393) into Eq ((2.397) above, we have

$$\dot{\hat{s}} - A\hat{s}'' = \frac{F_t}{T_0}\delta(\omega)\delta(t) + (B_i F_i + CF_e)\delta'(\omega)H(t) \tag{2.398}$$

where

$$A = \frac{k_{ij}n_i n_j g}{T_0} \tag{2.399}$$

$$B_k = \frac{k_{ij}n_i n_j v_k}{T_0} \tag{2.400}$$

$$C = \frac{k_{ij} n_i n_j w}{T_0} \tag{2.401}$$

In order to obtain Green's functions for each loading condition, consider first the effect of a unit force in the *i*th direction acting at the source point $\hat{\mathbf{x}}$ and beginning at time zero. Eq (2.398), in this case, becomes

$$\dot{\hat{s}} - A\hat{s}'' = B_i \delta'(\omega) H(t) \tag{2.402}$$

Its solution is well established in the literature [59]:

$$\hat{s}(\omega, t) = -\frac{B_i}{2A} \operatorname{erf}\left(\frac{\omega}{2\sqrt{At}} \right) \tag{2.403}$$

where erf represents the error function defined by

$$\operatorname{erf}(x) = \frac{2}{\sqrt{\pi}} \int_0^x \exp\left(-\frac{y^2}{2} \right) dy \tag{2.404}$$

Substituting Eq (2.403) into Eqs (2.382), (2.383) and (2.392) leads to the second-order derivative for displacements, electric potential, and temperature in the transform domain as

$$\hat{u}_{ij}'' = \frac{B_i c_j}{4\sqrt{tA^3}} \exp\left(-\frac{\omega^2}{4At} \right) - h_{ji} \delta(\omega) H(t) \tag{2.405}$$

$$\hat{\phi}_i'' = \frac{B_i f}{4\sqrt{tA^3}} \exp\left(-\frac{\omega^2}{4At} \right) - q_i \delta(\omega) H(t) \tag{2.406}$$

$$\hat{T}_i'' = \frac{B_i g \omega}{8\sqrt{t^3 A^5}} \exp\left(-\frac{\omega^2}{4At} \right) + v_i \delta'(\omega) H(t) \tag{2.407}$$

where

$$f = \frac{1}{a}\left(e_{ijk} + \frac{T_0 \lambda_{kj} \chi_i}{\rho c_v} \right) n_i n_j c_k + \frac{T_0 \chi_i n_i}{\rho c_v} \tag{2.408}$$

$$q_m = \frac{1}{a}\left(e_{ijk} + \frac{T_0 \lambda_{kj} \chi_i}{\rho c_v} \right) n_i n_j h_{km} \tag{2.409}$$

$$v_i = \frac{T_0}{c_v}\left(\lambda_{jk} n_k h_{ji} - \chi_j n_j q_i \right) \tag{2.410}$$

Similarly, Green's functions for a unit point charge acting at the point $\hat{\mathbf{x}}$ and beginning at time zero can be obtained as

$$\hat{u}_{4i}'' = \frac{C c_i}{4\sqrt{tA^3}} \exp\left(-\frac{\omega^2}{4At} \right) - d_i \delta(\omega) H(t) \tag{2.411}$$

$$\hat{\phi}_4'' = \frac{C e}{4\sqrt{tA^3}} \exp\left(-\frac{\omega^2}{4At} \right) - q \delta(\omega) H(t) \tag{2.412}$$

$$\hat{T}_4'' = \frac{Cg\omega}{8\sqrt{t^3A^5}}\exp\left(-\frac{\omega^2}{4At}\right) + w\delta'(\omega)H(t) \tag{2.413}$$

Finally, the infinite space response to a unit pulse heat source at the point $\hat{\mathbf{x}}$ and beginning at time zero is presented. Eq (2.398), in this case, becomes

$$\dot{\hat{s}} - A\hat{s}'' = \frac{1}{T_0}\delta(\omega)\delta(t) \tag{2.414}$$

The solution to this equation is well known and can be found in many text books [59]:

$$\hat{s}(\omega,t) = \frac{1}{2T_0\sqrt{\pi At}}\exp\left(-\frac{\omega^2}{4At}\right) \tag{2.415}$$

As a result, the derivatives of Green's function components in the transform domain are expressed in the following forms

$$\hat{u}_{5i}'' = \frac{\omega c_i}{4T_0\sqrt{\pi t^3A^3}}\exp\left(-\frac{\omega^2}{4At}\right) \tag{2.416}$$

$$\hat{\phi}_5'' = \frac{\omega e}{4T_0\sqrt{\pi t^3A^3}}\exp\left(-\frac{\omega^2}{4At}\right) \tag{2.417}$$

$$\hat{T}_5'' = \frac{(\omega^2 - 2At)g}{8T_0\sqrt{\pi t^5A^5}}\exp\left(-\frac{\omega^2}{4At}\right) \tag{2.418}$$

In order to obtain Green's functions u_{ij}, ϕ_i, and T_i in the space domain, it is necessary to apply the inverse Radon transform defined in Eq (A3) to Eqs (2.405)-(2.407), (2.411)-(2.413) and (2.416)-(2.418). As a result, the responses to the above three loading cases are obtained as

$$u_{ij}(\mathbf{x}-\hat{\mathbf{x}}) = -\frac{1}{8\pi^2}\oint_{|\mathbf{n}|=1}\frac{B_i(\mathbf{n})c_j(\mathbf{n})}{4\sqrt{tA^3(\mathbf{n})}}\exp\left(-\frac{[\mathbf{n}\cdot(\mathbf{x}-\hat{\mathbf{x}})]^2}{4tA(\mathbf{n})}\right)ds(\mathbf{n}) + \frac{H(t)}{8\pi^2 r}\int_0^{2\pi} h_{ji}d\psi$$

$$\phi_i(\mathbf{x}-\hat{\mathbf{x}}) = -\frac{1}{8\pi^2}\oint_{|\mathbf{n}|=1}\frac{B_i(\mathbf{n})f}{4\sqrt{tA^3(\mathbf{n})}}\exp\left(-\frac{[\mathbf{n}\cdot(\mathbf{x}-\hat{\mathbf{x}})]^2}{4tA(\mathbf{n})}\right)ds(\mathbf{n}) + \frac{H(t)}{8\pi^2 r}\int_0^{2\pi} q_i d\psi$$

$$T_i(\mathbf{x}-\hat{\mathbf{x}}) = -\frac{1}{8\pi^2}\oint_{|\mathbf{n}|=1}\frac{B_i(\mathbf{n})g\mathbf{n}\cdot(\mathbf{x}-\hat{\mathbf{x}})}{8\sqrt{t^3A^5(\mathbf{n})}}\exp\left(-\frac{[\mathbf{n}\cdot(\mathbf{x}-\hat{\mathbf{x}})]^2}{4tA(\mathbf{n})}\right)ds(\mathbf{n}) + \frac{H(t)}{8\pi^2 r^2}\int_0^{2\pi}\frac{\partial v_i}{\partial b}d\psi$$

$$u_{4i}(\mathbf{x}-\hat{\mathbf{x}}) = -\frac{1}{8\pi^2}\oint_{|\mathbf{n}|=1}\frac{Cc_j(\mathbf{n})}{4\sqrt{tA^3(\mathbf{n})}}\exp\left(-\frac{[\mathbf{n}\cdot(\mathbf{x}-\hat{\mathbf{x}})]^2}{4tA(\mathbf{n})}\right)ds(\mathbf{n}) + \frac{H(t)}{8\pi^2 r}\int_0^{2\pi} d_i d\psi$$

$$\phi_4(\mathbf{x}-\hat{\mathbf{x}}) = -\frac{1}{8\pi^2}\oint_{|\mathbf{n}|=1}\frac{eC}{4\sqrt{tA^3(\mathbf{n})}}\exp\left(-\frac{[\mathbf{n}\cdot(\mathbf{x}-\hat{\mathbf{x}})]^2}{4tA(\mathbf{n})}\right)ds(\mathbf{n}) + \frac{H(t)}{8\pi^2 r}\int_0^{2\pi} q d\psi$$

$$T_4(\mathbf{x}-\hat{\mathbf{x}}) = -\frac{1}{8\pi^2}\oint_{|\mathbf{n}|=1}\frac{Cg\mathbf{n}\cdot(\mathbf{x}-\hat{\mathbf{x}})}{8\sqrt{t^3A^5(\mathbf{n})}}\exp\left(-\frac{[\mathbf{n}\cdot(\mathbf{x}-\hat{\mathbf{x}})]^2}{4tA(\mathbf{n})}\right)ds(\mathbf{n}) + \frac{H(t)}{8\pi^2 r^2}\int_0^{2\pi}\frac{\partial w}{\partial b}d\psi$$

$$u_{5i}(\mathbf{x}-\bar{\mathbf{x}}) = -\frac{1}{8\pi^2}\oint_{|\mathbf{n}|=1} \frac{\mathbf{n}\cdot(\mathbf{x}-\bar{\mathbf{x}})c_i(\mathbf{n})}{4\sqrt{\pi t^3 A^3(\mathbf{n})}} \exp\left(-\frac{[\mathbf{n}\cdot(\mathbf{x}-\bar{\mathbf{x}})]^2}{4tA(\mathbf{n})}\right) ds(\mathbf{n})$$

$$\phi_5(\mathbf{x}-\bar{\mathbf{x}}) = -\frac{1}{8\pi^2}\oint_{|\mathbf{n}|=1} \frac{\mathbf{n}\cdot(\mathbf{x}-\bar{\mathbf{x}})e}{4\sqrt{\pi t^3 A^3(\mathbf{n})}} \exp\left(-\frac{[\mathbf{n}\cdot(\mathbf{x}-\bar{\mathbf{x}})]^2}{4tA(\mathbf{n})}\right) ds(\mathbf{n})$$

$$T_5(\mathbf{x}-\bar{\mathbf{x}}) = -\frac{1}{8\pi^2}\oint_{|\mathbf{n}|=1} \frac{[\mathbf{n}\cdot(\mathbf{x}-\bar{\mathbf{x}})]^2 g - 2Atg}{8\sqrt{t^5 A^5(\mathbf{n})}} \exp\left(-\frac{[\mathbf{n}\cdot(\mathbf{x}-\bar{\mathbf{x}})]^2}{4tA(\mathbf{n})}\right) ds(\mathbf{n}) \quad (2.419)$$

where $r = |\mathbf{x}-\bar{\mathbf{x}}|$, $\mathbf{n}\cdot(\mathbf{x}-\bar{\mathbf{x}}) = rb$, and r, b, and ψ are shown in Figs 2.13 and A1. During the derivation, the following identity is used

$$\oint \delta'(x-\bar{x}) f(x)dx = -\oint \delta(x-\bar{x})\frac{\partial f(x)}{\partial x}dx. \quad (2.420)$$

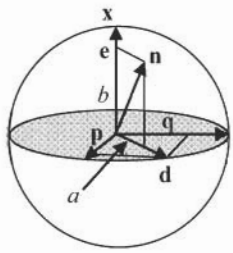

Fig. 2.13 Illustration of variables r, a, b, $\mathbf{n}$ used in Eq (2.419)

2.15.2 Evaluation of inverse Radon transform

In calculating Green's functions from Eq (2.419), one needs to evaluate the inverse Radon transform defined by [58,60]

$$f(\mathbf{x}) = -\frac{1}{8\pi^2}\int_{|\mathbf{n}|=1} \hat{f}(\omega,\mathbf{n})ds(\mathbf{n}) \quad (2.421)$$

To this end, let $\mathbf{e}$ (see Fig. 2.13) be a unit vector in the direction of $\mathbf{x}$ and $\mathbf{d}$ be a unit vector such that

$$\mathbf{d}\cdot\mathbf{e} = 0 \quad (2.422)$$

Thus $\mathbf{e}$ and $\mathbf{d}$ are two orthogonal vectors, and

$$\mathbf{x} = r\mathbf{e} \quad (2.423)$$

or

$$e_i = \frac{x_i}{r} \quad \text{and} \quad r = |\mathbf{x}| \tag{2.424}$$

In the **e**-**d** plane the unit vector **n** is decomposed into

$$\mathbf{n} = a\mathbf{d} + b\mathbf{e} \tag{2.425}$$

where

$$\sqrt{a^2 + b^2} = 1 \tag{2.426}$$

Therefore, $\omega = \mathbf{n} \cdot \mathbf{x} = rb$. It is noted that b ranges from -1 reflecting the negative **x** direction to 1. Furthermore, **d** may be expressed in terms of another parameter ψ (see Figs. 2.13 and A1). On the plane normal to **e**, we have

$$\mathbf{d} = \cos\psi\mathbf{p} + \sin\psi\mathbf{q} \tag{2.427}$$

where p, q, and e form a right-hand coordinate system. Hence,

$$\begin{aligned}\mathbf{n} = {} & \frac{r\sqrt{1-b^2}}{\sqrt{x_1^2 + x_2^2}}\left(\frac{x_2}{r}\cos\psi - \frac{x_1 x_3}{r^2}\sin\psi,\ -\frac{x_1}{r}\cos\psi - \frac{x_2 x_3}{r^2}\sin\psi,\ \frac{x_1^2 + x_2^2}{r^2}\sin\psi\right) \\ & + b\left(\frac{x_1}{r},\ \frac{x_2}{r},\ \frac{x_2}{r}\right)\end{aligned} \tag{2.428}$$

As a result, the surface integral can be expressed in terms of b and ψ as follows

$$f(\mathbf{x}) = -\frac{1}{8\pi^2}\int_0^{2\pi} d\psi \int_{-1}^{1} \hat{f}(rb, \mathbf{n}(b,\psi))db \tag{2.429}$$

Using the property of the Dirac delta function, $\delta(\omega) = \delta(rb) = \delta(b)/r$, we have

$$f(\mathbf{x}) = -\frac{1}{8\pi^2}\int_{|\mathbf{n}|=1} \hat{f}(\omega, \mathbf{n})\delta(\omega)ds(\mathbf{n}) = -\frac{1}{8\pi^2 r}\int_0^{2\pi} \hat{f}(0, \mathbf{n}(0,\psi))d\psi \tag{2.430}$$

If $\hat{f}(\omega, \mathbf{n}) = 1$ in Eq (2.430), we have

$$\int_{|\mathbf{n}|=1} \delta(\omega)ds(\mathbf{n}) = \int_0^{2\pi} d\psi \int_{-1}^{1} \delta(rb)db = \frac{2\pi}{r}. \tag{2.431}$$

References

[1] Mura T, Micromechanics of Defects in Solids, 2nd Edition, Dordrecht: Martinus Nijhoff Publishers, 1987
[2] Qin QH, Fracture mechanics of piezoelectric materials, Southampton: WIT Press, 2001
[3] Qin QH and Mai YW, BEM for crack-hole problems in thermopiezoelectric materials, Eng Frac Mech, 69, 577-588, 2002
[4] Benveniste Y, The determination of the elastic and electric-fields in a piezoelectric inhomogeneity, J Appl Phys, 72, 1086-1095, 1992
[5] Chen T, Green's functions and the non-uniform transformation problem in a piezoelectric medium. Mech Res Commun, 20, 271-278, 1993

[6] Chen T and Lin FZ, Numerical evaluation of derivatives of the anisotropic piezoelectric Green's function, Mech Res Commun, 20, 501-506, 1993
[7] Dunn ML, Electroelastic Green's functions for transversely isotropic media and their application to the solution of inclusion and inhomogeneity problems, Int J Eng Sci, 32, 119-131, 1994
[8] Lee JS and Jiang LZ, Boundary integral formulation and 2D fundamental solution for piezoelectric media, Mech Res Commun, 22, 47－54, 1994
[9] Sosa HA and Castro MA, On concentrated load at boundary of a piezoelectric half-plane, J Mech Phys Solids, 42, 1105-1122, 1994
[10] Dunn ML and Wienecke HA, Green's functions for transversely isotropic piezoelectric solids, Int J Solids Struct, 33, 4571-4581, 1996
[11] Ding HJ, Wang GQ and Chen WQ, A boundary integral formulation and 2D fundamental solutions for piezoelectric media, Comput Meth Appl Mech Eng, 158, 65-80, 1998
[12] Ding HJ, Wang GQ and Jiang AM, Green's function and boundary element method for transversely isotropic piezoelectric materials, Eng Anal Boun Elements, 28, 975-987, 2004
[13] Pan, E. A BEM analysis of fracture mechanics in 2D anisotropic piezoelectric solids, Eng Anal Boun Elements, 23, 67-76, 1999
[14] Gao CF and Fan WX, Green's functions for generalized 2D problems in piezoelectric media with an elliptic hole, Mech Res Commun, 25, 685-693, 1998
[15] Norris AN, Dynamic Green's functions in anisotropic, thermoelastic, and poroelastic solids, Proc R Soc Lond, A447, 175-188, 1994
[16] Khutoryansky NM and Sosa HA, Dynamic representation formulas and fundamental solutions for piezoelectricity, Int J Solids Struct, 32, 3307-3325, 1995
[17] Qin QH, Green's function and its application for piezoelectric plate with various openings, Arch Appl Mech, 69, 133-144, 1999
[18] Qin QH and Mai YW, Crack branch in piezoelectric bimaterial system, Int J Eng Sci, 38, 673-693, 2000
[19] Pan E and Yuan FG, Three-dimensional Green's functions in anisotropic piezoelectric bimaterials, Int J Eng Sci, 38, 1939-1960, 2000
[20] Pan E and Tonon F, Three-dimensional Green's functions in anisotropic piezoelectric solids, Int J Solids Struct, 37, 943-958, 2000
[21] Gao CF and Fan WX, Green's functions for the plane problem in a half-infinite piezoelectric medium, Mech Res Commun, 25, 69-74, 1998
[22] Dunn ML and Wienecke HA, Half-space Green's function for transversely isotropic piezoelectric solids, J Appl Mech, 66, 675-679, 1999
[23] Gao CF and YU JH, Two-dimensional analysis of a semi-infinite crack in piezoelectric media, Mech Res Commun, 25, 695-700, 1998
[24] Chen BJ, Xiao ZM and Liew KM, On the interaction between a semi-infinite anti-crack and a screw dislocation in piezoelectric solid, Int J Eng Sci, 42, 1-11, 2004
[25] Ding HJ, Chen B and Liang J, On the green's functions for two-phase transversely isotropic piezoelectric media, Int J Solids Struct, 34, 3041-3057, 1997
[26] Gao CF, Kessler H and Balke H, Green's function for anti-plane deformations of a circular arc-crack at the interface of piezoelectric materials, Arch Appl Mech, 73, 467-480, 2003
[27] Liu JX, Wang B and Du SY, Line force, charge and dislocation in anisotropic

piezoelectric materials with an elliptic hole or a crack, Mech Res Commun, 24, 399-405, 1997
[28] Lu P and Williams FW, Green's function of piezoelectric materials, with an elliptic hole or inclusion, Int J Solids Struct, 35, 651-664, 1998
[29] Lu P, Tan MJ and Liew KM, A further investigation of Green's functions for a piezoelectric media with a cavity or a crack, Int J Solids Struct, 37, 1065-1078, 2000
[30] Gao CF and Fan WX, A general solution for the plane problem in piezoelectric media with collinear cracks, Int J Eng Sci, 37, 347-363, 1999
[31] Gao CF and Wang MZ, Green's function of an interface crack between two dissimilar piezoelectric media, Int J Solids Struct, 38, 5323-5334, 2001
[32] Gao CF and Wang MZ, General treatment on mode III interfacial crack problems in piezoelectric materials. Arch Appl Mech, 71, 296-306, 2001
[33] Hill LR and Farris TN, Three-dimensional piezoelectric boundary element method, AIAA J, 36, 102-108, 1998
[34] Denda M, Araki Y and Yong YK, Time-harmonic BEM for 2-D piezoelectricity applied to eigenvalue problems, Int J Sloids Struct, 41, 7241-7265, 2004
[35] Ma H and Wang B, The scattering of electroelastic waves by an ellipsoidal inclusion in piezoelectric medium, Int J Sloids Struct, 42, 4541-4554, 2005
[36] Wang CY and Zhang Ch, 3-D and 2-D Dynamic Green's functions and time-domain BIEs for piezoelectric solids, Eng Anal Boun Elements, 29, 454-465, 2005
[37] Deeg, WF, The analysis of dislocation, crack, and inclusion problems in piezoelectric solids, PhD dissertation, Stanford University, 1980
[38] Synge JL, The hypercircle in mathematical physics: a method for the approximate solution of boundary value problems, Cambridge: Cambridge University Press, 1957
[39] Li XY and Wang MZ, Three-dimensional Green's functions for infinite anisotropic piezoelectric media, Int J Solids Struct (in press)
[40] Hadamard J, Lectures on Cauchy's problem in partial differential equations, New Haven: Yale University Press, 1923
[41] Liu JX, Wang B and Du S,Electro-elastic Green's functions for a piezoelectric half-space and their application, Appl Mathe Mech, 18, 1037-1043,1997
[42] Ding HJ, Wang GQ and Chen WQ, Green's functions for a piezoelectric half plane, Science in China Ser E, 41, 70-75, 1998
[43] Ting TCT, Image singularities of Green's functions for anisotropic elastic half-spaces and bimaterials, Q J Mech Appl Math, 45, 119-139, 1992
[44] Muskhelishvili NI, Some Basic Problems of Mathematical Theory of Elasticity, Noordhoff: Groningen, 1954
[45] Suo Z, Kuo CM, Barnett DM and Willis JR, Fracture mechanics for piezoelectric ceramics, J Mech Phys Solids, 40, 739-765, 1992
[46] Ting TCT and Chou SC, Edge singularities in anisotropic composites, Int J Solids Struct, 17, 1057-1068, 1981
[47] Chung MY and Ting TCT, Piezoelectric solid with an elliptic inclusion or hole, Int J Solids Struct, 33, 3343-3361, 1996
[48] Zhou ZD, Zhao SX and Kuang ZB, Stress and electric displacement analyses in piezoelectric media with an elliptic hole and a small crack, Int J Solids Struct, 42, 2803-2822, 2005
[49] Ting TCT, Green's functions for an anisotropic elliptic inclusion under

generalized plane strain deformations, Q J Mech Appl Math, 49, 1-18, 1996
[50] Chung MY and Ting TCT, The Green's function for a piezoelectric piezomagnetic magnetoelectric anisotropic elastic medium with an elliptic hole or rigid inclusion, Phil Mag Letters, 72, 405-410, 1995
[51] Chen BJ, Xiao ZM and Liew KM, A line dislocation interacting with a semi-infinite crack in piezoelectric solid, Int J Eng Sci, 42, 1-11, 2004
[52] Chen BJ, Liew KM and Xiao ZM, Green's function for anti-plane problems in piezoelectric media with a finite crack, Int J Solids Struct, 41, 5285-5300, 2004
[53] Wang X and Zhong Z, Two-dimensional time-harmonic dynamic Green's functions in transversely isotropic piezoelectric solids, Mech Res Commun, 30, 589-593, 2003
[54] Wang CY and Zhang C, 3-D and 2-D Dynamic Green's functions and time-domain BIEs for piezoelectric solids, Eng Anal Boun Elements, 29, 454-465, 2005
[55] Broida J and Williamson SG, A comprehensive introduction to linear algebra, California: Addison-Wesley, 1989
[56] Rajapakse RKND and Xu XL, Boundary element modeling of cracks in piezoelectric solids, Eng Anal Boun Elements, 25, 771-781, 2001
[57] Khutoryansky NM, Sosa HA and Zu WH, Approximate Green's functions and a boundary element method for electroelastic analysis of active materials, Computers & Structures, 66, 289-299, 1998
[58] Jiang LZ, Integral representation and Green's functions for 3D time-dependent thermo-piezoelectricity, Int J Solids Structures, 37, 6155-6171, 2000
[59] Carslaw HS and Jaeger JC, Conduction of heat in solids, 2nd ed., Clarendon Press, Oxford, 1959
[60] Wang CY and Achenbach JD, A new method to obtain 3D Green's functions for anisotropic solids, Wave Motion, 18, 273-289, 1993

Chapter 3 Green's function for thermoelectroelastic problems

3.1 Introduction

In the previous chapter we described Green's functions of piezoelectric material without or with defects such as cracks, holes, bimaterial interface, half-plane boundary, and inclusions. However, the widespread use of piezoelectric materials in structural applications has generated renewed interest in thermoelectroelastic behaviour. In particular, information about thermal stress concentrations around material or geometrical defects in piezoelectric solids has wide application in composite structures. Unlike in the cases of anisotropic elasticity and piezoelectricity, relatively little work has been reported regarding Green's functions in thermoelastic and thermopiezoelectric solids. Using Stroh's formalism and one-to-one mapping methods, Qin [1] obtained Green's functions in closed form for an infinite piezoelectric plate with an elliptic hole induced by temperature discontinuity. Qin and Mai [2,3] also investigated thermoelectroelastic Green's functions for half-plane and bimaterial problems. The studies in [4-6] further investigated thermoelectroelastic Green's functions for piezoelectric materials with various openings or an elliptic inclusion.

In this chapter, we begin with a discussion of Green's functions in free space of thermopiezoelectricity. The results are then extended to cases of infinite thermopiezoelectricity with a half-plane boundary, bimaterial interface, holes of various shapes, and an elliptic inclusion.

3.2 Green's function in free space

3.2.1 General solution in Stroh formalism

Consider an anisotropic piezoelectric solid in which all fields are assumed to depend on in-plane coordinates x_1 and x_2 only. The general solutions of stress and electric displacement (SED) $\mathbf{\Pi}_i$, elastic displacement and electric potential (EDEP) vector $\mathbf{U}$, temperature T, and heat flux h_i in the solid can be expressed in terms of complex analytic functions as follows [3]:

$$\begin{aligned} &T = 2\,\mathrm{Re}[g'(z_t)], \quad h_1 = -\vartheta_{,2}, \quad h_2 = \vartheta_{,1}, \\ &\mathbf{U} = 2\,\mathrm{Re}[\mathbf{A}\langle f(z_\alpha)\rangle \mathbf{q} + \mathbf{c}g(z_t)], \quad \mathbf{\Pi}_1 = -\boldsymbol{\varphi}_{,2}, \quad \mathbf{\Pi}_2 = \boldsymbol{\varphi}_{,1} \end{aligned} \tag{3.1}$$

where

$$\begin{aligned} &\vartheta = 2k\,\mathrm{Im}[g'(z_t)], \quad \boldsymbol{\varphi} = 2\,\mathrm{Re}[\mathbf{B}\langle f(z_\alpha)\rangle \mathbf{q} + \mathbf{d}g(z_t)], \\ &z_t = x_1 + p_1^* x_2, \quad z_\alpha = x_1 + p_\alpha x_2, \end{aligned} \tag{3.2}$$

where ϑ is the heat flux function, p_1^* represents the eigenvalue of heat conduction equation [7], $\langle f(z_\alpha)\rangle$ is defined in Eq (1.131), but it is a 4×4 matrix in this chapter rather than the original 5×5 matrix, an overbar denotes the complex conjugate, a prime represents the differentiation with respect to the argument, $\mathbf{q}$ is a constant vector to be determined by the boundary conditions, $i = \sqrt{-1}$, $k = \sqrt{k_{11}k_{22} - k_{12}^2}$, k_{ij} are the coefficients of heat conduction, and $f(z_i)$ and $g(z_t)$ are arbitrary functions with complex arguments z_i and z_t, respectively. $\mathbf{A}$, $\mathbf{B}$, $\mathbf{c}$ and $\mathbf{d}$ are associated with material constants and are well defined in the literature (see [7], for example).

3.2.2 Green's function in free space

For an infinite space subjected to a line heat source h^* and a line temperature discontinuity $\hat{T}$ both located at $z_{t0}(=x_{10}+p_1^* x_{20})$, the function $g'(z_t)$ can be chosen in the form [3]

$$g'(z_t) = q_0 \ln(z_t - z_{t0}) \tag{3.3}$$

where q_0 is a complex constant which can be determined from the conditions

$$\int_C dT = \hat{T} \qquad \textit{for any closed curve C enclosing the point } z_{t0}, \tag{3.4}$$

and

$$\int_C d\vartheta = -h^* \qquad \textit{for any closed curve C enclosing the point } z_{t0} \tag{3.5}$$

Substitution of Eq (3.3) into Eqs $(3.1)_1$ and $(3.2)_1$, and later into Eqs (3.4) and (3.5), yields

$$q_0 = \hat{T}/4\pi i - h^*/4\pi k \tag{3.6}$$

The function $g(z_t)$ in Eq $(3.1)_4$ or $(3.2)_2$ can be obtained by integrating Eq (3.3) with respect to z_t, which yields

$$g(z_t) = f^*(z_t - z_{t0})q_0 \tag{3.7}$$

where $f^*(x) = x(\ln x - 1)$.

Substituting Eq (3.7) into Eqs $(3.1)_4$ and $(3.2)_2$ and noting that $\mathbf{q} = 0$ for the current thermal problem, the Green's function for electroelastic field in free space is derived as

$$\mathbf{U} = 2\,\mathrm{Re}[\mathbf{c}f^*(z_t - z_{t0})q_0], \quad \boldsymbol{\varphi} = 2\,\mathrm{Re}[\mathbf{d}f^*(z_t - z_{t0})q_0] \tag{3.8}$$

3.3 Half-plane solid

In this section the Green's function in a half-plane piezoelectric solid subjected to loadings h^* and $\hat{T}$, both located at $z_{t0}(=x_{10}+p_1^* x_{20})$, are presented based on the concept of perturbation [8].

3.3.1 Green's function for thermal fields

If the infinite straight boundary of the half-plane solid is in the thermally insulated condition, we have

$$\vartheta = 0 \tag{3.9}$$

To satisfy the thermally insulated condition (3.9), the general solution of the thermal field can be assumed in the form from the concept of perturbation [8],

$$T = 2\,\mathrm{Re}[f_0(z_t) + f_1(z_t)], \qquad \vartheta = 2k\,\mathrm{Im}[f_0(z_t) + f_1(z_t)] \tag{3.10}$$

The function f_0 in Eq (3.10) can be chosen to represent the solutions associated with the unperturbed thermal fields (or the solution for an infinite homogeneous solid), and f_1 is the function corresponding to the perturbed field of the solid due to defects (a half-plane boundary in this Section). f_1=0 if there is no defect in a homogeneous solid. Therefore, f_0 is given by Eq (3.3) as

$$f_0(z_t) = g'(z_t) = q_0 \ln(z_t - z_{t0}) \tag{3.11}$$

Making use of Eq $(3.10)_2$, the thermally insulated condition on the surface $x_2 = 0$, i.e. $\vartheta = 0$, provides

$$f_1(z_t) = \overline{q}_0 \ln(z_t - \overline{z}_{t0}) \tag{3.12}$$

Further, if T= 0, rather than $\vartheta = 0$, on the surface x_2 = 0, we have

$$f_1(z_t) = -\overline{q}_0 \ln(z_t - \overline{z}_{t0}) \tag{3.13}$$

Having obtained the solutions of f_0 and f_1, the function $g'(z_t)$ can now be written as

$$g'(z_t) = q_0 \ln(z_t - z_{t0}) \pm \overline{q}_0 \ln(z_t - \overline{z}_{t0}) \tag{3.14}$$

where the symbol "+" before $\overline{q}_0$ stands for the condition ϑ=0 on the x_1-axis, and "-" stands for the condition T=0 on x_2=0. For the sake of clarity, we always use the symbol "+" in the following derivation. It should be understood that the symbol "+" is replaced by "-" if the boundary condition T=0 on x_2=0 is involved. Substitution of Eq (3.14) into Eq (3.10) yields the Green's functions of temperature and heat flux:

$$T(z_t) = 2\,\mathrm{Re}[q_0 \ln(z_t - z_{t0}) + \overline{q}_0 \ln(z_t - \overline{z}_{t0})], \tag{3.15}$$

$$\vartheta(z_t) = 2k\,\mathrm{Im}[q_0 \ln(z_t - z_{t0}) + \overline{q}_0 \ln(z_t - \overline{z}_{t0})] \tag{3.16}$$

3.3.2 Green's function for electroelastic fields

For linear thermopiezoelectric problems, the solution $(3.2)_2$ can be assumed to consist of a particular part $\boldsymbol{\varphi}_p$, atributable to thermal loading, and a modified part $\boldsymbol{\varphi}_m$, to ensure satisfaction of the half-plane boundary condition, as $\boldsymbol{\varphi} = \boldsymbol{\varphi}_m + \boldsymbol{\varphi}_p$. $\boldsymbol{\varphi}_p$ can be determined from the function $g(z_t)$ defined Eq (3.14). Therefore, the remaining task is to find the modified part $\boldsymbol{\varphi}_m$, which is related to $\boldsymbol{\varphi}_p$ through the traction-charge condition on the boundary x_2=0:

$$\boldsymbol{\varphi} = \boldsymbol{\varphi}_p + \boldsymbol{\varphi}_m = 0 \qquad \text{on } x_2\text{=}0 \tag{3.17}$$

On the basis of the expressions $(3.1)_4$ and $(3.2)_2$, the particular solutions $\mathbf{U}_p$ and $\boldsymbol{\varphi}_p$ for electroelastic fields can be written as

$$\mathbf{U}_p = 2\,\mathrm{Re}[\mathbf{c}g(z_t)], \qquad \boldsymbol{\varphi}_p = 2\,\mathrm{Re}[\mathbf{d}g(z_t)] \tag{3.18}$$

where subscript "p" refers to the particular solution. The function $g(z_t)$ in Eq (3.18) can be obtained by integrating Eq (3.14) with respect to z_t, which yields

$$g(z_t) = q_0 f^*(z_t - z_{t0}) + \overline{q}_0 f^*(z_t - \overline{z}_{t0}) \tag{3.19}$$

The particular solution $\boldsymbol{\varphi}_p$ induced by $g(z_t)$ [see Eq (3.18)] does not, generally, satisfy the traction-charge free condition (3.17) along the axis $x_2 = 0$. We therefore need to find a modified isothermal solution $\boldsymbol{\varphi}_m$ for a given problem such that when it is superposed on the particular electroelastic solution the traction-charge free condition along the axis $x_2 = 0$ will be satisfied. Owing to the fact that $f(z_k)$ and $g(z_t)$ have the same rule affecting the traction-charge in Eq $(3.2)_2$, possible function forms come from the partition of $g(z_t)$. This is

$$\boldsymbol{\varphi}_m = 2\,\mathrm{Re}[\mathbf{B}\langle f(z_\alpha)\rangle \mathbf{q}] \tag{3.20}$$

where

$$f(z_\alpha) = q_0 f^*(z_\alpha - z_{t0}) + \overline{q}_0 f^*(z_\alpha - \overline{z}_{t0}) \tag{3.21}$$

Substitution of Eqs $(3.18)_2$ and (3.20) into Eq (3.17) yields

$$\mathbf{q} = -\mathbf{B}^{-1}\mathbf{d} \tag{3.22}$$

Likewise, if **U**=0 on $x_2 = 0$, then

$$\mathbf{q} = -\mathbf{A}^{-1}\mathbf{c} \tag{3.23}$$

Thus, the resulting Green's function for the half-plane problem can be written as

$$T = 2\,\mathrm{Re}\{q_0 \ln y_t + \overline{q}_0 \ln y_t^*\}, \tag{3.24}$$

$$\mathbf{U} = 2\,\mathrm{Re}\{-\mathbf{A}\langle f(z_\alpha)\rangle \mathbf{B}^{-1}\mathbf{d} + \mathbf{c}[q_0 f^*(y_t) + \overline{q}_0 f^*(y_t^*)]\}, \tag{3.25}$$

$$\boldsymbol{\varphi} = 2\,\mathrm{Re}\{-\mathbf{B}\langle f(z_\alpha)\rangle \mathbf{B}^{-1}\mathbf{d} + \mathbf{d}[q_0 f^*(y_t) + \overline{q}_0 f^*(y_t^*)]\} \tag{3.26}$$

where $f(z_\alpha)$ is defined by Eq (3.21) and

$$y_t = z_t - z_{t0}, \qquad y_t^* = z_t - \overline{z}_{t0} \tag{3.27}$$

3.4 Bimaterial solid

Consider a bimaterial solid in which the upper half-plane $(x_2 > 0)$ is occupied by material 1 and the lower half-plane $(x_2 < 0)$ by material 2 (see Fig. 2.5). They are rigidly bonded together so that

$$T^{(1)} = T^{(2)}, \qquad \vartheta^{(1)} = \vartheta^{(2)}, \qquad \text{at } x_2 = 0 \tag{3.28}$$

$$\mathbf{U}^{(1)} = \mathbf{U}^{(2)}, \qquad \boldsymbol{\varphi}^{(1)} = \boldsymbol{\varphi}^{(2)}, \qquad \text{at } x_2 = 0 \tag{3.29}$$

where the superscripts (1) and (2) label the quantities relating to materials 1 and 2, respectively. In the rest of this section we present Green's functions of the bimaterial solid described above due to a line heat source h^* and a line temperature discontinuity $\hat{T}$ both located at $z_{t0}^{(1)} (= x_{10} + p_1^{*(1)} x_{20})$ in material 1.

3.4.1 Green's function for temperature fields

On the basis of the concept of perturbation given by Stagni [8], the general solution for the bimaterial solid can be assumed in the form [7]

$$T^{(1)} = 2\,\mathrm{Re}[f_0(z_t^{(1)}) + f_1(z_t^{(1)})], \quad \vartheta^{(1)} = 2k^{(1)}\,\mathrm{Im}[f_0(z_t^{(1)}) + f_1(z_t^{(1)})], \quad x_2 > 0, \tag{3.30}$$

$$T^{(2)} = 2\,\mathrm{Re}[f_2(z_t^{(2)})], \quad \vartheta^{(2)} = 2k^{(2)}\,\mathrm{Im}[f_2(z_t^{(2)})], \quad x_2 < 0 \tag{3.31}$$

where the function f_0 is defined by Eq (3.11), f_1 and f_2 are functions corresponding to the perturbed field of the solid due to the existence of the bimaterial interface, and

$$\begin{aligned} &z_t^{(1)} = x_1 + p_1^{*(1)} x_2, \quad z_t^{(2)} = x_1 + p_1^{*(2)} x_2, \\ &k^{(1)} = \sqrt{k_{11}^{(1)} k_{22}^{(1)} - \left(k_{12}^{(1)}\right)^2}, \quad k^{(2)} = \sqrt{k_{11}^{(2)} k_{22}^{(2)} - \left(k_{12}^{(2)}\right)^2} \end{aligned} \tag{3.32}$$

To satisfy the interface conditions (3.28), the functions f_1 and f_2 can be assumed in the form

$$f_1(z_t^{(1)}) = q_1 \ln y_2^{(1)}, \qquad f_2(z_t^{(2)}) = q_2 \ln y_1^{(2)} \tag{3.33}$$

where $y_2^{(1)} = z_t^{(1)} - \overline{z}_{t0}^{(1)}$, $y_1^{(2)} = z_t^{(2)} - z_{t0}^{(1)}$, and q_1 and q_2 are two constants to be determined. Substitution of Eq (3.33) into Eqs (3.30) and (3.31), and later into Eq (3.28), yields

$$q_1 = -b_1\overline{q}_0, \quad q_2 = b_2 q_0, \quad b_1 = \frac{k^{(2)} - k^{(1)}}{k^{(2)} + k^{(1)}}, \quad b_2 = \frac{2k^{(1)}}{k^{(2)} + k^{(1)}} \tag{3.34}$$

Therefore the Green's function for thermal fields can be written as

$$\begin{aligned} T^{(1)} &= 2\,\mathrm{Re}[q_0 \ln(z_t^{(1)} - z_{t0}^{(1)}) + q_1 \ln y_2^{(1)})], \\ \vartheta^{(1)} &= 2k^{(1)}\,\mathrm{Im}[q_0 \ln(z_t^{(1)} - z_{t0}^{(1)}) + q_1 \ln y_2^{(1)})], \end{aligned} \qquad x_2 > 0 \tag{3.35}$$

$$T^{(2)} = 2\,\mathrm{Re}[q_2 \ln y_1^{(2)}], \quad \vartheta^{(2)} = 2k^{(2)}\,\mathrm{Im}[q_2 \ln y_1^{(2)}], \qquad x_2 < 0 \tag{3.36}$$

3.4.2 Green's function for electroelastic fields

To use the interfacial condition (3.29) we first consider the particular solution due to the thermal field. This can be done by substituting Eq (3.33) into Eqs (3.30) and (3.31), and then integrating the result with respect to z_t, yielding the function $g(z_t)$, which is required when determining U and $\boldsymbol{\varphi}$ in Eqs (3.1) and (3.2), in the form

$$g_1(z_t^{(1)}) = q_0 f^*(y_1^{(1)}) - b_1\overline{q}_0 f^*(y_2^{(1)}) \tag{3.37}$$

for $x_2 > 0$, and

$$g_2(z_t^{(2)}) = b_2 q_0 f^*(y_1^{(2)}) \tag{3.38}$$

for $x_2 < 0$, where $y_1^{(1)} = z_t^{(1)} - z_{t0}^{(1)}$. The particular solution for electroelastic fields can then be given by

$$\mathbf{U}_p^{(1)}(z_t^{(1)}) = 2\,\mathrm{Re}[\mathbf{c}^{(1)} g_1(z_t^{(1)})] = 2\,\mathrm{Re}\{\mathbf{c}^{(1)}[q_0 f^*(y_1^{(1)}) - b_1\overline{q}_0 f^*(y_2^{(1)})]\}, \tag{3.39}$$

$$\boldsymbol{\varphi}_p^{(1)}(z_t^{(1)}) = 2\,\mathrm{Re}[\mathbf{d}^{(1)} g_1(z_t^{(1)})] = 2\,\mathrm{Re}\{\mathbf{d}^{(1)}[q_0 f^*(y_1^{(1)}) - b_1\overline{q}_0 f^*(y_2^{(1)})]\} \tag{3.40}$$

for $x_2 > 0$, and

$$\mathbf{U}_p^{(2)}(z_t^{(2)}) = 2\,\mathrm{Re}[\mathbf{c}^{(2)} g_2(z_t^{(2)})] = 2b_2\,\mathrm{Re}[\mathbf{c}^{(2)} q_0 f^*(y_1^{(2)})], \tag{3.41}$$

$$\boldsymbol{\varphi}_p^{(2)}(z_t^{(2)}) = 2\,\mathrm{Re}[\mathbf{d}^{(2)} g_2(z_t^{(2)})] = 2b_2\,\mathrm{Re}[\mathbf{d}^{(2)} q_0 f^*(y_1^{(2)})] \tag{3.42}$$

for $x_2 < 0$. The solutions (3.39)-(3.42) do not generally satisfy the interface condition (3.29). Therefore, development of a modified solution is needed such that when it is superposed on the particular solutions (3.39)-(3.42) the interface condition (3.29) will be satisfied.

Owing to the fact that $f(z_i)$ and $g(z_t)$ have the same rule affecting **U** and $\boldsymbol{\varphi}$ in Eqs $(3.1)_4$ and $(3.2)_2$, possible function forms come from the partition of solution $g(z_t)$. This is

$$\left\langle f(z_\alpha^{(j)})\right\rangle = \text{diag}[\, f(y_1^{*(j)})\ f(y_2^{*(j)})\ f(y_3^{*(j)})\ f(y_2^{*(j)})] \tag{3.43}$$

where

$$y_i^{*(j)} = z_i^{(j)} - z_{t0}^{(1)}, \qquad i\text{=1-4}, \quad j\text{=1, 2} \tag{3.44}$$

Thus the resulting expressions of $\mathbf{U}^{(i)}$ and $\boldsymbol{\varphi}^{(i)}$ can be given as

$$\mathbf{U}^{(1)} = 2\,\text{Re}\{\mathbf{A}^{(1)}\left\langle f(z_\alpha^{(1)})\right\rangle \mathbf{q}_1 + \mathbf{c}^{(1)}[q_0 f(y_1^{(1)}) - b_1\overline{q}_0 f(y_2^{(1)})]\}, \tag{3.45}$$

$$\boldsymbol{\varphi}^{(1)} = 2\,\text{Re}\{\mathbf{B}^{(1)}\left\langle f(z_\alpha^{(1)})\right\rangle \mathbf{q}_1 + \mathbf{d}^{(1)}[q_0 f(y_1^{(1)}) - b_1\overline{q}_0 f(y_2^{(1)})]\} \tag{3.46}$$

for $x_2 > 0$, and

$$\mathbf{U}^{(2)} = 2\,\text{Re}[\mathbf{A}^{(2)}\left\langle f(z_\alpha^{(2)})\right\rangle \mathbf{q}_2 + b_2 q_0 \mathbf{c}^{(2)} f(y_1^{(2)})], \tag{3.47}$$

$$\boldsymbol{\varphi}^{(2)} = 2\,\text{Re}[\mathbf{B}^{(2)}\left\langle f(z_\alpha^{(2)})\right\rangle \mathbf{q}_2 + b_2 q_0 \mathbf{d}^{(2)} f(y_1^{(2)})] \tag{3.48}$$

for $x_2 < 0$. The substitution of Eqs (3.45)-(3.48) into Eq (3.29) yields

$$\begin{aligned}\mathbf{q}_1 = q_0[&\mathbf{B}^{(1)} - \mathbf{B}^{(2)}\mathbf{A}^{(2)-1}\mathbf{A}^{(1)}]^{-1} \times \{[b_2\mathbf{d}^{(2)} + b_1\overline{\mathbf{d}}^{(1)} - \mathbf{d}^{(1)}] \\ &- \mathbf{B}^{(2)}\mathbf{A}^{(2)-1}[b_2\mathbf{c}^{(2)} + b_1\overline{\mathbf{c}}^{(1)} - \mathbf{c}^{(1)}]\},\end{aligned} \tag{3.49}$$

$$\begin{aligned}\mathbf{q}_2 = q_0[&\mathbf{B}^{(1)}\mathbf{A}^{(1)-1}\mathbf{A}^{(2)} - \mathbf{B}^{(2)}]^{-1} \times \{[b_2\mathbf{d}^{(2)} + b_1\overline{\mathbf{d}}^{(1)} - \mathbf{d}^{(1)}] \\ &- \mathbf{B}^{(1)}\mathbf{A}^{(1)-1}[b_2\mathbf{c}^{(2)} + b_1\overline{\mathbf{c}}^{(1)} - \mathbf{c}^{(1)}]\}\end{aligned} \tag{3.50}$$

Thus, the thermoelectroelastic Green's functions can be obtained by substituting Eqs (3.49) and (3.50) into Eqs (3.45)-(3.48).

3.5 Elliptic hole problems

3.5.1 Green's function of thermal field for insulated hole problems

Consider an infinite piezoelectric plate containing an elliptic hole subjected to loadings h^* and $\hat{T}$ at z_{t0}, as shown in Fig. 2.7 (it is noted that the loading vector here is $(h^*, \hat{T})$ rather than $(\mathbf{q}_0, \mathbf{b})$). If the hole is thermally insulated, the boundary conditions can be written as

$$\vartheta = 0, \tag{3.51}$$

$$h_i \to 0, \qquad \text{at infinity}, \tag{3.52}$$

in addition to the balance conditions (3.4) and (3.5).

The geometric equation of the elliptic hole Γ (see Fig. 2.7) is still defined by Eq (2.161), and the mapping function is given by Eq (2.162). Following the treatment in Section 2.8, a suitable function satisfying the boundary conditions (3.51) and (3.52) can be given in the form [7]:

$$\vartheta = 2k\,\text{Im}[g'(z_t)] = 2k\,\text{Im}[q_0\ln(\zeta_t - \zeta_{t0}) + q_1\ln(\zeta_t^{-1} - \overline{\zeta}_{t0})] \tag{3.53}$$

where ζ_t and ζ_{t0} are related to z_t and z_{t0} by

$$z_t = c_\tau\zeta_t + d_\tau\zeta_t^{-1}, \quad z_{t0} = c_\tau\zeta_{t0} + d_\tau\zeta_{t0}^{-1} \tag{3.54}$$

with

$$c_\tau = (a - ip_1^* b)/2, \quad d_\tau = (a + ip_1^* b)/2 \tag{3.55}$$

It should be mentioned that the function $\ln(\zeta_t^{-1} - \overline{\zeta}_{t0})$ is single valued since ζ_t^{-1} is always located inside the circle and $\overline{\zeta}_{t0}$ is a point outside the unit circle. When x_1 and x_2 are given by Eq $(2.161)_{1,2}$, $\zeta_t = e^{i\theta}$, and angle θ is defined in Fig. 2.7. Hence, the substitution of Eq (3.53) into Eq (3.51) yields

$$\vartheta = 2k\,\mathrm{Im}[g'(z_t)] = 2k\,\mathrm{Im}[q_0 \ln(e^{i\theta} - \zeta_{t0}) + q_1 \ln(e^{-i\theta} - \overline{\zeta}_{t0})] = 0 \tag{3.56}$$

The first term in Eq (3.56) can be replaced by the negative of its complex conjugate, that is,

$$\mathrm{Im}[q_0 \ln(e^{i\theta} - \zeta_{t0})] = -\mathrm{Im}[\overline{q}_0 \ln(e^{-i\theta} - \overline{\zeta}_{t0})] \tag{3.57}$$

Substituting Eq (3.57) into (3.56), we have

$$q_1 = \overline{q}_0 \tag{3.58}$$

3.5.2 Green's functions for electroelastic fields

Noting Eqs $(3.1)_4$ and $(3.2)_2$, the particular solution for the electroelastic field induced by the line heat source h^* and the line temperature discontinuity $\hat{T}$ can be written as

$$\mathbf{u}_p = 2\,\mathrm{Re}[\mathbf{c}g(z_t)], \quad \boldsymbol{\varphi}_p = 2\,\mathrm{Re}[\mathbf{d}g(z_t)] \tag{3.59}$$

The function $g(z_t)$ in Eq (3.59) above can be obtained by integrating $g'(z_t)$ in Eq (3.53) with respect to z_t, which yields

$$g(z_t) = q_0\{c_\tau F_1(\zeta_t) + d_\tau F_2(\zeta_t)\} + \overline{q}_0\{c_\tau F_4(\zeta_t) + d_\tau F_3(\zeta_t)\} \tag{3.60}$$

where

$$\begin{aligned} &F_1(s) = (s - \zeta_{t0})[\ln(s - \zeta_{t0}) - 1], \quad F_2(s) = (s^{-1} - \zeta_{t0}^{-1})\ln(s - \zeta_{t0}) + \zeta_{t0}^{-1}\ln s, \\ &F_3(s) = (s^{-1} - \overline{\zeta}_{t0})[\ln(s^{-1} - \overline{\zeta}_{t0}) - 1], \quad F_4(s) = (s - \overline{\zeta}_{t0}^{-1})\ln(s^{-1} - \overline{\zeta}_{t0}) - \overline{\zeta}_{t0}^{-1}\ln s \end{aligned} \tag{3.61}$$

For a zero traction-charge hole, the electroelastic boundary condition will be satisfied if [7]

$$\boldsymbol{\varphi} = 0 \tag{3.62}$$

To satisfy condition (3.62) along the hole boundary, possible function forms of $f(z_\alpha)$ come from the partition of $g(z_t)$, for the same reason as that stated for Eq (3.43). They are

$$f_i(z_\alpha) = F_i(\zeta_\alpha), \qquad (i\text{=}1\text{-}4) \tag{3.63}$$

where ζ_α is related to z_α by Eq (2.162).

The Green's functions for the electroelastic field can thus be chosen as

$$\mathbf{U} = 2\,\mathrm{Re}\sum_{k=1}^{4}[\mathbf{A}\langle f_k(\zeta_\alpha)\rangle\mathbf{q}_k + \mathbf{c}g(\zeta_t)] \tag{3.64}$$

$$\boldsymbol{\varphi} = 2\,\mathrm{Re}\sum_{k=1}^{4}[\mathbf{B}\langle f_k(\zeta_\alpha)\rangle\mathbf{q}_k + \mathbf{d}g(\zeta_t)] \tag{3.65}$$

Noting that $\zeta_\alpha = \zeta_t = e^{i\theta}$ on the hole boundary, we have

$$\mathbf{q}_1 = -q_0 c_\tau \mathbf{B}^{-1}\mathbf{d}, \quad \mathbf{q}_2 = -q_0 d_\tau \mathbf{B}^{-1}\mathbf{d}, \quad \mathbf{q}_3 = -\overline{q}_0 c_\tau \mathbf{B}^{-1}\mathbf{d}, \quad \mathbf{q}_4 = -\overline{q}_0 d_\tau \mathbf{B}^{-1}\mathbf{d} \tag{3.66}$$

Substituting Eq (3.66) into Eqs (3.64) and (3.65), the Green's functions can then be further written as

$$\begin{aligned}\mathbf{U} = &-2\,\mathrm{Re}[\mathbf{A}\{q_0 c_\tau \langle F_1(\zeta_\alpha)\rangle + q_0 d_\tau \langle F_2(\zeta_\alpha)\rangle + \overline{q}_0 c_\tau \langle F_4(\zeta_\alpha)\rangle + \overline{q}_0 d_\tau \langle F_3(\zeta_\alpha)\rangle\}\mathbf{B}^{-1}\mathbf{d}] \\ &+2\mathrm{Re}[\mathbf{c} q_0 \{c_\tau F_1(\zeta_t) + d_\tau F_2(\zeta_t)\} + \mathbf{c}\overline{q}_0 \{c_\tau F_4(\zeta_t) + d_\tau F_3(\zeta_t)\}]\end{aligned} \tag{3.67}$$

$$\begin{aligned}\boldsymbol{\varphi} = &-2\,\mathrm{Re}[\mathbf{B}\{q_0 c_\tau \langle F_1(\zeta_\alpha)\rangle + q_0 d_\tau \langle F_2(\zeta_\alpha)\rangle + \overline{q}_0 c_\tau \langle F_4(\zeta_\alpha)\rangle + \overline{q}_0 d_\tau \langle F_3(\zeta_\alpha)\rangle\}\mathbf{B}^{-1}\mathbf{d}] \\ &+2\mathrm{Re}[\mathbf{d} q_0 \{c_\tau F_1(\zeta_t) + d_\tau F_2(\zeta_t)\} + \mathbf{d}\overline{q}_0 \{c_\tau F_4(\zeta_t) + d_\tau F_3(\zeta_t)\}]\end{aligned} \tag{3.68}$$

3.6 Arbitrarily shaped hole problems

In Section 2.9, applications of Green's function to a piezoelectric plate containing an arbitrarily shaped hole were presented. Extension of the procedure to include thermal effects is described in this section. Green's functions in closed form for an infinite thermopiezoelectric plate with various holes induced by thermal loads are derived using Stroh formalism. The loads may be a point heat source or a temperature discontinuity.

3.6.1 Basic equations

As was treated in Section 2.9, we consider a plane strain analysis where the material is transversely isotropic and where coupling occurs between in-plane stresses and in-plane electric fields. For a Cartesian coordinate system *Oxyz*, choose the *z*-axis as the poling direction, and denote the coordinates *x* and *z* by x_1 and x_2 in order to obtain a compacted notation. The plane strain constitutive equations are expressed in matrix form as

$$h_i = k_{ij} q_j, \tag{3.69}$$

$$\begin{Bmatrix} \sigma_{11} \\ \sigma_{22} \\ \sigma_{12} \\ D_1 \\ D_2 \end{Bmatrix} = \begin{bmatrix} c_{11} & c_{12} & 0 & 0 & e_{21} \\ c_{12} & c_{22} & 0 & 0 & e_{22} \\ 0 & 0 & c_{33} & e_{13} & 0 \\ 0 & 0 & e_{13} & -\kappa_{11} & 0 \\ e_{21} & e_{22} & 0 & 0 & -\kappa_{22} \end{bmatrix} \begin{Bmatrix} \varepsilon_{11} \\ \varepsilon_{22} \\ 2\varepsilon_{12} \\ -E_1 \\ -E_2 \end{Bmatrix} - \begin{Bmatrix} \lambda_{11} \\ \lambda_{22} \\ 0 \\ 0 \\ \chi_2 \end{Bmatrix} T \tag{3.70}$$

or inversely

$$q_i = \rho_{ij} h_j, \tag{3.71}$$

$$\begin{Bmatrix} \varepsilon_{11} \\ \varepsilon_{22} \\ 2\varepsilon_{12} \\ -E_1 \\ -E_2 \end{Bmatrix} = \begin{bmatrix} f_{11} & f_{12} & 0 & 0 & g_{21} \\ f_{12} & f_{22} & 0 & 0 & g_{22} \\ 0 & 0 & f_{33} & g_{13} & 0 \\ 0 & 0 & g_{13} & -\beta_{11} & 0 \\ g_{21} & g_{22} & 0 & 0 & -\beta_{22} \end{bmatrix} \begin{Bmatrix} \sigma_{11} \\ \sigma_{22} \\ \sigma_{12} \\ D_1 \\ D_2 \end{Bmatrix} + \begin{Bmatrix} \alpha_{11} \\ \alpha_{22} \\ 0 \\ 0 \\ \lambda_2 \end{Bmatrix} T \tag{3.72}$$

where χ_2 and λ_2 are pyroelectric constants, λ_{ij} and α_{ij} are stress-temperature constants and thermal expansion constants respectively, q_j and h_j are heat intensity and heat flux,

k_{ij} and ρ_{ij} the coefficients of heat conductivity and heat resistivity.

The boundary conditions at the rim of the hole can be written as

$$\vartheta = \boldsymbol{\varphi} = 0, \tag{3.73}$$

if the hole is thermal-insulated, traction- and charge-free along the hole boundary. Besides, the infinite boundary condition

$$\mathbf{h} \to 0, \ \boldsymbol{\Pi} \to 0 \quad \text{at infinity} \tag{3.74}$$

and the balance conditions

$$\int_C dT = \hat{T} \quad \text{and} \quad \int_C d\vartheta = -h^* \quad \text{for any closed curve } C \text{ enclosing the point } \zeta_{t0} \tag{3.75}$$

should also be satisfied.

3.6.2 Green's function for thermal fields

Based on the one-to-one mapping described in Section 2.9 and the concept of perturbation [8], the general solution for temperature and heat-flow function can be assumed in the form

$$T = 2\,\mathrm{Re}[g'(z_t)] = 2\,\mathrm{Re}[f_0(\zeta_t) + f_1(\zeta_t)], \tag{3.76}$$

$$\vartheta = 2k\,\mathrm{Im}[g'(z_t)] = 2k\,\mathrm{Im}[f_0(\zeta_t) + f_1(\zeta_t)] \tag{3.77}$$

where z_t and ζ_t are related by the mapping function

$$z_t = a(a_{1\tau}\zeta_t + a_{2\tau}\zeta_t^{-1} + e_{m1}a_{3\tau}\zeta_t^{m} + e_{m1}a_{4\tau}\zeta_t^{-m}) \tag{3.78}$$

with

$$a_{1\tau} = (1 - ip_1^* e)/2, \ a_{2\tau} = (1 + ip_1^* e)/2,$$

$$a_{3\tau} = \gamma(1 + ip_1^* e)/2, \ a_{4\tau} = \gamma(1 - ip_1^* e)/2 \tag{3.79}$$

For an infinite piezoelectric plate containing a hole subjected to loadings h^* and $\hat{T}$ at z_{t0} (see Fig. 2.9), the function f_0 can be chosen in the form

$$f_0(\zeta_t) = q_0 \ln(\zeta_t - \zeta_{t0}) \tag{3.80}$$

where q_0 is given in Eq (3.6).

Thus the boundary condition $(3.73)_1$ requires that

$$f_1(\zeta_t) = \overline{q}_0 \ln(\zeta_t^{-1} - \overline{\zeta}_{t0}) \tag{3.81}$$

The function g in Eq $(3.2)_2$ can thus be obtained by integrating the functions f_0 and f_1 with respect to z_t, which leads to

$$\begin{aligned} g(z_t) = {} & aa_{1\tau}[q_0 F_1(\zeta_t, \zeta_{t0}) + \overline{q}_0 F_2(\zeta_t^{-1}, \overline{\zeta}_{t0})] + aa_{2\tau}[q_0 F_2(\zeta_t, \zeta_{t0}) + \overline{q}_0 F_1(\zeta_t^{-1}, \overline{\zeta}_{t0})] \\ & + ae_{j1}\{a_{3\tau}[q_0 F_3(\zeta_t, \zeta_{t0}) + \overline{q}_0 F_4(\zeta_t^{-1}, \overline{\zeta}_{t0})] + aa_{4\tau}[q_0 F_4(\zeta_t, \zeta_{t0}) + \overline{q}_0 F_3(\zeta_t^{-1}, \overline{\zeta}_{t0})]\} \end{aligned} \tag{3.82}$$

where

$$F_1(\zeta_t,\zeta_{t0})=(\zeta_t-\zeta_{t0})[\ln(\zeta_t-\zeta_{t0})-1], \tag{3.83}$$

$$F_2(\zeta_t,\zeta_{t0})=(\zeta_t^{-1}-\zeta_{t0}^{-1})\ln(\zeta_t-\zeta_{t0})+\zeta_{t0}^{-1}\ln\zeta_t, \tag{3.84}$$

$$F_3(\zeta_t,\zeta_{t0})=(\zeta_t^{m}-\zeta_{t0}^{m})\ln(\zeta_t-\zeta_{t0})-\zeta_{t0}^{m}\sum_{n=1}^{m}\frac{1}{n}\left(\frac{\zeta_t}{\zeta_{t0}}\right)^n, \tag{3.85}$$

$$F_4(\zeta_t,\zeta_{t0})=(\zeta_t^{-m}-\zeta_{t0}^{-m})\ln(\zeta_t-\zeta_{t0})+\zeta_{t0}^{-m}\ln\zeta_t-\zeta_{t0}^{-m}\sum_{n=1}^{m-1}\frac{1}{n}\left(\frac{\zeta_{t0}}{\zeta_t}\right)^n \tag{3.86}$$

3.6.3 Green's functions for electroelastic fields.

From Eqs $(3.1)_4$ and $(3.2)_2$ the particular solution for electroelastic fields induced by thermal loading can be written as

$$\mathbf{U}_p=2\,\mathrm{Re}[\mathbf{c}g(z_t)],\quad \varphi_p=2\,\mathrm{Re}[\mathbf{d}g(z_t)] \tag{3.87}$$

To satisfy the condition $(3.73)_2$ along the hole boundary, possible function forms of $f(z_k)$ should come from the partition of $g(z_t)$, for the same reason as that stated for Eq (3.43). They are

$$\begin{aligned}f_1(z_k)=a[&q_0F_1(\zeta_k,\zeta_{t0})+q_0F_2(\zeta_k,\zeta_{t0})+\overline{q}_0F_1(\zeta_k^{-1},\overline{\zeta}_{t0})+\overline{q}_0F_2(\zeta_k^{-1},\overline{\zeta}_{t0})]/2\\&+e_{j1}a\gamma[q_0F_3(\zeta_k,\zeta_{t0})+q_0F_4(\zeta_k,\zeta_{t0})+\overline{q}_0F_3(\zeta_k^{-1},\overline{\zeta}_{t0})+\overline{q}_0F_4(\zeta_k^{-1},\overline{\zeta}_{t0})]/2,\end{aligned} \tag{3.88}$$

$$\begin{aligned}f_2(z_k)=ip_kae[&-q_0F_1(\zeta_k,\zeta_{t0})+q_0F_2(\zeta_k,\zeta_{t0})+\overline{q}_0F_1(\zeta_k^{-1},\overline{\zeta}_t^{*})-\overline{q}_0F_2(\zeta_k^{-1},\overline{\zeta}_t^{*})]/2\\&+ie_{j1}p_kae\gamma[q_0F_3(\zeta_k,\zeta_{t0})-q_0F_4(\zeta_k,\zeta_{t0})-\overline{q}_0F_3(\zeta_k^{-1},\overline{\zeta}_{t0})+\overline{q}_0F_4(\zeta_k^{-1},\overline{\zeta}_{t0})]/2\end{aligned} \tag{3.89}$$

where functions f_1 and f_2 represent two different possible functions.

The Green's functions for electroelastic fields can thus be chosen as

$$\mathbf{U}=2\,\mathrm{Re}\left\{\sum_{k=1}^{2}[\mathbf{A}\langle f_k(z_\alpha)\rangle\mathbf{q}_k]+\mathbf{c}g(z_t)\right\},\quad \boldsymbol{\varphi}=2\,\mathrm{Re}\left\{\sum_{k=1}^{2}[\mathbf{B}\langle f_k(z_\alpha)\rangle\mathbf{q}_k]+\mathbf{d}g(z_t)\right\} \tag{3.90}$$

Substitution of Eqs (3.88) and (3.89) into Eq $(3.90)_2$ and later into Eq $(3.73)_2$ leads to

$$\mathbf{q}_1=-\mathbf{B}^{-1}\overline{\mathbf{d}},\quad \mathbf{q}_2=-\mathbf{P}^{-1}\mathbf{B}^{-1}\overline{\mathbf{d}}\overline{p}_1^{*}. \tag{3.91}$$

Substituting Eq (3.91) into Eq (3.90), the Green's functions can then be written as

$$\mathbf{U}=2\,\mathrm{Re}\{-\mathbf{A}[\langle f_1(z_\alpha)\rangle+\langle f_2(z_\alpha)\rangle\mathbf{P}^{-1}\overline{p}_1^{*}]\mathbf{B}^{-1}\overline{\mathbf{d}}+\mathbf{c}g(z_t)\}, \tag{3.92}$$

$$\boldsymbol{\varphi} = 2\,\mathrm{Re}\{-\mathbf{B}[\langle f_1(z_\alpha)\rangle + \langle f_2(z_\alpha)\rangle \mathbf{P}^{-1}\overline{p}_1^*]\mathbf{B}^{-1}\overline{\mathbf{d}} + \mathbf{d}g(z_t)\} \tag{3.93}$$

3.7 Elliptic inclusion problems

In this section fundamental solutions for thermal loading applied outside, inside or on the surface of an elliptic piezoelectric inclusion in an infinite piezoelectric matrix are presented. By combining the method of Stroh's formalism, the technique of one-to-one mapping, the concept of perturbation, and the method of analytical continuation, Green's functions are derived for an elliptic piezoelectric inclusion embedded in an infinite piezoelectric matrix subjected to a line heat source h^* and a line temperature discontinuity $\hat{T}$ (Fig. 3.1).

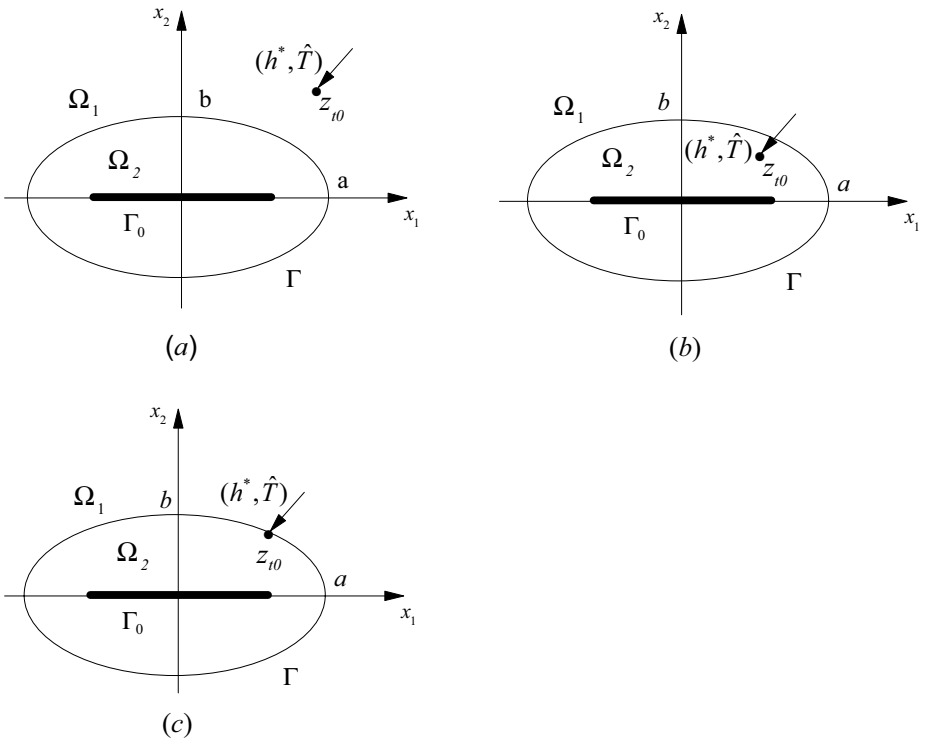

Fig. 3.1 Three loading cases: (*a*) outside the inclusion; (*b*) inside; (*c*) on the interface

To make the derivation tractable, consider again the one-to-one mapping defined by Eq (2.162). It will map the region outside the elliptic inclusion onto the exterior of a unit circle in the ζ_k-plane. Further, the transformation (2.162) has been proved in Section 2.8 to be single valued outside the ellipse, since the roots of equation (2.167) are located inside the unit circle $|\zeta_k|<1$, where ζ_k is related to z_k by Eq (2.162). However, the mapping (2.162) is not single valued inside the ellipse, because the roots of Eq (2.167) are located inside the unit circle, as indicated in Section 2.8. To

circumvent this problem, the mapping of Ω_2 (see Fig. 2.8) is done by excluding a slit, Γ_0, which represents a circle of radius $\sqrt{m_k}$ ($=\left|a_{2k}^{(2)}/a_{1k}^{(2)}\right|$) in the ζ_k-plane, from the ellipse [9]. In this case the function (2.162) will transform Γ and Γ_0 into a ring of outer and inner circles with radii $r_{out}=1$ and $r_{in}=\sqrt{m_k}$, respectively. Besides, anywhere inside the ellipse and on the slit Γ_0 a function $f(\zeta_k)$ must satisfy the condition [6]

$$f[\sqrt{m_k}\,\sigma(\theta)]=f[\sqrt{m_k}\,e^{2i\theta_k}/\sigma(\theta)] \tag{3.94}$$

to ensure that the field is single valued [9], where $\sigma(\theta)=e^{i\theta}$ stands for a point located on the unit circle in the ζ_k-plane, and θ is a polar angle defined in Fig. 2.7.

3.7.1 Green's functions of thermal loading applied outside the inclusion

Consider an elliptic inclusion embedded in an infinite piezoelectric matrix subjected to loadings h^* and $\hat{T}$ at a point (x_{10}, x_{20}) which is outside the inclusion (see Fig. 3.1a). If the inclusion and matrix are assumed to be perfectly bonded along the interface, the temperature, heat flow (h_n), elastic displacements, electric potential, stress and electric displacement($\mathbf{\Pi}_n$) across the interface should be continuous, i.e.,

$$T^{(1)}=T^{(2)},\quad \vartheta^{(1)}=\vartheta^{(2)},\quad \mathbf{U}^{(1)}=\mathbf{U}^{(2)},\quad \boldsymbol{\varphi}^{(1)}=\boldsymbol{\varphi}^{(2)}, \tag{3.95}$$

along the interface.

3.7.1.1 Green's functions for thermal fields. On the basis of the one-to-one mapping (3.54) and the concept of perturbation given by Stagni [8], the general solution for temperature and heat-flow function can be assumed in the form

$$\begin{aligned} T^{(1)} &= f_0(\zeta_t^{(1)})+\overline{f_0(\zeta_t^{(1)})}+f_1(\zeta_t^{(1)})+\overline{f_1(\zeta_t^{(1)})} \\ \vartheta^{(1)} &= -ik_1 f_0(\zeta_t^{(1)})+ik_1\overline{f_0(\zeta_t^{(1)})}-ik_1 f_1(\zeta_t^{(1)})+ik_1\overline{f_1(\zeta_t^{(1)})} \end{aligned} \qquad \zeta_t^{(1)}\in\Omega_1, \tag{3.96}$$

$$\begin{aligned} T^{(2)} &= f_2(\zeta_t^{(2)})+\overline{f_2(\zeta_t^{(2)})} \\ \vartheta^{(2)} &= -ik_2 f_2(\zeta_t^{(2)})+ik_2\overline{f_2(\zeta_t^{(2)})} \end{aligned} \qquad \zeta_t^{(2)}\in\Omega_2. \tag{3.97}$$

When an infinite space is subjected to loadings h^* and $\hat{T}$ at (x_{10}, x_{20}), the function f_0 can be chosen in the form

$$f_0(\zeta_t^{(1)})=q_0\ln(\zeta_t^{(1)}-\zeta_{t0}^{(1)}) \tag{3.98}$$

where $\zeta_t^{(1)}$ and $\zeta_{t0}^{(1)}$ are related to the complex arguments $z_t^{(1)}$ and $z_{t0}^{(1)}(=x_{10}+p_1^{*(1)}x_{20})$ through the following transformation functions:

$$\zeta_t^{(i)}=\frac{z_t^{(i)}+\sqrt{z_t^{(i)2}-a^2-p_1^{*(i)2}b^2}}{a-ip_1^{*(i)}b},\quad \zeta_{t0}^{(i)}=\frac{z_{t0}^{(i)}+\sqrt{z_{t0}^{(i)2}-a^2-p_1^{*(i)2}b^2}}{a-ip_1^{*(i)}b},\ (i=1,2) \tag{3.99}$$

and q_0 has the same form as that defined in Eq (3.6) in which k is replaced by $k^{(1)}$.

As for the function f_2, noting that it is holomorphic in the annular ring (see Fig. 2.8), it can be represented by Laurent's series,

$$f_2(\zeta_t^{(2)}) = \sum_{j=-\infty}^{\infty} c_j \zeta_t^{(2)j}, \tag{3.100}$$

whose coefficients c_{-j} can be related to c_j by means of Eq (3.94) in the following manner:

$$c_{-j} = \Gamma_j^* c_j, \quad \Gamma_j^* = \left(\frac{a + ibp_1^{*(2)}}{a - ibp_1^{*(2)}} \right)^j. \tag{3.101}$$

Inserting Eqs (3.98) and (3.100) into Eqs (3.96) and (3.97) and later into Eqs $(3.95)_{1,2}$ yields

$$f_1(\sigma) + \overline{f_0(\sigma)} - \sum_{j=1}^{\infty} [\overline{c}_j + \Gamma_j^* c_j]\sigma^{-j} = \sum_{j=1}^{\infty} [c_j + \overline{\Gamma}_j^* \overline{c}_j]\sigma^j - \overline{f_1(\sigma)} - f_0(\sigma), \tag{3.102}$$

$$-f_1(\sigma) + \overline{f_0(\sigma)} - \frac{k^{(2)}}{k^{(1)}} \sum_{j=1}^{\infty} [\overline{c}_j - \Gamma_j^* c_j]\sigma^{-j} = -\frac{k^{(2)}}{k^{(1)}} \sum_{j=1}^{\infty} [c_j - \overline{\Gamma}_j^* \overline{c}_j]\sigma^j + f_0(\sigma) - \overline{f_1(\sigma)} \tag{3.103}$$

One of the important properties of holomorphic functions used in the method of analytic continuation is that if the function $f(\zeta)$ is holomorphic in Ω_1 (or $\Omega_0 + \Omega_2$), then $\overline{f(1/\overline{\zeta})}$ is holomorphic in $\Omega_0 + \Omega_2$ (or Ω_1), Ω_0 denoting the region inside the circle of radius $\sqrt{m_t}$. Hence, put

$$\omega(\zeta) = \begin{cases} f_1(\zeta) + \overline{f_0(1/\overline{\zeta})} - \sum_{j=1}^{\infty} [\overline{c}_j + \Gamma_j^* c_j]\zeta^{-j}, & \zeta \in \Omega_1, \\ -\overline{f_1(1/\overline{\zeta})} - f_0(\zeta) + \sum_{j=1}^{\infty} [c_j + \overline{\Gamma}_j^* \overline{c}_j]\zeta^j, & \zeta \in \Omega_0 + \Omega_2, \end{cases} \tag{3.104}$$

where the function $\omega(\zeta)$ is holomorphic and single valued in the whole plane. By Liouville's theorem, we have $\omega(\zeta)$ = constant. However, constant function f does not produce stress and electric displacement (SED), which may be neglected. Thus, letting $\omega(\zeta)$=0, we have

$$\sum_{j=1}^{\infty} [\overline{c}_j + \Gamma_j^* c_j]\zeta^{-j} = f_1(\zeta) + \overline{f_0(1/\overline{\zeta})}, \qquad \zeta \in \Omega_1,$$

$$\sum_{j=1}^{\infty} [c_j + \overline{\Gamma}_j^* \overline{c}_j]\zeta^j = \overline{f_1(1/\overline{\zeta})} + f_0(\zeta), \qquad \zeta \in \Omega_0 + \Omega_2. \tag{3.105}$$

It should be mentioned that the superscripts (1) and (2) are omitted in Eqs (3.104) and (3.105). To further simplify subsequent writing, we shall omit them again in the related expressions when the distinction is unnecessary. Similar to the procedures in Eq (3.102), we can derive from Eq (3.103) that

$$\begin{aligned}
&\frac{k^{(2)}}{k^{(1)}}\sum_{j=1}^{\infty}[\overline{c}_j-\Gamma_j^* c_j]\zeta^{-j}=-f_1(\zeta)+\overline{f_0(1/\overline{\zeta})}, && \zeta\in\Omega_1,\\
&\frac{k^{(2)}}{k^{(1)}}\sum_{j=1}^{\infty}[c_j-\overline{\Gamma}_j^*\overline{c}_j]\zeta^{j}=-\overline{f_1(1/\overline{\zeta})}+f_0(\zeta), && \zeta\in\Omega_0+\Omega_2.
\end{aligned} \tag{3.106}$$

The equations $(3.105)_2$ and $(3.106)_2$ provide

$$f_0(\zeta)=\frac{1}{2}\sum_{j=1}^{\infty}[(1+k^{(2)}/k^{(1)})c_j+(1-k^{(2)}/k^{(1)})\overline{\Gamma}_j^*\overline{c}_j]\zeta^j. \tag{3.107}$$

With the use of the series representation

$$f_0(x)=\sum_{k=1}^{\infty}e_k x^k,\quad e_k=\frac{f_0^{(k)}(0)}{k!}=\frac{1}{2\pi i}\int_C\frac{f_0(x)}{x^{k+1}}dx, \tag{3.108}$$

the function $f_0(\zeta)$ given in Eq (3.98) can be expressed as

$$f_0(\zeta)=\sum_{j=1}^{\infty}e_j\zeta^j,\qquad e_j=-\frac{q_0\zeta_{t0}^{(1)-j}}{j} \tag{3.109}$$

where δ_{ij}=1, when i=j; δ_{ij}=0, when $i\neq j$.

Comparing the coefficients of corresponding terms in Eqs (3.107) and (3.109), one obtains

$$c_j=(G_0-\overline{G}_jG_j/G_0)^{-1}(e_j-\overline{G}_j\overline{e}_j/G_0),\qquad (j=1,\ 2,\cdots,\infty) \tag{3.110}$$

where $G_0=(1+k_2/k_1)/2,\ G_j=(1-k_2/k_1)\Gamma_j^*/2$.

With the solution obtained for c_k, the functions f_1, g_1' and g_2' can be further written as

$$f_1(\zeta)=\sum_{j=1}^{\infty}[\overline{c}_j+\Gamma_j^*c_j]\zeta_t^{(1)-j}-\overline{q}_0\ln(\zeta_t^{(1)-1}-\overline{\zeta}_{t0}^{(1)}), \tag{3.111}$$

$$g_1'(\zeta_t^{(1)})=q_0\ln(\zeta_t^{(1)}-\zeta_{t0}^{(1)})-\overline{q}_0\ln(\zeta_t^{(1)-1}-\overline{\zeta}_{t0}^{(1)})+\sum_{j=1}^{\infty}[\overline{c}_j+\Gamma_j^*c_j]\zeta_t^{(1)-j}, \tag{3.112}$$

$$g_2'(\zeta_t^{(2)})=\sum_{j=1}^{\infty}c_j[\zeta_t^{(2)j}+\Gamma_j^*\zeta_t^{(2)-j}]. \tag{3.113}$$

Substitution of Eqs (3.112) and (3.113) into Eqs$(3.1)_1$ and $(3.2)_1$ yields Green's functions for thermal fields.

3.7.1.2 Green's functions for electroelastic fields. From Eqs $(3.1)_4$ and $(3.2)_2$, the particular piezoelectric solution induced by the thermal loadings h^* and $\hat{T}$ can be written as

$$\mathbf{U}_p^{(i)}=2\,\mathrm{Re}[\mathbf{c}^{(i)}g_i(\zeta_t^{(i)})],\quad \boldsymbol{\varphi}_p^{(i)}=2\,\mathrm{Re}[\mathbf{d}^{(i)}g_i(\zeta_t^{(i)})],\qquad (i=1,2), \tag{3.114}$$

The function $g(z_t)$ in Eq (3.114) can be obtained by integrating Eqs (3.112) and (3.113) with respect to z_t,, which yields

$$g_1(\zeta_t^{(1)}) = a_{1\tau}^{(1)}[q_0 F_1(\zeta_t^{(1)}, \zeta_{t0}^{(1)}) - \overline{q}_0 F_2(\zeta_t^{(1)-1}, \overline{\zeta}_{t0}^{(1)})] + a_{2\tau}^{(1)}[q_0 F_2(\zeta_t^{(1)}, \zeta_{t0}^{(1)}) - \overline{q}_0 F_1(\zeta_t^{(1)-1}, \overline{\zeta}_{t0}^{(1)})] + (\overline{c}_1 + \Gamma_1^* c_1) a_{1\tau}^{(1)} \ln \zeta_t^{(1)} + \sum_{j=1}^{\infty} G_{1j} \zeta_t^{(1)-j}, \tag{3.115}$$

$$g_2(\zeta_t^{(2)}) = \sum_{j=1}^{\infty} [G_{2j} \zeta_t^{(1)j} + G_{3j} \zeta_t^{(2)-j}], \tag{3.116}$$

where

$$F_1(\zeta_t, \zeta_{t0}) = (\zeta_t - \zeta_{t0})[\ln(\zeta_t - \zeta_{t0}) - 1],$$

$$F_2(\zeta_t, \zeta_{t0}) = (\zeta_t^{-1} - \zeta_{t0}^{-1}) \ln(\zeta_t - \zeta_{t0}) + \zeta_{t0}^{-1} \ln \zeta_t,$$

$$\begin{aligned} &a_{1\tau}^{(k)} = (a - i p_1^{*(k)} b)/2, \quad a_{2\tau}^{(k)} = (a + i p_1^{*(k)} b)/2, \qquad (k = 1, 2), \\ &G_{1j} = -[(\overline{c}_{j+1} + \Gamma_{j+1}^* c_{j+1}) a_{1\tau}^{(1)} - a_{2\tau}^{(1)} (\overline{c}_{j-1} + \Gamma_{j-1}^* c_{j-1}) s_{j1}]/j, \\ &G_{2j} = (a_{1\tau}^{(2)} c_{j-1} s_{j1} - a_{2\tau}^{(2)} c_{j+1})/j, \\ &G_{3j} = -(a_{1\tau}^{(2)} \Gamma_{j+1}^* c_{j+1} - a_{2\tau}^{(2)} \Gamma_{j-1}^* c_{j-1} s_{j1})/j, \end{aligned} \tag{3.117}$$

and $s_{ij} = 1$ for $i \neq j$, $s_{ij} = 0$ for $i = j$.

To satisfy the condition $(3.95)_{3,4}$ along the interface, the function $f(\zeta_m)$ can be assumed in the form [6]:

$$\begin{aligned} f_{1m}^{(j)}(\zeta_m^{(j)}) &= a[q_0 F_1(\zeta_m^{(j)}, \zeta_{t0}^{(j)}) + q_0 F_2(\zeta_m^{(j)}, \zeta_{t0}^{(j)}) \\ &\quad - \overline{q}_0 F_1(\zeta_m^{(j)-1}, \overline{\zeta}_{t0}^{(j)}) - \overline{q}_0 F_2(\zeta_m^{(j)-1}, \overline{\zeta}_{t0}^{(j)})]/2, \\ f_{2m}^{(j)}(\zeta_m^{(j)}) &= i p_m^{(j)} b[-q_0 F_1(\zeta_m^{(j)}, \zeta_{t0}^{(j)}) + q_0 F_2(\zeta_m^{(j)}, \zeta_{t0}^{(j)}) \\ &\quad - \overline{q}_0 F_1(\zeta_m^{(j)-1}, \overline{\zeta}_{t0}^{(j)}) + \overline{q}_0 F_2(\zeta_m^{(j)-1}, \overline{\zeta}_{t0}^{(j)})]/2, \end{aligned} \qquad (j=1, 2), \tag{3.118}$$

$$f_{3m}^{(j)}(\zeta_m^{(j)}) = a_{1m}^{(j)} \ln \zeta_m^{(j)}, \qquad (j=1, 2), \tag{3.119}$$

$$\mathbf{f}_4^{(j)}(\zeta^{(j)}) = \sum_{k=1}^{\infty} \left\langle \zeta_\alpha^{(j)k} \right\rangle \mathbf{r}_k^{(j)}, \quad \mathbf{f}_5^{(j)}(\zeta^{(j)}) = \sum_{k=1}^{\infty} \left\langle \zeta_\alpha^{(j)-k} \right\rangle \mathbf{s}_k^{(j)}, \qquad (j=1, 2) \tag{3.120}$$

where $\mathbf{f}_k^{(j)}$ are four component vectors, and $\mathbf{r}_k^{(j)}$ and $\mathbf{s}_k^{(j)}$ are constant vectors with four components to be determined. It should be pointed out that the vector $\mathbf{s}_k^{(j)}$ is different from the symbol s_{ij} appearing in Eq (3.117).

The Green's functions for the electroelastic fields can thus be chosen as

$$\mathbf{U}^{(j)} = 2\,\mathrm{Re}\left\{ \sum_{k=1}^{3} \mathbf{A}^{(j)} \left\langle f_{k\alpha}^{(j)}(\zeta_\alpha^{(j)}) \right\rangle \mathbf{q}_k^{(j)} + \sum_{k=4}^{5} \mathbf{A}^{(j)} \mathbf{f}_k^{(j)}(\boldsymbol{\zeta}^{(j)}) + \mathbf{c}^{(j)} g_j(\zeta_t^{(j)}) \right\}, \tag{3.121}$$

$$\varphi^{(j)} = 2\,\mathrm{Re}\left\{ \sum_{k=1}^{3} \mathbf{B}^{(j)} \left\langle f_{k\alpha}^{(j)}(\zeta_\alpha^{(j)}) \right\rangle \mathbf{q}_k^{(j)} + \sum_{k=4}^{5} \mathbf{B}^{(j)} \mathbf{f}_k^{(j)}(\boldsymbol{\zeta}^{(j)}) + \mathbf{d}^{(j)} g_j(\zeta_t^{(j)}) \right\} \tag{3.122}$$

The above two expressions, together with the interface condition $(3.95)_{3,4}$, provide

$$\mathbf{q}_1^{(1)} = \mathbf{X}_1 (\mathbf{A}^{(2)-1} \overline{\mathbf{c}}^{(1)} - \mathbf{B}^{(2)-1} \overline{\mathbf{d}}^{(1)}), \tag{3.123}$$

$$\mathbf{q}_1^{(2)} = \mathbf{X}_2(\mathbf{B}^{(1)-1}\overline{\mathbf{d}}^{(1)} - \mathbf{A}^{(1)-1}\overline{\mathbf{c}}^{(1)}), \tag{3.124}$$

$$\mathbf{q}_2^{(1)} = \overline{p}_1^{*(1)}\mathbf{P}^{(1)-1}\mathbf{q}_1^{(1)}, \tag{3.125}$$

$$\mathbf{q}_2^{(2)} = \overline{p}_1^{*(1)}\mathbf{P}^{(2)-1}\mathbf{q}_1^{(2)}, \tag{3.126}$$

$$\mathbf{q}_3^{(1)} = \left\langle a_{1\alpha}^{(1)} \right\rangle^{-1} \overline{a}_{1\tau}^{(1)}(c_1 + \overline{\Gamma}_1^{*}\overline{c}_1)\mathbf{q}_1^{(1)}, \tag{3.127}$$

$$\mathbf{q}_3^{(2)} = \left\langle a_{1\alpha}^{(2)} \right\rangle^{-1} \overline{a}_{1\tau}^{(1)}(c_1 + \overline{\Gamma}_1^{*}\overline{c}_1)\mathbf{q}_1^{(2)}, \tag{3.128}$$

$$\begin{aligned}&\mathbf{A}^{(1)}\mathbf{f}_5^{(1)}(\sigma) + \overline{\mathbf{A}}^{(1)}\overline{\mathbf{f}_4^{(1)}(\sigma)} - \mathbf{A}^{(2)}\mathbf{f}_5^{(2)}(\sigma) - \overline{\mathbf{A}}^{(2)}\overline{\mathbf{f}_4^{(2)}(\sigma)} + \sum_{j=1}^{\infty}(\mathbf{c}^{(1)}G_{1j} - \overline{\mathbf{c}}^{(2)}\overline{G}_{2j} - \mathbf{c}^{(2)}G_{3j})\sigma^{-j} \\ =&\mathbf{A}^{(2)}\mathbf{f}_4^{(2)}(\sigma) + \overline{\mathbf{A}}^{(2)}\overline{\mathbf{f}_5^{(2)}(\sigma)} - \mathbf{A}^{(1)}\mathbf{f}_4^{(1)}(\sigma) - \overline{\mathbf{A}}^{(1)}\overline{\mathbf{f}_5^{(1)}(\sigma)} - \sum_{j=1}^{\infty}(\overline{\mathbf{c}}^{(1)}\overline{G}_{1j} - \mathbf{c}^{(2)}G_{2j} - \overline{\mathbf{c}}^{(2)}\overline{G}_{3j})\sigma^{j}\end{aligned} \tag{3.129}$$

$$\begin{aligned}&\mathbf{B}^{(1)}\mathbf{f}_5^{(1)}(\sigma) + \overline{\mathbf{B}}^{(1)}\overline{\mathbf{f}_4^{(1)}(\sigma)} - \mathbf{B}^{(2)}\mathbf{f}_5^{(2)}(\sigma) - \overline{\mathbf{B}}^{(2)}\overline{\mathbf{f}_4^{(2)}(\sigma)} + \sum_{j=1}^{\infty}(\mathbf{d}^{(1)}G_{1j} - \overline{\mathbf{d}}^{(2)}\overline{G}_{2j} - \mathbf{d}^{(2)}G_{3j})\sigma^{-j} \\ =&\mathbf{B}^{(2)}\mathbf{f}_4^{(2)}(\sigma) + \overline{\mathbf{B}}^{(2)}\overline{\mathbf{f}_5^{(2)}(\sigma)} - \mathbf{B}^{(1)}\mathbf{f}_4^{(1)}(\sigma) - \overline{\mathbf{B}}^{(1)}\overline{\mathbf{f}_5^{(1)}(\sigma)} - \sum_{j=1}^{\infty}(\overline{\mathbf{d}}^{(1)}\overline{G}_{1j} - \mathbf{d}^{(2)}G_{2j} - \overline{\mathbf{d}}^{(2)}\overline{G}_{3j})\sigma^{j}\end{aligned} \tag{3.130}$$

where

$$\mathbf{X}_1 = (\mathbf{A}^{(2)-1}\mathbf{A}^{(1)} - \mathbf{B}^{(2)-1}\mathbf{B}^{(1)})^{-1}, \quad \mathbf{X}_2 = (\mathbf{A}^{(1)-1}\mathbf{A}^{(2)} - \mathbf{B}^{(1)-1}\mathbf{B}^{(2)})^{-1}. \tag{3.131}$$

Therefore, by Liouville's theorem, Eqs (3.129) and (3.130) yield

$$\mathbf{A}^{(1)}\mathbf{f}_5^{(1)}(\sigma) + \overline{\mathbf{A}}^{(1)}\overline{\mathbf{f}_4^{(1)}(\sigma)} = \mathbf{A}^{(2)}\mathbf{f}_5^{(2)}(\sigma) + \overline{\mathbf{A}}^{(2)}\overline{\mathbf{f}_4^{(2)}(\sigma)} - \sum_{j=1}^{\infty}(\mathbf{c}^{(1)}G_{1j} - \overline{\mathbf{c}}^{(2)}\overline{G}_{2j} - \mathbf{c}^{(2)}G_{3j})\sigma^{-j}, \tag{3.132}$$

$$\mathbf{A}^{(1)}\mathbf{f}_4^{(1)}(\sigma) + \overline{\mathbf{A}}^{(1)}\overline{\mathbf{f}_5^{(1)}(\sigma)} = \mathbf{A}^{(2)}\mathbf{f}_4^{(2)}(\sigma) + \overline{\mathbf{A}}^{(2)}\overline{\mathbf{f}_5^{(2)}(\sigma)} - \sum_{j=1}^{\infty}(\overline{\mathbf{c}}^{(1)}\overline{G}_{1j} - \mathbf{c}^{(2)}G_{2j} - \overline{\mathbf{c}}^{(2)}\overline{G}_{3j})\sigma^{j}, \tag{3.133}$$

$$\mathbf{B}^{(1)}\mathbf{f}_5^{(1)}(\sigma) + \overline{\mathbf{B}}^{(1)}\overline{\mathbf{f}_4^{(1)}(\sigma)} = \mathbf{B}^{(2)}\mathbf{f}_5^{(2)}(\sigma) + \overline{\mathbf{B}}^{(2)}\overline{\mathbf{f}_4^{(2)}(\sigma)} - \sum_{j=1}^{\infty}(\mathbf{d}^{(1)}G_{1j} - \overline{\mathbf{d}}^{(2)}\overline{G}_{2j} - \mathbf{d}^{(2)}G_{3j})\sigma^{-j}, \tag{3.134}$$

$$\mathbf{B}^{(1)}\mathbf{f}_4^{(1)}(\sigma) + \overline{\mathbf{B}}^{(1)}\overline{\mathbf{f}_5^{(1)}(\sigma)} = \mathbf{B}^{(2)}\mathbf{f}_4^{(2)}(\sigma) + \overline{\mathbf{B}}^{(2)}\overline{\mathbf{f}_5^{(2)}(\sigma)} - \sum_{j=1}^{\infty}(\overline{\mathbf{d}}^{(1)}\overline{G}_{1j} - \mathbf{d}^{(2)}G_{2j} - \overline{\mathbf{d}}^{(2)}\overline{G}_{3j})\sigma^{j} \tag{3.135}$$

The above four equations are not completely independent. For example, Eqs (3.132) and (3.134) can be obtained from Eqs (3.133) and (3.135). Thus only two of the equations are independent. However, there are four sets of constant vectors, i.e., $\mathbf{r}_k^{(j)}$ and $\mathbf{s}_k^{(j)}(j=1,2)$, to be determined. We need two more equations to make the solution unique. Through use of the relation (3.94) and Eqs (3.121) and (3.122), the

unknown vectors $\mathbf{r}_j^{(2)}$ and $\mathbf{s}_j^{(2)}$ appearing in $\mathbf{f}_4^{(2)}$ and $\mathbf{f}_5^{(2)}$ can be determined as follows:

$$\begin{aligned}\mathbf{r}_j^{(2)} = (\mathbf{A}^{(2)-1}\left\langle\Gamma_{j\alpha}^{(2)}\right\rangle\mathbf{A}^{(2)} - \mathbf{B}^{(2)-1}\left\langle\Gamma_{j\alpha}^{(2)}\right\rangle\mathbf{B}^{(2)})^{-1}[\mathbf{A}^{(2)-1}(\mathbf{c}^{(2)}G_{3j} - \left\langle\Gamma_{j\alpha}^{(2)}\right\rangle\mathbf{c}^{(2)}G_{2j}) \\ - \mathbf{B}^{(2)-1}(\mathbf{d}^{(2)}G_{3j} - \left\langle\Gamma_{j\alpha}^{(2)}\right\rangle\mathbf{d}^{(2)}G_{2j})], \qquad (j=1,\cdots,\infty),\end{aligned} \tag{3.136}$$

$$\mathbf{s}_j^{(2)} = \mathbf{B}^{(2)-1}[\left\langle\Gamma_{j\alpha}^{(2)}\right\rangle(\mathbf{B}^{(2)}\mathbf{r}_j^{(2)} + \mathbf{d}^{(2)}G_{2j}) - \mathbf{d}^{(2)}G_{3j}] \qquad (j=1,\cdots,\infty), \tag{3.137}$$

where $\left\langle\Gamma_{j\alpha}^{(i)}\right\rangle = \left\langle\left(\dfrac{a+ibp_\alpha^{(i)}}{a-ibp_\alpha^{(i)}}\right)^j\right\rangle$.

Once the constant vectors $\mathbf{r}_j^{(2)}$ and $\mathbf{s}_j^{(2)}$ are obtained, the unknown vectors $\mathbf{r}_j^{(1)}$ and $\mathbf{s}_j^{(1)}$ appearing in functions $\mathbf{f}_4^{(1)}$ and $\mathbf{f}_5^{(1)}$ can be determined from Eqs (3.132) and (3.134) [or(3.133) and (3.135)]. They are

$$\begin{aligned}\mathbf{r}_j^{(1)} = i\mathbf{A}^{(1)T}\{(\mathbf{M}_2 + \overline{\mathbf{M}}_1)\mathbf{A}^{(2)}\mathbf{r}_j^{(2)} + (\overline{\mathbf{M}}_1 - \overline{\mathbf{M}}_2)\overline{\mathbf{A}}^{(2)}\overline{\mathbf{s}}_j^{(2)} \\ - \overline{\mathbf{M}}_1(\overline{\mathbf{c}}^{(1)}\overline{G}_{1j} - \mathbf{c}^{(2)}G_{2j} - \overline{\mathbf{c}}^{(2)}\overline{G}_{3j}) + i(\overline{\mathbf{d}}^{(1)}\overline{G}_{1j} - \mathbf{d}^{(2)}G_{2j} - \overline{\mathbf{d}}^{(2)}\overline{G}_{3j})\},\end{aligned} \tag{3.138}$$

$$\begin{aligned}\mathbf{s}_j^{(1)} = i\mathbf{A}^{(1)T}\{(\mathbf{M}_2 + \overline{\mathbf{M}}_1)\mathbf{A}^{(2)}\mathbf{s}_j^{(2)} + (\overline{\mathbf{M}}_1 - \overline{\mathbf{M}}_2)\overline{\mathbf{A}}^{(2)}\overline{\mathbf{r}}_j^{(2)} \\ - \overline{\mathbf{M}}_1(\mathbf{c}^{(1)}G_{1j} - \overline{\mathbf{c}}^{(2)}\overline{G}_{2j} - \mathbf{c}^{(2)}G_{3j}) + i(\mathbf{d}^{(1)}G_{1j} - \overline{\mathbf{d}}^{(2)}\overline{G}_{2j} - \mathbf{d}^{(2)}G_{3j})\}\end{aligned} \tag{3.139}$$

where

$$\mathbf{M}_k = -i\mathbf{B}^{(k)}\mathbf{A}^{(k)-1} = \mathbf{H}^{(k)-1}(\mathbf{I} + i\mathbf{S}^{(k)}),\ \ \mathbf{H}^{(k)} = 2i\mathbf{A}^{(k)}\mathbf{A}^{(k)T},\ \ \mathbf{S}^{(k)} = i(2\mathbf{A}^{(k)}\mathbf{B}^{(k)T} - \mathbf{I}),$$

$$(k=1,2) \tag{3.140}$$

3.7.2 Green's functions for thermal loads applied inside the inclusion

3.7.2.1 Green's functions for thermal fields. For the case of thermal loads h^* and $\hat{T}$ located at a point (x_{10}, x_{20}) inside the inclusion, the general solution for temperature and heat-flow function can be assumed in the form [5]

$$\begin{aligned}T^{(1)} &= f_0(\zeta_t^{(1)}) + f_1(\zeta_t^{(1)}) + \overline{f_0(\zeta_t^{(1)})} + \overline{f_1(\zeta_t^{(1)})}, \\ \vartheta^{(1)} &= -ik^{(1)}f_0(\zeta_t^{(1)}) - ik^{(1)}f_1(\zeta_t^{(1)}) + ik^{(1)}\overline{f_0(\zeta_t^{(1)})} + ik^{(1)}\overline{f_1(\zeta_t^{(1)})}\end{aligned} \tag{3.141}$$

$$\begin{aligned}T^{(2)} &= f_0^*(\zeta_t^{(2)}) + f_2(\zeta_t^{(2)}) + \overline{f_0^*(\zeta_t^{(2)})} + \overline{f_2(\zeta_t^{(2)})}, \\ \vartheta^{(2)} &= -ik^{(2)}f_0^*(\zeta_t^{(2)}) - ik^{(2)}f_2(\zeta_t^{(2)}) + ik^{(2)}\overline{f_0^*(\zeta_t^{(2)})} + ik^{(2)}\overline{f_2(\zeta_t^{(2)})}\end{aligned} \tag{3.142}$$

Here, f_0 and f_0^* can be chosen to represent the solutions associated with the unperturbed thermal fields caused by thermal load. f_1 and f_2 are the functions corresponding to the perturbed field of matrix and inclusion, respectively. Since (x_{10}, x_{20}) is inside the inclusion, there is a branch cut extending from (x_{10}, x_{20}) to infinity. Thus the choice of f_0 and f_0^* should take into account the discontinuity across this branch cut. A proper form of f_0 and f_0^* may be chosen as [10]:

$$f_0(\zeta_t^{(1)}) = d \ln \zeta_t^{(1)}, \quad f_0^*(\zeta_t^{(2)}) = q_0[\ln(z_t^{(2)} - z_{t0}^{(2)}) - \ln a_{1\tau}^{(2)}] \tag{3.143}$$

$$f_2(\zeta_t^{(2)}) = \sum_{j=-\infty}^{\infty} c_j \zeta_t^{(2)j}, \quad c_{-j} = \Gamma_j^* c_j \tag{3.144}$$

where $a_{1\tau}^{(k)}$ is defined in Eq (3.117), d and c_j are unknowns to be determined, $\zeta_t^{(i)}$ and $\zeta_{t0}^{(2)}$ are related to the complex arguments $z_t^{(i)}$ and $z_{t0}^{(2)} (= x_{10} + p_1^{*(2)} x_{20})$ by Eq (3.99), and q_0 is a complex number which can be determined from the conditions

$$\int_C dT = \hat{T} \quad \text{for any closed curve } C \text{ enclosing the point } \zeta_{t0}^{(2)} \tag{3.145}$$

$$\int_C d\vartheta = -h^* \quad \text{for any closed curve } C \text{ enclosing the point } \zeta_{t0}^{(2)} \tag{3.146}$$

Substitution of Eqs (3.143) and (3.144) into (3.141) and (3.142) and later into (3.145) and (3.146) yields

$$q_0 = T_0 / 4\pi i - h^* / 4\pi k^{(2)} \tag{3.147}$$

As for the unknowns d, c_j and the function f_1, they can be derived in the following way. Noting the relation

$$\ln[(z_t - z_{t0}) / a_{1\tau}] = \ln(\zeta_t - \zeta_{t0}) + \ln(1 - \frac{a_{2\tau} / a_{1\tau}}{\zeta_t \zeta_{t0}}) \tag{3.148}$$

where $a_{1\tau} = (a - ip_1^* b)/2$, $a_{2\tau} = (a + ip_1^* b)/2$, we have the series representation

$$f_0^*(\zeta_t^{(2)}) = q_0\{\ln \zeta_t^{(2)} - \sum_{j=1}^{\infty} e_j \zeta_t^{(2)-j}\} \qquad \text{for } |\zeta_t^{(2)}| > |\zeta_{t0}^{(2)}| \tag{3.149}$$

in which $e_j = [\zeta_{t0}^{(2)j} + (a_{2\tau}^{(2)} / a_{1\tau}^{(2)})^j \zeta_{t0}^{(2)-j}] / j$. Imposition of the continuity conditions (3.95) on the interface leads to

$$f_1(\sigma) + \bar{d}\overline{\ln \sigma} + \overline{f_1(\sigma)} + d \ln \sigma = \sum_{j=1}^{\infty} [\bar{c}_j + \Gamma_j^* c_j]\sigma^{-j} + \sum_{j=1}^{\infty} [c_j + \bar{\Gamma}_j^* \bar{c}_j]\sigma^j$$

$$+ q_0\{\ln \sigma - \sum_j^{\infty} e_j \sigma^{-j}\} + \bar{q}_0\{\overline{\ln \sigma} - \sum_j^{\infty} \bar{e}_j \sigma^j\} \tag{3.150}$$

$$-f_1(\sigma) + \bar{d}\overline{\ln \sigma} + \overline{f_1(\sigma)} - d \ln \sigma = \frac{k^{(2)}}{k^{(1)}} \sum_{j=1}^{\infty} [\bar{c}_j - \Gamma_j^* c_j]\sigma^{-j} - \frac{k^{(2)}}{k^{(1)}} \sum_{j=1}^{\infty} [c_j - \bar{\Gamma}_j^* \bar{c}_j]\sigma^j$$

$$- \frac{k^{(2)} q_0}{k^{(1)}}\{\ln \sigma - \sum_j^{\infty} e_j \sigma^{-j}\} + \frac{k^{(2)} \bar{q}_0}{k^{(1)}}\{\overline{\ln \sigma} - \sum_j^{\infty} \bar{e}_j \sigma^j\} \tag{3.151}$$

where $\sigma = e^{i\theta}$ stands for a point located on the unit circle in the ζ_t-plane, and θ is a polar angle. Comparison of the coefficients of the "ln" terms on both sides of Eqs (3.150) and (3.151) yields

$$d = \frac{1}{2}(1+\frac{k^{(2)}}{k^{(1)}})q_0 - \frac{1}{2}(1-\frac{k^{(2)}}{k^{(1)}})\overline{q}_0 \tag{3.152}$$

In order to use the analytical continuation method, Eqs (3.150) and (3.151) are rewritten, by deleting the "ln" terms, as

$$f_1(\sigma) - \sum_{j=1}^{\infty}[\overline{c}_j + \Gamma_j^* c_j - q_0 e_j]\sigma^{-j} = -\overline{f_1(\sigma)} + \sum_{j=1}^{\infty}[c_j + \overline{\Gamma}_j^* \overline{c}_j - \overline{q}_0 \overline{e}_j]\sigma^j \tag{3.153}$$

$$-f_1(\sigma) - \frac{k^{(2)}}{k^{(1)}}\sum_{j=1}^{\infty}[\overline{c}_j - \Gamma_j^* c_j + q_0 e_j]\sigma^{-j} = -\overline{f_1(\sigma)} - \frac{k^{(2)}}{k^{(1)}}\sum_{j=1}^{\infty}[c_j - \overline{\Gamma}_j^* \overline{c}_j + \overline{q}_0 \overline{e}_j]\sigma^j \tag{3.154}$$

Similar to the treatment for the case of loading applied outside the inclusion, application of the method of analytical continuation to Eqs (3.153) and (3.154) yields

$$\begin{aligned} f_1(\zeta) &= \sum_{j=1}^{\infty}[\overline{c}_j + \mathbf{\Gamma}_j^* c_j - q_0 e_j]\zeta^{-j} \qquad \zeta \in \mathbf{\Omega}_1 \\ \overline{f_1(\zeta)} &= \sum_{j=1}^{\infty}[c_j + \overline{\mathbf{\Gamma}}_j^* \overline{c}_j - \overline{q}_0 \overline{e}_j]\zeta^j \qquad \zeta \in \mathbf{\Omega}_2 \end{aligned} \tag{3.155}$$

for Eq (3.153), and

$$\begin{aligned} f_1(\zeta) &= -\frac{k^{(2)}}{k^{(1)}}\sum_{j=1}^{\infty}[\overline{c}_j - \Gamma_j^* c_j + q_0 e_j]\zeta^{-j} \qquad \zeta \in \Omega_1 \\ \overline{f_1(\zeta)} &= -\frac{k^{(2)}}{k^{(1)}}\sum_{j=1}^{\infty}[c_j - \overline{\Gamma}_j^* \overline{c}_j + \overline{q}_0 \overline{e}_j]\zeta^j \qquad \zeta \in \Omega_2 \end{aligned} \tag{3.156}$$

for Eq (3.154). Solving Eqs (3.155) and (3.156) for c_j yields

$$c_j = \frac{k^{(1)} - k^{(2)}}{2k^{(1)}}(G_0 - \overline{G}_j G_j / G_0)^{-1}(\overline{q}_0 \overline{e}_j - \overline{G}_j q_0 e_j / G_0), \qquad (j = 1, 2, \cdots, \infty) \tag{3.157}$$

where

$$G_0 = (1 + k^{(2)}/k^{(1)})/2, \; G_j = (1 - k^{(2)}/k^{(1)})\Gamma_j^*/2 \tag{3.158}$$

Having obtained the solution of c_k, the functions g_i in Eqs $(3.1)_4$ and $(3.2)_2$ can be given by

$$\begin{aligned} g_1(z_t^{(1)}) = q_0\{&a_{1\tau}^{(1)}\zeta_t^{(1)}(\ln\zeta_t^{(1)} - 1) + a_{2\tau}^{(1)}(1 + \ln\zeta_t^{(1)})/\zeta_t^{(1)}\} \\ &+ (\overline{c}_1 + \Gamma_1^* c_1 - q_0 e_1)a_{1\tau}^{(1)}\ln\zeta_t^{(1)} + \sum_{j=1}^{\infty} G_{4j}\zeta_t^{(1)-j} \end{aligned} \tag{3.159}$$

$$\begin{aligned} g_2(z_t^{(2)}) = q_0\{&a_{1\tau}^{(2)}\zeta_t^{(2)}(\ln\zeta_t^{(2)} - 1) + a_{2\tau}^{(2)}(1 + \ln\zeta_t^{(2)})/\zeta_t^{(2)}\} \\ &- q_0 e_1 a_{1\tau}^{(2)}\ln\zeta_t^{(2)} + \sum_{j=1}^{\infty}[G_{5j}\zeta_t^{(2)j} + G_{6j}\zeta_t^{(2)-j}] \end{aligned} \tag{3.160}$$

where

$$
\begin{aligned}
G_{4j} &= -[(\overline{c}_{j+1} + \Gamma^*_{j+1} c_{j+1} - q_0 e_{j+1}) a^{(1)}_{1\tau} - a^{(1)}_{2\tau} (\overline{c}_{j-1} + \Gamma^*_{j-1} c_{j-1} - q_0 e_{j-1}) t_{j1} / j \\
G_{5j} &= (a^{(2)}_{1\tau} c_{j-1} t_{j1} - a^{(2)}_{2\tau} c_{j+1}) / j \\
G_{6j} &= [a^{(2)}_{1\tau} (\Gamma^*_{j+1} c_{j+1} - q_0 e_{j+1}) - a^{(2)}_{2\tau} (\Gamma^*_{j-1} c_{j-1} - q_0 e_{j-1}) t_{j1}] / j
\end{aligned} \tag{3.161}
$$

with $t_{ij} = 1$ for $i \neq j$, $t_{ij} = 0$ for $i = j$.

3.7.2.2 Green's functions for electroelastic fields. From Eqs $(3.1)_4$ and $(3.2)_2$ the particular piezoelectric solution induced by thermal load can be written as

$$
\mathbf{U}^{(i)}_p = 2\,\mathrm{Re}[\mathbf{c}^{(i)} g_i(\zeta^{(i)}_t)], \quad \boldsymbol{\varphi}^{(i)}_p = 2\,\mathrm{Re}[\mathbf{d}^{(i)} g_i(\zeta^{(i)}_t)] \quad (i=1,2) \tag{3.162}
$$

As stated previously, the particular solutions (3.162) do not generally satisfy the conditions $(3.95)_{3,4}$ along the interface. We therefore need to find a corrective isothermal solution for a given problem so that, when it is superimposed on the particular thermoelectroelastic solution, the interface conditions $(3.95)_{3,4}$ will be satisfied. Owing to the fact that $f(\zeta_\alpha)$ and $g(\zeta_t)$ have the same order to affect the SED in Eq $(3.2)_2$, possible function forms may be taken from the partition of $g(\zeta_t)$ in order to satisfy the boundary conditions considered. They are

$$
\begin{aligned}
&f^{(j)}_1(z^{(j)}_k) = aF_1(\zeta^{(j)}_k)/2, \quad f^{(j)}_2(z^{(j)}_k) = ip^{(j)}_k bF_2(\zeta^{(j)}_k)/2, \\
&f^{(j)}_3(z^{(j)}_k) = a^{(j)}_{1k} \ln \zeta^{(j)}_k,
\end{aligned} \quad (j=1,2) \tag{3.163}
$$

$$
\mathbf{f}^{(j)}_4(\boldsymbol{\zeta}^{(j)}) = \sum_{k=1}^{\infty} \left\langle \zeta^{(j)k}_\alpha \right\rangle \mathbf{r}^{(j)}_k, \quad \mathbf{f}^{(j)}_5(\boldsymbol{\zeta}^{(j)}) = \sum_{k=1}^{\infty} \left\langle \zeta^{(j)-k}_\alpha \right\rangle \mathbf{s}^{(j)}_k \qquad (j=1,2) \tag{3.164}
$$

where $\mathbf{f}^{(j)}_k$ are 4-component vectors, $\mathbf{r}^{(j)}_k$ and $\mathbf{s}^{(j)}_k$ are constant vectors with 4-componants to be determined, and

$$
\begin{aligned}
F_1(\zeta) &= \zeta^{-1}(1 + \ln \zeta) - \zeta(1 - \ln \zeta), \\
F_2(\zeta) &= \zeta^{-1}(1 + \ln \zeta) + \zeta(1 - \ln \zeta),
\end{aligned} \tag{3.165}
$$

The Green's functions for the electroelastic fields can thus be chosen as

$$
\mathbf{U}^{(j)} = 2\,\mathrm{Re}\{\sum_{k=1}^{3} \mathbf{A}^{(j)} \left\langle f^{(j)}_k(\zeta^{(j)}_\alpha) \right\rangle \mathbf{q}^{(j)}_k + \sum_{k=4}^{5} \mathbf{A}^{(j)} \mathbf{f}^{(j)}_k(\boldsymbol{\zeta}^{(j)}) + \mathbf{c}^{(j)} g_j(\zeta^{(j)}_t)] \tag{3.166}
$$

$$
\boldsymbol{\varphi}^{(j)} = 2\,\mathrm{Re}\{\sum_{k=1}^{3} \mathbf{B}^{(j)} \left\langle f^{(j)}_k(\zeta^{(j)}_\alpha) \right\rangle \mathbf{q}^{(j)}_k + \sum_{k=4}^{5} \mathbf{B}^{(j)} \mathbf{f}^{(j)}_k(\boldsymbol{\zeta}^{(j)}) + \mathbf{d}^{(j)} g_j(\zeta^{(j)}_t)] \tag{3.167}
$$

Substituting Eqs (3.166) and (3.167) into Eq (3.95) provides

$$
\mathbf{q}^{(1)}_1 = q_0 \mathbf{X}_1 [\mathbf{A}^{(2)-1}(\mathbf{c}^{(2)} - \mathbf{c}^{(1)}) - \mathbf{B}^{(2)-1}(\mathbf{d}^{(2)} - \mathbf{d}^{(1)})], \tag{3.168}
$$

$$
\mathbf{q}^{(2)}_1 = q_0 \mathbf{X}_2 [\mathbf{A}^{(1)-1}(\mathbf{c}^{(1)} - \mathbf{c}^{(2)}) - \mathbf{B}^{(1)-1}(\mathbf{d}^{(1)} - \mathbf{d}^{(2)})], \tag{3.169}
$$

$$
\mathbf{q}^{(1)}_2 = q_0 \mathbf{P}^{(1)-1} \mathbf{X}_1 [\mathbf{A}^{(2)-1}(p^{*(2)}_1 \mathbf{c}^{(2)} - p^{*(1)}_1 \mathbf{c}^{(1)}) - \mathbf{B}^{(2)-1}(p^{*(2)}_1 \mathbf{d}^{(2)} - p^{*(1)}_1 \mathbf{d}^{(1)})], \tag{3.170}
$$

$$\mathbf{q}_2^{(2)} = q_0 \mathbf{P}^{(2)-1} \mathbf{X}_2 [\mathbf{A}^{(1)-1}(p_1^{*(1)}\mathbf{c}^{(1)} - p_1^{*(2)}\mathbf{c}^{(2)}) - \mathbf{B}^{(1)-1}(p_1^{*(1)}\mathbf{d}^{(1)} - p_1^{*(2)}\mathbf{d}^{(2)})], \tag{3.171}$$

$$\mathbf{q}_3^{(1)} = \left\langle a_{1k}^{(1)} \right\rangle^{-1} \mathbf{X}_1 [\mathbf{A}^{(2)-1}(b_*^{(1)}\mathbf{c}^{(1)} - b_*^{(2)}\mathbf{c}^{(2)}) - \mathbf{B}^{(2)-1}(b_*^{(1)}\mathbf{d}^{(1)} - b_*^{(2)}\mathbf{d}^{(2)})], \tag{3.172}$$

$$\mathbf{q}_3^{(2)} = \left\langle a_{1k}^{(2)} \right\rangle^{-1} \mathbf{X}_1 [\mathbf{A}^{(1)-1}(b_*^{(2)}\mathbf{c}^{(2)} - b_*^{(1)}\mathbf{c}^{(1)}) - \mathbf{B}^{(1)-1}(b_*^{(2)}\mathbf{d}^{(2)} - b_*^{(1)}\mathbf{d}^{(1)})], \tag{3.173}$$

$$\mathbf{A}^{(1)}\mathbf{f}_5^{(1)}(\sigma) + \overline{\mathbf{A}}^{(1)}\overline{\mathbf{f}_4^{(1)}(\sigma)} - \mathbf{A}^{(2)}\mathbf{f}_5^{(2)}(\sigma) - \overline{\mathbf{A}}^{(2)}\overline{\mathbf{f}_4^{(2)}(\sigma)} + \sum_{j=1}^{\infty}(\mathbf{c}^{(1)}G_{4j} - \overline{\mathbf{c}}^{(2)}\overline{G}_{5j} - \mathbf{c}^{(2)}G_{6j})\sigma^{-j}$$

$$= \mathbf{A}^{(2)}\mathbf{f}_4^{(2)}(\sigma) + \overline{\mathbf{A}}^{(2)}\overline{\mathbf{f}_5^{(2)}(\sigma)} - \mathbf{A}^{(1)}\mathbf{f}_4^{(1)}(\sigma) - \overline{\mathbf{A}}^{(1)}\overline{\mathbf{f}_5^{(1)}(\sigma)} - \sum_{j=1}^{\infty}(\overline{\mathbf{c}}^{(1)}\overline{G}_{4j} - \mathbf{c}^{(2)}G_{5j} - \overline{\mathbf{c}}^{(2)}\overline{G}_{6j})\sigma^{j} \tag{3.174}$$

$$\mathbf{B}^{(1)}\mathbf{f}_5^{(1)}(\sigma) + \overline{\mathbf{B}}^{(1)}\overline{\mathbf{f}_4^{(1)}(\sigma)} - \mathbf{B}^{(2)}\mathbf{f}_5^{(2)}(\sigma) - \overline{\mathbf{B}}^{(2)}\overline{\mathbf{f}_4^{(2)}(\sigma)} + \sum_{j=1}^{\infty}(\mathbf{d}^{(1)}G_{4j} - \overline{\mathbf{d}}^{(2)}\overline{G}_{5j} - \mathbf{d}^{(2)}G_{6j})\sigma^{-j}$$

$$= \mathbf{B}^{(2)}\mathbf{f}_4^{(2)}(\sigma) + \overline{\mathbf{B}}^{(2)}\overline{\mathbf{f}_5^{(2)}(\sigma)} - \mathbf{B}^{(1)}\mathbf{f}_4^{(1)}(\sigma) - \overline{\mathbf{B}}^{(1)}\overline{\mathbf{f}_5^{(1)}(\sigma)} - \sum_{j=1}^{\infty}(\overline{\mathbf{d}}^{(1)}\overline{G}_{4j} - \mathbf{d}^{(2)}G_{5j} - \overline{\mathbf{d}}^{(2)}\overline{G}_{6j})\sigma^{j} \tag{3.175}$$

where

$$\mathbf{P}^{(j)} = \text{diag}[p_1^{(j)}\ p_2^{(j)}\ p_3^{(j)}\ p_4^{(j)}],\ \ b_*^{(1)} = a_{1\tau}^{(1)}(\bar{c}_1 + \Gamma_1^* c_1 - q_0 e_1),\ b_*^{(2)} = -q_0 a_{1\tau}^{(2)} e_1 \tag{3.176}$$

It is found that Eqs (3.175) and (3.176) can be obtained from Eqs (3.129) and (3.130) by replacing G_{1j} by G_{4j}, G_{2j} by G_{5j}, and G_{3j} by G_{6j}. Therefore, the procedure for determining the four sets of constant vectors, i.e., $\mathbf{r}_k^{(j)}$ and $\mathbf{s}_k^{(j)}(j=1,2)$, operates in the same way as that treated in Section 3.7.1.2. The results of $\mathbf{r}_k^{(j)}$ and $\mathbf{s}_k^{(j)}$ in Eq (3.164) have the same form as those in Eqs (3.136)-(3.139), but G_{1j}, G_{2j}, G_{3j} in those equations are now replaced by G_{4j}, G_{5j}, and G_{6j}.

3.7.3 Green's functions for thermal loads applied on the interface

3.7.3.1 Green's functions for thermal fields. When (x_{10}, x_{20}) is on the interface, say $x_{10} = a\cos\theta_0$, $x_{20} = b\sin\theta_0$, $\zeta_{t0}^{(1)} = \zeta_{t0}^{(2)} = e^{i\theta_0}$, the proper choice of f_0 and f_0^* should reflect the singularity properties of both inclusion and matrix. By referring to the Eq (20) given in Yen et al [10], they may be assumed in the form

$$f_0(\zeta_t^{(1)}) = q_0 \ln(\zeta_t^{(1)} - e^{i\theta_0}) \tag{3.177}$$

$$f_1(\zeta_t^{(1)}) = \sum_{j=1}^{\infty} a_{*j}\zeta_t^{(1)-j} + q_1 \ln(\zeta_t^{(1)-1} - e^{-i\theta_0}) \tag{3.178}$$

$$f_0^*(\zeta_t^{(2)}) = q_2 \ln[(z_t^{(2)} - z_{t0}^{(2)})/a_{1\tau}^{(2)}] \tag{3.179}$$

With the use of the series representation

$$\ln(1-x) = -\sum_{j=1}^{\infty} x^j / j \tag{3.180}$$

and the relation (3.148), Eq (3.179) may be rewritten as

$$f_0^*(\zeta_t^{(2)}) = q_2\{\ln(\zeta_t^{(2)} - e^{i\theta_0}) - \sum_{j=1}^{\infty}[(a_{2\tau}^{(2)}e^{-i\theta_0}/a_{1\tau}^{(2)})^j \zeta_t^{(2)-j}/j]\} \tag{3.181}$$

The continuity conditions $(3.95)_{1,2}$ on the interface give

$$q_1 = \frac{k^{(1)} - k^{(2)}}{k^{(1)} + k^{(2)}} \overline{q}_0, \quad q_2 = \frac{2k^{(1)}}{k^{(1)} + k^{(2)}} q_0 \tag{3.182}$$

To determine the remaining unknown functions, f_1 and f_2, the method of analytical continuation presented in the previous sections will be used. As described in Eqs (3.105) and (3.106), the holomorphic properties provide

$$\begin{aligned}
&f_{11}(\zeta) = f_{22}(\zeta) + \overline{f_{21}(\zeta)}, && \zeta \in \Omega_1 \\
&\overline{f_{11}(\zeta)} = \overline{f_{22}(\zeta)} + f_{21}(\zeta), && \zeta \in \Omega_2 \\
&f_{11}(\zeta) = k^{(2)}[f_{22}(\zeta) - \overline{f_{21}(\zeta)}]/k^{(1)}, && \zeta \in \Omega_1 \\
&\overline{f_{11}(\zeta)} = k^{(2)}[\overline{f_{22}(\zeta)} - f_{21}(\zeta)]/k^{(1)}, && \zeta \in \Omega_2
\end{aligned} \tag{3.183}$$

where

$$\begin{aligned}
&f_{11}(\zeta) = \sum_{j=1}^{\infty} a_{*j} \zeta^{-j}, \quad f_{21}(\zeta) = \sum_{j=1}^{\infty} c_j \zeta^j, \\
&f_{22}(\zeta) = \sum_{j=1}^{\infty} [\Gamma_j^* c_j - e_{*j}] \zeta^{-j}
\end{aligned} \tag{3.184}$$

where $e_{*j} = q_2 (a_{2\tau}^{(2)} e^{-i\theta_0} / a_{1\tau}^{(2)})^j / j$.

Solving Eq (3.183) yields

$$a_{*j} = \overline{c}_j + \Gamma_j^* c_j - e_{*j}, \tag{3.185}$$

$$c_j = \frac{k^{(1)} - k^{(2)}}{2k^{(1)}} (G_0 - \overline{G}_j G_j / G_0)^{-1} (\overline{e}_{*j} - \overline{G}_j e_{*j} / G_0), \qquad j = 1, 2, \cdots, \infty \tag{3.186}$$

Thus the corresponding functions g_i are given as

$$\begin{aligned}
g_1(z_t^{(1)}) = \{&a_{1\tau}^{(1)} [q_0 F_3(\zeta_t^{(1)}, e^{i\theta_0}) + q_1 F_4(\zeta_t^{(1)-1}, e^{-i\theta_0})] + a_{2\tau}^{(1)} [q_0 F_4(\zeta_t^{(1)}, e^{i\theta_0}) \\
&+ q_1 F_3(\zeta_t^{(1)-1}, e^{-i\theta_0})] + a_{*1} a_{1\tau}^{(1)} \ln \zeta_t^{(1)} + \sum_{j=1}^{\infty} G_{7j} \zeta_t^{(1)-j}\}
\end{aligned} \tag{3.187}$$

$$\begin{aligned}
g_2(z_t^{(2)}) = &q_2 \{a_{1\tau}^{(2)} F_3(\zeta_t^{(2)}, e^{i\theta_0}) + a_{2\tau}^{(2)} F_4(\zeta_t^{(2)}, e^{i\theta_0})\} - e_{*1} a_{1\tau}^{(2)} \ln \zeta_t^{(2)} \\
&+ \sum_{j=1}^{\infty} [G_{8j} \zeta_t^{(2)j} + G_{9j} \zeta_t^{(2)-j}]
\end{aligned} \tag{3.188}$$

where

$$F_3(x, y) = (x - y)[\ln(x - y) - 1] \tag{3.189}$$

$$F_4(x, y) = (\frac{1}{x} - \frac{1}{y}) \ln(x - y) + \frac{1}{y} \ln x \tag{3.190}$$

$$
\begin{aligned}
G_{7j} &= -[a_{1\tau}^{(1)} a_{*(j+1)} - t_{j1} a_{2\tau}^{(1)} a_{*(j-1)}]/\, j, \\
G_{8j} &= (a_{1\tau}^{(2)} c_{j-1} t_{j1} - a_{2\tau}^{(2)} c_{j+1})/\, j = G_{5j}, \\
G_{9j} &= -[a_{1\tau}^{(2)} (\Gamma_{j+1}^{*} c_{j+1} - e_{*(j+1)}) - a_{2\tau}^{(2)} (\Gamma_{j-1}^{*} c_{j-1} - e_{*(j-1)}) t_{j1}]/\, j
\end{aligned}
\tag{3.191}
$$

For the same reason as given in relation to Eqs (3.166) and (3.167), the corresponding electroelastic solutions may be assumed in the form

$$
\mathbf{U}^{(j)} = 2\,\mathrm{Re}\{\sum_{k=1}^{5} \mathbf{A}^{(j)} \left\langle f_k^{(j)}(\zeta_\alpha^{(j)}) \right\rangle \mathbf{q}_k^{(j)} + \sum_{k=6}^{7} \mathbf{A}^{(j)} \mathbf{f}_k^{(j)}(\boldsymbol{\zeta}^{(j)}) + \mathbf{c}^{(j)} g_j(\zeta_t^{(j)})\} \tag{3.192}
$$

$$
\boldsymbol{\varphi}^{(j)} = 2\,\mathrm{Re}\{\sum_{k=1}^{5} \mathbf{B}^{(j)} \left\langle f_k^{(j)}(\zeta_\alpha^{(j)}) \right\rangle \mathbf{q}_k^{(j)} + \sum_{k=6}^{7} \mathbf{B}^{(j)} \mathbf{f}_k^{(j)}(\boldsymbol{\zeta}^{(j)}) + \mathbf{d}^{(j)} g_j(\zeta_t^{(j)})\} \tag{3.193}
$$

where

$$
\begin{aligned}
f_1^{(j)}(\zeta_\alpha^{(j)}) &= a[q_0 F_3(\zeta_\alpha^{(j)}, e^{i\theta_0}) + q_0 F_4(\zeta_\alpha^{(j)}, e^{i\theta_0}) \\
&\quad + q_1 F_3(\zeta_\alpha^{(j)-1}, e^{-i\theta_0}) + q_1 F_4(\zeta_\alpha^{(j)-1}, e^{-i\theta_0})]/2 \\
f_2^{(j)}(\zeta_\alpha^{(j)}) &= i p_\alpha^{(j)} b[-q_0 F_3(\zeta_\alpha^{(j)}, e^{i\theta_0}) + q_0 F_4(\zeta_\alpha^{(j)}, e^{i\theta_0}) \\
&\quad + q_1 F_3(\zeta_\alpha^{(j)-1}, e^{-i\theta_0}) - q_1 F_4(\zeta_\alpha^{(j)-1}, e^{-i\theta_0})]/2
\end{aligned}
\qquad (j=1,2) \tag{3.194}
$$

$$
\begin{aligned}
f_3^{(j)}(\zeta_\alpha^{(j)}) &= a[q_2 F_3(\zeta_\alpha^{(j)}, e^{i\theta_0}) + q_2 F_4(\zeta_\alpha^{(j)}, e^{i\theta_0})]/2 \\
f_4^{(j)}(\zeta_\alpha^{(j)}) &= i p_\alpha^{(j)} b[-q_2 F_3(\zeta_\alpha^{(j)}, e^{i\theta_0}) + q_2 F_4(\zeta_\alpha^{(j)}, e^{i\theta_0})]/2
\end{aligned}
\qquad (j=1,2) \tag{3.195}
$$

$$
f_5^{(j)}(\zeta_\alpha^{(j)}) = a_{1\alpha}^{(j)} \ln \zeta_\alpha^{(j)} \qquad (j=1,2) \tag{3.196}
$$

$$
\mathbf{f}_6^{(j)}(\boldsymbol{\zeta}^{(j)}) = \sum_{k=1}^{\infty} \left\langle \zeta_\alpha^{(j)k} \right\rangle \mathbf{r}_k^{(j)}, \quad \mathbf{f}_7^{(j)}(\boldsymbol{\zeta}^{(j)}) = \sum_{k=1}^{\infty} \left\langle \zeta_\alpha^{(j)-k} \right\rangle \mathbf{s}_k^{(j)} \qquad (j=1,2) \tag{3.197}
$$

The continuity conditions $(3.95)_{3,4}$ now provide

$$
\mathbf{q}_1^{(1)} = \mathbf{X}_1(\mathbf{B}^{(2)-1}\mathbf{d}^{(1)} - \mathbf{A}^{(2)-1}\mathbf{c}^{(1)}), \quad \mathbf{q}_1^{(2)} = \mathbf{X}_2(\mathbf{A}^{(1)-1}\mathbf{c}^{(1)} - \mathbf{B}^{(1)-1}\mathbf{d}^{(1)}), \tag{3.198}
$$

$$
\mathbf{q}_2^{(1)} = p_1^{*(1)} \mathbf{P}^{(1)-1} \mathbf{q}_1^{(1)}, \qquad \mathbf{q}_2^{(2)} = p_1^{*(1)} \mathbf{P}^{(2)-1} \mathbf{q}_1^{(2)}, \tag{3.199}
$$

$$
\mathbf{q}_3^{(1)} = \mathbf{X}_1(\mathbf{A}^{(2)-1}\mathbf{c}^{(2)} - \mathbf{B}^{(2)-1}\mathbf{d}^{(2)}), \quad \mathbf{q}_3^{(2)} = \mathbf{X}_2(\mathbf{B}^{(1)-1}\mathbf{d}^{(2)} - \mathbf{A}^{(1)-1}\mathbf{c}^{(2)}), \tag{3.200}
$$

$$
\mathbf{q}_4^{(1)} = p_1^{*(2)} \mathbf{P}^{(1)-1} \mathbf{q}_3^{(1)}, \qquad \mathbf{q}_4^{(2)} = p_1^{*(2)} \mathbf{P}^{(2)-1} \mathbf{q}_3^{(2)}, \tag{3.201}
$$

$$
\mathbf{q}_5^{(1)} = \left\langle a_{1k}^{(1)} \right\rangle^{-1} \mathbf{X}_1[\mathbf{A}^{(2)-1}(b_{**}^{(1)}\mathbf{c}^{(1)} - b_{**}^{(2)}\mathbf{c}^{(2)}) - \mathbf{B}^{(2)-1}(b_{**}^{(1)}\mathbf{d}^{(1)} - b_{**}^{(2)}\mathbf{d}^{(2)})], \tag{3.202}
$$

$$
\mathbf{q}_5^{(2)} = \left\langle a_{1k}^{(2)} \right\rangle^{-1} \mathbf{X}_2[\mathbf{A}^{(1)-1}(b_{**}^{(2)}\mathbf{c}^{(2)} - b_{**}^{(1)}\mathbf{c}^{(1)}) - \mathbf{B}^{(1)-1}(b_{**}^{(2)}\mathbf{d}^{(2)} - b_{**}^{(1)}\mathbf{d}^{(1)})] \tag{3.203}
$$

while the remaining unknown coefficients have the same form as those in Eqs (3.136)~(3.139) except that G_{1j}, G_{2j} and G_{3j} should be replaced by G_{7j}, G_{8j} and G_{9j}.

3.7.3 Green's functions for an elliptic hole

3.7.3.1 Boundary conditions. When the inclusion becomes an elliptic hole with finite permittivity and thermal conductivity but vanishing elastic stiffness, the Green's function can be derived based on the results in the last section. In this case, the thermal and electric fields are still continuous across the hole surface, but the hole is free of traction. The boundary conditions on the hole can thus be written as

$$\vartheta^{(1)} = \vartheta^{(0)}; \quad \mathbf{t}_{\mathrm{n}}^{(1)} = \{t_1\ t_2\ t_3\ D_n\}^T = \mathbf{t}_0 = \mathbf{I}_4 D_0 \tag{3.204}$$

where $\mathbf{I}_4=\{0\ 0\ 0\ 1\}^T$, t_i (i=1,2,3) are the rectangular coordinates of surface force, $\mathbf{t}_0$ is surface traction-charge vector in the hole, the subscript "0" stands for the quantity associated with hole material, and D_n and D_0 are the normal components of electric displacement in the matrix and the hole, respectively. Noting that $\mathbf{t}_n=\boldsymbol{\varphi}_{,s}$, the boundary condition $(3.204)_2$ can be further written as

$$\boldsymbol{\varphi}^{(1)}\big|_s = \mathbf{I}_4 \int_s D_0 ds = \mathbf{I}_4 \int_s (D_{20} dx_1 - D_{10} dx_2) \tag{3.205}$$

By writing the electric potential $\phi^{(0)}(z)$, where $z_0=x_1+ix_2$, inside the hole as

$$\phi^{(0)}(z_0) = 2\,\mathrm{Re}\, f_0(z_0) \tag{3.206}$$

the electric displacement D_{i0} can be expressed as

$$D_{10} = -2\kappa_0\,\mathrm{Re}[df_0/dz_0], \quad D_{20} = 2\kappa_0\,\mathrm{Im}[df_0/dz_0] \tag{3.207}$$

where κ_0 is the dielectric constant of the hole material. Using the above relations, Eq (3.205) can be further written as

$$\boldsymbol{\varphi}^{(1)}\big|_s = 2\kappa_0 \mathbf{I}_4\,\mathrm{Im}[f_0(z_0)] \tag{3.208}$$

In addition, the continuous condition of electric potential across the hole surface requires

$$\phi^{(1)} = 2\,\mathrm{Re}\, f_0(z_0) \tag{3.209}$$

3.7.3.2 Green's function for holes. Since the interface condition for thermal field is the same as that in section 3.7.2, the Green's functions given in Eqs (3.187) and (3.188) are still available, but Eq (3.188) should be rewritten in the following form, using the subscript "0" here instead of the subscript "2":

$$\begin{aligned} g_0(z_t^{(0)}) = {} & q_2\{a_{1\tau}^{(0)} F_3(\zeta_t^{(0)}, e^{i\theta_0}) + a_{2\tau}^{(0)} F_4(\zeta_t^{(0)}, e^{i\theta_0})\} - e_{*1} a_{1\tau}^{(0)} \ln \zeta_t^{(0)} \\ & + \sum_{j=1}^{\infty} [G_{8j} \zeta_t^{(0)j} + G_{9j} \zeta_t^{(0)-j}] \end{aligned} \tag{3.210}$$

and $\zeta_t^{(0)}$ is related to $z_t^{(0)}$ ($x_1+ p_1^{*(0)} x_2$) by

$$z_t^{(0)} = a_{1\tau}^{(0)} \zeta_t^{(0)} + a_{2\tau}^{(0)} \zeta_t^{(0)-1} \tag{3.211}$$

The boundary conditions (3.208) and (3.209) together with Eqs (3.187) and (3.210) suggest that the solutions $\phi^{(0)}$, $\phi^{(1)}$ and $\boldsymbol{\varphi}^{(1)}$ be chosen as

$$\phi^{(0)}(\zeta_0) = 2\,\mathrm{Re}[\sum_{k=1}^{5} f_{k0}(\zeta_0) q_{k0} + f_{60}(\zeta_0) + f_{70}(\zeta_0) + c_4^{(0)} g_0(\zeta_t^{(0)})] \tag{3.212}$$

$$\phi^{(1)}(\boldsymbol{\zeta}) = 2\,\mathrm{Re}[\mathbf{A}_4^{(1)}\{\sum_{k=1}^{5}\left\langle f_{k\alpha}(\zeta_\alpha)\right\rangle \mathbf{q}_k^{(1)} + \mathbf{f}_6(\boldsymbol{\zeta}) + \mathbf{f}_7(\boldsymbol{\zeta})\} + c_4^{(1)} g_1(\zeta_t^{(1)})] \tag{3.213}$$

$$\boldsymbol{\varphi}^{(1)} = 2\,\mathrm{Re}[\mathbf{B}_1\{\sum_{k=1}^{5}\left\langle f_{k\alpha}(\zeta_\alpha)\right\rangle \mathbf{q}_k^{(1)} + \mathbf{f}_6(\boldsymbol{\zeta}) + \mathbf{f}_7(\boldsymbol{\zeta})\} + \mathbf{d}^{(1)} g_1(\zeta_t^{(1)})] \tag{3.214}$$

where $\zeta_\alpha = \zeta_\alpha^{(1)}$, q_{k0} and $\mathbf{q}_k^{(1)} = \{q_{k1}\ q_{k2}\ q_{k3}\ q_{k4}\}^T$ are constants to be determined, $\mathbf{A}_4^{(1)} = (A_{41}^{(1)}\ A_{42}^{(1)}\ A_{43}^{(1)}\ A_{44}^{(1)}\}$, A_{ij} are the components of matrix $\mathbf{A}$, and

$$\begin{aligned} f_{1\alpha}(\zeta_\alpha) = a[&q_0 F_3(\zeta_\alpha, e^{i\theta_0}) + q_0 F_4(\zeta_\alpha, e^{i\theta_0}) \\ &+ q_1 F_3(\zeta_\alpha^{-1}, e^{-i\theta_0}) + q_1 F_4(\zeta_\alpha^{-1}, e^{-i\theta_0})]/2 \end{aligned} \qquad (\alpha = 0\text{-}4) \tag{3.215}$$

$$\begin{aligned} f_{2\alpha}(\zeta_\alpha) = ip_\alpha b[&-q_0 F_3(\zeta_\alpha, e^{i\theta_0}) + q_0 F_4(\zeta_\alpha, e^{i\theta_0}) \\ &+ q_1 F_3(\zeta_\alpha^{-1}, e^{-i\theta_0}) - q_1 F_4(\zeta_\alpha^{-1}, e^{-i\theta_0})]/2 \end{aligned} \qquad (\alpha = 0\text{-}4) \tag{3.215}$$

$$\begin{aligned} f_{3\alpha}(\zeta_\alpha) &= a[q_2 F_3(\zeta_\alpha, e^{i\theta_0}) + q_2 F_4(\zeta_\alpha, e^{i\theta_0})]/2 \\ f_{4\alpha}(\zeta_\alpha) &= ip_\alpha b[-q_2 F_3(\zeta_\alpha, e^{i\theta_0}) + q_2 F_4(\zeta_\alpha, e^{i\theta_0})]/2 \end{aligned} \qquad (\alpha = 0\text{-}4) \tag{3.217}$$

$$f_{5\alpha}(\zeta_\alpha) = a_{1\alpha}^{(1)} \ln \zeta_\alpha;\ \ f_{50}(\zeta_0) = \ln \zeta_0 \qquad (\alpha = 1\text{-}4) \tag{3.218}$$

$$\mathbf{f}_6(\boldsymbol{\zeta}) = \sum_{k=1}^{\infty}\left\langle \zeta_m^k \right\rangle \mathbf{r}_k^{(1)},\ \ \mathbf{f}_7(\boldsymbol{\zeta}) = \sum_{k=1}^{\infty}\left\langle \zeta_m^{-k} \right\rangle \mathbf{s}_k^{(1)} \qquad (\alpha = 1\text{-}4) \tag{3.219}$$

$$f_{60}(\zeta_0) = \sum_{k=1}^{\infty} \zeta_0^k r_{k0},\ \ f_{70}(\zeta_0) = \sum_{k=1}^{\infty} \zeta_0^{-k} s_{k0} \tag{3.220}$$

where $p_m = p_m^{(1)}$, $p_0 = i$, $r_k^{(1)} = \{r_{k1}\ r_{k2}\ r_{k3}\ r_{k4}\}^T$ and $s_k^{(1)} = \{s_{k1}\ s_{k2}\ s_{k3}\ s_{k4}\}^T$ are two four-component vectors to be determined.

The interface condition (3.209) provides

$$q_{10} = \mathbf{A}_4^{(1)} \mathbf{q}_1^{(1)} + c_4^{(1)}, \qquad q_{20} = -i\sum_{j=1}^{4} A_{4j}^{(1)} p_j q_{2j}^{(1)} - i\tau_1 c_4^{(1)} \tag{3.221}$$

$$q_{30} = \mathbf{A}_4^{(1)} \mathbf{q}_3^{(1)} + c_4^{(1)}, \qquad q_{40} = -i\sum_{j=1}^{4} A_{4j}^{(1)} p_j q_{4j}^{(1)} + i\tau_2 c_4^{(1)} \tag{3.222}$$

$$q_{50} = \mathbf{A}_4^{(1)}\left\langle a_{1m}^{(1)} \right\rangle \mathbf{q}_5^{(1)} + a_{*1} a_{1\tau}^{(1)} c_4^{(1)} + e_{*1} a_{1\tau}^{(0)} c_4^{(0)} \tag{3.223}$$

The remaining unknowns r_{j0}, s_{j0}, $\mathbf{q}_k^{(1)}$, $\mathbf{r}_j^{(1)}$ and $\mathbf{s}_j^{(1)}$ can also be determined through use of the boundary conditions (3.208), (3.209) and Eq (3.94), and we will omit those details, which are tedious and algebraic.

3.7.3.3 Cracks. By letting $b \to 0$ in Eq (3.55), the problem discussed above becomes an infinite piezoelectric solid containing a slit crack of length 2*a*. In this case, Eqs

(3.187) and (3.188) are reduced to

$$g_1(z_t^{(1)}) = \frac{a}{2}\{q_0 F_3(\zeta_t^{(1)}, e^{i\theta_0}) + q_1 F_4(\zeta_t^{(1)-1}, e^{-i\theta_0}) + q_0 F_4(\zeta_t^{(1)}, e^{i\theta_0}) + q_1 F_3(\zeta_t^{(1)-1}, e^{-i\theta_0}) + a_{*1} \ln \zeta_t^{(1)}\} + \sum_{j=1}^{\infty} G_{7j} \zeta_t^{(1)-j}\} \tag{3.224}$$

$$g_0(z_t^{(0)}) = \frac{aq_2}{2}\{F_3(\zeta_t^{(0)}, e^{i\theta_0}) + F_4(\zeta_t^{(0)}, e^{i\theta_0})\} - e_{*1} \ln \zeta_t^{(0)} + \sum_{j=1}^{\infty}[G_{8j} \zeta_t^{(0)j} + G_{9j} \zeta_t^{(0)-j}] \tag{3.225}$$

Therefore the solutions $\phi^{(0)}$, $\phi^{(1)}$ and $\boldsymbol{\varphi}^{(1)}$ should be chosen as

$$\phi^{(0)}(\zeta_0) = 2\,\mathrm{Re}[\sum_{k=1,3,5} f_{k0}(\zeta_0) q_{k0} + f_{60}(\zeta_0) + f_{70}(\zeta_0) + c_4^{(0)} g_0(\zeta_t^{(0)})] \tag{3.226}$$

$$\phi^{(1)}(\boldsymbol{\zeta}) = 2\,\mathrm{Re}[\mathbf{A}_4^{(1)}\{\sum_{k=1,3,5} \langle f_{k\alpha}(\zeta_\alpha)\rangle \mathbf{q}_k^{(1)} + \mathbf{f}_6(\boldsymbol{\zeta}) + \mathbf{f}_7(\boldsymbol{\zeta})\} + c_4^{(1)} g_1(\zeta_t^{(1)})] \tag{3.227}$$

$$\boldsymbol{\varphi}^{(1)} = 2\,\mathrm{Re}[\mathbf{B}^{(1)}\{\sum_{k=1,3,5} \langle f_{k\alpha}(\zeta_\alpha)\rangle \mathbf{q}_k^{(1)} + \mathbf{f}_6(\boldsymbol{\zeta}) + \mathbf{f}_7(\boldsymbol{\zeta})\} + \mathbf{d}_1 g_1(\zeta_t^{(1)})] \tag{3.228}$$

Similarly, the unknown constants in Eqs (3.226)-(3.228) can be determined by using the boundary conditions (3.208) and (3.209).

References

[1] Qin QH, Thermoelectroelastic Green's function for a piezoelectric plate containing an elliptic hole, Mech Mat, 30, 21-29, 1998

[2] Qin QH and Mai YW, Thermoelectroelastic Green's function and its application for bimaterial of piezoelectric materials, Arch Appl Mech, 68, 433-444, 1998

[3] Qin QH, Thermoelectroelastic analysis of cracks in piezoelectric half-plane by BEM, Compu Mech, 23, 353-360, 1999

[4] Qin QH, Green's function for thermopiezoelectric materials with holes of various shapes, Arch Appl Mech, 69, 406-418, 1999

[5] Qin QH, Thermoelectroelastic Green's function for thermal load inside or on the boundary of an elliptic inclusion, Mech Mat, 31, 611-626, 1999

[6] Qin QH, Thermoelectroelastic solution on elliptic inclusions and its application to crack-inclusion problems, Appl Math Modelling 25, 1-23, 2000

[7] Qin QH, Fracture mechanics of piezoelectric materials, Southampton: WIT Press, 2001

[8] Stagni L, On the elastic field perturbation by inhomogeneous in plane elasticity, ZAMP, 33, 313-325, 1982

[9] Hwu C and Yen WJ, On the anisotropic elastic inclusions in plane elastostatics. J Appl Mech, 60, 626-632, 1993

[10] Yen WJ, Hwu C and LiangYK, Dislocation inside, outside or on the interface of an anisotropic elliptical inclusion, J Appl Mech, 306-311, 1995

Chapter 4 Green's function for magnetoelectroelastic problems

4.1 Introduction

This chapter deals with applications of the Green's function approach to solving coupled magnetoelectroelastic problems. Green's functions by Radon transform in full space are described first, followed by a discussion of Green's functions of magnetoelectroelastic problems using the potential function approach. The discussion is then extended to the cases of magnetoelectric plate, magnetoelectroelastic solid with half-plane boundary, bimaterial interface, and elliptic hole. Finally, Green's functions for thermomagnetoelectroelastic solids with various defects are presented.

Application of the Green's function approach to the analysis of magnetoelectroelastic solids has been considered by many distinguished researchers over the past decades [1-13]. For example, Pan [1] derived three-dimensional Green's functions in anisotropic magnetoelectroelastic full-space, half-space, bimaterials based on the extended Stroh formalism and two-dimensional Fourier transforms. Soh et al [2] presented explicitly a 3D Green's function for an infinite three-dimensional transversely isotropic magnetoelectroelastic solid based on the potential theory. Huang et al [3] obtained magnetoelectroelastic Eshelby tensors in an inclusion resulting from the constraint of the surrounding matrix of piezoelectric-piezomagnetic composites. Liu et al [4] obtained Green's functions for an infinite 2D anisotropic magnetoelectroelastic medium containing an elliptic cavity or a crack. Li [5] presented explicit expressions of Green's function for magnetoelectric problems. Researchers in [6-8] used the potential function approach to derive Green's functions for various magnetoelectroelastic problems. Alshtis et al [9] obtained the Green's functions of an angularly inhomogeneous magnetoelectroelastic medium subjected to a line defect at the origin of the coordinate system. Jiang and Pan [10] derived Green's functions for a 2D polygonal inclusion problem in magnetoelectroelastic full-, half-, and bimaterial-planes. Recently, Qin [11-13] obtained Green's functions for magnetoelectroelastic solids with various defects. The defects may be an elliptic hole or a Griffith crack, a half-plane boundary, a bimaterial interface, wedge boundary, or a rigid inclusion. Chen et al [14] derived a set of dynamic Green's functions of magnetoelectroelastic medium based on potential approach. For the present, we restrict our attention to the problems treated in [1, 4, 5, 8, 10-14].

4.2 3D Green's functions by Radon transform

4.2.1 Integral expressions for the Green's function

In this section, the results presented in [1] for 3D Green's functions developed using Radon transform are described. In doing so, we consider an anisotropic magnetoelectroelastic solid subjected to an extended concentrated force **f** at the origin (0,0,0). The governing equations and constitutive relations of this problem are defined by Eqs (1.112) and (1.113), respectively. By comparing Eq (1.112) with Eq (1.33), the governing equation for determining Green's function corresponding to Eq (1.112) can be written as

$$E_{iJMn}G_{MR,in}(\mathbf{x}) + \delta_{JR}\delta(\mathbf{x}) = 0 \tag{4.1}$$

which is in the same form as that of Eq (2.4), but has different components, where the components $G_{IJ}(\mathbf{x})$ represent the elastic displacement at $\mathbf{x}$ in the x_I-direction (for I=1,2,3) or electric potential (for I=4) or magnetic potential (for I=5) due to a unit point force in the x_J-direction (for J=1,2,3) or a unit point charge (for J=4) or a point electric current (for J=5) at the origin, δ_{JR} is the fifth-rank Kronecker delta [1].

To make the derivation tractable, the 5×5 matrix, $K_{JM}(\mathbf{n}) = E_{iJMl} n_i n_l$, defined in Section 2.2 [just after Eq (2.5)] is again used here. By integrating $K_{JM}^{-1}(\mathbf{n})\delta(\mathbf{n}\cdot\mathbf{x})$ with respect to $\mathbf{n}$, taking its second derivatives with respect to $\mathbf{x}$, and multiplying the results by E_{iJMl}, we obtain the identity [1]

$$E_{iJMl}\frac{\partial^2}{\partial x_i \partial x_l}\int_{\mathbf{n}\cdot\mathbf{x}=0} K_{JM}^{-1}(\mathbf{n})\delta(\mathbf{n}\cdot\mathbf{x})d\Omega(\mathbf{n}) = \delta_{JR}\nabla_3 \int_{\mathbf{n}\cdot\mathbf{x}=0}\frac{\delta(\mathbf{n}\cdot\mathbf{x})}{|\mathbf{n}|^2}d\Omega(\mathbf{n}) \tag{4.2}$$

Making use of the plane representation of the Dirac delta function [15]

$$\delta(\mathbf{x}) = \frac{1}{8\pi^2}\nabla_3 \int_{\mathbf{n}\cdot\mathbf{x}=0}\frac{\delta(\mathbf{n}\cdot\mathbf{x})}{|\mathbf{n}|^2}d\Omega(\mathbf{n}), \tag{4.3}$$

where $\mathbf{n}$ is defined in Appendix A, Eq (4.2) can be rewritten as

$$E_{iJMl}\frac{\partial^2}{\partial x_i \partial x_l}\int_{\mathbf{n}\cdot\mathbf{x}=0} K_{JM}^{-1}(\mathbf{n})\delta(\mathbf{n}\cdot\mathbf{x})d\Omega(\mathbf{n}) = -8\pi^2\ \delta_{JR}\delta(\mathbf{x}) \tag{4.4}$$

The comparison between Eqs (4.1) and (4.4) provides

$$G_{JM}(\mathbf{x}) = \frac{1}{8\pi^2}\int_{\mathbf{n}\cdot\mathbf{x}=0} K_{JM}^{-1}(\mathbf{n})\delta(\mathbf{n}\cdot\mathbf{x})d\Omega(\mathbf{n}) \tag{4.5}$$

4.2.2 Explicit expression for Green's functions

As was pointed out in [15], the integral (4.5) can be transformed into a one-dimensional infinite integral and the results can then be reduced to a summation of five residues. This is achieved by expressing the vector $\mathbf{n}$ in terms of a new, orthogonal, and normalized system (**d**-**m**-**t**) as shown in Fig. 2.1. The new base (**d**-**m**-**t**) is chosen as

$$\mathbf{t} = \frac{\mathbf{x}}{r}, \quad r = |\mathbf{x}| \tag{4.6}$$

The remaining two unit vector orthogonal to $\mathbf{t}$ can be obtained as

$$\mathbf{d} = \frac{\mathbf{t}\times\mathbf{v}}{|\mathbf{t}\times\mathbf{v}|}, \quad \mathbf{m} = \mathbf{t}\times\mathbf{d}, \tag{4.7}$$

where $\mathbf{v}$ is an arbitrary unit vector different from $\mathbf{t}$ (i.e, $\mathbf{v}\neq\mathbf{t}$), and the symbol '×' represents cross product of any two vectors. The vector $\mathbf{n}$ can thus be expressed in terms of the new system (**d**-**m**-**t**) as

$$\mathbf{n} = \xi\mathbf{d} + \zeta\mathbf{m} + \eta\mathbf{t} \tag{4.8}$$

It is clear that

$$\mathbf{n}\cdot\mathbf{x} = \xi\mathbf{d}\cdot\mathbf{x} + \zeta\mathbf{m}\cdot\mathbf{x} + \eta\mathbf{t}\cdot\mathbf{x} = r\eta \tag{4.9}$$

Therefore, in the new system (**d**-**m**-**t**), the integral (4.5) becomes

$$\begin{aligned} G_{JM}(\mathbf{x}) &= \frac{1}{8\pi^2}\int_{\mathbf{n}\cdot\mathbf{x}=0} K_{JM}^{-1}(\xi\mathbf{d}+\zeta\mathbf{m}+\eta\mathbf{t})\delta(r\eta)d\Omega(\xi,\zeta,\eta) \\ &= \frac{1}{8\pi^2}\int_{\mathbf{n}\cdot\mathbf{x}=0} \frac{A_{JM}(\xi\mathbf{d}+\zeta\mathbf{m}+\eta\mathbf{t})}{D(\xi\mathbf{d}+\zeta\mathbf{m}+\eta\mathbf{t})}\delta(r\eta)d\Omega(\xi,\zeta,\eta) \end{aligned} \tag{4.10}$$

where $A_{JM}(\mathbf{n})$ is the adjoint matrix of $K_{JM}(\mathbf{n})$ and $D(\mathbf{n}) = \det\left|K_{JM}(\mathbf{n})\right|$ is the determinant of $K_{JM}(\mathbf{n})$. Carrying out the integration of $(4.10)_2$ with respect to η provides [15]

$$G_{JM}(\mathbf{x}) = \frac{1}{4\pi^2 r}\int_{-\infty}^{\infty} \frac{A_{JM}(\mathbf{d}+\zeta\mathbf{m})}{D(\mathbf{d}+\zeta\mathbf{m})}d\zeta \tag{4.11}$$

Since the inverse of K_{JM} exists [15], its determinant $D(\mathbf{n})$ does not have real roots. Therefore, the tenth-order polynomial equation of ζ

$$D(\mathbf{d}+\zeta\mathbf{m}) = 0 \tag{4.12}$$

has ten roots, five of them being the conjugate of the remainder. With these roots, we can write the polynomial (4.12) as

$$D(\mathbf{d}+\zeta\mathbf{m}) = \sum_{k=0}^{10} a_{k+1}\zeta^k = a_{11}\prod_{k=1}^{5}(\zeta-\zeta_k)(\zeta-\overline{\zeta}_k), \tag{4.13}$$

where a_{11} is the coefficient of ζ^{10}. In terms of the residues at the poles, the Green's function (4.11) can finally be expressed explicitly as

$$G_{JM}(\mathbf{x}) = -\frac{1}{2\pi r}\,\mathrm{Im}\sum_{m=1}^{5}\left[\frac{A_{JM}(\mathbf{d}+\zeta_m\mathbf{m})}{a_{11}(\zeta_k-\overline{\zeta}_k)\prod\limits_{k=1(k\neq m)}^{5}(\zeta_m-\zeta_k)(\zeta_m-\overline{\zeta}_k),}\right] \tag{4.14}$$

4.3 3D Green's functions by potential function approach

In the previous section, we discussed Green's functions for magnetoelectroelastic solids by the Radon transform approach. This section describes Green's functions for the same problem but derived through use of the potential function approach. The discussion below follows the results presented in [8].

4.3.1 General solutions for magnetoelectroelastic solids

Consider a transversely isotropic magnetoelectroelastic solid subjected to an extended concentrated force **f** at the origin (0,0,0). The governing equations and constitutive relations of this problem are defined by Eqs (1.90)-(1.97). The general solution for the solid with distinct eigenvalues can be assumed in the form

$$U=\Delta\left(i\varpi_0+\sum_{j=1}^{4}\varpi_j\right),\quad w_m=\sum_{j=1}^{4}s_jk_{mj}\frac{\partial\varpi_j}{\partial z_j},$$

$$\sigma_1=2\sum_{j=1}^{4}(c_{66}-\omega_{1j}s_j^2)\frac{\partial^2\varpi_j}{\partial z_j^2},\quad \sigma_2=2c_{66}\Delta^2\left(i\varpi_0+\sum_{j=1}^{4}\varpi_j\right),\qquad (m=1,2,3)\quad (4.15)$$

$$\sigma_{zm}=\sum_{j=1}^{4}\omega_{mj}\frac{\partial^2\varpi_j}{\partial z_j^2},\qquad \tau_{zm}=\Delta\left(s_0\rho_m i\frac{\partial\varpi_0}{\partial z_0}+\sum_{j=1}^{4}s_j\omega_{mj}\frac{\partial\varpi_j}{\partial z_j}\right),$$

where ϖ_0 and ϖ_j are potential functions to be determined,

$$U=u_x+iu_y=e^{i\theta}(u_r+iu_\theta),\quad w_1=u_z,\quad w_2=\phi,\quad w_3=\psi,\quad z_j=s_jz$$

$$\sigma_1=\sigma_x+\sigma_y,\quad \sigma_2=\sigma_x-\sigma_y+2i\tau_{xy}=e^{2i\theta}(\sigma_r-\sigma_\theta+2i\tau_{r\theta}),$$

$$\tau_{z1}=\tau_{xz}+i\tau_{yz}=e^{i\theta}(\tau_{rz}+i\tau_{\theta z}),\quad \tau_{z2}=D_x+iD_y=e^{i\theta}(D_r+iD_\theta),$$

$$\tau_{z3}=B_x+iB_y=e^{i\theta}(B_r+iB_\theta),\quad \sigma_{z1}=\sigma_z,\quad \sigma_{z2}=D_z,\quad \sigma_{z3}=B_z,$$

$$\rho_1=c_{44},\quad \rho_2=e_{15},\quad \rho_3=\tilde{e}_{15},\quad k_{mj}=\frac{\beta_{mj}}{\alpha_j s_j^2},\quad \Delta=\frac{\partial}{\partial x}+i\frac{\partial}{\partial y},$$

$$\omega_{1j}=c_{44}(1+k_{1j})+e_{15}k_{2j}+\tilde{e}_{15}k_{3j},\quad \omega_{2j}=e_{15}(1+k_{1j})-\kappa_{11}k_{2j}-\alpha_{11}k_{3j},$$

$$\omega_{3j}=\tilde{e}_{15}(1+k_{1j})-\alpha_{11}k_{2j}-\mu_{11}k_{3j},\qquad (4.16)$$

and α_j, s_j, β_{mj} are constants listed in Appendix B.

4.3.2 Green's function for 3D magnetoelectroelastic solids

For a transversely isotropic magnetoelectroelastic solid subjected to an extended concentrated force **f** at the origin (0,0,0), the corresponding Green's functions can be obtained based on the general solution presented above. We consider below the case in which all eigenvalues are distinct. For problems with multiple eigenvalues the details of the solution procedure are similar to the case with distinct eigenvalues, and have been documented in [8].

4.3.2.1 Solution due to a point force P_z in z-direction, a point charge Q, and a magnetic monopole J. In this case the problem is axially symmetric about the *z*-axis and the related potential functions can be assumed in the form [8]:

$$\varpi_0=0,\quad \varpi_j=\mathfrak{M}_j\,\mathrm{sign}(z)\ln R_j^*\qquad (j=1\text{-}4)\qquad (4.17)$$

where $\mathfrak{M}_j$ are constants to be determined, sign(*z*) is the signum function defined by Eq (2.225), and R_j^* is defined in Eq (2.17).

Substituting Eq (4.17) into Eq (4.15) we have

$$U=\mathrm{sign}(z)\sum_{j=1}^{4}\mathfrak{M}_j\frac{x+iy}{R_jR_j^*},\quad w_m=\sum_{j=1}^{4}\mathfrak{M}_js_jk_{mj}\frac{1}{R_j},$$

$$\sigma_{zm}=-\sum_{j=1}^{4}\mathfrak{M}_j\omega_{mj}\frac{z_j}{R_j^3},\quad \tau_{zm}=-\sum_{j=1}^{4}\mathfrak{M}_js_j\omega_{mj}\frac{x+iy}{R_j^3}$$

$$\sigma_1 = 2c_{66}\text{sign}(z)\sum_{j=1}^{4}\mathfrak{M}_j\left[\frac{2}{R_jR_j^*}-\frac{x^2+y^2}{R_j^2R_j^*}\left(\frac{1}{R_j}+\frac{1}{R_j^*}\right)\right]-2\sum_{j=1}^{4}\mathfrak{M}_j(2c_{66}-\omega_{1j}s_j^2)\frac{z_j}{R_j^3},$$

$$\sigma_2 = 2c_{66}\text{sign}(z)\sum_{j=1}^{4}\mathfrak{M}_j\left[\frac{y^2-x^2-2ixy}{R_j^2R_j^*}\left(\frac{1}{R_j}+\frac{1}{R_j^*}\right)\right] \tag{4.18}$$

There are four unknowns $\mathfrak{M}_j$ in Eq (4.18). We need to find four conditions to determine the four unknowns. The displacements u_x and u_y are bounded on the z-axis, which provides

$$\sum_{j=1}^{4}\mathfrak{M}_j = 0 \tag{4.19}$$

The remaining three equations can be established by considering the requirements of the force, charge, and electric current balances. These requirements are enforced by integrating the traction, the normal component of the electric displacement, and magnetic induction over the surface of a small spherical cavity centered at the origin, and requiring these to balance the point force P_z, the point charge Q, and a *magnetic monopole J*. These conditions lead to

$$\sum_{j=1}^{4}\omega_{1j}\mathfrak{M}_j = \frac{P_z}{4\pi},\quad \sum_{j=1}^{4}\omega_{2j}\mathfrak{M}_j = \frac{-Q}{4\pi},\quad \sum_{j=1}^{4}\omega_{2j}\mathfrak{M}_j = \frac{-J}{4\pi} \tag{4.20}$$

Solving Eqs (4.19) and (4.20), yields

$$\mathfrak{M}_j = \upsilon_j P_z + \beta_j Q + \gamma_j J, \qquad (j\text{=}1\text{-}4) \tag{4.21}$$

where

$$\begin{Bmatrix}\upsilon_1\\ \upsilon_2\\ \upsilon_3\\ \upsilon_4\end{Bmatrix} = \begin{bmatrix}1 & 1 & 1 & 1\\ \omega_{11} & \omega_{12} & \omega_{13} & \omega_{14}\\ \omega_{21} & \omega_{22} & \omega_{23} & \omega_{24}\\ \omega_{31} & \omega_{32} & \omega_{33} & \omega_{34}\end{bmatrix}^{-1}\begin{Bmatrix}0\\1\\0\\0\end{Bmatrix},\quad \begin{Bmatrix}\beta_1\\ \beta_2\\ \beta_3\\ \beta_4\end{Bmatrix} = \begin{bmatrix}1 & 1 & 1 & 1\\ \omega_{11} & \omega_{12} & \omega_{13} & \omega_{14}\\ \omega_{21} & \omega_{22} & \omega_{23} & \omega_{24}\\ \omega_{31} & \omega_{32} & \omega_{33} & \omega_{34}\end{bmatrix}^{-1}\begin{Bmatrix}0\\0\\1\\0\end{Bmatrix},$$

$$\begin{Bmatrix}\gamma_1\\ \gamma_2\\ \gamma_3\\ \gamma_4\end{Bmatrix} = \begin{bmatrix}1 & 1 & 1 & 1\\ \omega_{11} & \omega_{12} & \omega_{13} & \omega_{14}\\ \omega_{21} & \omega_{22} & \omega_{23} & \omega_{24}\\ \omega_{31} & \omega_{32} & \omega_{33} & \omega_{34}\end{bmatrix}^{-1}\begin{Bmatrix}0\\0\\0\\1\end{Bmatrix} \tag{4.22}$$

4.3.2.2 Solution due to point forces P_x in x-direction and P_y in y-direction. For a point force P_x applied at the origin, the solution can be assumed in the form

$$\varpi_0 = \frac{\Upsilon_0 y}{R_0^*},\quad \varpi_j = \frac{\Upsilon_j x}{R_j^*},(j\text{=}1\text{-}4) \tag{4.23}$$

where Υ_j (j=0-4) are constants to be determined.

Substituting Eq (4.23) into Eq (4.15) we have

$$U = -\Upsilon_0\left[\frac{1}{R_0^*} - \frac{y(y-ix)}{R_0 R_0^{*2}}\right] + \sum_{j=1}^{4}\Upsilon_j\left[\frac{1}{R_j^*} - \frac{x(x+iy)}{R_j R_j^{*2}}\right],,$$

$$\sigma_1 = 2x\sum_{j=1}^{4}\Upsilon_j\left\{(2c_{66} - \omega_{1j}s_j^2)\frac{1}{R_j^3} - c_{66}\left[\frac{4}{R_j R_j^{*2}} - \frac{x^2+y^2}{R_j^2 R_j^{*2}}\left(\frac{1}{R_j} + \frac{2}{R_j^*}\right)\right]\right\},$$

$$\sigma_2 = 4c_{66}\Upsilon_0\left[\frac{iy}{2R_0^3} + \frac{x-iy}{R_0 R_0^{*2}} - \frac{xy(y-ix)}{R_0^2 R_0^{*2}}\left(\frac{1}{R_0} + \frac{2}{R_0^*}\right)\right]$$

$$-2c_{66}\sum_{j=1}^{4}\Upsilon_j\left[\frac{2(x+iy)}{R_j R_j^{*2}} + \frac{x(x-iy)^2}{R_j^2 R_j^{*2}}\left(\frac{1}{R_j} + \frac{2}{R_j^*}\right)\right],$$

$$\tau_{zm} = s_0\rho_m \mathrm{sign}(z)\Upsilon_0\left[\frac{1}{R_0 R_0^*} - \frac{y(y-ix)}{R_0^2 R_0^*}\left(\frac{1}{R_0} + \frac{1}{R_0^*}\right)\right]$$

$$-\mathrm{sign}(z)\sum_{j=1}^{4}s_j\omega_{mj}\Upsilon_j\left[\frac{1}{R_j R_j^*} - \frac{x(x+iy)}{R_j^2 R_j^*}\left(\frac{1}{R_j} + \frac{1}{R_j^*}\right)\right],$$

$$w_m = -\mathrm{sign}(z)\sum_{j=1}^{4}\Upsilon_j s_j k_{mj}\frac{x}{R_j R_j^*}, \quad \sigma_{zm} = \sum_{j=1}^{4}\Upsilon_j\omega_{mj}\frac{x}{R_j^3}, \tag{4.24}$$

There are five unknowns Υ_j (j=0-4) in Eq (4.24), which can be determined by enforcing the requirement that the solution be continuous on z = 0, plus the force balance condition.

Consideration of the continuity of w_m and τ_{mz} on z = 0 yields [8]

$$\sum_{j=1}^{4}s_j k_{mj}\Upsilon_j = 0, \quad s_0\rho_m\Upsilon_0 + \sum_{j=1}^{4}s_j\omega_{mj}\Upsilon_j = 0, \quad (m\text{=}1\text{-}3) \tag{4.25}$$

By substituting ρ_m and ω_{mj} in Eq (4.16) into Eq $(4.25)_2$ and after some manipulation, Eq $(4.25)_2$ can be simplified to only one independent equation as

$$\sum_{j=1}^{4}s_j\Upsilon_j = 0 \tag{4.26}$$

which together with Eq $(4.25)_1$ consists of four independent equations for determining the unknown constants Υ_j. Consideration of the equilibrium of a layer cut by two planes of $z = \pm\varepsilon$ in the neighborhood of the plane of z = 0 gives

$$\int_{-\infty}^{\infty}[\tau_{zx}(x,y,\varepsilon) - \tau_{zx}(x,y,-\varepsilon)]dxdy + P_x = 0 \tag{4.27}$$

Substitution of τ_{z1} in Eq (4.24) into Eq (4.27), after some manipulation, yields

$$2\pi c_{44}s_0\Upsilon_0 - 2\pi c_{44}\sum_{j=1}^{4}s_j\Upsilon_j = -P_x \tag{4.28}$$

Solving Eqs $(4.25)_1$, (4.26) and (4.28) for unknown constants Υ_j, we obtain

$$\Upsilon_j = \lambda_j P_x \quad (j\text{=}0\text{-}4) \tag{4.29}$$

where

$$\lambda_0 = -\frac{1}{4\pi s_0 c_{44}}, \quad \begin{Bmatrix} \lambda_1 \\ \lambda_2 \\ \lambda_3 \\ \lambda_4 \end{Bmatrix} = \frac{1}{4\pi c_{44}} \begin{bmatrix} s_1 k_{11} & s_2 k_{12} & s_3 k_{13} & s_4 k_{14} \\ s_1 k_{21} & s_2 k_{22} & s_3 k_{23} & s_4 k_{24} \\ s_1 k_{31} & s_2 k_{32} & s_3 k_{33} & s_4 k_{34} \\ s_1 & s_2 & s_3 & s_4 \end{bmatrix}^{-1} \begin{Bmatrix} 0 \\ 0 \\ 0 \\ 1 \end{Bmatrix} \tag{4.30}$$

The solution (4.29) is for the point force P_x applied at the origin. When the point forces P_x and P_y are simultaneously applied at the origin, the corresponding potential functions are

$$\varpi_0 = \lambda_0 \frac{P_x y - P_y x}{R_0^*}, \quad \varpi_j = \lambda_j \frac{P_x x + P_y y}{R_j^*} \quad (j=1\text{-}4) \tag{4.31}$$

from which the Green's functions of the magnetoelectroelastic field can be determined.

4.4 Green's functions for magnetoelectric problems

In this section we consider the coupling between magnetic and electric fields only. The discussion follows the results presented in [5]. In the case of static linear magnetoelectric problems where there is no free electric charge and current, the basic equations governing the magnetic and electric fields are [5]

$$\begin{aligned} &D_{i,i} = 0, && B_{i,i} = 0 \\ &D_i = \kappa_{ij} E_j + \alpha_{ij} H_j, && B_i = \alpha_{ij} E_j + \mu_{ij} H_j \\ &E_i = -\phi_{,i}, && H_i = -\psi_{,i} \end{aligned} \tag{4.32}$$

Using the shorthand notation described in Section 1.5, the constitutive equations, Gaussian equations, and gradient equations can be written as

$$\Pi_{iJ,i} = E_{iJMn} U_{J,in} = 0, \quad \Pi_{iJ} = E_{iJMn} U_{M,n} \tag{4.33}$$

where the magnetoelectric fields U_J, generalized stress Π_{iJ}, and stiffness constant E_{iJMn} are defined as

$$U_J = \begin{cases} -\phi, & J=1, \\ -\psi, & J=2, \end{cases} \quad \Pi_{iJ} = \begin{cases} D_i, & J=1, \\ B_i & J=2, \end{cases} \tag{4.34}$$

$$E_{iJMn} = \begin{cases} \kappa_{in}, & J=M=1, \\ \alpha_{in}, & J=1, M=2, \\ \alpha_{in}, & J=2, M=1, \\ \mu_{in}, & J=2, M=2 \end{cases} \tag{4.35}$$

By comparing with Eq (1.33), the Green's function corresponding to Eq (4.33) is defined by the differential equation

$$E_{iJMn} G_{MR,in}(\mathbf{x}-\hat{\mathbf{x}}) + \delta_{JR}\delta(\mathbf{x}-\hat{\mathbf{x}}) = 0 \tag{4.36}$$

The Green's function $G_{MR}(\mathbf{x}-\hat{\mathbf{x}})$ can be obtained by applying the Radon transform defined in Appendix A to Eq (4.36) above [5]:

$$E_{iJMl} z_i z_l \frac{\partial^2}{\partial \omega^2} \hat{G}_{MR}(\mathbf{n}, \omega - \mathbf{n} \cdot \hat{\mathbf{x}}) + \delta_{JR} \delta(\omega - \mathbf{n} \cdot \hat{\mathbf{x}}) = 0 \tag{4.37}$$

Multiplying the inverse of $K_{JM}(\mathbf{n}) = E_{iJMl} n_i n_l$ to both sides of Eq (4.37) and then taking its inverse transform, we obtain

$$G_{MR}(\mathbf{x} - \hat{\mathbf{x}}) = \frac{1}{8\pi^2} \int_{|\mathbf{n}|=1} K_{MR}^{-1}(\mathbf{n}) \delta[\mathbf{n} \cdot (\mathbf{x} - \hat{\mathbf{x}})] dS(\mathbf{n}) \tag{4.38}$$

Denoting $\mathbf{t} = (\mathbf{x} - \hat{\mathbf{x}}) / |\mathbf{x} - \hat{\mathbf{x}}|$ (see Fig. 2.1), and utilizing the property of the Dirac delta function given in Eq (1.43), we have

$$G_{MR}(\mathbf{x} - \hat{\mathbf{x}}) = \frac{1}{8\pi^2 |\mathbf{x} - \hat{\mathbf{x}}|} \int_{|\mathbf{n}|=1} K_{MR}^{-1}(\mathbf{n}) \delta[\mathbf{n} \cdot \mathbf{t}] dS(\mathbf{n}) \tag{4.39}$$

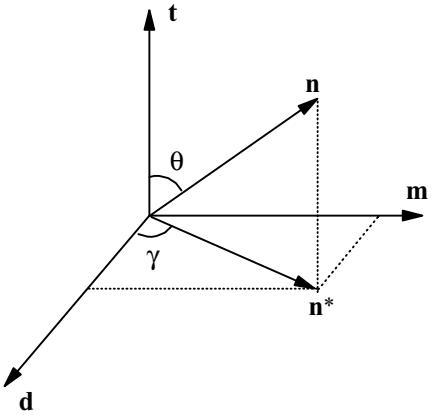

Fig. 4.1 Relationship between $\mathbf{t}$, $\mathbf{n}$, and $\mathbf{n}^*$

The relationship between vectors **n** and **t** is shown in Fig. 4.1, where $\mathbf{n}^*$ lies in the plane **m**-**d** normal to **t**. Making use of the property of the Dirac delta function again, Eq (4.39) can be further written as

$$G_{MR}(\mathbf{x} - \hat{\mathbf{x}}) = \frac{1}{8\pi^2 |\mathbf{x} - \hat{\mathbf{x}}|} \int_{|\mathbf{n}|=1} K_{MR}^{-1}(\mathbf{n}^*) d\gamma(\mathbf{n}^*) \tag{4.40}$$

where $|\mathbf{n}| = 1$ represents a unit circle, which is the intersection of the unit sphere with plane **m**-**d** (see Fig. 4.1).

For the Green's functions defined by the integral (4.40), Li [5] obtained their explicit expressions for transversely isotropic media. The discussion here follows his results. For a transversely isotropic magnetoelectric medium, the matrix K_{JM} is a 2×2 matrix given by

$$K_{JM} = \begin{bmatrix} \kappa_{11}(n_1^2 + n_2^2) + \kappa_{33} n_3^2 & \alpha_{11}(n_1^2 + n_2^2) + \alpha_{33} n_3^2 \\ \alpha_{11}(n_1^2 + n_2^2) + \alpha_{33} n_3^2 & \mu_{11}(n_1^2 + n_2^2) + \mu_{33} n_3^2 \end{bmatrix} \tag{4.41}$$

The inverse of K_{JM} can then be obtained as

$$K_{JM}^{-1}=\frac{1}{\det|K_{JM}|}\begin{bmatrix}\mu_{11}(n_1^2+n_2^2)+\mu_{33}n_3^2 & -\alpha_{11}(n_1^2+n_2^2)-\alpha_{33}n_3^2\\ -\alpha_{11}(n_1^2+n_2^2)-\alpha_{33}n_3^2 & \kappa_{11}(n_1^2+n_2^2)+\kappa_{33}n_3^2\end{bmatrix} \tag{4.42}$$

For the sake of simplicity, assume the source point is located at the origin, i.e., $\hat{\mathbf{x}}=(0,0,0)$, and the field point is lying in the x_1-x_3 plane, with $\tan\theta=x_1/x_3$. For such a configuration, the intersection between the unit sphere $|\mathbf{n}|=1$ and the plane **m-d** (see Fig. 4.1) is a unit circle represented by $\eta_1^2+\eta_2^2=1$, with η_3=0 corresponding to the plane **m-d**. Without loss of generality, choose η_2 to coincide with a unit vector in the x_2-direction. Thus the variable **n** is related to η_i by

$$n_1=\eta_1\cos\theta,\quad n_2=\eta_2,\quad n_3=-\eta_1\sin\theta \tag{4.43}$$

By introducing a complex variable $\zeta=\eta_1+i\eta_2=e^{i\gamma}$, we have

$$\eta_1=\frac{\zeta+\zeta^{-1}}{2},\quad \eta_2=\frac{\zeta-\zeta^{-1}}{2i},\quad d\gamma=\frac{d\zeta}{i\zeta} \tag{4.44}$$

Making use of Eq (4.44), the integral (4.40) can be expressed in terms of the complex variable ζ and then evaluated using Cauchy's residue theorem. To use the Cauchy's residue theorem, express $g=\det|K_{JM}|$ in terms of ζ and θ as [5]

$$g=\frac{(\kappa_{33}\mu_{33}-\alpha_{33}^2)\sin^4\theta}{16\zeta^4}(1-A_1)(1-A_2)h_1(\zeta)h_2(\zeta), \tag{4.45}$$

where

$$\begin{aligned}
&h_i(\zeta)=\zeta^4+2B_i\zeta^2+1,\quad B_i=\frac{A_i\cos^2\theta+\sin^2\theta+A_i}{(1-A_i)\sin^2\theta},\\
&A_1=\frac{-b-\sqrt{b^2-4(\alpha_{11}^2-\kappa_{11}\mu_{11})(\alpha_{33}^2-\kappa_{33}\mu_{33})}}{2(\alpha_{33}^2-\kappa_{33}\mu_{33})},\\
&A_2=\frac{-b+\sqrt{b^2-4(\alpha_{11}^2-\kappa_{11}\mu_{11})(\alpha_{33}^2-\kappa_{33}\mu_{33})}}{2(\alpha_{33}^2-\kappa_{33}\mu_{33})},
\end{aligned} \tag{4.46}$$

with

$$b=\kappa_{33}\mu_{11}+\kappa_{11}\mu_{33}-2\alpha_{11}\alpha_{33} \tag{4.47}$$

Noting that if ζ^* is a root of $h_i(\zeta)=0$, so are $-\zeta^*$, $1/\zeta^*$, and $-1/\zeta^*$ [5], so in general, there two sets of roots: (i) $\pm\chi_i$ with modulus less than unity; and (ii) $\pm\beta_i$ with moduli great than unity. Eq (4.45) can thus be factored as

$$g=\frac{(\kappa_{33}\mu_{33}-\alpha_{33}^2)\sin^4\theta}{16\zeta^4}(1-A_1)(1-A_2)(\zeta^2-\chi_1^2)(\zeta^2-\chi_2^2)(\zeta^2-\beta_1^2)(\zeta^2-\beta_2^2) \tag{4.48}$$

Substituting Eq (4.48) into Eq (4.40) yields

$$G_{MR}(\mathbf{x})=C\int_{|\mathbf{n}|=1}\frac{\zeta L_{MR}(\zeta)d\zeta}{(\zeta^2-\chi_1^2)(\zeta^2-\chi_2^2)(\zeta^2-\beta_1^2)(\zeta^2-\beta_2^2)}, \tag{4.49}$$

where

$$L_{MR}(\zeta)=\begin{cases}(1+\zeta^2)^2(\mu_{11}\cos^2\theta+\mu_{33}\sin^2\theta)-(1-\zeta^2)^2\mu_{11}, & MR=11\\ -(1+\zeta^2)^2(\alpha_{11}\cos^2\theta+\alpha_{33}\sin^2\theta)+(1-\zeta^2)^2\alpha_{11}, & MR=12\\ -(1+\zeta^2)^2(\alpha_{11}\cos^2\theta+\alpha_{33}\sin^2\theta)+(1-\zeta^2)^2\alpha_{11}, & MR=21\\ (1+\zeta^2)^2(\kappa_{11}\cos^2\theta+\kappa_{33}\sin^2\theta)-(1-\zeta^2)^2\kappa_{11}, & MR=22\end{cases} \tag{4.50}$$

and

$$C=\frac{1}{2i\pi^2|\mathbf{x}|(\kappa_{33}\mu_{33}-\alpha_{33}^2)\sin^4\theta(1-A_1)(1-A_2)} \tag{4.51}$$

Now define

$$t_{MR}(\zeta)=\frac{\zeta L_{MR}(\zeta)}{(\zeta^2-\beta_1^2)(\zeta^2-\beta_2^2)}, \tag{4.52}$$

which is analytical inside $|\zeta|=1$. Since $|\beta_i|>1$, Eq (4.49) can be rewritten as

$$G_{MR}(\mathbf{x})=C\int_{|\mathbf{n}|=1}\frac{t_{MR}(\zeta)d\zeta}{(\zeta^2-\chi_1^2)(\zeta^2-\chi_2^2)}, \tag{4.53}$$

According to Cauchy's residue theorem, Eq (4.53) can be further written as

$$G_{MR}(\mathbf{x})=8i\pi C\left[\frac{t_{MR}(\chi_1)-t_{MR}(\chi_2)}{(\chi_1^2-\chi_2^2)}\right] \tag{4.54}$$

4.5 Half-plane problems

4.5.1 Green's function for magnetoelectroelastic plate with horizontal half-plane boundary

The Green's functions for a half-plane magnetoelectroelastic plate subjected to loadings $\mathbf{q}_0$ and **b** can be obtained in the same way as that treated in Section 2.5 if the half-plane boundary is in horizontal direction. Accordingly, the generalized displacement vector **U** and stress function $\boldsymbol{\varphi}$ can be assumed in the form:

$$\mathbf{U}=\frac{1}{\pi}\mathrm{Im}\{\mathbf{A}\langle\ln(z_\alpha-z_{\alpha 0})\rangle\mathbf{q}^*\}+\sum_{\beta=1}^{5}\frac{1}{\pi}\mathrm{Im}\{\mathbf{A}\langle\ln(z_\alpha-\bar{z}_{\beta 0})\rangle\mathbf{q}_\beta\}, \tag{4.55}$$

$$\boldsymbol{\varphi}=\frac{1}{\pi}\mathrm{Im}\{\mathbf{B}\langle\ln(z_\alpha-z_{\alpha 0})\rangle\mathbf{q}^*\}+\sum_{\beta=1}^{5}\frac{1}{\pi}\mathrm{Im}\{\mathbf{B}\langle\ln(z_\alpha-\bar{z}_{\beta 0})\rangle\mathbf{q}_\beta\} \tag{4.56}$$

where $\mathbf{q}^*$ and $\mathbf{q}_\beta$ are in the same form as those in Eqs (2.86) and (2.91), respectively, but now each of them has five components instead of four.

4.5.2 Green's function for magnetoelectroelastic plate with vertical half-plane boundary

4.5.2.1 Coordinate transformation. When the half-plane boundary is in the vertical direction (or even arbitrarily oriented) instead of the horizontal direction (Fig. 4.2), the approach described in Section 2.5 is no longer applicable. The reason is that,

unlike in the case of horizontal boundary where $z_\alpha = x_1 + p_\alpha x_2$ becomes a real number on the boundary $x_2 = 0$, z_α is, in general, neither a real number nor a pure imaginary number on the vertical boundary $x_1 = 0$, which complicates the related mathematical derivation. To circumvent this problem, a new coordinate variable is introduced [11]:

$$z_\alpha^* = z_\alpha / p_\alpha \tag{4.57}$$

In this case z_α^* is a real number on the vertical boundary $x_1 = 0$. This coordinate transformation can be used for both half-plane and bimaterial problems with a vertical boundary.

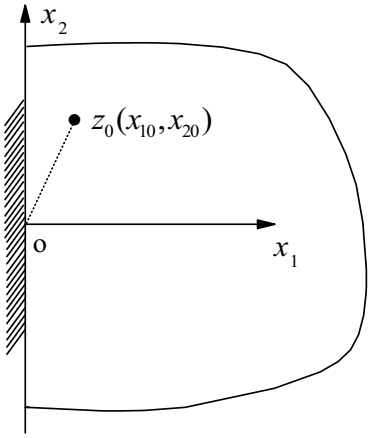

Fig. 4.2 Magnetoelectroelastic plate with vertical half-plane boundary

4.5.2.2 Green's function for magnetoelectroelastic plate with vertical half-plane boundary. Let the material occupy the region $x_1 > 0$, and a line force-charge $\mathbf{q}_0$ and a line dislocation **b** be applied at $z_0(x_{10}, x_{20})$ (see Fig. 4.2). To satisfy the boundary conditions on $x_1 = 0$, the solution can be assumed in the form [11]

$$\mathbf{U} = \frac{1}{\pi}\mathrm{Im}\{\mathbf{A}\left\langle \ln(z_\alpha^* - z_{\alpha 0}^*)\right\rangle \mathbf{q}^*\} + \sum_{\beta=1}^{5}\frac{1}{\pi}\mathrm{Im}\{\mathbf{A}\left\langle \ln(z_{\alpha 0}^* - \bar{z}_{\beta 0}^*)\right\rangle \mathbf{q}_\beta\}, \tag{4.58}$$

$$\boldsymbol{\varphi} = \frac{1}{\pi}\mathrm{Im}\{\mathbf{B}\left\langle \ln(z_\alpha^* - z_{\alpha 0}^*)\right\rangle \mathbf{q}^*\} + \sum_{\beta=1}^{5}\frac{1}{\pi}\mathrm{Im}\{\mathbf{B}\left\langle \ln(z_{\alpha 0}^* - \bar{z}_{\beta 0}^*)\right\rangle \mathbf{q}_\beta\} \tag{4.59}$$

where $\mathbf{q}^*$ is given in Eq (2.86) and $\mathbf{q}_\beta$ are unknown constants to be determined.

Consider first the case in which the surface $x_1 = 0$ is traction-free, so that

$$\boldsymbol{\varphi} = 0 \qquad \text{for} \quad x_1 = 0 \tag{4.60}$$

Substituting Eq (4.59) into Eq (4.60) yields

$$\boldsymbol{\varphi} = \frac{1}{\pi}\mathrm{Im}\{\mathbf{B}\left\langle \ln(x_2 - z_{\alpha 0}^*)\right\rangle \mathbf{q}^*\} + \sum_{\beta=1}^{5}\frac{1}{\pi}\mathrm{Im}\{\mathbf{B}\left\langle \ln(x_2 - \bar{z}_{\beta 0}^*)\right\rangle \mathbf{q}_\beta\} = 0 \tag{4.61}$$

Using the following relations

$$\mathrm{Im}\{\mathbf{B}\left\langle \ln(x_2 - z^*_{\alpha 0})\right\rangle \mathbf{q}^*\} = -\mathrm{Im}\{\overline{\mathbf{B}}\left\langle \ln(x_2 - \overline{z}^*_{\alpha 0})\right\rangle \overline{\mathbf{q}}\}, \tag{4.62}$$

and

$$\left\langle \ln(x_2 - z^*_{\alpha 0})\right\rangle = \sum_{\beta=1}^{5} \ln(x_2 - z^*_{\beta 0})\mathbf{I}_\beta, \tag{4.63}$$

where

$$\mathbf{I}_\beta = \left\langle \delta_{\beta\alpha}\right\rangle = \mathrm{diag}[\delta_{\beta 1}, \delta_{\beta 2}, \delta_{\beta 3}, \delta_{\beta 4}, \delta_{\beta 5}], \tag{4.64}$$

Eq (4.61) yields

$$\mathbf{q}_\beta = \mathbf{B}^{-1}\overline{\mathbf{B}}\mathbf{I}_\beta \overline{\mathbf{q}}^* = \mathbf{B}^{-1}\overline{\mathbf{B}}\mathbf{I}_\beta(\overline{\mathbf{A}}^T\mathbf{q}_0 + \overline{\mathbf{B}}^T\mathbf{b}) \tag{4.65}$$

If the boundary $x_1 = 0$ is a rigid surface, then

$$\mathbf{U} = 0, \qquad \text{at } x_1 = 0 \tag{4.66}$$

The same procedure shows that the solution is given by Eqs (4.58) and (4.59) with

$$\mathbf{q}_\beta = \mathbf{A}^{-1}\overline{\mathbf{A}}\mathbf{I}_\beta(\overline{\mathbf{A}}^T\mathbf{q}_0 + \overline{\mathbf{B}}^T\mathbf{b}) \tag{4.67}$$

It is noted that Eqs (4.65) and (4.67) have the same forms as those of Eqs (2.91) and (2.93). The final version of the Green's function can thus be written in terms of z_k as

$$\mathbf{U} = \frac{1}{\pi}\mathrm{Im}\{\mathbf{A}\left\langle \ln(z_\alpha - z_{\alpha 0})/p_\alpha\right\rangle \mathbf{q}^*\} + \sum_{\beta=1}^{5}\frac{1}{\pi}\mathrm{Im}\{\mathbf{A}\left\langle \ln(z_\alpha/p_\alpha - \overline{z}_{\beta 0}/\overline{p}_\beta)\right\rangle \mathbf{q}_\beta\} \tag{4.68}$$

$$\boldsymbol{\varphi} = \frac{1}{\pi}\mathrm{Im}\{\mathbf{B}\left\langle \ln(z_\alpha - z_{\alpha 0})/p_\alpha\right\rangle \mathbf{q}^*\} + \sum_{\beta=1}^{5}\frac{1}{\pi}\mathrm{Im}\{\mathbf{B}\left\langle \ln(z_\alpha/p_\alpha - \overline{z}_{\beta 0}/\overline{p}_\beta)\right\rangle \mathbf{q}_\beta\} \tag{4.69}$$

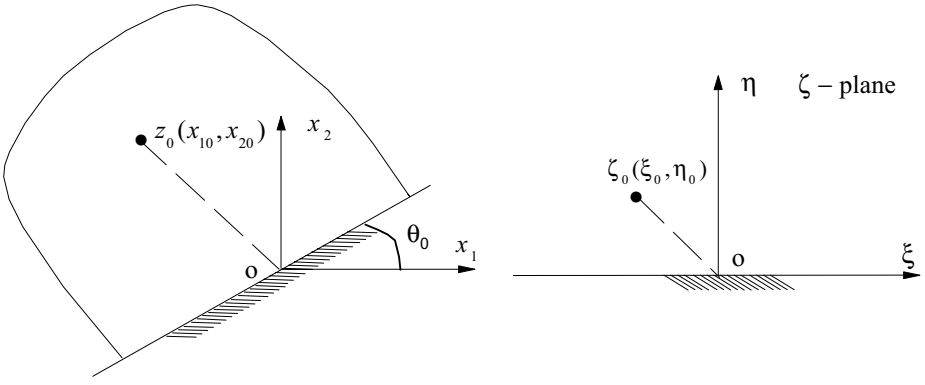

Fig. 4.3 Magnetoelectroelastic solid with arbitrarily oriented half-plane boundary

4.5.2.2 Green's function for a solid with an arbitrarily oriented half-plane boundary. If the half-plane boundary is in an angle θ_0 ($\theta_0 \neq 0$) with positive x_1-axis, the corresponding Green's function can be obtained by introducing a new mapping function [11]

$$z = \zeta^{\theta_0/\pi} \qquad (\theta_0 \neq 0) \tag{4.70}$$

which maps the boundary $\theta = \theta_0$ in the z-plane onto the real axis in the ζ-plane ($\xi+i\eta$) (Fig. 4.3).

Following the procedure in section 4.5.2.1 it can be shown that the resulting Green's functions can be expressed as

$$\mathbf{U} = \frac{1}{\pi}\mathrm{Im}\{\mathbf{A}\left\langle \ln(z_\alpha^{\pi/\theta_0} - z_{\alpha 0}^{\pi/\theta_0})\right\rangle \mathbf{q}^*\} + \sum_{\beta=1}^{5}\frac{1}{\pi}\mathrm{Im}\{\mathbf{A}\left\langle \ln(z_\alpha^{\pi/\theta_0} - \bar{z}_{\beta 0}^{\pi/\theta_0})\right\rangle \mathbf{q}_\beta\} \tag{4.71}$$

$$\boldsymbol{\varphi} = \frac{1}{\pi}\mathrm{Im}\{\mathbf{B}\left\langle \ln(z_\alpha^{\pi/\theta_0} - z_{\alpha 0}^{\pi/\theta_0})\right\rangle \mathbf{q}^*\} + \sum_{\beta=1}^{5}\frac{1}{\pi}\mathrm{Im}\{\mathbf{B}\left\langle \ln(z_\alpha^{\pi/\theta_0} - \bar{z}_{\beta 0}^{\pi/\theta_0})\right\rangle \mathbf{q}_\beta\} \tag{4.72}$$

where $\mathbf{q}^*$ and $\mathbf{q}_\beta$ have, respectively, the same forms as those given in Eqs (2.86) and (4.65).

4.6 Bimaterial problems

4.6.1 Green's function for magnetoelectroelastic bimaterial with horizontal interface

Similar to the discussion of half-plane problems in the previous section, the Green's functions for a magnetoelectroelastic bimaterial solid subjected to loadings $\mathbf{q}_0$ and $\mathbf{b}$ can also be obtained in the same way as that treated in Section 2.6 if the interface is in the horizontal direction. Consider a bimaterial magnetoelectroelastic plate subjected to loadings $\mathbf{q}_0$ and $\mathbf{b}$ applied in the upper half-plane at $z_0(x_{10}, x_{20})$, in which the upper half-plane $(x_2 > 0)$ is occupied by material 1 and the lower half-plane $(x_2 < 0)$ is occupied by material 2 (see Fig. 2.5). Following the procedure described in Section 2.6, the generalized displacement vector $\mathbf{U}$ and stress function $\boldsymbol{\varphi}$ are, in this case, assumed in the form

$$\mathbf{U}^{(1)} = \frac{1}{\pi}\mathrm{Im}\{\mathbf{A}^{(1)}\left\langle \ln(z_\alpha^{(1)} - z_{\alpha 0}^{(1)})\right\rangle \mathbf{q}^{(1)*}\} + \sum_{\beta=1}^{5}\frac{1}{\pi}\mathrm{Im}\{\mathbf{A}^{(1)}\left\langle \ln(z_\alpha^{(1)} - \bar{z}_{\beta 0}^{(1)})\right\rangle \mathbf{q}_\beta^{(1)}\}, \tag{4.73}$$

$$\boldsymbol{\varphi}^{(1)} = \frac{1}{\pi}\mathrm{Im}\{\mathbf{B}^{(1)}\left\langle \ln(z_\alpha^{(1)} - z_{\alpha 0}^{(1)})\right\rangle \mathbf{q}^{(1)*}\} + \sum_{\beta=1}^{5}\frac{1}{\pi}\mathrm{Im}\{\mathbf{B}^{(1)}\left\langle \ln(z_\alpha^{(1)} - \bar{z}_{\beta 0}^{(1)})\right\rangle \mathbf{q}_\beta^{(1)}\} \tag{4.74}$$

for material 1 in $x_2>0$ and

$$\mathbf{U}^{(2)} = \sum_{\beta=1}^{5}\frac{1}{\pi}\mathrm{Im}\{\mathbf{A}^{(2)}\left\langle \ln(z_\alpha^{(2)} - z_{\beta 0}^{(1)})\right\rangle \mathbf{q}_\beta^{(2)}\}, \tag{4.75}$$

$$\varphi^{(2)} = \sum_{\beta=1}^{5}\frac{1}{\pi}\mathrm{Im}\{\mathbf{B}^{(2)}\left\langle \ln(z_\alpha^{(2)} - z_{\beta 0}^{(1)})\right\rangle \mathbf{q}_\beta^{(2)}\} \tag{4.76}$$

for material 2 in $x_2<0$, where $\mathbf{q}^{(1)*}$, $\mathbf{q}_\beta^{(1)}$, and $\mathbf{q}_\beta^{(2)}$ have the same forms as those in Eqs (2.95), (2.100) and (2.101), but now each of these three vectors has five components instead of four.

4.6.2 Green's function for magnetoelectroelastic bimaterial with vertical interface.

For a magnetoelectroelastic bimaterial plate with a vertical interface subjected to loadings $\mathbf{q}_0$ and $\mathbf{b}$ in the left half-plane at $z_0(x_{10}, x_{20})$ (Fig. 4.4), the solution may be

assumed, in a way similar to that for half-plane problem, in the form

$$\mathbf{U}^{(1)} = \frac{1}{\pi}\mathrm{Im}\{\mathbf{A}^{(1)}\left\langle \ln(z_\alpha^{*(1)} - z_{\alpha 0}^{*(1)})\right\rangle \mathbf{q}^{(1)*}\} + \sum_{\beta=1}^{5}\frac{1}{\pi}\mathrm{Im}\{\mathbf{A}^{(1)}\left\langle \ln(z_\alpha^{*(1)} - \overline{z}_{\beta 0}^{*(1)})\right\rangle \mathbf{q}_\beta^{(1)}\}, \tag{4.77}$$

$$\boldsymbol{\varphi}^{(1)} = \frac{1}{\pi}\mathrm{Im}\{\mathbf{B}^{(1)}\left\langle \ln(z_\alpha^{*(1)} - z_{\alpha 0}^{*(1)})\right\rangle \mathbf{q}^{(1)*}\} + \sum_{\beta=1}^{5}\frac{1}{\pi}\mathrm{Im}\{\mathbf{B}^{(1)}\left\langle \ln(z_\alpha^{*(1)} - \overline{z}_{\beta 0}^{*(1)})\right\rangle \mathbf{q}_\beta^{(1)}\} \tag{4.78}$$

for material 1 in the region $x_1 < 0$ and

$$\mathbf{U}^{(2)} = \sum_{\beta=1}^{5}\frac{1}{\pi}\mathrm{Im}\{\mathbf{A}^{(2)}\left\langle \ln(z_\alpha^{*(2)} - z_{\beta 0}^{*(1)})\right\rangle \mathbf{q}_\beta^{(2)}\}, \tag{4.79}$$

$$\boldsymbol{\varphi}^{(2)} = \sum_{\beta=1}^{5}\frac{1}{\pi}\mathrm{Im}\{\mathbf{B}^{(2)}\left\langle \ln(z_\alpha^{*(2)} - z_{\beta 0}^{*(1)})\right\rangle \mathbf{q}_\beta^{(2)}\} \tag{4.80}$$

for material 2 in the region $x_1 > 0$, where $z_{\beta 0}^{*(1)} = z_{\beta 0}^{(1)} / p_\beta^{(1)}$, $z_\alpha^{*(i)} = z_\alpha^{(i)} / p_\alpha^{(i)}$ (i = 1,2), $\mathbf{q}^{(1)*}$, $\mathbf{q}_\beta^{(1)}$, and $\mathbf{q}_\beta^{(2)}$ are the same as in Eqs (4.73)-(4.76). It is found that Eqs (4.77)-(4.80) can be obtained from Eqs (4.73)-(4.76) by replacing $z_\alpha^{(1)}$, $z_{\alpha 0}^{(1)}$, $\overline{z}_{\beta 0}^{(1)}$, $z_\alpha^{(2)}$, and $z_{\beta 0}^{(1)}$ with $z_\alpha^{*(1)}$, $z_{\alpha 0}^{*(1)}$, $\overline{z}_{\beta 0}^{*(1)}$, $z_\alpha^{*(2)}$, and $z_{\beta 0}^{*(1)}$.

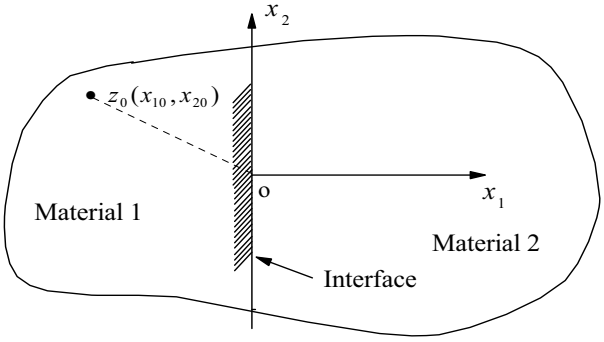

Fig. 4.4 Magnetoelectroelastic bimaterial with vertical interface

Finally, if the interface is in an angle θ_0 ($\theta_0 \neq 0$) with positive x_1-axis, the corresponding Green's function can be obtained from Eqs (4.73)-(4.76) by replacing $z_\alpha^{(1)}$, $z_{\alpha 0}^{(1)}$, $\overline{z}_{\beta 0}^{(1)}$, $z_\alpha^{(2)}$, and $z_{\beta 0}^{(1)}$ with $z_\alpha^{(1)\pi/\theta_0}$, $z_{\alpha 0}^{(1)\pi/\theta_0}$, $\overline{z}_{\beta 0}^{(1)\pi/\theta_0}$, $z_\alpha^{(2)\pi/\theta_0}$, and $z_{\beta 0}^{(1)\pi/\theta_0}$ [11].

4.7 Problems with an elliptic hole or a crack

In the previous two sections, Green's functions for magnetoelectroelastic solids with half-plane boundary and bimaterial interface were discussed. Extension of the procedure to the case of magnetoelectroelastic solids containing an elliptic hole is described in this section. Green's functions for an infinite magnetoelectroelastic solid with an elliptic hole induced by electroelastic loads are derived using Stroh formalism. The loads may be a generalized line force $\mathbf{q}_0$ and a generalized line dislocation **b**. The discussion here is based on the results presented in [4].

4.7.1 Basic formulation of the hole problem

Consider an infinite magnetoelectroelastic solid with an elliptic hole subjected to a generalized line dislocation **b** and a generalized line force $\mathbf{q}_0$ at a point $z_0(x_{10},x_{20})$ outside the ellipse (see Fig. 2.7). The hole is assumed to be free of force, charge and electric current along its surface, but to be filled with a homogeneous gas of dielectric constant κ^c and permeability μ^c.

As indicated in [4], electric and magnetic fields can permeate in a vacuum and can exist inside the hole of a magnetoelectroelastic material. The electric and magnetic potentials in the hole satisfy the Laplace equation

$$\nabla_2\phi^c = 0, \quad \nabla_2\psi^c = 0 \quad \text{in } \Omega_c \tag{4.81}$$

and the constitutive relations are

$$D_i^c = \kappa^c E_i^c = -\kappa^c \frac{\partial\phi^c}{\partial x_i},\ B_i^c = \mu^c H_i^c = -\mu^c \frac{\partial\psi^c}{\partial x_i}, \quad i=1,2 \tag{4.82}$$

where superscript *c* refers to the variables associated with hole medium. As treated in Section 2.8, the general solution to Eq (4.81) can be assumed in the form

$$\phi^c(z) = 2\,\mathrm{Re}[f_\phi^c(z)],\ \psi^c(z) = 2\,\mathrm{Re}[f_\psi^c(z)], \tag{4.83}$$

Making use of Eqs (4.82) and (4.83), the resultants of the normal components of electric displacement and magnetic induction along an arc can be written as

$$S_D^c = -2\kappa^c\,\mathrm{Im}[f_\phi^c(z)],\ \ S_B^c = -2\mu^c\,\mathrm{Im}[f_\psi^c(z)] \tag{4.84}$$

If we define

$$\mathbf{\Psi}^c = \{\phi^c,\psi^c\}^T = 2\,\mathrm{Re}\{\mathbf{f}^c(z)\},\ \ \mathbf{S}^c = \{S_D^c, S_B^c\}^T = -2\mathbf{\Pi}^c\,\mathrm{Im}\{\mathbf{f}^c(z)\} \tag{4.85}$$

with

$$\mathbf{f}^c(z) = \{f_\phi^c(z), f_\psi^c(z)\}^T,\ \ \mathbf{\Pi}^c = \begin{bmatrix} \kappa^c & 0 \\ 0 & \mu^c \end{bmatrix}, \tag{4.86}$$

the boundary conditions of the hole problem can be expressed as

$$\mathbf{g}^T\mathbf{U} = \mathbf{\Psi}^c,\ \boldsymbol{\varphi} = -\mathbf{g}\mathbf{S}^c \ \text{ along the hole boundary,} \tag{4.87}$$

$$\{\sigma_{ij}, D_i, B_i\} \to 0 \ \text{ at infinity,} \tag{4.88}$$

and the balance equations are defined by Eq (2.77), where

$$\mathbf{g} = \begin{bmatrix} 0 & 0 & 0 & 1 & 0 \\ 0 & 0 & 0 & 0 & 1 \end{bmatrix}^T \tag{4.89}$$

4.7.2 Green's function for the hole problem

Using the mapping functions (2.162), (2.182), and superposition principle of linear problems, the general expressions for the fields outside and inside the ellipse can be written in the form

$$\mathbf{U} = 2\,\mathrm{Re}\{\mathbf{A}[\mathbf{f}_0(\zeta)+\mathbf{f}_1(\zeta)],\quad \boldsymbol{\varphi} = 2\,\mathrm{Re}\{\mathbf{B}[\mathbf{f}_0(\zeta)+\mathbf{f}_1(\zeta)] \ \text{ in } \Omega \tag{4.90}$$

and

$$\mathbf{\Psi}^c == 2\,\mathrm{Re}\{\mathbf{f}^c(\zeta_0)\}\,,\quad \mathbf{S}^c = -2\mathbf{\Pi}^c\,\mathrm{Im}\{\mathbf{f}^c(\zeta_0)\}\quad \text{in } \Omega_c \tag{4.91}$$

where Ω and Ω_c are defined in Fig. 2.7, ζ_α and ζ_0 are related to z_α and z by Eqs (2.162) and (2.182), respectively. Following the procedure in Section 2.8, functions $\mathbf{f}_0$, $\mathbf{f}_1$, and $\mathbf{f}^c$ are assumed in the form

$$\mathbf{f}_0 = \langle f_0(\zeta_\alpha)\rangle = \langle \ln(z_\alpha - z_{\alpha 0}\rangle \mathbf{q}_f\,, \tag{4.92}$$

$$\mathbf{f}_1(\boldsymbol{\zeta}) = \langle f_1(\zeta_\alpha)\rangle = \sum_{k=1}^{\infty}\langle \zeta_\alpha^{-k}\rangle \mathbf{d}_k\,,\quad |\zeta_\alpha| \ge 1\,, \tag{4.93}$$

$$\mathbf{f}^c(\zeta_0) = \sum_{k=1}^{\infty}(\zeta_0^k + r_{in}^{2k}\zeta_0^{-k})\mathbf{e}_k\,,\quad r_{in} \le |\zeta_0| \le 1\,, \tag{4.94}$$

where $\mathbf{q}_f$ is defined by Eq (2.80), $\mathbf{d}_k$ and $\mathbf{e}_k$ are constants to be determined, $r_{in} = \sqrt{\dfrac{a-b}{a+b}}$, a and b are defined in Fig. 2.7.

In order to obtain $\mathbf{d}_k$ and $\mathbf{e}_k$ from the boundary condition (4.87), the function $\mathbf{f}_0$ should also be expressed in terms of $\boldsymbol{\zeta}^k$. As treated in Section 2.8, Eq (4.92) is written in terms of Laurent series expansions in the form

$$\mathbf{f}_0 = \sum_{k=1}^{\infty}\left(\langle \zeta_\alpha^k\rangle \mathbf{c}_k + \langle \zeta_\alpha^{-k}\rangle \mathbf{c}_{-k}\right),\qquad 1 \le |\zeta_\alpha| \le |\zeta_{\alpha 0}| \tag{4.95}$$

where

$$\mathbf{c}_k = -\frac{1}{k}\left\langle \left(\frac{1}{\zeta_{\alpha 0}}\right)^k \right\rangle \mathbf{q}_f,\quad \mathbf{c}_{-k} = -\frac{1}{k}\left\langle \left(\frac{d_\alpha}{c_\alpha \zeta_{\alpha 0}}\right)^k \right\rangle \mathbf{q}_f\,, \tag{4.96}$$

while c_α and d_α are defined by Eq (2.164), and $\zeta_{\alpha 0}$ is defined by Eq (2.172).

Substituting Eqs (4.93)-(4.95) and noting that $\zeta_0 = \zeta_\alpha = e^{i\theta}$ on the hole boundary, the condition (4.87) yields

$$\mathbf{g}^T\,\mathrm{Re}\sum_{k=1}^{\infty}\{\mathbf{A}[\mathbf{c}_k e^{ik\theta} + (\mathbf{c}_{-k} + \mathbf{d}_k)e^{-ik\theta}]\} = \mathrm{Re}\sum_{k=1}^{\infty}(e^{ik\theta} + r_{in}^{2k}e^{-ik\theta})\mathbf{e}_k, \tag{4.97}$$

$$\mathrm{Re}\sum_{k=1}^{\infty}\{\mathbf{B}[\mathbf{c}_k e^{ik\theta} + (\mathbf{c}_{-k} + \mathbf{d}_k)e^{-ik\theta}]\} = \mathbf{g}\mathbf{\Pi}^c\,\mathrm{Im}\sum_{k=1}^{\infty}(e^{ik\theta} + r_{in}^{2k}e^{-ik\theta})\mathbf{e}_k \tag{4.98}$$

Comparing the coefficients of $e^{ik\theta}$ and $e^{-ik\theta}$ in Eqs (4.97) and (4.98), we have

$$\begin{aligned}
&\mathbf{g}^T\mathbf{A}\mathbf{d}_k - (r_{in}^{2k}\mathbf{e}_k + \overline{\mathbf{e}}_k) = -\mathbf{g}^T(\overline{\mathbf{A}}\,\overline{\mathbf{c}}_k + \mathbf{A}\mathbf{c}_{-k}),\\
&\mathbf{g}^T\overline{\mathbf{A}}\,\overline{\mathbf{d}}_k - (\mathbf{e}_k + r_{in}^{2k}\overline{\mathbf{e}}_k) = -\mathbf{g}^T(\overline{\mathbf{A}}\,\overline{\mathbf{c}}_{-k} + \mathbf{A}\mathbf{c}_k),\\
&\mathbf{B}\mathbf{d}_k + i\mathbf{g}\mathbf{\Pi}^c(r_{in}^{2k}\mathbf{e}_k - \overline{\mathbf{e}}_k) = -(\overline{\mathbf{B}}\,\overline{\mathbf{c}}_k + \mathbf{B}\mathbf{c}_{-k}),\\
&\overline{\mathbf{B}}\,\overline{\mathbf{d}}_k + i\mathbf{g}\mathbf{\Pi}^c(\mathbf{e}_k - r_{in}^{2k}\overline{\mathbf{e}}_k) = -(\overline{\mathbf{B}}\,\overline{\mathbf{c}}_{-k} + \mathbf{B}\mathbf{c}_k)
\end{aligned} \tag{4.99}$$

Solving Eq (4.99) for $\mathbf{d}_k$ and $\mathbf{e}_k$, we obtain

$$\begin{aligned}\mathbf{d}_k &= -\mathbf{c}_{-k} - \mathbf{B}^{-1}\overline{\mathbf{B}}\overline{\mathbf{c}}_k + i\mathbf{B}^{-1}\mathbf{g}\boldsymbol{\Pi}^c(\overline{\mathbf{e}}_k - r_{in}^{2k}\mathbf{e}_k),\\ \mathbf{e}_k &= (r_{in}^{4k}\mathbf{W} - \mathbf{V}\mathbf{W}^{-1}\overline{\mathbf{V}})^{-1}(r_{in}^{2k}\overline{\mathbf{Y}}_k - \mathbf{V}\mathbf{W}^{-1}\mathbf{Y}_k)\end{aligned} \tag{4.100}$$

where

$$\mathbf{W} = \mathbf{I} + \mathbf{g}^T\mathbf{M}\mathbf{g}\boldsymbol{\Pi}^c, \quad \mathbf{V} = \mathbf{I} - \mathbf{g}^T\mathbf{M}\mathbf{g}\boldsymbol{\Pi}^c, \quad \mathbf{Y}_k = 2i\mathbf{g}^T\mathbf{L}^{-1}\mathbf{B}\mathbf{c}_k \tag{4.101}$$

with $\mathbf{I}$ being the 2×2 unit matrix, $\mathbf{M}$ and $\mathbf{L}$ being defined by Eqs (2.217) and (1.142).

Substituting Eq (4.100) into Eq (4.93) and using relation (2.193), $\mathbf{f}_1$ can be expressed in the form

$$\begin{aligned}\mathbf{f}_1 = &-\left\langle \ln\left(1 - \frac{d_\alpha / c_\alpha}{\zeta_\alpha \overline{\zeta}_{\alpha 0}}\right)\right\rangle \mathbf{q}_f - \sum_{\beta=1}^{5}\left\langle \ln\left(1 - \frac{1}{\zeta_\alpha \overline{\zeta}_{\beta 0}}\right)\right\rangle \mathbf{B}^{-1}\overline{\mathbf{B}}\mathbf{I}_\beta \overline{\mathbf{q}}_f\\ &+ i\sum_{k=1}^{\infty}\left\langle \zeta_\alpha^{-k}\right\rangle \mathbf{B}^{-1}\mathbf{g}\boldsymbol{\Pi}^c(\overline{\mathbf{e}}_k - r_{in}^{2k}\mathbf{e}_k)\end{aligned} \tag{4.102}$$

The corresponding Green's functions can thus be obtained by substituting Eqs (4.92) and (4.102) into Eqs (4.90) and (4.91).

When the minor axis 2b of the ellipse approaches zero, the elliptic hole reduces to a slit crack of length 2a. In this case, the Green's function can be obtained by considering that $c_0 = d_0 = c_\alpha = d_\alpha = a/2$. When b=0, Eq (4.102) reduces

$$\begin{aligned}\mathbf{f}_1 = &-\left\langle \ln\left(1 - \frac{d_\alpha / c_\alpha}{\zeta_\alpha \overline{\zeta}_{\alpha 0}}\right)\right\rangle \mathbf{q}_f - \sum_{\beta=1}^{5}\left\langle \ln\left(1 - \frac{1}{\zeta_\alpha \overline{\zeta}_{\beta 0}}\right)\right\rangle \mathbf{B}^{-1}[(\mathbf{L}\mathbf{M})^{-1} - \mathbf{I})\overline{\mathbf{B}}\mathbf{I}_\beta \overline{\mathbf{q}}_f\\ &+ \sum_{\beta=1}^{5}\left\langle \ln\left(1 - \frac{1}{\zeta_\alpha \zeta_{\beta 0}}\right)\right\rangle \mathbf{B}^{-1}(\mathbf{L}\mathbf{M})^{-1}\mathbf{B}\mathbf{I}_\beta \mathbf{q}_f\end{aligned} \tag{4.103}$$

where

$$a\zeta_\alpha = z_\alpha + \sqrt{z_\alpha^2 - a^2}, \quad a\zeta_{\alpha 0} = z_{\alpha 0} + \sqrt{z_{\alpha 0}^2 - a^2} \tag{4.104}$$

Eq (4.103) indicates that $\mathbf{f}_1$ is independent of $\boldsymbol{\Pi}^c$. This means that the Green's functions for a magnetoelectroelastic plate with a crack are not related to $\boldsymbol{\Pi}^c$.

4.8 Green's functions for thermomagnetoelectroelastic problems

In the previous chapter, applications of Green's function to thermopiezoelectric problems were presented. Extension of the procedure to including a magnetic field is described in this section. The discussion here follows the results presented in [12,13].

4.8.1 Basic equation for thermomagnetoelectroelastic problems

For a thermomagnetoelectroelastic solid where all fields are functions of x_1 and x_2 only, the complete set of governing equations for coupled thermo-electro-magneto-elastic problems is defined by Eqs (1.98)-(1.101). Using the shorthand notation described in Section 1.5.1 and assuming that no free electric charge, electric current, body force, and heat source exist, Eqs (1.98) and (1.99) can be rewritten as [12,13]:

$$q_{i,i} = 0, \quad \Pi_{iJ,i} = 0 \tag{4.105}$$

together with

$$q_i = -k_{ij}T_{,j}, \quad \Pi_{iJ} = E_{iJMn}U_{M,n} - \chi_{iJ}T \tag{4.106}$$

in which

$$\chi_{iJ} = \begin{cases} \lambda_{ij}, & J \le 3, \\ \chi_i, & J = 4, \\ \nu_i, & J = 5, \end{cases} \tag{4.107}$$

The general solution to Eq (4.105) is in the same form as that of Eq (3.1), but the vectors here have five components.

4.8.2 Green's function for half-plane problems

4.8.2.1 Green's function for thermal field. The half-plane boundary considered here is in the vertical direction (x_1=0 on the boundary in our analysis, see Fig. 4.2). In the analysis the boundary faces of the half-plane are assumed to be thermal-insulated, free of traction force, external electric current and charge. The boundary condition along the half-plane boundary can thus be written as

$$\vartheta = \varphi = 0 \tag{4.108}$$

The half-plane solution can be obtained by considering the full-space solution plus some modification term to satisfy the condition on the boundary of the half-plane [Eq (4.107)]. To this end, the general solution for temperature and heat-flow function can be assumed in the form [12]

$$T = 2\,\mathrm{Re}[g'(z_t^*)] = 2\,\mathrm{Re}[f_0(z_t^*) + f_1(z_t^*)] \tag{4.109}$$

$$\vartheta = 2k\,\mathrm{Im}[g'(z_t^*)] = 2k\,\mathrm{Im}[f_0(z_t^*) + f_1(z_t^*)] \tag{4.110}$$

where $z_t^* = z_t / p_1^*$, and f_0 is in the form [12]

$$f_0(z_t^*) = q_0 \ln(z_t^* - z_{t0}^*) \tag{4.111}$$

with q_0 defined by Eq (3.6). For the half-plane in the $z_t^* = z_t / p_1^*$ system, the perturbation function can be assumed in the form

$$f_1(z_t^*) = q_1 \ln(z_t^* - \bar{z}_{t0}^*) \tag{4.112}$$

Substituting Eqs (4.111) and (4.112) into Eq (4.110), the condition $(4.108)_1$ yields

$$\mathrm{Im}[q_0 \ln(x_2 - z_{t0}^*) + q_1 \ln(x_2 - \bar{z}_{t0}^*)] = 0 \tag{4.113}$$

Noting that $z_t^* = x_2$ on the half-plane boundary and $\mathrm{Im}(f) = -\mathrm{Im}(\bar{f})$, we have

$$\mathrm{Im}[q_0 \ln(x_2 - z_{t0}^*)] = -\mathrm{Im}[\bar{q}_0 \ln(x_2 - \bar{z}_{t0}^*)] \tag{4.114}$$

Eq (4.113) now yields

$$q_1 = \bar{q}_0 \tag{4.115}$$

The function g in Eq (3.1) can then be obtained by integrating f_0 and f_1 with respect to z_t, which yields

$$g(z_t) = q_0 f^*(z_t^*, z_{t0}^*) + \bar{q}_0 f^*(z_t^*, \bar{z}_{t0}^*) \tag{4.116}$$

where the function f^* is defined by Eq (3.7).

4.8.2.2 Green's function for magnetoelectroelastic field. As treated previously, the general solution of the thermomagnetoelectroelastic problem can be written as

$$\mathbf{U} = \mathbf{U}_p + \mathbf{U}_h, \quad \boldsymbol{\varphi} = \boldsymbol{\varphi}_p + \boldsymbol{\varphi}_h \tag{4.117}$$

where subscripts 'p' and 'h' refer, respectively, to the particular and homogeneous solutions.

From Eqs (3.1) and (3.2) the particular solution of a magnetoelectroelastic field induced by thermal loading can be written as

$$\mathbf{U}_p = 2\,\mathrm{Re}[\mathbf{c}g(z_t)], \quad \boldsymbol{\varphi}_p = 2\,\mathrm{Re}[\mathbf{d}g(z_t)] \tag{4.118}$$

To satisfy the boundary condition (4.108), the homogeneous solution $\mathbf{U}_h$ and $\boldsymbol{\varphi}_h$ can be assumed in the form [12]

$$\mathbf{U}_h = 2\,\mathrm{Re}[\mathbf{c}q_0 f^*(z_k^*, z_{t0}^*) + \mathbf{c}\bar{q}_0[f^*(z_k^*, \bar{z}_{t0}^*)] \tag{4.119}$$

$$\boldsymbol{\varphi}_h = 2\,\mathrm{Re}[\mathbf{d}q_0 f^*(z_k^*, z_{t0}^*)] + \mathbf{d}\bar{q}_0 f^*(z_k^*, \bar{z}_{t0}^*)] \tag{4.120}$$

where z_k^* is defined by Eq (4.57). For simplicity, denote

$$f(z_k^*) = q_0 f^*(z_k^*, z_{t0}^*) + \bar{q}_0 f^*(z_k^*, \bar{z}_{t0}^*) \tag{4.121}$$

Substitution of Eqs (4.119)-(4.121) into $(3.2)_2$, and then into $(4.108)_2$, leads to

$$\mathbf{q} = -\mathbf{B}^{-1}\mathbf{d} \tag{4.122}$$

Thus Green's functions for the magnetoelectroelastic field of the half-plane problem can be written as

$$\mathbf{U} = 2\,\mathrm{Re}[-\mathbf{A}\mathbf{f}(\mathbf{z}^*)\mathbf{B}^{-1}\mathbf{d} + \mathbf{c}g(z_t)], \qquad \boldsymbol{\varphi} = 2\,\mathrm{Re}[-\mathbf{B}\mathbf{f}(\mathbf{z}^*)\mathbf{B}^{-1}\mathbf{d} + \mathbf{d}g(z_t)] \tag{4.123}$$

where $\mathbf{f}(\mathbf{z}^*) = \mathrm{diag}[f(z_1^*)\, f(z_2^*)\, f(z_3^*)\, f(z_4^*)\, f(z_5^*)]$.

4.8.3 Green's function for bimaterial problems

We now consider a bimaterial solid whose interface is on x_2-axis (x_1=0). It is assumed that the left half-plane (x_1<0) is occupied by material 1, and the right half-plane (x_1>0) is occupied by material 2 (Fig. 4.4). They are rigidly bonded together so that

$$T^{(1)} = T^{(2)}, \quad \vartheta^{(1)} = \vartheta^{(2)}, \quad \mathbf{U}^{(1)} = \mathbf{U}^{(2)}, \quad \boldsymbol{\varphi}^{(1)} = \boldsymbol{\varphi}^{(2)}, \quad \text{at } x_1=0 \tag{4.124}$$

where the superscripts (1) and (2) label the quantities relating to materials 1 and 2 respectively.

4.8.3.1 Green's function for thermal field in bimaterial solids. For a bimaterial subjected to a line temperature discontinuity $\hat{T}$ and a line heat source h^*, both located in the left half-plane at $z_0(x_{10}, x_{20})$ as shown in Fig. 4.4, the general solution for the bimaterial solid can be assumed in the form [12]

$$T^{(1)} = 2\,\mathrm{Re}[f_0(z_t^{(1)*}) + f_1(z_t^{(1)*})], \quad \vartheta^{(1)} = 2k^{(1)}\,\mathrm{Im}[f_0(z_t^{(1)*}) + f_1(z_t^{(1)*})], \quad x_1 < 0, \tag{4.125}$$

$$T^{(2)} = 2\,\mathrm{Re}[f_2(z_t^{(2)*})], \quad \vartheta^{(2)} = 2k^{(2)}\,\mathrm{Im}[f_2(z_t^{(2)*})], \quad x_1 > 0 \tag{4.126}$$

where the function f_0 is again given in Eq (4.111). To satisfy the interface condition $(4.124)_{1,2}$, the functions f_1 and f_2 are taken as

$$f_1(z_t^{(1)*}) = q_1 \ln(z_t^{(1)*} - \bar{z}_{t0}^{(1)*}), \tag{4.127}$$

$$f_2(z_t^{(2)*}) = q_2 \ln(z_t^{(2)*} - z_{t0}^{(1)*}) \tag{4.128}$$

With the substitution of Eqs (4.111), (4.127), and (4.128) into Eqs (4.125) and (4.126), the continuity condition $(4.124)_{1,2}$ provides

$$q_1 = \frac{k^{(1)} - k^{(2)}}{k^{(2)} + k^{(1)}} \bar{q}_0, \quad q_2 = \frac{2k^{(1)}}{k^{(1)} + k^{(2)}} q_0 \tag{4.129}$$

Therefore the function g for the present bimaterial problem can be written in the form

$$g_1(z_t^{(1)*}) = q_0 f^*(z_t^{(1)*}, z_{t0}^{(1)*}) + q_1 f^*(z_t^{(1)*}, \bar{z}_{t0}^{(1)*}) \tag{4.130}$$

$$g_2(z_t^{(2)*}) = q_2 f^*(z_t^{(2)*}, z_{t0}^{(1)*}) \tag{4.131}$$

4.8.3.2 Green's function for magnetoelectroelastic field in bimaterial solids. To use the condition $(4.124)_{3,4}$ we first consider the particular solution due to the thermal field. Using Eqs (4.130) and (4.131), the particular solution for the magnetoelectroelastic field can be written as

$$\mathbf{U}_p^{(1)}(z_t^{(1)*}) = 2\,\mathrm{Re}[q_0 \mathbf{c}^{(1)} f^*(z_t^{(1)*}, z_{t0}^{(1)*}) + \mathbf{c}^{(1)} q_1 [f^*(z_t^{(1)*}, \bar{z}_{t0}^{(1)*})], \tag{4.132}$$

$$\boldsymbol{\varphi}_p^{(1)}(z_t^{(1)*}) = 2\,\mathrm{Re}[q_0 \mathbf{d}^{(1)} f^*(z_t^{(1)*}, z_{t0}^{(1)*}) + \mathbf{d}^{(1)} q_1 f^*(z_t^{(1)*}, \bar{z}_{t0}^{(1)*})] \tag{4.133}$$

for $x_1 < 0$, and

$$\mathbf{U}_p^{(2)}(z_t^{(2)*}) = 2\,\mathrm{Re}[\mathbf{c}^{(2)} q_2 f^*(z_t^{(2)*}, z_{t0}^{(1)*})], \tag{4.134}$$

$$\boldsymbol{\varphi}_p^{(2)}(z_t^{(2)*}) = 2\,\mathrm{Re}[\mathbf{d}^{(2)} q_2 f^*(z_t^{(2)*}, z_{t0}^{(1)*})] \tag{4.135}$$

for $x_1 > 0$. For the same reason as in Section 3.3.2, a corrective solution needs to be constructed in such a way that when it is superimposed on the particular solutions (4.132)-(4.135) the interface condition (4.124) will be satisfied. Owing to the fact that $f(z_k)$ and $g(z_t)$ have the same rule affecting **U** and **φ** in Eqs (3.1) and (3.2), possible function forms come from the partition of solution $g(z_t)$. This is

$$f_1(z_\alpha^{(1)*}) = f^*(z_\alpha^{(1)*}, z_{t0}^{(1)*}), \quad f_2(z_\alpha^{(1)*}) = f^*(z_\alpha^{(1)*}, \bar{z}_{t0}^{(1)*}) \tag{4.136}$$

$$f_3(z_\alpha^{(2)*}) = f^*(z_\alpha^{(2)*}, z_{t0}^{(1)*}), f_4(z_\alpha^{(2)*}) = f^*(z_\alpha^{(2)*}, \bar{z}_{t0}^{(1)*}) \tag{4.137}$$

Thus the resulting expressions of $\mathbf{U}^{(i)}$ and $\boldsymbol{\varphi}^{(i)}$ can be given as

$$\begin{aligned}\mathbf{U}^{(1)} = 2\,\mathrm{Re}\{&\mathbf{A}^{(1)}[\langle f_1(z_\alpha^{(1)*})\rangle \mathbf{q}_{11} + \langle f_2(z_\alpha^{(1)*})\rangle \mathbf{q}_{12}] + q_0 \mathbf{c}^{(1)} f^*(z_t^{(1)*}, z_{t0}^{(1)*}) \\ &+ \mathbf{c}^{(1)} q_1 f^*(z_t^{(1)*}, \bar{z}_{t0}^{(1)*})\},\end{aligned} \tag{4.138}$$

$$\begin{aligned}\boldsymbol{\varphi}^{(1)} = 2\,\mathrm{Re}\{&\mathbf{B}^{(1)}[\langle f_1(z_\alpha^{(1)*})\rangle \mathbf{q}_{11} + \langle f_2(z_\alpha^{(1)*})\rangle \mathbf{q}_{12}] + q_0 \mathbf{d}^{(1)} f^*(z_t^{(1)*}, z_{t0}^{(1)*}) \\ &+ \mathbf{d}^{(1)} q_1 f^*(z_t^{(1)*}, \bar{z}_{t0}^{(1)*})\}\end{aligned} \tag{4.139}$$

for $x_1 < 0$, and

$$\mathbf{U}^{(2)} = 2\,\mathrm{Re}\{\mathbf{A}^{(2)}[\langle f_3(z_\alpha^{(2)*})\rangle \mathbf{q}_{21} + \langle f_4(z_\alpha^{(2)*})\rangle \mathbf{q}_{22}] + \mathbf{c}^{(2)} q_2 f^*(z_t^{(2)*}, z_{t0}^{(1)*})\}, \quad (4.140)$$

$$\boldsymbol{\varphi}^{(2)} = 2\,\mathrm{Re}\{\mathbf{B}^{(2)} \langle f_3(z_\alpha^{(2)*})\rangle \mathbf{q}_{21} + \langle f_4(z_\alpha^{(2)*})\rangle \mathbf{q}_{22}] + \mathbf{d}^{(2)} q_2 f^*(z_t^{(2)*}, z_{t0}^{(1)*})\} \quad (4.141)$$

for $x_1 > 0$. The substitution of Eqs (4.138)-(4.141) into Eq $(4.124)_{3,4}$ yields

$$\mathbf{q}_{11} = \mathbf{M}_1[(\mathbf{B}^{(2)-1}\mathbf{d}^{(2)} - \mathbf{A}^{(2)-1}\mathbf{c}^{(2)})q_2 - (\mathbf{B}^{(2)-1}\mathbf{d}^{(1)} - \mathbf{A}^{(2)-1}\mathbf{c}^{(1)})q_0] \quad (4.142)$$

$$\mathbf{q}_{21} = \mathbf{M}_2[(\mathbf{B}^{(1)-1}\mathbf{d}^{(1)} - \mathbf{A}^{(1)-1}\mathbf{c}^{(1)})q_0 - (\mathbf{B}^{(1)-1}\mathbf{d}^{(2)} - \mathbf{A}^{(1)-1}\mathbf{c}^{(2)})q_2] \quad (4.143)$$

$$\mathbf{q}_{12} = -\mathbf{M}_1(\mathbf{B}^{(2)-1}\mathbf{d}^{(1)} - \mathbf{A}^{(2)-1}\mathbf{c}^{(1)})q_1 \quad (4.144)$$

$$\mathbf{q}_{22} = \mathbf{M}_2(\mathbf{B}^{(1)-1}\mathbf{d}^{(1)} - \mathbf{A}^{(1)-1}\mathbf{c}^{(1)})q_1 \quad (4.145)$$

where $\mathbf{M}_1 = (\mathbf{B}^{(2)-1}\mathbf{B}^{(1)} - \mathbf{A}^{(2)-1}\mathbf{A}^{(1)})^{-1}$, $\mathbf{M}_2 = (\mathbf{B}^{(1)-1}\mathbf{B}^{(2)} - \mathbf{A}^{(1)-1}\mathbf{A}^{(2)})^{-1}$. Thus, the explicit expression of the thermomagnetoelectroelastic Green's functions for the bimaterial solid can be obtained by substituting Eqs (4.142)-(4.145) into Eqs (4.138)-(4.141).

4.8.4 Green's function for elliptic hole problems

The hole problem to be considered here is illustrated in Fig. 2.7, showing an infinite two-dimensional thermomagnetoelectroelastic plate containing an elliptic hole (with the limit *b*=0, a crack) with semi-major axis *a* and semi-minor axis *b*. The plate is subjected to a line heat source h^* and a line temperature discontinuity $\hat{T}$, both located at $z_0(x_{10},x_{20})$ (Fig. 2.7). In this subsection, the hole is assumed to be filled with a homogeneous gas (air or vacuum) of permittivity (κ^c) and permeability (μ^c), where superscript '*c*' refers to the quantities associated with the hole medium [12]. Therefore, induced electric and magnetic fields exist in the hole, denoted by Ω_c, and can be governed by the equations

$$\nabla^2\phi^c = 0, \qquad \nabla^2\psi^c = 0, \qquad \text{in } \Omega_c \quad (4.146)$$

with the constitutive relations

$$D_i^c = \kappa^c E_i^c = -\kappa^c \phi_{,i}^c, \qquad B_i^c = \kappa^c H_i^c = -\mu^c \psi_{,i}^c \quad i=1,2 \quad \text{in } \Omega_c \quad (4.147)$$

The general solutions to Eqs (4.146) and (4.147) are thus given by

$$\phi^c = 2\,\mathrm{Re}[f_1^c(z)], \qquad \psi^c = 2\,\mathrm{Re}[f_2^c(z)], \qquad z = x_1 + ix_2 \quad (4.148)$$

Defining the potential, electric displacement and magnetic induction function

$$\mathbf{U}^c = \begin{Bmatrix} \phi^c \\ \psi^c \end{Bmatrix} = 2\,\mathrm{Re}\begin{Bmatrix} f_1^c(z) \\ f_2^c(z) \end{Bmatrix}, \qquad \boldsymbol{\varphi}^c = 2\,\mathrm{Re}\{\begin{bmatrix} b_1^c & 0 \\ 0 & b_2^c \end{bmatrix}\begin{Bmatrix} f_1^c(z) \\ f_2^c(z) \end{Bmatrix}\} \quad (4.149)$$

where $b_1^c = -i\kappa^c$, $b_2^c = -i\mu^c$, we have

$$\boldsymbol{\Pi}_1^c = \{D_1^c, B_1^c\}^T = -\boldsymbol{\varphi}_{,2}^c, \quad \boldsymbol{\Pi}_2^c = \{D_2^c, B_2^c\}^T = \boldsymbol{\varphi}_{,1}^c \quad (4.150)$$

Using the above expression, the magnetoelectroelastic boundary conditions along the surface of the hole can be written as

$$\mathbf{g}^T\mathbf{U} = \mathbf{U}^c, \quad \boldsymbol{\varphi} = \mathbf{g}\boldsymbol{\varphi}^c \qquad \text{on } \Gamma \tag{4.151}$$

$$\Pi_{ij} \to 0 \quad \text{at infinity} \tag{4.152}$$

where **g** is defined by Eq (4.89). As in Section 2.8, single-valued mapping (2.182)

$$z = c_0\zeta_0 + d_0\zeta_0^{-1} \tag{4.153}$$

is used here.

The Green's functions for thermal field here are the same as those in Section 3.5. We will not repeat that here. To satisfy the conditions (4.151), the solutions **U** and **φ** can be chosen to be Eqs (3.64) and (3.65), i.e.

$$\mathbf{U} = 2\,\mathrm{Re}[\sum_{k=1}^{4}\mathbf{A}\langle f_k(\zeta_\alpha)\rangle\mathbf{q}_k + \mathbf{c}g(\zeta_t)] \tag{4.154}$$

$$\boldsymbol{\varphi} = 2\,\mathrm{Re}[\sum_{k=1}^{4}\mathbf{B}\langle f_k(\zeta_\alpha)\rangle\mathbf{q}_k + \mathbf{d}g(\zeta_t)] \tag{4.155}$$

and $\mathbf{U}^c$ and $\boldsymbol{\varphi}^c$ are assumed in the form

$$\mathbf{U}^c = 2\,\mathrm{Re}\sum_{k=1}^{4}[\langle f_k^c(\zeta_0)\rangle\mathbf{q}_{ck}] \tag{4.156}$$

$$\boldsymbol{\varphi}^c = 2\,\mathrm{Re}\sum_{k=1}^{4}[\mathbf{B}^c\langle f_k^c(\zeta_0)\rangle\mathbf{q}_{ck}] \tag{4.157}$$

where f_k is defined by Eq (3.63), and

$$\mathbf{B}^c = \begin{bmatrix} -i\boldsymbol{\kappa}^c & 0 \\ 0 & -i\boldsymbol{\mu}^c \end{bmatrix}, \quad f_k^c(\zeta_0) = F_k(\zeta_0) \tag{4.158}$$

in which F_k is given in Eq (3.61). The condition (4.151) provides

$$2\,\mathrm{Re}[\mathbf{g}^T(\mathbf{A}\mathbf{q}_i + \mathbf{c}r_i)] = 2\,\mathrm{Re}[\mathbf{q}_{ci}], \quad 2\,\mathrm{Re}[\mathbf{B}\mathbf{q}_i + \mathbf{d}r_i] = 2\,\mathrm{Re}[\mathbf{g}\mathbf{B}^c\mathbf{q}_{ci}], \ (i\text{=}1\text{-}4) \tag{4.159}$$

where

$$r_1 = c_\tau q_0, \quad r_2 = d_\tau q_0, \quad r_3 = d_\tau\overline{q}_0, \quad r_4 = c_\tau\overline{q}_0 \tag{4.160}$$

Solving Eqs (4.159) yields

$$\mathbf{q}_i = (\mathbf{B} - \mathbf{g}\mathbf{B}^c\mathbf{g}^T\mathbf{A})^{-1}(\mathbf{g}\mathbf{B}^c\mathbf{g}^T\mathbf{c} - \mathbf{d})r_i, \quad \mathbf{q}_{ci} = \mathbf{g}^T(\mathbf{A}\mathbf{q}_i + \mathbf{c}r_i), \quad (i\text{=}1\text{-}4) \tag{4.161}$$

A crack of length 2*a* can be formed by letting the minor axis *b* of the ellipse approach zero. The solutions for a crack in an infinite magnetoelectroelastic plate can then be obtained from the formulation above by setting *b*=0. In this case, Eqs (2.162), (3.54), and (4.153) are reduced to

$$z_\alpha = \frac{a}{2}\left(\zeta_\alpha + \zeta_\alpha^{-1}\right), \quad c_\alpha = d_\alpha = \frac{a}{2} \tag{4.162}$$

$$z_t = \frac{a}{2}\left(\zeta_t + \zeta_t^{-1}\right), \quad c_\tau = d_\tau = \frac{a}{2} \tag{4.163}$$

$$z = \frac{a}{2}\left(\zeta_0 + \zeta_0^{-1}\right), \quad c_0 = d_0 = \frac{a}{2} \tag{4.164}$$

4.8.5 Green's functions for a wedge or semi-infinite crack

Consider an infinite magnetoelectroelastic wedge whose symmetric line extends infinitely in the negative direction of the x_1-axis (Fig. 4.5). The wedge angle is denoted by $2\theta_0$. The solid is subjected to a temperature discontinuity $\hat{T}$ and a heat source h^*, both at a point z_0 (x_{10}, x_{20}) as shown in Fig. 4.5. The wedge faces are assumed to be thermal-insulated, free of force, external electric current and charge. The boundary condition along the two wedge faces can thus be written as

$$\vartheta = \boldsymbol{\varphi} = 0 \tag{4.167}$$

4.8.5.1 General solution for thermal field

As in Section 4.8.2, the general solution for temperature and heat-flow function can be assumed in the form

$$T = 2\,\mathrm{Re}[g'(z_t)] = 2\,\mathrm{Re}[f_0(\zeta_t) + f_1(\zeta_t)] \tag{4.168}$$

$$\vartheta = 2k\,\mathrm{Im}[g'(z_t)] = 2k\,\mathrm{Im}[f_0(\zeta_t) + f_1(\zeta_t)] \tag{4.169}$$

where f_0 is chosen to represent the solutions associated with the unperturbed thermal fields and f_1 is a function corresponding to the perturbed field due to the wedge boundary. Here ζ_t and ζ_{t0} are related to z_t and $z_{t0}(= x_{10} + p_1^* x_{20})$ by the mapping functions [13]

$$z_t = \zeta_t^{1/\lambda} \quad \text{and} \quad z_{t0} = \zeta_{t0}^{1/\lambda} \tag{4.170}$$

where $\lambda = \pi/(2\pi - 2\theta_0)$ and $\zeta_t = \xi + i\eta$ maps the wedge boundary $\theta = \pm(\pi - \theta_0)$ in the z_t-plane into the imaginary axis in the ζ_t-plane (Fig. 4.5). Therefore the solution domain is mapped into the right half plane axis in the ζ_t-plane.

For a given loading condition, the function f_0 can be obtained easily since it is related to the solution of homogeneous media. When an infinite space is subjected to a line heat source h^* and the thermal analog of a line temperature discontinuity T_0, both located at (x_{10}, x_{20}), the function f_0 can be chosen in the form

$$f_0(\zeta_t) = q_0 \ln(\zeta_t - \zeta_{t0}) \tag{4.171}$$

and q_0 is defined by Eq (3.6).

For the half-plane in the $\zeta_t = \xi + i\eta$ system, the perturbation function can be assumed in the form [13]:

$$f_1(\zeta_t) = q_1 \ln(-\zeta_t - \overline{\zeta}_{t0}) \tag{4.172}$$

Substituting Eqs (4.171) and (4.172) into Eq (4.169), the condition $(4.167)_1$ yields

$$\mathrm{Im}[q_0 \ln(i\eta - \zeta_{t0}) + q_1 \ln(-i\eta - \overline{\zeta}_{t0})] = 0 \tag{4.173}$$

Noting that $\mathrm{Im}(f) = -\mathrm{Im}(\bar{f})$, we have

$$\mathrm{Im}[q_0 \ln(i\eta - \zeta_{t0})] = -\mathrm{Im}[\overline{q}_0 \ln(-i\eta - \overline{\zeta}_{t0})] \tag{4.174}$$

Equation (4.173) now yields

$$q_1 = \overline{q}_0 \tag{4.175}$$

Having obtained the solution of f_0 and f_1, the function $g'(z_t)$ can now be written as

$$g'(z_t) = q_0 \ln(z_t^\lambda - z_{t0}^\lambda) + \overline{q}_0 \ln(-z_t^\lambda - \overline{z}_{t0}^\lambda) \tag{4.176}$$

Substituting Eq (4.176) into Eqs (4.168) and (4.169) yields

$$T = 2\,\mathrm{Re}[q_0 \ln(z_t^\lambda - z_{t0}^\lambda) + \overline{q}_0 \ln(-z_t^\lambda - \overline{z}_{t0}^\lambda)] \tag{4.177}$$

$$\vartheta = 2k\,\mathrm{Im}[q_0 \ln(z_t^\lambda - z_{t0}^\lambda) + \overline{q}_0 \ln(-z_t^\lambda - \overline{z}_{t0}^\lambda)] \tag{4.178}$$

The function g in Eq (3.1) can thus be obtained by integrating the functions of f_0 and f_1 with respect to z_t, which leads to

$$g(z_t) = q_0 \hat{f}_1(z_t) + \overline{q}_0 \hat{f}_2(z_t) \tag{4.179}$$

where

$$\hat{f}_1(z_t) = \lambda z_t(-1 + {}_2F_1(1/\lambda, 1, 1+1/\lambda, z_t^\lambda / z_{t0}^\lambda) + z_t \ln(z_t^\lambda - z_{t0}^\lambda)$$

$$\hat{f}_2(z_t) = \lambda z_t(-1 + {}_2F_1(1/\lambda, 1, 1+1/\lambda, -z_t^\lambda / \overline{z}_{t0}^\lambda) + z_t \ln(-z_t^\lambda - \overline{z}_{t0}^\lambda) \tag{4.180}$$

with ${}_2F_1(a,b,c,z)$ being a hypergeometric function defined in [16]

$${}_2F_1(a,b,c,z) = \frac{\Gamma(c)}{\Gamma(b)\Gamma(c-b)} \int_0^1 \frac{t^{b-1}(1-t)^{c-b-1}}{(1-tz)^a} dt \tag{4.181}$$

or series expansion

$${}_2F_1(a,b,c,z) = 1 + \frac{ab}{1!c} z + \frac{a(a+1)b(b+1)}{2!c(c+1)} z^2 + \cdots = \sum_{n=0}^{\infty} \frac{(a)_n (b)_n}{n!(c)_n} z^n \tag{4.182}$$

where $\Gamma(x)$ is a gamma function.

3.2 Green's functions for magnetoelectroelastic fields

The general solution of the thermomagnetoelectroelastic problem can be written as

$$\mathbf{U} = \mathbf{U}_p + \mathbf{U}_h, \quad \boldsymbol{\varphi} = \boldsymbol{\varphi}_p + \boldsymbol{\varphi}_h \tag{4.183}$$

where subscripts 'p' and 'h' refer, respectively, to the particular and homogeneous solutions.

From Eqs (3.1) and (3.2) the particular solution of magnetoelectroelastic field induced by thermal loading can be written as

$$\mathbf{U}_p = 2\,\mathrm{Re}[\mathbf{c}g(z_t)], \quad \boldsymbol{\varphi}_p = 2\,\mathrm{Re}[\mathbf{d}g(z_t)] \tag{4.184}$$

To satisfy the boundary condition $(4.167)_2$ along the wedge boundary, a corrective isothermal solution is required so that, when superimposed on the particular

thermomagnetoelectroelastic solution, the surface conditions $(4.167)_2$ will be satisfied. Owing to the fact that $f(z_\alpha)$ and $g(z_t)$ have the same order of effect on stress and electric displacement in Eqs (3.1) and (3.2) [note that the term **Bf(z)q** in Eq (3.2) is now replaced by $\mathbf{B}(\langle f_1(z_\alpha)\rangle \mathbf{q}_1 + \langle f_2(z_\alpha)\rangle \mathbf{q}_2)$], possible function forms come from the partition of $g(z_t)$. They are

$$f_1(z_\alpha) = \lambda z_\alpha(-1 + {}_2F_1(1/\lambda, 1, 1+1/\lambda, z_\alpha^\lambda / z_{t0}^\lambda) + z_\alpha \ln(z_\alpha^\lambda - \bar{z}_{t0}^\lambda)$$

$$f_2(z_\alpha) = \lambda z_\alpha(-1 + {}_2F_1(1/\lambda, 1, 1+1/\lambda, -z_\alpha^\lambda / \bar{z}_{t0}^\lambda) + z_\alpha \ln(-z_\alpha^\lambda - \bar{z}_{t0}^\lambda) \qquad (4.185)$$

The substitution of Eqs (4.184) and (4.185) into (3.2), and then into (4.167), leads to

$$\mathbf{q}_1 = -\mathbf{B}^{-1}\mathbf{d}q_0, \qquad \mathbf{q}_2 = -\mathbf{B}^{-1}\mathbf{d}\bar{q}_0 \qquad (4.186)$$

Substituting Eq (4.186) into Eqs (3.1) and (3.2), the Green's functions can then be written as

$$\mathbf{U} = 2\,\mathrm{Re}[-\mathbf{A}(\langle f_1(z_\alpha)\rangle q_0 + \langle f_2(z_\alpha)\rangle \bar{q}_0)\mathbf{B}^{-1}\mathbf{d} + \mathbf{c}g(z_t)],$$

$$\boldsymbol{\varphi} = 2\,\mathrm{Re}[-\mathbf{B}(\langle f_1(z_\alpha)\rangle q_0 + \langle f_2(z_\alpha)\rangle \bar{q}_0)\mathbf{B}^{-1}\mathbf{d} + \mathbf{d}g(z_t)] \qquad (4.187)$$

When $\theta_0=0$, i.e, $\lambda=1/2$, Eq (4.187) represents Green's functions for the case of a semi-infinite crack in an infinite magnetoelectroelastic solid.

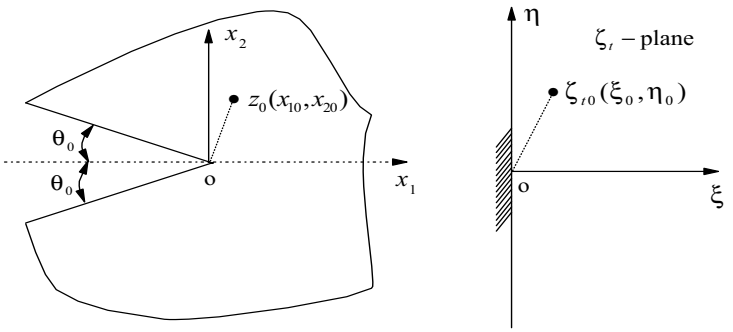

Fig. 4.5: Wedge-shaped magnetoelectroelastic plate and its mapping in the ζ-plane

4.9 Dynamic Green's functions of magnetoelectroelastic media

In this section, the potential approach is used to derive dynamic Green's functions of magnetoelectroelastic problems. The discussion follows the results presented in [14].

4.9.1 Dynamic potentials

Consider a linear transversely isotropic magnetoelectroelastic medium with the poling direction along the x_3-axis being perpendicular to the isotropic plane, whose motion in Euclidean space is described in terms of the independent variables $\mathbf{x} = \{x_i\}$ and t. The governing equations of electric and magnetic fields are still given by Eqs $(1.98)_{2,3}$, while the elastic equilibrium equations $(1.98)_1$ are, in this case, modified as

$$\sigma_{ij,j} + b_i = \rho \ddot{u}_i \tag{4.188}$$

where ρ is the mass density of the magnetoelectroelastic medium, and the dots over a variable represent temporal derivatives.

For simplicity, the discussion below considers an infinite two-dimensional 'quasi-plane' magnetoelectroelastic medium with transversely isotropic symmetry only. All field quantities depend only on the plane space vector $\mathbf{r} = (x,y)$ in the plane of transverse isotropy. These assumptions mean that

$$\begin{aligned} &\mathbf{U} = \{u_1, u_2, u_3, \phi, \psi\} = \{u_1, u_2, u_3, \phi, \psi\}(x, y) \\ &\frac{\partial}{\partial x_3}(\cdot) = 0 \end{aligned} \tag{4.189}$$

In view of Eq (4.189), Eqs (4.188), $(1.59)_2$ and $(1.82)_1$ can be reduced to

$$\begin{aligned} &\frac{\partial \sigma_{11}}{\partial x} + \frac{\partial \sigma_{12}}{\partial y} + b_1 = \rho \frac{\partial^2 u_1}{\partial t^2} \\ &\frac{\partial \sigma_{12}}{\partial x} + \frac{\partial \sigma_{22}}{\partial y} + b_2 = \rho \frac{\partial^2 u_2}{\partial t^2} \\ &\frac{\partial \sigma_{13}}{\partial x} + \frac{\partial \sigma_{23}}{\partial y} + b_3 = \rho \frac{\partial^2 u_3}{\partial t^2} \\ &\frac{\partial D_1}{\partial x} + \frac{\partial D_2}{\partial y} + b_e = 0 \\ &\frac{\partial B_1}{\partial x} + \frac{\partial B_2}{\partial y} + b_m = 0 \end{aligned} \tag{4.190}$$

Substituting Eqs (1.90)-(1.92) into Eq (4.190) leads to the following governing equation

$$T(\nabla, \frac{\partial}{\partial t})\mathbf{U} + \mathbf{F} = 0 \tag{4.191}$$

where

$$T(\nabla, \frac{\partial}{\partial t}) = \begin{bmatrix} T_I(\nabla, \frac{\partial}{\partial t}) & 0 \\ 0 & T_{II}(\nabla, \frac{\partial}{\partial t}) \end{bmatrix} \tag{4.192}$$

$$T_I(\nabla, \frac{\partial}{\partial t}) = \begin{bmatrix} c_{11}\frac{\partial^2}{\partial x^2} + \frac{c_{11}-c_{12}}{2}\frac{\partial^2}{\partial y^2} - \rho\frac{\partial^2}{\partial t^2} & \frac{c_{11}+c_{12}}{2}\frac{\partial^2}{\partial x \partial y} \\ \frac{c_{11}+c_{12}}{2}\frac{\partial^2}{\partial x \partial y} & c_{11}\frac{\partial^2}{\partial y^2} + \frac{c_{11}-c_{12}}{2}\frac{\partial^2}{\partial x^2} - \rho\frac{\partial^2}{\partial t^2} \end{bmatrix} \tag{4.193}$$

$$T_{II}(\nabla,\frac{\partial}{\partial t})=\begin{bmatrix} c_{44}\nabla_2-\rho\dfrac{\partial^2}{\partial t^2} & e_{15}\nabla_2 & \tilde{e}_{15}\nabla_2 \\ e_{15}\nabla_2 & -\kappa_{11}\nabla_2 & -\alpha_{11}\nabla_2 \\ \tilde{e}_{15}\nabla_2 & -\alpha_{11}\nabla_2 & -\mu_{11}\nabla_2 \end{bmatrix} \tag{4.194}$$

$$\nabla_2=\frac{\partial^2}{\partial x^2}+\frac{\partial^2}{\partial y^2} \tag{4.195}$$

$$\mathbf{F}=\{b_1,\ b_2,\ b_3,\ b_e,\ b_m\}^T \tag{4.196}$$

Introducing following notations

$$\begin{aligned} &\mathbf{U}_I=\{u_1,\ u_2\}^T, \quad \mathbf{U}_{II}=\{u_3,\ \phi,\ \psi\}^T, \\ &\mathbf{F}_I=\{b_1,\ b_2\}^T, \quad \mathbf{F}_{II}=\{b_3,\ b_e,\ b_m\}^T \end{aligned} \tag{4.197}$$

Eq (4.191) can be further written as

$$\begin{bmatrix} T_I(\nabla,\dfrac{\partial}{\partial t}) & 0 \\ 0 & T_{II}(\nabla,\dfrac{\partial}{\partial t}) \end{bmatrix}\begin{Bmatrix}\mathbf{U}_I\\ \mathbf{U}_{II}\end{Bmatrix}+\begin{Bmatrix}\mathbf{F}_I\\ \mathbf{F}_{II}\end{Bmatrix}=\mathbf{0} \tag{4.198}$$

where the operator matrix T is divided into two parts in which T_I corresponds to a pure elastic part which acts on u_1 and u_2 in the isotropic plane and T_{II} corresponds to the magnetoelectroelastic coupling of u_3, ϕ and ψ.

The magnetoelectroelastic potentials $\hat{\mathbf{G}}(\mathbf{r},t)$ of Eq (4.191) are thus determined by the following differential equations[14]:

$$T(\nabla,\frac{\partial}{\partial t})\hat{\mathbf{G}}(\mathbf{r},t)+\mathbf{I}_5\Theta_s(\mathbf{r})\delta(t)=0 \tag{4.199}$$

where $\mathbf{I}_5$ represents a 5×5 unit matrix, $\Theta_s(\mathbf{r})$ denotes the characteristic function of the inclusion S embedded in the medium, characterizing the spatial distribution of generalized unit forces. Based on this explanation, the dynamic magnetoelectroelastic potential can be regarded as generalized displacement due to a source distribution of generalized forces represented by an inclusion.

On the other hand, the dynamic Green's function $\mathbf{G}(\mathbf{r},t)$ for Eq (4.191) can be defined as

$$T(\nabla,\frac{\partial}{\partial t})\mathbf{G}(\mathbf{r},t)+\mathbf{I}_5\delta^2(\mathbf{r})\delta(t)=0 \tag{4.200}$$

Making use of Eqs (4.199) and (4.200), dynamic potential and Green's function can be related by

$$\hat{\mathbf{G}}(\mathbf{r},t)=\int_{-\infty}^{\infty}\mathbf{G}(\mathbf{r}-\mathbf{r}',t)\Theta_s(\mathbf{r}')d\mathbf{r}'=\int_S\mathbf{G}(\mathbf{r}-\mathbf{r}',t)d\mathbf{r}' \tag{4.201}$$

where S denotes the surface of the inclusion under consideration. Similar to the character of the operator T in Eq (4.192), the dynamic potential can also be decomposed as

$$\hat{\mathbf{G}}(\mathbf{r},t)=\begin{bmatrix}\hat{\mathbf{G}}_I(\mathbf{r},t) & 0\\ 0 & \hat{\mathbf{G}}_{II}(\mathbf{r},t)\end{bmatrix} \tag{4.202}$$

where $\hat{\mathbf{G}}_I(\mathbf{r},t)$ and $\hat{\mathbf{G}}_{II}(\mathbf{r},t)$ satisfy, respectively[14]

$$\begin{aligned} T_I(\nabla,\frac{\partial}{\partial t})\hat{\mathbf{G}}_I(\mathbf{r},t)+\mathbf{I}_2\Theta_s(\mathbf{r})\delta(t)=0,\\ T_{II}(\nabla,\frac{\partial}{\partial t})\hat{\mathbf{G}}_{II}(\mathbf{r},t)+\mathbf{I}_3\Theta_s(\mathbf{r})\delta(t)=0 \end{aligned} \tag{4.203}$$

As presented in [14,17], $\hat{\mathbf{G}}_I(\mathbf{r},t)$ is written in matrix form as

$$\hat{\mathbf{G}}_I(\mathbf{r},t)=\frac{1}{\rho}\begin{bmatrix}\dfrac{\partial^2}{\partial x^2} & \dfrac{\partial^2}{\partial x\partial y}\\ \dfrac{\partial^2}{\partial x\partial y} & \dfrac{\partial^2}{\partial y^2}\end{bmatrix}(\hat{h}_1-\hat{h}_2)+\frac{1}{c_{66}}\mathbf{I}_2\hat{g}_2 \tag{4.204}$$

where functions $\hat{h}_1$, $\hat{h}_2$ and $\hat{g}_2$ are determined by the equations [14]

$$\left(\nabla_2-\frac{1}{c_i^2}\frac{\partial^2}{\partial t^2}\right)\hat{g}_i+\Theta_s(\mathbf{r})\delta(t)=0 \qquad (i=1,2) \tag{4.205}$$

$$\left(\nabla_2-\frac{1}{c_i^2}\frac{\partial^2}{\partial t^2}\right)\frac{\partial^2}{\partial t^2}\hat{h}_i+\Theta_s(\mathbf{r})\delta(t)=0 \qquad (i=1,2) \tag{4.206}$$

where

$$\hat{g}_i=\frac{\partial^2\hat{h}_i}{\partial t^2} \quad (i=1,2) \tag{4.207}$$

$$c_1=\sqrt{\frac{c_{11}}{\rho}}, \quad c_1=\sqrt{\frac{c_{66}}{\rho}}, \quad c_{66}=\frac{c_{11}-c_{12}}{2} \tag{4.208}$$

The solution of the second equation of Eq (4.203) can be obtained by taking inverse of the operator matrix [14]

$$\hat{\mathbf{G}}_{II}(\mathbf{r},t)=T_{II}^*(\nabla,\frac{\partial}{\partial t})\hat{g}_{II}(\mathbf{r},t)\mathbf{I}_3 \tag{4.209}$$

where $T_{II}^*(\nabla,\frac{\partial}{\partial t})$ is the adjoint matrix of $T_{II}(\nabla,\frac{\partial}{\partial t})$ and $\hat{g}_{II}(\mathbf{r},t)$ satisfies

$$Q_{II}(\nabla,\frac{\partial}{\partial t})\hat{g}_{II}(\mathbf{r},t)+\Theta_s(\mathbf{r})\delta(t)=0 \tag{4.210}$$

in which $Q_{II}(\nabla,\frac{\partial}{\partial t})$ is the determinant of $T_{II}(\nabla,\frac{\partial}{\partial t})$:

$$Q_{II}(\nabla,\frac{\partial}{\partial t})=\det\left[T_{II}(\nabla,\frac{\partial}{\partial t})\right]=(\kappa_{11}\mu_{11}-\alpha_{11}^2)\hat{c}_{44}\left(\nabla_2-\frac{1}{c_3^2}\frac{\partial^2}{\partial t^2}\right)\nabla_2^2 \tag{4.211}$$

$$\hat{c}_{44} = c_{44} + \frac{\tilde{e}_{15}^2 \kappa_{11} + e_{15}^2 \mu_{11} - 2e_{15}\tilde{e}_{15}\alpha_{11}}{\kappa_{11}\mu_{11} - \alpha_{11}^2} \tag{4.212}$$

$$c_3 = \sqrt{\frac{\hat{c}_{44}}{\rho}} \tag{4.213}$$

Using two new functions defined by [14]

$$\begin{aligned} \hat{g}_3 &= (\kappa_{11}\mu_{11} - \alpha_{11}^2)\hat{c}_{44}\nabla_2^2 \hat{g}_{II} \\ \hat{g}_s &= (\kappa_{11}\mu_{11} - \alpha_{11}^2)\hat{c}_{44}\left(\nabla_2 - \frac{1}{c_3^2}\frac{\partial^2}{\partial t^2}\right)\nabla_2 \hat{g}_{II} \end{aligned} \tag{4.214}$$

two new equations can be induced from Eq (4.210) as

$$\begin{aligned} &\left(\nabla_2 - \frac{1}{c_3^2}\frac{\partial^2}{\partial t^2}\right)\hat{g}_3 + \Theta_s(\mathbf{r})\delta(t) = 0 \\ &\nabla_2 \hat{g}_s + \Theta_s(\mathbf{r})\delta(t) = 0 \end{aligned} \tag{4.215}$$

Considering the character of Eq $(4.215)_2$, it is reasonable to assume that $\hat{g}_s = \hat{g}_4(\mathbf{r})\delta(t)$. Thus we have

$$\nabla_2 \hat{g}_4 + \Theta_s(\mathbf{r}) = 0 \tag{4.216}$$

Substituting the expression of $T_{II}^*(\nabla, \frac{\partial}{\partial t})$ into Eq (4.209) and making use of Eq (4.214), the dynamic potential $\hat{\mathbf{G}}_{II}(\mathbf{r},t)$ becomes

$$\begin{aligned} \hat{\mathbf{G}}_{II}(\mathbf{r},t) = &\begin{bmatrix} a_* & b_* & c_* \\ b_* & 0 & 0 \\ c_* & 0 & 0 \end{bmatrix} \frac{\hat{g}_3(\mathbf{r},t)}{a_* \hat{c}_{44}} \\ &- \frac{1}{a_*}\begin{bmatrix} 0 & 0 & 0 \\ 0 & 1 & 0 \\ 0 & 0 & 0 \end{bmatrix}\left\{\mu_{11}\hat{g}_4(\mathbf{r})\delta(t) + \frac{\hat{g}_3(\mathbf{r},t)}{\hat{c}_{44}}[\tilde{e}_{15}^2 - \mu_{11}(\hat{c}_{44} - c_{44})]\right\} \\ &+ \frac{1}{a_*}\begin{bmatrix} 0 & 0 & 0 \\ 0 & 0 & 1 \\ 0 & 1 & 0 \end{bmatrix}\left\{\alpha_{11}\hat{g}_4(\mathbf{r})\delta(t) + \frac{\hat{g}_3(\mathbf{r},t)}{\hat{c}_{44}}[e_{15}\tilde{e}_{15} - \alpha_{11}(\hat{c}_{44} - c_{44})]\right\} \\ &- \frac{1}{a_*}\begin{bmatrix} 0 & 0 & 0 \\ 0 & 0 & 0 \\ 0 & 0 & 1 \end{bmatrix}\left\{\kappa_{11}\hat{g}_4(\mathbf{r})\delta(t) + \frac{\hat{g}_3(\mathbf{r},t)}{\hat{c}_{44}}[e_{15}^2 - \kappa_{11}(\hat{c}_{44} - c_{44})]\right\} \end{aligned} \tag{4.217}$$

where

$$a_* = \kappa_{11}\mu_{11} - \alpha_{11}^2, \quad b_* = e_{15}\mu_{11} - \tilde{e}_{15}\alpha_{11}, \quad c_* = \tilde{e}_{15}\kappa_{11} - e_{15}\alpha_{11} \tag{4.218}$$

4.9.2 Green's functions

Based on the discussion above, the dynamic Green's function $\mathbf{G}(\mathbf{r},t)$ is governed by the functions g_i (i=1,2,3,4) and h_i (i=1,2) which are similar to the functions $\hat{g}_i$ (i=1,2,3,4) and $\hat{h}_i$ (i=1,2). The functions g_i (i=1,2,3,4) and h_i (i=1,2) are, in this case, determined by replacing $\Theta_s(\mathbf{r})$ by $\delta(\mathbf{r})$:

$$\left(\nabla_2 - \frac{1}{c_i^2}\frac{\partial^2}{\partial t^2}\right) g_i + \delta(\mathbf{r})\delta(t) = 0 \quad (i=1,2,3) \tag{4.219}$$

$$\left(\nabla_2 - \frac{1}{c_i^2}\frac{\partial^2}{\partial t^2}\right)\frac{\partial^2}{\partial t^2} h_i + \delta(\mathbf{r})\delta(t) = 0 \quad (i=1,2) \tag{4.220}$$

$$\nabla_2 g_4 + \delta(\mathbf{r}) = 0 \tag{4.221}$$

Eq (4.221) is the Laplace equation and its fundamental solution can be found in many text books as

$$g_4(r) = -\frac{1}{2\pi}\ln r \tag{4.222}$$

where $r = (x^2 + y^2)^{1/2}$.

The functions $g_i(\mathbf{r},t)$ and $h_i(\mathbf{r},t)$ have been presented in [18] as

$$g_i(r,t) = \frac{1}{2\pi}\frac{H(t - r/c_i)}{\sqrt{t^2 + r^2/c_i^2}}, \quad (i=1,2,3) \tag{4.223}$$

$$h_i(r,t) = \frac{H(t - r/c_i)}{2\pi}\left[t\ln\left(\frac{ct}{r} + \sqrt{\frac{c^2t^2}{r^2} - 1}\right) - \sqrt{t^2 - \frac{r^2}{c^2}}\right], \quad (i=1,2) \tag{4.224}$$

where $H(x)$ is the Heaviside step function defined by

$$H(x) = \begin{cases} 1 & \text{if } x > 0 \\ 0 & \text{if } x < 0 \end{cases} \tag{4.225}$$

Similar to Eqs (4.204) and (4.217), the corresponding expressions of dynamic Green's function are given by

$$\mathbf{G}_1(\mathbf{r},t) = \frac{1}{\rho}\begin{bmatrix} \dfrac{\partial^2}{\partial x^2} & \dfrac{\partial^2}{\partial x \partial y} \\ \dfrac{\partial^2}{\partial x \partial y} & \dfrac{\partial^2}{\partial y^2} \end{bmatrix}(h_1 - h_2) + \frac{1}{c_{66}}\mathbf{I}_2 g_2 \tag{4.226}$$

$$\begin{aligned}\mathbf{G}_{II}(\mathbf{r},t)=&\begin{bmatrix}a_* & b_* & c_*\\ b_* & 0 & 0\\ c_* & 0 & 0\end{bmatrix}\frac{g_3(\mathbf{r},t)}{a_*\hat{c}_{44}}\\ &-\frac{1}{a_*}\begin{bmatrix}0&0&0\\0&1&0\\0&0&0\end{bmatrix}\left\{\mu_{11}g_4(\mathbf{r})\delta(t)+\frac{g_3(\mathbf{r},t)}{\hat{c}_{44}}[\tilde{e}_{15}^2-\mu_{11}(\hat{c}_{44}-c_{44})]\right\}\\ &+\frac{1}{a_*}\begin{bmatrix}0&0&0\\0&0&1\\0&1&0\end{bmatrix}\left\{\alpha_{11}g_4(\mathbf{r})\delta(t)+\frac{g_3(\mathbf{r},t)}{\hat{c}_{44}}[e_{15}\tilde{e}_{15}-\alpha_{11}(\hat{c}_{44}-c_{44})]\right\}\\ &-\frac{1}{a_*}\begin{bmatrix}0&0&0\\0&0&0\\0&0&1\end{bmatrix}\left\{\kappa_{11}g_4(\mathbf{r})\delta(t)+\frac{g_3(\mathbf{r},t)}{\hat{c}_{44}}[e_{15}^2-\kappa_{11}(\hat{c}_{44}-c_{44})]\right\}\end{aligned} \tag{4.227}$$

By means of the Fourier transform, expressions of g_i (i=1,2,3,4) and h_i (i=1,2) in the space-frequency domain can also be obtained [14,17], namely

$$g_j(r,\omega+i\xi)=\frac{1}{4}iH_0^{(1)}(\frac{\omega+i\xi}{c_j}r), \qquad (j=1,2,3) \tag{4.228}$$

$$h_j(r,\omega+i\xi)=-\frac{1}{4(\omega+i\xi)^2}H_0^{(1)}(\frac{\omega+i\xi}{c_j}r), \qquad (j=1,2) \tag{4.229}$$

where $i=\sqrt{-1}$ and the infinitesimal damping constant $\xi\to 0^+$ is introduced in order to guarantee the causality of the derived Green's function [18] and $H_0^{(1)}(\cdot)$ is the Hankel function of the first kind.

On the basis of the expressions of $g_j(r,\omega+i\xi)$ and $h_j(r,\omega+i\xi)$, the dynamic Green's functions in the space-frequency domain can be obtained as

$$\mathbf{G}_I(\mathbf{r},t)=\frac{i}{\rho\omega^2}\begin{bmatrix}\dfrac{\partial^2}{\partial x^2} & \dfrac{\partial^2}{\partial x\partial y}\\ \dfrac{\partial^2}{\partial x\partial y} & \dfrac{\partial^2}{\partial y^2}\end{bmatrix}\{H_0^{(1)}(k_2r)-H_0^{(1)}(k_1r)\}+k_2^2\mathbf{I}_2H_0^{(1)}(k_2r) \tag{4.230}$$

$$\begin{aligned}\mathbf{G}_{II}(\mathbf{r},t)=&\begin{bmatrix}a_* & b_* & c_*\\ b_* & 0 & 0\\ c_* & 0 & 0\end{bmatrix}\frac{ik_3^2H_0^{(1)}(k_3r)}{4a_*\rho\omega^2}\\ &-\frac{1}{a_*}\begin{bmatrix}0&0&0\\0&1&0\\0&0&0\end{bmatrix}\left\{-\frac{\mu_{11}}{2\pi}\ln r+\frac{ik_3^2H_0^{(1)}(k_3r)}{4\rho\omega^2}[\tilde{e}_{15}^2-\mu_{11}(\hat{c}_{44}-c_{44})]\right\}\\ &+\frac{1}{a_*}\begin{bmatrix}0&0&0\\0&0&1\\0&1&0\end{bmatrix}\left\{-\frac{\alpha_{11}}{2\pi}\ln r+\frac{ik_3^2H_0^{(1)}(k_3r)}{4\rho\omega^2}[e_{15}\tilde{e}_{15}-\alpha_{11}(\hat{c}_{44}-c_{44})]\right\}\\ &-\frac{1}{a_*}\begin{bmatrix}0&0&0\\0&0&0\\0&0&1\end{bmatrix}\left\{-\frac{\kappa_{11}}{2\pi}\ln r+\frac{ik_3^2H_0^{(1)}(k_3r)}{4\rho\omega^2}[e_{15}^2-\kappa_{11}(\hat{c}_{44}-c_{44})]\right\}\end{aligned}\tag{4.231}$$

where $k_j=\omega/c_j+i\xi$ (j=1,2,3) and the result when $\xi\to 0^+$ has been used, which is omitted in the derivation process.

It is easy to prove that the dynamic functions $\mathbf{G}_I(\mathbf{r},\omega)$ and $\mathbf{G}_{II}(\mathbf{r},\omega)$ defined in Eqs (4.230) and (4.231) fulfil

$$\begin{aligned}&T_I(\nabla,\omega)\mathbf{G}_I(\mathbf{r},\omega)+\mathbf{I}_2\delta(\mathbf{r})=0,\\ &T_{II}(\nabla,\omega)\mathbf{G}_{II}(\mathbf{r},\omega)+\mathbf{I}_3\delta(\mathbf{r})=0\end{aligned}\tag{4.232}$$

References

[1] Pan E, Three dimensional Green's functions in anisotropic magnetoelectroelastic bimaterials. Z Angew Math Phys, 53, 815-838, 2002

[2] Soh AK, Liu JX, Hoon KH. Three-dimensional Green's functions for transversely isotropic magnetoelectroelastic solids. Int J Non Sci Num Simulation, 4, 139-148, 2003

[3] Huang JH, Chiu YH, Liu HK. Magneto-electro-elastic Eshelby tensors for a piezoelectric-piezomagnetic composite reinforced by ellipsoidal inclusions. J Appl Phys, 83, 5364-5370, 1998

[4] Liu J, Liu X, Zhao Y. Green's functions for anisotropic magnetoelectroelastic solids with an elliptical cavity or a crack. Int J Eng Sci, 39, 1405-1418, 2001

[5] Li JY, Magnetoelectric Green's functions and their application to the inclusion and inhomogeneity problems, Int J Solids Struct, 39, 4201-4213, 2002

[6] Wang X and Shen YP, The general solution of three-dimensional problems in magnetoelectroelastic media, Int J Eng Sci, 40, 1069-1080,2002

[7] Ding HJ, Jiang A, Hou PF and Chen WQ, Green's function for two-phase transversely isotropic magnetoelectroelastic media, Eng Ana Boun Elements, 29, 551-561, 2005

[8] Hou PF, Ding HJ and Chen JY, Green's function for transversely isotropic magnetoelectroelastic media, Int J Eng Sci, 43, 826-858, 2005

[9] Alshits VI, Kirchner HOK and Ting TCT, Angularly inhomogeneous piezoelectric piezomagnetic magnetoelectric anisotropic media, Philos Mag Lett,

71, 285-288, 1995
[10] Jiang X and Pan E, Exact solution for 2D polygonal inclusion problem in anisotropic magnetoelectroelastic full-, half-, and bimaterial-planes, Int J Solids Struct, 41, 4361-4382, 2004
[11] Qin QH, Green's functions of magnetoelectroelastic solids with a half-plane boundary or bimaterial interface, Philos Mag Lett, 84, 771-779, 2004
[12] Qin QH, 2D Green's functions of defective magnetoelectroelastic solids under thermal loading, Eng Ana Boun Elements, 29, 577-585, 2005
[13] Qin QH, Green's functions of magnetoelectroelastic solids and applications to fracture analysis, pp93-106, in Proc. of 9th Int Conf on Inspection, Appraisal, Repairs & Maintenance of Structures, Fuzhou, China on 20-21 October, 2005, Ed. Ren WX, K.C. Gary Ong and John S.Y. Tan, CI-Premier PTE LTD
[14] Chen P, Shen YP and Tian XG, Dynamic potentials and green's functions of a quasi-plane magnetoelectroelastic medium with inclusion, Int J Eng Sci, 44, 540-553, 2006
[15] Pan E and Tonon F, Three-dimensional Green's functions in anisotropic piezoelectric solids, Int J Solids Struct, 37, 943-958, 2000
[16] Seaborn JB, *Hypergeometric functions and their applications*, New York, Springer-Verlag, 1991
[17] Michelitsch TM, Levin VM and Gao HJ, Dynamic potentials and Green's functions of a quasi-plane piezoelectric medium with inclusion, Proc R Soc London A, 458, 2393-2415, 2002
[18] Levin VM, Michelitsch TM and Gao HJ, Propagation of electroacoustic waves in the transversely isotropic piezoelectric medium reinforced by randomly distributed cylindrical inhomogeneities, Int J Solids Struct, 39, 5013-5051

Chapter 5 Boundary element method for piezoelectricity

5.1 Introduction

In the previous four chapters we described Green's functions in piezoelectric and piezomagnetic materials. Applications of these Green's functions to boundary element method (BEM) are described in this and next chapter. It should be noted that application of BEM to piezoelectric materials has been the subject of fruitful scientific attention by many a distinguished researcher (e.g. Lee and Jiang [1], Lee [2], Denda and Mansukh [3], Sanz et al [4], and others). Lee and Jiang [1] derived the boundary integral equation of piezoelectric media by the method of weighted residuals for plane piezoelectricity. Lu and Mahrenholtz [5] presented a variational boundary integral equation for the same problem. Ding et al [6] developed a boundary integral formulation which is efficient for analyzing crack problems in piezoelectric material. Rajapakse [7] discussed three boundary element methods (direct boundary method, indirect boundary element method and fictitious stress-electric charge method) in coupled electroelastic problems. Xu and Rajapakse [8] and Rajapakse and Xu [9] extended the formulations in [7,8] to the case of piezoelectric solids with various defects (cavities, inclusions, cracks, etc.). Liu and Fan [10] established a boundary integral equation in a rigorous way and addressed the question of degeneration for problems of cracks and thin shell-like structures. Pan [11] derived a single domain BE formulation for 2D static crack problems. Denda and Lua [12] developed a BEM formulation using Stroh's formalism to derive the fundamental solution but did not show any numerical results. Davi and Molazo [13] used the known subdomain method to formulate a multidomain BEM, well suited for crack problems, by modeling crack faces as boundaries of the different subdomains. Groh and Kuma [14] developed a direct collocation boundary element code with a subdomain technique for analyzing crack problems and calculating stress intensity factors. Zhao et al [15] presented a boundary integral-differential model for interfacial cracks in 3D piezoelectric solids. Liew and Liang [16] presented Green's functions for transversely isotropic piezoelectric bimaterials based on the solution of Ding et al [17] for distinct eigenvalue materials and applied them to the solution of the problem of cavities in an infinite domain. Sanz et al [4] presented a general BEM for 3D fracture problems in piezoelectric materials. Khutoryaansky et al [18] introduced a BE formulation for time-dependent problems of linear piezoelectricity. Time-dependent BEM for piezoelectricity was also discussed in [19,20]. Recently, Ding and Jiang [21] extended the BEM approach to 2D problems in magnetoelectroelastic media. In addition, for the application of BEM in piezoelectric materials, the work presented in [22-29] should also be mentioned.

5.2 Boundary integral equation

5.2.1 Governing equations

In this section, the theory of piezoelectricity presented in Chapter 1 is briefly summarized for deriving the corresponding boundary integral equation. Under the condition of a static deformation, the governing equations for a linear and generally anisotropic piezoelectric solid consist of [11]

(i) Equilibrium equations

$$\sigma_{ij,j} + b_i = 0, \quad D_{i,i} + b_e = 0 \tag{5.1}$$

(ii) Constitutive relations

$$\sigma_{ij} = c_{ijkl}\varepsilon_{kl} - e_{mij}E_m, \quad D_k = e_{kij}\varepsilon_{ij} + \kappa_{mk}E_m \tag{5.2}$$

(iii) Elastic strain-displacement and electric field-potential relations

$$\varepsilon_{ij} = \frac{1}{2}(u_{i,j} + u_{j,i}), \quad E_i = -\phi_{,i} \tag{5.3}$$

(iv) Boundary conditions

$$\left.\begin{array}{ll} u_i = \bar{u}_i & \text{on } \Gamma_u \\ t_i = \sigma_{ij}n_j = \bar{t}_i & \text{on } \Gamma_t \end{array}\right\}, \quad \left.\begin{array}{ll} \phi = \bar{\phi} & \text{on } \Gamma_\phi \\ D_n = D_i n_i = -\bar{q}_s & \text{on } \Gamma_D \end{array}\right\} \tag{5.4}$$

5.2.2 Boundary integral equation for piezoelectricity

Several approaches have been used in the literature to establish boundary integral equations of piezoelectric materials, such as the variational approach [5], weighted residual approach [1,2,19,30], and Betti's reciprocity theorem [11,14,18,20,22,31,32]. A brief discussion of the above three approaches which have been widely used in BE analysis is given here.

(1) Variational method. The generalized variational principle below is due to Lu and Mahrenholtz [5] and is applicable to any boundary value problems of piezoelectric materials. It is based on a modified functional with six kinds of independent variable, i.e. displacements and electric potential in the domain, and displacements, tractions, electric potential and surface charge on the boundary. Since all the boundary conditions considered have been introduced into the framework of the modified variational expression, no additional constraints have to be satisfied when assuming the variables on the boundary. The functional used for deriving boundary integral equation is of the form

$$\begin{aligned} \Pi(\mathbf{u},\phi,\tilde{\mathbf{u}},\tilde{\mathbf{t}},\tilde{\phi},\tilde{q}_s) = & \int_\Omega [\frac{1}{2}c_{ijkl}u_{i,j}u_{k,l} - \frac{1}{2}\kappa_{ij}\phi_{,i}\phi_{,j} + e_{ikl}\phi_{,i}u_{k,l} - b_i u_i - b_e\phi]d\Omega \\ & - \int_\Gamma [\tilde{t}_i(u_i - \tilde{u}_i) - \tilde{q}_s(\phi - \tilde{\phi})]d\Gamma - \int_{\Gamma_t} \bar{t}_i\tilde{u}_i d\Gamma + \int_{\Gamma_D} \bar{q}_s\tilde{\phi}d\Gamma \\ & - \int_{\Gamma_u} \tilde{t}_i(\tilde{u}_i - \bar{u}_i)d\Gamma + \int_{\Gamma_\phi} \tilde{q}_s(\tilde{\phi} - \bar{\phi})d\Gamma, \end{aligned} \tag{5.5}$$

in which the variables assumed to be independent are:

(a) displacement field, $\mathbf{u}$, with components u_i;
(b) electric potential in the domain, ϕ;
(c) boundary displacement field, $\tilde{\mathbf{u}}$, with components, $\tilde{u}_i$;
(d) boundary traction, $\tilde{\mathbf{t}}$, with components, $\tilde{t}_i$;
(e) boundary electric potential, $\tilde{\phi}$;
(f) boundary surface charge, $\tilde{q}_s$.

Lu and Mahrenholtz [5] showed that the stationary condition of the functional (5.5) leads to Eqs (5.1), (5.4), and

$$u_i = \tilde{u}_i, \quad \phi = \tilde{\phi}, \quad t_j = \tilde{t}_j, \quad D_n = -\tilde{q}_s \quad \text{on } \Gamma \tag{5.6}$$

The proof can be made by taking variations with respect to the independent variables as

$$\begin{aligned}\delta\Pi(\mathbf{u},\phi,\tilde{\mathbf{u}},\tilde{\mathbf{t}},\tilde{\phi},\tilde{q}_s) = &-\int_\Omega[(\sigma_{ij,j}+b_i)\delta u_i+(D_{i,i}+b_e)\delta\phi]d\Omega\\ &+\int_\Gamma[(t_i-\tilde{t}_i)\delta u_i+(D_n+\tilde{q}_s)\delta\phi+(\phi-\tilde{\phi})\delta\tilde{q}_s-(u_i-\tilde{u}_i)\delta\tilde{t}_j]d\Gamma\\ &+\int_{\Gamma_t}(\tilde{t}_i-\bar{t}_i)\delta\tilde{u}_i d\Gamma-\int_{\Gamma_D}(\tilde{q}_s-\bar{q}_s)\delta\tilde{\phi}d\Gamma\\ &-\int_{\Gamma_u}(\tilde{u}_i-\bar{u}_i)\delta\tilde{t}_i d\Gamma+\int_{\Gamma_\phi}(\tilde{\phi}-\bar{\phi})\delta\tilde{q}_s d\Gamma=0\end{aligned} \tag{5.7}$$

Therefore, the Eular equations for expression (5.7) are Eqs (5.1), (5.4), and (5.6), as the quantities δu_i, $\delta\phi$, $\delta\tilde{u}_i$, $\delta\tilde{\phi}$, $\delta\tilde{t}_i$, and $\delta\tilde{q}_s$ may be arbitrary. This indicates that the boundary conditions (5.4) and (5.6) have been included in the framework of the variational formulation (5.5). The independent boundary variables $\tilde{u}_i$, $\tilde{\phi}$, $\tilde{t}_i$, and $\tilde{q}_s$ in Eq (5.5) are, in this case, not required to satisfy the boundary conditions (5.6). Therefore, the continuity requirements of the boundary variables are relaxed in the variational expression (5.5) which may be convenient for interpolating boundary variables. To convert the variational expression (5.5) into a boundary expression, the first integration in Eq (5.5) is transformed into a boundary integral. This can be done by integrating by parts and making use of relations (5.2) and (5.3). Then Eq (5.5) can be rewritten as

$$\begin{aligned}\Pi(\mathbf{u},\phi,\tilde{\mathbf{u}},\tilde{\mathbf{t}},\tilde{\phi},\tilde{q}_s) = &\int_\Omega[-\frac{1}{2}\sigma_{ij,j}u_i-\frac{1}{2}D_{i,i}\phi-b_i u_i-b_e\phi]d\Omega\\ &\frac{1}{2}\int_\Gamma[(t_i-2\tilde{t}_i)u_i+(D_n+2\tilde{q}_s)\phi]d\Gamma-\int_{\Gamma_t}\bar{t}_i\tilde{u}_i d\Gamma+\int_{\Gamma_D}\bar{q}_s\tilde{\phi}d\Gamma\\ &+\int_{\Gamma_u}\tilde{t}_i\bar{u}_i d\Gamma-\int_{\Gamma_\phi}\tilde{q}_s\bar{\phi}d\Gamma+\int_{\Gamma-\Gamma_u}\tilde{t}_i\tilde{u}_i d\Gamma-\int_{\Gamma-\Gamma_\phi}\tilde{q}_s\tilde{\phi}d\Gamma,\end{aligned} \tag{5.8}$$

The functional (5.8) can be taken as the basis for the deriving BE formulation.

(2) Weighted residual method. The method of weighted residuals can also be used to establish the boundary integral equations presented above. As indicated in [1,2], the electroelastic weighted residual statement for the boundary value problem (5.1) and (5.4) may be expressed as

$$\int_\Omega(\sigma_{ij,i}+b_j)u_i^* d\Omega=\int_{\Gamma_t}(t_i-\bar{t}_i)u_i^* d\Gamma+\int_{\Gamma_u}(\bar{u}_i-u_i)t_i^* d\Gamma \tag{5.9}$$

where u_i^* and $t_i^*=\sigma_{ij}^* n_j$ are the displacement and traction respectively corresponding to the weighted field. By carrying out integration by parts and using the constitutive equation (5.2) and noting that $-q_s^*=D_i^* n_i$, Eq (5.9) can be written as [1]

$$\begin{aligned}\int_\Omega(\sigma_{ij,j}^* u_i+D_{i,i}^*\phi+b_i u_i^*+b_e\phi^*)d\Omega=&\int_{\Gamma_t}(t_i^* u_i-\bar{t}_i u_i^*)d\Gamma+\int_{\Gamma_u}(\bar{u}_i t_i^*-u_i^* t_i)d\Gamma\\ &+\int_{\Gamma_\phi}(q_s^*\bar{\phi}-\phi^* q_s)d\Gamma-\int_{\Gamma_D}(\bar{q}_s\phi^*-q_s^*\phi)d\Gamma\end{aligned} \tag{5.10}$$

Lee and Jiang [1] mentioned that Eq (5.10) can also obtained by choosing Eqs $(5.1)_2$ and $(5.4)_2$ instead of Eqs $(5.1)_1$ and $(5.4)_1$ in the weighted residual statement (5.9).

To convert Eq (5.10) into a boundary integral equation, choose the weighted functions such that they satisfy Eq (5.1), i.e.,

$$\sigma_{ij,j}^*+\delta(\mathbf{x}-\hat{\mathbf{x}})e_i=0,\qquad D_{i,i}^*+\delta(\mathbf{x}-\hat{\mathbf{x}})=0 \tag{5.11}$$

where e_i is the unit vector in x_i-direction. Then, the first two terms of the first integral in Eq (5.10) reduce to

$$\int_\Omega \sigma^*_{ij,j} u_i d\Omega = -u_i(\bar{\mathbf{x}})e_i, \qquad \int_\Omega D^*_{j,j}\phi d\Omega = -\phi(\bar{\mathbf{x}}) \tag{5.12}$$

Further, if the point force in each direction and the point charge are taken as independent of each other, the weighting functions can be written in the following form

$$u^*_j = u^*_{ij}(\mathbf{x}-\bar{\mathbf{x}})e_i,\ t^*_j = t^*_{ij}(\mathbf{x}-\bar{\mathbf{x}})e_i,\ \phi^* = \phi^*_i(\mathbf{x}-\bar{\mathbf{x}})e_i,\ q^*_s = q^*_{si}(\mathbf{x}-\bar{\mathbf{x}})e_i \tag{5.13}$$

After some mathematical manipulation [1,2], the boundary integral equation for the three displacement components and for the electric potential can be obtained as follows

$$\begin{aligned} u_I(\bar{\mathbf{x}}) &+ \int_\Gamma (t^*_{ij}(\mathbf{x},\bar{\mathbf{x}})u_j(\mathbf{x})d\Gamma(\mathbf{x}) - \int_\Gamma q^*_{si}(\mathbf{x},\bar{\mathbf{x}})\phi(\mathbf{x})d\Gamma(\mathbf{x}) \\ &= \int_\Omega u^*_{ij}(\mathbf{x},\bar{\mathbf{x}})b_j(\mathbf{x})d\Omega\ (\mathbf{x}) + \int_\Omega \phi^*_i(\mathbf{x},\bar{\mathbf{x}})b_e(\mathbf{x})d\Omega\ (\mathbf{x}) \\ &+ \int_\Gamma u^*_{ij}(\mathbf{x},\bar{\mathbf{x}})t_j(\mathbf{x})d\Gamma(\mathbf{x}) - \int_\Gamma \phi^*_i(\mathbf{x},\bar{\mathbf{x}})q_s(\mathbf{x})d\Gamma(\mathbf{x}) \end{aligned} \tag{5.14}$$

where $\mathbf{u} = \{u_I\} = \{u_1,\ u_2,\ u_3,\ -\phi\}$. Eq (5.14) is the piezoelectric analogue of Somigliana's identity and gives values of the displacement and electric potential at any internal point in terms of the boundary field values, the body forces and charge, and the fundamental solution. Note that if $\bar{\mathbf{x}}$ is taken to the boundary, the integrals have a singularity which needs to be taken into account. For example, if $\bar{\mathbf{x}}$ lies on a smooth boundary, $u_I(\bar{\mathbf{x}})$ is replaced by $u_I(\bar{\mathbf{x}})/2$.

The boundary integral equation (5.14) applies for static elastoelastic problems only. To solve time-dependent thermo-piezoelectric problems, a boundary integral equation developed in [19] is presented below. Note that for time-dependent thermo-piezoelectric problems, Eqs (2.375) and (5.1)-(5-4) are both space- and time-dependent. To eliminate the time variable in these equations, applying the Laplace transform [33] with respect to time to Eqs (2.375) and (5.1) leads to

$$\breve{\sigma}_{ij,j} + \breve{b}_i = 0 \tag{5.15}$$

$$\breve{D}_{i,i} + \breve{b}_e = 0 \tag{5.16}$$

$$\breve{h}_{i,i} + T_0\beta\breve{s} + \breve{b}_t = 0 \tag{5.17}$$

where the symbol $(\breve{})$ over a variable indicates that the variable is expressed in the transform domain, β is the Laplace transformed variable, and s(0) is assumed to be zero without loss of generality. In the transformed domain, the electroelastic weighted residual statement for the boundary value problem (5.15) and (5.16) may be expressed as [19]

$$\int_\Omega (\breve{\sigma}_{ij,j} + \breve{b}_i)\breve{u}^*_i d\Omega = 0 \tag{5.18}$$

where $\breve{u}^*_i$ is the displacement in the transformed domain corresponding to the weighting field. By using integration by parts, divergence theorem and constitutive equations, the following expression can be obtained

$$\int_\Omega (\breve{\sigma}^*_{ij,j}\breve{u}_i + \breve{D}^*_{i,i}\breve{\phi} + \breve{b}_i\breve{u}^*_i + \breve{b}_e\breve{\phi}^*)d\Omega + \int_\Gamma (\breve{u}^*_i\breve{t}_i - \breve{t}^*_i\breve{u}_i - \breve{\phi}^*\breve{q}_s + \breve{\phi}\breve{q}^*_s)d\Gamma + \int_\Omega (\chi_m\breve{E}^*_m\breve{T} - \chi_m\breve{E}_m\breve{T}^* + \lambda_{ij}\breve{\varepsilon}^*_{ij}\breve{T} - \lambda_{ij}\breve{\varepsilon}_{ij}\breve{T}^*)d\Omega = 0 \tag{5.19}$$

In order to eliminate the last two volume integrals as required in the boundary integral equation, apply the weighting function field and actual field to the linear heat conduction equation such that

$$k_{ij}\breve{T}_{,ij} - T_0\beta\breve{s} - \breve{b}_t = 0 \tag{5.20}$$

$$k_{ij}\breve{T}^*_{,ij} - T_0\beta\breve{s}^* - \breve{b}^*_t = 0 \tag{5.21}$$

Then, making use of Eqs (5.20) and (5.21), and after somewhat lengthy mathematical manipulation, the following expression is obtained [19]

$$\int_\Omega (\chi_m\breve{E}^*_m\breve{T} - \chi_m\breve{E}_m\breve{T}^* + \lambda_{ij}\breve{\varepsilon}^*_{ij}\breve{T} - \lambda_{ij}\breve{\varepsilon}_{ij}\breve{T}^*)d\Omega = \frac{1}{\beta T_0}\left[\int_\Omega (\breve{b}^*_t\breve{T} - \breve{b}_t\breve{T}^*)d\Omega - \int_\Gamma (\breve{q}^*_n\breve{T} - \breve{q}_n\breve{T}^*)d\Gamma\right] \tag{5.22}$$

where $\breve{q}_n = -k_{ij}T_{,j}n_i$.

Substituting Eq (5.22) into Eq (5.19) and applying the inverse Laplace transform to Eq(5.19), yields [19]

$$\int_\Omega (\dot{\sigma}^*_{ij,j} \times u_i + \dot{D}^*_{i,i} \times \breve{\phi} + b_i \times \dot{u}^*_i + b_e \times \dot{\phi}^*)d\Omega + \frac{1}{T_0}\int_\Omega (b^*_t \times T - b_t \times T^* - q^*_n \times T - q_n \times T^*)d\Omega + \int_\Gamma (q^*_s \times \phi + q_s \times \phi^* - t_i \times u^*_i - t^*_i \times u_i)d\Gamma = 0 \tag{5.23}$$

in which the notation of the convolution integral

$$f \times g = \int_0^t f(t-\tau)g(\tau)d(\tau) \tag{5.24}$$

and the property of the inverse Laplace transform

$$L^{-1}(\beta\breve{f}) = \dot{f}\,, \quad (L^{-1}(\breve{f}) = f) \tag{5.25}$$

have been used.

To make the first three volume integrals vanish, Jiang [19] considered the weighting field as an infinite thermo-piezoelectric body subjected to unit forces, electric charge, and pulse heat source equal to the following three states separately:

$$(1)\ b^*_i = \delta(\mathbf{x} - \hat{\mathbf{x}})H(t)\delta_{ij}e_j, \quad b^*_e = b^*_t = 0 \tag{5.26}$$

$$(2)\ b^*_e = \delta(\mathbf{x} - \hat{\mathbf{x}})H(t), \quad b^*_i = b^*_t = 0 \tag{5.27}$$

$$(3)\ b^*_t = \delta(\mathbf{x} - \hat{\mathbf{x}})\delta(t), \quad b^*_i = b^*_e = 0 \tag{5.28}$$

Jiang [19] also mentioned that the heat source with respect to time *t* is subjected to the Dirac delta function while the other two loads are subjected to the step function of time. This is purely a mathematical consideration and can be easily explained by noting that b^*_t in the integral does not involve the time derivative while both

$\dot{\sigma}^*_{ij,j}$ and $\dot{D}^*_{i,i}$ do. If no body forces, volume charge, and heat source are considered, the boundary integral equation (5.23) becomes

$$u_I(\hat{\mathbf{x}}) + \int_\Omega [t^*_{Ij}(\mathbf{x},\hat{\mathbf{x}}) \times u_j(\mathbf{x}) - q^*_{sI}(\mathbf{x},\hat{\mathbf{x}}) \times \phi(\mathbf{x}) + \frac{1}{T_0} q^*_{nI}(\mathbf{x},\hat{\mathbf{x}}) \times T(\mathbf{x})] d\Gamma(\mathbf{x}) \\ = \int_\Gamma [u^*_{Ij}(\mathbf{x},\hat{\mathbf{x}}) \times t_j(\mathbf{x}) - \phi^*_I(\mathbf{x},\hat{\mathbf{x}}) \times q_s(\mathbf{x}) + \frac{1}{T_0} T^*_I(\mathbf{x},\hat{\mathbf{x}}) \times q_n(\mathbf{x})] d\Gamma(\mathbf{x}) \tag{5.29}$$

where $\mathbf{u} = \{u_I\} = \{u_1,\ u_2,\ u_3,\ -\phi,\ -T/T_0\}$, u^*_{ij} represents the displacement in the *j*th direction at field point $\mathbf{x}$ due to a point force in the *i*th direction applied at the source point $\hat{\mathbf{x}}$ interior to Γ, u^*_{4i} denotes the *i*th displacement at $\mathbf{x}$ due to a point electric charge at $\hat{\mathbf{x}}$, u^*_{5i} stands for the *i*th displacement at $\mathbf{x}$ due to a pulse heat source acting at time zero at $\hat{\mathbf{x}}$, and so on.

(3) Reciprocity theorem method. In addition to the variational approach and weighted residual methods discussed above, the reciprocity theorem can also be used to establish the boundary integral equation. The presentation below is from the development in [12,18,31,32,34].

(a) reciprocity theorem in electroelastic problems [12,18]
Consider two electroelastic states, namely

State 1: $\{U^{(1)}_I\}^T = \{u^{(1)}_1,\ u^{(1)}_2,\ u^{(1)}_3,\ \phi^{(1)}\}^T$; $\{b^{(1)}_I\}^T = \{b^{(1)}_1,\ b^{(1)}_2,\ b^{(1)}_3,\ b^{(1)}_e\}^T$; (5.30)

$\{t^{(1)}_I\}^T = \{t^{(1)}_1,\ t^{(1)}_2,\ t^{(1)}_3,\ -q^{(1)}_s\}^T$.

State 2: $\{U^{(2)}_I\}^T = \{u^{(2)}_1,\ u^{(2)}_2,\ u^{(2)}_3,\ \phi^{(2)}\}^T$; $\{b^{(2)}_I\}^T = \{b^{(2)}_1,\ b^{(2)}_2,\ b^{(2)}_3,\ b^{(2)}_e\}^T$; (5.31)

$\{t^{(2)}_I\}^T = \{t^{(2)}_1,\ t^{(2)}_2,\ t^{(2)}_3,\ -q^{(2)}_s\}^T$.

The first state represents the solution to piezoelectric problems with finite domains and general loading conditions; the second state is of an artificial nature and represents the fundamental solution to the case of a fictitious infinite body subjected to a point force or a point charge. Further, introduce the compatible field $\{\tilde{\varepsilon}_{ij},\ \tilde{u}_i,\ \tilde{E}_i,\ \tilde{\phi}\}$, which satisfies Eqs (5.3). The principle of virtual work is given by

$$\int_\Omega b^{(1)}_I \tilde{U}_I d\Omega + \int_\Gamma t^{(1)}_I \tilde{U}_I d\Gamma = \int_\Omega (\sigma^{(1)}_{ij} \tilde{\varepsilon}_{ij} - D^{(1)}_i \tilde{E}_i) d\Omega \tag{5.32}$$

On the other hand, for a linear piezoelectric solid, one can show that the following reciprocal property of Betti type holds

$$\sigma^{(1)}_{ij} \varepsilon^{(2)}_{ij} - D^{(1)}_i E^{(2)}_i = \sigma^{(2)}_{ij} \varepsilon^{(1)}_{ij} - D^{(2)}_i E^{(1)}_i \tag{5.33}$$

By substituting Eq (5.33) into Eq (5.32), the following reciprocal relation can be obtained

$$\int_\Omega b^{(1)}_I U^{(2)}_I d\Omega + \int_\Gamma t^{(1)}_I U^{(2)}_I d\Gamma = \int_\Omega b^{(2)}_I U^{(1)}_I d\Omega + \int_\Gamma t^{(2)}_I U^{(1)}_I d\Gamma \tag{5.34}$$

(b) static boundary integral equation
To convert Eq (5.34) into a boundary integral equation, assume that state (1) is the actual solution for a body Ω with the boundary Γ and state (2) is the solution for a

fictitious infinite body subjected to a point force at $\hat{\mathbf{x}}$ in the x_m direction with no bulk charge distribution (i.e. $b_e^{(2)} = 0$), namely

$$b_i^{(2)}(\mathbf{x}) = \delta(\mathbf{x} - \hat{\mathbf{x}})\delta_{im}, \quad (m=1, 2, 3) \tag{5.35}$$

The displacement, electric potential, stress, and electric displacement induced by the abovementioned point force were discussed in Chapter 2. Using the solution given in Chapter 2, the variables $u_i^{(2)}$, $\phi^{(2)}$, $\sigma_{ij}^{(2)}$, and $D_i^{(2)}$ can be written in the form

$$\begin{aligned}
u_i^{(2)} &= u_{ij}^*(\mathbf{x}, \hat{\mathbf{x}})e_j, \\
\phi^{(2)} &= \phi_j^*(\mathbf{x}, \hat{\mathbf{x}})e_j = u_{4j}^*(\mathbf{x}, \hat{\mathbf{x}})e_j, \\
\sigma_{ij}^{(2)} &= \Sigma_{ijm}^*(\mathbf{x}, \hat{\mathbf{x}})e_m = [c_{ijkl}u_{km,l}^*(\mathbf{x}, \hat{\mathbf{x}}) - e_{lij}u_{4m,l}^*(\mathbf{x}, \hat{\mathbf{x}})]e_m, \\
D_i^{(2)} &= D_{im}^*(\mathbf{x}, \hat{\mathbf{x}})e_m = [e_{ikl}u_{km,l}^*(\mathbf{x}, \hat{\mathbf{x}}) + \kappa_{il}u_{4m,l}^*(\mathbf{x}, \hat{\mathbf{x}})]e_m
\end{aligned} \tag{5.36}$$

Making use of Eq (5.4), the traction and surface charge can be obtained as

$$\begin{aligned}
t_i^{(2)} &= t_{im}^*(\mathbf{x}, \hat{\mathbf{x}})e_m = \Sigma_{ijm}^*(\mathbf{x}, \hat{\mathbf{x}})n_j e_m, \\
-q_s^{(2)} &= t_{4m}^*(\mathbf{x}, \hat{\mathbf{x}})e_m = D_{im}^*(\mathbf{x}, \hat{\mathbf{x}})n_i e_m
\end{aligned} \tag{5.37}$$

Substituting all the above quantities associated with state (2) into Eq (5.34) yields

$$\begin{aligned}
u_i(\hat{\mathbf{x}}) = &\int_\Omega u_{Ji}^*(\mathbf{x}, \hat{\mathbf{x}})b_J(\mathbf{x})d\Omega(\mathbf{x}) - \int_\Gamma t_{Ji}^*(\mathbf{x}, \hat{\mathbf{x}})u_J(\mathbf{x})d\Gamma(\mathbf{x}) \\
&+ \int_\Gamma u_{Ji}^*(\mathbf{x}, \hat{\mathbf{x}})t_J(\mathbf{x})d\Gamma(\mathbf{x})
\end{aligned} \tag{5.38}$$

where i=1,2,3, J=1-4, $u_4 = -\phi$, $b_4 = b_e$, and $t_4 = -q_s$.

Next, assume that state (2) of the fictitious infinite body is subjected to a point charge at $\hat{\mathbf{x}}$ with no body force distribution, i.e.

$$b_e^{(2)}(\mathbf{x}) = \delta(\mathbf{x} - \hat{\mathbf{x}}), \quad b_i^{(2)}(\mathbf{x}) = 0 \quad (m=1, 2, 3) \tag{5.39}$$

The resulting displacement and electric potential induced by this point charge are given by

$$\begin{aligned}
u_i^{(2)} &= u_{i4}^*(\mathbf{x}, \hat{\mathbf{x}}), \\
\phi^{(2)} &= \phi_4^*(\mathbf{x}, \hat{\mathbf{x}}) = u_{44}^*(\mathbf{x}, \hat{\mathbf{x}})
\end{aligned} \tag{5.40}$$

Substituting the solution in Eq (5.40) into Eqs (5.2) and (5.4), we have

$$\begin{aligned}
\sigma_{ij}^{(2)} &= \Sigma_{ij4}^*(\mathbf{x}, \hat{\mathbf{x}}) = c_{ijkl}u_{k4,l}^*(\mathbf{x}, \hat{\mathbf{x}}) - e_{lij}u_{44,l}^*(\mathbf{x}, \hat{\mathbf{x}}), \\
D_i^{(2)} &= D_{i4}^*(\mathbf{x}, \hat{\mathbf{x}}) = e_{ikl}u_{k4,l}^*(\mathbf{x}, \hat{\mathbf{x}}) + \kappa_{il}u_{44,l}^*(\mathbf{x}, \hat{\mathbf{x}}), \\
t_i^{(2)} &= t_{i4}^*(\mathbf{x}, \hat{\mathbf{x}}) = \Sigma_{ij4}^*(\mathbf{x}, \hat{\mathbf{x}})n_j, \\
-q_s^{(2)} &= t_{44}^*(\mathbf{x}, \hat{\mathbf{x}}) = D_{i4}^*(\mathbf{x}, \hat{\mathbf{x}})n_i
\end{aligned} \tag{5.41}$$

Substituting Eqs (5.39)-(5.41) into Eq (5.34), we obtain

$$\begin{aligned}
\phi(\hat{\mathbf{x}}) = &\int_\Omega u_{J4}^*(\mathbf{x}, \hat{\mathbf{x}})b_J(\mathbf{x})d\Omega(\mathbf{x}) - \int_\Gamma t_{J4}^*(\mathbf{x}, \hat{\mathbf{x}})u_J(\mathbf{x})d\Gamma(\mathbf{x}) \\
&+ \int_\Gamma u_{J4}^*(\mathbf{x}, \hat{\mathbf{x}})t_J(\mathbf{x})d\Gamma(\mathbf{x})
\end{aligned} \tag{5.42}$$

Combining Eq (5.38) with Eq (5.42), we have

$$u_I(\hat{\mathbf{x}}) = \int_\Omega u^*_{JI}(\mathbf{x},\hat{\mathbf{x}}) b_J(\mathbf{x}) d\Omega(\mathbf{x}) - \int_\Gamma t^*_{JI}(\mathbf{x},\hat{\mathbf{x}}) u_J(\mathbf{x}) d\Gamma(\mathbf{x}) + \int_\Gamma u^*_{JI}(\mathbf{x},\hat{\mathbf{x}}) t_J(\mathbf{x}) d\Gamma(\mathbf{x}) \tag{5.43}$$

where I, J =1-4. Obviously, the outcome of Eq (5.43) is identical to that of Eq (5.14) which was obtained from the weighted residual method.

Making use of Eqs (5.2) and (5.43), the corresponding stresses and electric displacements are expressed as

$$\Pi_{iJ}(\hat{\mathbf{x}}) = \int_\Omega D^*_{KiJ}(\mathbf{x},\hat{\mathbf{x}}) b_K(\mathbf{x}) d\Omega(\mathbf{x}) - \int_\Gamma S^*_{KiJ}(\mathbf{x},\hat{\mathbf{x}}) u_K(\mathbf{x}) d\Gamma(\mathbf{x}) + \int_\Gamma D^*_{KiJ}(\mathbf{x},\hat{\mathbf{x}}) t_K(\mathbf{x}) d\Gamma(\mathbf{x}) \tag{5.44}$$

where

$$S^*_{KiJ}(\mathbf{x},\hat{\mathbf{x}}) = E_{iJMn} \frac{\partial t^*_{MK}(\mathbf{x},\hat{\mathbf{x}})}{\partial x_n}, \quad D^*_{KiJ}(\mathbf{x},\hat{\mathbf{x}}) = E_{iJMn} \frac{\partial u^*_{MK}(\mathbf{x},\hat{\mathbf{x}})}{\partial x_n} \tag{5.45}$$

The integral representation formula for the generalized traction components can be obtained from Eqs (5.4) and (5.44) as

$$t_J(\hat{\mathbf{x}}) = \int_\Omega V^*_{IJ}(\mathbf{x},\hat{\mathbf{x}}) b_I(\mathbf{x}) d\Omega(\mathbf{x}) - \int_\Gamma W^*_{IJ}(\mathbf{x},\hat{\mathbf{x}}) u_I(\mathbf{x}) d\Gamma(\mathbf{x}) + \int_\Gamma V^*_{IJ}(\mathbf{x},\hat{\mathbf{x}}) t_I(\mathbf{x}) d\Gamma(\mathbf{x}) \tag{5.46}$$

where

$$V^*_{IJ}(\mathbf{x},\hat{\mathbf{x}}) = D^*_{IkJ}(\mathbf{x},\hat{\mathbf{x}}) n_k(\hat{\mathbf{x}}), \quad W^*_{IJ}(\mathbf{x},\hat{\mathbf{x}}) = S^*_{IkJ}(\mathbf{x},\hat{\mathbf{x}}) n_k(\hat{\mathbf{x}}) \tag{5.47}$$

It can be seen from Eq (5.38), (5.42), (5.47) that to obtain the fields at internal points, the boundary data of traction, displacement, electric potential and the normal component of electric displacement need to be known throughout the boundary Γ. For this purpose, one can examine the limiting forms of Eqs (5.38), (5.42) and (5.47) as $\hat{\mathbf{x}}$ approaches the boundary. To properly circumvent the singular behaviour when $\mathbf{x}$ approaches $\hat{\mathbf{x}}$, Chen and Lin [22] assumed a singular point $\hat{\mathbf{x}}$ on the boundary surrounded by a small hemispherical surface of radius ε, say Γ_ε, centred at the point $\hat{\mathbf{x}}$ with $\varepsilon \to 0$. Since the asymptotic behaviour of Green's function in piezoelectric solids at $r = |\mathbf{x} - \hat{\mathbf{x}}| \to 0$ is mathematically similar to that of uncoupled elasticity, Eqs (5.38), (5.42), and (5.47) can be rewritten as [22]

$$c_{ki} u_k(\hat{\mathbf{x}}) = \int_\Omega u^*_{Ji}(\mathbf{x},\hat{\mathbf{x}}) b_J(\mathbf{x}) d\Omega(\mathbf{x}) - \int_\Gamma t^*_{Ji}(\mathbf{x},\hat{\mathbf{x}}) u_J(\mathbf{x}) d\Gamma(\mathbf{x}) + \int_\Gamma u^*_{Ji}(\mathbf{x},\hat{\mathbf{x}}) t_J(\mathbf{x}) d\Gamma(\mathbf{x}) \tag{5.48}$$

$$b\phi(\hat{\mathbf{x}}) = \int_\Omega u^*_{J4}(\mathbf{x},\hat{\mathbf{x}}) b_J(\mathbf{x}) d\Omega(\mathbf{x}) - \int_\Gamma t^*_{J4}(\mathbf{x},\hat{\mathbf{x}}) u_J(\mathbf{x}) d\Gamma(\mathbf{x}) + \int_\Gamma u^*_{J4}(\mathbf{x},\hat{\mathbf{x}}) t_J(\mathbf{x}) d\Gamma(\mathbf{x}) \tag{5.49}$$

$$c_{ki} t_k(\hat{\mathbf{x}}) = \int_\Omega V^*_{Ji}(\mathbf{x},\hat{\mathbf{x}}) b_J(\mathbf{x}) d\Omega(\mathbf{x}) - \int_\Gamma W^*_{Ji}(\mathbf{x},\hat{\mathbf{x}}) u_J(\mathbf{x}) d\Gamma(\mathbf{x}) + \int_\Gamma V^*_{Ji}(\mathbf{x},\hat{\mathbf{x}}) t_J(\mathbf{x}) d\Gamma(\mathbf{x}) \tag{5.50}$$

$$-bq_s(\hat{\mathbf{x}}) = \int_\Omega V_{J4}^*(\mathbf{x},\hat{\mathbf{x}})b_J(\mathbf{x})d\Omega(\mathbf{x}) - \int_\Gamma W_{J4}^*(\mathbf{x},\hat{\mathbf{x}})u_J(\mathbf{x})d\Gamma(\mathbf{x}) + \int_\Gamma V_{J4}^*(\mathbf{x},\hat{\mathbf{x}})t_J(\mathbf{x})d\Gamma(\mathbf{x}) \tag{5.51}$$

where $\hat{\mathbf{x}} \in \Gamma$, and the coefficients c_{ki} and b are defined as

$$c_{ki}(\hat{\mathbf{x}}) = \delta_{ki} + \lim_{\varepsilon\to 0}\int_{\Gamma_\varepsilon} t_{ki}^*(\mathbf{x},\hat{\mathbf{x}})d\Gamma(\mathbf{x}) \tag{5.52}$$

$$b(\hat{\mathbf{x}}) = 1 + \lim_{\varepsilon\to 0}\int_{\Gamma_\varepsilon} t_{44}^*(\mathbf{x},\hat{\mathbf{x}})d\Gamma(\mathbf{x}) \tag{5.53}$$

In the field of BEM, the coefficients c_{ki} and b are usually known as boundary shape coefficients, $c_{ii}(\hat{\mathbf{x}}) = b(\hat{\mathbf{x}}) = 1$ if $\hat{\mathbf{x}} \in \Omega$, $c_{ii}(\hat{\mathbf{x}}) = b(\hat{\mathbf{x}}) = 1/2$ if $\hat{\mathbf{x}}$ is on the smooth boundary [29]. Using the concept of boundary shape coefficients, Eq (5.43) can be rewritten as

$$c_{KI}u_K(\hat{\mathbf{x}}) = \int_\Omega u_{JI}^*(\mathbf{x},\hat{\mathbf{x}})b_J(\mathbf{x})d\Omega(\mathbf{x}) - \int_\Gamma t_{JI}^*(\mathbf{x},\hat{\mathbf{x}})u_J(\mathbf{x})d\Gamma(\mathbf{x}) + \int_\Gamma u_{JI}^*(\mathbf{x},\hat{\mathbf{x}})t_J(\mathbf{x})d\Gamma(\mathbf{x}) \tag{5.54}$$

where $\hat{\mathbf{x}} \in \Gamma$, and $c_{K4} = c_{4K} = b\delta_{K4}$.

It is more convenient to work with matrices rather than continue with the indicial notation. To this effect the generalized displacement **U,** traction **T**, body force **b**, and boundary shape coefficients **C** are defined as [6]

$$\mathbf{U} = \begin{Bmatrix} u_1 \\ u_2 \\ u_3 \\ -\phi \end{Bmatrix}, \quad \mathbf{T} = \begin{Bmatrix} t_1 \\ t_2 \\ t_3 \\ -q_s \end{Bmatrix}, \quad \mathbf{b} = \begin{Bmatrix} b_1 \\ b_2 \\ b_3 \\ b_e \end{Bmatrix}, \quad \mathbf{C} = \begin{bmatrix} c_{11} & c_{12} & c_{13} & 0 \\ c_{21} & c_{22} & c_{23} & 0 \\ c_{31} & c_{32} & c_{33} & 0 \\ 0 & 0 & 0 & b \end{bmatrix}^T \tag{5.55}$$

Similarly, the fundamental solution coefficients can be defined in matrix form as

$$\mathbf{U}^* = \begin{bmatrix} u_{11}^* & u_{12}^* & u_{13}^* & u_{14}^* \\ u_{21}^* & u_{22}^* & u_{23}^* & u_{24}^* \\ u_{31}^* & u_{32}^* & u_{33}^* & u_{34}^* \\ u_{41}^* & u_{42}^* & u_{43}^* & u_{44}^* \end{bmatrix}^T, \quad \mathbf{T}^* = \begin{bmatrix} t_{11}^* & t_{12}^* & t_{13}^* & t_{14}^* \\ t_{21}^* & t_{22}^* & t_{23}^* & t_{24}^* \\ t_{31}^* & t_{32}^* & t_{33}^* & t_{34}^* \\ t_{41}^* & t_{42}^* & t_{43}^* & t_{44}^* \end{bmatrix}^T \tag{5.56}$$

where u_{ij}^* and t_{ij}^* (i=1,2,3) represent the elastic displacement and traction, respectively, in the jth direction at a field point **x** due to a unit point load acting at the source point $\hat{\mathbf{x}}$, u_{4j}^* and t_{4j}^* denote the jth elastic displacement and traction, respectively, at **x** due to a unit electric charge at $\hat{\mathbf{x}}$, ϕ_i^* and $-q_{si}^*$ (i=1,2,3) stand for the electric potential and surface charge, respectively, at **x** corresponding to a unit force in the ith direction at $\hat{\mathbf{x}}$, ϕ_4^* and $-q_{s4}^*$ represent the electric potential and surface charge, respectively, at **x** due to a unit electric charge at $\hat{\mathbf{x}}$. Using the matrix notation defined in Eqs (5.55) and (5.56), the integral equation (5.54) can be written in matrix form as

$$\mathbf{CU} = \int_\Omega \mathbf{U}^*\mathbf{b}d\Omega - \int_\Gamma \mathbf{T}^*\mathbf{U}d\Gamma + \int_\Gamma \mathbf{U}^*\mathbf{T}d\Gamma \tag{5.57}$$

Using Eq (5.57), the generalized displacement at point, say point $\hat{\mathbf{x}}_i$, can be obtained

by enforcing a point load at the same point. In this case Eq (5.57) becomes

$$\mathbf{C}(\hat{\mathbf{x}}_i)\mathbf{U}(\hat{\mathbf{x}}_i) = \int_\Omega \mathbf{U}^*(\hat{\mathbf{x}}_i,\mathbf{x})\mathbf{b}(\mathbf{x})d\Omega(\mathbf{x}) - \int_\Gamma \mathbf{T}^*(\hat{\mathbf{x}}_i,\mathbf{x})\mathbf{U}(\mathbf{x})d\Gamma(\mathbf{x}) + \int_\Gamma \mathbf{U}^*(\hat{\mathbf{x}}_i,\mathbf{x})\mathbf{T}(\mathbf{x})d\Gamma(\mathbf{x}) \tag{5.58}$$

(c) boundary integral equation for crack problems [34]

Consider a finite three-dimensional piezoelectric solid containing several cracks. Let L be the union of all cracks, L^+ and L^- represent the union of the positive side and negative side of the cracks. The displacements and electric potential can, in this case, still be evaluated using Eq (5.43) if the boundary Γ is replaced by $\Gamma+L$, i.e.

$$\begin{aligned} u_I(\hat{\mathbf{x}}) &+ \int_\Gamma t^*_{JI}(\mathbf{x},\hat{\mathbf{x}})u_J(\mathbf{x})d\Gamma(\mathbf{x}) + \int_{L^+L^-} t^*_{JI}(\mathbf{x},\hat{\mathbf{x}})u_J(\mathbf{x})d\Gamma(\mathbf{x}) \\ &= \int_\Omega u^*_{JI}(\mathbf{x},\hat{\mathbf{x}})b_J(\mathbf{x})d\Omega(\mathbf{x}) + \int_\Gamma u^*_{JI}(\mathbf{x},\hat{\mathbf{x}})t_J(\mathbf{x})d\Gamma(\mathbf{x}) \\ &+ \int_{L^+L^-} u^*_{JI}(\mathbf{x},\hat{\mathbf{x}})t_J(\mathbf{x})d\Gamma(\mathbf{x}) \end{aligned} \tag{5.59}$$

To simplify the integral equation (5.59), denote the elastic displacements and electric potential discontinuities as

$$\Delta u_J = \begin{cases} \Delta u_j = u_j^+ - u_j^- & \text{for } J = 1,2,3 \\ \Delta\phi = \phi^+ - \phi^- & \text{for} \quad J = 4 \end{cases} \tag{5.60}$$

Then, using the relations $t^*_{IJ}(\hat{\mathbf{x}},\mathbf{x}^+) = -t^*_{IJ}(\hat{\mathbf{x}},\mathbf{x}^-) = t^{*+}_{IJ}(\hat{\mathbf{x}},\mathbf{x})$ and $u^*_{IJ}(\hat{\mathbf{x}},\mathbf{x}^+) = u^*_{IJ}(\hat{\mathbf{x}},\mathbf{x}^-)$, Eq (5.59) can be simplified as

$$\begin{aligned} u_I(\hat{\mathbf{x}}) &+ \int_\Gamma t^*_{JI}(\mathbf{x},\hat{\mathbf{x}})u_J(\mathbf{x})d\Gamma(\mathbf{x}) + \int_{L^+} t^{*+}_{JI}(\mathbf{x},\hat{\mathbf{x}})\Delta u_J(\mathbf{x})d\Gamma(\mathbf{x}) \\ &= \int_\Omega u^*_{JI}(\mathbf{x},\hat{\mathbf{x}})b_J(\mathbf{x})d\Omega(\mathbf{x}) + \int_\Gamma u^*_{JI}(\mathbf{x},\hat{\mathbf{x}})t_J(\mathbf{x})d\Gamma(\mathbf{x}) \end{aligned} \tag{5.61}$$

As indicated in [34], for a finite piezoelectric solid with several embedded flat cracks, there two parts of the boundary. One is the external boundary Γ, and the other is the union of cracks L. If the source point $\hat{\mathbf{x}}$ is taken to the boundary Γ, the boundary integral equation can be derived from Eq (5.61) as

$$\begin{aligned} c_{IK}u_K(\hat{\mathbf{x}}) &+ \int_\Gamma t^*_{JI}(\mathbf{x},\hat{\mathbf{x}})u_J(\mathbf{x})d\Gamma(\mathbf{x}) + \int_{L^+} t^{*+}_{JI}(\mathbf{x},\hat{\mathbf{x}})\Delta u_J(\mathbf{x})d\Gamma(\mathbf{x}) \\ &= \int_\Omega u^*_{JI}(\mathbf{x},\hat{\mathbf{x}})b_J(\mathbf{x})d\Omega(\mathbf{x}) + \int_\Gamma u^*_{JI}(\mathbf{x},\hat{\mathbf{x}})t_J(\mathbf{x})d\Gamma(\mathbf{x}) \end{aligned} \qquad \hat{\mathbf{x}} \in \Gamma \tag{5.62}$$

When the source point $\hat{\mathbf{x}}$ is taken to the boundary L, using the free boundary conditions of traction and surface charge on crack faces, the hypersingular integral equation can be obtained as

$$\begin{aligned} \oint_{L^+} S^{*+}_{KiJ}(\mathbf{x},\hat{\mathbf{x}})\Delta u_K(\mathbf{x})d\Gamma(\mathbf{x}) &+ \int_\Gamma S^*_{KiJ}(\mathbf{x},\hat{\mathbf{x}})u_K(\mathbf{x})d\Gamma(\mathbf{x}) \\ &= \int_\Omega D^*_{KiJ}(\mathbf{x},\hat{\mathbf{x}})b_K(\mathbf{x})d\Omega(\mathbf{x}) + \int_\Gamma D^*_{KiJ}(\mathbf{x},\hat{\mathbf{x}})t_K(\mathbf{x})d\Gamma(\mathbf{x}) \end{aligned} \qquad \hat{\mathbf{x}} \in L^+ \tag{5.63}$$

where $\oint$ means that the integral must be interpreted as a finite-part integral. The first integral in Eq (5.63) has the singular order r^{-3} and a hypersingular order. Eqs (5.62) and (5.63) form the basis for developing the BE formulation.

(d) dynamic boundary integral equation [31,32]

The reciprocity theorem approach described above can also be used to derive the dynamic boundary integral equation. To doing this, consider the following two dynamic electroelastic states

$$\text{State 1: } \{U_I^{(1)}\}^T = \{u_1^{(1)},\ u_2^{(1)},\ u_3^{(1)},\ \phi^{(1)}\}^T;\ \{b_I^{(1)}\}^T = \{b_1^{(1)},\ b_2^{(1)},\ b_3^{(1)},\ b_e^{(1)}\}^T; \tag{5.64}$$

$$\{t_I^{(1)}\}^T = \{t_1^{(1)},\ t_2^{(1)},\ t_3^{(1)},\ -q_s^{(1)}\}^T,\ \sigma_{ij,j}^{(1)} + b_i^{(1)} = \rho\ddot{u}_i^{(1)},\ D_{j,j}^{(1)} + b_e^{(1)} = 0.$$

$$\text{State 2: } \{U_I^{(2)}\}^T = \{u_1^{(2)},\ u_2^{(2)},\ u_3^{(2)},\ \phi^{(2)}\}^T;\ \{b_I^{(2)}\}^T = \{b_1^{(2)},\ b_2^{(2)},\ b_3^{(2)},\ b_e^{(2)}\}^T; \tag{5.65}$$

$$\{t_I^{(2)}\}^T = \{t_1^{(2)},\ t_2^{(2)},\ t_3^{(2)},\ -q_s^{(2)}\}^T,\ \sigma_{ij,j}^{(2)} + b_i^{(2)} = \rho\ddot{u}_i^{(2)},\ D_{j,j}^{(2)} + b_e^{(2)} = 0.$$

State (1) again represents the solution to piezoelectric problems with finite domains and general loading conditions. The second state stands for the fundamental solution to the case of an infinite piezoelectric solid subjected to an impulsive point force and an impulsive point charge. Furthermore, define a function Ξ_{ij} as

$$\Xi_{ij} = \int_\Omega b_k^{(i)} \times u_k^{(j)} d\Omega + \int_\Gamma t_k^{(i)} \times u_k^{(j)} d\Gamma + \int_\Omega b_e^{(i)} \times \phi^{(j)} d\Omega - \int_\Gamma q_s^{(i)} \times \phi^{(j)} d\Gamma \tag{5.66}$$

where the first two terms represent mechanical work and the last two terms represent electrical work. It is easy to show that $\Xi_{12} = \Xi_{21}$. The proof can be accomplished by recognizing that

$$\begin{aligned}\int_\Gamma (t_k^{(1)} \times u_k^{(2)} - q_s^{(1)} \times \phi^{(2)}) d\Gamma = &\int_\Omega (-b_k^{(1)} \times u_k^{(2)} + \rho\ddot{u}_k^{(1)} \times u_k^{(2)} + \sigma_{ij}^{(1)} \times u_{i,j}^{(2)}) d\Omega \\ &+ \int_\Omega (-b_e^{(1)} \times \phi^{(2)} + D_i^{(1)} \times \phi_{,i}^{(2)}) d\Omega\end{aligned} \tag{5.67}$$

as a consequence of the divergence theorem and the field equations (5.1)-(5.4). Inserting this relation into Eq (5.66) with i=1 and j=2 leads to

$$\Xi_{12} = \int_\Omega (\rho\ddot{u}_k^{(1)} \times u_k^{(2)} + \sigma_{ij}^{(1)} \times u_{i,j}^{(2)} + D_i^{(1)} \times \phi_{,i}^{(2)}) d\Omega \tag{5.68}$$

Furthermore, for linear piezoelectricity the following relation holds true:

$$\sigma_{ij}^{(1)} \times u_{i,j}^{(2)} + D_i^{(1)} \times \phi_{,i}^{(2)} = \sigma_{ij}^{(2)} \times u_{i,j}^{(1)} + D_i^{(2)} \times \phi_{,i}^{(1)} \tag{5.69}$$

and since

$$\rho\ddot{u}_k^{(1)} \times u_k^{(2)} = \rho\ddot{u}_k^{(2)} \times u_k^{(1)} \tag{5.70}$$

it follows that

$$\Xi_{12} = \Xi_{21} \tag{5.71}$$

Eq (5.71) is the starting point for derivation of the dynamic boundary integral equation for piezoelectricity using the reciprocity theorem approach. This derivation is based on two independent loading conditions for the second state, where a unit force and a unit charge are applied at a source point $\hat{\mathbf{x}}$. We first consider that state (2) is subjected to a point force at $\hat{\mathbf{x}}$ in the x_m direction with no bulk charge distribution (i.e. $b_e^{(2)} = 0$), namely

$$b_i^{(2)}(\mathbf{x}) = \delta(\mathbf{x} - \hat{\mathbf{x}})\delta(t)\delta_{im}, \quad (m=1, 2, 3) \tag{5.72}$$

The displacement, electric potential, stress, and electric displacement induced by the abovementioned point force were discussed in Chapter 2. Using the solution given in

Chapter 2, the variables $u_i^{(2)}$, $\phi^{(2)}$, $\sigma_{ij}^{(2)}$, and $D_i^{(2)}$ can be written in the form

$$\begin{aligned} u_i^{(2)} &= u_{ij}^*(\mathbf{x},\hat{\mathbf{x}},t)e_j, \\ \phi^{(2)} &= \phi_j^*(\mathbf{x},\hat{\mathbf{x}},t)e_j = u_{4j}^*(\mathbf{x},\hat{\mathbf{x}},t)e_j, \\ \sigma_{ij}^{(2)} &= \Sigma_{ijm}^*(\mathbf{x},\hat{\mathbf{x}},t)e_m = [c_{ijkl}u_{km,l}^*(\mathbf{x},\hat{\mathbf{x}},t) - e_{lij}u_{4m,l}^*(\mathbf{x},\hat{\mathbf{x}},t)]e_m, \\ D_i^{(2)} &= D_{im}^*(\mathbf{x},\hat{\mathbf{x}},t)e_m = [e_{ikl}u_{km,l}^*(\mathbf{x},\hat{\mathbf{x}},t) + \kappa_{il}u_{4m,l}^*(\mathbf{x},\hat{\mathbf{x}},t)]e_m \end{aligned} \tag{5.73}$$

Making use of Eq (5.4), the traction and surface charge can be obtained as

$$\begin{aligned} t_i^{(2)} &= t_{im}^*(\mathbf{x},\hat{\mathbf{x}},t)e_m = \Sigma_{ijm}^*(\mathbf{x},\hat{\mathbf{x}},t)n_j e_m, \\ -q_s^{(2)} &= t_{4m}^*(\mathbf{x},\hat{\mathbf{x}},t)e_m = D_{im}^*(\mathbf{x},\hat{\mathbf{x}},t)n_i e_m \end{aligned} \tag{5.74}$$

Substituting all the above quantities associated with state (2) into Eq (5.71) leads to

$$\begin{aligned} u_j(\hat{\mathbf{x}},t) = &\int_\Gamma \int_0^t u_{Ij}^*(\hat{\mathbf{x}},\mathbf{x},t-\tau)t_I(\mathbf{x},\tau)d\tau d\Gamma(\mathbf{x}) \\ &- \int_\Gamma \int_0^t t_{Ij}^*(\hat{\mathbf{x}},\mathbf{x},t-\tau)u_I(\mathbf{x},\tau)d\tau d\Gamma(\mathbf{x}) \qquad \hat{\mathbf{x}}\in\Omega \\ &+ \int_\Omega \int_0^t [u_{Ij}^*(\hat{\mathbf{x}},\mathbf{x},t-\tau)b_I(\mathbf{x},\tau)d\tau d\Omega(\mathbf{x}) \end{aligned} \tag{5.75}$$

which is the representation formula for the elastic displacements.

Similarly, the representation formula for the electric potential can be obtained by considering following loading condition:

$$b_e^{(2)}(\mathbf{x}) = \delta(\mathbf{x}-\hat{\mathbf{x}})\delta(t), \quad b_i^{(2)} = 0 \quad (m=1, 2, 3) \tag{5.76}$$

The resulting displacement and electric potential induced by this point charge are given by

$$\begin{aligned} u_i^{(2)} &= u_{i4}^*(\mathbf{x},\hat{\mathbf{x}},t), \\ \phi^{(2)} &= \phi_4^*(\mathbf{x},\hat{\mathbf{x}},t) = u_{44}^*(\mathbf{x},\hat{\mathbf{x}},t) \end{aligned} \tag{5.77}$$

Substituting the solution in Eq (5.77) into Eq (5.4), we have

$$\begin{aligned} \sigma_{ij}^{(2)} &= \Sigma_{ij4}^*(\mathbf{x},\hat{\mathbf{x}},t) = c_{ijkl}u_{k4,l}^*(\mathbf{x},\hat{\mathbf{x}},t) - e_{lij}u_{44,l}^*(\mathbf{x},\hat{\mathbf{x}},t), \\ D_i^{(2)} &= D_{i4}^*(\mathbf{x},\hat{\mathbf{x}},t) = e_{ikl}u_{k4,l}^*(\mathbf{x},\hat{\mathbf{x}},t) + \kappa_{il}u_{44,l}^*(\mathbf{x},\hat{\mathbf{x}},t), \\ t_i^{(2)} &= t_{i4}^*(\mathbf{x},\hat{\mathbf{x}},t) = \Sigma_{ij4}^*(\mathbf{x},\hat{\mathbf{x}},t)n_j, \\ -q_s^{(2)} &= t_{44}^*(\mathbf{x},\hat{\mathbf{x}},t) = D_{i4}^*(\mathbf{x},\hat{\mathbf{x}},t)n_i \end{aligned} \tag{5.78}$$

Substituting Eqs (5.76)-(5.78) into Eq (5.71), we obtain

$$\begin{aligned} \phi(\hat{\mathbf{x}},t) = &\int_\Gamma \int_0^t u_{I4}^*(\hat{\mathbf{x}},\mathbf{x},t-\tau)t_I(\mathbf{x},\tau)d\tau d\Gamma(\mathbf{x}) \\ &- \int_\Gamma \int_0^t t_{I4}^*(\hat{\mathbf{x}},\mathbf{x},t-\tau)u_I(\mathbf{x},\tau)d\tau d\Gamma(\mathbf{x}) \qquad \hat{\mathbf{x}}\in\Omega \\ &+ \int_\Omega \int_0^t [u_{I4}^*(\hat{\mathbf{x}},\mathbf{x},t-\tau)b_I(\mathbf{x},\tau)d\tau d\Omega(\mathbf{x}) \end{aligned} \tag{5.79}$$

Combining Eq (5.75) with Eq (5.79), we have

$$
\begin{aligned}
u_J(\hat{\mathbf{x}},t) = & \int_\Gamma \int_0^t u_{IJ}^*(\hat{\mathbf{x}},\mathbf{x},t-\tau) t_I(\mathbf{x},\tau) d\tau d\Gamma(\mathbf{x}) \\
& - \int_\Gamma \int_0^t t_{IJ}^*(\hat{\mathbf{x}},\mathbf{x},t-\tau) u_I(\mathbf{x},\tau) d\tau d\Gamma(\mathbf{x}) \qquad \hat{\mathbf{x}} \in \Omega \\
& + \int_\Omega \int_0^t [u_{IJ}^*(\hat{\mathbf{x}},\mathbf{x},t-\tau) b_I(\mathbf{x},\tau) d\tau d\Omega(\mathbf{x})
\end{aligned} \tag{5.80}
$$

where I, J =1-4.

Making use of Eqs (5.2) and (5.80), the corresponding stresses and electric displacements are expressed as

$$
\begin{aligned}
\Pi_{iJ}(\hat{\mathbf{x}},t) = & \int_\Omega \int_0^t D_{KiJ}^*(\mathbf{x},\hat{\mathbf{x}},t-\tau) b_K(\mathbf{x},\tau) d\tau d\Omega(\mathbf{x}) \\
& - \int_\Gamma \int_0^t S_{KiJ}^*(\mathbf{x},\hat{\mathbf{x}},t-\tau) u_K(\mathbf{x},\tau) d\tau d\Gamma(\mathbf{x}) \\
& + \int_\Gamma \int_0^t D_{KiJ}^*(\mathbf{x},\hat{\mathbf{x}},t-\tau) t_K(\mathbf{x},\tau) d\tau d\Gamma(\mathbf{x})
\end{aligned} \tag{5.81}
$$

The corresponding integral representation formula for the generalized traction components can be obtained from Eqs (5.4) and (5.81) as [31]

$$
\begin{aligned}
t_J(\hat{\mathbf{x}},t) = & \int_\Omega \int_0^t V_{IJ}^*(\mathbf{x},\hat{\mathbf{x}},t-\tau) b_I(\mathbf{x},\tau) d\tau d\Omega(\mathbf{x}) \\
& - \int_\Gamma \int_0^t W_{IJ}^*(\mathbf{x},\hat{\mathbf{x}},t-\tau) u_I(\mathbf{x},\tau) d\tau d\Gamma(\mathbf{x}) \\
& + \int_\Gamma \int_0^t V_{IJ}^*(\mathbf{x},\hat{\mathbf{x}},t-\tau) t_I(\mathbf{x},\tau) d\tau d\Gamma(\mathbf{x})
\end{aligned} \tag{5.82}
$$

where

$$
\begin{aligned}
V_{IJ}^*(\mathbf{x},\hat{\mathbf{x}},t-\tau) &= D_{IkJ}^*(\mathbf{x},\hat{\mathbf{x}},t-\tau) n_k(\hat{\mathbf{x}}), \\
W_{IJ}^*(\mathbf{x},\hat{\mathbf{x}},t-\tau) &= S_{IkJ}^*(\mathbf{x},\hat{\mathbf{x}},t-\tau) n_k(\hat{\mathbf{x}})
\end{aligned} \tag{5.83}
$$

As with the treatment in Eqs (5.48)-(5.51), the dynamic boundary integral equations corresponding to Eqs (5.80) and (5.82) can be obtained by examining the limiting process when $\hat{\mathbf{x}} \to \Gamma$:

$$
\begin{aligned}
c_{JK} u_K(\hat{\mathbf{x}},t) = & \int_\Gamma \int_0^t u_{IJ}^*(\hat{\mathbf{x}},\mathbf{x},t-\tau) t_I(\mathbf{x},\tau) d\tau d\Gamma(\mathbf{x}) \\
& - \int_\Gamma \int_0^t t_{IJ}^*(\hat{\mathbf{x}},\mathbf{x},t-\tau) u_I(\mathbf{x},\tau) d\tau d\Gamma(\mathbf{x}) \qquad \hat{\mathbf{x}} \in \Gamma \\
& + \int_\Omega \int_0^t [u_{IJ}^*(\hat{\mathbf{x}},\mathbf{x},t-\tau) b_I(\mathbf{x},\tau) d\tau d\Omega(\mathbf{x})
\end{aligned} \tag{5.84}
$$

$$
\begin{aligned}
c_{JK} t_K(\hat{\mathbf{x}},t) = & \int_\Omega \int_0^t V_{IJ}^*(\mathbf{x},\hat{\mathbf{x}},t-\tau) b_I(\mathbf{x},\tau) d\tau d\Omega\ (\mathbf{x}) \\
& - \int_\Gamma \int_0^t W_{IJ}^*(\mathbf{x},\hat{\mathbf{x}},t-\tau) u_I(\mathbf{x},\tau) d\tau d\Gamma(\mathbf{x}) \qquad \hat{\mathbf{x}} \in \Gamma \\
& + \int_\Gamma \int_0^t V_{IJ}^*(\mathbf{x},\hat{\mathbf{x}},t-\tau) t_I(\mathbf{x},\tau) d\tau d\Gamma(\mathbf{x})
\end{aligned} \tag{5.85}
$$

5.2.3 Boundary integral equation for magnetoelectroelastic solid

The boundary integral equations discussed in Section 5.2.2 above apply for electroelastic problems only. For magnetoelectroelastic materials, the corresponding boundary integral equation can be obtained similarly [21]. To this end, consider a

magnetoelectroelastic solid with the domain Ω and its boundary Γ. The basic equations governing this problem are Eqs (1.82), (1.83), (1.88), (1.89), (5.1), (5.3), and (5.4). Eq (5.54) still applies for this boundary value problem if we replace **U**, $\mathbf{U}^*$, **T**, $\mathbf{T}^*$, and **b** by [21]

$$\mathbf{U}=\begin{Bmatrix} u_1 \\ u_2 \\ u_3 \\ -\phi \\ -\psi \end{Bmatrix}, \qquad \mathbf{T}=\begin{Bmatrix} t_1 \\ t_2 \\ t_3 \\ -q_s \\ m \end{Bmatrix}, \qquad \mathbf{b}=\begin{Bmatrix} b_1 \\ b_2 \\ b_3 \\ b_e \\ b_m \end{Bmatrix}, \quad \mathbf{C}=\begin{bmatrix} c_{11} & c_{12} & c_{13} & 0 & 0 \\ c_{21} & c_{22} & c_{23} & 0 & 0 \\ c_{31} & c_{32} & c_{33} & 0 & 0 \\ 0 & 0 & 0 & b & 0 \\ 0 & 0 & 0 & 0 & c \end{bmatrix}^T \tag{5.86}$$

$$\mathbf{U}^*=\begin{bmatrix} u_{11}^* & u_{12}^* & u_{13}^* & u_{14}^* & u_{15}^* \\ u_{21}^* & u_{22}^* & u_{23}^* & u_{24}^* & u_{25}^* \\ u_{31}^* & u_{32}^* & u_{33}^* & u_{34}^* & u_{35}^* \\ u_{41}^* & u_{42}^* & u_{43}^* & u_{44}^* & u_{45}^* \\ u_{51}^* & u_{52}^* & u_{53}^* & u_{54}^* & u_{55}^* \end{bmatrix}^T, \qquad \mathbf{T}^*=\begin{bmatrix} t_{11}^* & t_{12}^* & t_{13}^* & t_{14}^* & t_{15}^* \\ t_{21}^* & t_{22}^* & t_{23}^* & t_{24}^* & t_{25}^* \\ t_{31}^* & t_{32}^* & t_{33}^* & t_{34}^* & t_{35}^* \\ t_{41}^* & t_{42}^* & t_{43}^* & t_{44}^* & t_{45}^* \\ t_{51}^* & t_{52}^* & t_{53}^* & t_{54}^* & t_{55}^* \end{bmatrix}^T \tag{5.87}$$

where

$$c(\hat{\mathbf{x}})=1+\lim_{\varepsilon\to 0}\int_{\Gamma_\varepsilon} t_{55}^*(\mathbf{x},\hat{\mathbf{x}})d\Gamma(\mathbf{x}) \tag{5.88}$$

and where u_{4j}^* and t_{4j}^* (j=1-3) are, respectively, displacement components and surface tractions in the x_j-direction at **x** due to a unit electric charge at $\hat{\mathbf{x}}$, u_{5j}^* and t_{5j}^* (j=1-3) are, respectively, displacement components and surface tractions in the x_j-direction at **x** due to a unit current at $\hat{\mathbf{x}}$, u_{i4}^*, t_{i4}^*, u_{i5}^*, and t_{i5}^* (i=1-3) are, respectively, electric potential, surface charge, magnetic potential, and surface magnetic induction at **x** due to a unit force at $\hat{\mathbf{x}}$, u_{44}^*, u_{45}^*, t_{44}^*, and t_{45}^* are, respectively, electric potential, magnetic potential, surface charge, and surface magnetic induction at **x** due to a unit electric charge at $\hat{\mathbf{x}}$, u_{54}^*, u_{55}^*, t_{54}^*, and t_{55}^* are, respectively, electric potential, magnetic potential, surface charge, and surface magnetic induction at **x** due to a unit current at $\hat{\mathbf{x}}$.

5.3 BE formulation

The analytical solution to the boundary integral equations developed in Section 5.2 is not, in general, possible to obtain due to the complexity of the geometry, loading condition and the kernels. Therefore a numerical procedure via discretization of the boundary into a number of elements must be used to solve the equations. In the following, we consider first the BE implementation of Eq (5.8), and then discuss the discretization form of Eqs (5.48)-(5.51).

5.3.1 BE implementation of Eq (5.8) [5]

In order to obtain a weak solution of Eq (5.8), the independent functions in Eq (5.8) are approximated as the product of known functions by unknown parameters. To eliminate the first domain integrals in Eq (5.8), the displacement **u** and electric potential ϕ in the domain are expressed in terms of linear combinations of fundamental solutions:

$$\mathbf{u} = \mathbf{U}_u^{*T}\mathbf{s}_u + \mathbf{U}_\phi^{*T}\mathbf{s}_\phi,\ \phi = \mathbf{\Phi}_u^{*T}\mathbf{s}_u + \mathbf{\Phi}_\phi^{*T}\mathbf{s}_\phi \tag{5.89}$$

where the notation in Eq (5.89) has the same form and meaning as in [5], i.e. $\mathbf{s}_u$ and $\mathbf{s}_\phi$ are unknown parameters, $\mathbf{U}_u^*$ and $\mathbf{U}_\phi^*$ are the matrices whose coefficients are displacements at $\mathbf{x}$ due to a unit force acting in one of the x_i directions and a unit electric charge at $\hat{\mathbf{x}}$ on the boundary, respectively, while the coefficients of $\mathbf{\Phi}_u^*$ and $\mathbf{\Phi}_\phi^*$ are electric potentials at $\mathbf{x}$ due to a unit force acting in one of the x_i directions and a unit electric charge at $\hat{\mathbf{x}}$ on the boundary, respectively. The fundamental solutions given in Chapter 2 can be used for this purpose. Similarly, the boundary variables in Eq (5.8) may be interpolated as follows

$$\begin{aligned} \tilde{\mathbf{u}} &= \mathbf{N}_{\tilde{u}\tilde{u}}^T\mathbf{d}_{\tilde{u}} + \mathbf{N}_{\tilde{u}\tilde{\phi}}^T\mathbf{d}_{\tilde{\phi}}, \qquad \tilde{\phi} = \mathbf{N}_{\tilde{\phi}\tilde{u}}^T\mathbf{d}_{\tilde{u}} + \mathbf{N}_{\tilde{\phi}\tilde{\phi}}^T\mathbf{d}_{\tilde{\phi}}, \\ \tilde{\mathbf{t}} &= \mathbf{N}_{\tilde{t}\tilde{t}}^T\mathbf{p}_{\tilde{t}} + \mathbf{N}_{\tilde{t}\tilde{q}_s}^T\mathbf{p}_{\tilde{q}_s}, \qquad \tilde{q}_s = \mathbf{N}_{\tilde{q}_s\tilde{u}}^T\mathbf{p}_{\tilde{t}} + \mathbf{N}_{\tilde{q}_s\tilde{q}_s}^T\mathbf{p}_{\tilde{q}_s} \end{aligned} \tag{5.90}$$

where $\mathbf{N}_{ij}$ are the matrices whose components are nonsingular interpolation functions of the type used in standard BEs, and $\mathbf{d}_{\tilde{u}}$, $\mathbf{d}_{\tilde{\phi}}$, $\mathbf{p}_{\tilde{t}}$, and $\mathbf{p}_{\tilde{q}_s}$ are unknown vectors. As $\mathbf{u}$ and ϕ are defined by Eq (5.89), the first integrals in Eq (5.8) vanish if one excludes from the domain Ω the singularities occurring at the source points on the boundary.

Substituting Eqs (5.89) and (5.90) into Eq (5.8) and using following notation

$$\mathbf{s} = \begin{Bmatrix} \mathbf{s}_u \\ \mathbf{s}_\phi \end{Bmatrix}, \quad \mathbf{d} = \begin{Bmatrix} \mathbf{d}_{\tilde{u}} \\ \mathbf{d}_{\tilde{\phi}} \end{Bmatrix}, \quad \mathbf{p} = \begin{Bmatrix} \mathbf{p}_{\tilde{t}} \\ \mathbf{p}_{\tilde{q}_s} \end{Bmatrix} \tag{5.91}$$

$$\mathbf{F} = \begin{bmatrix} \mathbf{F}_{uu} & \mathbf{F}_{u\phi} \\ \mathbf{F}_{\phi u} & \mathbf{F}_{\phi\phi} \end{bmatrix} = \int_\Gamma \begin{bmatrix} \mathbf{U}_u^* & \mathbf{\Phi}_u^* \\ \mathbf{U}_\phi^* & \mathbf{\Phi}_\phi^* \end{bmatrix} \begin{bmatrix} \mathbf{T}_u^* & \mathbf{\Omega}_u^* \\ \mathbf{T}_\phi^* & \mathbf{\Omega}_\phi^* \end{bmatrix}^T d\Gamma \tag{5.92}$$

$$\mathbf{G} = \begin{bmatrix} \mathbf{G}_{uu} & \mathbf{G}_{u\phi} \\ \mathbf{G}_{\phi u} & \mathbf{G}_{\phi\phi} \end{bmatrix} = \int_\Gamma \begin{bmatrix} \mathbf{U}_u^* & \mathbf{\Phi}_u^* \\ \mathbf{U}_\phi^* & \mathbf{\Phi}_\phi^* \end{bmatrix} \begin{bmatrix} \mathbf{N}_{\tilde{t}\tilde{t}} & -\mathbf{N}_{\tilde{q}_s\tilde{t}} \\ \mathbf{N}_{\tilde{t}\tilde{q}_s} & -\mathbf{N}_{\tilde{q}_s\tilde{q}_s} \end{bmatrix}^T d\Gamma \tag{5.93}$$

$$\mathbf{L} = \begin{bmatrix} \mathbf{L}_{uu} & \mathbf{L}_{u\phi} \\ \mathbf{L}_{\phi u} & \mathbf{L}_{\phi\phi} \end{bmatrix} = \int_{\Gamma-\Gamma_u} \begin{bmatrix} \mathbf{N}_{\tilde{t}\tilde{t}} \\ \mathbf{N}_{\tilde{t}\tilde{q}_s} \end{bmatrix} \begin{bmatrix} \mathbf{N}_{\tilde{u}\tilde{u}} \\ \mathbf{N}_{\tilde{u}\tilde{\phi}} \end{bmatrix}^T d\Gamma - \int_{\Gamma-\Gamma_\phi} \begin{bmatrix} \mathbf{N}_{\tilde{q}_s\tilde{t}} \\ \mathbf{N}_{\tilde{q}_s\tilde{q}_s} \end{bmatrix} \begin{bmatrix} \mathbf{N}_{\tilde{\phi}\tilde{u}} \\ \mathbf{N}_{\tilde{\phi}\tilde{\phi}} \end{bmatrix}^T d\Gamma \tag{5.94}$$

$$\bar{\mathbf{U}} = \begin{bmatrix} \bar{\mathbf{U}}_u \\ \bar{\mathbf{U}}_\phi \end{bmatrix} = \int_{\Gamma_u} \begin{bmatrix} \mathbf{N}_{\tilde{t}\tilde{t}} \\ \mathbf{N}_{\tilde{t}\tilde{q}_s} \end{bmatrix} \bar{\mathbf{u}} d\Gamma - \int_{\Gamma_\phi} \begin{bmatrix} \mathbf{N}_{\tilde{q}_s\tilde{t}} \\ \mathbf{N}_{\tilde{q}_s\tilde{q}_s} \end{bmatrix} \bar{\phi} d\Gamma \tag{5.95}$$

$$\bar{\mathbf{T}} = \begin{bmatrix} \bar{\mathbf{T}}_t \\ \bar{\mathbf{T}}_{q_s} \end{bmatrix} = \int_{\Gamma_t} \begin{bmatrix} \mathbf{N}_{\tilde{u}\tilde{u}} \\ \mathbf{N}_{\tilde{u}\tilde{\phi}} \end{bmatrix} \bar{\mathbf{t}} d\Gamma - \int_{\Gamma_\phi} \begin{bmatrix} \mathbf{N}_{\tilde{\phi}\tilde{u}} \\ \mathbf{N}_{\tilde{\phi}\tilde{\phi}} \end{bmatrix} \bar{q}_s d\Gamma \tag{5.96}$$

$$\mathbf{B} = \begin{bmatrix} \mathbf{B}_u \\ \mathbf{B}_\phi \end{bmatrix} = \int_\Omega \begin{bmatrix} \mathbf{U}_u^* & \mathbf{\Phi}_u^* \\ \mathbf{U}_\phi^* & \mathbf{\Phi}_\phi^* \end{bmatrix} \begin{Bmatrix} \mathbf{b} \\ b_e \end{Bmatrix} d\Omega \tag{5.97}$$

we have

$$\Pi = -\mathbf{s}^T\mathbf{B} + \frac{1}{2}\mathbf{s}^T\mathbf{F}\mathbf{s} - \mathbf{s}^T\mathbf{G}\mathbf{p} + \mathbf{p}^T\mathbf{L}\mathbf{d} - \mathbf{d}^T\bar{\mathbf{T}} + \mathbf{p}^T\bar{\mathbf{U}} \tag{5.98}$$

where $\mathbf{T}_u^*$, $\mathbf{T}_\phi^*$ and $\mathbf{\Omega}_u^*$, $\mathbf{\Omega}_\phi^*$ are the matrices whose components are the tractions and surface charges obtained from the displacements $\mathbf{U}_u^*$, $\mathbf{U}_\phi^*$ and the electric potentials $\mathbf{\Phi}_u^*$, $\mathbf{\Phi}_\phi^*$, respectively.

Performing the vanishing variation of Π with respect to **s**, **d**, and **p**, we have

$$\hat{\mathbf{F}}\mathbf{s} - \mathbf{G}\mathbf{p} - \mathbf{B} = 0 \tag{5.99}$$

$$-\mathbf{G}^T\mathbf{s} + \mathbf{L}\mathbf{d} + \bar{\mathbf{U}} = 0 \tag{5.100}$$

$$\mathbf{L}^T\mathbf{p} - \bar{\mathbf{T}} = 0 \tag{5.101}$$

where

$$\hat{\mathbf{F}} = \frac{1}{2}(\mathbf{F}^T + \mathbf{F}) \tag{5.102}$$

The unknowns **s** and **p** can be obtained by solving Eqs (5.99) and (5.101). Then substituting the solution **s** into Eq (5.100), the final system of equations for the solution of the problem can be written as

$$\mathbf{K}\mathbf{d} = \mathbf{Q} \tag{5.103}$$

where

$$\mathbf{K} = \mathbf{R}^T\hat{\mathbf{F}}\mathbf{R}, \quad \mathbf{R} = (\mathbf{G}^{-1})^T\mathbf{L}, \quad \mathbf{Q} = \bar{\mathbf{T}} + \mathbf{R}^T\mathbf{B} - \mathbf{K}\mathbf{L}^{-1}\bar{\mathbf{U}} \tag{5.104}$$

5.3.2 BE implementation for Eqs (5.48)-(5.51)

In order to obtain a numerical solution of Eqs (5.48)-(5.51), as in the usual BE approach, the boundary Γ and the domain Ω are discretized into a series of boundary elements and internal cells, respectively. The boundary vectors **U** and **T** are defined at each element "*j*" in terms of their values at nodal points of the element as

$$\mathbf{U} = \mathbf{N}\mathbf{U}_j, \quad \mathbf{T} = \mathbf{N}\mathbf{T}_j \tag{5.105}$$

where $\mathbf{U}_j$ and $\mathbf{T}_j$ are the element nodal displacements, electric potential, tractions, and surface charge of dimensions $4\times M$ for a three-dimensional electroelastic solid, M being the number of nodes within the element. The interpolation function matrix **N** is a $4\times 4M$ array of shape functions, i.e. [29]

$$\mathbf{N} = \begin{bmatrix} N_1 & 0 & 0 & 0 & \cdots & N_M & 0 & 0 & 0 \\ 0 & N_1 & 0 & 0 & \cdots & 0 & N_M & 0 & 0 \\ 0 & 0 & N_1 & 0 & \cdots & 0 & 0 & N_M & 0 \\ 0 & 0 & 0 & N_1 & \cdots & 0 & 0 & 0 & N_M \end{bmatrix} \tag{5.106}$$

in which components N_i represent the shape function which is the same as that in conventional finite element formulation. For example, for an 8-node isoparametric element as shown in Fig. 5.1, the shape functions N_i (i =1-8) may be given in the form

$$N_1 = \frac{1}{4}(1-s)(1-t)(-s-t-1), \quad N_2 = \frac{1}{4}(1+s)(1-t)(s-t-1), \tag{5.107a}$$

$$N_3 = \frac{1}{4}(1+s)(1+t)(s+t-1), \quad N_4 = \frac{1}{4}(1-s)(1+t)(-s+t-1), \tag{5.107b}$$

$$N_5=\frac{1}{2}\left(1-s^2\right)\left(1-t\right), \qquad N_6=\frac{1}{2}\left(1+s\right)\left(1-t^2\right), \tag{5.107c}$$

$$N_7=\frac{1}{2}\left(1-s^2\right)\left(1+t\right), \qquad N_8=\frac{1}{2}\left(1-s\right)\left(1-t^2\right) \tag{5.107d}$$

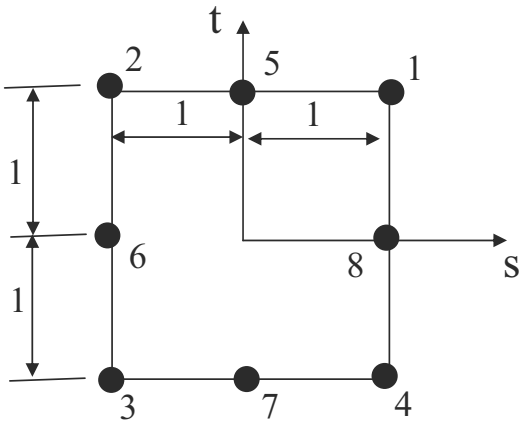

Fig. 5.1 8-node isoparametric element

Substitution of the approximation (5.105) into Eqs (5.48)-(5.51) yields

$$\begin{aligned}\mathbf{C}_u(\hat{\mathbf{x}}_i)\mathbf{U}_u(\hat{\mathbf{x}}_i)=&\sum_{s=1}^{K}\left\{\int_{\Omega_s}\mathbf{U}_u^*(\mathbf{x},\hat{\mathbf{x}}_i)\mathbf{b}(\mathbf{x})d\Omega(\mathbf{x})\right\}\\&-\sum_{k=1}^{NE}\left\{\int_{\Gamma_k}\mathbf{T}_u^*(\mathbf{x},\hat{\mathbf{x}}_i)\mathbf{N}d\Gamma(\mathbf{x})\right\}\mathbf{U}_k+\sum_{k=1}^{NE}\left\{\int_{\Gamma_k}\mathbf{U}_u^*(\mathbf{x},\hat{\mathbf{x}}_i)\mathbf{N}d\Gamma(\mathbf{x})\right\}\mathbf{T}_k\end{aligned} \tag{5.109}$$

$$\begin{aligned}b(\hat{\mathbf{x}}_i)\phi(\hat{\mathbf{x}}_i)=&\sum_{s=1}^{K}\left\{\int_{\Omega_s}\mathbf{U}_\phi^*(\mathbf{x},\hat{\mathbf{x}}_i)\mathbf{b}(\mathbf{x})d\Omega(\mathbf{x})\right\}\\&-\sum_{k=1}^{NE}\left\{\int_{\Gamma_k}\mathbf{T}_\phi^*(\mathbf{x},\hat{\mathbf{x}}_i)\mathbf{N}d\Gamma(\mathbf{x})\right\}\mathbf{U}_k+\sum_{k=1}^{NE}\left\{\int_{\Gamma_k}\mathbf{U}_\phi^*(\mathbf{x},\hat{\mathbf{x}}_i)\mathbf{N}d\Gamma(\mathbf{x})\right\}\mathbf{T}_k\end{aligned} \tag{5.110}$$

$$\begin{aligned}\mathbf{C}_u(\hat{\mathbf{x}}_i)\mathbf{T}_t(\hat{\mathbf{x}}_i)=&\sum_{s=1}^{K}\left\{\int_{\Omega_s}\mathbf{V}_t^*(\mathbf{x},\hat{\mathbf{x}}_i)\mathbf{b}(\mathbf{x})d\Omega(\mathbf{x})\right\}\\&-\sum_{k=1}^{NE}\left\{\int_{\Gamma_k}\mathbf{W}_t^*(\mathbf{x},\hat{\mathbf{x}}_i)\mathbf{N}d\Gamma(\mathbf{x})\right\}\mathbf{U}_k+\sum_{k=1}^{NE}\left\{\int_{\Gamma_k}\mathbf{V}_t^*(\mathbf{x},\hat{\mathbf{x}}_i)\mathbf{N}d\Gamma(\mathbf{x})\right\}\mathbf{T}_k\end{aligned} \tag{5.111}$$

$$\begin{aligned}-b(\hat{\mathbf{x}}_i)q_s(\hat{\mathbf{x}}_i)=&\sum_{s=1}^{K}\left\{\int_{\Omega_s}\mathbf{V}_{q_s}^*(\mathbf{x},\hat{\mathbf{x}}_i)\mathbf{b}(\mathbf{x})d\Omega(\mathbf{x})\right\}\\&-\sum_{k=1}^{NE}\left\{\int_{\Gamma_k}\mathbf{W}_{q_s}^*(\mathbf{x},\hat{\mathbf{x}}_i)\mathbf{N}d\Gamma(\mathbf{x})\right\}\mathbf{U}_k+\sum_{k=1}^{NE}\left\{\int_{\Gamma_k}\mathbf{V}_{q_s}^*(\mathbf{x},\hat{\mathbf{x}}_i)\mathbf{N}d\Gamma(\mathbf{x})\right\}\mathbf{T}_k\end{aligned} \tag{5.112}$$

where the summation from 1 to *NE* indicates summation over the NE boundary elements, Γ_k is the surface of the *k*th element, and the summation from 1 to *K* indicates summation over the *K* internal cells where the body force integrals are to be computed. Eqs (5.109) and (5.110) are usually suitable for problems without cracks or

discontinuities, and Eqs (5.111) and (5.112) are effective for solving crack problems. The matrices $\mathbf{U}_u, \mathbf{U}_u^*, \mathbf{T}_u^*, \mathbf{U}_\phi^*, \mathbf{T}_\phi^*, \mathbf{T}_t, \mathbf{V}_t^*, \mathbf{W}_t^*, \mathbf{V}_{q_s}^*, \mathbf{W}_{q_s}^*$ are defined by

$$\mathbf{U}_u = \begin{Bmatrix} u_1 \\ u_2 \\ u_3 \end{Bmatrix}, \mathbf{U}_u^* = \begin{bmatrix} u_{11}^* & u_{21}^* & u_{31}^* & u_{41}^* \\ u_{12}^* & u_{22}^* & u_{32}^* & u_{42}^* \\ u_{13}^* & u_{23}^* & u_{33}^* & u_{43}^* \end{bmatrix}, \; T_u^* = \begin{bmatrix} t_{11}^* & t_{21}^* & t_{31}^* & t_{41}^* \\ t_{12}^* & t_{22}^* & t_{32}^* & t_{41}^* \\ t_{13}^* & t_{23}^* & t_{33}^* & t_{43}^* \end{bmatrix}$$

$$\mathbf{U}_\phi^* = \{u_{14}^*,\ u_{24}^*,\ u_{34}^*,\ u_{44}^*\}, \quad \mathbf{T}_\phi^* = \{t_{14}^*,\ t_{24}^*,\ t_{34}^*,\ t_{44}^*\}$$

$$\mathbf{T}_t = \begin{Bmatrix} t_1 \\ t_2 \\ t_3 \end{Bmatrix}, \mathbf{V}_t^* = \begin{bmatrix} V_{11}^* & V_{21}^* & V_{31}^* & V_{41}^* \\ V_{12}^* & V_{22}^* & V_{32}^* & V_{42}^* \\ V_{13}^* & V_{23}^* & V_{33}^* & V_{43}^* \end{bmatrix}, \mathbf{W}_t^* = \begin{bmatrix} W_{11}^* & W_{21}^* & W_{31}^* & W_{41}^* \\ W_{12}^* & W_{22}^* & W_{32}^* & W_{41}^* \\ W_{13}^* & W_{23}^* & W_{33}^* & W_{43}^* \end{bmatrix}$$

$$\mathbf{V}_{q_s}^* = \{V_{14}^*,\ V_{24}^*,\ V_{34}^*,\ V_{44}^*\}, \quad \mathbf{W}_{q_s}^* = \{W_{14}^*,\ W_{24}^*,\ W_{34}^*,\ W_{44}^*\} \tag{5.113}$$

Combining Eq (5.109) with Eq (5.110), and Eq (5.111) with Eq (5.112), we have

$$\begin{aligned} \mathbf{C}(\hat{\mathbf{x}}_i)\mathbf{U}(\hat{\mathbf{x}}_i) &= \sum_{s=1}^{K}\left\{\int_{\Omega_s} \mathbf{U}^*(\mathbf{x},\hat{\mathbf{x}}_i)\mathbf{b}(\mathbf{x})d\Omega(\mathbf{x})\right\} \\ &- \sum_{k=1}^{NE}\left\{\int_{\Gamma_k} \mathbf{T}^*(\mathbf{x},\hat{\mathbf{x}}_i)\mathbf{N}d\Gamma(\mathbf{x})\right\}\mathbf{U}_k + \sum_{k=1}^{NE}\left\{\int_{\Gamma_k} \mathbf{U}^*(\mathbf{x},\hat{\mathbf{x}}_i)\mathbf{N}d\Gamma(\mathbf{x})\right\}\mathbf{T}_k \end{aligned} \tag{5.114}$$

$$\begin{aligned} \mathbf{C}(\hat{\mathbf{x}}_i)\mathbf{T}(\hat{\mathbf{x}}_i) &= \sum_{s=1}^{K}\left\{\int_{\Omega_s} \mathbf{V}^*(\mathbf{x},\hat{\mathbf{x}}_i)\mathbf{b}(\mathbf{x})d\Omega(\mathbf{x})\right\} \\ &- \sum_{k=1}^{NE}\left\{\int_{\Gamma_k} \mathbf{W}^*(\mathbf{x},\hat{\mathbf{x}}_i)\mathbf{N}d\Gamma(\mathbf{x})\right\}\mathbf{U}_k + \sum_{k=1}^{NE}\left\{\int_{\Gamma_k} \mathbf{V}^*(\mathbf{x},\hat{\mathbf{x}}_i)\mathbf{N}d\Gamma(\mathbf{x})\right\}\mathbf{T}_k \end{aligned} \tag{5.115}$$

After performing the discretization with boundary elements and internal cells and carrying out the integrals, Eq (5.14) is reduced to a system of algebraic equations:

$$\mathbf{C}(\hat{\mathbf{x}}_i)\mathbf{U}(\hat{\mathbf{x}}_i) + \sum_{j=1}^{N} H_{ij}\mathbf{U}^j = \sum_{j=1}^{N} G_{ij}\mathbf{T}^j + \sum_{s=1}^{K} B_{is}^{(u)} \tag{5.116}$$

$$\mathbf{C}\hat{\mathbf{x}}_i)\mathbf{T}(\hat{\mathbf{x}}_i) + \sum_{j=1}^{N} W_{ij}\mathbf{U}^j = \sum_{j=1}^{N} V_{ij}\mathbf{T}^j + \sum_{s=1}^{K} B_{is}^{(t)} \tag{5.117}$$

where N is the number of nodes, and $\mathbf{U}^j$ and $\mathbf{T}^j$ are the generalized displacement and traction at node j. The inference matrices **H**, **G**, **V**, and **W** are evaluated by

$$H_{ij} = \sum_t \int_{\Gamma_t} \mathbf{T}^*(\hat{\mathbf{x}}_i,\mathbf{x})\mathbf{N}_q(\mathbf{x})d\Gamma(\mathbf{x}), \quad G_{ij} = \sum_t \int_{\Gamma_t} \mathbf{U}^*(\hat{\mathbf{x}}_i,\mathbf{x})\mathbf{N}_q(\mathbf{x})d\Gamma(\mathbf{x})$$

$$V_{ij} = \sum_t \int_{\Gamma_t} \mathbf{V}^*(\hat{\mathbf{x}}_i,\mathbf{x})\mathbf{N}_q(\mathbf{x})d\Gamma(\mathbf{x}), \quad W_{ij} = \sum_t \int_{\Gamma_t} \mathbf{W}^*(\boldsymbol{\xi}_i,\mathbf{x})\mathbf{N}_q(\mathbf{x})d\Gamma(\mathbf{x}) \tag{5.118}$$

where the summation extends to all the elements to which node j belongs and q is the number of order of the node j within element t, and

$$\mathbf{V}^* = \begin{bmatrix} \mathbf{V}_t^* \\ \mathbf{V}_{q_s}^* \end{bmatrix}, \qquad \mathbf{W}^* = \begin{bmatrix} \mathbf{W}_t^* \\ \mathbf{W}_{q_s}^* \end{bmatrix} \tag{5.119}$$

The pseudo-loading component $B_{is}^{(u)}$ and $B_{is}^{(t)}$ is defined as

$$B_{is}^{(u)} = \int_{\Omega_s} \mathbf{U}^*(\boldsymbol{\xi}_i, \mathbf{x})\mathbf{b}(\mathbf{x})d\Omega(\mathbf{x}), \quad B_{is}^{(t)} = \int_{\Omega_s} \mathbf{V}^*(\boldsymbol{\xi}_i, \mathbf{x})\mathbf{b}(\mathbf{x})d\Omega(\mathbf{x}) \tag{5.120}$$

If we define $H_{ij} = H_{ij} + \delta_{ij}C(\hat{\mathbf{x}}_i)$ and $V_{ij} = V_{ij} + \delta_{ij}C(\hat{\mathbf{x}}_i)$, Eqs (5.116) and (5.117) can be further written in matrix form as

$$\mathbf{HU}=\mathbf{GT}+\mathbf{B}^{(\mathrm{u})} \tag{5.121}$$

$$\mathbf{WU}=\mathbf{VT}+\mathbf{B}^{(\mathrm{t})} \tag{5.122}$$

The vectors **U** and **T** represent all the values of generalized displacements and tractions before applying boundary conditions. These conditions can be introduced by collecting the unknown terms to the left-hand side and the known terms to the right-hand side of Eqs (5.121) and (5.122). This gives the final system of equations, i.e.

$$\mathbf{EX}=\mathbf{R} \tag{5.123}$$

By solving the above system all boundary variables are fully determined.

5.4 Evaluation of u_{ij}^* and t_{ij}^*

For illustration, we list below the explicit expressions of fundamental solutions presented in [28], although the Green's functions presented in Chapter 2 can also be used for evaluating integrals (5.118) and (5.120). For a two-dimensional piezoelectric solid, the corresponding fundamental solution is given by [28]

$$u_{IJ}^*(\hat{z}_K, z_K) = -\frac{1}{\pi}\mathrm{Re}\left\{\sum_{R=1}^{3} A_{JR}M_{RI}\ln(z_R - \hat{z}_R)\right\} \tag{5.124}$$

$$t_{IJ}^*(\hat{z}_K, z_K) = \frac{1}{\pi}\mathrm{Re}\left\{\sum_{R=1}^{3} F_{JR}M_{RI}\frac{p_R n_1 - n_2}{z_R - \hat{z}_R}\right\} \tag{5.125}$$

where z_K is defined in Eq (1.126), $\mathbf{n} = \{n_1, n_2\}$ is the outward unit normal at the observation point **x**, p_R and the matrix **A** is determined by Eqs (1.118) and (1.130), and F_{ij} is given by

$$F_{IK} = \sum_{R=1}^{3}[c_{2IR1} + c_{2IR2}p_K]A_{RK} \tag{5.126}$$

and the matrix **M** is obtained from

$$\mathbf{M} = \mathbf{A}^{-1}(\mathbf{B}^{-1} + \overline{\mathbf{B}}^{-1})^{-1}, \text{ with } \mathbf{B} = i\mathbf{A}\mathbf{F}^{-1} \tag{5.127}$$

The terms D_{KiJ}^* and S_{KiJ}^* appearing in Eq (5.44) are obtained by differentiation of u_{ij}^* and t_{ij}^* as

$$D_{KiJ}^* = E_{iJMl}u_{MK,l}^*, \quad S_{KiJ}^* = E_{iJMl}t_{MK,l}^*, \tag{5.128}$$

while V_{KJ}^*, and W_{KJ}^* in Eq (5.46) are related to D_{KiJ}^* and S_{KiJ}^* by Eq (5.47).

The derivatives of u_{ij}^* and t_{ij}^* are evaluated from

$$u^*_{IJ,k}(\hat{z}_M, z_M) = \frac{1}{\pi}\mathrm{Re}\left\{\sum_{R=1}^{3} A_{JR} M_{RI} \frac{\delta_{k1} + p_R \delta_{k2}}{z_R - \hat{z}_R}\right\} \tag{5.129}$$

$$t^*_{IJ,k}(\hat{z}_M, z_M) = \frac{1}{\pi}\mathrm{Re}\left\{\sum_{R=1}^{3} F_{JR} M_{RI} (\delta_{k1} + p_R \delta_{k2}) \frac{p_R n_1 - n_2}{(z_R - \hat{z}_R)^2}\right\} \tag{5.130}$$

5.5 Evaluation of singular integrals

The accuracy of BEM for piezoelectric problems is critically dependent upon proper evaluation of the boundary integrals. The integrals (5.118) and (5.120) present a singular behavior of the order $O(1/r)$ and $O(1/r^2)$ for the generalized displacement and traction fundamental solutions, where r is the distance from a source point to the element under evaluation. The discussion which follows illustrates the basic procedure in treating singular integrals, taken from the results in [20, 28, 29, 31].

5.5.1 Weakly singular integrals

Integrals of the kernels $\mathbf{U}^*$ in Eq (5.118) show a weak singularity of the type $O[\ln(z_K - z_{K0})]$ when the source point and the field point are coincident or they are a short distance apart in comparison with the size of the element, which can be numerically integrated without difficulty by using a special quadrature including a logarithm (see Appendix C for details of Gauss quadrature formulae).

5.5.2 Non-hypersingular integrals [28]

The kernels T* appearing in Eq (5.118) show a strong singularity of $O[1/(z_K - \hat{z}_K)]$ as $\hat{\mathbf{x}} \to \mathbf{x}$. Integration of such kernels over the element Γ_j that contains the source point $\hat{\mathbf{x}}$ can be achieved as follows:

It is obvious that integrals of the type

$$\int_{\Gamma_j} \mathbf{T}^*(\hat{\mathbf{x}}_j, \mathbf{x}) \mathbf{N}_q(\mathbf{x}) d\Gamma(\mathbf{x}) \tag{5.131}$$

contain the basic integral as

$$I_K = \int_{\Gamma_j} [p_K n_1(\mathbf{x}) - n_2(\mathbf{x})] \frac{1}{z_K - \hat{z}_K} \mathbf{N}_q(\mathbf{x}) d\Gamma(\mathbf{x}) \quad (K=1\text{-}4) \tag{5.132}$$

where n_1, n_2 are the components of the external unit normal to the boundary at the observation point $\mathbf{x}$ (see Fig. 5.2). Define

$$r_K = z_K - \hat{z}_K = (x_1 - \hat{x}_1) + p_K (x_2 - \hat{x}_2) \tag{5.133}$$

It follows that

$$\frac{dr_K}{d\Gamma} = \frac{dr_K}{dx_1}\frac{dx_1}{d\Gamma} + \frac{dr_K}{dx_2}\frac{dx_2}{d\Gamma} = -n_2 + p_K n_1 \tag{5.134}$$

Eq (5.134) is the key for all the transformations proposed below, and this illustrates that the Jacobian $dr_K / d\Gamma$ of the coordinate transformation that maps the geometry of the boundary element Γ_j onto the complex plane r_K is included in the fundamental solution itself for the piezoelectric case.

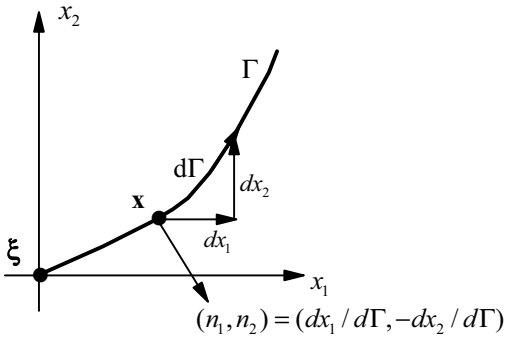

Fig. 5.2 Outward unit normal at boundary point **x**

Making use of Eq (5.134), Eq (5.132) can be rewritten as

$$I_K = \int_{\Gamma_j} \frac{1}{r_K} \mathbf{N}_q(\mathbf{x}) dr_K \tag{5.135}$$

which can be decomposed into the sum of a regular integral plus a singular integral with a known analytical solution

$$I_K = \int_{\Gamma_j} \frac{1}{r_K} (\mathbf{N}_q(\mathbf{x}) - 1) dr_K + \int_{\Gamma_j} \frac{1}{r_K} dr_K \tag{5.136}$$

Integration of the kernels D^*_{KiJ} and V^*_{IJ} can be achieved in a similar way as for $\mathbf{T}^*$ kernels since they contain singularities of the same type when $\hat{\mathbf{x}} \to \mathbf{x}$. From Eq (5.129), we have the singular integral of the type [28]

$$I'_K = \int_{\Gamma_j} [p_K n_1(\hat{\mathbf{x}}) - n_2(\hat{\mathbf{x}})] \frac{1}{r_K} \mathbf{N}_q(\mathbf{x}) d\Gamma(\mathbf{x}) \quad (K\text{=1-4}) \tag{5.137}$$

which can be regularized as follows

$$I'_K = \int_{\Gamma_j} [p_K n_1(\hat{\mathbf{x}}) - n_2(\hat{\mathbf{x}}) - \frac{dr_K}{d\Gamma}] \frac{1}{r_K} \mathbf{N}_q(\mathbf{x}) d\Gamma(\mathbf{x}) + \int_{\Gamma_j} \frac{1}{r_K} \mathbf{N}_q(\mathbf{x}) dr_K \tag{5.138}$$

The first integral in Eq (5.138) is regular and the second integral can be easily evaluated.

5.5.3 Hypersingular integrals [28]

Note that the integration of W^*_{IJ} in Eq (5.118) has a hypersingularity of the order $O(1/r^2)$ as $\mathbf{x} \to \hat{\mathbf{x}}$. From Eq (5.130) it follows that the hypersingular integral in Eq (5.118) is of the form

$$I''_K = \int_{\Gamma_j} [p_K n_1(\mathbf{x}) - n_2(\mathbf{x})] \frac{1}{r_K^2} \mathbf{N}_q(\mathbf{x}) d\Gamma(\mathbf{x}) = \int_{\Gamma_j} \frac{1}{r_K^2} \mathbf{N}_q(\mathbf{x}) dr_K \quad (K\text{=1-4}) \tag{5.139}$$

As indicated in [28], the integral (5.139) can be again decomposed into the sum of a regular integral plus singular integrals with known analytical solutions by using Eq (5.134) and the first two terms of the series expansion of the shape function N_q at $\hat{\mathbf{x}}$, considered as a function of the complex space variable r_K

$$N_q(r_K) = N_q\big|_{r_K=0} + \left.\frac{dN_q}{dr_K}\right|_{r_K=0} r_K + 0(r_K^2) \approx N_{q0} + N'_{q0} r_K \tag{5.140}$$

Thus, I''_K can be written as

$$\begin{aligned} I''_K &= \int_{\Gamma_j} \frac{1}{r_K^2} \mathbf{N}_q(\mathbf{x}) dr_K = \int_{\Gamma_j} \frac{1}{r_K^2} [\mathbf{N}_q(\mathbf{x}) - N_{q0} - N'_{q0} r_K) dr_K \\ &+ N_{q0} \int_{\Gamma_j} \frac{1}{r_K^2} \mathbf{N}_q(\mathbf{x}) dr_K + N'_{q0} \int_{\Gamma_j} \frac{1}{r_K} \mathbf{N}_q(\mathbf{x}) dr_K \end{aligned} \tag{5.141}$$

The first integral in (5.141) is regular and the other two can be easily evaluated analytically.

5.5.4 Self-adaptive subdivision method

An alternative method presented in [29] for evaluating singular integrals is introduced in this section. As was pointed out in [29], the advantage of this technique is the possibility of monitoring the convergence of the matrix coefficients. The basic steps of the method are as follows:

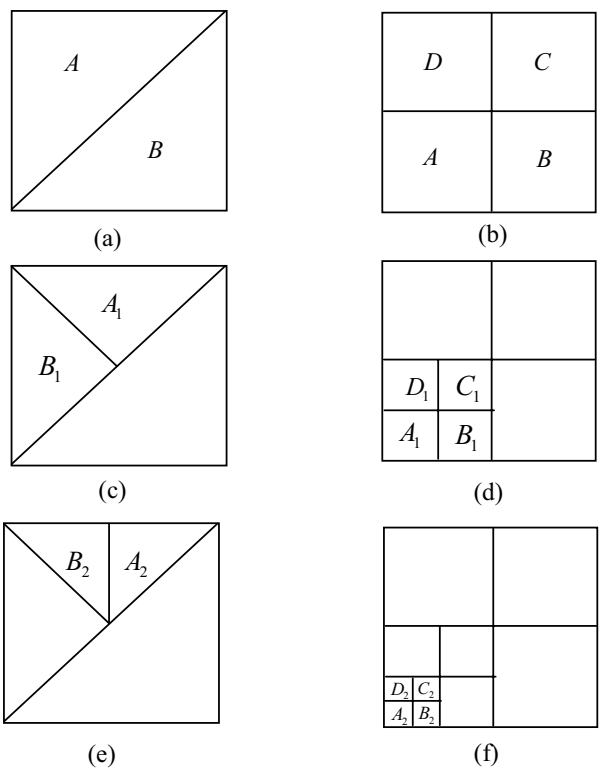

Fig. 5.3 Self-adaptive subdivision scheme

(i) The normalized element is divided into two triangles or four rectangles (see Fig. 5.3a,b) and the matrices **H** and **G** are evaluated over one of them, for example sub-element A.

(ii) The sub-element is divided (see Fig. 5.3c,d) and the the matrices **H** and **G** are are obtained as the sum of the integrals evaluated over each of these new sub-elements.

(iii) If the difference in the sum of the absolute values of the coefficients of **H** and **G** calculated in step 1 and step 2 is greater than a prescribed tolerance, the procedure is repeated over each new sub-element until convergence is achieved (see Fig. 5.3e,f).

(iv) The procedure is repeated in the rest of the element, i.e., triangle B and rectangles B, C, and D, respectively.

5.5.5 Singular integral in time-domain boundary integral equation [31]
It is noted that Eq (5.84) have a Cauchy-type singularity of the order

$$t_{IJ}^{*}(\hat{\mathbf{x}},\mathbf{x},t-\tau)\propto\begin{cases}\dfrac{1}{\left|\mathbf{x}-\hat{\mathbf{x}}\right|^{2}} & \text{when } \hat{\mathbf{x}}\to\mathbf{x}, \text{ for 3D,}\\ \dfrac{1}{\left|\mathbf{x}-\hat{\mathbf{x}}\right|} & \text{when } \hat{\mathbf{x}}\to\mathbf{x}, \text{ for 2D}\end{cases} \tag{5.142}$$

The time-domain singular integrals can be evaluated by using a two-state conservation integral presented in [31]. The two-state conservation integral for linear dynamic piezoelectricity is stated as

$$\begin{aligned}\int_{\Gamma}\left\{\varepsilon_{rki}\varepsilon_{rst}\Pi_{iJ}^{(2)}\times U_{J,t}^{(1)}n_{s}-\left[\Pi_{jI}^{(1)}\times U_{I,k}^{(2)}-\rho\delta_{IM}^{*}\ddot{U}_{M}^{(1)}\times U_{I}^{(2)}\delta_{jk}\right]n_{j}\right\}d\Gamma\\ -\int_{\Omega}\left[b_{I}^{(1)}\times U_{I,k}^{(2)}+b_{I}^{(2)}\times U_{I,k}^{(1)}\right]d\Omega=0\end{aligned} \tag{5.143}$$

where ε_{rki} is the permutation tensor, and

$$\delta_{IM}^{*}=\begin{cases}\delta_{im}, & \text{for } I,M=1,2,3,\\ 0, & \text{otherwise}\end{cases} \tag{5.144}$$

Proof of the state can be obtained by considering the following conservation integral of linear dynamic piezoelectricity:

$$\begin{aligned}J_{k}^{D}=\int_{\Gamma}\left[\frac{1}{2}(\Pi_{mN}\times U_{N,m}+\rho\delta_{IM}^{*}\ddot{U}_{M}\times U_{I})\delta_{jk}-\Pi_{jI}\times U_{I,k}\right]n_{j}d\Gamma\\ -\int_{\Omega}b_{I}\times U_{I,k}d\Omega=0\end{aligned} \tag{5.145}$$

Wang and Zhang [31] indicated that the conditions for the validity of Eq (5.145) are the zero initial conditions:

$$U_{I}(x,t)=\dot{U}_{I}(x,t)=0 \quad \text{for } t=0 \tag{5.146}$$

and the absence of singularities with the piezoelectric solid under consideration. The proof of Eq (5.145) is straightforward by applying the divergence theorem and the properties of the Riemann convolution. To this end, let U_{I}, Π_{iJ}, and b_{I} be in the form

$$U_I = U_I^{(1)} + U_I^{(2)}, \quad \Pi_{jI} = \Pi_{jI}^{(1)} + \Pi_{jI}^{(2)}, \quad b_I = b_I^{(1)} + b_I^{(2)} \tag{5.147}$$

Substituting Eq (5.147) into Eq (5.145), we have

$$\begin{aligned} J_k^D(U_I) &= J_k^D(U_I^{(1)}) + J_k^D(U_I^{(2)}) \\ &= \int_\Gamma \left\{ \varepsilon_{rki}\varepsilon_{rst}\Pi_{iJ}^{(2)} \times U_{J,t}^{(1)} n_s - \left[\Pi_{jI}^{(1)} \times U_{I,k}^{(2)} - \rho\delta_{IM}^* \ddot{U}_M^{(1)} \times U_I^{(2)} \delta_{jk} \right] n_j \right\} d\Gamma \\ &\quad - \int_\Omega \left[b_I^{(1)} \times U_{I,k}^{(2)} + b_I^{(2)} \times U_{I,k}^{(1)} \right] d\Omega = 0 \end{aligned} \tag{5.148}$$

Since the first two terms in Eq (5.148) vanish identically, the two-state conversation integral (5.143) holds true for linear piezoelectric solids.

Consider that the abovementioned state (1) represents the solution to piezoelectric problems with finite domains and general loading conditions. The second state stands for the fundamental solution to the case of an infinite piezoelectric solid subjected to an impulsive point force and an impulsive point charge. By using Eq (5.148) and the sifting property of the Dirac delta function, a representation formula for the generalized displacement gradients $U_{L,k}(\hat{\mathbf{x}}, t)$ can be obtained, as

$$U_{L,k}(\hat{\mathbf{x}}, t) = \int_\Gamma \left\{ \varepsilon_{rki}\varepsilon_{rst} D_{JiL}^* \times U_{J,t} n_s - \left[u_{IL,k}^* \times \Pi_{jI} - \rho\delta_{IM}^* u_{IL}^* \times \ddot{U}_M \delta_{jk} \right] n_j \right\} d\Gamma \tag{5.149}$$

where $\hat{\mathbf{x}} \notin \Gamma$.

Making use of the constitutive equation (5.2) and the expression of t_i and q_s in Eq (5.4), the following 3D dynamic boundary integral equation on generalized traction can be obtained as

$$t_I(\hat{\mathbf{x}}, t) = E_{pILk} n_p(\hat{\mathbf{x}}, t) \int_\Gamma \left\{ \varepsilon_{rkm}\varepsilon_{rst} D_{JmL}^* \times U_{J,t} n_s - \left[u_{JL,k}^* \times t_J - \rho\delta_{IM}^* u_{IL}^* \times \ddot{U}_M n_k \right] \right\} d\Gamma \tag{5.150}$$

The corresponding 2D time-domain boundary integral equation can be obtained from Eq (5.150) as

$$t_I(\hat{\mathbf{x}}, t) = E_{\alpha IL\beta} n_\alpha(\hat{\mathbf{x}}, t) \int_\Gamma \left\{ D_{J\gamma L}^* \times (n_\beta \partial_\gamma - n_\gamma \partial_\beta) U_J - \left[u_{JL,\beta}^* \times t_J - \rho\delta_{IM}^* u_{IL}^* \times \ddot{U}_M n_\beta \right] \right\} d\Gamma \tag{5.151}$$

5.6 Crack tip singularity by evaluating hypersingular integrals

Based on the Green's functions presented in Section 2.3, Qin and Noda [34] developed an approach for evaluating the hypersingular integrals appearing in Eq (5.63) and provided explicit expressions of stress and electric displacement field near the crack tip. It should be mentioned that the Green's functions presented in Section 2.3 are for a point force or charge applied at origin only. For the case of a point load acting at $\hat{\mathbf{x}} = (\hat{x}, \hat{y}, \hat{z})$ rather than $\mathbf{0}$, the solution still applies if x, y, z in Section 2.3 are replaced by $x - \hat{x}$, $y - \hat{y}$, $z - \hat{z}$. Using the solution given in Section 2.3, the hypersingular integral in Eq (5.63) can be rewritten as

$$\oint_{L^+} \frac{1}{r^3} [c_{44}^2 D_0 v_0 (2\delta_{\alpha\beta} - 3r_{,\alpha} r_{,\beta}) + k_{11}(\delta_{\alpha\beta} - 3r_{,\alpha} r_{,\beta})] \Delta u_\beta(\mathbf{x}) d\Gamma(\mathbf{x}) = -t_{\alpha 0}(\bar{\mathbf{x}}) \tag{5.152}$$

$$\oint_{L^+} \frac{1}{r^3} [k_{33} \Delta u_3(\mathbf{x}) + k_{34} \Delta\phi(\mathbf{x})] d\Gamma(\mathbf{x}) = -t_{30}(\bar{\mathbf{x}}) \tag{5.153}$$

$$\oint_{L^+} \frac{1}{r^3} [k_{43} \Delta u_3(\mathbf{x}) + k_{44} \Delta\phi(\mathbf{x})] d\Gamma(\mathbf{x}) = -q_{s0}(\bar{\mathbf{x}}) \tag{5.154}$$

where $\alpha, \beta = 1,2$, $\hat{\mathbf{x}} \in L^+$, t_{i0} and q_{s0} stand for the mechanical and electric loads on the crack surfaces due to internal or external loads and can be obtained from the solution for the loads of the uncracked solid, and k_{ij} is given by

$$k_{11} = \sum_{i=1}^{3} [c_{44}(A_i + D_i v_i) + e_{15} B_i][c_{44}(v_i \lambda_i^{uv} + \lambda_i^{w}) + e_{15} \lambda_i^{\phi}] \tag{5.155}$$

$$k_{33} = \sum_{i=1}^{3} (-c_{13} \lambda_i^{uv} + c_{33} \lambda_i^{w} v_i + e_{33} v_i \lambda_i^{\phi})(c_{33} A_i v_i + e_{33} B_i v_i - c_{13} D_i) \tag{5.156}$$

$$k_{34} = \sum_{i=1}^{3} (-c_{13} \lambda_i^{uv} + c_{33} \lambda_i^{w} v_i + e_{33} v_i \lambda_i^{\phi})(e_{33} A_i v_i - \kappa_{33} B_i v_i - e_{31} D_i) \tag{5.157}$$

$$k_{43} = \sum_{i=1}^{3} (-e_{31} \lambda_i^{uv} + e_{33} \lambda_i^{w} v_i - \kappa_{33} v_i \lambda_i^{\phi})(c_{33} A_i v_i + e_{33} B_i v_i - c_{13} D_i) \tag{5.158}$$

$$k_{34} = \sum_{i=1}^{3} (-e_{31} \lambda_i^{uv} + e_{33} \lambda_i^{w} v_i - \kappa_{33} v_i \lambda_i^{\phi})(e_{33} A_i v_i - \kappa_{33} B_i v_i - e_{31} D_i) \tag{5.157}$$

with A_i, B_i, D_i, v_i, $\lambda_i^{uv}, \lambda_i^{w}$, and λ_i^{ϕ} being defined in Section 2.3.

When using Eqs (5.152)-(5.154) for analyzing singularity of generalized stress near a crack tip, it is convenient to use a local coordinate system as shown in Fig. 5.4. That is, the x_1-axis is the tangent line of the crack front at point $\mathbf{x}_0$, x_2-axis is the internal normal line in the crack plane, and x_3-axis is normal to the crack. Then the displacement and electric potential discontinuities between crack surfaces near the point $\mathbf{x}_0$ can be assumed as

$$\Delta u_i(\mathbf{x}) = g_k(\mathbf{x}_0) x_2^{\lambda_k}, \quad \Delta\phi(\mathbf{x}) = \Phi(\mathbf{x}_0) x_2^{\lambda_4}, \qquad 0 < \mathrm{Re}(\lambda_k) < 1 \tag{5.158}$$

where $g_k(\mathbf{x}_0)$ and $\Phi(\mathbf{x}_0)$ are non-zero constants related to point $\mathbf{x}_0$, λ_k is the singular index at the crack front. Consider now the singular point $\mathbf{x}_0$ on the boundary surrounded by a small semi-circular surface of radius ε, say Γ_ε, centred at the point $\mathbf{x}_0$ with $\varepsilon \to 0$. Using the main-part analytical method [35], the following relations can be obtained

$$\oint_{\Gamma_\varepsilon} \frac{\Delta u_1}{r^3} dx_1 dx_2 \cong -2\pi\lambda_1 g_1(\mathbf{x}_0) \hat{x}_2^{\lambda_1 - 1} \cot(\lambda_1 \pi) \tag{1.159}$$

$$\oint_{\Gamma_\varepsilon} \frac{\Delta u_1}{r^5} (x_1 - \hat{x}_1)^2 dx_1 dx_2 \cong -\frac{2}{3} \pi\lambda_1 g_1(\mathbf{x}_0) \hat{x}_2^{\lambda_1 - 1} \cot(\lambda_1 \pi) \tag{1.160}$$

$$\oint_{\Gamma_\varepsilon} \frac{\Delta u_2}{r^5} (x_2 - \hat{x}_2)^2 dx_1 dx_2 \cong -\frac{4}{3} \pi\lambda_2 g_2(\mathbf{x}_0) \hat{x}_2^{\lambda_2 - 1} \cot(\lambda_2 \pi) \tag{1.161}$$

$$\oint_{\Gamma_\varepsilon} \frac{\Delta u_1}{r^5} (x_1 - \hat{x}_1)(x_2 - \hat{x}_2) dx_1 dx_2 \cong 0 \tag{1.162}$$

$$\oint_{\Gamma_\varepsilon} \frac{\Delta u_3}{r^3} dx_1 dx_2 \cong -2\pi\lambda_3 g_3(\mathbf{x}_0) \hat{x}_2^{\lambda_3 - 1} \cot(\lambda_3 \pi) \tag{1.163}$$

$$\oint_{\Gamma_\varepsilon} \frac{\Delta \phi}{r^3} dx_1 dx_2 \cong -2\pi\lambda_4 \Phi(\mathbf{x}_0) \hat{x}_2^{\lambda_4 - 1} \cot(\lambda_4 \pi) \tag{1.164}$$

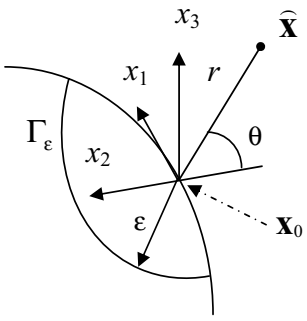

Fig. 5.4 A semi-circular domain Γ_ε on the crack surface

Making use of the above relations, Eqs (5.152) and (5.154) yield

$$\cot(\lambda_i \pi) = 0, \ (i\text{=1-4}) \tag{5.165}$$

Then the singular index is obtained as

$$\lambda_1 = \lambda_2 = \lambda_3 = \lambda_4 = \frac{1}{2} \tag{5.166}$$

Considering Eq (5.158) and the main-part analytical method, the following relations can be obtained, which are necessary for deriving crack-tip fields:

$$\int_{\Gamma_\varepsilon} \frac{1}{R_0^3}\left(1-\frac{3(x_1-\hat{x}_1)^2}{R_0^2}\right)\Delta u_1 dx_1 dx_2 \cong 0 \tag{5.167}$$

$$\int_{\Gamma_\varepsilon} \frac{1}{R_0^3}\left(1-\frac{3(x_2-\hat{x}_2)^2}{R_0^2}\right)\Delta u_1 dx_1 dx_2 \cong \frac{\pi g_1(\mathbf{x}_0)}{\sqrt{r_0 r}}\cos\frac{\theta_0}{2} \tag{5.168}$$

$$\int_{\Gamma_\varepsilon} \frac{1}{R_0^3}\left(1-\frac{3v_0^2 x_3^2}{R_0^2}\right)\Delta u_1 dx_1 dx_2 \cong \frac{\pi g_1(\mathbf{x}_0)}{\sqrt{r_0 r}}\cos\frac{\theta_0}{2} \tag{5.169}$$

$$\int_{\Gamma_\varepsilon} \frac{1}{R_j^3}\left(1-\frac{3(x_2-\hat{x}_2)^2}{R_j^2}\right)\Delta u_3 dx_1 dx_2 \cong \frac{\pi g_3(\mathbf{x}_0)}{\sqrt{r_j r}}\cos\frac{\theta_j}{2}, \ (j\text{=1,2,3}) \tag{5.170}$$

$$\int_{\Gamma_\varepsilon} \frac{1}{R_j^3}\left(1-\frac{3v_j^2 x_3^2}{R_j^2}\right)\Delta u_i dx_1 dx_2 \cong \frac{\pi g_i(\mathbf{x}_0)}{\sqrt{r_j r}}\cos\frac{\theta_j}{2} \tag{5.171}$$

$$\int_{\Gamma_\varepsilon} \frac{3v_j x_3 (x_2-\hat{x}_2)}{R_j^5}\Delta u_3 dx_1 dx_2 \cong -\frac{\pi g_3(\mathbf{x}_0)}{\sqrt{r_j r}}\sin\frac{\theta_j}{2}, \ (j\text{=1,2,3}) \tag{5.172}$$

where $r_0 = (\cos^2\theta + v_0^2 \sin^2\theta)^{1/2}$, $\theta_0 = \mathrm{tg}^{-1}(v_0 \mathrm{tg}\theta)$, $r_j e^{i\theta_j} = \cos\theta + i v_j \sin\theta$. Using the relations (5.167)-(5.172), the singular stresses and electric displacement near the crack front can be expressed as

$$\sigma_{13} = c_{44}^2 D_0 v_0^2 \frac{\pi g_1(\mathbf{x}_0)}{\sqrt{r_0 r}} \cos\frac{\theta_0}{2} \tag{5.173}$$

$$\sigma_{23} = -\frac{\pi g_2(\mathbf{x}_0)}{\sqrt{r}} \sum_{i=1}^{3} A_i^u \gamma_i^u \frac{1}{\sqrt{r_i}} \cos\frac{\theta_i}{2} + \frac{\pi}{\sqrt{r}} \sum_{i=1}^{3} [g_3(\mathbf{x}_0) A_i^w + \Phi(\mathbf{x}_0) A_i^\phi] \gamma_i^u \frac{1}{\sqrt{r_i}} \sin\frac{\theta_i}{2} \tag{5.174}$$

$$\sigma_{33} = -\frac{\pi g_2(\mathbf{x}_0)}{\sqrt{r}} \sum_{i=1}^{3} A_i^u \gamma_i^w \frac{1}{\sqrt{r_i}} \sin\frac{\theta_i}{2} - \frac{\pi}{\sqrt{r}} \sum_{i=1}^{3} [g_3(\mathbf{x}_0) A_i^w + \Phi(\mathbf{x}_0) A_i^\phi] \gamma_i^w \frac{1}{\sqrt{r_i}} \cos\frac{\theta_i}{2} \tag{5.175}$$

$$D_3 = -\frac{\pi g_2(\mathbf{x}_0)}{\sqrt{r}} \sum_{i=1}^{3} A_i^u \gamma_i^\phi \frac{1}{\sqrt{r_i}} \sin\frac{\theta_i}{2} - \frac{\pi}{\sqrt{r}} \sum_{i=1}^{3} [g_3(\mathbf{x}_0) A_i^w + \Phi(\mathbf{x}_0) A_i^\phi] \gamma_i^\phi \frac{1}{\sqrt{r_i}} \cos\frac{\theta_i}{2} \tag{5.176}$$

where

$$\begin{aligned}
&A_i^u = c_{44}(A_i + D_i v_i) + e_{15} B_i, \quad A_i^w = c_{33} A_i v_i + e_{33} B_i v_i - c_{13} D_i, \\
&A_i^\phi = e_{33} A_i v_i - \kappa_{33} B_i v_i - e_{31} D_i, \; \gamma_i^u = c_{44}(v_i \lambda_i^{uv} + \lambda_i^w) + e_{15} \lambda_i^\phi, \\
&\gamma_i^w = c_{13} \lambda_i^{uv} - c_{33} v_i \lambda_i^w) - e_{33} v_i \lambda_i^\phi \; \gamma_i^\phi = e_{31} \lambda_i^{uv} - e_{33} \lambda_i^w v_i + \kappa_{33} v_i \lambda_i^\phi
\end{aligned} \tag{5.177}$$

Using the traditional definitions of the stress intensity factors and the electric field intensity factor

$$\begin{cases}
K_I = \lim\limits_{r\to 0} \sigma_{33}(r,\theta)\big|_{\theta=0} \sqrt{2r}, \\
K_{II} = \lim\limits_{r\to 0} \sigma_{32}(r,\theta)\big|_{\theta=0} \sqrt{2r}, \\
K_{III} = \lim\limits_{r\to 0} \sigma_{31}(r,\theta)\big|_{\theta=0} \sqrt{2r}, \\
K_{IV} = \lim\limits_{r\to 0} D_3(r,\theta)\big|_{\theta=0} \sqrt{2r},
\end{cases} \tag{5.178}$$

The above singular stresses and electric displacement can be rewritten in terms of field intensity factor as

$$\sigma_{13} = \frac{K_{III}}{\sqrt{2r}} \frac{1}{\sqrt{r_0}} \cos\frac{\theta}{2} \tag{5.179}$$

$$\sigma_{23} = \frac{K_I}{\sqrt{2r}} f_{21}(\theta) + \frac{K_{II}}{\sqrt{2r}} f_{22}(\theta) + \frac{K_{IV}}{\sqrt{2r}} f_{24}(\theta) \tag{5.180}$$

$$\sigma_{33} = \frac{K_I}{\sqrt{2r}} f_{31}(\theta) + \frac{K_{II}}{\sqrt{2r}} f_{32}(\theta) + \frac{K_{IV}}{\sqrt{2r}} f_{34}(\theta) \tag{5.181}$$

$$D_3 = \frac{K_I}{\sqrt{2r}} f_{41}(\theta) + \frac{K_{II}}{\sqrt{2r}} f_{42}(\theta) + \frac{K_{IV}}{\sqrt{2r}} f_{44}(\theta) \tag{5.182}$$

where

$$f_{21}(\theta) = -\frac{1}{k_{33}k_{44} - k_{34}k_{43}} \sum_{i=1}^{3} (k_{44} A_i^w - k_{43} A_i^\phi) \gamma_i^u \frac{1}{\sqrt{r_i}} \sin\frac{\theta_i}{2} \tag{5.183}$$

$$f_{22}(\theta) = \frac{1}{k_{11}} \sum_{i=1}^{3} A_i^u \gamma_i^u \frac{1}{\sqrt{r_i}} \cos\frac{\theta_i}{2} \tag{5.184}$$

$$f_{24}(\theta) = -\frac{1}{k_{33}k_{44} - k_{34}k_{43}} \sum_{i=1}^{3} (k_{33}A_i^w - k_{34}A_i^\phi)\gamma_i^u \frac{1}{\sqrt{r_i}} \sin\frac{\theta_i}{2} \tag{5.185}$$

$$f_{31}(\theta) = -\frac{1}{k_{33}k_{44} - k_{34}k_{43}} \sum_{i=1}^{3} (k_{44}A_i^w - k_{43}A_i^\phi)\gamma_i^w \frac{1}{\sqrt{r_i}} \cos\frac{\theta_i}{2} \tag{5.186}$$

$$f_{32}(\theta) = \frac{1}{k_{11}} \sum_{i=1}^{3} A_i^u \gamma_i^w \frac{1}{\sqrt{r_i}} \sin\frac{\theta_i}{2} \tag{5.187}$$

$$f_{34}(\theta) = -\frac{1}{k_{33}k_{44} - k_{34}k_{43}} \sum_{i=1}^{3} (k_{34}A_i^w - k_{33}A_i^\phi)\gamma_i^w \frac{1}{\sqrt{r_i}} \cos\frac{\theta_i}{2} \tag{5.188}$$

$$f_{41}(\theta) = \frac{1}{k_{33}k_{44} - k_{34}k_{43}} \sum_{i=1}^{3} (k_{44}A_i^w - k_{43}A_i^\phi)\gamma_i^\phi \frac{1}{\sqrt{r_i}} \cos\frac{\theta_i}{2} \tag{5.189}$$

$$f_{42}(\theta) = \frac{1}{k_{11}} \sum_{i=1}^{3} A_i^u \gamma_i^\phi \frac{1}{\sqrt{r_i}} \sin\frac{\theta_i}{2} \tag{5.190}$$

$$f_{41}(\theta) = -\frac{1}{k_{33}k_{44} - k_{34}k_{43}} \sum_{i=1}^{3} (k_{34}A_i^w - k_{33}A_i^\phi)\gamma_i^\phi \frac{1}{\sqrt{r_i}} \cos\frac{\theta_i}{2} \tag{5.191}$$

5.7 Multi-domain problems

Eq (5.18) is suitable for problems with a single solution domain only. If the solution domain is made up piece-wise of different materials the problem can be solved by the multi-domain BEM [13]. The multi-domain approach presented in [13] is based on the division of the origin domain into homogeneous subregions (see Fig. 5.5) so that Eq (5.121) still holds for each single subdomain, and one can write

$$\mathbf{H}^{(i)}\mathbf{U}^{(i)} - \mathbf{G}^{(i)}\mathbf{T}^{(i)} = \mathbf{B}^{(i)}, \quad (i = 1, 2, \ldots, J) \tag{5.192}$$

where J is the number of subregions and the superscript (i) indicates quantities associated with the ith subregion. To obtain the solution it is necessary to restore domain unity by enforcing the generalized displacement and traction continuity conditions along the interfaces between contiguous subdomains. Let us introduce a partition of the linear algebraic system given by Eq (5.192) in such a way that the generic vector can be written as [13]

$$y^{(i)} = \left\{ y_{\Gamma_{i1}}^{(i)} \quad \cdots \quad y_{\Gamma_{iJ}}^{(i)} \right\}^T \tag{5.193}$$

where the vector $y_{\Gamma_{ij}}^{(i)}$ collects the components of $y^{(i)}$ associated with the nodes belonging to the interface Γ_{ij} between the ith and jth subdomain, with the convention that Γ_{ii} stands for the external boundary of the ith subdomain (see Fig. 5.5). Based on this arrangement, the interface compatibility and equilibrium conditions are given by [13]

$$\mathbf{U}_{\Gamma_{ij}}^{(i)} = \mathbf{U}_{\Gamma_{ij}}^{(j)}, \quad \mathbf{T}_{\Gamma_{ij}}^{(i)} = -\mathbf{T}_{\Gamma_{ij}}^{(j)}, \quad (i = 1, \cdots J-1;\ j = i+1, \cdots J) \tag{5.194}$$

It should be noted that if the ith and jth subdomain have no common boundary, $y_{\Gamma_{ij}}^{(i)}$ is

a zero-order vector and Eq (5.194) is no longer valid. The system of Eq (5.192) and the interface continuity conditions (5.194) provide a set of relationships which, together with the external boundary conditions, allows derivation of the electroelastic solution in terms of generalized displacement and traction on the boundary of each subdomain. It should be mentioned that the multi-domain approach described here is suitable for modeling general fracture problems in piezoelectric media [13].

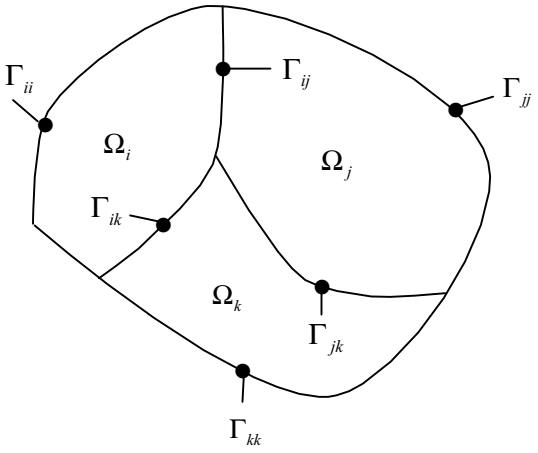

Fig. 5.5 Multi-domain configuration

5.8 Application of BEM to fracture analysis

Over the years, several special boundary elements have been presented to capture the crack-tip singularity of piezoelectric materials. For illustration, three typical boundary elements presented in [11,28, 36] are discussed here.

5.8.1 One quarter-point quadratic crack-tip element

The boundary element formulation described in Section 5.3 is inefficient for modeling crack-tip elements. To capture the square root characteristics of the generalized relative crack displacement (GRCD) near the crack-tip, a quarter-point quadratic crack-tip element is developed by setting [28]

$$\zeta = 2\sqrt{\frac{r}{L}} - 1 \tag{5.195}$$

where ζ is the boundary element natural coordinate, r is the distance from a field point to the crack-tip, and L the element length (see Fig. 5.6). In the element, the collocation points NC1, NC2, and NC3 for the quarter-point element are located at $\zeta_1 = -3/4$, $\zeta_2 = 0$, and $\zeta_3 = 3/4$, respectively (see Fig. 5.6). In such a case, the distance r from the collocation nodes of the quarter-point element to the crack-tip follows from Eq (5.195)

$$r_1 = \frac{L}{64} \text{ at NC1}, \; r_2 = \frac{L}{4} \text{ at NC2}, \; r_3 = \frac{49L}{64} \text{ at NC3} \tag{5.196}$$

If we use the conventional polar coordinate system (r,θ), centered at the crack-tip and such that $\theta = \pm\pi$ are the crack faces, the GRCD $\Delta\mathbf{U}$ across the two opposite crack faces may be written in terms of the generalized stress intensity factors (GSIF), as

[28]

$$\Delta\mathbf{U}=\begin{Bmatrix}\Delta u_1\\ \Delta u_2\\ \Delta\phi\end{Bmatrix}=\sqrt{\frac{8r}{\pi}}\,\mathrm{Re}[\mathbf{B}]\begin{Bmatrix}K_{II}\\ K_I\\ K_{IV}\end{Bmatrix} \tag{5.197}$$

where K_I and K_{II} are the conventional mode I and mode II SIF, respectively, and K_{IV} is the electric displacement intensity factor. Particularizing Eq (5.197) for the collocation node NC1, the following one-point formula for direct evaluation of the GSIF can be obtained

$$\mathbf{K}=\begin{Bmatrix}K_{II}\\ K_I\\ K_{IV}\end{Bmatrix}=2\sqrt{\frac{2\pi}{L}}(\mathrm{Re}[\mathbf{B}])^{-1}\begin{Bmatrix}\Delta u_1^{NC1}\\ \Delta u_2^{NC1}\\ \Delta\phi^{NC1}\end{Bmatrix} \tag{5.198}$$

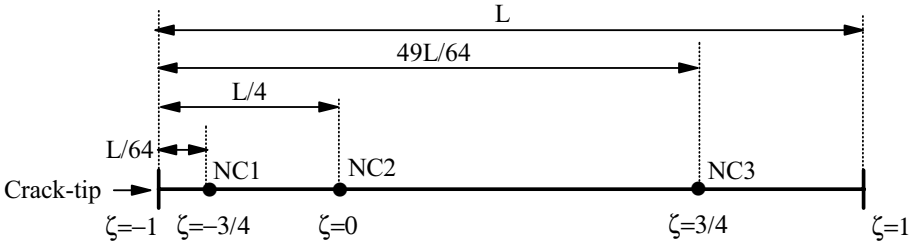

Fig. 5.6 Configuration of quarter-point element

5.8.2 An alternative crack-tip element

To effectively evaluate crack-tip fields, Pan [11] constructed the following crack-tip element with its tip at ζ=-1

$$\Delta\mathbf{U}=\sum_{k=1}^{3}\Phi_k\Delta\mathbf{U}^k \tag{5.199}$$

where the superscript k (k=1,2,3) denotes the GRCD at nodes ζ=-2/3,0,2/3, respectively. The shape functions Φ_k are defined by [11]

$$\begin{aligned}\Phi_1&=\frac{3\sqrt{3}}{8}\sqrt{\zeta+1}[-5+18(\zeta+1)-9(\zeta+1)^2],\\ \Phi_2&=\frac{1}{4}\sqrt{\zeta+1}[5-8(\zeta+1)+3(\zeta+1)^2],\\ \Phi_3&=\frac{3\sqrt{3}}{8\sqrt{5}}\sqrt{\zeta+1}[1-4(\zeta+1)+3(\zeta+1)^2],\end{aligned} \tag{5.200}$$

For the GSIF calculation, Pan [11] employed the extrapolation method of the GRCD, which requires an analytical relation between the generalized displacement and the GSIF. This relation can be expressed as

$$\Delta\mathbf{U}(r)=2\sqrt{\frac{2r}{\pi}}(i\mathbf{A}\mathbf{B}^{-1})\mathbf{K} \tag{5.201}$$

where **K** is defined in Eq (5.198).

5.8.3 8-node crack element

For a 3D cracked piezoelectric solid, Wippler and Kuna [36] developed a set of 8-node quadrilateral elements including regular elements and non-conformal elements. The regular element is used to model a smooth surface, while the non-conformal element is used to model surfaces with edges and corners. Special crack front elements modeling the radial dependence of the field quantities around the crack front are used in the vicinity of cracks. Fig. 5.7 shows the possible element types and their node and side numbering for the geometry discretization.

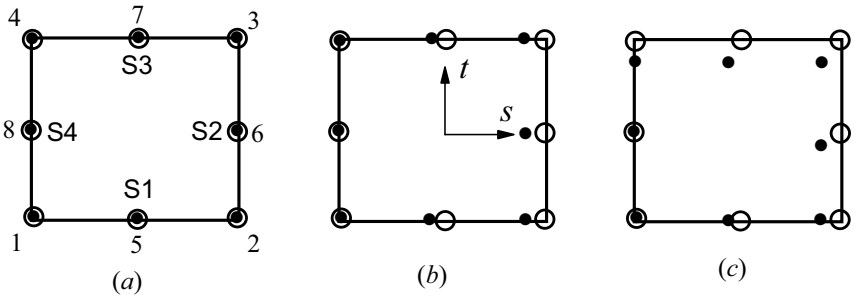

Fig. 5.7 Types of conformal and non-conformal boundary elements

In this setting the shape functions for a regular element are defined by Eq (5.107). For non-conformal interpolation the node coordinates depend on the discontinuous side. If, for example, element four (S4) is the discontinuous element, the node coordinates are

$$\begin{aligned} s_N &= \{-\Delta,\ 1,\ 1,\ -\Delta,\ 0.5(-\Delta+1),\ 1,\ 0.5(-\Delta+1),\ -\Delta\} \\ t_N &= \{-1,\ -1,\ 1,\ 1,\ -1,\ 0,\ 1,\ 0\} \end{aligned} \tag{5.202}$$

which leads the discontinuous shape functions used near edges and corners. Δ is the discontinuity parameter ($\Delta<1$). Following this scheme the discontinuities required for each side can be established separately. To emphasize again, the geometry is still interpolated with respect to the unshifted nodes.

To obtain the r-dependent discontinuous shape functions for displacement interpolation $N_i^{(U)}$ Wippler and Kuna [36] assumed

$$N_i^{(U)}(r,t) = a_1^i + a_2^i\sqrt{r} + a_3^i t + a_4^i r + a_5^i t^2 + a_6^i t\sqrt{r} + a_7^i rt + a_8^i t^2\sqrt{r} \tag{5.203}$$

where $r=1+s$, and a_j^i are determined by the condition [37]

$$N_i(s_j,t_j) = \delta_{ij}\ \ (i,j=1,2,\ldots 8) \tag{5.204}$$

with

$$N_i\,(s,t) = a_1^i + a_2^i s + a_3^i t + a_4^i s^2 + a_5^i t^2 + a_6^i st + a_7^i s^2 t + a_8^i t^2 s \tag{5.205}$$

These crack front elements possess $\sqrt{r}$ behavior of displacement and electric potential with respect to one element side. Depending on the side which is adjacent to the crack front, r can also be (1-s), (1+t), or (1-t). To incorporate the $r^{-1/2}$ behavior of the generalized tractions at the ligament ahead of the crack front, Eq (5.203) is divided by $\sqrt{r}$, giving the shape function $N_i^{(T)}$ [36]:

$$N_i^{(T)}(r,t)=\frac{a_1^i}{\sqrt{r}}+a_2^i+\frac{a_3^i t}{\sqrt{r}}+a_4^i\sqrt{r}+\sqrt{r}+a_6^i t+a_7^i t\sqrt{r}+a_8^i t^2 \tag{5.206}$$

If symmetry planes and free faces intersect the crack front, a new element is required with the *r*-dependence being with respect to one corner node only [36]:

$$N_i^{(SU)}(r,\alpha)=a_1^i+a_2^i\sqrt{r}+a_3^i\alpha+a_4^i r+a_5^i\alpha^2+a_6^i\alpha\sqrt{r}+a_7^i r\alpha+a_8^i\alpha^2\sqrt{r} \tag{5.207}$$

where $r=\sqrt{(1+s)^2+(1+t)^2}$ and $\alpha=\arctan[(1+t)/(1+s)]$, the superscript *S* here standing for symmetry plane or surface. The corresponding generalized traction can be approximated by the following shape functions

$$N_i^{(SU)}(r,\alpha)=\frac{a_1^i}{\sqrt{r}}+a_2^i+\frac{a_3^i\alpha}{\sqrt{r}}+a_4^i\sqrt{r}+\frac{a_5^i\alpha^2}{\sqrt{r}}+a_6^i\alpha+a_7^i\alpha\sqrt{r}+a_8^i\alpha^2 \tag{5.208}$$

where α is the angle around the node of singularity.

5.9 Mixed BEM-homogenization method

The BE formulation described in the previous sections can be used to predict effective material properties of piezoelectric composites by means of the homogenization approach. The homogenization model is used to establish the relationship between overall material properties and boundary fields for composites with inhomogeneities, and introducing the BE formulation can predict the numerical results of the boundary fields.

5.9.1 Basic concept of effective material properties

Let us consider a piezoelectric composite in which the inclusions or holes are of cylindrical shape. In this case both the matrix and the inclusion can be viewed as transversely isotropic, and coupling occurs between in-plane stresses and in-plane electric fields. For a Cartesian coordinate system *Oxyz*, choose the *z*-axis as the poling direction, and denote the coordinates *x* and *z* by x_1 and x_2 to achieve a compact notation. The plane strain constitutive equations are expressed by Eqs (1.144) and (1.145). These two equations can be written in matrix form as follows [38]

$$\mathbf{\Pi}=\mathbf{C}\mathbf{Z},\quad \mathbf{Z}=\mathbf{F}\mathbf{\Pi} \tag{5.209}$$

where $\mathbf{F}=\mathbf{C}^{-1}$, and

$$\mathbf{\Pi}=\{\Pi_i\}^T=\{\sigma_{11}\sigma_{22}\sigma_{12}D_1D_2\}^T,\ \mathbf{Z}=\{Z_i\}^T=\{\varepsilon_{11}\varepsilon_{22}2\varepsilon_{12}-E_1-E_2\}^T \tag{5.210}$$

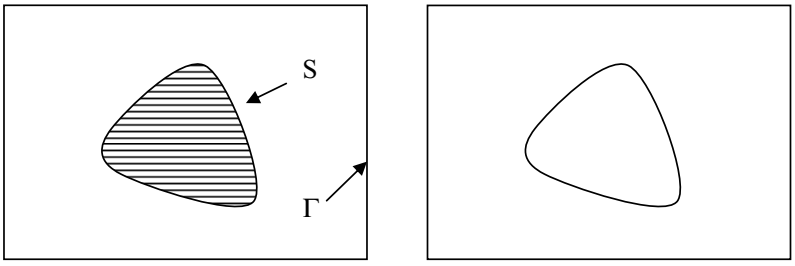

(a) RVE with an inclusion (b) RVE with a void

Fig. 5.8 Two RVE models

The homogenization formulation is established by considering a representative volume element (RVE) Ω which is chosen so as to be statistically representative of the two-phase composite. In particular, the characteristic size of the heterogeneities needs to be small with respect to the dimension of the RVE, which in turn needs to be small compared to the wavelength of the macroscopic structure.

To understand the key point of the homogenization procedure, consider a RVE consisting of the matrix material and inclusion phase (see Fig. 5.8). As the RVE is comprised of different materials, the micro-constitutive law that governs each material or phase in a RVE is given by the standard constitutive law. On the other hand, the stress and electric displacement (SED) and strain and electric field (SEF) on the macro-level are directly associated with the global analysis of a two-phase composite. On the macro-level, the RVE is regarded as just a point with a homogenized constitutive law. The macro SED, $\overline{\Pi}_i$, is usually defined as the volume average of SED in a RVE, $\langle \Pi_i \rangle$, as follows

$$\overline{\Pi}_i = \langle \Pi_i \rangle_\Omega = \frac{1}{V} \int_\Omega \Pi_i d\Omega \tag{5.211}$$

where Ω represents the domain of the RVE and V is its volume. Similarly, the volume average of SEF $\overline{Z}_i$ and the volume average of free energy density $\overline{W}$ in a RVE is defined by

$$\overline{Z}_i = \langle Z_i \rangle_\Omega = \frac{1}{V} \int_\Omega Z_i d\Omega \tag{5.212}$$

$$\begin{aligned} \overline{W} &= \frac{1}{V} \int_\Omega W d\Omega = \frac{1}{2V} \int_\Omega \Pi_i Z_i d\Omega \\ &= \frac{1}{2V} \int_\Omega C_{ij} Z_i Z_j d\Omega = \frac{1}{2V} \int_\Omega F_{ij} \Pi_i \Pi_j d\Omega \end{aligned} \tag{5.213}$$

where $(\mathbf{C})_{ij} = C_{ij}$ and $(\mathbf{F})_{ij} = F_{ij}$ are, respectively, local stiffness and local compliance coefficients which are different from phase to phase. Moreover, the macroscopic strain energy should satisfy

$$\overline{W} = \frac{1}{2} \overline{\Pi}_i \overline{Z}_i \tag{5.214}$$

The effective properties represented by effective stiffness C_{ij}^* or compliancy F_{ij}^* of the piezoelectric composites can be defined by the average SED and SEF as

$$\overline{\Pi}_i = C_{ij}^* \overline{Z}_j, \quad \overline{Z}_i = F_{ij}^* \overline{\Pi}_j \tag{5.215}$$

or by the equivalence of the free strain energy

$$\frac{1}{2} \overline{\Pi}_i \overline{Z}_i = \frac{1}{2V} \int_\Omega \Pi_i Z_i d\Omega \tag{5.216}$$

or

$$\frac{1}{2} \overline{C}_{ij} \overline{Z}_i \overline{Z}_j = \frac{1}{2V} \int_\Omega C_{ij} Z_i Z_j d\Omega \tag{5.217}$$

The linearity of the stress-strain relation for elastic bodies leads to

$$\overline{C}_{ij} = \frac{\partial^2 \overline{W}}{\partial \overline{Z}_i \partial \overline{Z}_j} \tag{5.218}$$

Then an explicit form of the effective stiffness components can be evaluated as below.

5.9.2 Homogenization model

The homogenization method for a composite with defects has been discussed in [39,40]. For the reader's convenience we describe the method here briefly.

For piezoelectric materials with inclusions or microcavities, the homogenization theory may be applied based on some fundamental results in the theory of two-phase linear piezoelectric media. In the case of two-phase materials, the volume average of SED and SEF tensors is defined by [38]

$$\langle \mathbf{\Pi} \rangle = v^{(1)} \langle \mathbf{\Pi}^{(1)} \rangle + v^{(2)} \langle \mathbf{\Pi}^{(2)} \rangle, \quad \langle \mathbf{Z} \rangle = v^{(1)} \langle \mathbf{Z}^{(1)} \rangle + v^{(2)} \langle \mathbf{Z}^{(2)} \rangle \tag{5.219}$$

where superscripts $^{(1)}$ and $^{(2)}$ denote the matrix and inclusion phases, $v^{(1)}$ and $v^{(2)}$ their volume fractions. Substituting Eq (5.219) into Eq (5.215) and noting that $\mathbf{\Pi}^{(i)} = \mathbf{C}^{(i)}\mathbf{Z}^{(i)}$, we have

$$\mathbf{C}^* = \mathbf{C}^{(1)} + (\mathbf{C}^{(2)} - \mathbf{C}^{(1)})\mathbf{A}^{(2)} v^{(2)}, \quad \mathbf{F}^* = \mathbf{F}^{(1)} + (\mathbf{F}^{(2)} - \mathbf{F}^{(1)})\mathbf{B}^{(2)} v^{(2)} \tag{5.220}$$

in which the symmetric tensors $\mathbf{A}^{(2)}$ and $\mathbf{B}^{(2)}$ are defined by the linear relations

$$\langle \mathbf{Z}^{(2)} \rangle = \mathbf{A}^{(2)} \mathbf{Z}^0, \qquad \langle \mathbf{\Pi}^{(2)} \rangle = \mathbf{B}^{(2)} \mathbf{\Pi}^0 \tag{5.221}$$

with $\mathbf{Z}^0$ and $\mathbf{\Pi}^0$ being remote SEF and SED fields applied on the effective medium. The interpretation of $\langle \mathbf{Z}^{(2)} \rangle$ in Eq (5.221) follows from the average strain theorem

$$\langle Z_{ij}^{(2)} \rangle = \frac{1}{2\Omega_2} \int_{\partial\Omega_2} \{[1 + H(i-3)] U_i n_j + U_j n_i) d\Omega \tag{5.222}$$

where Ω_2 and $\partial\Omega_2$ are the total volume and boundary of the inclusion or void, $H(i)$ is the Heaviside step function, $\mathbf{n}=\{n_1,n_2,0\}^T$ is the normal local to inclusion surface, and

$$\{Z_{11}, Z_{22}, 2Z_{12}, Z_{31}, Z_{32}\} = \{\varepsilon_{11}, \varepsilon_{22}, 2\varepsilon_{12}, -E_1, -E_2\}, \qquad \{U_i\} = \{u_1, u_2, \phi\} \tag{5.223}$$

We now consider the case when inclusions become voids which are thought of as being filled with air. This implies that $\mathbf{C}^{(2)} \to 0$, $\mathbf{F}^{(2)} \to \infty$. Thus we assume that $\mathbf{C}^{(2)}=0$, where $\mathbf{C}^{(2)}$ stands for the stiffness constants of the void-phase. Then Eq (5.220) become

$$\mathbf{C}^* = \mathbf{C}^{(1)}(\mathbf{I} - \mathbf{A}^{(2)} v^{(2)}), \quad \mathbf{F}^* = \mathbf{F}^{(1)}(\mathbf{I} + \mathbf{B}^{(0)} v^{(2)}) \tag{5.224}$$

where $\mathbf{I}$ is the unit tensor and $\mathbf{B}^{(0)}$ is defined by

$$\langle \mathbf{Z}^{(2)} \rangle = \mathbf{F}^{(1)} \mathbf{B}^{(0)} \mathbf{\Pi}^0 \tag{5.225}$$

Therefore, the estimation of integral (5.222) and thus $\mathbf{A}^{(2)}$ is the key to predicting the effective electroelastic moduli $\mathbf{C}^*$. The calculation of integral (5.222) through use of BEM is the subject of the next section.

5.9.3 BE equations

Noting that Eq (5.222) contains unknown variables on the boundary only, the BE equation (5.116) can be used to evaluate the displacements and electric potential on the boundary $\partial\Omega$. The two subdomains of the RVE shown in Fig. 5.8 are separated by the interfaces *S* between fiber and matrix (see Fig. 1). Each subdomain can be separately modeled by Eq (5.116). Global assembly of the BE subdomains is then performed by enforcing continuity of the DEP and SED at the subdomain interface.

In a two-phase piezoelectric composite, the BE formulation (5.116) takes the form

$$\mathbf{C}^{(\alpha)}(\hat{\mathbf{x}}_i)\mathbf{U}^{(\alpha)}(\hat{\mathbf{x}}_i)+\sum_{j=1}^{N} H_{ij}^{(\alpha)}\mathbf{U}^{(\alpha)j}=\sum_{j=1}^{N} G_{ij}^{(\alpha)}\mathbf{T}^{(\alpha)j} \tag{5.226}$$

where no generalized body force is assumed, the superscript (α) stands for the quantity associated with the αth phase, (α=1 being matrix and α=2 being fiber), and

$$S^{(\alpha)}=\begin{cases} S+\Gamma & \alpha=1 \\ S & \alpha=2 \end{cases} \quad c^{(\alpha)}(\boldsymbol{\xi})=\begin{cases} 1 & \text{if } \boldsymbol{\xi}\in\Omega^{(\alpha)} \\ 0.5 & \text{if } \boldsymbol{\xi}\in S^{(\alpha)}\ (S^{(\alpha)} \text{ smooth}) \\ 0 & \text{if } \boldsymbol{\xi}\notin\Omega^{(\alpha)}\cup S^{(\alpha)} \end{cases} \tag{5.227}$$

in which Γ and *S* are the boundaries of the RVE and inclusions, respectively (see Fig. 5.8a).

When the inclusion in Fig. 5.8a becomes a hole, the boundary integral equation (5.226) still holds true if one takes α=1 only. In this case the interfacial continuity condition is replaced by the hole boundary condition: $\mathbf{T}^{j}=0$ along the boundary S (Fig. 5.8b).

5.9.4 Algorithms for self-consistent and Mori-Tanaka approaches

(a) Self-consistent BEM approach.

As stated in [41,42], in the self-consistent method, for each inclusion (or hole), the effect of inclusion (or hole) interaction is taken into account approximately by embedding each inclusion (or hole) in the effective medium whose properties are unknown. In this case, the material constants appearing in the BE formulation (5.226) are unknown. Consequently, a set of initial trial values of the effective properties is needed and an iteration algorithm is required. The algorithm is described in detail here.

(a) Assume initial values of material constants $\mathbf{C}^{*}_{(0)}$

(b) Solve Eq (5.226) for $\mathbf{U}_{(i)}$ using the values of $\mathbf{C}^{*}_{(i-1)}$, where the subscript "(*i*)" stands for the variable associated with the *i*th iterative cycle.

(c) Calculate $\mathbf{A}^{(2)}_{(i)}$ in Eq (5.221) by way of Eq (5.222) and using the current values of $\mathbf{U}_{(i)}$, and then determine $\mathbf{C}^{*}_{(i)}$ by way of Eq (5.224).

(d) If $\varepsilon_{(i)}=\left\|\mathbf{C}^{*}_{(i)}-\mathbf{C}^{*}_{(i-1)}\right\|/\left\|\mathbf{C}^{*}_{(0)}\right\|\le\varepsilon$, where ε is a convergent tolerance, terminate the iteration; otherwise take $\mathbf{C}^{*}_{(i)}$ as the initial value and go to step (b).

(b) Mori-Tanaka-BEM approach

The key assumption in Mori-Tanaka theory [40] is that the concentration matrix $\mathbf{A}^{(2)}_{MT}$ (here we use $\mathbf{A}^{(2)}_{MT}$, rather than $\mathbf{A}^{(2)}$ to distinguish it from $\mathbf{A}^{(2)}$ in Section 5.8.2) is given by the solution for a single inclusion (or void) embedded in an intact solid subject to an applied strain field equal to the as yet unknown average field in the

composite, which means that the introduction of inclusions in the composite results in a value of $\overline{\mathbf{Z}}^{(2)}$ given by

$$\overline{\mathbf{Z}}^{(2)} = \mathbf{A}_{DIL}^{(2)} \overline{\mathbf{Z}}^{(1)} \tag{5.228}$$

where $\mathbf{A}_{DIL}^{(2)}$ is the concentration matrix related to the dilute model, which can be calculated by way of Eqs (5.221), (5.222) and (5.226). In this case, the material constants appearing in the BE formulation (5.226) are all known. As such, it is easy to prove that [40,41]

$$\mathbf{A}_{MT}^{(2)} = \mathbf{A}_{DIL}^{(2)} (v_1 \mathbf{I} + v_2 \mathbf{A}_{DIL}^{(2)})^{-1} \tag{5.229}$$

It can be seen from Eq (5.229) that the Mori-Tanaka approach provides explicit expressions for effective constants of a defective piezoelectric solid. Therefore, no iteration is required with the Mori-Tanaka-BEM.

5.10 Numerical assessments

To illustrate the application of the element model described above, three examples are presented. The first example deals with a piezoelectric column subjected to tension at the two ends of the column, the second treats an infinite piezoelectric solid with a horizontal finite crack, and the third illustrates the behavior of crack tip fields in a skew-cracked rectangular panel.

5.10.1 A piezoelectric column under uniaxial tension [6]

In this example, a piezoelectric prism under simple extension is considered (see Fig. 5.9). The size of the prism is $2a \times 2a \times 2b$. The corresponding boundary conditions are given by

$$\sigma_z = p, \quad \sigma_{xz} = \sigma_{yz} = D_z = 0, \quad \text{for } z = \pm b,$$

$$\phi = 0, \quad \text{for } z = 0$$

$$\sigma_x = \sigma_{xz} = D_x = 0, \quad \text{for } x = \pm a$$

$$\sigma_y = \sigma_{yz} = D_y = 0, \quad \text{for } y = \pm a$$

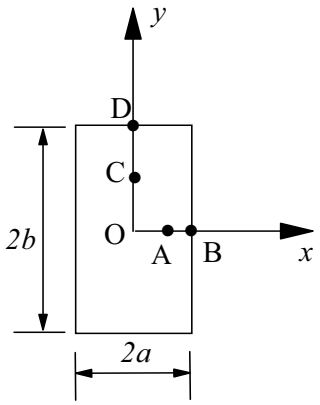

Fig. 5.9 Geometry of the piezoelectric prism

In the calculation, $2a$=3m, $2b$=10m, and $p = 100\text{Nm}^2$ are assumed and 32 elements

are used [6]. The material considered is PZT-4 whose material parameters are

$$c_{11} = 13.9\times10^{10}\,\mathrm{Nm}^{-2},\ c_{12} = 7.78\times10^{10}\,\mathrm{Nm}^{-2},\ c_{13} = 7.43\times10^{10}\,\mathrm{Nm}^{-2}$$

$$c_{33} = 11.5\times10^{10}\,\mathrm{Nm}^{-2},\ c_{44} = 2.56\times10^{10}\,\mathrm{Nm}^{-2},\ e_{15} = 12.7\mathrm{Cm}^{-2}$$

$$e_{31} = -5.2\mathrm{Cm}^{-2},\ e_{33} = 15.1\mathrm{Cm}^{-2},\ \kappa_{11} = 730\kappa_0,\ \kappa_{33} = 635\kappa_0$$

where $\kappa_0 = 8.854\times10^{-12}\,\mathrm{C}^2/\mathrm{Nm}^2$. Table 5.1 lists the displacements and electric potential at points A(2,0), B(3,0), C(0,5), and D(0,10) using BEM, and comparison is made with analytical results. It is found that the BEM results are in good agreement with the analytical results even when only six boundary elements are used in the calculation [6].

Table 5.1 u_1, u_2 and ϕ of BEM results and comparison with exact solution [6]

Point		A(2,0)	B(3,0)	C(0,5)	D(0,10)
BEM	$u_1\times10^{10}$ (m)	-0.9665	-1.4502	0	0
	$u_2\times10^{9}$ (m)	0	0	0.4997	1.0004
	ϕ(V)	0	0	0.6879	1.3762
Exact [6]	$u_1\times10^{10}$ (m)	-0.9672	-1.4508	0	0
	$u_2\times10^{9}$ (m)	0	0	0.5006	1.0011
	ϕ(V)	0	0	0.6888	1.3775

5.10.2 A horizontal finite crack in an infinite piezoelectric solid [11]

The second example is a finite horizontal crack along the *x*-direction in an infinite PZT-4 medium under a uniform far-field stress or electric displacement. Pan [11] used 20 discontinuous quadratic elements as described in Section 5.7.2 to discretize the crack surface which has a length of 2*a* (=1m). Tables 5.2 and 5.3 list the GRCD caused by a far-field stress σ_{yy} (=1N/m^2) and a far-field electric displacement D_y (=1C/m^2), and comparison is made with analytical results. It is obvious that a far-field stress induces a non-zero $\Delta\phi$ even though the corresponding K_{IV} is zero. Similarly, a far-field electric displacement can induce a non-zero Δu_y.

5.10.3 A rectangular piezoelectric solid with a central inclined crack [13]

The third example is a rectangular piezoelectric solid with a central crack (a =0.1m) inclined $\theta = 45^\circ$ with respect to the positive *x*-direction. The ratios of crack length to width and of height to width are a/w = 0.2 and h/w = 2, respectively (see Fig. 5.10). The analysis is carried out for the rectangle loaded by a uniform tension and electric displacement applied in the *y*-direction. Table 5.4 lists the normalized GSIF for the two loading conditions considered and the results obtained are compared with those given by Pan [11], who used 10 discontinuous quadratic elements on the crack surfaces and 32 quadratic elements on the outside boundaries in his analysis. Tables 5.5 and 5.6 give the corresponding GRCD. In Table 5.4, D^* is a nominal electric displacement expressed in the unit of C/m^2 with its amplitude equal to that of σ_{yy} expressed in N/m^2, and σ^* is a nominal stress expressed in the unit of N/m^2 with its amplitude equal to that of D_y expressed in C/m^2.

Table 5.2 GRCD caused by a far-field σ_{yy} (=1N/m^2)[11]

	Δu_y (10^{-12} m)		$\Delta\phi$(10^{-1} V)	
x(m)	BEM	analytical	BEM	analytical
0.492	0.032	0.032	0.040	0.040
0.425	0.094	0.093	0.116	0.116
0.358	0.124	0.124	0.154	0.154
0.292	0.144	0.144	0.179	0.179
0.225	0.158	0.158	0.197	0.197
0.158	0.168	0.168	0.210	0.210
0.092	0.174	0.174	0.217	0.217
0.025	0.177	0.177	0.221	0.221

Table 5.3 GRCD caused by a far-field D_y (=1C/m^2) [11]

	$\Delta\phi$(10^8 V)		Δu_y (10^{-1} m)	
x(m)	BEM	analytical	BEM	analytical
0.492	0.161	0.160	0.040	0.040
0.425	0.466	0.465	0.116	0.116
0.358	0.616	0.616	0.154	0.154
0.292	0.717	0.717	0.179	0.179
0.225	0.789	0.789	0.197	0.197
0.158	0.838	0.838	0.210	0.210
0.092	0.868	0.868	0.217	0.217
0.025	0.882	0.882	0.221	0.221

Table 5.4 GSIF for cracked rectangle loaded by σ_y or D_y

		$K_I / \sigma_y\sqrt{\pi a}$	$K_{II} / \sigma_y\sqrt{\pi a}$	$K_{IV} / D^*\sqrt{\pi a}$
Loaded by σ_y	Ref[11]	0.5303	0.5151	-2.97×10^{-12}
	Ref[13]	0.5292	0.5163	-2.79×10^{-12}
		$K_I / \sigma^*\sqrt{\pi a}$	$K_{II} / \sigma^*\sqrt{\pi a}$	$K_{IV} / D_y\sqrt{\pi a}$
Loaded by D_y	Ref[11]	-1.42×10^6	1.69×10^5	-0.7278
	Ref[13]	-1.44×10^6	1.64×10^5	-0.7283

It can be seen from Table 5.4 that an electric load of D_y (=1C/m2) can produce very large mechanical stress intensity factors. Conversely, the electric displacement intensity factor due to mechanical loads is usually negligible. This phenomenon indicates clearly that crack initiation criteria based on a single SIF cannot be simply extended to the piezoelectric case. It is also found from Tables 5.5 and 5.6 that a mechanical load can induce relative crack electric potential and, vice versa, an electric load can give rise to relative crack displacement.

Table 5.5 GRCD for cracked rectangle caused by a far-field σ_{yy} (=1N/m^2) [13]

$x=y(10^{-1}\text{m})$	$\Delta u_x(10^{-13}\text{m})$	$\Delta u_y(10^{-11}\text{m})$	$\Delta\phi(10^{-2}\text{V})$
0.477	0.256	-0.190	0.232
0.424	0.279	-0.206	0.252
0.371	0.299	-0.219	0.268
0.318	0.315	-0.230	0.281
0.265	0.328	-0.239	0.292
0.212	0.339	-0.246	0.300
0.159	0.347	-0.251	0.307
0.106	0.352	-0.255	0.312
0.053	0.356	-0.257	0.314

Table 5.6 GRCD for cracked rectangle caused by a far-field D_y (=1C/m^2) [13]

$x=y(10^{-1}\text{m})$	$\Delta u_x(10^{-5}\text{m})$	$\Delta u_y(10^{-2}\text{m})$	$\Delta\phi(10^{8}\text{V})$
0.477	0.353	0.232	0.093
0.424	0.371	0.252	0.100
0.371	0.385	0.268	0.107
0.318	0.391	0.281	0.112
0.265	0.406	0.292	0.116
0.212	0.410	0.300	0.120
0.159	0.416	0.307	0.123
0.106	0.420	0.312	0.125
0.053	0.431	0.314	0.126

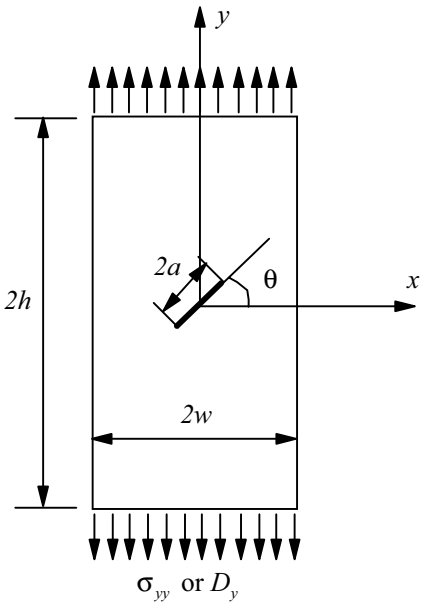

Fig. 5.10 Finite rectangular solid with an inclined crack under uniform tension or electric displacement in the *y*-direction

5.10.4 A magneto-electro-elastic column [21]

The example taken from Ding and Jiang [21] is a magneto-electro-elastic column of size $a\times b$ under uniform axial tension, electric displacement or magnetic induction. The problem is treated as a plane-strain one and three load cases are considered. The material properties used in the numerical calculation are as follows

$$c_{11}=16.6\times10^{10}\ \text{Nm}^{-2},\ c_{12}=7.7\times10^{10}\ \text{Nm}^{-2},\ c_{13}=7.8\times10^{10}\ \text{Nm}^{-2}$$

$$c_{33}=16.2\times10^{10}\ \text{Nm}^{-2},\ c_{44}=4.3\times10^{10}\ \text{Nm}^{-2},\ c_{66}=4.45\times10^{10}\ \text{Nm}^{-2},$$

$$e_{15}=11.6\ \text{Cm}^{-2},\ e_{31}=-4.4\ \text{Cm}^{-2},\ e_{33}=18.6\ \text{Cm}^{-2},$$

$$\tilde{e}_{15}=550\ \text{N/(A m)},\ \tilde{e}_{31}=580.3\ \text{N/(A m)},\ \tilde{e}_{33}=699.7\ \text{N/(A m)},$$

$$\kappa_{11}=1.12\times10^{-8}\ \text{C/(V m)},\ \kappa_{33}=1.26\times10^{-8}\ \text{C/(V m)},$$

$$\alpha_{11}=5.0\times10^{-12}\ \text{N s/(V C)},\ \alpha_{33}=3.0\times10^{-12}\ \text{N s/(V C)},$$

$$\mu_{11}=5.0\times10^{-6}\ \text{N s}^2/\text{C}^2,\ \mu_{33}=10\times10^{-6}\ \text{N s}^2/\text{C}^2,$$

and the boundary conditions of this problem can be written as

$z=\pm b/2$:

$$\sigma_{zz}=P_0,\ D_z=0,\ B_z=0,\quad \text{(for load case 1)}$$
$$\sigma_{zz}=0,\ D_z=D_0,\ B_z=0,\quad \text{(for load case 2)}$$
$$\sigma_{zz}=0,\ D_z=0,\ B_z=B_0,\quad \text{(for load case 3)}$$

$x=\pm a/2$:

$$\sigma_{xx}=\sigma_{xz}=D_x=B_x=0\quad \text{(for all load cases)}$$

In the numerical analysis, the solution domain is modeled by 28 linear boundary elements. The values of a, b, P_0, D_0, and B_0 are assumed to be:

$$a=0.6\ \text{m},\ b=0.02\ \text{m},\ P_0=10\ \text{Pa},\ D_0=10^{-10}\ \text{C m}^{-2},B_0=10^{-8}\ \text{N/(A m)}$$

The numerical results at the central point (a/2, b/2) obtained from the boundary formulation described in Section 5.2.3 are listed in Table 5.7 and comparison is made with the exact results.

Table 5.7 Numerical and analytical results of column

variables	Load case 1		2		3	
	BEM	Exact[21]	BEM	Exact[21]	BEM	Exact[21]
$u\times10^{12}$	-9.501	-9.500	-0.2107	-0.2108	0.5077	0.5077
$w\times10^{12}$	0.5680	0.5683	0.0095	0.0095	0.0214	0.0214
$\phi\times10^{4}$	9.495	9.495	-0.6289	-0.6289	0.2564	0.2567
$\psi\times10^{5}$	2.138	2.139	0.0257	0.0257	-0.7520	-0.7521

5.10.5 A simply supported beam of magneto-electro-elastic material [21]

This example is also taken from [21] in which a simply supported rectangular beam of length L, height h and width b is considered. It is subjected to uniformly distributed loads on the upper and lower surfaces. The problem is treated as a plane-stress one and the boundary conditions are

$z=h/2$: $\sigma_{zz}=q_0\sin(\pi x/L),\quad \sigma_{xz}=D_z=B_z=0,$

$z = -h/2$: $\sigma_{zz} = \sigma_{xz} = D_z = B_z = 0,$

$x = 0,\ L$: $\sigma_{xx} = w = \phi = \psi = 0.$

The material properties are the same as those used in Section 5.9.4, and other parameters are assumed to be L=0.2 m, h =0.02 m, b =0.001 m, and $q_0 = -10$ Pa. Eight linear elements are used to model this problem. Table 5.8 lists the boundary element results at four reference points and comparison is made with the analytical results. Coordinates of the four points are, respectively, A(0.1, 0), B(0.125, 0), and C(0.15, 0).

Table 5.8 Numerical and analytical results of rectangular beam

variables	point A		B		C	
	BEM	Exact[21]	BEM	Exact[21]	BEM	Exact[21]
$w\times10^{9}$	-1.977	-2.000	-1.796	-1.847	-1.378	-1.414
$\phi\times10^{2}$	-2.300	-2.314	-2.123	-2.138	-1.625	-1.637
$\psi\times10^{3}$	-1.794	-1.808	-1.588	-1.671	-1.258	-1.279
σ_{zz}	-4.9969	-5.0000	-4.6168	-4.6190	-3.5336	-3.5351
$D_z\times10^{11}$	-1.113	-1.114	-1.032	-1.029	-0.7896	-0.7875
$B_z\times10^{10}$	-2.254	-2.282	-2.114	-2.109	-1.619	-1.614
$\sigma_{xx}\times10^{2}$	2.796	2.818	2.583	2.604	1.976	1.993

References

[1] Lee JS and Jiang, LZ, A boundary integral formulation and 2D fundamental solution for piezoelectric media, Mech Res Comm, 21, 47-54, 1994

[2] Lee JS, Boundary element method for electroelastic interaction in piezoceramics, Eng Analysis Boun Elements, 15, 321-328, 1995

[3] Denda M and Mansukh M, Upper and lower bounds analysis of electric induction intensity factors for multiple piezoelectric cracks by the BEM, Eng Analysis Boun Elements, 29, 533-550, 2005

[4] Sanz JA, Ariza MP and Dominquez J, Three-dimensional BEM for piezoelectric fracture analysis, Eng Analysis Boun Elements, 29, 586-596, 2005

[5] Lu P and Mahrenholtz O, A variational boundary element formulation for piezoelectricity, Mech Res Comm, 21, 605-611, 1994

[6] Ding HJ, Wang GP and Chen WQ, Boundary integral formulation and 2D fundamental solutions for piezoelectric media, Comp Meth Appl Mech Eng, 158, 65-80, 1998

[7] Rajapakse RK, Boundary element methods for piezoelectric solids, *Procs of SPIE, Mathematics and Control in Smart Structures*, 3039, 418-428, 1997

[8] Xu XL and Rajapakse RKND, Boundary element analysis of piezoelectric solids with defects, *Composites Part B: Engineering*, 29, 655-669, 1998

[9] Rajapakse RKND and Xu XL, Boundary element modeling of cracks in piezoelectric solids, Eng Analysis Boun Elements, 25, 771-781, 2001

[10] Liu YJ and Fan H, On the conventional boundary integral formulation for piezoelectric solids with defects or of thin shapes, Eng Analysis Boun Elements, 25, 77-91, 2001

[11] Pan E, A BEM analysis of fracture mechanics in 2D anisotropic piezoelectric

solids, Eng Analysis Boun Elements, 23, 67-76, 1999
[12] Denda M and Lua J, Development of the boundary element method for 2D piezoelectricity, Composites: Part B, 30, 699-707, 1999
[13] Davi G and Milazzo A, Multidomain boundary integral formulation for piezoelectric materials fracture mechanics, Int J Solids Srtuc, 38, 7065-7078, 2001
[14] Groh U and Kuna M, Efficient boundary element analysis of cracks in 2D piezoelectric structures, Int J Solids Srtuc, 42, 2399-2416, 2005
[15] Zhao MH, Fang PZ and Shen YP, Boundary integral-differential equations and boundary element method for interfacial cracks in three-dimensional piezoelectric media, Eng Analysis Boun Elements, 28, 753-762, 2004
[16] Liew KM and Liang J, Modeling of 3D transversely piezoelectric and elastic bimaterials using the boundary element method, Computa Mech, 29, 151-162, 2002
[17] Ding HJ, Chen B and Liang J, On the Green's functions for two-phase transversely isotropic piezoelectric media, Int J Solids Srtuc, 34, 3041-3057, 1997
[18] Khutoryaansky N, Sosa H and Zu WH, Approximate Green's functions and a boundary element method for electroelastic analysis of active materials, Compu Struct, 66, 289-299, 1998
[19] Jiang LZ, Integral representation and Green's functions for 3D time-dependent thermo-piezoelectricity, Int J Solids Struc, 37, 6155-6171, 2000
[20] Kogl M and Gaul L, A boundary element method for transient piezoelectric analysis, Eng Analysis Boun Elements, 24, 591-598, 2000
[21] Ding HJ and Jiang AM, A boundary integral formulation and solution for 2D problems in magnetoelectroelastic media, Comput Struct, 82, 1599-1607, 2004
[22] Chen T and Lin FZ, Boundary integral formulations for three-dimensional anisotropic piezoelectric solids, Computa Mech, 15, 485-496, 1995
[23] Ding HJ and Jiang J, The fundamental solution for transversely isotropic piezoelectricity and boundary element method, Comput Struct, 71, 447-455, 1999
[24] Ding HJ, Chen WQ and Jiang AM, Green's functions and boundary element method for transversely isotropic piezoelectric materials, Eng Analysis Boun Elements, 28, 975-987, 2004
[25] Chen MC, Application of finite part integrals to the three-dimensional fracture problems for piezoelectric media, Part I: hypersingular integral equation and theoretical analysis. Int J Frac, 121, 133-148, 2003
[26] Chen MC, Application of finite part integrals to the three-dimensional fracture problems for piezoelectric media, Part II: numerical analysis. Int J Frac, 121, 149-161, 2003
[27] Liew KM and Liang J, Three-dimensional piezoelectric boundary element analysis of transversely isotropic half-place, Computa Mech, 32, 29-39, 2003
[28] Garcia-Sanchez F, Saez A and Dominguez J, Anisotropic and piezoelectric materials fracture analysis by BEM, Comput Struct, 83, 804-820, 2005
[29] Schclar NA, Anisotropic analysis using boundary elements, Computational Mechanics Publications, Southampton, 1994
[30] Tanaka K and Tanaka M, A boundary element formulation in linear piezoelectric problems, J Appl Math Phys (ZAMP), 31, 568-580, 1980
[31] Wang CY and Zhang Ch, 3-D and 2-D dynamic Green's functions and time domain BIEs for piezoelectric solids, Eng Analysis Boun Elem, 29, 454-465, 2005

[32] Khutoryaansky N and Sosa H, Dynamic representation formulas and fundamental solutions for piezoelectricity, Int J Solids Structures, 32, 3307-3325, 1995
[33] Courant R and Hilbert D, Methods of Mathematical Physics, vol II. New York, Interscience, 1962
[34] Qin TY and Noda NA, Application of hypersingular integral equation method to a three-dimensional crack in piezoelectric materials, JSME International, Series A, 47, 173-180, 2004
[35] Qin TY and Noda NA, Analysis of a three-dimensional crack terminating at an interface using a hypersingular integral equation method, J Appl Mech, 69, 626-631, 2002
[36] Wippler K and Kuna M, Crack analyses in three-dimensioanl piezoelectric structures by the BEM, Computational Materials Science (2006, in press)
[37] Mi Y and Aliabadi MH, Discontinuous crack-tip elements: Application to 3D boundary element method, Int J Fracture, 67, R67-R71, 1994
[38] Qin QH, Material Properties of Piezoelectric Composites by BEM and Homogenization Method, *Composite Structures*, 66, 295-299, 2004
[39] Hashin Z, Analysis of composite materials—A survey, J Appl Mech, 50, 481-505, 1983
[40] Qin QH, Mai YW and Yu SW, Effective moduli for thermopiezoelectric materials with microcracts, Int J Fracture, 91, 359-371, 1998
[41] Nemat-Nasser S and Hori M. Micromechanics: Overall properties of heterogeneous materials. Amsterdam, North Holland Publ, 1993
[42] Qin QH and Yu SW, Effective moduli of thermopiezoelectric material with microcavities, Int J Solids Struct, 35, 5085-5095, 1998

Chapter 6 Boundary element method for discontinuity problems

6.1 Introduction

In the previous chapter we described the BE formulations derived based on reciprocity theorem. These formulations are useful for electroelastic problems in which no discontinuity of load is involved. This chapter deals with applications of BEM to thermoelectroelastic problems with discontinuous loadings, especially discontinuity of thermal loading. Although the BEM has been widely used for modeling various engineering problems, analysis of discontinuity problems with this approach has been very limited [1-4]. Qin [1] and Qin and Lu [2] proposed a BE formulation for fracture analysis of thermo-piezoelectricity with a half-plane boundary and an inclusion, respectively, based on the dislocation method and the potential variational principle. Later Qin and Mai [3] and Qin [4] extended this procedure to the discontinuity problem of thermopiezoelectricity with holes and thermomagnetoelectroelastic problems. The developments in [1-4] are briefly described in this chapter.

6.2 BEM for thermopiezoelectric problems

Consider a two-dimensional thermoelectroelastic solid inside of which there exists a number of defects such as cracks and holes. The numerical approach to such a problem will involve two major steps: (i) first solve a heat transfer problem to obtain the steady-state temperature field; (ii) calculate the stress and electric displacement (SED) caused by the temperature field, then calculate an isothermal solution to satisfy the corresponding mechanical and electric boundary conditions, and finally, solve the modified problem for elastic displacement and electric potential (EDEP) and SED fields. In what follows, we begin by deriving a variational principle for temperature discontinuity and then extend it to the case of thermoelectroelastic problems.

6.2.1 BEM for temperature discontinuity problems

Let us consider a finite region Ω_1 bounded by Γ, as shown in Fig. 6.1(a). The heat transfer problem to be considered is stated as

$$k_{ij}T_{,ij} = 0 \qquad \text{in } \Omega_1 \tag{6.1}$$

$$h_n = h_i n_i = \overline{h}_n \qquad \text{on } \Gamma_h \tag{6.2}$$

$$T = \overline{T} \qquad \text{on } \Gamma_T \tag{6.3}$$

$$h_i n_i = 0 \qquad \text{on } L \tag{6.4}$$

where n_i is the normal to the boundary Γ, $\overline{h}_n$ and $\overline{T}$ are the prescribed values of heat flow and temperature, which act on the boundaries Γ_h and Γ_T, respectively. For simplicity, we define $\hat{T} = T\big|_{L^+} - T\big|_{L^-}$ on L ($=L^+ + L^-$), where $\hat{T}$ is the temperature discontinuity, L is the union of all cracks, and L^+ and L^- are defined in Fig. 6.1b.

Further, if we let Ω_2 be the complementary region of Ω_1 (i.e., the union of Ω_1 and Ω_2 forms the infinite region Ω) and $\hat{T} = T\big|_{\Gamma^+} - T\big|_{\Gamma^-} = \overline{T}$, the problem shown in Fig. 6.1a can be extended to the infinite case (see Fig. 6.1b). Here $\Gamma = \Gamma^+ + \Gamma^-$, in which Γ^+ and Γ^- stand for the boundaries of Ω_1 and Ω_2, respectively (see Fig. 6.1b).

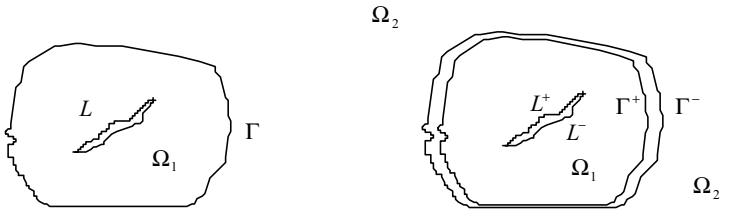

(a) (b)

Fig. 6.1 Configuration of piezoelectric plate for BEM analysis

6.2.1.1 Potential variational principle

In a manner similar to that of Yin and Ehrlacher [5], the total generalized potential energy for the thermal problem defined above can be given as

$$P(T,\hat{T}) = \frac{1}{2}\int_{\Omega} k_{ij}T_{,i}T_{,j}d\Omega + \int_{\Gamma} h_n\hat{T}dL \tag{6.5}$$

By transforming the region integral in Eq (6.5) into a boundary integral, we have

$$P(T,\hat{T}) = -\frac{1}{2}\int_{L} \vartheta(T)\hat{T}_{,s}ds + \int_{\Gamma} h_n\hat{T}ds \tag{6.6}$$

in which the relations

$$h_i = -k_{ij}T_{,j}, \qquad \int_L h_n\hat{T}ds = \int_L [(\vartheta\hat{T})_{,s} - \vartheta\hat{T}_{,s}]ds \tag{6.7}$$

have been used and the temperature discontinuity is assumed to be continuous over L and zero at the ends of L. Moreover, temperature T in Eq (6.6) can be expressed in terms of $\hat{T}$ through use of Green's function presented in Chapter 3. Thus, the potential energy can be further written as

$$P(\hat{T}) = -\frac{1}{2}\int_{L} \vartheta(\hat{T})\hat{T}_{,s}ds + \int_{\Gamma} h_n\hat{T}ds \tag{6.8}$$

6.2.1.2 Boundary element formulation

Analytical results for the minimum potential (6.8) are not, in general, possible, and therefore a numerical procedure must be used to solve the problem. As in conventional BEM, the boundaries Γ and L are divided into M_Γ and M_L linear boundary elements, for which the temperature discontinuity may be approximated by the sum of elemental temperature discontinuities:

$$\hat{T}(s) = \sum_{m=1}^{M} \hat{T}_m F_m(s) \tag{6.9}$$

where $\hat{T}_m$ is the temperature discontinuity at node m, $M = M_\Gamma + M_L + N$, and N is the number of cracks. It should be mentioned that the appearance of N is due to the number of nodes being one more than the number of elements in each crack. s is a length coordinate ($s>0$ in the element located at the right of the node m, $s<0$ in the element located at the left of the node), $F_m(s)$ is a global shape function associated with the node m. $F_m(s)$ is zero-valued over the whole mesh except within two

elements connected to the node m (see Fig. 6.2). Since $F_m(s)$ is assumed to be linear within each element, it has three possible forms:

$$F_m(s) = (l_{m-1} + s)/l_{m-1} \tag{6.10}$$

for a node located at the left end of a line (see Fig. 6.2a), or

$$F_m(s) = (l_m - s)/l_m \tag{6.11}$$

for a node located at the right end of a line (see Fig. 6.2b), or

$$F_m(s) = \begin{cases} (l_{m-1} + s)/l_{m-1}, & \text{if } s \in \text{element } l_{m-1}, \\ (l_m - s)/l_m, & \text{if } s \in \text{element } l_m, \end{cases} \tag{6.12}$$

where l_m and l_{m-1} are the lengths of the two elements connected to the mth node, l_m being to the right and l_{m-1} being to the left (see Fig. 6.2c). While

$$s = \begin{cases} 0, & \text{at node } m, \\ l_m, & \text{at node } m+1, \\ -l_{m-1}, & \text{at node } m-1 \end{cases} \tag{6.13}$$

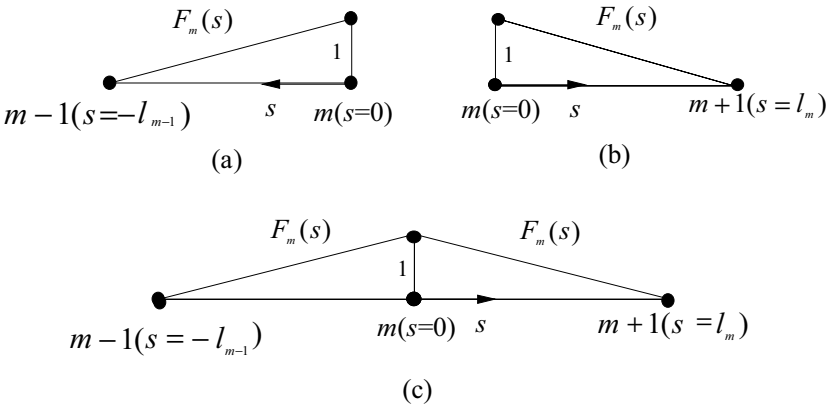

Fig. 6.2 Definition of $F_m(s)$

With the use of Green's functions presented in Chapter 3 and the approximation (6.9), the temperature and heat-flow function at point z_t (or $\zeta_t(z_t)$ can be given as

$$T(\zeta_t) = \sum_{m=1}^{M} \mathrm{Im}[a_m(\zeta_t)]\hat{T}_m \tag{6.14}$$

$$\vartheta(\zeta_t) = -k\sum_{m=1}^{M} \mathrm{Re}[a_m(\zeta_t)]\hat{T}_m \tag{6.15}$$

where $a_m(\zeta_t)$ has a different form for different problems. For example, we have for the problems of

(i) a bimaterial solid (see Fig. 2.5 and formulation in Section 3.4.1):

$$\begin{aligned} a_m(z_t^{(1)}) &= \frac{1}{2\pi}\int_{l_{m-1}} \{\ln(z_t^{(1)} - z_{t0}^{(1)(m-1)}) + b_1 \ln(z_t^{(1)} - \overline{z}_{t0}^{(1)(m-1)})\} \frac{l_{m-1}+s}{l_{m-1}} ds \\ &+ \frac{1}{2\pi}\int_{l_m} \{\ln(z_t^{(1)} - z_{t0}^{(1)(m)}) + b_1 \ln(z_t^{(1)} - \overline{z}_{t0}^{(1)(m)})\} \frac{l_m - s}{l_m} ds; \end{aligned} \tag{6.16}$$

(ii) a plate containing an elliptic hole (see Fig. 2.7 and formulation in Section 3.5):

$$\begin{aligned} a_m(\zeta_t) &= \frac{1}{2\pi}\int_{l_{m-1}} \left\{\ln(\zeta_t - \zeta_{t0}^{(m-1)}) - \ln(\zeta_t^{-1} - \overline{\zeta}_{t0}^{(m-1)})\right\} \frac{l_{m-1}+s}{l_{m-1}} ds \\ &+ \frac{1}{2\pi}\int_{l_m} \left\{\ln(\zeta_t - \zeta_{t0}^{(m)}) - \ln(\zeta_t^{-1} - \overline{\zeta}_{t0}^{(m)})\right\} \frac{l_m - s}{l_m} ds \end{aligned} \tag{6.17}$$

where

$$\zeta_t = f(z_t) = \frac{z_t + \sqrt{z_t^2 - a^2 - p_1^{*2} b^2}}{a - i p_1^{*2} b}, \quad \zeta_{t0}^{(m-1)} = f(z_{t0}^{(m-1)}), \quad \zeta_{t0}^{(m)} = f(z_{t0}^{(m)}); \tag{6.18}$$

(iii) a half-plane plate (see Fig. 2.4 and formulation in Section 3.3):

$$\begin{aligned} a_m(z_t) &= \frac{1}{2\pi}\int_{l_{m-1}} \{\ln(z_t - z_{t0}^{(m-1)}) - \ln(z_t - \overline{z}_{t0}^{(m-1)})\} \frac{l_{m-1}+s}{l_{m-1}} ds \\ &+ \frac{1}{2\pi}\int_{l_m} \{\ln(z_t - z_{t0}^{(m)}) - \ln(z_t - \overline{z}_{t0}^{(m)})\} \frac{l_m - s}{l_m} ds; \end{aligned} \tag{6.19}$$

(iv) a plate containing a hole of various shapes (see Fig. 2.9 and formulation in Section 3.7):

$$\begin{aligned} a_m(\zeta_t) &= \frac{1}{2\pi}\int_{l_{m-1}} \{\ln(\zeta_t - \zeta_{t0}^{(m-1)}) - \ln(\zeta_t^{-1} - \overline{\zeta}_{t0}^{(m-1)})\} \frac{l_{m-1}+s}{l_{m-1}} ds \\ &+ \frac{1}{2\pi}\int_{l_m} \{\ln(\zeta_t - \zeta_{t0}^{(m)}) - \ln(\zeta_t^{-1} - \overline{\zeta}_{t0}^{(m)})\} \frac{l_m - s}{l_m} ds \end{aligned} \tag{6.20}$$

where ζ_t and z_t are related by Eq (3.78);

(v) a plate with a wedge boundary (see Fig. 4.5 and formulation in Section 4.8.5)

$$\begin{aligned} a_m(z_t) &= \frac{1}{2\pi}\int_{l_{m-1}} \{\ln(z_t^{\lambda} - z_{t0}^{(m-1)\lambda}) - \ln(-z_t^{\lambda} - \overline{z}_{t0}^{(m-1)\lambda})\} \frac{l_{m-1}+s}{l_{m-1}} ds \\ &+ \frac{1}{2\pi}\int_{l_m} \{\ln(z_t^{\lambda} - z_{t0}^{(m)\lambda}) - \ln(-z_t^{\lambda} - \overline{z}_{t0}^{(m)\lambda})\} \frac{l_m - s}{l_m} ds \end{aligned} \tag{6.21}$$

where λ is defined in Eq (4.170).

In the formulations listed above $z_{t0}^{(m)}$ is defined as

$$z_{t0}^{(m-1)} = d_{tm} + s(\cos\alpha_{m-1} + p_1^* \sin\alpha_{m-1}), \quad z_{t0}^{(m)} = d_{tm} + s(\cos\alpha_m + p_1^* \sin\alpha_m) \tag{6.22}$$

and $d_{tm} = x_{1m} + p_1^* x_{2m}$, (x_{1m}, x_{2m}) represent the coordinates at node m, α_{m-1} is the angle between the element in the left of node m and the x_1-axis, with α_m defined

similarly. It should be pointed out that the superscript "(1)" for variables ζ_t and z_t has been dropped in Eq (6.17) in order to simplify the writing. Hereafter, we again omit the superscript "(1)" when the distinction is unnecessary.

In particular the temperature at node *j* can be written as

$$T_j[f(d_j)] = \sum_{m=1}^{M} \mathrm{Im}\{a_m[f(d_j)]\}\hat{T}_m \tag{6.23}$$

where $d_j = x_{1j} + p_1^* x_{2j}$, (x_{1j}, x_{2j}) are the coordinates at node *j*.

For the total potential energy (6.8), substituting Eqs (6.9) and (6.15) into it yields

$$P(\hat{T}) \approx \sum_{j=1}^{M}\left[\sum_{m=1}^{M}\left(-\frac{1}{2}K_{mj}\hat{T}_m\hat{T}_j\right) + G_j\hat{T}_j\right] \tag{6.24}$$

where K_{mj} is the so-called stiffness matrix and G_j the equivalent nodal heat flow vector, with the form

$$K_{mj} = -\frac{k}{l_{j-1}}\int_{l_{j-1}} \mathrm{Re}[a_m(x^{(j-1)})]ds + \frac{k}{l_j}\int_{l_j} \mathrm{Re}[a_m(x^{(j)})]ds, \tag{6.25}$$

$$G_j = \int_{l_{j-1}+l_j} h_{*0}F_j(s)ds, \tag{6.26}$$

where $h_{*0} = h_0$ when $s \in \Gamma_h$, and $h_{*0} = 0$ for other cases, $x^{(k)} = z_{t0}^{(k)}$ for the cases (i), (iii) and (v), and $x^{(k)} = \zeta_{t0}^{(k)}$ for the remaining two cases.

The minimization of $P(\hat{T})$ yields

$$\sum_{j=1}^{M} K_{mj}\hat{T}_j = G_m \tag{6.27}$$

The final form of linear equation to be solved is obtained by selecting the appropriate equation from Eqs (6.23) and (6.27). Equation (6.23) will be chosen for those nodes at which the temperature is prescribed, and Eq (6.27) will be chosen for the remaining nodes. After the nodal temperature discontinuities have been calculated, the displacement and stress at any point in the region can be evaluated through use of Eqs (3.1) and (3.2). They are

$$\mathbf{U} = \sum_{j=1}^{M}\mathbf{u}_j\hat{T}_j, \quad \mathbf{\Pi}_1 = \sum_{j=1}^{M}\mathbf{x}_j\hat{T}_j, \quad \mathbf{\Pi}_2 = \sum_{j=1}^{M}\mathbf{y}_j\hat{T}_j \tag{6.28}$$

where $\mathbf{u}_j$, $\mathbf{x}_j$ and $\mathbf{y}_j$ have different forms for different problems. They are

(i) bimaterial problems

$$\begin{aligned}\mathbf{u}_j = {} & \frac{1}{2\pi}\mathrm{Im}\int_{l_{j-1}}\{\mathbf{A}^{(1)}\left\langle f(z_\alpha^{(1)})\right\rangle\mathbf{q}_{1*} + \mathbf{c}^{(1)}[f(y_1^{(1)}) + b_1 f(y_2^{(1)})]\}\frac{l_{j-1}+s}{l_{j-1}}ds \\ & + \frac{1}{2\pi}\mathrm{Im}\int_{l_j}\{\mathbf{A}^{(1)}\left\langle f(z_\alpha^{(1)})\right\rangle\mathbf{q}_1 + \mathbf{c}^{(1)}[f(y_1^{(1)}) + b_1 f(y_2^{(1)})]\}\frac{l_j - s}{l_j}ds,\end{aligned} \tag{6.29}$$

$$\mathbf{x}_j = -\frac{1}{2\pi}\mathrm{Im}\int_{l_{j-1}}\{\mathbf{B}^{(1)}\left\langle p_\alpha^{(1)} f'(z_\alpha^{(1)})\right\rangle \mathbf{q}_{1*} + \mathbf{d}^{(1)} p_1^{*(1)}[f'(y_1^{(1)}) + b_1 f'(y_2^{(1)})]\}\frac{l_{j-1}+s}{l_{j-1}}ds$$
$$-\frac{1}{2\pi}\mathrm{Im}\int_{l_j}\{\mathbf{B}^{(1)}\left\langle p_\alpha^{(1)} f'(z_\alpha^{(1)})\right\rangle \mathbf{q}_{1*} + \mathbf{d}^{(1)} p_1^{*(1)}[f'(y_1^{(1)}) + b_1 f'(y_2^{(1)})]\}\frac{l_j - s}{l_j}ds, \tag{6.30}$$

$$\mathbf{y}_j = \frac{1}{2\pi}\mathrm{Im}\int_{l_{j-1}}\{\mathbf{B}^{(1)}\left\langle f'(z_\alpha^{(1)})\right\rangle \mathbf{q}_{1*} + \mathbf{d}^{(1)}[f'(y_1^{(1)}) + b_1 f'(y_2^{(1)})]\}\frac{l_{j-1}+s}{l_{j-1}}ds$$
$$+\frac{1}{2\pi}\mathrm{Im}\int_{l_j}\{\mathbf{B}^{(1)}\left\langle f'(z_\alpha^{(1)})\right\rangle \mathbf{q}_{1*} + \mathbf{d}^{(1)}[q_0 f'(y_1^{(1)}) + b_1 f'(y_2^{(1)})]\}\frac{l_j - s}{l_j}ds \tag{6.31}$$

where $\mathbf{q}_{1*} = \mathbf{q}_1 / q_0$, $\mathbf{q}_1$ being defined in Eq (3.49), and all other functions and constants used are defined in Section 3.4.

(ii) a plate containing an elliptic hole and multiple cracks

$$\mathbf{u}_j = \frac{1}{2\pi}\mathrm{Im}\int_{l_{j-1}}\left[\sum_{k=1}^{4}\mathbf{A}\left\langle f_k(\zeta_\alpha)\right\rangle \mathbf{B}^{-1}\mathbf{d}q_k + \mathbf{c}g_*(\zeta_t)\right]\frac{l_{j-1}+s}{l_{j-1}}ds$$
$$+\frac{1}{2\pi}\mathrm{Im}\int_{l_j}\left[\sum_{k=1}^{5}\mathbf{A}\left\langle f_k(\zeta_\alpha)\right\rangle \mathbf{B}^{-1}\mathbf{d}q_k + \mathbf{c}g_*(\zeta_t)\right]\frac{l_j - s}{l_j}ds, \tag{6.32}$$

$$\mathbf{x}_j = -\frac{1}{2\pi}\mathrm{Im}\int_{l_{j-1}}\left[\sum_{k=1}^{4}\mathbf{B}\left\langle p_\alpha f_k'(\zeta_\alpha)\frac{\partial\zeta_\alpha}{\partial z_\alpha}\right\rangle \mathbf{B}^{-1}\mathbf{d}q_k + \mathbf{c}p_1^* g_*'(\zeta_t)\frac{\partial\zeta_t}{\partial z_t}\right]\frac{l_{j-1}+s}{l_{j-1}}ds$$
$$-\frac{1}{2\pi}\mathrm{Im}\{\int_{l_j}\left[\sum_{k=1}^{4}\mathbf{B}\left\langle p_\alpha f_k'(\zeta_\alpha)\frac{\partial\zeta_\alpha}{\partial z_\alpha}\right\rangle \mathbf{B}^{-1}\mathbf{d}q_k + \mathbf{c}p_1^* g_*'(\zeta_t)\frac{\partial\zeta_t}{\partial z_t}\right]\frac{l_j - s}{l_j}ds, \tag{6.33}$$

$$\mathbf{y}_j = \frac{1}{2\pi}\mathrm{Im}\int_{l_{j-1}}\left[\sum_{k=1}^{4}\mathbf{B}\left\langle f_k'(\zeta_\alpha)\frac{\partial\zeta_\alpha}{\partial z_\alpha}\right\rangle \mathbf{B}^{-1}\mathbf{d}q_k + \mathbf{c}g_*'(\zeta_t)\frac{\partial\zeta_t}{\partial z_t}\right]\frac{l_{j-1}+s}{l_{j-1}}ds$$
$$+\frac{1}{2\pi}\mathrm{Im}\{\int_{l_j}\left[\sum_{k=1}^{4}\mathbf{B}\left\langle f_k'(\zeta_\alpha)\frac{\partial\zeta_\alpha}{\partial z_\alpha}\right\rangle \mathbf{B}^{-1}\mathbf{d}q_k + \mathbf{c}g_*'(\zeta_t)\frac{\partial\zeta_t}{\partial z_t}\right]\frac{l_j - s}{l_j}ds, \tag{6.34}$$

where f_k is difined in Eq (3.63), and

$$q_1 = -q_4 = -c_\tau \quad q_2 = -q_3 = -d_\tau \tag{6.35}$$

$$g_*(\zeta_t) = c_\tau F_1(\zeta_t) + d_\tau F_2(\zeta_t) - c_\tau F_4(\zeta_t) - d_\tau F_3(\zeta_t). \tag{6.36}$$

with F_i being defined in Eq (3.61);

(iii) half-plane problems with multiple cracks

$$\mathbf{u}_j = \frac{1}{2\pi}\mathrm{Im}\int_{l_{j-1}}[\mathbf{A}\left\langle f_*(z_\alpha)\right\rangle(-\mathbf{B}^{-1}\mathbf{d}) + \mathbf{c}f_*(z_t)]\frac{l_{j-1}+s}{l_{j-1}}ds$$
$$+\frac{1}{2\pi}\mathrm{Im}\int_{l_j}[\mathbf{A}\left\langle f_*(z_\alpha)\right\rangle(-\mathbf{B}^{-1}\mathbf{d}) + \mathbf{c}f_*(z_t)]\frac{l_j - s}{l_j}ds, \tag{6.37}$$

$$\mathbf{x}_j = \frac{1}{2\pi}\mathrm{Im}\int_{l_{j-1}} [\mathbf{B}\langle p_\alpha f_*'(z_\alpha)\rangle(\mathbf{B}^{-1}\mathbf{d}) - \mathbf{d}p_1^* f_*'(z_t)]\frac{l_{j-1}+s}{l_{j-1}}ds + \frac{1}{2\pi}\mathrm{Im}\int_{l_j} [\mathbf{B}\langle p_\alpha f_*'(z_\alpha)\rangle(\mathbf{B}^{-1}\mathbf{d}) - \mathbf{d}p_1^* f_*'(z_t)]\frac{l_j-s}{l_j}ds, \tag{6.38}$$

$$\mathbf{y}_j = -\frac{1}{2\pi}\mathrm{Im}\int_{l_{j-1}} [\mathbf{B}\langle f_*'(z_\alpha)\rangle(\mathbf{B}^{-1}\mathbf{d}) - \mathbf{d}f_*'(z_t)]\frac{l_{j-1}+s}{l_{j-1}}ds - \frac{1}{2\pi}\mathrm{Im}\int_{l_j} [\mathbf{B}\langle f_*'(z_\alpha)\rangle(\mathbf{B}^{-1}\mathbf{d}) - \mathbf{d}f_*'(z_t)]\frac{l_j-s}{l_j}ds \tag{6.39}$$

where

$$f_*(z_x) = (z_x - z_{t0})[\ln(z_x - z_{t0}) - 1] - (z_x - \overline{z}_{t0})[\ln(z_x - \overline{z}_{t0}) - 1] \tag{6.40}$$

(iv) a plate containing multiple cracks and a hole of various shapes (see Fig. 2.9 and formulation in Section 3.7)

$$\mathbf{u}_j = -\frac{1}{2\pi}\mathrm{Im}\int_{l_{j-1}} [\mathbf{A}(\langle f_{1*}(\zeta_\alpha)\rangle + \overline{p}_1^*\langle p_\alpha f_{2*}(\zeta_\alpha)\rangle)\mathbf{B}^{-1}\overline{\mathbf{d}} - \mathbf{c}g_*(z_t)]\frac{l_{j-1}+s}{l_{j-1}}ds - \frac{1}{2\pi}\mathrm{Im}\int_{l_j} [\mathbf{A}(\langle f_{1*}(\zeta_\alpha)\rangle + \overline{p}_1^*\langle p_\alpha f_{2*}(\zeta_\alpha)\rangle)\mathbf{B}^{-1}\overline{\mathbf{d}} - \mathbf{c}g_*(z_t)]\frac{l_j-s}{l_j}ds, \tag{6.41}$$

$$\mathbf{x}_j = \frac{1}{2\pi}\mathrm{Im}\int_{l_{j-1}} [\mathbf{B}\left\langle \{f_{1*}'(\zeta_\alpha) + \overline{p}_1^* p_\alpha f_{2*}'(\zeta_\alpha)\}p_\alpha\frac{\partial\zeta_\alpha}{\partial z_\alpha}\right\rangle\mathbf{B}^{-1}\overline{\mathbf{d}} - \mathbf{c}p_1^* g_*'(z_t)]\frac{l_{j-1}+s}{l_{j-1}}ds + \frac{1}{2\pi}\mathrm{Im}\int_{l_j} [\mathbf{B}\left\langle \{f_{1*}'(\zeta_\alpha) + \overline{p}_1^* p_\alpha f_{2*}'(\zeta_\alpha)\}p_\alpha\frac{\partial\zeta_\alpha}{\partial z_\alpha}\right\rangle\mathbf{B}^{-1}\overline{\mathbf{d}} - \mathbf{c}p_1^* g_*'(z_t)]\frac{l_j-s}{l_j}ds, \tag{6.42}$$

$$\mathbf{y}_j = -\frac{1}{2\pi}\mathrm{Im}\int_{l_{j-1}} [\mathbf{B}\left\langle \{f_{1*}'(\zeta_\alpha) + \overline{p}_1^* p_\alpha f_{2*}'(\zeta_\alpha)\}\frac{\partial\zeta_\alpha}{\partial z_\alpha}\right\rangle\mathbf{B}^{-1}\overline{\mathbf{d}} - \mathbf{c}g_*'(z_t)]\frac{l_{j-1}+s}{l_{j-1}}ds - \frac{1}{2\pi}\mathrm{Im}\int_{l_j} [\mathbf{B}\left\langle \{f_{1*}'(\zeta_\alpha) + \overline{p}_1^* p_\alpha f_{2*}'(\zeta_\alpha)\}\frac{\partial\zeta_\alpha}{\partial z_\alpha}\right\rangle\mathbf{B}^{-1}\overline{\mathbf{d}} - \mathbf{c}g_*'(z_t)]\frac{l_j-s}{l_j}ds, \tag{6.43}$$

where

$$f_{1*}(\zeta_\alpha) = a[F_1(\zeta_\alpha,\zeta_{t0}) + F_2(\zeta_\alpha,\zeta_{t0}) - F_1(\zeta_\alpha^{-1},\overline{\zeta}_{t0}) - F_2(\zeta_\alpha^{-1},\overline{\zeta}_{t0})]/2 + e_{j1}a\gamma[F_3(\zeta_\alpha,\zeta_{t0}) + F_4(\zeta_\alpha,\zeta_{t0}) - F_3(\zeta_\alpha^{-1},\overline{\zeta}_{t0}) - F_4(\zeta_\alpha^{-1},\overline{\zeta}_{t0})]/2,$$

$$f_{2*}(\zeta_\alpha) = ip_\alpha ae[-F_1(\zeta_\alpha,\zeta_{t0}) + F_2(\zeta_\alpha,\zeta_{t0}) - F_1(\zeta_\alpha^{-1},\overline{\zeta}_t^*) + F_2(\zeta_\alpha^{-1},\overline{\zeta}_t^*)]/2 + ie_{j1}p_\alpha ae\gamma[F_3(\zeta_\alpha,\zeta_{t0}) - F_4(\zeta_\alpha,\zeta_{t0}) + F_3(\zeta_\alpha^{-1},\overline{\zeta}_{t0}) - F_4(\zeta_\alpha^{-1},\overline{\zeta}_{t0})]/2$$

$$g_*(z_t) = aa_{1\tau}[F_1(\zeta_t,\zeta_{t0}) - F_2(\zeta_t^{-1},\overline{\zeta}_{t0})] + aa_{2\tau}[F_2(\zeta_t,\zeta_{t0}) - F_1(\zeta_t^{-1},\overline{\zeta}_{t0})] + ae_{j1}\{a_{3\tau}[F_3(\zeta_t,\zeta_{t0}) - F_4(\zeta_t^{-1},\overline{\zeta}_{t0})] + aa_{4\tau}[F_4(\zeta_t,\zeta_{t0}) - F_3(\zeta_t^{-1},\overline{\zeta}_{t0})]\}$$

(v) a plate containing multiple cracks and a wedge boundary (see Fig. 4.5 and formulation in Section 4.8.5)

$$\mathbf{u}_j = \frac{1}{2\pi}\mathrm{Im}\{\int_{l_{j-1}}[-\mathbf{A}(\langle f_1(z_\alpha)\rangle - \langle f_2(z_\alpha)\rangle)\mathbf{B}^{-1}\mathbf{d} + \mathbf{c}g_*(z_t)]\frac{l_{j-1}+s}{l_{j-1}}ds\} + \frac{1}{2\pi}\mathrm{Im}\{\int_{l_j}[-\mathbf{A}(\langle f_1(z_\alpha)\rangle - \langle f_2(z_\alpha)\rangle)\mathbf{B}^{-1}\mathbf{d} + \mathbf{c}g_*(z_t)]\frac{l_j - s}{l_j}ds\} \tag{6.44}$$

$$\mathbf{x}_j = \frac{1}{2\pi}\mathrm{Im}\{\int_{l_{j-1}}[\mathbf{B}(\langle p_\alpha f_1'(z_\alpha)\rangle - \langle p_\alpha f_2'(z_\alpha)\rangle)\mathbf{B}^{-1} - p_1^* g_*'(\zeta_t)]\mathbf{d}\frac{l_{j-1}+s}{l_{j-1}}ds\} + \frac{1}{2\pi}\mathrm{Im}\{\int_{l_j}[\mathbf{B}(\langle p_\alpha f_1'(z_\alpha)\rangle - \langle p_\alpha f_2'(z_\alpha)\rangle)\mathbf{B}^{-1} - p_1^* g_*'(\zeta_t)]\mathbf{d}\frac{l_j - s}{l_j}ds\} \tag{6.45}$$

$$\mathbf{y}_j = \frac{1}{2\pi}\mathrm{Im}\{\int_{l_{j-1}}[-\mathbf{B}(\langle f_1'(z_\alpha)\rangle - \langle f_2'(z_\alpha)\rangle)\mathbf{B}^{-1} + g_*'(\zeta_t)]\mathbf{d}\frac{l_{j-1}+s}{l_{j-1}}ds\} + \frac{1}{2\pi}\mathrm{Im}\{\int_{l_j}[-\mathbf{B}(\langle f_1'(z_\alpha)\rangle - \langle f_2'(z_\alpha)\rangle)\mathbf{B}^{-1} + g_*'(\zeta_t)]\mathbf{d}\frac{l_j - s}{l_j}ds\} \tag{6.46}$$

where f_1 and f_2 are defined in Eq (4.185), and $g_*(z_t) = \hat{f}_1(z_t) - \hat{f}_2(z_t)$.

Thus, the SED and EDEP on a boundary induced by temperature discontinuity are of the form

$$\mathbf{t}_n^\theta(s) = \Pi_i n_i = \sum_{j=1}^{M}(\mathbf{x}_j n_1 + \mathbf{y}_j n_2)\hat{T}_j, \qquad \mathbf{U}_T^\theta(s) = \sum_{j=1}^{M}\mathbf{u}_j\hat{T}_j. \tag{6.47}$$

In general, $\mathbf{t}_n^\theta(s) \neq 0$ and $\mathbf{U}_T^\theta(s) \neq 0$. To eliminate these quantities on the corresponding boundaries, we must superimpose a solution of the corresponding isothermal problem with a SED (or an EDEP) equal and opposite to those of Eq (6.47). The details are given in the following sub-section.

6.2.2 BEM for displacement and potential discontinuity problems

Consider again the domain Ω_1, in which the governing equation and its boundary conditions are described as follows:

$$\Pi_{ij,j} = 0, \qquad \text{in } \Omega_1, \tag{6.48}$$

$$t_{ni} = \Pi_{ij} n_j = \bar{t}_i - (\mathbf{t}_n^\theta)_i, \qquad \text{on } \Gamma_t, \tag{6.49}$$

$$u_i = \bar{u}_i - (\mathbf{U}_T^\theta)_i, \qquad \text{on } \Gamma_u, \tag{6.50}$$

$$t_{ni}\big|_{L^+} = -t_{ni}\big|_{L^-} = -(\mathbf{t}_n^\theta)_i, \quad b_i = u_i\big|_{L^+} - u_i\big|_{L^-} - (\mathbf{U}_T^\theta)_i\big|_{L^+} + (\mathbf{U}_T^\theta)_i\big|_{L^-}, \quad \text{on } L \tag{6.51}$$

where Γ_t and Γ_u are the boundaries on which the prescribed values of stress $\bar{t}_i$ and displacement $\bar{u}_i$ are imposed. Similarly, the related potential energy for the elastic problem can be given as

$$P(\mathbf{b}) = \frac{1}{2}\int_L[\boldsymbol{\varphi}(\mathbf{b})\cdot\mathbf{b}_{,s} + 2\bar{\mathbf{t}}_n\cdot\mathbf{b}]ds - \int_\Gamma(\bar{\mathbf{t}}_n - \mathbf{t}_n^\theta)\cdot\mathbf{b}ds \tag{6.52}$$

where the electroelastic solutions of functions $\boldsymbol{\varphi}(\mathbf{b})$ and $\mathbf{U}(\mathbf{b})$ appearing later have been discussed in Chapter 2 and are listed for the readers' convenience:

(i) bimaterial problems
For a bimaterial plate subjected to a line dislocation $\mathbf{b}$ located in the upper half-plane at $z_0(x_{10}, x_{20})$, the solution is given by

$$\mathbf{U}^{(1)} = \frac{1}{\pi}\mathrm{Im}\{\mathbf{A}^{(1)}\left\langle \ln(z_\alpha^{(1)} - z_{\alpha 0}^{(1)})\right\rangle \mathbf{B}^{T}\}\mathbf{b} + \sum_{\beta=1}^{4}\frac{1}{\pi}\mathrm{Im}\{\mathbf{A}^{(1)}\left\langle \ln(z_\alpha^{(1)} - \bar{z}_{\beta 0}^{(1)})\right\rangle \mathbf{q}_\beta^{(1)}\}, \quad (6.53)$$

$$\boldsymbol{\varphi}^{(1)} = \frac{1}{\pi}\mathrm{Im}\{\mathbf{B}^{(1)}\left\langle \ln(z_\alpha^{(1)} - z_{\alpha 0}^{(1)})\right\rangle \mathbf{B}^{T}\}\mathbf{b} + \sum_{\beta=1}^{4}\frac{1}{\pi}\mathrm{Im}\{\mathbf{B}^{(1)}\left\langle \ln(z_\alpha^{(1)} - \bar{z}_{\beta 0}^{(1)})\right\rangle \mathbf{q}_\beta^{(1)}\} \quad (6.54)$$

for material 1 in $x_2>0$ and

$$\mathbf{U}^{(2)} = \sum_{\beta=1}^{4}\frac{1}{\pi}\mathrm{Im}\{\mathbf{A}^{(2)}\left\langle \ln(z_\alpha^{(2)} - z_{\beta 0}^{(1)})\right\rangle \mathbf{q}_\beta^{(2)}\}, \quad (6.55)$$

$$\boldsymbol{\varphi}^{(2)} = \sum_{\beta=1}^{4}\frac{1}{\pi}\mathrm{Im}\{\mathbf{B}^{(2)}\left\langle \ln(z_\alpha^{(2)} - z_{\beta 0}^{(1)})\right\rangle \mathbf{q}_\beta^{(2)}\} \quad (6.56)$$

where

$$\mathbf{q}_\beta^{(1)} = \mathbf{B}^{(1)-1}[\mathbf{I} - 2(\mathbf{M}^{(1)-1} + \bar{\mathbf{M}}^{(2)-1})^{-1}\mathbf{L}^{(1)-1}]\bar{\mathbf{B}}^{(1)}\mathbf{I}_\beta\bar{\mathbf{B}}^{T}\mathbf{b}, \quad (6.57)$$

$$\mathbf{q}_\beta^{(2)} = 2\mathbf{B}^{(2)-1}(\bar{\mathbf{M}}^{(1)-1} + \mathbf{M}^{(2)-1})^{-1}\mathbf{L}^{(1)-1}\mathbf{B}^{(1)}\mathbf{I}_\beta\mathbf{B}^{T}\mathbf{b}, \quad (6.58)$$

with $\mathbf{M}^{(j)} = -i\mathbf{B}^{(j)}\mathbf{A}^{(j)-1}$ as the surface impedance matrix.

(ii) a plate containing an elliptic hole and multiple cracks

$$\mathbf{U}(\mathbf{b}) = \frac{1}{\pi}\mathrm{Im}[\mathbf{A}\left\langle \ln(\zeta_\alpha - \zeta_{\alpha 0})\right\rangle \mathbf{B}^{T}]\mathbf{b} + \frac{1}{\pi}\sum_{\beta=1}^{4}\mathrm{Im}[\mathbf{A}\left\langle \ln(\zeta_\alpha^{-1} - \bar{\zeta}_{\beta 0})\right\rangle \mathbf{B}^{-1}\bar{\mathbf{B}}\mathbf{I}_\beta\bar{\mathbf{B}}^{T}]\mathbf{b} \quad (6.59)$$

$$\boldsymbol{\varphi}(\mathbf{b}) = \frac{1}{\pi}\mathrm{Im}[\mathbf{B}\left\langle \ln(\zeta_\alpha - \zeta_{\alpha 0})\right\rangle \mathbf{B}^{T}]\mathbf{b} + \frac{1}{\pi}\sum_{\beta=1}^{4}\mathrm{Im}[\mathbf{B}\left\langle \ln(\zeta_\alpha^{-1} - \bar{\zeta}_{\beta 0})\right\rangle \mathbf{B}^{-1}\bar{\mathbf{B}}\mathbf{I}_\beta\bar{\mathbf{B}}^{T}]\mathbf{b} \quad (6.60)$$

(iii) half-plane problems

$$\mathbf{U}(\mathbf{b}) = \frac{1}{\pi}\mathrm{Im}[\mathbf{A}\left\langle \ln(z_\alpha - z_{\alpha 0})\right\rangle \mathbf{B}^{T}]\mathbf{b} + \frac{1}{\pi}\sum_{\beta=1}^{4}\mathrm{Im}[\mathbf{A}\left\langle \ln(z_\alpha - \bar{z}_{\beta 0})\right\rangle \mathbf{B}^{-1}\bar{\mathbf{B}}\mathbf{I}_\beta\bar{\mathbf{B}}^{T}]\mathbf{b} \quad (6.61)$$

$$\boldsymbol{\varphi}(\mathbf{b}) = \frac{1}{\pi}\mathrm{Im}[\mathbf{B}\left\langle \ln(z_\alpha - z_{\alpha 0})\right\rangle \mathbf{B}^{T}]\mathbf{b} + \frac{1}{\pi}\sum_{\beta=1}^{4}\mathrm{Im}[\mathbf{B}\left\langle \ln(z_\alpha - \bar{z}_{\beta 0})\right\rangle \mathbf{B}^{-1}\bar{\mathbf{B}}\mathbf{I}_\beta\bar{\mathbf{B}}^{T}]\mathbf{b} \quad (6.62)$$

(iv) a plate containing a hole of various shapes
For the case of a plate containing a hole of various shapes the expressions of $\boldsymbol{\varphi}(\mathbf{b})$ and $\mathbf{U}(\mathbf{b})$ have the same form as those of Eqs (6.59) and (6.60), but the relation between ζ_α and z_α is defined by Eq (2.223)

(v) wedge problems

$$\mathbf{U}(\mathbf{b}) = \frac{1}{\pi}\mathrm{Im}[\mathbf{A}\left\langle \ln(z_k^{\lambda} - z_{k0}^{\lambda})\right\rangle \mathbf{B}^T]\mathbf{b} + \frac{1}{\pi}\sum_{\beta=1}^{4}\mathrm{Im}[\mathbf{A}\left\langle \ln(-z_k^{\lambda} - \bar{z}_{\beta 0}^{\lambda})\right\rangle \mathbf{B}^{-1}\bar{\mathbf{B}}\mathbf{I}_{\beta}\bar{\mathbf{B}}^T]\mathbf{b} \quad (6.63)$$

$$\boldsymbol{\varphi}(\mathbf{b}) = \frac{1}{\pi}\mathrm{Im}[\mathbf{B}\left\langle \ln(z_k^{\lambda} - z_{k0}^{\lambda})\right\rangle \mathbf{B}^T]\mathbf{b} + \frac{1}{\pi}\sum_{\beta=1}^{4}\mathrm{Im}[\mathbf{B}\left\langle \ln(-z_k^{\lambda} - \bar{z}_{\beta 0}^{\lambda})\right\rangle \mathbf{B}^{-1}\bar{\mathbf{B}}\mathbf{I}_{\beta}\bar{\mathbf{B}}^T]\mathbf{b} \quad (6.64)$$

As treated earlier, the boundaries L and Γ are divided into a series of boundary elements, for which the EDEP discontinuity may be approximated through linear interpolation as

$$\mathbf{b}(s) = \sum_{m=1}^{M}\mathbf{b}_m F_m(s)\,. \quad (6.65)$$

With the approximation (6.65), the EDEP and SED functions can be expressed in the form

$$\mathbf{U}(\zeta) = \sum_{m=1}^{M}\mathrm{Im}[\mathbf{A}\mathbf{D}_m(\zeta)]\mathbf{b}_m, \qquad \boldsymbol{\varphi}(\zeta) = \sum_{m=1}^{M}\mathrm{Im}[\mathbf{B}\mathbf{D}_m(\zeta)]\mathbf{b}_m \quad (6.66)$$

where $\mathbf{D}_m$ has different forms for different problems. The function $\mathbf{D}_m$ is given below for five typical problems.

(i) bimaterial problems

$$\begin{aligned}\mathbf{D}_m(\mathbf{z}) = {} & \frac{1}{\pi}\int_{l_{m-1}}\left\{\left\langle \ln(z_{\alpha\alpha 0}^{(m-1)})\right\rangle \mathbf{B}^T + \sum_{\beta=1}^{4}\left\langle \ln(z_{\alpha\beta 0}^{(m-1)})\right\rangle \mathbf{B}^*\bar{\mathbf{B}}\mathbf{I}_{\beta}\bar{\mathbf{B}}^T\right\}\frac{l_{m-1}+s}{l_{m-1}}ds \\ & + \frac{1}{\pi}\int_{l_m}\left\{\left\langle \ln(z_{\alpha\alpha 0}^{(m)})\right\rangle \mathbf{B}^T + \sum_{\beta=1}^{4}\left\langle \ln(z_{\alpha\beta 0}^{(m)})\right\rangle \mathbf{B}^*\bar{\mathbf{B}}\mathbf{I}_{\beta}\bar{\mathbf{B}}^T\right\}\frac{l_m-s}{l_m}ds\end{aligned} \quad (6.67)$$

where $z_{\alpha\alpha 0}^{(m)} = z_{\alpha} - z_{\alpha 0}^{(m)}$, $z_{\alpha\beta 0}^{(m)} = z_{\alpha} - \bar{z}_{\beta 0}^{(m)}$, $\mathbf{B}^* = \mathbf{B}^{(1)-1}[\mathbf{I} - 2(\mathbf{M}^{(1)-1} + \bar{\mathbf{M}}^{(2)-1})^{-1}\mathbf{L}^{(1)-1}]$.

(i) a plate containing an elliptic hole

$$\begin{aligned}\mathbf{D}_m(\boldsymbol{\zeta}) = {} & \frac{1}{\pi}\int_{l_{m-1}}\left\{\left\langle \ln(\zeta_{\alpha} - \zeta_{\alpha 0}^{(m-1)})\right\rangle \mathbf{B}^T + \sum_{\beta=1}^{4}\left\langle \ln(\zeta_{\alpha}^{-1} - \bar{\zeta}_{\beta 0}^{(m-1)})\right\rangle \mathbf{B}^{-1}\bar{\mathbf{B}}\mathbf{I}_{\beta}\bar{\mathbf{B}}^T\right\}\frac{l_{m-1}+s}{l_{m-1}}ds \\ & + \frac{1}{\pi}\int_{l_m}\left\{\left\langle \ln(\zeta_{\alpha} - \zeta_{\alpha 0}^{(m)})\right\rangle \mathbf{B}^T + \sum_{\beta=1}^{4}\left\langle \ln(\zeta_{\alpha}^{-1} - \bar{\zeta}_{\beta 0}^{(m)})\right\rangle \mathbf{B}^{-1}\bar{\mathbf{B}}\mathbf{I}_{\beta}\bar{\mathbf{B}}^T\right\}\frac{l_m-s}{l_m}ds\end{aligned} \quad (6.68)$$

(ii) half-plane problems

$$\begin{aligned}\mathbf{D}_m(\mathbf{z}) = {} & \frac{1}{\pi}\int_{l_{m-1}}\left\{\left\langle \ln(z_{\alpha\alpha 0}^{m-1})\right\rangle \mathbf{B}^T + \sum_{\beta=1}^{4}\left\langle \ln(z_{\alpha\beta 0}^{m-1})\right\rangle \mathbf{B}^{-1}\bar{\mathbf{B}}\mathbf{I}_{\beta}\bar{\mathbf{B}}^T\right\}\frac{l_{m-1}+s}{l_{m-1}}ds \\ & + \frac{1}{\pi}\int_{l_m}\left\{\left\langle \ln(z_{\alpha\alpha 0}^{m})\right\rangle \mathbf{B}^T + \sum_{\beta=1}^{4}\left\langle \ln(z_{\alpha\beta 0}^{m})\right\rangle \mathbf{B}^{-1}\bar{\mathbf{B}}\mathbf{I}_{\beta}\bar{\mathbf{B}}^T\right\}\frac{l_m-s}{l_m}ds\end{aligned} \quad (6.69)$$

(iv) a plate containing multiple cracks and a hole of various shapes (see Section 4.11). It has the same form as that in Eq (6.68), but ζ_{α} is related to z_{α} by Eq (2.223).

(v) wedge problems

$$\mathbf{D}_m(\mathbf{z}) = \frac{1}{\pi}\int_{l_{m-1}} \{\left\langle \ln(z_\alpha^\lambda - z_{\alpha 0}^{\lambda(m-1)})\right\rangle \mathbf{B}^T + \sum_{\beta=1}^{5} \left\langle \ln(-z_\alpha^\lambda - \bar{z}_{\beta 0}^{\lambda(m-1)})\right\rangle \mathbf{B}^{-1}\bar{\mathbf{B}}\mathbf{I}_\beta \bar{\mathbf{B}}^T\} \frac{l_{m-1}+s}{l_{m-1}} ds$$
$$+\frac{1}{\pi}\int_{l_m} \{\left\langle \ln(z_\alpha^\lambda - z_{\alpha 0}^{\lambda(m)})\right\rangle \mathbf{B}^T + \sum_{\beta=1}^{5} \left\langle \ln(-z_\alpha^\lambda - \bar{z}_{\beta 0}^{\lambda(m)})\right\rangle \mathbf{B}^{-1}\bar{\mathbf{B}}\mathbf{I}_\beta \bar{\mathbf{B}}^T\} \frac{l_m - s}{l_m} ds \tag{6.70}$$

In particular the displacement at node j is given by

$$\mathbf{U}[\left\langle f(d_{\alpha j})\right\rangle] = \sum_{m=1}^{M} \mathrm{Im}\{\mathbf{A}\mathbf{D}_m[\left\langle f(d_{\alpha j})\right\rangle]\}\mathbf{b}_m . \tag{6.71}$$

Substituting Eq (6.66) into Eq (6.52), we have

$$P(\mathbf{b}) = \sum_{i=1}^{M}\left[\mathbf{b}_i^T \cdot \left(\sum_{j=1}^{M} \mathbf{k}_{ij}\mathbf{b}_j\right)/2 - \mathbf{g}_i\right] \tag{6.72}$$

where

$$\mathbf{k}_{ij} = \frac{1}{l_{j-1}}\int_{l_{j-1}} \mathrm{Im}[\mathbf{D}_i^T(\boldsymbol{\zeta}_0^{j-1})\mathbf{B}^T]ds - \frac{1}{l_j}\int_{l_j} \mathrm{Im}[\mathbf{D}_i^T(\boldsymbol{\zeta}_0^{j})\mathbf{B}^T]ds \tag{6.73}$$

$$\mathbf{g}_j = \int_{l_{j-1}+l_j} \mathbf{G}_j F_j(s) ds \tag{6.74}$$

and $\mathbf{G}_j = -\mathbf{t}_n^\theta$ when node j is located at the boundary L, $\mathbf{G}_j = \mathbf{t}^0 - \mathbf{t}_n^\theta$ for the other nodes. The minimization of Eq (6.72) leads to a set of linear equations:

$$\sum_{j=1}^{M} \mathbf{k}_{ij}\mathbf{b}_j = \mathbf{g}_i . \tag{6.75}$$

Similarly, the final form of the linear equations to be solved is obtained by selecting the appropriate equation from Eqs (6.71) and (6.75). Equation (6.71) will be chosen for those nodes at which the EDEP is prescribed, and Eq (6.75) will be chosen for the remaining nodes. Once the EDEP discontinuity **b** has been found, the SED at any point can be expressed as

$$\boldsymbol{\Pi}_1 = -\sum_{m=1}^{M} \mathrm{Im}[\mathbf{B}\mathbf{P}\mathbf{D}'_m(\zeta)]\mathbf{b}_m, \quad \boldsymbol{\Pi}_2 = \sum_{m=1}^{M} \mathrm{Im}[\mathbf{B}\mathbf{D}'_m(\zeta)]\mathbf{b}_m \tag{6.76}$$

Therefore, the surface traction-charge vector $\boldsymbol{\Pi}_n$ in a coordinate system local to a particular crack line, say the ith crack, can be expressed in the form

$$\boldsymbol{\Pi}_n = \Omega(\alpha_i)\{-\boldsymbol{\Pi}_1 \sin\alpha_i + \boldsymbol{\Pi}_2 \cos\alpha_i\}^T \tag{6.77}$$

where $\Omega(\alpha_i)$ is defined by

$$\Omega(\alpha) = \begin{bmatrix} \cos\alpha & \sin\alpha & 0 & 0 \\ -\sin\alpha & \cos\alpha & 0 & 0 \\ 0 & 0 & 1 & 0 \\ 0 & 0 & 0 & 1 \end{bmatrix} \tag{6.78}$$

Using Eq (6.77) we can evaluate the SED intensity factors by the following definition

$$\mathbf{K}(c) = \{K_{II}\ K_I\ K_{III}\ K_D\}^T = \lim_{r\to 0}\sqrt{2\pi r}\boldsymbol{\Pi}_n(r) \tag{6.79}$$

6.3 Application of BEM to determine SED intensity factors

In practical computations the SED intensity factors may be evaluated in several ways, such as extrapolation formulae, traction formulae, *J*-integral formulae [6], least-square method [7,8], and others [6]. In our analysis, the method of least-square is used, since only the EDEP field obtained from the BEM is required in the procedure. Therefore not much computer time is required for the calculation of *K*-factors. Moreover, it is very easy to implement the method into our BEM computer program. That is why we select the least-square method rather than any other to calculate SED intensity factors.

6.3.1 Relation between SED function and SED intensity factors

In order to take into account the crack-tip singularity of the SED field we choose the mapping function [9]

$$z_k - z_{k0} = w(\xi_k) = \xi_k^2, \qquad (k=1, 2, 3, 4, t) \tag{6.80}$$

where z_{k0} is the coordinate of the crack tip under consideration. Recall that the general expressions for the EDEP field and SED function of a linear thermopiezoelectric solid are [2]

$$\mathbf{U} = 2\,\mathrm{Re}[\mathbf{A}\mathbf{f}(\mathbf{z}) + \mathbf{c}g(z_t)], \quad \boldsymbol{\varphi} = 2\,\mathrm{Re}[\mathbf{B}\mathbf{f}(\mathbf{z}) + \mathbf{d}g(z_t)] \tag{6.81}$$

The EDEP and SED fields in ξ-plane can then be written as

$$\mathbf{U} = 2\,\mathrm{Re}[\mathbf{A}\mathbf{f}(\xi) + \mathbf{c}g(\xi_t)], \quad \boldsymbol{\Pi}_2 = 2\,\mathrm{Re}[\mathbf{B}\mathbf{f}'(\xi)/\xi + \mathbf{d}g'(\xi_t)/\xi_t] \tag{6.82}$$

With the usual definition, the vector of SED intensity factor, **K,** is evaluated by

$$\mathbf{K} = \lim_{\xi\to 0}\xi\sqrt{2\pi}\Pi_2 = 2\sqrt{2\pi}\lim_{\xi\to 0}\mathrm{Re}[\mathbf{B}\mathbf{f}'(\xi) + \mathbf{d}g'(\xi_t)] \tag{6.83}$$

The functions **f** and *g* near the crack tip can be assumed as simple polynomials of $\boldsymbol{\xi}$

$$\mathbf{f}(\xi) \approx \sum_{j=1}^{2n}(\mathbf{s}_j + i\mathbf{s}_{2n+j})\xi^j, \quad g(\xi_t) \approx \sum_{j=1}^{2n} r_j \xi_t^j \tag{6.84}$$

where r_j (j=1, 2, 3,…, 2n) are known complex constants, and $\mathbf{s}_j$ are real constant vectors to be determined.

On the crack surface which is traction-charge free, i.e., $\boldsymbol{\varphi}$ =0, substitution of Eq (6.84) into Eq $(6.81)_2$ yields

$$\boldsymbol{\varphi} = 2\,\mathrm{Re}\sum_{j=1}^{2n}[\mathbf{B}(\mathbf{s}_j + i\mathbf{s}_{2n+j})\xi^j + \mathbf{d}r_j\xi_t^j] = 0 \tag{6.85}$$

Noting that $\boldsymbol{\xi}^j = \xi_t^j = (-x)^{j/2}$ along the crack surface, where x is the distance from crack tip to the point concerned, we have

$$\mathbf{s}_{2n+j} = \mathbf{B}_R^{-1}[-\mathbf{B}_I\mathbf{s}_j + \mathrm{Im}\{\mathbf{d}r_j\}], \qquad \text{for } j=1, 3, 5,\ldots, 2n\text{-}1, \tag{6.86}$$

$$\mathbf{s}_{2n+j} = \mathbf{B}_I^{-1}[\mathbf{B}_R\mathbf{s}_j + \mathrm{Re}\{\mathbf{d}r_j\}], \qquad \text{for } j=2, 4, 6,\ldots, 2n, \tag{6.87}$$

in which $\mathbf{B}_R$=Re($\mathbf{B}$), $\mathbf{B}_I$=Im($\mathbf{B}$).

Substituting Eqs (6.86) and (6.87) into Eq (6.84), and then into Eqs (6.82) and (6.83), yields

$$\begin{aligned}\mathbf{U} &= \sum_{j=1}^{2n}[\mathbf{Q}_j(\xi)\mathbf{s}_j + \mathbf{S}_j(\xi,\xi_t)],\\ \mathbf{K} &= 2\sqrt{2\pi}\,\mathrm{Re}[\mathbf{B}(\mathbf{I}-i\mathbf{B}_R^{-1}\mathbf{B}_I)\mathbf{s}_1 + i\mathbf{B}\mathbf{B}_R^{-1}\,\mathrm{Im}(\mathbf{d}r_1) + \mathbf{d}r_1]\end{aligned} \tag{6.88}$$

where

$$\mathbf{Q}_j(\xi) = [\mathbf{I} - i\mathbf{B}_R^{-1}\mathbf{B}_I]\xi^j,\ \ \mathbf{S}_j(\xi,\xi_t) = i\mathbf{B}_R^{-1}\mathrm{Im}[\mathbf{d}r_j]\xi^j + \mathbf{d}r_j\xi_t^j,\ \ (j=1,\ 3,\ldots,\ 2n-1), \tag{6.89}$$

$$\mathbf{Q}_j(\xi) = [\mathbf{I} + i\mathbf{B}_I^{-1}\mathbf{B}_R]\xi^j,\ \ \mathbf{S}_j(\xi,\xi_t) = i\mathbf{B}_I^{-1}\mathrm{Re}[\mathbf{d}r_j]\xi^j + \mathbf{d}r_j\xi_t^j,\ \ (j=2,\ 4,\ldots,\ 2n) \tag{6.90}$$

6.3.2 Simulating K by BEM and least-square method

The least-square method may be developed by considering the residual vector for EDEP field at point k (k=1, 2, …, m)

$$\mathbf{R}_k = \sum_{j=1}^{2n}[\mathbf{Q}_j(\xi_k)\mathbf{s}_j + \mathbf{S}_j(\xi_k,\xi_{tk})] - \mathbf{U}_k, \qquad (k=1, 2,\ldots, m) \tag{6.91}$$

where $\mathbf{U}_k$ is the EDEP vector at point k obtained from the BEM given in the previous section.

The minimum for the sum of the squares of the residual vector

$$\pi = \{\mathbf{s}\}^T[\mathbf{Q}]^T[\mathbf{Q}]\{\mathbf{s}\} - 2\{\mathbf{s}\}^T[\mathbf{Q}]^T(\{\mathbf{U}\} - \{\mathbf{S}\}) + \text{terms without } \{\mathbf{s}\} \tag{6.92}$$

provides

$$[\mathbf{Q}]^T[\mathbf{Q}]\{\mathbf{s}\} = [\mathbf{Q}]^T(\{\mathbf{U}\} - \{\mathbf{S}\}), \tag{6.93}$$

where

$$\{\mathbf{s}\}=\{\mathbf{s}_1, \mathbf{s}_2,\ldots,\mathbf{s}_{2n}\}^T, \quad \{\mathbf{U}\} = \{\mathbf{U}_1, \mathbf{U}_2,\ldots,\mathbf{U}_m\}^T, \tag{6.94}$$

$$\{\mathbf{S}\} = \{\mathbf{S}_1^*, \mathbf{S}_2^*,\ldots,\mathbf{S}_m^*\}^T, \quad \mathbf{S}_k^* = \sum_{j=1}^{2n}\mathbf{S}_j(\xi_k,\xi_{tk}), \tag{6.95}$$

$$[\mathbf{Q}] = \begin{bmatrix} \mathbf{Q}_{11} & \mathbf{Q}_{21} & \cdots & \mathbf{Q}_{2n,1} \\ \mathbf{Q}_{12} & \mathbf{Q}_{22} & \cdots & \mathbf{Q}_{2n,2} \\ \cdots & \cdots & \cdots & \cdots \\ \mathbf{Q}_{1m} & \mathbf{Q}_{2m} & \cdots & \mathbf{Q}_{2n,m} \end{bmatrix}, \tag{6.96}$$

$$\mathbf{Q}_{jk} = \mathbf{Q}_j(\xi_k) \tag{6.97}$$

Once the unknown vector $\{\mathbf{s}\}$ has been obtained from Eq (6.93), the SED intensity factor $\mathbf{K}$ can be evaluated from Eq $(6.88)_2$. In the calculation, an appropriate number m can be set to obtain the required accuracy.

6.4 Effective properties of cracked piezoelectricity

6.4.1 Effective properties and concentration matrix $\mathbf{P}$

In Section 5.8 we presented formulations for predicting effective properties of

piezoelectricity with inclusions or holes. For piezoelectricity weakened by cracks, the effective material properties can be analyzed by the combination of micromechanics models presented in Section 5.8 and the BE Eqs (6.71) and (6.75). To this end, define the overall elastic, piezoelectric, and dielectric constants of the piezoelectric solid by [10]

$$\begin{aligned} \overline{\boldsymbol{\sigma}} &= \mathbf{C}^* \overline{\boldsymbol{\varepsilon}} - (\mathbf{e}^*)^T \overline{\mathbf{E}} \\ \overline{\mathbf{D}} &= \mathbf{e}^* \overline{\boldsymbol{\varepsilon}} + \boldsymbol{\kappa}^* \overline{\mathbf{E}} \end{aligned} \tag{6.98}$$

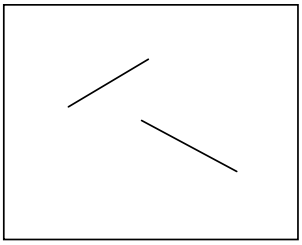

Fig. 6.3 A typical RVE with cracks

Using the definition (6.98), the following two types of boundary condition can be used to evaluate overall material properties:

a) Uniform traction, $\boldsymbol{\sigma}^0$, and electric displacement, $\mathbf{D}^0$, on boundary Γ of the RVE (see Fig. 6.3):

$$\boldsymbol{\sigma} = \boldsymbol{\sigma}^0, \quad \mathbf{D} = \mathbf{D}^0 \tag{6.99}$$

b) Uniform strain, $\boldsymbol{\varepsilon}^0$, and electric field, $\mathbf{E}^0$, on boundary Γ of the RVE:

$$\boldsymbol{\varepsilon} = \boldsymbol{\varepsilon}^0, \quad \mathbf{E} = \mathbf{E}^0 \tag{6.100}$$

Since the material behavior is linear, the principle of superposition is used to decompose the load ($\boldsymbol{\varepsilon}^0$, $\mathbf{E}^0$) into two elementary loadings ($\boldsymbol{\varepsilon}^0$, $\mathbf{E}^0$=0) and ($\boldsymbol{\varepsilon}^0$=0, $\mathbf{E}^0$). For the loading case ($\boldsymbol{\varepsilon}^0$, $\mathbf{E}^0$=0), Eq (6.98) becomes

$$\begin{aligned} \overline{\boldsymbol{\sigma}} &= \mathbf{C}^* \boldsymbol{\varepsilon}^0 \\ \overline{\mathbf{D}} &= \mathbf{e}^* \boldsymbol{\varepsilon}^0 \end{aligned} \tag{6.101}$$

Using relations (5.219) and (6.101), we have

$$\begin{aligned} \mathbf{C}^* &= \mathbf{C}_1 + (\mathbf{C}_2 - \mathbf{C}_1)\mathbf{A}_2 v_2 \\ \mathbf{e}^* &= \mathbf{e}_1 + (\mathbf{e}_2 - \mathbf{e}_1)\mathbf{A}_2 v_2 \end{aligned} \tag{6.102}$$

where the concentration tensor $\mathbf{A}_2$ is defined by the linear relation

$$\overline{\boldsymbol{\varepsilon}}_2 = \mathbf{A}_2 \boldsymbol{\varepsilon}^0 \tag{6.103}$$

Following the average strain theorem [11], the strain tensor, $\overline{\boldsymbol{\varepsilon}}_2$, can be expressed as

$$(\bar{\boldsymbol{\varepsilon}}_2)_{ij} = \frac{1}{2\Omega_2}\int_{\partial\Omega_2}(u_i n_j + u_j n_i)dS \tag{6.104}$$

where u_i is the ith component displacement vector, and n_i the ith component of unit outward vector normal to the boundary. When inclusions become cracks, Eq (6.104) cannot be directly used to calculate the average strain. This problem can be bypassed by considering cracks to be very flat voids of vanishing height and thus also of vanishing volume. Multiplying both sides of Eq (6.104) by v_2 and considering the limit of flattening out into cracks, i.e. $v_2 = \Omega_2/\Omega \to 0$, one obtains

$$\lim_{v_2\to 0}(\bar{\boldsymbol{\varepsilon}}_2 v_2)_{ij} = \frac{v_2}{2\Omega_2}\int_L(\Delta u_i n_j + \Delta u_j n_i)dS = \frac{1}{2\Omega}\int_L(\Delta u_i n_j + \Delta u_j n_i)dS \tag{6.105}$$

where Δu_i is the jump of displacement across the crack faces, $L = l_1 \cup l_2 \cup \ldots \cup l_N$, l_i is the length of the ith crack, N the number of cracks within the RVE under consideration. For convenience, we define

$$\mathbf{P} = \lim_{v_2\to 0}(\mathbf{A}_2 v_2) \tag{6.106}$$

where **P** can be calculated by the relation:

$$(\mathbf{P}\boldsymbol{\varepsilon}^0)_{ij} = \lim_{v_2\to 0}(\bar{\boldsymbol{\varepsilon}}_2 v_2)_{ij} = \frac{1}{2\Omega}\int_L(\Delta u_i n_j + \Delta u_j n_i)dS \tag{6.107}$$

Substituting Eq (6.106) into Eq (6.102) and considering $\mathbf{C}_2 \to 0$ and $\mathbf{e}_2 \to 0$ when inclusions become cracks, yields

$$\begin{aligned}\mathbf{C}^* &= \mathbf{C}_1(\mathbf{I}-\mathbf{P})\\ \mathbf{e}^* &= \mathbf{e}_1(\mathbf{I}-\mathbf{P})\end{aligned} \tag{6.108}$$

On the other hand, for the loading case ($\boldsymbol{\varepsilon}^0$=0, $\mathbf{E}^0$), Eq (6.98) leads to

$$\begin{aligned}\bar{\boldsymbol{\sigma}} &= -(\mathbf{e}^*)^T\mathbf{E}^0\\ \bar{\mathbf{D}} &= \boldsymbol{\kappa}^*\mathbf{E}^0\end{aligned} \tag{6.109}$$

Similar to the treatment in Eq (6.102), we have

$$\begin{aligned}\mathbf{e}^* &= \mathbf{e}_1 + \mathbf{B}_2^T(\mathbf{e}_2-\mathbf{e}_1)v_2\\ \boldsymbol{\kappa}^* &= \boldsymbol{\kappa}_1 + (\boldsymbol{\kappa}_2-\boldsymbol{\kappa}_1)\mathbf{B}_2 v_2\end{aligned} \tag{6.110}$$

where the tensor $\mathbf{B}_2$ is defined by

$$\bar{\mathbf{E}}_2 = \mathbf{B}_2\mathbf{E}_0 \tag{6.111}$$

By comparing Eqs $(6.102)_2$ and $(6.110)_1$, it is evident that

$$(\mathbf{e}_2-\mathbf{e}_1)\mathbf{A}_2 = \mathbf{B}_2^T(\mathbf{e}_2-\mathbf{e}_1) \tag{6.112}$$

Therefore the effective constitutive law (6.98) is completely defined once the concentration factor $\mathbf{A}_2$ has been determined.

The estimation of integral (6.104) or (6.105) and thus $\mathbf{A}_2$ (or $\mathbf{P}$) is the key to predicting the effective electroelastic moduli $\mathbf{C}^*$, $\mathbf{e}^*$, and $\boldsymbol{\kappa}^*$. Calculation of integral (6.104) or (6.105) through the use of the BEM is the subject of the following section. Eqs (6.71) and (6.75) are used to evaluate Δu_i in Eq (6.107). The matrix $\mathbf{P}$ can then be predicted through use of Eq (6.107).

6.4.2 Algorithms for self-consistent and Mori-Tanaka approaches

The algorithm used for predicting effective properties of cracked piezoelectricity based on the self-consistent or Mori-Tanaka approach is similar to that in Section 5.8 and is described in detail as below.

(a) Algorithms for self-consistent BEM approach

(a) Assume initial values of material constants $\mathbf{C}^*_{(0)}$, $\mathbf{e}^*_{(0)}$, and $\boldsymbol{\kappa}^*_{(0)}$ ($\mathbf{C}^*_{(0)}=\mathbf{C}^0$, $\mathbf{e}^*_{(0)}=\mathbf{e}^0$ and $\boldsymbol{\kappa}^*_{(0)}=\boldsymbol{\kappa}^0$ are used as initial value in our analysis)

(b) Solve Eqs (6.71) and (6.75) for $\mathbf{b}_{m(i)}$ ($=\Delta u_{m(i)}$) using the values of $\mathbf{C}^*_{(i-1)}$, $\mathbf{e}^*_{(i-1)}$, and $\boldsymbol{\kappa}^*_{(i-1)}$, where the subscript ($i$) stands for the variable associated with the the ith iterative cycle.

(c) Calculate $\mathbf{P}_{(i)}$ in Eq (6.106)) by way of Eq (6.107) using the current values of $\mathbf{b}_{m(i)}$, and then determine $\mathbf{C}^*_{(i)}$, $\mathbf{e}^*_{(i)}$, and $\boldsymbol{\kappa}^*_{(i)}$ by way of Eqs (6.102) and (6.110).

(d) If $\varepsilon_{(i)} = \left\|\mathbf{F}^*_{(i)} - \mathbf{F}^*_{(i-1)}\right\| / \left\|\mathbf{F}^*_{(0)}\right\| \le \varepsilon$, where ε is a convergent tolerance, terminate the iteration; $\mathbf{F}$ may be $\mathbf{C}$, $\mathbf{e}$ or $\boldsymbol{\kappa}$, otherwise take $\mathbf{C}^*_{(i)}$, $\mathbf{e}^*_{(i)}$, and $\boldsymbol{\kappa}^*_{(i)}$ as the initial values and go to Step (b).

(b) Mori-Tanaka-BEM approach

As indicated in Section 5.8.4, the key assumption in the Mori-Tanaka theory is that the concentration matrix $\mathbf{P}^{MT}$ is given by the solution for a single crack embedded in an intact solid subject to an applied strain field equal to the as yet

unknown average field in the solid, which means that the introduction of cracks in the solid results in a value of $\bar{\boldsymbol{\varepsilon}}_2$ given by

$$\bar{\boldsymbol{\varepsilon}}_2 = \mathbf{A}_2^{DIL}\bar{\boldsymbol{\varepsilon}}_1 \tag{6.113}$$

where $\mathbf{A}_2^{DIL}$ is the concentration matrix related to the dilute model. As such, it is easy to prove that [11]

$$\mathbf{P}^{MT} = \mathbf{P}^{DIL}(\mathbf{I} + \mathbf{P}^{DIL})^{-1} \tag{6.114}$$

where **I** is unit matrix. It can be seen from Eq (6.114) that the Mori-Tanaka approach provides explicit expressions for effective constants of defective piezoelectric solids. Therefore, no iteration is required with the mixed Mori-Tanaka-BEM.

6.5 Numerical examples

As an illustration, the proposed BE model is applied to the following two numerical examples in which an inclusion and a crack are involved. In all the calculations, the materials for the matrix and the elliptic inclusion are assumed to be $BaTiO_3$ and Cadmium Selenide, respectively. The material constants for the two materials are as follows:

(i) Material constants for $BaTiO_3$

$c_{11} = 150$ GPa, $c_{12} = 66$ GPa, $c_{13} = 66$ GPa, $c_{33} = 146$ GPa, $c_{44} = 44$ GPa,
$\alpha_{11}^* = 8.53\times10^{-6}\,\mathrm{K}^{-1}$, $\alpha_{33}^* = 1.99\times10^{-6}\,\mathrm{K}^{-1}$, $\lambda_3 = 0.133\times10^5$ N/CK,
$e_{31} = -4.35$ C/m^2, $e_{33} = 17.5$ C/m^2, $e_{15} = 11.4$ C/m^2, $\kappa_{11} = 1115\,\kappa_0$,
$\kappa_{33} = 1260\,\kappa_0$, $\kappa_0 = 8.85\times10^{-12}$ C^2/Nm^2 = permittivity of free space

(ii) Material constants for Cadmium Selenide

$c_{11} = 74.1$ GPa, $c_{12} = 45.2$ GPa, $c_{13} = 39.3$ GPa, $c_{33} = 83.6$ GPa,
$c_{44} = 13.2$ GPa, $\gamma_{11} = 0.621\times10^6$ NK^{-1}m^{-2}, $\gamma_{33} = 0.551\times10^6$ NK^{-1}m^{-2},
$g_3 = -0.294\times10^5$ CK^{-1}m^{-2}, $e_{31} = -0.160$ Cm^{-2}, $e_{33} = 0.347$ Cm^{-2},
$e_{15} = 0.138$ Cm^{-2}, $\kappa_{11} = 82.6\times10^{-12}$ C^{2}N^{-1}m^{-2}, $\kappa_{33} = 90.3\times10^{-12}$ C^{2}N^{-1}m^{-2}

where c_{ij} is elastic stiffness, α_{11}^* and α_{33}^* are thermal expansion constants, λ_3 and g_3 are pyroelectric constants, e_{ij} is piezoelectric constants, and γ_{ij} is a piezothermal constant.

Since the values of the coefficient of heat conduction for $BaTiO_3$ and Cadmium Selenide could not be found in the literature, the values $k_{33}/k_{11}=1.5$ for $BaTiO_3$ and $k_{33}/k_{11}=1.8$ for Cadmium Selenide, $k_{13}=0$ and $k_{11}=1$ W/mK are assumed.

In our analysis, plane strain deformation is assumed and the crack line is assumed to be in the x_1-x_2 plane, i.e., $D_3=u_3=0$. Therefore the stress intensity factor vector $\mathbf{K}^*$ now has only three components (K_I, K_{II}, K_D).

In the least-square method, the SED intensity factors are affected by the parameters n, d_{max} and d_{min}, where n is the number of terms in Eq (6.91), d_{max} is the

maximum distance from crack tip to the *n*-point at which the residual vectors are calculated, and d_{min} is the minimum distance. In our analysis d_{min} is set to be $0.05c$.

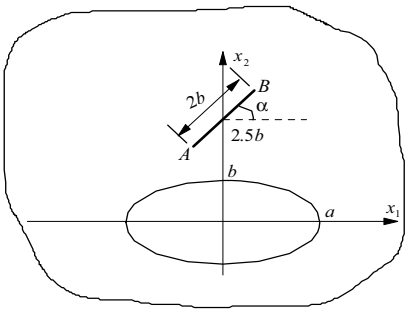

Fig. 6.4 Geometry of the crack-inclusion system

Example 1: Consider a crack of length $2b$ and an inclusion embedded in an infinite plate as shown in Fig. 6.4. The uniform heat flow h_{n0} is applied on the crack face only. In our analysis, the crack was modelled by 40 linear elements. Table 1 shows that the numerical results for the coefficients of stress intensity factors β_i at point A (see Fig. 6.4) vary with d_{max} when the crack angle $\alpha = 0^\circ$ and n=5, 10, 15, respectively, where β_i are defined by

$$\begin{aligned} K_I &= h_{n0} c\sqrt{\pi c}\gamma_{33}\beta_1 / k_1 , \\ K_{II} &= h_{n0} c\sqrt{\pi c}\gamma_{11}\beta_2 / k_1 , \\ K_D &= h_{n0} c\sqrt{\pi c}\chi_3\beta_D / k_1 \end{aligned} \tag{6.115}$$

Table 6.1 The BEM results for coefficients β_i vs d_{max} in Example 1

d_{max}/c	n	β_1	β_2	β_D
0.5	5	1.230	0.328	0.755
	10	1.224	0.323	0.747
	15	1.222	0.322	0.745
1.0	5	1.225	0.321	0.749
	10	1.221	0.318	0.745
	15	1.220	0.318	0.743
1.5	5	1.231	0.328	0.757
	10	1.227	0.324	0.752
	15	1.226	0.323	0.750
SIEM		1.207	0.311	0.732

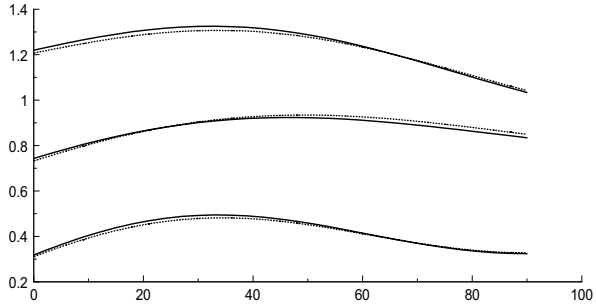

Fig. 6.5 The coefficients β_i versus crack angle α

For comparison, the singular integral equation method (SIEM) given in [12,13] was used to obtain corresponding results. It can be seen from Table 6.1 that the results obtained using $d_{max}=c$ are often closer to those obtained by SIEM than by using $d_{max}=0.5c$ or $d_{max}=1.5c$. This is because more data can be included into the least-square method for a large d_{max}, but a too large d_{max} may not represent the crack-tip properties and can cause errors.

Figure 6.5 shows the results of coefficients β_i as a function of crack angle α when $d_{max}=c$ and n=15. It is evident from the figure that all the coefficients β_i are not very sensitive to the crack angle, but vary slightly with it. It is also evident that the two numerical models (BEM and SIEM) provide almost the same results.

Example 2: Consider a rectangular thermopiezoelectric plate containing a crack and an inclusion as shown in Fig. 6.6. In the calculation, each side of the outer boundary is modelled by 50 linear elements and the crack is divided into 40 linear elements, and $d_{max}=b$ and n=15 are used. In Fig. 6.6 the coefficients of SED intensity factors β_i at point A (see Fig. 6.6) are presented as a function of crack orientation angle α. Numerical results for such a problem are not yet available in the literature. Therefore for comparison, the well-known finite element method [14] is used to obtain corresponding results. In the calculation, an eight-node quadrilateral element model has been used. In addition, the three nodes along one of the sides of each of the quadrilateral elements are collapsed at the crack tip and the two adjoining mid-points are moved to the quarter distances [15], in order to produce $1/r^{1/2}$ type of singularity. It can be seen from Fig. 6.7 that the values of β_i are more sensitive to crack orientation than those in Example 1. They reach their peak values at $\alpha = 37^\circ$ for β_1, $\alpha = 42^\circ$ for β_2, and $\alpha = 50^\circ$ for β_D, respectively. It is also evident from Fig. 6.7 that the maximum discrepancy between the numerical results obtained from the two models is less than 5%.

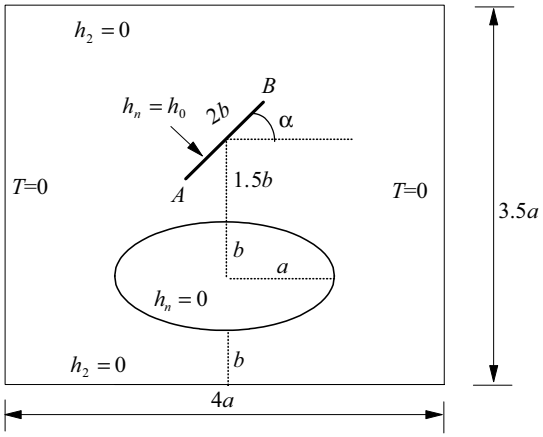

Fig. 6.6 Configuration of the crack-inclusion system in Example 2 (a=2b)

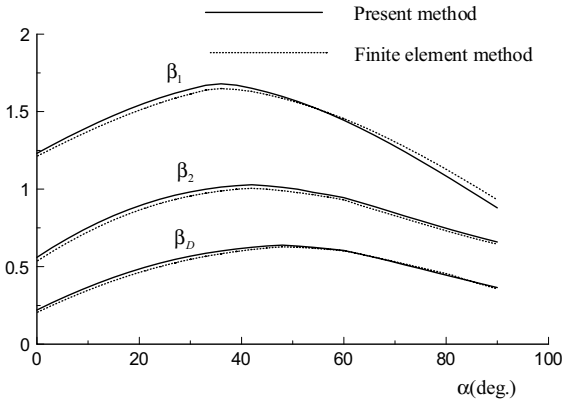

Fig. 6.7 SED intensity factors versus crack angle α

References

[1] Qin QH, Thermoelectroelastic analysis of cracks in piezoelectric half-plane by BEM, *Computa Mech*, 23, 353-360, 1999

[2] Qin QH and Lu M, BEM for crack-inclusion problems of plane thermo-piezoelectric solids, Int J Numer Meth Eng, 48, 1071-1088, 2000

[3] Qin QH and Mai YW, BEM for crack-hole problems in thermopiezoelectric materials, Eng Frac Mech, 69, 577-588, 2002

[4] Qin QH, Green's functions of magnetoelectroelastic solids and applications to fracture analysis, pp93-106, in Proc. of 9th Int Conf on Inspection, Appraisal, Repairs & Maintenance of Structures, Fuzhou, China, 20-21 Oct, 2005

[5] Yin HP and Ehrlacher A, Variational approach of displacement discontinuity method and application to crack problems, Int J Frac, 63, 135-153, 1993

[6] Aliabadi MH and Rooke DP, Numerical Fracture Mechanics, Computational Mechanics Publications: Southampton, 1991
[7] Ju SH, Simulating stress intensity factors for anisotropic materials by the least-square method, Int J Frac, 81, 283-397, 1996
[8] Ju SH, Simulating three-dimensional stress intensity factors by the least-square method, Int J Numer Meth Eng, 43, 1437-1451, 1998
[9] Khalil SA, Sun CT and Kwang WC, Application of a hybrid finite element method to determine stress intensity factors in unidirectional composites, Int J Frac, 31, 37-51, 1986
[10] Qin QH, Micromechanics-BE solution for properties of piezoelectric materials with defects, Eng Anal Boundary Elements, 28, 809-814, 2004
[11] Qin QH and Yu SW, Effective moduli of thermopiezoelectric material with microcavities, Int J Solids Struct, 35, 5085-5095, 1998
[12] Hill LR and Farris TN, Three dimensional piezoelectric boundary elements. Proceedings of SPIE, Mathematics and Control in Smart Structures, 3039, 406-417, 1997
[13] Khutoryaansky N, Sosa H and Zu WH, Approximate Green's functions and a boundary element method for electroelastic analysis of active materials, Compu & Struct, 66, 289-299, 1998
[14] Oden JT and Kelley BE, Finite element formulation of general electrothermo-elasticity problems, Int J Numer Meth Eng, 3, 161-179, 1971
[15] Anderson JL, Fracture Mechanics: Fundamentals and Applications, CRC Press: Boston, 1991

Chapter 7 Trefftz Boundary Element Method

7.1 Introduction

In the previous two chapters, we presented boundary element formulation of piezoelectric problem using Green's function and generalized dislocation solution. The boundary element formulation can also be established using the Trefftz function approach [1-4]. The name 'Trefftz function' here indicates that the regular trial functions, in contrast to the singular Green's function, satisfy all governing differential equations. To distinguish the above two types of boundary element formulations, we refer to the former as Somigliana boundary element formulation (SBEF) and the latter as Trefftz boundary element method (TBEM). The TBEM can, in general, be classified as either indirect and direct formulations. In the indirect formulation [1,2], which is thought to be the original one presented by Trefftz, the solution of the problem is approximated by the superposition of the functions satisfying the governing differential equation, and then the unknown parameters are determined so that the approximate solution satisfies the boundary condition by means of the collocation, least square or Galerkin method. In the direct formulation, a relatively new formulation presented by Cheung and his co-workers [5,6], the weighted residual expression of the governing equation is derived by taking the regular Trefftz functions satisfying the governing equation as the weighting function, and then the boundary integral equation is obtained by applying the Gauss divergence formula to it twice. The resulting boundary integral equation, as in the boundary element method, is discretized and solved for the boundary unknowns. It should be mentioned that the basic distinction between the Trefftz and the conventional (sometimes known as Somigliana) BEM, presented in the previous two chapters, is that while Trefftz methods are based on the use of Trefftz functions which are regular functions, Somigliana methods make use of Green's functions which are either singular or hyper-singular functions. As a consequence, whenever an integration is carried out, it is always simpler and more economical in the Trefftz method than in the Somigliana method. This is an important advantage that makes the TBEM so powerful when compared with conventional BEM. In this chapter, the two alternative techniques (indirect and direct formulations) are described briefly in order to provide an introduction to the TBEM.

7.2 Anti-plane piezoelectric problems

In this section the application of the TBEM to anti-plane electroelastic problems is described. In particular, both direct and indirect methods with domain decomposition are considered. The TBEM discussed here is based on a weighted residual formulation presented in [1].

7.2.1 Trefftz functions

To show how the Trefftz functions of anti-plane piezoelectric problems can be generated, consider an anti-plane shear deformation involving only out-of-plane displacement u_z and in-plane electric fields as defined by Eqs (2.278)-(2.285). The boundary conditions corresponding to the boundary value problem (2.278)-(2.285) can be written:

$$u_z = \bar{u}_z \qquad \text{on } \Gamma_u \tag{7.1}$$

$$t = \sigma_{3j} n_j = \bar{t} \qquad \text{on } \Gamma_t \tag{7.2}$$

$$D_n = D_i n_i = -\bar{q}_s = \bar{D}_n \qquad \text{on } \Gamma_D \tag{7.3}$$

$$\phi = \bar{\phi} \qquad \text{on } \Gamma_\phi \tag{7.4}$$

where $\bar{u}$, $\bar{t}$, $\bar{D}_n$ and $\bar{\phi}$ are, respectively, prescribed boundary displacement, traction force, surface charge and electric potential, an overhead bar denotes prescribed value, and $\Gamma=\Gamma_u+\Gamma_t=\Gamma_D+\Gamma_\phi$ is the boundary of the solution domain Ω.

It is well known that the solutions of the Laplace equation (2.285) may be found using the method of variable separation. By this method, the Trefftz functions corresponding to Eq (2.285) are obtained as [7]

$$u_z(r,\theta) = \sum_{m=0}^{\infty} r^m (a_m \cos m\theta + b_m \sin m\theta) \tag{7.5}$$

$$\phi(r,\theta) = \sum_{m=0}^{\infty} r^m (c_m \cos m\theta + d_m \sin m\theta) \tag{7.6}$$

for a bounded region and

$$u_z(r,\theta) = a_0^* + a_0 \ln r + \sum_{m=1}^{\infty} r^{-m} (a_m \cos m\theta + b_m \sin m\theta), \tag{7.7}$$

$$\phi(r,\theta) = c_0^* + c_0 \ln r + \sum_{m=1}^{\infty} r^{-m} (c_m \cos m\theta + d_m \sin m\theta) \tag{7.8}$$

for an unbounded region, where r and θ are a pair of polar coordinates. Thus, the associated Trefftz function sets of Eqns (7.5)-(7.8) can be expressed in the form

$$N = \{1, r\cos\theta, r\sin\theta, ..., r^m \cos m\theta, r^m \sin m\theta, ...\} = \{N_i\}, \tag{7.9}$$

$$N = \{1, \ln r, r^{-1} \cos\theta, r^{-1} \sin\theta, ..., r^{-m} \cos m\theta, r^{-m} \sin m\theta, ...\} = \{N_i\} \tag{7.10}$$

7.2.2 Special solution set for a subdomain containing an angular corner

It is well known that singularities induced by local defects such as angular corners, cracks, and so on, can be accurately accounted for in the conventional FE or BEM model by way of appropriate local refinement of the element mesh. However, an important feature of the Trefftz method is that such problems can be far more efficiently handled by the use of particular solutions [7]. In this sub-section we show how particular solutions can be constructed to satisfy both the Laplace equation (2.285) and the traction-free boundary conditions on angular corner faces (Fig. 7.1). The derivation of such functions is based on the general solution of the two-dimensional Laplace equation:

$$u_z(r,\theta) = a_0 + \sum_{n=1}^{\infty} (a_n r^{\lambda_n} + c_n r^{-\lambda_n}) \cos(\lambda_n \theta) + \sum_{n=1}^{\infty} (d_n r^{\lambda_n} + g_n r^{-\lambda_n}) \sin(\lambda_n \theta), \tag{7.11}$$

$$\phi(r,\theta) = b_0 + \sum_{n=1}^{\infty} (b_n r^{\lambda_n} + f_n r^{-\lambda_n}) \cos(\lambda_n \theta) + \sum_{n=1}^{\infty} (e_n r^{\lambda_n} + h_n r^{-\lambda_n}) \sin(\lambda_n \theta) \tag{7.12}$$

Appropriate trial functions for a sub-domain containing a singular corner are obtained by considering an infinite wedge (Fig. 7.1) with particular boundary conditions prescribed along the sides $\theta=\pm\theta_0$ forming the angular corner. The boundary conditions

on the upper and lower surfaces of the wedge are free of surface traction and surface charge:

$$\sigma_{z\theta} = c_{44}\frac{\partial u_z}{r\partial\theta} + e_{15}\frac{\partial\phi}{r\partial\theta} = 0, \quad D_\theta = e_{15}\frac{\partial u_z}{r\partial\theta} - \kappa_{11}\frac{\partial\phi}{r\partial\theta} = 0 \tag{7.13}$$

This leads to

$$\frac{\partial u_z}{\partial\theta} = 0, \quad \frac{\partial\phi}{\partial\theta} = 0 \qquad (\text{for } \theta = \pm\theta_0) \tag{7.14}$$

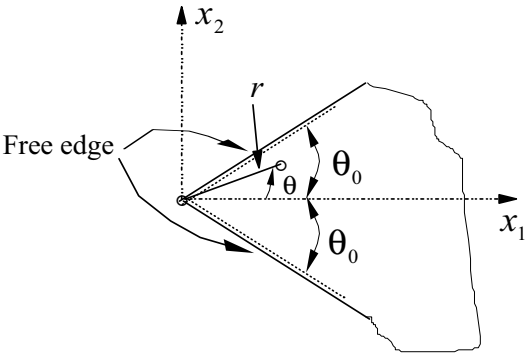

Fig. 7.1 Typical subdomain containing a singular corner

Considering the symmetry of the free boundary condition on the x_1-axis of the singular corner and the different properties of sin- and cos- functions, which should depend on different variables in order to satisfy the same boundary conditions, introduce a set of new constants β_n and rewrite the general solutions (7.11) as

$$u_z(r,\theta) = a_0 + \sum_{n=1}^{\infty}(a_n r^{\lambda_n} + c_n r^{-\lambda_n})\cos(\lambda_n\theta) + \sum_{n=1}^{\infty}(d_n r^{\beta_n} + g_n r^{-\beta_n})\sin(\beta_n\theta) \tag{7.15}$$

where λ_n and β_n are two sets of constants which are assumed to be greater than zero. Differentiating the solution (7.15) and substituting it into Eq (7.14) yields

$$\frac{\partial u_z}{\partial\theta}\Big|_{\theta=\pm\theta_0} = -\sum_{n=1}^{\infty}\lambda_n(a_n r^{\lambda_n} + c_n r^{-\lambda_n})\sin(\pm\lambda_n\theta_0)$$

$$+\sum_{n=1}^{\infty}\beta_n(d_n r^{\beta_n} + g_n r^{-\beta_n})\cos(\pm\beta_n\theta_0) = 0 \tag{7.16}$$

Since the solution must be limited for $r = 0$, we should specify

$$c_n = g_n = 0 \tag{7.17}$$

From Eq (7.16) it can be deduced that

$$\sin(\pm\lambda_n\theta_0) = 0, \qquad \cos(\pm\beta_n\theta_0) = 0, \tag{7.18}$$

leading to

$$\lambda_n \theta_0 = n\pi, \qquad (n=1,2,3,\ldots), \tag{7.19}$$

$$2\beta_n \theta_0 = n\pi, \qquad (n=1,3,5,\ldots) \tag{7.20}$$

Thus, for an element containing an edge crack (in this case $\theta_0 = \pi$), the solution can be written in the form

$$u_z(r,\theta) = a_0 + \sum_{n=1}^{\infty} a_n r^n \cos(n\theta) + \sum_{n=1,3,5}^{\infty} d_n r^{\frac{n}{2}} \sin(\frac{n}{2}\theta) = \sum_{n=1}^{\infty} a_n r_n^* + \sum_{n=1,3,5}^{\infty} d_n f_n^* \tag{7.21}$$

where $r_n^* = r^n \cos(n\theta)$ and $f_n^* = r^{\frac{n}{2}} \sin(\frac{n}{2}\theta)$.

It is obvious that the displacement function (7.21) includes the term proportional to $r^{1/2}$, whose derivative is singular at the crack tip. The solution for the second equation of (7.14) can be obtained similarly and denoted as

$$\phi(r,\theta) = b_0 + \sum_{n=1}^{\infty} b_n r^n \cos(n\theta) + \sum_{n=1,3,5}^{\infty} e_n r^{\frac{n}{2}} \sin(\frac{n}{2}\theta) = \sum_{n=1}^{\infty} b_n r_n^* + \sum_{n=1,3,5}^{\infty} e_n f_n^* \tag{7.22}$$

Thus, the associated T-complete sets of Eqs (7.21) and (7.22) can be expressed in the form

$$N = \{1, r\cos\theta, r^{\frac{1}{2}} \sin(\frac{\theta}{2}), \ldots, r^m \cos m\theta, r^{\frac{2m-1}{2}} \sin(\frac{2m-1}{2}\theta), \ldots\} = \{N_i\} \tag{7.23}$$

7.2.3 Stress intensity factor

Generally, stress intensity factors (SIF) can be evaluated by analysing stress and displacement fields near crack-tips using various numerical methods such as conventional FEM and BEM. These procedures are usually complicated and time-consuming as they cannot calculate the SIF directly from basic variables like the coefficients d_i and e_i. But in the light of the special purpose function for the crack-tip element, local field distributions can be easily obtained in crack problems, such as stress and electric displacement fields. Thus, the high efficiency in solving singular problems by the HTBE approach creates the attractive possibility of straightforwardly evaluating SIF K_{III} and K_D from d_i and e_i, which are associated with the singular factors in particular solutions (7.21) and (7.22). To show this, considering the $r^{-1/2}$ type of stress singularity, the corresponding SIF K_{III} can be defined as

$$\sigma_{32} = \frac{K_{III}}{\sqrt{2\pi r}} \cos\frac{\theta}{2} \quad \Rightarrow \quad K_{III} = \lim_{r\to 0} \sqrt{2\pi r}\,\sigma_{32} / \cos\frac{\theta}{2} \tag{7.24}$$

and when $\theta = 0$

$$K_{III} = \lim_{r\to 0} \sqrt{2\pi r}\,\sigma_{32} \tag{7.25}$$

Substituting Eqs (2.281), (2.282), and (7.21) into Eq (7.25), we have

$$K_{III} = \lim_{r\to 0}\sqrt{2\pi r}\left\{\sum_{n=1}^{\infty}\left(c_{44}a_n + e_{15}b_n\right)\frac{\partial r_n^*}{\partial y} + \sum_{n=1,3,5}^{\infty}\left(c_{44}d_n + e_{15}e_n\right)\frac{\partial f_n^*}{\partial y}\right\} \tag{7.26}$$

When the crack tip is defined at the origin of the polar coordinate system (see Fig. 7.1), Eq (7.26) can be written as

$$K_{III} = \lim_{r\to 0}\frac{\sqrt{2\pi r}}{r}\left(\sum_{n=1}^{\infty}\left(c_{44}a_n + e_{15}b_n\right)\frac{\partial r_n^*}{\partial \theta} + \sum_{n=1,3,5}^{\infty}\left(c_{44}d_n + e_{15}e_n\right)\frac{\partial f_n^*}{\partial \theta}\right) \tag{7.27}$$

Substituting Eq (7.27) into Eq (7.26), we can obtain the expression of the stress singular factor

$$K_{III} = \sqrt{\frac{\pi}{2}}\left(c_{44}d_1 + e_{15}e_1\right) \tag{7.28}$$

In general, when $\theta_0 \neq \pi$, the singularity becomes the type $r^{\lambda-1}$, where $\lambda = 1-\pi/2\theta_0$, and the general expression of stress intensity factors corresponding to stress singularity is defined as

$$K_{III} = \lim_{r\to 0}\left[\frac{(2\pi)^{1/2}}{r^{1-\lambda}}\sigma_{32}(r,0)\right] \tag{7.29}$$

and it can be also written as:

$$K_{III} = \sqrt{2\pi}\left(c_{44}d_1 + e_{15}e_1\right)\frac{\pi}{2\theta_0} \tag{7.30}$$

Similarly, the singularity factor K_D can also be written as

$$K_D = \sqrt{2\pi}\left(e_{15}d_1 - \kappa_{11}e_1\right)\frac{\pi}{2\theta_0} \tag{7.31}$$

7.2.4. Indirect formulation

In the indirect method, the unknown displacement u_z and electric potential ϕ are approximated by the expansions as

$$\mathbf{u} = \begin{Bmatrix} u_z \\ \phi \end{Bmatrix} = \sum_{j=1}^{m}\begin{bmatrix} N_{1j} & 0 \\ 0 & N_{2(m+j)} \end{bmatrix}\begin{Bmatrix} c_j \\ c_{m+j} \end{Bmatrix} = \begin{bmatrix} \mathbf{N}_1 \\ \mathbf{N}_2 \end{bmatrix}\mathbf{c} = \mathbf{N}\mathbf{c} \tag{7.32}$$

where N_{ij} is taken from Eq (7.9) for subdomains without cracks and from Eq (7.23) for the rest, and **c** denotes the unknown vector. Using the definitions (2.280), (2.282), (7.2) and (7.3), the generalized boundary force and electric displacements can be given by

$$\mathbf{T} = \begin{Bmatrix} t \\ D_n \end{Bmatrix} = \begin{Bmatrix} \sigma_{3j}n_j \\ D_j n_j \end{Bmatrix} = \sum_{j=0}^{m}\begin{bmatrix} Q_{1j} & Q_{1(m+j)} \\ Q_{2j} & Q_{2(m+j)} \end{bmatrix}\begin{Bmatrix} c_j \\ c_{m+j} \end{Bmatrix} = \begin{bmatrix} \mathbf{Q}_1 \\ \mathbf{Q}_2 \end{bmatrix}\mathbf{c} = \mathbf{Q}\mathbf{c} \tag{7.33}$$

With the expressions above, the indirect formulation corresponding to the anti-plane problem can be expressed by

$$\int_{\Gamma_u}(\bar{u}_z - u_z)w_1 ds + \int_{\Gamma_\phi}(\bar{\phi} - \phi)w_2 ds + \int_{\Gamma_t}(\bar{t} - t)w_3 ds + \int_{\Gamma_D}(\bar{D}_n - D_n)w_4 ds = 0 \tag{7.34}$$

where w_i (i=1-4) are arbitrary weighting functions and u_z, ϕ, t, D_n have the series representations (7.32) and (7.33).

(a) Galerkin method

If we use the Galerkin method, the weighting functions are chosen as arbitrary variations of the expressions (7.32) and (7.33), that is:

$$w_1 = \mathbf{Q}_1 \delta\mathbf{c}\,,\ w_2 = \mathbf{Q}_2 \delta\mathbf{c}\,,\ w_3 = -\mathbf{N}_1 \delta\mathbf{c}\,,\ w_4 = -\mathbf{N}_2 \delta\mathbf{c} \tag{7.35}$$

Substituting Eq (7.35) into Eq (7.34), yields

$$\mathbf{K}\mathbf{c} = \mathbf{f} \tag{7.36}$$

where

$$\mathbf{K} = \int_{\Gamma_u} \mathbf{Q}_1^T \mathbf{N}_1 ds - \int_{\Gamma_t} \mathbf{N}_1^T \mathbf{Q}_1 ds + \int_{\Gamma_\phi} \mathbf{Q}_2^T \mathbf{N}_2 ds - \int_{\Gamma_D} \mathbf{N}_2^T \mathbf{Q}_2 ds \tag{7.37}$$

$$\mathbf{f} = \int_{\Gamma_u} \mathbf{Q}_1^T \overline{u}_z ds - \int_{\Gamma_t} \mathbf{N}_1^T \overline{t}\, ds + \int_{\Gamma_\phi} \mathbf{Q}_2^T \overline{\phi} ds - \int_{\Gamma_D} \mathbf{N}_2^T \overline{D}_n ds \tag{7.38}$$

It is noted that the formulation above applies only to the solution domain containing one semi-infinite crack, when the particular solution (7.23) is used as the weighting function. For multi-crack problems, the domain decomposition approach is required. In this case, the solution domain is divided into several sub-domains (Fig. 7.2). For example, a domain containing two cracks can be divided into four sub-domains (Fig. 7.2), In the figure, Ω_i (i=1-4) denote the sub-domains, Γ the outer boundary, and Γ_{Iij} the inner boundaries between sub-domains. For each sub-domain, the indirect method leads to

$$\mathbf{K}_i \mathbf{c}_i = \mathbf{f}_i \qquad (i\text{=}1\text{-}4) \tag{7.39}$$

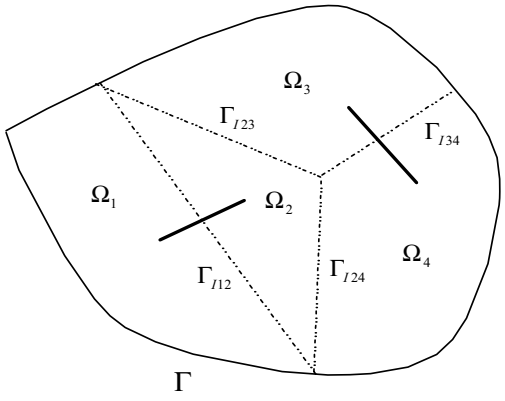

Fig. 7.2 Four sub-domain problem

On the inner boundary Γ_{Ij}, the continuity conditions provide

$$u_{zI}^{i} = u_{zI}^{j}, \quad \phi_I^i = \phi_I^j, \quad t_I^i = -t_I^j, \; D_{nI}^i = -D_{nI}^j \tag{7.40}$$

where the subscript I stands for the inner boundary, and superscript i (or j) means the ith (or jth) subdomain. Eqs (7.39) and (7.40) can be used to solve multiple crack problems.

(b) Point-collocation formulation

The collocation technique is obtained when the four weighting functions in Eq (7.34) are chosen as the Dirac delta function:

$$w_j = \delta(P - P_i) \quad (j\text{=}1\text{-}4) \tag{7.41}$$

where P_i is the collocation point. Substituting Eq (7.41) into Eq (7.34) yields

$$u_z(P_i) = \mathbf{N}_1(P_i)\mathbf{c} = \bar{u}_z(P_i), \qquad (P_i \in \Gamma_u, \; i = 1,2,\cdots M_1) \tag{7.42}$$

$$\phi(P_i) = \mathbf{N}_2(P_i)\mathbf{c} = \bar{\phi}(P_i), \qquad (P_i \in \Gamma_\phi, \; i = 1,2,\cdots M_2) \tag{7.44}$$

$$t(P_i) = \mathbf{Q}_1(P_i)\mathbf{c} = \bar{t}(P_i), \qquad (P_i \in \Gamma_t, \; i = 1,2,\cdots M_3) \tag{7.43}$$

$$D_n(P_i) = \mathbf{Q}_2(P_i)\mathbf{c} = \bar{D}_n(P_i), \qquad (P_i \in \Gamma_D, \; i = 1,2,\cdots M_4) \tag{7.45}$$

where M_1-M_4 are the numbers of the collocation points placed on Γ_u, Γ_t, Γ_ϕ and Γ_D, respectively. Using matrix notation, Eqs (7.42)-(7.45) can be written as

$$K_{ij} c_j = f_i \quad \text{or} \quad \mathbf{Kc} = \mathbf{f} \tag{7.46}$$

where the unknown c_j represents the constant coefficient of the jth term in the expansion (7.32), and K_{ij} and f_i are respectively given by

$$K_{ij} = \begin{cases} N_{1j}(P_i) & \text{if } P_i \in \Gamma_u, \\ N_{2j}(P_i) & \text{if } P_i \in \Gamma_\phi, \\ Q_{1j}(P_i) & \text{if } P_i \in \Gamma_t, \\ Q_{2j}(P_i) & \text{if } P_i \in \Gamma_D \end{cases} \tag{7.47}$$

$$f_i = \begin{cases} \bar{u}_z(P_i) & \text{if } P_i \in \Gamma_u, \\ \bar{\phi}(P_i) & \text{if } P_i \in \Gamma_\phi, \\ \bar{t}(P_i) & \text{if } P_i \in \Gamma_t, \\ \bar{D}_n(P_i) & \text{if } P_i \in \Gamma_D \end{cases} \tag{7.48}$$

(c) Least square method

The least square method formulation can be obtained by considering the residual function

$$R(\mathbf{c}) = \int_{\Gamma_u} (N_1\mathbf{c} - \bar{u}_z)^2 ds + \alpha_1 \int_{\Gamma_\phi} (N_2\mathbf{c} - \bar{\phi})^2 ds + \alpha_2 \int_{\Gamma_t} (\mathbf{Q}_1\mathbf{c} - \bar{t})^2 ds + \alpha_3 \int_{\Gamma_D} (\mathbf{Q}_2\mathbf{c} - \bar{D}_n)^2 ds \tag{7.49}$$

where α_i (i=1,2,3) are three weighting parameters which preserve the numerical equivalence between the first and the remaining terms on the right hand side of the above equation. In the least square method, the derivative of the residual function with respect to **c** is forced to vanish:

$$\frac{R(\mathbf{c})}{\partial \mathbf{c}} = 2\int_{\Gamma_u} \mathbf{N}_1^T(\mathbf{N}_1\mathbf{c} - \bar{u}_z)ds + 2\alpha_1 \int_{\Gamma_\phi} \mathbf{N}_2^T(\mathbf{N}_2\mathbf{c} - \bar{\phi})ds$$

$$+ 2\alpha_2 \int_{\Gamma_t} \mathbf{Q}_1^T(\mathbf{Q}_1\mathbf{c} - \bar{t})^2 ds + 2\alpha_3 \int_{\Gamma_D} \mathbf{Q}_2^T(\mathbf{Q}_2\mathbf{c} - \overline{D}_n)ds = 0 \tag{7.50}$$

Rearranging the above equations, we have

$$\left[\int_{\Gamma_u} \mathbf{N}_1^T\mathbf{N}_1 ds + \alpha_1 \int_{\Gamma_\phi} \mathbf{N}_2^T\mathbf{N}_2 ds + \alpha_2 \int_{\Gamma_t} \mathbf{Q}_1^T\mathbf{Q}_1 ds + \alpha_3 \int_{\Gamma_D} \mathbf{Q}_2^T\mathbf{Q}_2 ds\right]\mathbf{c}$$
$$= \int_{\Gamma_u} \mathbf{N}_1^T\bar{u}_z ds + \alpha_1 \int_{\Gamma_\phi} \mathbf{N}_1^T\bar{\phi} ds + \alpha_2 \int_{\Gamma_t} \mathbf{Q}_1^T\bar{t} ds + \alpha_3 \int_{\Gamma_D} \mathbf{Q}_2^T\overline{D}_n ds \tag{7.51}$$

or in matrix form

$$K_{ij}c_j = f_i \quad \text{or} \quad \mathbf{Kc} = \mathbf{f} \tag{7.52}$$

where

$$K_{ij} = \int_{\Gamma_u} N_{1i}N_{1j} ds + \alpha_1 \int_{\Gamma_\phi} N_{2i}N_{2j} ds + \alpha_2 \int_{\Gamma_t} Q_{1i}Q_{1j} ds + \alpha_3 \int_{\Gamma_D} Q_{2i}Q_{2j} ds \tag{7.53}$$

$$f_i = \int_{\Gamma_u} N_{1i}\bar{u} ds + \alpha_1 \int_{\Gamma_\phi} N_{2i}\bar{\phi} ds + \alpha_2 \int_{\Gamma_t} Q_{1i}\bar{u} ds + \alpha_3 \int_{\Gamma_D} Q_{2i}\overline{D}_n ds \tag{7.54}$$

In this formulation, it is important to choose the proper value of α_i. How to choose the value of α_i is, however, still an open question, and there is no general rule for that choice at present. Generally, the optimal value of α_i for a given type of problem should be found by numerical experimentation.

(d) Modified Trefftz formulation

Another indirect formulation called the 'modified Trefftz formulation' appears to be due to Oliveira [7] and Patterson and Sheikh [8,9]. In this approach, the approximate solutions u and q_n are expressed in terms of a linear combination of the singular fundamental solution, and then the unknown parameters are determined so that the approximate solution satisfies the boundary conditions by using the collocation method.

It is well known that the fundamental solution of the two-dimensional Laplace equation (2.285)

$$u_z^*(r_{PQ}) = \frac{1}{2\pi}\ln\left(\frac{1}{r_{PQ}}\right), \quad \phi^*(r_{PQ}) = \frac{1}{2\pi}\ln\left(\frac{1}{r_{PQ}}\right) \tag{7.55}$$

has a singularity at P=Q, where P and Q stand for the observation point and source point, respectively. To avoid this singularity, the source points Q_i (i=1,2,…,N) are placed on an imaginary boundary outside the solution domain and $u(P)$ is approximated as follows:

$$\mathbf{u}(P)=\begin{Bmatrix}u_z(P)\\ \phi(P)\end{Bmatrix}=\sum_{j=1}^{m}\begin{bmatrix}u_z^*(r_{PQ_j}) & 0\\ 0 & \phi^*(r_{PQ_j})\end{bmatrix}\begin{Bmatrix}c_j\\ c_{m+j}\end{Bmatrix}=\begin{bmatrix}\mathbf{N}_1^*\\ \mathbf{N}_2^*\end{bmatrix}\mathbf{c}=\mathbf{N}^*\mathbf{c} \tag{7.56}$$

where m is the total number of the source points, and

$$r_{PQ_i}=\sqrt{(x_P-x_{Q_i})^2+(y_P-y_{Q_i})^2}\,. \tag{7.57}$$

Differentiating eqn (10.27) with respect to the normal direction n, we have

$$\mathbf{T}=\begin{Bmatrix}t\\ D_n\end{Bmatrix}=\begin{Bmatrix}\sigma_{3j}n_j\\ D_jn_j\end{Bmatrix}=\sum_{j=0}^{m}\begin{bmatrix}Q_{1j}^* & Q_{1(m+j)}^*\\ Q_{2j}^* & Q_{2(m+j)}^*\end{bmatrix}\begin{Bmatrix}c_j\\ c_{m+j}\end{Bmatrix}=\begin{bmatrix}\mathbf{Q}_1^*\\ \mathbf{Q}_2^*\end{bmatrix}\mathbf{c}=\mathbf{Q}^*\mathbf{c} \tag{7.58}$$

The collocation method leads to the following equations:

$$u_z(P_i)=\mathbf{N}_1^*(P_i)\mathbf{c}=\bar{u}_z(P_i),\qquad (P_i\in\Gamma_u,\ i=1,2,\cdots M_1) \tag{7.59}$$

$$t(P_i)=\mathbf{Q}_1^*(P_i)\mathbf{c}=\bar{t}(P_i),\qquad (P_i\in\Gamma_t,\ i=1,2,\cdots M_2) \tag{7.60}$$

$$\phi(P_i)=\mathbf{N}_2^*(P_i)\mathbf{c}=\bar{\phi}(P_i),\qquad (P_i\in\Gamma_\phi,\ i=1,2,\cdots M_3) \tag{7.61}$$

$$D_n(P_i)=\mathbf{Q}_2^*(P_i)\mathbf{c}=\bar{D}_n(P_i),\qquad (P_i\in\Gamma_D,\ i=1,2,\cdots M_4) \tag{7.62}$$

or in matrix form

$$\mathbf{Kc}=\mathbf{f} \tag{7.63}$$

where **K** and **f** are determined in a way similar to the treatment in Eqs (7.46)-(7.48), and $N=M_1+M_2+M_3+M_4$. In this approach, it is important to select the appropriate points Q_i (i=1,2,…N).

7.2.5 Direct formulation

The Trefftz direct formulation is obtained by considering [1]

$$\iint_\Omega[\nabla^2u_zv_1+\nabla^2\phi v_2]d\Omega=0 \tag{7.64}$$

Performing the integration by parts and taking the expression (7.32) as weighting function, that is:

$$\mathbf{v}=\begin{Bmatrix}v_1\\ v_2\end{Bmatrix}=\sum_{j=1}^{m}\begin{bmatrix}N_{1j} & 0\\ 0 & N_{2j}\end{bmatrix}\begin{Bmatrix}c_j\\ c_{m+j}\end{Bmatrix}=\begin{bmatrix}\mathbf{N}_1\\ \mathbf{N}_2\end{bmatrix}\mathbf{c}=\mathbf{Nc} \tag{7.65}$$

we have

$$\mathbf{c}^T\int_\Gamma(\mathbf{N}_1^Tt-\mathbf{Q}_1^{\mathrm{T}}u_z+\mathbf{N}_2^TD_n-\mathbf{Q}_2^{\mathrm{T}}\phi)ds=0 \tag{7.66}$$

Since the equation is valid for arbitrary vectors **c**, we have

$$\int_\Gamma(\mathbf{N}_{1i}^Tt-\mathbf{Q}_{1i}^{\mathrm{T}}u_z+\mathbf{N}_{2i}^TD_n-\mathbf{Q}_{2i}^{\mathrm{T}}\phi)ds=0 \tag{7.67}$$

The analytical results for Eq (7.67) are, in general, impossible, and therefore a numerical procedure must be used to solve the problem. As in the conventional BEM, the boundary Γ is divided into k linear elements, for which u_z, t, ϕ, and D_n are approximated by

$$u_z(s)=\sum_{i=1}^{k}u_{zi}F_i(s),\ t(s)=\sum_{i=1}^{k}t_iF_i(s),\ \phi(s)=\sum_{i=1}^{k}\phi_iF_i(s),\ D_n(s)=\sum_{i=1}^{k}D_{ni}F_i(s) \quad (7.68)$$

where u_{zi}, t_i, ϕ and D_n are, respectively, their values at node i, s is a length coordinate defined in Fig. 6.2, F_i(s) is defined in Eqs (6.10)-(6.12) and is a global shape function associated with the ith-node. F_i(s) is zero-valued over the whole mesh except within two elements connected to the ith-node (see Fig. 6.2). Following the abovementioned discretization, Eq (7.67) becomes

$$\mathbf{Gu}=\mathbf{Ht} \quad (7.69)$$

Applying the boundary conditions, we have

$$\begin{bmatrix}\mathbf{G}_1 & \mathbf{G}_2 & \mathbf{G}_3 & \mathbf{G}_4\end{bmatrix}\begin{Bmatrix}\overline{\mathbf{u}}_z\\ \mathbf{u}_z\\ \overline{\boldsymbol{\varphi}}\\ \boldsymbol{\varphi}\end{Bmatrix}=\begin{bmatrix}\mathbf{H}_1 & \mathbf{H}_2 & \mathbf{H}_3 & \mathbf{H}_4\end{bmatrix}\begin{Bmatrix}\overline{\mathbf{t}}\\ \mathbf{t}\\ \overline{\mathbf{D}}_\mathbf{n}\\ \mathbf{D}_\mathbf{n}\end{Bmatrix} \quad (7.70)$$

or simply

$$\mathbf{Kx}=\mathbf{f} \quad (7.71)$$

The direct formulation above is only suitable for single crack problems. For multi-crack problems, as in Section 7.2.4, the domain decomposition approach is used to convert them into several single crack problems. For a particular single crack problem with sub-domain i (see Fig. 7.2), Eq (7.71) becomes

$$\mathbf{K}_i\mathbf{x}_i=\mathbf{f}_i \qquad \text{in } \Omega_i \quad (7.72)$$

while on the inner boundary Γ_{Ij}, the continuity condition is again defined in Eq (7.40).

7.3 Plane piezoelectricity

The application of the Trefftz boundary element method to plane piezoelectricity was discussed in [2-4,11,12]. Sheng and Sze's formulation was based on the multi-region approach and a special set of Trefftz functions that satisfy the traction-free and charge-free conditions at free surfaces such as crack faces [4]. Sheng et al [3] presented the same TBEM as in [4] but used a different approach to derive the Trefftz function. Yao and Wang [11] and Li and Yao [12] developed a modified TBEM which is based on the concept of an imaginary boundary and Green's functions of plane piezoelectricity.

7.3.1 Governing equations

For convenience, the basic equations of plane piezoelectricity presented in Chapter 1 are briefly summarized as follows:

$$\sigma_{11,1}+\sigma_{12,2}+b_1=0,\quad \sigma_{12,1}+\sigma_{22,2}+b_2=0,\quad D_{1,1}+D_{2,2}+b_e=0,\quad (\text{in } \Omega) \quad (7.73)$$

$$\varepsilon_{i,j}=\frac{1}{2}(u_{i,j}+u_{j,i}),\quad E_i=-\phi_{,i} \qquad (\text{in } \Omega) \quad (7.74)$$

$$\begin{Bmatrix} \sigma_{11} \\ \sigma_{22} \\ \sigma_{12} \\ D_1 \\ D_2 \end{Bmatrix} = \begin{bmatrix} c_{11} & c_{12} & 0 & 0 & e_{21} \\ c_{12} & c_{22} & 0 & 0 & e_{22} \\ 0 & 0 & c_{33} & e_{13} & 0 \\ 0 & 0 & e_{13} & -\kappa_{11} & 0 \\ e_{21} & e_{22} & 0 & 0 & -\kappa_{22} \end{bmatrix} \begin{Bmatrix} \varepsilon_{11} \\ \varepsilon_{22} \\ 2\varepsilon_{12} \\ -E_1 \\ -E_2 \end{Bmatrix}, \qquad (\text{in } \Omega) \qquad (7.75)$$

$$\left.\begin{matrix} u_i = \overline{u}_i & \text{on } \Gamma_u \\ t_i = \sigma_{ij} n_j = \overline{t}_i & \text{on } \Gamma_t \end{matrix}\right\}, \qquad \left\{\begin{matrix} \phi = \overline{\phi} & \text{on } \Gamma_\phi \\ D_n = D_i n_i = -\overline{q}_s & \text{on } \Gamma_D \end{matrix}\right\} \qquad (7.76)$$

7.3.2 Trefftz functions

For the boundary value problem (7.73)-(7.76), its Trefftz functions can be constructed based on the solutions (1.160) and (1.163). It should be noted that the constants ω_0, u_0, v_0 in Eq (1.163) represent rigid body displacements, and ϕ_0 is a reference potential. These constants are ignored in the following development. Using the solutions (1.160) and (1.163), the plane strain piezoelectric problem is reduced to the one of finding three complex potentials, Φ_1, Φ_2 and Φ_3, in some region Ω of the material. Each potential is a function of a different generalized complex variable $z_k = x_1 + p_k x_2$. The discussion in this subsection is from the development in [3,13].

(a) Trefftz functions for domain without defects

For an interior domain problem without any flux singularities, Φ_1, Φ_2 and Φ_3 can be represented by the Talor series as [3,13]

$$\Phi_k(z_k) = \sum_{n=1}^{\infty} (\alpha_k^{(n)} + i\beta_k^{(n)}) z_k^n \quad (k=1,2,3) \qquad (7.77)$$

where $i = \sqrt{-1}$, and α's and β's are real constants to be determined. By substituting the expression (7.77) into Eq (1.163) and using the polar coordinate systems (r_k, θ_k) defined by

$$z_k = x_1 + p_k x_2 = r_k(\cos\theta_k + i\sin\theta_k), \qquad (7.78)$$

the basic set of Trefftz functions for interior domain problems can be obtained as

$$\begin{aligned} \mathbf{S}_{\text{int}}^u = \{ & \text{Re}(\mathbf{D}_1) r_1^n \cos n\theta_1 - \text{Im}(\mathbf{D}_1) r_1^n \sin n\theta_1, -\text{Re}(\mathbf{D}_1) r_1^n \sin n\theta_1 - \text{Im}(\mathbf{D}_1) r_1^n \cos n\theta_1, \\ & \text{Re}(\mathbf{D}_2) r_2^n \cos n\theta_2 - \text{Im}(\mathbf{D}_2) r_2^n \sin n\theta_2, -\text{Re}(\mathbf{D}_2) r_2^n \sin n\theta_2 - \text{Im}(\mathbf{D}_2) r_2^n \cos n\theta_2, \\ & \text{Re}(\mathbf{D}_3) r_3^n \cos n\theta_3 - \text{Im}(\mathbf{D}_3) r_3^n \sin n\theta_3, -\text{Re}(\mathbf{D}_3) r_3^n \sin n\theta_3 - \text{Im}(\mathbf{D}_3) r_3^n \cos n\theta_3 \} \end{aligned}$$

$$\text{for } n=1,2,3\ldots \qquad (7.79)$$

which corresponds to the coefficients $\alpha_k^{(n)}$ and $\beta_k^{(n)}$, where $\mathbf{D}_k = \{p_k^*, q_k^*, t_k^*\}^T$, and the superscript u indicates that the basic solution set is for the vector of primary variables u_1, u_2, and ϕ.

In the case of exterior domain problems without flux singularity, Sheng et al [3] expressed the potential functions Φ_k in terms of the following Laurent series as

$$\Phi_k(z_k) = \sum_{n=1}^{\infty} (\alpha_k^{(-n)} + i\beta_k^{(-n)}) z_k^{-n} \qquad (k=1,2,3) \qquad (7.80)$$

Substituting Eq (7.80) into Eq (1.163), the basic set of Trefftz functions for exterior domain problems can be obtained as

$$\begin{aligned}\mathbf{S}_{ext}^{u} = \{&\mathrm{Re}(\mathbf{D}_1)\,\mathrm{Re}(z_1^{-n}) - \mathrm{Im}(\mathbf{D}_1)\,\mathrm{Im}(z_1^{-n}), -\mathrm{Re}(\mathbf{D}_1)\,\mathrm{Im}(z_1^{-n}) - \mathrm{Im}(\mathbf{D}_1)\,\mathrm{Re}(z_1^{-n}),\\ &\mathrm{Re}(\mathbf{D}_2)\,\mathrm{Re}(z_2^{-n}) - \mathrm{Im}(\mathbf{D}_2)\,\mathrm{Im}(z_2^{-n}), -\mathrm{Re}(\mathbf{D}_2)\,\mathrm{Im}(z_2^{-n}) - \mathrm{Im}(\mathbf{D}_2)\,\mathrm{Re}(z_2^{-n}),\\ &\mathrm{Re}(\mathbf{D}_3)\,\mathrm{Re}(z_3^{-n}) - \mathrm{Im}(\mathbf{D}_3)\,\mathrm{Im}(z_3^{-n}), -\mathrm{Re}(\mathbf{D}_3)\,\mathrm{Im}(z_3^{-n}) - \mathrm{Im}(\mathbf{D}_3)\,\mathrm{Re}(z_3^{-n})\}\end{aligned} \tag{7.81}$$

which corresponds to the unknown coefficients $\alpha_k^{(-n)}$ and $\beta_k^{(-n)}$.

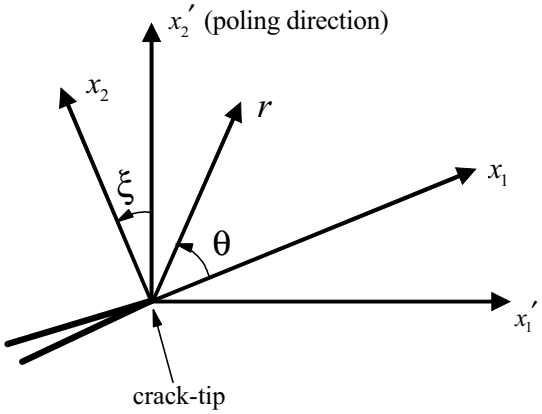

Fig. 7.3 An arbitrarily oriented crack

(b) Trefftz functions for domain with an impermeable crack

Consider a domain with an arbitrarily oriented impermeable crack as shown in Fig. 7.3. In the figure, the system (x_1', x_2') represents the principal material coordinate system, and (x_1, x_2) is the coordinate system defined on the crack-tip with the x_1-axis along the crack line. ξ stands for the angle between the crack line and the x_1'-axis. The special set of Trefftz functions can be constructed by considering the following complex potential functions

$$\Phi_k(z_k) = \sum_{\eta}(\alpha_k^{(\eta)} + i\beta_k^{(\eta)}) z_k^{(\eta)} = \sum_{\eta}(\alpha_k^{(\eta)} + i\beta_k^{(\eta)}) r_k^{\eta}(\cos\eta\theta_k + i\sin\eta\theta_k) \tag{7.82}$$

satisfying the boundary conditions on crack faces

$$\sigma_{22}\big|_{\theta=\pm\pi} = \sigma_{12}\big|_{\theta=\pm\pi} = D_2\big|_{\theta=\pm\pi} = 0 \tag{7.83}$$

where η's are eigenvalues to be determined. Substituting Eq (7.82) into Eqs (1.160) and (1.163), we have [3]

$$\phi = 2\sum_{k=1}^{3}\sum_{\eta} r_k^{\eta}(\alpha_k^{(\eta)}[A_{tk}\cos\eta\theta_k - B_{tk}\sin\eta\theta_k] - \beta_k^{(\eta)}[A_{tk}\sin\eta\theta_k + B_{tk}\cos\eta\theta_k]) \tag{7.84}$$

$$\sigma_{22} = 2\sum_{k=1}^{3}\sum_{\eta}\eta r_k^{\eta-1}(\alpha_k^{(\eta)}\cos(\eta-1)\theta_k - \beta_k^{(\eta)}\sin(\eta-1)\theta_k) \tag{7.85}$$

$$\sigma_{12} = 2\sum_{k=1}^{3}\sum_{\eta}\eta r_k^{\eta-1}(\alpha_k^{(\eta)}[A_{pk}\cos(\eta-1)\theta_k - B_{pk}\sin(\eta-1)\theta_k] - \beta_k^{(\eta)}[A_{pk}\sin(\eta-1)\theta_k + B_{pk}\cos(\eta-1)\theta_k]) \tag{7.86}$$

$$D_2 = 2\sum_{k=1}^{3}\sum_{\eta}\eta r_k^{\eta-1}(\alpha_k^{(\eta)}[A_{\varpi k}\cos(\eta-1)\theta_k - B_{\varpi k}\sin(\eta-1)\theta_k] - \beta_k^{(\eta)}[A_{\varpi k}\sin(\eta-1)\theta_k + B_{\varpi k}\cos(\eta-1)\theta_k]) \tag{7.87}$$

where $A_{tk} = \mathrm{Re}(t_k^*)$, $B_{tk} = \mathrm{Im}(t_k^*)$, $A_{pk} = \mathrm{Re}(p_k)$, $B_{pk} = \mathrm{Im}(p_k)$, $A_{\varpi k} = \mathrm{Re}(\varpi_k)$, and $B_{\varpi k} = \mathrm{Im}(\varpi_k)$. Noting that $\theta_k = \pm\pi$ and $r_k = r$ at $\theta = \pm\pi$, substituting Eqs (7.85)-(7.87) into Eq (7.83) leads to

$$\mathbf{X}(\eta)\mathbf{G}\mathbf{q} = 0 \tag{7.88}$$

where

$$\mathbf{X}(\eta) = \mathrm{diag}[\cos\eta\pi, \sin\eta\pi, \cos\eta\pi, \sin\eta\pi, \cos\eta\pi, \sin\eta\pi] \tag{7.89}$$

$$\mathbf{q} = \begin{Bmatrix} \alpha_1^{(\eta)} \\ \beta_1^{(\eta)} \\ \alpha_2^{(\eta)} \\ \beta_2^{(\eta)} \\ \alpha_3^{(\eta)} \\ \beta_3^{(\eta)} \end{Bmatrix}, \qquad \mathbf{G} = \begin{bmatrix} 1 & 0 & 1 & 0 & 1 & 0 \\ 0 & 1 & 0 & 1 & 0 & 1 \\ A_{p1} & -B_{p1} & A_{p2} & -B_{p2} & A_{p3} & -B_{p3} \\ B_{p1} & A_{p1} & B_{p2} & A_{p2} & B_{p3} & A_{p3} \\ A_{\varpi 1} & -B_{\varpi 1} & A_{\varpi 2} & -B_{\varpi 2} & A_{\varpi 3} & -B_{\varpi 3} \\ B_{\varpi 1} & A_{\varpi 1} & B_{\varpi 2} & A_{\varpi 2} & B_{\varpi 3} & A_{\varpi 3} \end{bmatrix} \tag{7.90}$$

As was pointed out in [3], **G** is in full rank for most practical piezoelectric materials. In this case, the non-trivial solution of **q** is determined by setting the determinant of $\mathbf{X}(\eta)$ to zero. Thus, the eigenvalues η's are solved to be

$$\eta = n/2, \qquad \text{for } n = 0,1,2,3,\cdots \tag{7.91}$$

As was done in [3], taking $\alpha_1^{(\eta)}$, $\eta_1^{(\eta)}$, and $\alpha_2^{(\eta)}$ as independent coefficients, the following relationships can be found from Eq (7.88) as

$$\begin{aligned} \beta_2^{(\eta)} &= J_1\alpha_1^{(\eta)} + J_2\beta_1^{(\eta)} + J_3\alpha_2^{(\eta)}, \\ \alpha_3^{(\eta)} &= J_4\alpha_1^{(\eta)} + J_5\beta_1^{(\eta)} + J_6\alpha_2^{(\eta)}, \\ \beta_3^{(\eta)} &= J_7\alpha_1^{(\eta)} + J_8\beta_1^{(\eta)} + J_9\alpha_2^{(\eta)} \end{aligned} \tag{7.92}$$

where

$$J_1 = (B_{\varpi 3}B_{p1} - B_{\varpi 1}B_{p3})/J_0, \qquad J_2 = [B_{\varpi 3}(A_{p1} - A_{p3}) - B_{p3}(A_{\varpi 1} - A_{\varpi 3})]/J_0, \tag{7.93}$$

$$J_3 = (B_{\varpi 3}B_{p2} - B_{\varpi 2}B_{p3})/J_0, \qquad J_4 = [B_{\varpi 1}(A_{p2} - A_{p3}) - B_{p1}(A_{\varpi 2} - A_{\varpi 3})]/J_0, \tag{7.94}$$

$$J_5 = [A_{p1}(A_{\varpi 3} - A_{\varpi 2}) + A_{p2}(A_{\varpi 1} - A_{\varpi 3}) + A_{p3}(A_{\varpi 2} - A_{\varpi 1})]/J_0, \tag{7.95}$$

$$J_6 = [B_{\varpi 2}(A_{p2} - A_{p3}) - B_{p2}(A_{\varpi 2} - A_{\varpi 3})]/J_0, \qquad J_7 = -J_1, \tag{7.96}$$

$$J_8 = [B_{\varpi 3}(A_{p1} - A_{p2}) - B_{p3}(A_{\varpi 1} - A_{\varpi 2})]/J_0, \qquad J_9 = -J_3, \tag{7.97}$$

$$J_0 = B_{\varpi 3}(A_{p3} - A_{p2}) - B_{p3}(A_{\varpi 3} - A_{\varpi 2}) \tag{7.98}$$

for odd n, i.e. $\eta = 1/2, 3/2, 5/2, \cdots$, and

$$J_1 = [B_{\varpi 3}(A_{p1} - A_{p3}) - B_{p3}(A_{\varpi 1} - A_{\varpi 3})]/J_0, \quad J_2 = (B_{\varpi 1}B_{p3} - B_{\varpi 3}B_{p1})/J_0, \tag{7.99}$$

$$J_3 = [B_{\varpi 3}(A_{p2} - A_{p3}) - B_{p3}(A_{\varpi 2} - A_{\varpi 3})]/J_0, \quad J_4 = J_6 = -1, \quad J_5 = 0, \tag{7.100}$$

$$J_7 = [B_{\varpi 2}(A_{p3} - A_{p1}) - B_{p2}(A_{\varpi 3} - A_{\varpi 1})]/J_0, \quad J_8 = (B_{\varpi 2}B_{p1} - B_{\varpi 1}B_{p2})/J_0, \tag{7.101}$$

$$J_9 = [B_{\varpi 2}(A_{p3} - A_{p2}) - B_{p2}(A_{\varpi 3} - A_{\varpi 2})]/J_0, \quad J_0 = B_{\varpi 3}B_{p2} - B_{\varpi 2}B_{p3}, \tag{7.102}$$

for even n, i.e. $\eta = 0, 1, 2, 3, \cdots$.

Incorporating Eqs (7.82), (7.91), and (7.92) into Eq (1.163), the following special solution set for impermeable crack-tip fields can be obtained as

$$\begin{aligned}\mathbf{S}^{u}_{crack-im} = \{&\mathbf{S}^{(n/2)}_{\alpha_1} + J_1\mathbf{S}^{(n/2)}_{\beta_2} + J_4\mathbf{S}^{(n/2)}_{\alpha_3} + J_7\mathbf{S}^{(n/2)}_{\beta_3},\ \mathbf{S}^{(n/2)}_{\beta_1} + J_2\mathbf{S}^{(n/2)}_{\beta_2} + J_5\mathbf{S}^{(n/2)}_{\alpha_3} + J_8\mathbf{S}^{(n/2)}_{\beta_3},\\ &\mathbf{S}^{(n/2)}_{\alpha_2} + J_3\mathbf{S}^{(n/2)}_{\beta_2} + J_6\mathbf{S}^{(n/2)}_{\alpha_3} + J_9\mathbf{S}^{(n/2)}_{\beta_3}\}, \qquad \text{for } n = 0, 1, 2, 3, \cdots\end{aligned} \tag{7.103}$$

which corresponds to the independent coefficients $\{\alpha_1^{(n/2)}, \beta_1^{(n/2)}, \alpha_2^{(n/2)}\}$, where

$$\begin{aligned}\mathbf{S}^{(n/2)}_{\alpha_k} &= 2\,\mathrm{Re}(\mathbf{D}_k)r_k^{n/2}\cos\frac{n}{2}\theta_k - 2\,\mathrm{Im}(\mathbf{D}_k)r_k^{n/2}\sin\frac{n}{2}\theta_k,\\ \mathbf{S}^{(n/2)}_{\beta_k} &= -2\,\mathrm{Re}(\mathbf{D}_k)r_k^{n/2}\sin\frac{n}{2}\theta_k - 2\,\mathrm{Im}(\mathbf{D}_k)r_k^{n/2}\cos\frac{n}{2}\theta_k\end{aligned} \tag{7.104}$$

(c) Treffitz functions for domain with a permeable crack

In addition to the impermeable boundary condition, Sheng et al [3] also consider a domain with a permeable crack. In the case of a permeable crack, the boundary conditions along the crack faces (7.83) become

$$\sigma_{22}\big|_{\theta=\pm\pi} = \sigma_{12}\big|_{\theta=\pm\pi} = 0, \quad \phi\big|_{\theta=\pi} = \phi\big|_{\theta=-\pi}, \quad D_2\big|_{\theta=\pi} = D_2\big|_{\theta=-\pi} \tag{7.105}$$

Making use of Eqs (7.84)-(7.87) and (7.105), an equation analogous to Eq (7.88) can be obtained. The pertinent eigenvalues η's are again solved to be Eq (7.91). However, the eigenfunctions are different:

(i) For odd n, i.e. $\eta = 1/2, 3/2, 5/2, \cdots$, and with $\alpha_1^{(\eta)}$ and $\beta_1^{(\eta)}$ taken as independent coefficients, the following relationships can be found as

$$\begin{aligned}\alpha_2^{(\eta)} &= J_{11}\alpha_1^{(\eta)} + J_{12}\beta_1^{(\eta)}, \quad \beta_2^{(\eta)} = J_{13}\alpha_1^{(\eta)} + J_{14}\beta_1^{(\eta)},\\ \alpha_3^{(\eta)} &= J_{15}\alpha_1^{(\eta)} + J_{16}\beta_1^{(\eta)}, \quad \beta_3^{(\eta)} = J_{17}\alpha_1^{(\eta)} + J_{18}\beta_1^{(\eta)}\end{aligned} \tag{7.106}$$

where

$$\begin{aligned}J_{11} = [&(A_{p3} - A_{p2})(B_{\varpi 3}B_{t1} - B_{\varpi 1}B_{t3}) + (A_{\varpi 3} - A_{\varpi 2})(B_{p1}B_{t3} - B_{p3}B_{t1})\\ &+ (A_{t3} - A_{t2})(B_{\varpi 1}B_{p3} - B_{\varpi 3}B_{p1})]/J_{10}\end{aligned} \tag{7.107}$$

$$\begin{aligned}J_{12} = [&(A_{p3} - A_{p2})(B_{\varpi 3}A_{t1} - A_{\varpi 1}B_{t3}) + (A_{p3} - A_{p1})(A_{\varpi 2}B_{t3} - B_{\varpi 3}A_{t2}) + (A_{p2} - A_{p1})\\ &\times(B_{\varpi 3}A_{t3} - A_{\varpi 3}B_{t3}) + A_{\varpi 3}B_{p3}(A_{t2} - A_{t1}) + A_{\varpi 2}B_{p3}(A_{t1} - A_{t3}) + A_{\varpi 1}B_{p3}(A_{t3} - A_{t2})]/J_{10}\end{aligned} \tag{7.108}$$

$$J_{13}=[B_{\varpi 3}(B_{p2}B_{t1}-B_{p1}B_{t2})+B_{\varpi 2}(B_{p1}B_{t3}-B_{p3}B_{t1})+B_{\varpi 1}(B_{p3}B_{t2}-B_{p2}B_{t3})]/J_{10} \quad (7.109)$$

$$\begin{aligned}J_{14}=[&(A_{p3}-A_{p1})(B_{\varpi 3}B_{t2}-B_{\varpi 2}B_{t3})+(A_{\varpi 3}-A_{\varpi 1})(B_{p2}B_{t3}-B_{p3}B_{t2})\\&+(A_{t3}-A_{t1})(B_{\varpi 2}B_{p3}-B_{\varpi 3}B_{p2})]/J_{10}\end{aligned} \quad (7.110)$$

$$\begin{aligned}J_{15}=[&(A_{p3}-A_{p2})(B_{\varpi 1}B_{t2}-B_{\varpi 2}B_{t1})+(A_{\varpi 3}-A_{\varpi 2})(B_{p2}B_{t1}-B_{p1}B_{t2})\\&+(A_{t3}-A_{t2})(B_{\varpi 2}B_{p1}-B_{\varpi 1}B_{p2})]/J_{10}\end{aligned} \quad (7.111)$$

$$\begin{aligned}J_{16}=&[(A_{t2}-A_{t1})(B_{\varpi 2}A_{p3}-B_{p2}A_{\varpi 3})+(A_{t3}-A_{t2})(A_{p1}B_{\varpi 2}-B_{p2}A_{\varpi 1})+(A_{t3}-A_{t1})\\&\times(B_{p2}A_{\varpi 2}-B_{\varpi 2}A_{p2})+A_{p1}B_{t2}(A_{\varpi 2}-A_{\varpi 3})+A_{p2}B_{t2}(A_{\varpi 3}-A_{\varpi 1})+A_{p3}B_{t2}(A_{\varpi 1}-A_{\varpi 2})]/J_{10}\end{aligned} \quad (7.112)$$

$$J_{17}=-J_{13} \quad (7.113)$$

$$\begin{aligned}J_{18}=[&(A_{p2}-A_{p1})(B_{\varpi 2}B_{t3}-B_{\varpi 3}B_{t2})+(A_{\varpi 2}-A_{\varpi 1})(B_{p3}B_{t2}-B_{p2}B_{t3})\\&+(A_{t2}-A_{t1})(B_{\varpi 3}B_{p2}-B_{\varpi 2}B_{p3})]/J_{10}\end{aligned} \quad (7.114)$$

$$\begin{aligned}J_{10}=&(A_{p3}-A_{p2})(B_{\varpi 2}B_{t3}-B_{\varpi 3}B_{t2})+(A_{\varpi 3}-A_{\varpi 2})(B_{p3}B_{t2}-B_{p2}B_{t3})\\&+(A_{t3}-A_{t2})(B_{\varpi 3}B_{p2}-B_{\varpi 2}B_{p3})\end{aligned} \quad (7.115)$$

(ii) for even n, i.e. $\eta=0,1,2,3,\cdots$ and with $\alpha_1^{(\eta)}$, $\beta_1^{(\eta)}$, $\alpha_2^{(\eta)}$, and $\beta_2^{(\eta)}$ taken as independent coefficients, we have

$$\alpha_3^{(\eta)}=-\alpha_1^{(\eta)}-\alpha_2^{(\eta)}, \qquad \beta_3^{(\eta)}=J_{19}\alpha_1^{(\eta)}+J_{20}\beta_1^{(\eta)}+J_{21}\alpha_2^{(\eta)}+J_{22}\beta_2^{(\eta)} \quad (7.116)$$

where

$$J_{19}=\frac{(A_{p1}-A_{p3})}{B_{p3}},\ \ J_{20}=-\frac{B_{p1}}{B_{p3}},\ \ J_{21}=\frac{(A_{p2}-A_{p3})}{B_{p3}},\ \ J_{22}=-\frac{B_{p2}}{B_{p3}} \quad (7.117)$$

Incorporating Eqs (7.82), (7.91), (7.106), and (7.117) into Eq (1.163) yields

$$\mathbf{S}^u_{crack-p}=\mathbf{S}^u_{n_1}\cup\mathbf{S}^u_{n_2} \quad (7.118)$$

where

$$\begin{aligned}\mathbf{S}^u_{n_1}=\{&\mathbf{S}^{(n_1/2)}_{\alpha_1}-\mathbf{S}^{(n_1/2)}_{\alpha_3}+J_{19}\mathbf{S}^{(n_1/2)}_{\beta_3},\ \mathbf{S}^{(n_1/2)}_{\beta_1}+J_{20}\mathbf{S}^{(n_1/2)}_{\beta_3},\\&\mathbf{S}^{(n_1/2)}_{\alpha_2}-\mathbf{S}^{(n_1/2)}_{\alpha_3}+J_{21}\mathbf{S}^{(n_1/2)}_{\beta_3},\ \mathbf{S}^{(n_1/2)}_{\beta_2}+J_{22}\mathbf{S}^{(n_1/2)}_{\beta_3}\},\quad \text{for } n_1=0,2,4,\cdots\end{aligned} \quad (7.119)$$

$$\begin{aligned}\mathbf{S}^u_{n_2}=\{&\mathbf{S}^{(n_2/2)}_{\alpha_1}+J_{11}\mathbf{S}^{(n_2/2)}_{\alpha_2}+J_{13}\mathbf{S}^{(n_2/2)}_{\beta_2}+J_{15}\mathbf{S}^{(n_2/2)}_{\alpha_3}+J_{17}\mathbf{S}^{(n_2/2)}_{\beta_3},\\&\mathbf{S}^{(n_2/2)}_{\beta_1}+J_{12}\mathbf{S}^{(n_2/2)}_{\alpha_2}+J_{14}\mathbf{S}^{(n_2/2)}_{\beta_2}+J_{16}\mathbf{S}^{(n_2/2)}_{\alpha_3}+J_{18}\mathbf{S}^{(n_2/2)}_{\beta_3}\},\quad \text{for } n_2=1,3,5,\cdots\end{aligned} \quad (7.120)$$

and **S**'s are defined by Eq (7.104).

(d) Trefftz functions for domain with an impermeable elliptic hole

Consider a piezoelectric plate containing an impermeable elliptic hole as shown in Fig. 7.4. To apply the hole boundary conditions conveniently, the conformal mappings defined by Eq (2.162) are used and rewritten as

$$z_k = \frac{c - ip_k b}{2}\zeta_k + \frac{c + ip_k b}{2}\frac{1}{\zeta_k} \tag{7.121}$$

where a and b are the semi-axis of the elliptic hole (Fig. 7.4). The inverse mappings of ζ_k are given by

$$\zeta_{k1,2} = \frac{z_k \pm (z_k^2 - a^2 - p_k^2 b^2)^{1/2}}{a - ip_k b} \tag{7.122}$$

in which the sign of the square root ($\pm$) is chosen in such a way that $|\zeta_k| \geq 1$. In terms of the variables, Eqs (1.160) and (1.163) are rewritten as

$$\begin{Bmatrix} u_1 \\ u_2 \\ \phi \end{Bmatrix} = 2\,\mathrm{Re}\sum_{k=1}^{3} \begin{Bmatrix} p_k^* \\ q_k^* \\ t_k^* \end{Bmatrix} \Phi_k(\zeta_k) \tag{7.123}$$

$$\begin{Bmatrix} \sigma_{11} \\ \sigma_{22} \\ \sigma_{12} \end{Bmatrix} = 2\,\mathrm{Re}\sum_{k=1}^{3} \begin{Bmatrix} p_k^2 \\ 1 \\ -p_k \end{Bmatrix} \frac{\Phi_k'(\zeta_k)}{z_k'(\zeta_k)}, \qquad \begin{Bmatrix} D_1 \\ D_2 \end{Bmatrix} = 2\,\mathrm{Re}\sum_{k=1}^{3} \begin{Bmatrix} \varpi_k p_k \\ -\varpi_k \end{Bmatrix} \frac{\Phi_k'(\zeta_k)}{z_k'(\zeta_k)} \tag{7.124}$$

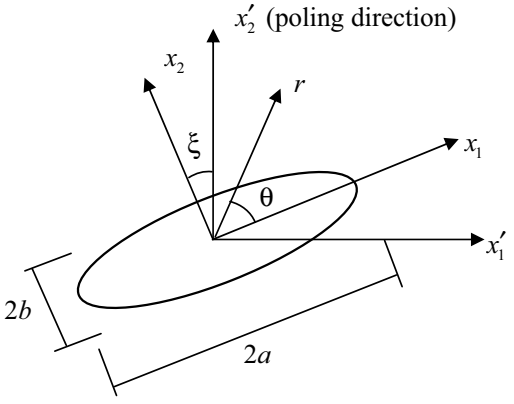

Fig. 7.4 Coordinate systems for elliptic hole

For the traction-free and charge-free conditions along the hole boundary, we have

$$\mathrm{Re}\sum_{k=1}^{3} \Phi_k(\zeta_k) = 0, \quad \mathrm{Re}\sum_{k=1}^{3} p_k \Phi_k(\zeta_k) = 0, \quad \mathrm{Re}\sum_{k=1}^{3} \varpi_k \Phi_k(\zeta_k) = 0, \quad \text{for } |\zeta_k| = 1 \tag{7.125}$$

which can be expressed in matrix form [3,13]

$$\begin{bmatrix} 1 & 1 & 1 \\ \bar{p}_1 & \bar{p}_2 & \bar{p}_3 \\ \bar{\varpi}_1 & \bar{\varpi}_2 & \bar{\varpi}_3 \end{bmatrix} \begin{Bmatrix} \bar{\Phi}_1 \\ \bar{\Phi}_2 \\ \bar{\Phi}_3 \end{Bmatrix} = \begin{bmatrix} 1 & 1 & 1 \\ p_1 & p_2 & p_3 \\ \varpi_1 & \varpi_2 & \varpi_3 \end{bmatrix} \begin{Bmatrix} \Phi_1 \\ \Phi_2 \\ \Phi_3 \end{Bmatrix} \tag{7.126}$$

Eq (7.126) can be further written as

$$\begin{Bmatrix} \bar{\Phi}_1 \\ \bar{\Phi}_2 \\ \bar{\Phi}_3 \end{Bmatrix} = \begin{bmatrix} E_{11} & E_{12} & E_{13} \\ E_{21} & E_{22} & E_{23} \\ E_{31} & E_{32} & E_{33} \end{bmatrix} \begin{Bmatrix} \Phi_1 \\ \Phi_2 \\ \Phi_3 \end{Bmatrix} \tag{7.127}$$

where

$$\begin{bmatrix} E_{11} & E_{12} & E_{13} \\ E_{21} & E_{22} & E_{23} \\ E_{31} & E_{32} & E_{33} \end{bmatrix} = \begin{bmatrix} 1 & 1 & 1 \\ \bar{p}_1 & \bar{p}_2 & \bar{p}_3 \\ \bar{\varpi}_1 & \bar{\varpi}_2 & \bar{\varpi}_3 \end{bmatrix}^{-1} \begin{bmatrix} 1 & 1 & 1 \\ p_1 & p_2 & p_3 \\ \varpi_1 & \varpi_2 & \varpi_3 \end{bmatrix} \tag{7.128}$$

The complex potential functions $\Phi_k(\zeta_k)$ for the elliptic hole problem can thus be chosen in the following form [3,13]

$$\Phi_k(z_k) = \sum_{n=1}^{\infty} [(\alpha_k^{(n)} + i\beta_k^{(n)})\zeta_k^n + (\alpha_k^{(-n)} + i\beta_k^{(-n)})\zeta_k^{-n}] \quad \text{for } k=1,2,3 \tag{7.129}$$

It is noted that at any point along the hole boundary, ζ_k's can be expressed as

$$\zeta_1 = \zeta_2 = \zeta_3 = e^{i\theta} \tag{7.130}$$

where $\theta \in [-\pi, \pi]$. By incorporating Eqs (7.129) and (7.130) into Eq (7.127), six constraints on the 12 real coefficients α's and β's can be established. Taking $\alpha_k^{(n)}$'s and $\beta_k^{(n)}$'s as the independent coefficients and substituting Eq (7.129) into Eq (7.123) yields the special set of Trefftz functions in the form [3]

$$\mathbf{S}_{hole}^u = \{\boldsymbol{\Theta}_{\alpha_1}^{(n)}, \boldsymbol{\Theta}_{\beta_1}^{(n)}, \boldsymbol{\Theta}_{\alpha_2}^{(n)}, \boldsymbol{\Theta}_{\beta_2}^{(n)}, \boldsymbol{\Theta}_{\alpha_3}^{(n)}, \boldsymbol{\Theta}_{\beta_3}^{(n)}\} \quad \text{for } n = 0,1,2,3,\cdots \tag{7.131}$$

where

$$\begin{aligned} \boldsymbol{\Theta}_{\alpha_k}^{(n)} &= \boldsymbol{\chi}_{\alpha_k}^{(n)} + \sum_{i=1}^{3} \mathrm{Re}(E_{ik}) \boldsymbol{\chi}_{\alpha_i}^{(-n)} - \sum_{i=1}^{3} \mathrm{Im}(E_{ik}) \boldsymbol{\chi}_{\beta_i}^{(-n)}, \\ \boldsymbol{\Theta}_{\beta_k}^{(n)} &= \boldsymbol{\chi}_{\beta_k}^{(n)} + \sum_{i=1}^{3} \mathrm{Im}(E_{ik}) \boldsymbol{\chi}_{\alpha_i}^{(-n)} - \sum_{i=1}^{3} \mathrm{Re}(E_{ik}) \boldsymbol{\chi}_{\beta_i}^{(-n)}, \end{aligned} \tag{7.132}$$

with

$$\begin{aligned} \boldsymbol{\chi}_{\alpha_k}^{(n)} &= 2\,\mathrm{Re}(\mathbf{D}_k)\,\mathrm{Re}(\zeta_k^n) - 2\,\mathrm{Im}(\mathbf{D}_k)\,\mathrm{Im}(\zeta_k^n), \\ \boldsymbol{\chi}_{\alpha_k}^{(-n)} &= 2\,\mathrm{Re}(\mathbf{D}_k)\,\mathrm{Re}(\zeta_k^{-n}) - 2\,\mathrm{Im}(\mathbf{D}_k)\,\mathrm{Im}(\zeta_k^{-n}), \\ \boldsymbol{\chi}_{\beta_k}^{(n)} &= -2\,\mathrm{Re}(\mathbf{D}_k)\,\mathrm{Im}(\zeta_k^n) - 2\,\mathrm{Im}(\mathbf{D}_k)\,\mathrm{Re}(\zeta_k^n), \\ \boldsymbol{\chi}_{\beta_k}^{(-n)} &= 2\,\mathrm{Re}(\mathbf{D}_k)\,\mathrm{Im}(\zeta_k^{-n}) - 2\,\mathrm{Im}(\mathbf{D}_k)\,\mathrm{Re}(\zeta_k^{-n}) \end{aligned} \tag{7.133}$$

7.3.3 Indirect formulations

In the indirect techniques the generalized displacement **u** is approximated as

$$\mathbf{u} = \begin{Bmatrix} u_1 \\ u_2 \\ \phi \end{Bmatrix} = \begin{Bmatrix} \mathbf{N}_1 \\ \mathbf{N}_2 \\ \mathbf{N}_3 \end{Bmatrix} \mathbf{c} + \begin{Bmatrix} \breve{u}_1 \\ \breve{u}_2 \\ \breve{\phi} \end{Bmatrix} = \mathbf{N}\mathbf{c} + \breve{\mathbf{u}} \tag{7.134}$$

where $\mathbf{c}_j$ stands for undetermined coefficient (denoted as α's and β's in the last subsection), $\mathbf{N}_j$ are the Trefftz functions extracted from the basic or special solution sets given in Section 7.3.2, and $\breve{\mathbf{u}}\,(=\{\breve{u}_1, \breve{u}_2, \breve{\phi}\}^T)$ are known special solutions due to generalized body force. If the governing differential equation (7.73) is rewritten in a general form

$$\Re\mathbf{u}(\mathbf{x}) + \mathbf{b}(\mathbf{x}) = 0 \tag{7.135}$$

where $\Re$ stands for the differential operator matrix for Eq (7.73), $\mathbf{x}$ for the position vector, $\mathbf{b}\,(=\{b_1, b_2, b_e\}^T)$ for the known generalized body force term. Then $\breve{\mathbf{u}} = \breve{\mathbf{u}}(\mathbf{x})$ and $\mathbf{N} = \mathbf{N}(\mathbf{x})$ in eqn (7.134) have to be chosen such that

$$\Re\breve{\mathbf{u}} + \mathbf{b} = 0 \quad \text{and} \quad \Re\mathbf{N} = 0 \tag{7.136}$$

Using the above definitions the generalized boundary forces and electric displacements can be derived from Eqs (8), (9) and (7.134), and denoted as

$$\mathbf{T} = \begin{Bmatrix} t_1 \\ t_2 \\ D_n \end{Bmatrix} = \begin{Bmatrix} \sigma_{1j} n_j \\ \sigma_{2j} n_j \\ D_j n_j \end{Bmatrix} = \begin{Bmatrix} \breve{t}_1 \\ \breve{t}_2 \\ \breve{D}_n \end{Bmatrix} + \begin{Bmatrix} \mathbf{Q}_1 \\ \mathbf{Q}_2 \\ \mathbf{Q}_3 \end{Bmatrix} \mathbf{c} = \mathbf{Q}\mathbf{c} + \breve{\mathbf{T}} \tag{7.137}$$

where $\breve{t}_i$ and $\breve{D}_n$ are derived from $\breve{\mathbf{u}}$.

Since the displacement $\mathbf{u}$ is approximated by Trefftz functions that satisfy Eq (7.136), the weighted residual statement for the plane piezoelectric problem can be written as

$$\int_{\Gamma_u} (u_i - \overline{u}_i) w_{1i} ds + \int_{\Gamma_\phi} (\phi - \overline{\phi}) w_2 ds + \int_{\Gamma_t} (t_i - \overline{t}_i) w_{3i} ds + \int_{\Gamma_t} (D_n - \overline{D}_n) w_4 ds = 0 \tag{7.138}$$

(a) Galerkin formulation

The Galerkin formulation is obtained when both the weighting and trial functions are chosen from Eqs (7.134) and (7.137) such that

$$w_{1i} = \mathbf{Q}_i \delta\mathbf{c}, \quad w_2 = \mathbf{Q}_3 \delta\mathbf{c}, \quad w_{3i} = -\mathbf{N}_i \delta\mathbf{c}, \quad w_4 = -\mathbf{N}_3 \delta\mathbf{c} \tag{7.139}$$

$$u_i = \mathbf{N}_i \mathbf{c} + \breve{u}_i, \quad \phi = \mathbf{N}_3 \mathbf{c} + \breve{\phi}, \quad t_i = \mathbf{Q}_i \mathbf{c} + \breve{t}_i, \quad D_n = \mathbf{Q}_3 \mathbf{c} + \breve{D}_n \tag{7.140}$$

Substituting these expressions into Eq (7.138), we have

$$\begin{aligned} &\int_{\Gamma_u} \mathbf{Q}_i^T (\mathbf{N}_i \mathbf{c} + \breve{u}_i - \overline{u}_i) ds + \int_{\Gamma_\phi} \mathbf{Q}_3^T (\mathbf{N}_3 \mathbf{c} + \breve{\phi} - \overline{\phi}) w_2 ds \\ &\quad - \int_{\Gamma_t} \mathbf{N}_i^T (\mathbf{Q}_i \mathbf{c} + \breve{t}_i - \overline{t}_i) ds - \int_{\Gamma_t} \mathbf{N}_3^T (\mathbf{Q}_3 \mathbf{c} + \breve{D}_n - \overline{D}_n) ds = 0 \end{aligned} \tag{7.141}$$

where the repeated index i represents the conventional summation from 1 to 2. Eq (7.141) can be conveniently written as the matrix form

$$\mathbf{K}\mathbf{c} = \mathbf{f} \tag{7.142}$$

with

$$\mathbf{K} = \int_{\Gamma_u} \mathbf{Q}_i^T \mathbf{N}_i ds - \int_{\Gamma_t} \mathbf{N}_i^T \mathbf{Q}_i ds + \int_{\Gamma_\phi} \mathbf{Q}_3^T \mathbf{N}_3 ds - \int_{\Gamma_D} \mathbf{N}_3^T \mathbf{Q}_3 ds \tag{7.143}$$

$$\mathbf{f} = \int_{\Gamma_u} \mathbf{Q}_i^T (\bar{u}_i - \breve{u}_i) ds - \int_{\Gamma_t} \mathbf{N}_i^T (\bar{t}_i - \breve{t}_i) ds + \int_{\Gamma_\phi} \mathbf{Q}_3^T (\bar{\phi} - \breve{\phi}) ds - \int_{\Gamma_D} \mathbf{N}_3^T (\bar{D}_n - \breve{D}_n) ds \tag{7.144}$$

(b) Point-collocation technique

The point collocation formulation is obtained when the weighting functions w_{ij} and w_i in Eq (7.138) are chosen to be the Dirac delta function:

$$w_{1i} = w_{3i} = w_2 = w_4 = \delta(P - P_i) \tag{7.145}$$

Substituting Eq (7.145) into Eq (7.138) yields

$$u_j(P_i) = \mathbf{N}_j(P_i)\mathbf{c} + \breve{u}_j(P_i) - \bar{u}_j(P_i) = 0, \quad (\text{for } P_i \in \Gamma_u, \ i = 1,2,\cdots M_1) \tag{7.146}$$

$$\phi(P_i) = \mathbf{N}_3(P_i)\mathbf{c} + \breve{\phi}(P_i) - \bar{\phi}(P_i) = 0, \quad (\text{for } P_i \in \Gamma_\phi, \ i = 1,2,\cdots M_2) \tag{7.147}$$

$$t_j(P_i) = \mathbf{Q}_j(P_i)\mathbf{c} + \breve{t}_j(P_i) - \bar{t}_j(P_i) = 0, \quad (\text{for } P_i \in \Gamma_\phi, \ i = 1,2,\cdots M_3) \tag{7.148}$$

$$D_n(P_i) = \mathbf{Q}_3(P_i)\mathbf{c} + \breve{D}_n(P_i) - \bar{D}_n(P_i) = 0, \quad (\text{for } P_i \in \Gamma_D, \ i = 1,2,\cdots M_4) \tag{7.149}$$

The above two equations may be written in matrix form as

$$\mathbf{K}_{ij}\mathbf{c}_j = \mathbf{f}_i \quad \text{or} \quad \mathbf{K}\mathbf{c} = \mathbf{f} \tag{7.150}$$

in which $\mathbf{K}_{ij}$ and $\mathbf{f}_i$ are given by

$$K_{ij} = \begin{cases} N_{1j}(P_i) & \text{if } j \le M_1 \text{ and } P_i \in \Gamma_u \\ N_{2j}(P_i) & \text{if } j > M_1 \text{ and } P_i \in \Gamma_u \\ N_{3j}(P_i) & \text{if } P_i \in \Gamma_\phi \\ Q_{1j}(P_i) & \text{if } j \le 2M_1 + M_2 + M_3 \text{ and } P_i \in \Gamma_t \\ Q_{2j}(P_i) & \text{if } j > 2M_1 + M_2 + M_3 \text{ and } P_i \in \Gamma_t \\ Q_{3j}(P_i) & \text{if } P_i \in \Gamma_D \end{cases} \tag{7.151}$$

and

$$f_i = \begin{cases} \bar{u}_1(P_i) - \breve{u}_1(P_i) & \text{if } i \le M_1 \text{ and } P_i \in \Gamma_u \\ \bar{u}_2(P_i) - \breve{u}_2(P_i) & \text{if } i > M_1 \text{ and } P_i \in \Gamma_u \\ \bar{\phi}(P_i) - \breve{\phi}(P_i) & \text{if } P_i \in \Gamma_\phi \\ \bar{t}_1(P_i) - \breve{t}_1(P_i) & \text{if } i \le 2M_1 + M_2 + M_3 \text{ and } P_i \in \Gamma_t \\ \bar{t}_2(P_i) - \breve{t}_2(P_i) & \text{if } i > 2M_1 + M_2 + M_3 \text{ and } P_i \in \Gamma_t \\ \bar{D}_n(P_i) - \breve{D}_n(P_i) & \text{if } P_i \in \Gamma_D \end{cases} \tag{7.152}$$

The points of collocation can be set at any location where a boundary value is known.

(c) Least-square formulation

The least-square formulation can be obtained by choosing w_{ij} and w_i in Eq (7.138) as arbitrary variations of the respective boundary residues, i.e.

$$w_{1i} = \delta(u_i - \bar{u}_i) = \mathbf{N}_i \delta\mathbf{c}, \quad w_2 = \delta(\phi - \bar{\phi}) = \mathbf{N}_3 \delta\mathbf{c} \tag{7.153}$$

$$w_{3i} = \delta(t_i - \bar{t}_i) = \mathbf{Q}_i \delta\mathbf{c}, \quad w_4 = \delta(D_n - \bar{D}_n) = \mathbf{Q}_3 \delta\mathbf{c} \tag{7.154}$$

Through substitution of Eqs (7.153) and (7.154) into Eq (7.138), we have

$$\begin{aligned} \delta\mathbf{c}^T [& \int_{\Gamma_u} \mathbf{N}_i^T (\mathbf{N}_i \mathbf{c} + \breve{u}_i - \bar{u}_i) ds + \alpha_1 \int_{\Gamma_\phi} \mathbf{N}_3^T (\mathbf{N}_3 \mathbf{c} + \breve{\phi} - \bar{\phi}) ds \\ & + \alpha_2 \int_{\Gamma_t} \mathbf{Q}_i^T (\mathbf{Q}_i \mathbf{c} + \breve{t}_i - \bar{t}_i) ds + \alpha_3 \int_{\Gamma_D} \mathbf{Q}_3^T (\mathbf{Q}_3 \mathbf{c} + \breve{D}_n - \bar{D}_n) ds] = 0 \end{aligned} \tag{7.155}$$

which leads to

$$\begin{aligned} [& \int_{\Gamma_u} \mathbf{N}_i^T \mathbf{N}_i ds + \alpha_1 \int_{\Gamma_\phi} \mathbf{N}_3^T \mathbf{N}_3 ds + \alpha_2 \int_{\Gamma_t} \mathbf{Q}_i^T \mathbf{Q}_i ds + \alpha_3 \int_{\Gamma_D} \mathbf{Q}_3^T \mathbf{Q}_3 ds] \mathbf{c} = \int_{\Gamma_u} \mathbf{N}_i^T (\breve{u}_i - \bar{u}_i) ds \\ & + \alpha_1 \int_{\Gamma_\phi} \mathbf{N}_3^T (\breve{\phi} - \bar{\phi}) ds + \alpha_2 \int_{\Gamma_t} \mathbf{Q}_i^T (\breve{t}_i - \bar{t}_i) ds + \alpha_3 \int_{\Gamma_D} \mathbf{Q}_3^T (\breve{D}_n - \bar{D}_n) ds \end{aligned} \tag{7.156}$$

where α_i again represents the weighting parameters serving the purpose of restoring the homogeneity of the physical dimensions.

This system of equations may be written in the same matrix form as Eq (7.150), in which the elements of matrix **K** are given by

$$\mathbf{K}_{jm} = \int_{\Gamma_u} \mathbf{N}_{ij}^T \mathbf{N}_{im} ds + \alpha_1 \int_{\Gamma_\phi} \mathbf{N}_{3j}^T \mathbf{N}_{3m} ds + \alpha_2 \int_{\Gamma_t} \mathbf{Q}_{ij}^T \mathbf{Q}_{im} ds + \alpha_3 \int_{\Gamma_D} \mathbf{Q}_{3j}^T \mathbf{Q}_{3m} ds \tag{7.157}$$

and the right-hand term $\mathbf{f}_i$ is in the form

$$f_j = \int_{\Gamma_u} \mathbf{N}_{ij}^T (\breve{u}_i - \bar{u}_i) ds + \alpha_1 \int_{\Gamma_\phi} \mathbf{N}_{3j}^T (\breve{\phi} - \bar{\phi}) ds + \alpha_2 \int_{\Gamma_t} \mathbf{Q}_{ij}^T (\breve{t}_i - \bar{t}_i) ds + \alpha_3 \int_{\Gamma_D} \mathbf{Q}_{3j}^T (\breve{D}_n - \bar{D}_n) ds \tag{7.158}$$

7.3.4 Direct formulation

The derivation of the direct Trefftz formulation is based on the following weighted residual statement

$$\int_\Omega [(\sigma_{ij,j} + b_i) u_i^* + (D_{i,i} + b_e) \phi^*] d\Omega = 0 \tag{7.159}$$

Integrating by parts for the term containing $\sigma_{ij,j}$ and $D_{i,i}$ in Eq (7.159), we obtain the following expression:

$$\int_\Omega (\sigma_{ij,j} u_i^* + D_{i,i} \phi^*] d\Omega = \int_\Gamma (t_i u_i^* + D_n \phi^*) ds - \int_\Omega (\sigma_{ij} u_{i,j}^* + D_i \phi_{,i}^*] d\Omega \tag{7.160}$$

Noting that

$$\sigma_{ij} u_{i,j}^* + D_i \phi_{,i}^* = \sigma_{ij}^* u_{i,j} + D_i^* \phi_{,i} \tag{7.161}$$

for linear piezoelectric material and integrating by parts to the second integral on the

right-hand side of Eq (7.160), we obtain

$$\int_\Omega (\sigma^*_{ij}u_{i,j} + D^*_i\phi_{,i})d\Omega = \int_\Gamma (t^*_i u_i + D^*_n\phi)ds - \int_\Omega (\sigma^*_{ij,j}u_i + D^*_{i,i}\phi)d\Omega \tag{7.162}$$

Making use of Eqs (7.160) and (7.162) yields

$$\int_\Omega (\sigma^*_{ij,j}u_i + D^*_{i,i}\phi + b_i u^*_i + b_e\phi^*)d\Omega = \int_\Gamma (t^*_i u_i + D^*_n\phi - t_i u^*_i - D_n\phi^*)ds \tag{7.163}$$

Notice that the four terms on the right-hand side are integrals on the Γ surface of the solution domain. Let us now consider that the boundary Γ is divided into two parts, Γ_u and Γ_t (Γ_ϕ and Γ_D), on each of which the boundary conditions (7.76) apply. Hence, Eq (7.163) can be written as

$$\begin{aligned}\int_\Omega (\sigma^*_{ij,j}u_i + D^*_{i,i}\phi + b_i u^*_i + b_e\phi^*)d\Omega &= \int_{\Gamma_u} (t^*_i\overline{u}_i - t_i u^*_i)ds \\ + \int_{\Gamma_t} (t^*_i u_i - \overline{t}_i u^*_i)ds &+ \int_{\Gamma_\phi} (D^*_n\overline{\phi} - D_n\phi^*)ds + \int_{\Gamma_D} (D^*_n\phi - \overline{D}_n\phi^*)ds\end{aligned} \tag{7.164}$$

which can be used as the starting point for the direct Trefftz boundary element formulation.

In the direct technique, the weighting function u^*_i and ϕ^* is chosen as

$$u^*_i = \mathbf{N}_i\delta\mathbf{c}, \quad \phi^* = \mathbf{N}_3\delta\mathbf{c}, \quad t^*_i = \mathbf{Q}_i\delta\mathbf{c}, \quad D^*_n = \mathbf{Q}_3\delta\mathbf{c} \tag{7.165}$$

Hence, Eq (7.164) reduces to

$$\begin{aligned}\int_\Omega (\mathbf{N}^T_i b_i + \mathbf{N}^T_3 b_e)d\Omega &= \int_{\Gamma_u} (\mathbf{Q}^T_i\overline{u}_i - \mathbf{N}^T_i t_i)ds \\ + \int_{\Gamma_t} (\mathbf{Q}^T_i u_i - \mathbf{N}^T_i\overline{t}_i)ds &+ \int_{\Gamma_\phi} (\mathbf{Q}^T_3\overline{\phi} - \mathbf{N}^T_3 D_n)ds + \int_{\Gamma_D} (\mathbf{Q}^T_3\phi - \mathbf{N}^T_3\overline{D}_n)ds\end{aligned} \tag{7.166}$$

which is free of the unknown vector **c**.

Similar to the treatment in Section 7.2.5, the boundary Γ is divided into a number of elements, for which u_z, t, ϕ, and D_n over a particular element, say element e, are approximated by the following interpolation functions:

$$u_{ie} = \tilde{\mathbf{N}}_{ie}\hat{\mathbf{u}}_{ie}, \qquad (\text{if element } e \in \Gamma_t) \tag{7.167}$$

$$t_{ie} = \tilde{\mathbf{Q}}_{ie}\hat{\mathbf{t}}_{ie}, \qquad (\text{if element } e \in \Gamma_u) \tag{7.168}$$

$$\phi_e = \tilde{\mathbf{N}}_{3e}\hat{\boldsymbol{\varphi}}_e, \qquad (\text{if element } e \in \Gamma_D) \tag{7.169}$$

$$D_{ne} = \tilde{\mathbf{Q}}_{3e}\hat{\mathbf{D}}_{ne}, \qquad (\text{if element } e \in \Gamma_\phi) \tag{7.170}$$

$\hat{\mathbf{u}}_{ie}$, $\hat{\mathbf{t}}_{ie}$, $\hat{\boldsymbol{\varphi}}_e$, and $\hat{\mathbf{D}}_{ne}$ are the nodal displacements, tractions, electric potential, and electric displacement over the related elements, and $\tilde{\mathbf{N}}_{ie}$ and $\tilde{\mathbf{Q}}_{ie}$ are suitable interpolation functions, which may be of the following form:

Constant element:

$$N(\xi) = 1 \tag{7.171}$$

Linear element:

$$N_1(\xi)=\frac{\xi_2-\xi}{\xi_2-\xi_1},\qquad N_2(\xi)=\frac{\xi-\xi_1}{\xi_2-\xi_1} \tag{7.172}$$

Quadratic element:

$$N_1(\xi)=\frac{(\xi-\xi_2)(\xi-\xi_3)}{(\xi_1-\xi_2)(\xi_1-\xi_3)}, \tag{7.173}$$

$$N_2(\xi)=\frac{(\xi-\xi_1)(\xi-\xi_3)}{(\xi_2-\xi_1)(\xi_2-\xi_3)}, \tag{7.174}$$

$$N_3(\xi)=\frac{(\xi-\xi_1)(\xi-\xi_2)}{(\xi_3-\xi_1)(\xi_3-\xi_2)} \tag{7.175}$$

where ξ varies from 0 to 1, and ξ_i is the value of ξ at node *i*.

Assembling all the elements, we can obtain the global interpolation functions for $\hat{\mathbf{u}}$ and $\hat{\mathbf{t}}$ over the whole boundary such that

$$u_i=\tilde{\mathbf{N}}_i\hat{\mathbf{u}}_i,\qquad (\text{if element } e\in\Gamma_t) \tag{7.176}$$

$$t_i=\tilde{\mathbf{Q}}_i\hat{\mathbf{t}}_i,\qquad (\text{if element } e\in\Gamma_u) \tag{7.177}$$

$$\phi=\tilde{\mathbf{N}}_3\hat{\boldsymbol{\varphi}},\qquad (\text{if element } e\in\Gamma_D) \tag{7.178}$$

$$D_n=\tilde{\mathbf{Q}}_3\hat{\mathbf{D}}_n,\qquad (\text{if element } e\in\Gamma_\phi) \tag{7.179}$$

with $\tilde{\mathbf{N}}_i$ and $\tilde{\mathbf{T}}_i$ being the global polynomial expansions defined only on Γ, and $\hat{\mathbf{u}}_i$, $\hat{\mathbf{t}}_i$, $\hat{\boldsymbol{\varphi}}$, and $\hat{\mathbf{D}}_n$ standing for vectors of nodal parameters on the boundary.

The final result of the algebraic equation system can be written as

$$\mathbf{K}\mathbf{x}=\mathbf{f} \tag{7.180}$$

where $\mathbf{x}$ is a vector of unknown values, and $\mathbf{K}$ and $\mathbf{f}$ are given by

$$\mathbf{K}=-\int_{\Gamma_u}\mathbf{N}_i^T\tilde{\mathbf{Q}}_i ds+\int_{\Gamma_t}Q_i^T\tilde{\mathbf{N}}_i ds-\int_{\Gamma_\phi}\mathbf{N}_3^T\tilde{\mathbf{Q}}_3 ds+\int_{\Gamma_t}Q_3^T\tilde{\mathbf{N}}_3 ds \tag{7.181}$$

$$\mathbf{f}=\int_\Omega(\mathbf{N}_i^T b_i+\mathbf{N}_3^T b_e)d\Omega-\int_{\Gamma_u}\mathbf{Q}_i^T\overline{u}_i ds+\int_{\Gamma_t}\mathbf{N}_i^T\overline{t}_i ds-\int_{\Gamma_\phi}\mathbf{Q}_3^T\overline{\phi} ds+\int_{\Gamma_t}\mathbf{N}_3^T\overline{D}_n ds \tag{7.182}$$

7.3.5 Modified Trefftz formulation

The modified Trefftz method presented in [11] is based on the principle of superposition and the basic idea of virtual BEM for elasticity. The use of a virtual boundary can obviate the need for computation of a singular integral on the real boundary. This subsection briefly summarizes the development in [11].

To obtain a weak solution of the boundary value problem (7.73)-(7.76), Yao and Wang [11] assumed that there are L points $\mathbf{x}_k^0$ $(k=1,2,3,\cdots,L)$ within the domain Ω, at which there are *x*- and *z*-direction point loads and point charge F_{k1}, F_{k2}, F_{k3},

respectively. Suppose also that there are distributed unknown virtual source loads $\boldsymbol{\Phi}(\bar{\mathbf{x}}) = \{\varphi_1(\bar{\mathbf{x}}), \varphi_2(\bar{\mathbf{x}}), \varphi_3(\bar{\mathbf{x}})\}$ on the virtual boundary Γ' (see Fig. 7.5), where φ_1, φ_2, φ_3 denote *x*- and *z*-direction loads and charge at source point $\bar{\mathbf{x}}$, respectively.

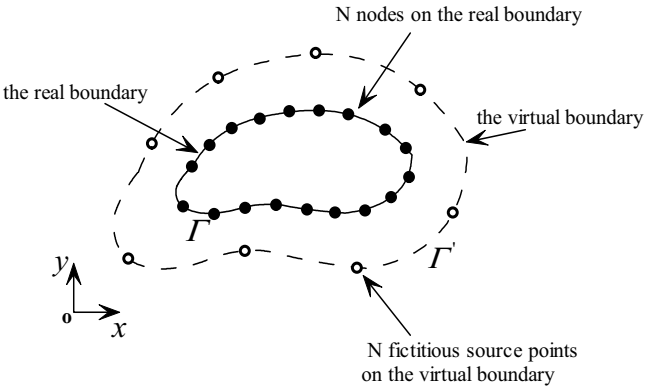

Fig. 7.5 Illustration of a computational domain and point discretization on real and virtual boundaries

In the absence of body forces and free electric volume charge, according to the principle of superposition the elastic displacements, electric potential, stress, and electric displacement at field point **x** induced by the loads mentioned above can be expressed as

$$u_I(\mathbf{x}) = \int_{\Gamma'} \left[\sum_{J=1}^{3} u_{IJ}^*(\mathbf{x}, \bar{\mathbf{x}}) \varphi_J(\bar{\mathbf{x}}) \right] d\Gamma' + \sum_{k=1}^{L} \sum_{J=1}^{3} u_{IJ}^*(\mathbf{x}, \mathbf{x}_k^0) F_{kJ} \tag{7.183}$$

$$\Pi_{iJ}(\mathbf{x}) = \int_{\Gamma'} \left[\sum_{J=1}^{3} S_{KiJ}^*(\mathbf{x}, \bar{\mathbf{x}}) \varphi_K(\bar{\mathbf{x}}) \right] d\Gamma' + \sum_{k=1}^{L} \sum_{J=1}^{3} S_{MiJ}^*(\mathbf{x}, \mathbf{x}_k^0) F_{kM} \tag{7.184}$$

where i=1,2,3, u_{IJ}^* was explained in the paragraph just after Eq (5.29), and S_{KiJ}^* was defined by Eq (5.45).

To evaluate the boundary integral in Eq (7.183) numerically, divide the virtual boundary Γ' into n elements. Assume that the total number of nodes is N and there are m nodal points on a particular element, say element p. Therefore, the value of the distributed loads and charge at any point on the element p can be expressed as

$$\varphi_J = \sum_{l=1}^{m} N_l(\xi) \varphi_J^l \tag{7.185}$$

where $N_l(\xi)$ are the conventional interpolation functions, ξ is the dimensionless coordinate explained after Eq (7.175), and φ_J^l represents the value of loads and charge at the lth nodal point.

Substituting Eq (7.185) into Eqs (7.183) and (7.184) yields

$$\begin{aligned} u_I(\mathbf{x}) &= \sum_{p=1}^{n}\int_{\Gamma_p'}\left[\sum_{J=1}^{3}u_{IJ}^{*}(\mathbf{x},\hat{\mathbf{x}})\varphi_J(\hat{\mathbf{x}})\right]d\Gamma' + \sum_{k=1}^{L}\sum_{J=1}^{3}u_{IJ}^{*}(\mathbf{x},\mathbf{x}_k^0)F_{kJ} \\ &= \sum_{p=1}^{n}\sum_{l=1}^{m}\sum_{J=1}^{3}\left[\int_{\Gamma_p'}u_{IJ}^{*}(\mathbf{x},\hat{\mathbf{x}})N_l(\xi)d\Gamma'\right]\varphi_J^l + \sum_{k=1}^{L}\sum_{J=1}^{3}u_{IJ}^{*}(\mathbf{x},\mathbf{x}_k^0)F_{kJ} \end{aligned} \tag{7.186}$$

$$\begin{aligned} \Pi_{iJ}(\mathbf{x}) &= \sum_{p=1}^{n}\int_{\Gamma_p'}\left[\sum_{J=1}^{3}S_{KiJ}^{*}(\mathbf{x},\hat{\mathbf{x}})\varphi_K(\hat{\mathbf{x}})\right]d\Gamma' + \sum_{k=1}^{L}\sum_{J=1}^{3}S_{MiJ}^{*}(\mathbf{x},\mathbf{x}_k^0)F_{kM} \\ &= \sum_{p=1}^{n}\sum_{l=1}^{m}\sum_{J=1}^{3}\left[\int_{\Gamma_p'}S_{KiJ}^{*}(\mathbf{x},\hat{\mathbf{x}})N_l(\xi)d\Gamma'\right]\varphi_K^l + \sum_{k=1}^{L}\sum_{J=1}^{3}S_{MiJ}^{*}(\mathbf{x},\mathbf{x}_k^0)F_{kM} \end{aligned} \tag{7.187}$$

To determine the $3N$ unknowns φ_J^l, the N collocation points $\mathbf{x}_q$ (q=1,2,3,…,N) on the real boundary are selected. Then, using Eqs (7.186) and (7.187), the generalized displacement and stress at point $\mathbf{x}_q$ can be expressed as

$$u_I(\mathbf{x}_q) = \sum_{p=1}^{n}\sum_{l=1}^{m}\sum_{J=1}^{3}h_{iJl}^{pq}(\mathbf{x}_q)\varphi_J^l + \sum_{k=1}^{L}\sum_{J=1}^{3}u_{IJ}^{*}(\mathbf{x}_q,\mathbf{x}_k^0)F_{kJ} \tag{7.188}$$

$$\Pi_{iJ}(\mathbf{x}_p) = \sum_{p=1}^{n}\sum_{l=1}^{m}\sum_{J=1}^{3}g_{KiJl}^{pq}(\mathbf{x}_p)\varphi_K^l + \sum_{k=1}^{L}\sum_{J=1}^{3}S_{MiJ}^{*}(\mathbf{x}_q,\mathbf{x}_k^0)F_{kM} \tag{7.189}$$

where

$$h_{ijl}^{pq} = \int_{\Gamma_p'}u_{IJ}^{*}(\mathbf{x},\hat{\mathbf{x}})N_l(\xi)d\Gamma' \tag{7.190}$$

$$g_{KiJl}^{pq} = \int_{\Gamma_p'}S_{KiJ}^{*}(\mathbf{x},\hat{\mathbf{x}})N_l(\xi)d\Gamma' \tag{7.191}$$

A linear equation system for the unknowns φ_J^l can thus be obtained by enforcing the given boundary conditions at $\mathbf{x}_q$ (q=1,2,3,…,N) as

$$\mathbf{HA} = \mathbf{Y} \tag{7.192}$$

where $\mathbf{A} = \{\varphi_1^1, \varphi_2^1, \varphi_3^1, \varphi_1^2, \cdots, \varphi_3^N\}^T$, $\mathbf{Y}$ designates a vector with $3N$ components, which is formed according to the given boundary conditions at collocation points $\mathbf{x}_q$ (q=1,2,3,…,N) on the real boundary, and $\mathbf{H}$ stands for the influence matrix of $3N\times3N$.

As was noted in [14], the effectiveness of the modified Trefftz method depends strongly on following three aspects:

--- shape of the virtual boundary

--- distance between the virtual and physical boundaries

--- investigation of the conditioning number of the solution matrix

Firstly, any shape of virtual boundary can, theoretically, be used in the calculation. However, due to inherent limitations of computer precision, the shape of the virtual boundary may influence the numerical accuracy of the output results. It has been proved that a circular virtual boundary [15] and a similar virtual boundary [16] are suitable for the modified Trefftz method. Based on these two schemes, for a rectangular domain for example, the shape of a virtual boundary can be chosen as either a rectangle or a circle (see Fig. 7.6). The effectiveness of the two schemes is assessed in [14].

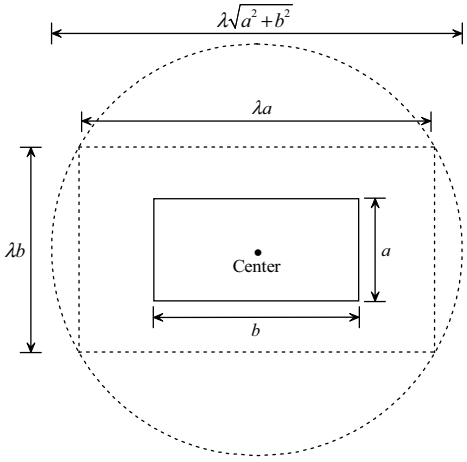

Fig. 7.6 Rectangular and circular virtual boundaries of a simple rectangular domain

The distance between fictitious source points and the physical boundary also has an important effect on the accuracy of the modified Trefftz method. To determine the location of the virtual boundary, a parameter λ representing the ratio between the characteristic lengths of the virtual and physical boundaries is introduced [16,17], defined by

$$\lambda = \frac{\text{characteristic length of virtual boundary}}{\text{characteristic length of physical boundary}} \tag{7.193}$$

From the computational viewpoint, the accuracy of the numerical results will deteriorate if the distance between the virtual and physical boundaries is too small (i.e., the similarity ratio λ is close to one), as that may cause problems due to singularity of the fundamental solutions. Conversely, round-off error in C/Fortran floating point arithmetic may be a serious problem when the source points are far from the real boundary. In that case, the coefficient matrix of the system of equations is nearly zero [18]. The similarity ratio λ is generally selected to be in the range of 1.8-4.0 for internal problems and 0.6-0.8 for external problems in practical computation [16,17].

The condition number of the solution matrix may be influenced by the location and shape of the virtual boundary as well as by the number of fictitious source points. In general, th coefficient matrix formed by using the virtual boundary collocation method has a large condition number. In this case, the standard Gauss elimination or LU decomposition (i.e. a procedure for decomposing a matrix **A** into a product of a lower triangular matrix **L** and an upper triangular matrix **U**) solutions may be invalid and the singular value decomposition is recommended to keep results stable for ill-conditioned systems [19].

References

[1] Qin QH, Mode III fracture analysis of piezoelectric materials by Trefftz BEM, Struc Eng Mech, 20, 225-239, 2005

[2] Jin WG, Sheng N, Sze KY, and Li J, Trefftz indirect methods for plane piezoelectricity, Int J Numer Meth Eng, 63, 2113-2138, 2006
[3] Sheng N, Sze KY and Cheung YK, Trefftz solutions for piezoelectricity by Lekhnitskii's formalism and boundary-collocation method, Int J Numer Meth Eng, 65, 139-158, 2005
[4] Sheng N and Sze KY, Multi-region Trefftz boundary element method for fracture analysis in plane piezoelectricity, Computational Mech, 37, 381-393, 2006
[5] Cheung YK, Jin WG and Zienkiewicz OC, Direct solution procedure for solution of harmonic problems using complete, non-singular, Trefftz functions, Commun Appl Numer Meth, 5, 159-169, 1989
[6] Jin WG, Cheung YK and Zienkiewicz OC, Application of the Trefftz method in plane elasticity problems, Int J Numer Meth Eng, 30, 1147-1161, 1990
[7] Qin QH, *The Trefftz Finite and Boundary Element Method*, WIT Press, Southampton, UK, 2000
[8] Oliveira ERA, Plane stress analysis by a general integral method, J Eng Mech Div, Proc ASCE, 94, 79-101, 1968
[9] Patterson C and Sheikh MA, On the use of fundamental solutions in Trefftz method for potential and elasticity problems, in: Boundary Element Methods in Engineering, Proc. 4th Int. Conf. on BEM, ed. C.A. Brebbia, Springer, pp. 43-57, 1982
[10] Patterson C and Sheikh MA, A modified Trefftz method for three dimensional elasticity, in: Boundary Elements, Proc. 5th Int. Conf. on BEM, eds. C.A. Brebbia, T. Futagami & M. Tanaka, Compu Mech Pub/Springer, pp. 427-437, 1983
[11] Yao WA and Wang H, Virtual boundary element integral method for 2-D piezoelectric media, Finite Elements in Analysis and Design, 41, 875-891, 2005
[12] Li XC and Yao WA, Virtual boundary element integral collocation method for the plane magnetoelectroelastic solids, Eng Analysis Bound Elements, 30, 709-717, 2006
[13] Wang XW, Zhou Y and Zhou WL, A novel hybrid finite element with a hole for analysis of plane piezoelectric medium with defects, Int J Solids Struct, 41, 7111-7128, 2004
[14] Wang H and Qin QH, A meshless method for generalized linear or nonlinear Poisson-type problems, Eng Analy Boun Elements, 30, 515-521, 2006
[15] Bogomolny A, Fundamental solutions method for elliptic boundary value problems. SIAM J Num Aanl, 22, 644-669, 1985
[16] Wang H, Qin QH and Kang YL, A new meshless method for steady-state heat conduction problems in anisotropic and inhomogeneous media, Arch Appl Mech. 74, 563-579, 2005
[17] Sun HC and Yao WA, Virtual boundary element-linear complementary equations for solving the elastic obstacle problems of thin plate, Finite Elements in Analysis and Design, 27, 153-161, 1997
[18] Mitic P and Rashed YF, Convergence and stability of the method of meshless fundamental solutions using an array of randomly distributed sources, Eng Analy Boun Elements, 28, 143-153, 2004
[19] Ramachandran PA, Method of fundamental solutions: singular value decomposition analysis, Commun. Numer. Meth. Engng, 18, 789–801, 2002

Appendix A: Radon Transform

In this Appendix, the Radon transform of f on Euclidean space is discussed. The discussion includes 2D and 3D Radon transform, their inverse representation, and some important properties of Radon transform. This appendix follows the relevant results presented in [1,2].

A.1 2D Radon transform

Let $\mathbf{x}=(x,y)$ and $\mathbf{n}=(\cos\psi,\sin\psi)$ be vectors in a 2D space (see Fig. A1), and consider an arbitrary function $f(\mathbf{x})$ defined on some domain Ω (the domain Ω may include the entire plane or some region of the plane, as shown in Fig. A1). If L is any line in the plane defined by

$$\omega = \mathbf{x}\cdot\mathbf{n} = x\cos\psi + y\sin\psi\,, \tag{A1}$$

then the mapping defined by the projection or line integral of f along all possible line lines L is the 2D Radon transform of f provided the integral exists. Based on the statement above, the 2D Radon transform may be written as an integral over Ω by allowing the Dirac delta function to select the line $\omega = \mathbf{x}\cdot\mathbf{n}$ from Ω[2]:

$$\hat{f}(\omega,\mathbf{n}) = R[f(\mathbf{x})] = \int_{\omega=\mathbf{x}\cdot\mathbf{n}} f(\mathbf{x})\delta(\omega-\mathbf{x}\cdot\mathbf{n})d\mathbf{x} \tag{A2}$$

Keep in mind that the unit vector $\mathbf{n}$ defines the direction in terms of the angle ψ, as shown in Fig. A1.

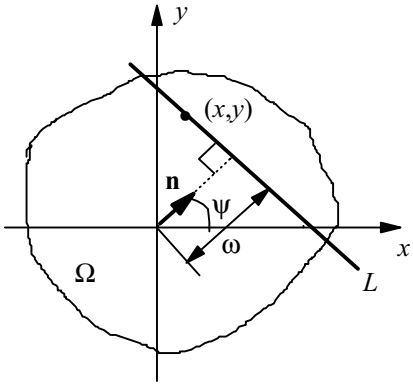

Fig. A1 The line L and coordinates ω and ψ

The inverse Radon transform is an integration in the $\mathbf{n}$-space over the surface Ω containing the origin, which can be given by[1,2]

$$f(\mathbf{x}) = R^{*}[\hat{f}(\omega,\mathbf{n})] = \frac{-1}{4\pi^2}\int_0^{2\pi} d\psi \int_{-\infty}^{\infty} \frac{\partial \hat{f}(\omega,\mathbf{n})/\partial\omega}{\omega-\mathbf{n}\cdot\mathbf{x}} d\omega \tag{A3}$$

Example: Let $f(x,y) = e^{-x^2-y^2}$. The Radon transform is then

$$\hat{f}(\omega,\mathbf{n}) = R[f(\mathbf{x})] = \int_{-\infty}^{\infty}\int_{-\infty}^{\infty} e^{-x^2-y^2}\delta(\omega-\mathbf{n}\cdot\mathbf{x})d\mathbf{x} \tag{A4}$$

Using the orthogonal linear transformation[1]

$$\begin{Bmatrix} u \\ v \end{Bmatrix} = \begin{bmatrix} n_1 & n_2 \\ -n_2 & n_1 \end{bmatrix} \begin{Bmatrix} x \\ y \end{Bmatrix} \tag{A5}$$

We have from Eq (A4)

$$\hat{f}(\omega, \mathbf{n}) = \int_{-\infty}^{\infty} \int_{-\infty}^{\infty} e^{-u^2 - v^2} \delta(\omega - u) du dv = e^{-\omega^2} \int_{-\infty}^{\infty} e^{-v^2} dv = \sqrt{\pi} e^{-\omega^2} \tag{A6}$$

A.2 3D extension

The generalization of Eq (A2) to 3D is accomplished by letting **x** be a vector in 3D, **x**=(*x*,*y*,*z*) and d**x**=*dxdydz*. The vector **n** is still a vector, but in 3D (Fig. A2). The line *L* is now replaced by a plane, as shown in Fig. A2. The plane is defined by

$$\omega = \mathbf{n} \cdot \mathbf{x} = n_1 x + n_2 y + n_3 z \tag{A7}$$

The corresponding Radon transform is exactly in the same form as that of Eq (A2), but the integrations are over planes rather than lines. Geometrically, as indicated in Fig. A2, ω is the distance from the origin to the plane and **n** is a unit vector along ω that defines the orientation of the plane.

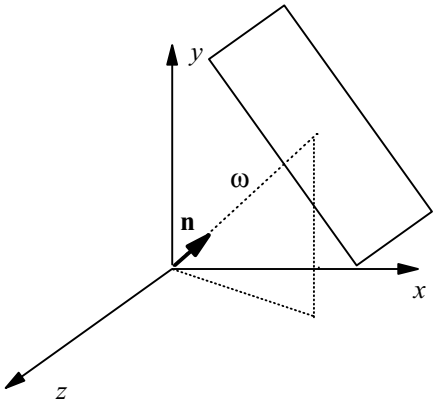

Fig. A2 Grometry for the Radon transform in 3D

Inverse of 3D Radon transform is defined by[1]

$$f(\mathbf{x}) = R^*[\hat{f}(\omega, \mathbf{n})] = \frac{-1}{8\pi^2} \int_{|\mathbf{n}|=1} \frac{\partial^2 \hat{f}(\omega, \mathbf{n})}{\partial \omega^2} d\mathbf{n} \tag{A8}$$

A.3 Basic properties of Radon transform[1,2]

A brief discussion of some basic properties treated here follows the results presented in [1]. From the definition (A2), we have following properties of Radon transform:

(i) Homogeneity

$$\hat{f}(s\omega, s\mathbf{n}) = \int_{\omega = \mathbf{x} \cdot \mathbf{n}} f(\mathbf{x}) \delta(s\omega - \mathbf{x} \cdot s\mathbf{n}) d\mathbf{x} = |s|^{-1} \hat{f}(\omega, \mathbf{n}) \tag{A9}$$

(ii)Linearity

$$R[cf + dg] = c\hat{f} + d\hat{g} \tag{A10}$$

(iii) Shifting property

$$R[f(\mathbf{x}+\mathbf{a})] = \hat{f}(\omega+\mathbf{n}\cdot\mathbf{a},\mathbf{n}) \tag{A11}$$

(iv)Transform of a linear transformation

$$R[f(\mathbf{A}^{-1}\mathbf{x})] = \left|\det \mathbf{A}\right| \hat{f}(\omega,\mathbf{A}^{T}\mathbf{n}) \tag{A12}$$

where $\det \mathbf{A} \neq 0$, and 'det' represents the determinant.

(v)Transform of derivatives

$$R\left[\frac{\partial f(\mathbf{x})}{\partial x_i}\right] = n_i \frac{\partial \hat{f}(\omega,\mathbf{n})}{\partial \omega}, \quad R\left[\frac{\partial^2 f(\mathbf{x})}{\partial x_i \partial x_j}\right] = n_i n_j \frac{\partial^2 \hat{f}(\omega,\mathbf{n})}{\partial \omega^2} \tag{A13}$$

(vi) Derivatives of the transform

$$\frac{\partial}{\partial n_i} R\left[f(\mathbf{x})\right] = -\frac{\partial}{\partial \omega} R\left[x_i f(\mathbf{x})\right], \quad \frac{\partial^2}{\partial n_i \partial n_j} R\left[f(\mathbf{x})\right] = \frac{\partial^2}{\partial \omega^2} R\left[x_i x_j f(\mathbf{x})\right] \tag{A14}$$

(vii) Transform of convolution
Let f be the convolution of g and h,

$$f(\mathbf{x}) = g * h = \int g(\mathbf{y}) h(\mathbf{x}-\mathbf{y}) d\mathbf{y}, \tag{A15}$$

then

$$R[f(\mathbf{x})] = R[g * h] = \hat{g} * \hat{h} \tag{A16}$$

References

[1] Dears SR, The Radon transform and some of its applications, New York: Wiley-Interscience Publication, 1983
[2] Pan E and Tonon F, Three-dimensional Green's functions in anisotropic piezoelectric solids, Int J Solids Struct, 37, 943-958, 2000

Appendix B: The constants α_j, s_j, and β_{mj} appeared in Section 4.3

(i) The constants α_j is given by[1,2]

$$\alpha_j = -n_1 + n_2 s_j^2 - n_3 s_j^4, \tag{B1}$$

where[2]

$$n_1 = (c_{13}+c_{44})(\kappa_{11}\mu_{11}-\alpha_{11}^2)+(e_{15}+e_{31})(e_{15}\mu_{11}-\alpha_{11}\tilde{e}_{15})-(\tilde{e}_{15}+\tilde{e}_{31})(e_{15}\alpha_{11}-\kappa_{11}\tilde{e}_{15}),$$

$$n_2 = (c_{13}+c_{44})(\kappa_{11}\mu_{33}+\kappa_{33}\mu_{11}-2\alpha_{11}\alpha_{33})+(e_{15}+e_{31})(e_{15}\mu_{33}+e_{33}\mu_{11}-\alpha_{11}\tilde{e}_{33}-\alpha_{33}\tilde{e}_{15})$$
$$-(\tilde{e}_{15}+\tilde{e}_{31})(e_{15}\alpha_{33}+e_{33}\alpha_{11}-\kappa_{11}\tilde{e}_{33}-\kappa_{33}\tilde{e}_{15}),$$

$$n_3 = (c_{13}+c_{44})(\kappa_{33}\mu_{33}-\alpha_{33}^2)+(e_{15}+e_{31})(e_{33}\mu_{33}-\alpha_{33}\tilde{e}_{33})-(\tilde{e}_{15}+\tilde{e}_{31})(e_{33}\alpha_{33}-\kappa_{33}\tilde{e}_{33}), \tag{B2}$$

and $s_0 = (c_{66}/c_{44})^{1/2}$, $s_j\,(j=1-4)$ are four characteristic roots of the following equation

$$a_1 s^8 - a_2 s^6 + a_3 s^4 - a_4 s^2 + a_5 = 0 \tag{B3}$$

with

$$a_1 = c_{44}[c_{33}(\kappa_{33}\mu_{33}-\alpha_{33}^2)-2e_{33}\alpha_{33}\tilde{e}_{33}+\mu_{33}e_{33}^2+\kappa_{33}\tilde{e}_{33}^2],$$

$$a_2 = c_{11}a_1/c_{44}+c_{44}[c_{44}(\kappa_{33}\mu_{33}-\alpha_{33}^2)+c_{33}(\kappa_{11}\mu_{33}+\kappa_{33}\mu_{11}-2\alpha_{11}\alpha_{33})$$
$$-2e_{15}\alpha_{33}\tilde{e}_{33}-2e_{33}(\alpha_{11}\tilde{e}_{33}+\alpha_{33}\tilde{e}_{15})+\mu_{11}e_{33}^2+2\mu_{33}e_{15}e_{33}+\kappa_{11}\tilde{e}_{33}^2+2\kappa_{33}\tilde{e}_{15}\tilde{e}_{33}]$$
$$-(c_{13}+c_{44})[(c_{13}+c_{44})(\kappa_{33}\mu_{33}-\alpha_{33}^2)+(e_{15}+e_{31})(e_{33}\mu_{33}-\alpha_{33}\tilde{e}_{33})$$
$$-(\tilde{e}_{15}+\tilde{e}_{31})(e_{33}\alpha_{33}-\kappa_{33}\tilde{e}_{33})]-(e_{15}+e_{31})[(c_{13}+c_{44})(e_{33}\mu_{33}-\alpha_{33}\tilde{e}_{33})$$
$$-(e_{15}+e_{31})(c_{33}\mu_{33}+\tilde{e}_{33}^2)+(\tilde{e}_{15}+\tilde{e}_{31})(c_{33}\alpha_{33}+e_{33}\tilde{e}_{33})]$$
$$-(\tilde{e}_{15}+\tilde{e}_{31})[(c_{13}+c_{44})(\kappa_{33}\tilde{e}_{33}-e_{33}\alpha_{33})+(e_{15}+e_{31})(c_{33}\alpha_{33}+e_{33}\tilde{e}_{33})$$
$$-(\tilde{e}_{15}+\tilde{e}_{31})(c_{33}\kappa_{33}+e_{33}^2)],$$

$$a_3 = c_{11}[c_{44}(\kappa_{33}\mu_{33}-\alpha_{33}^2)+c_{33}(\kappa_{11}\mu_{33}+\kappa_{33}\mu_{11}-2\alpha_{11}\alpha_{33})-2e_{15}\alpha_{33}\tilde{e}_{33}$$
$$-2e_{33}(\alpha_{11}\tilde{e}_{33}+\alpha_{33}\tilde{e}_{15})+\mu_{11}e_{33}^2+2\mu_{33}e_{15}e_{33}+\kappa_{11}\tilde{e}_{33}^2+2\kappa_{33}\tilde{e}_{15}\tilde{e}_{33}]$$
$$+c_{44}[c_{44}(\kappa_{11}\mu_{33}+\kappa_{33}\mu_{11}-2\alpha_{11}\alpha_{33})+c_{33}(\kappa_{11}\mu_{11}-\alpha_{11}^2)-2e_{15}(\alpha_{11}\tilde{e}_{33}+\alpha_{33}\tilde{e}_{15})$$
$$-2e_{33}\alpha_{11}\tilde{e}_{15}+2\mu_{11}e_{15}e_{33}+\mu_{33}e_{15}^2+2\kappa_{11}\tilde{e}_{15}\tilde{e}_{33}+\kappa_{33}\tilde{e}_{15}^2]$$
$$-(c_{13}+c_{44})[(c_{13}+c_{44})(\kappa_{11}\mu_{33}+\kappa_{33}\mu_{11}-2\alpha_{11}\alpha_{33})+(e_{15}+e_{31})(e_{15}\mu_{33}+e_{33}\mu_{11}$$
$$-\tilde{e}_{15}\alpha_{33}-\tilde{e}_{33}\alpha_{11})-(\tilde{e}_{15}+\tilde{e}_{31})(\alpha_{33}e_{15}+\alpha_{11}e_{33}-\tilde{e}_{15}\kappa_{33}-\tilde{e}_{33}\kappa_{11})]$$
$$-(e_{15}+e_{31})[(c_{13}+c_{44})(\mu_{33}e_{15}+\mu_{11}e_{33}-\alpha_{11}\tilde{e}_{33}-\tilde{e}_{15}\alpha_{33})$$
$$-(e_{15}+e_{31})(c_{44}\mu_{33}+c_{33}\mu_{11}+2\tilde{e}_{15}\tilde{e}_{33})+(\tilde{e}_{15}+\tilde{e}_{31})(c_{44}\alpha_{33}+c_{33}\alpha_{11}$$
$$+\tilde{e}_{15}e_{33}+e_{15}\tilde{e}_{33})]-(\tilde{e}_{15}+\tilde{e}_{31})[(c_{13}+c_{44})(\kappa_{11}\tilde{e}_{33}+\kappa_{33}\tilde{e}_{15}-\alpha_{33}e_{15}-\alpha_{11}e_{33})$$
$$+(e_{15}+e_{31})(c_{44}\alpha_{33}+c_{33}\alpha_{11}+e_{15}\tilde{e}_{33}+\tilde{e}_{15}e_{33})$$
$$-(\tilde{e}_{15}+\tilde{e}_{31})(c_{44}\kappa_{33}+c_{33}\kappa_{11}+2e_{15}e_{33})],$$

$$
\begin{aligned}
a_4 &= c_{11}[c_{44}(\kappa_{11}\mu_{33}+\kappa_{33}\mu_{11}-2\alpha_{11}\alpha_{33})+c_{33}(\kappa_{11}\mu_{11}-\alpha_{11}^2)-2e_{15}(\alpha_{11}\tilde{e}_{33}+\alpha_{33}\tilde{e}_{15})\\
&\quad -2e_{33}\alpha_{11}\tilde{e}_{15}+2\mu_{11}e_{15}e_{33}+\mu_{33}e_{15}^2+2\kappa_{11}\tilde{e}_{15}\tilde{e}_{33}+\kappa_{33}\tilde{e}_{15}^2]\\
&\quad +c_{44}[c_{44}(\kappa_{11}\mu_{11}-\alpha_{11}^2)-2\alpha_{11}e_{15}\tilde{e}_{15}+\mu_{11}e_{15}^2+\kappa_{11}\tilde{e}_{15}^2]\\
&\quad -(c_{13}+c_{44})[(c_{13}+c_{44})(\kappa_{11}\mu_{11}-\alpha_{11}^2)+(e_{15}+e_{31})(e_{15}\mu_{11}-\tilde{e}_{15}\alpha_{11})\\
&\quad -(\tilde{e}_{15}+\tilde{e}_{31})(\alpha_{11}e_{15}-\kappa_{11}\tilde{e}_{15})]-(e_{15}+e_{31})[(c_{13}+c_{44})(\mu_{11}e_{15}-\tilde{e}_{15}\alpha_{11})\\
&\quad -(e_{15}+e_{31})(c_{44}\mu_{11}+\tilde{e}_{15}^2)+(\tilde{e}_{15}+\tilde{e}_{31})(c_{44}\alpha_{11}+e_{15}\tilde{e}_{15})]\\
&\quad -(\tilde{e}_{15}+\tilde{e}_{31})[(c_{13}+c_{44})(\kappa_{11}\tilde{e}_{15}-e_{15}\alpha_{11})+(e_{15}+e_{31})(c_{44}\alpha_{11}+e_{15}\tilde{e}_{15})\\
&\quad -(\tilde{e}_{15}+\tilde{e}_{31})(c_{44}\kappa_{11}+e_{15}^2)],\\
a_5 &= c_{11}[c_{44}(\kappa_{11}\mu_{11}-\alpha_{11}^2)-2\alpha_{11}e_{15}\tilde{e}_{15}+\mu_{11}e_{15}^2+\kappa_{11}\tilde{e}_{15}^2]
\end{aligned}
\tag{B4}
$$

(ii) The constants β_{mj} are defined by

$$\beta_{mj}=-n_{4m}+n_{5m}s_j^2-n_{6m}s_j^4+n_{7m}s_j^6,\quad (m\text{=1-3}) \tag{B5}$$

where

$$
\begin{aligned}
&n_{41}=c_{11}(\kappa_{11}\mu_{11}-\alpha_{11}^2),\ \ n_{42}=c_{11}(e_{15}\mu_{11}-\tilde{e}_{15}\alpha_{11}),\ \ n_{43}=c_{11}(\kappa_{11}\tilde{e}_{15}-e_{15}\alpha_{11}),\\
&n_{51}=c_{11}(\kappa_{11}\mu_{33}+\kappa_{33}\mu_{11}-2\alpha_{11}\alpha_{33})+c_{44}(\kappa_{11}\mu_{11}-\alpha_{11}^2)+\mu_{11}(e_{15}+e_{31})^2\\
&\qquad +\kappa_{11}(\tilde{e}_{15}+\tilde{e}_{31})^2-2\alpha_{11}(e_{15}+e_{31})(\tilde{e}_{15}+\tilde{e}_{31}),\\
&n_{52}=c_{11}(e_{15}\mu_{33}+e_{33}\mu_{11}-\alpha_{11}\tilde{e}_{33}-\alpha_{33}\tilde{e}_{15})+c_{44}(e_{15}\mu_{11}-\alpha_{11}\tilde{e}_{15})-(e_{15}+e_{31})[\mu_{11}(c_{13}+c_{44})\\
&\qquad +\tilde{e}_{15}(\tilde{e}_{15}+\tilde{e}_{31})]+(\tilde{e}_{15}+\tilde{e}_{31})[\alpha_{11}(c_{13}+c_{44})+e_{15}(\tilde{e}_{15}+\tilde{e}_{31})],\\
&n_{53}=c_{11}(\kappa_{11}\tilde{e}_{33}+\kappa_{33}\tilde{e}_{15}-e_{15}\alpha_{33}-e_{33}\alpha_{11})+c_{44}(\kappa_{11}\tilde{e}_{15}-e_{15}\alpha_{11})+(e_{15}+e_{31})[\alpha_{11}(c_{13}+c_{44})\\
&\qquad +\tilde{e}_{15}(e_{15}+e_{31})]-(\tilde{e}_{15}+\tilde{e}_{31})[\kappa_{11}(c_{13}+c_{44})+e_{15}(e_{15}+e_{31})],\\
&n_{61}=c_{11}(\kappa_{33}\mu_{33}-\alpha_{33}^2)+c_{44}(\kappa_{11}\mu_{33}+\kappa_{33}\mu_{11}-2\alpha_{11}\alpha_{33})+\mu_{33}(e_{15}+e_{31})^2\\
&\qquad +\kappa_{33}(\tilde{e}_{15}+\tilde{e}_{31})^2-2\alpha_{33}(e_{15}+e_{31})(\tilde{e}_{15}+\tilde{e}_{31}),\\
&n_{62}=c_{44}(e_{15}\mu_{33}+e_{33}\mu_{11}-\alpha_{11}\tilde{e}_{33}-\alpha_{33}\tilde{e}_{15})+c_{11}(e_{33}\mu_{33}-\alpha_{33}\tilde{e}_{33})-(e_{15}+e_{31})[\mu_{33}(c_{13}+c_{44})\\
&\qquad +\tilde{e}_{33}(\tilde{e}_{15}+\tilde{e}_{31})]+(\tilde{e}_{15}+\tilde{e}_{31})[\alpha_{33}(c_{13}+c_{44})+e_{33}(\tilde{e}_{15}+\tilde{e}_{31})],\\
&n_{63}=c_{44}(\kappa_{11}\tilde{e}_{33}+\kappa_{33}\tilde{e}_{15}-e_{15}\alpha_{33}-e_{33}\alpha_{11})+c_{11}(\kappa_{33}\tilde{e}_{33}-e_{33}\alpha_{33})+(e_{15}+e_{31})[\alpha_{33}(c_{13}+c_{44})\\
&\qquad +\tilde{e}_{33}(e_{15}+e_{31})]-(\tilde{e}_{15}+\tilde{e}_{31})[\kappa_{33}(c_{13}+c_{44})+e_{33}(e_{15}+e_{31})],\\
&n_{71}=c_{44}(\kappa_{33}\mu_{33}-\alpha_{33}^2),\ \ n_{72}=c_{44}(e_{33}\mu_{33}-\alpha_{33}\tilde{e}_{33}),\ \ n_{73}=-c_{44}(e_{33}\alpha_{33}-\kappa_{33}\tilde{e}_{33})
\end{aligned}
\tag{B6}
$$

References

[1] Hou PF, Ding HJ and Chen JY, Green's function for transversely isotropic magnetoelectroelastic media, Int J Eng Sci, 43, 826-858, 2005

[2] Hou PF, Leung YTA and Ding HJ, The elliptical Hertzian contact of transversely isotropic magnetoelectroelastic bodies, Int J Solids Struct, 40, 2833-2850, 2003

Appendix C: Numerical Integration

C.1 Introduction

In this Appendix, guidelines for numerical computation of the element and its boundary integrals are presented. Since Gaussian integration formulae are general, simple and very accurate for a given number of points, attention is given to this type of numerical integration procedure.

C.2 One dimensional Gaussian quadrature [3]

The integrals in this case can be written as

$$I_1 = \int_{-1}^{1} f(\xi) d\xi = \sum_{i=1}^{n} f(\xi_i) w_i + E_n \tag{C1}$$

where ξ_i is the coordinate of the *i*th integration point, w_i is the associated weighting factor, and n is the total number of integration points. They are listed in Table C.1. Notice that ξ_i values are symmetric with respect to $\xi = 0$, w_i being the same for the two symmetric values. E_n is the error defined as [1]

$$E_n = \frac{2^{2n+1}(n!)^4}{(2n+1)(2n!)^3} \frac{d^{2n} f(\xi)}{d\xi^{2n}}, \quad (-1<\xi<1) \tag{C2}$$

Formula (C1) is based on the representation of $f(\xi)$ by means of Legendre polynomials $P_n(\xi)$. The ξ_i value is the coordinate at a point *i* where P_n is zero and for which the weights are given by

$$w_i = 2/(1-\xi_i^2) \left[\frac{dP_n(\xi)}{d\xi} \right]^2_{\xi=\xi_i} \tag{C3}$$

C.3 Two- and three-dimensional quadrature for rectangles and rectangular hexahedra

Two- and three-dimensional formulae are obtained by combining expression (C1) in the form

$$I_2 = \int_{-1}^{1} \int_{-1}^{1} f(\xi, \eta) d\xi d\eta \cong \sum_{j=1}^{n} \sum_{i=1}^{n} f(\xi_i, \eta_j) w_i w_j \tag{C4}$$

$$I_3 = \int_{-1}^{1} \int_{-1}^{1} \int_{-1}^{1} f(\xi, \eta, \zeta) d\xi d\eta d\zeta \cong \sum_{k=1}^{n} \sum_{j=1}^{n} \sum_{i=1}^{n} f(\xi_i, \eta_j, \zeta_k) w_i w_j w_k \tag{C5}$$

where the integration point coordinates and weighting factors are listed in Table C.1.

Table C1. Coefficients $\pm\xi_i$ and w_i in eqn (C1).

$\pm\xi_i$	w_i	$\pm\xi_i$	w_i
n =2		n=8	
0.57735 02691 89626	1.00000 00000 00000	0.18343 46424 95650	0.36268 37833 78362
		0.52553 24099 16329	0.31370 66458 77887
n=3		0.79666 64774 13627	0.22238 10344 53374
0.00000 00000 00000	0.88888 88888 88888	0.96028 98564 97536	0.10122 85362 90376
0.77459 66692 41483	0.55555 55555 55555		
		n=9	
n=4		0.00000 00000 00000	0.33023 93550 01260
0.33998 10435 84856	0.65214 51548 62546	0.32425 34234 03809	0.31234 70770 40003
0.86113 63115 94053	0.34785 48451 37454	0.61337 14327 00590	0.26061 06964 02935
		0.83603 11073 26636	0.18064 81606 94857
n=5		0.96816 02395 07626	0.08127 43883 61574
0.00000 00000 00000	0.56888 88888 88889		
0.53846 93101 05683	0.47862 86704 99366	n=10	
0.90617 98459 38664	0.23692 68850 56189	0.14887 43389 81631	0.29552 42247 14753
		0.43339 53941 29247	0.26926 67193 09996
n=6		0.67940 95682 99024	0.21908 63625 15982
0.23861 91860 83197	0.46791 39345 72691	0.86506 33666 88985	0.14945 13491 50581
0.66120 93864 66265	0.36076 15730 48139	0.97390 65285 17172	0.06667 13443 08688
0.93246 95142 03152	0.17132 44923 79170		
		n=12	
n=7		0.12523 34085 11469	0.24914 70458 13403
0.00000 00000 00000	0.41795 91836 73469	0.36783 14989 98180	0.23349 25365 38355
0.40584 51513 77397	0.38183 00505 05119	0.58731 79542 86617	0.20316 74267 23066
0.74153 11855 99394	0.27970 53914 89277	0.76990 26741 94305	0.16007 83285 43346
0.94910 79123 42759	0.12948 49661 68870	0.90411 72563 70475	0.10693 93259 95318
		0.98156 06342 46719	0.04717 53363 86512

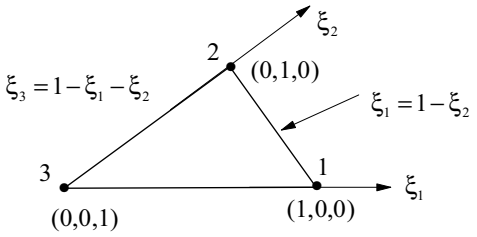

Fig. C1: Definition of triangular coordinates (ξ_1, ξ_2).

C.4 Triangular domain [1]

Numerical integration over a triangle can be carried out using triangular coordinates as shown in Fig. C1. This gives

$$I = \int_0^1 \left(\int_0^{1-\xi_2} f(\xi_1, \xi_2, \xi_3) d\xi_1 \right) d\xi_2 = \sum_{i=1}^{n} w_i f(\xi_1^i, \xi_2^i, \xi_3^i) \qquad \text{(C6)}$$

where n is the number of integration points, ξ_1^i, ξ_2^i and ξ_3^i are the coordinates of the ith integration point and w_i the associated weighting factor. Values of ξ_1^i, ξ_2^i, ξ_3^i and w_i compiled from Hammer [2] are given in Table C2.

By combining expression (C6) with (C1), numerical integration formulae for three-dimensional pentahedral cells can be obtained as before.

Table C2. Coefficients ξ_j^i $(j=1,2,3)$ and w_i in Eq (C6).

n	i	ξ_1^i	ξ_2^i	ξ_3^i	$2w_i$
1(linear)	1	1/3	1/3	1/3	1
3(quadratic)	1	1/2	1/2	0	1/3
	2	0	1/2	1/2	1/3
	3	1/2	0	1/2	1/3
4(cubic)	1	1/3	1/3	1/3	-9/16
	2	3/5	1/5	1/5	25/48
	3	1/5	3/5	1/5	25/48
	4	1/5	1/5	3/5	25/48
7(quintic)	1	0.333 333 33	0.333 333 33	0.333 333 33	0.225 000 00
	2	0.797 426 99	0.101 286 51	0.101 286 51	0.125 939 18
	3	0.101 286 51	0.797 426 99	0.101 286 51	0.125 939 18
	4	0.101 286 51	0.101 286 51	0.797 426 99	0.125 939 18
	5	0.059 715 87	0.470 142 06	0.470 142 06	0.132 394 15
	6	0.470 142 06	0.059 715 87	0.470 142 06	0.132 394 15
	7	0.470 142 06	0.470 142 06	0.059 715 87	0.132 394 15

References

[1] Brebbia C.A. & Dominguez J. *Boundary Elements: An Introductory Course*, 2nd Edition, Comp. Mech. Pub./McGraw-Hill Inc.: Southampton & New York, 1992.

[2] Hammer, P.C., Marlowe, O.J. & Stroud, A.H. Numerical Integration over simplexes and cones, *Math. Tables and Other Aids to Computation*, Vol. 10, 1956.

[3] Stroud, A.H. & Secrest, D. *Gaussian Quadrature Formulas,* Prentice-Hall: New York, 1966.

Index